THEORETICAL MODEL AND DYNAMIC SIMULATION OF VARIABLE FILL HYDRAULIC DYNAMOMETERS

P.G. Hodgson

May 1991

THEORETICAL MODEL AND DYNAMIC SIMULATION OF VARIABLE FILL HYDRAULIC DYNAMOMETERS

A thesis submitted for the Degree of
Doctor of Philosophy
in Mechanical Engineering at the
University of Canterbury,
Christchurch, New Zealand.

P.G. Hodgson

May 1991

To J.M.H.

ABSTRACT

The torque characteristics of variable fill hydraulic dynamometers are investigated, particularly the phenomenon of self-emptying of Froude F type machines under open loop control. An integrated one-dimensional model is adapted from fluid coupling and torque converter theory to cover the steady-state case, and extended to the non-linear open loop dynamic cases by incorporating varying fluid fill and the dynamic governing equations for dynamometers. Two feedback systems are included to predict the closed loop behaviour of the machines.

The effect of geometric variations on the steady-state torque capacity of dynamometers is given and the cause of the self-emptying phenomenon determined. It is found that the increase in working compartment fluid pressure with shaft speed leads to the fluid outflow rate becoming greater than the supplied inflow rate. Thus the fluid fill decreases. This phenomenon is further investigated using a dynamic model, consisting of a system of first order differential equations. The Adams-Bashforth Predictor Adams-Moulton Corrector numerical method is used to solve the system of equations. In addition to the self-emptying characteristic investigation, the differences between steady state and dynamic model predictions and the system responses to changes of set point and disturbances of its inputs (driving torque, outflow valve position, fluid inflow rate) are studied.

To enable closed loop performance prediction, models of two feedback system are incorporated: a back pressure water outlet valve driven by a machine-speed oil-pump, and an electrohydraulic butterfly valve governed by direct digital control. The latter model is used to investigate controller tuning around the dynamometer's operating envelope. It is also subjected to input disturbances and the responses compared to the open loop behaviour.

ACKNOWLEDGEMENTS

The author wishes to thank:

Dr. J.K. Raine for his supervision and guidance throughout the course of this research.

My parents, Ken and Joy, for their support and encouragement during my university career.

Murray Aitken for his friendship, tutelage and inspiration.

Professor H. McCallion for the use of the Department's facilities. Phillip Smith for his considerable assistance with the use of the Department's computing resources. Bruce Sparks for his drafting expertise. Diane Sanders for text entry.

All my friends for making existence through this work bearable.

Most importantly, Jilly for making it all worth while.

The financial support of the University Grants Committee Postgraduate Scholarship is gratefully acknowledged.

TABLE OF CONTENTS

LIST OF FIGURES

LIST OF TABLES

NOMENCLATURE

a	acceleration; working compartment radius
a_Y	air pocket radius
A	flow area
b	working compartment radius in axial plane
b_Y	air pocket radius in axial plane
B	bulk modulus of control hydraulic fluid
c	gap between rotor backs; damping constant
C	loss coefficient; cross product cofactor; integration constant
C_S	control surface
C_V	control volume
$C(r)$	circumference as a function of r
$c(t+h)$	corrected numerical valve of $y(t)$
d	hydraulic diameter
D	diameter; outer streamtube thickness
f	friction factor
F_P	pressure force
F_S	surface force
$f(x)$, $g(x)$	functions defining working compartment surface
$fy(x)$, $gy(x)$	functions defining air-water interface surface
g	body force
$G(s)$	first order approximate model of sigmoidal responses
h	conservation of mass for stator as a function of R_{CO} and R_{CI}
j	percentage fill definition as a function of R_{CO} and R_{CI}
J	Jacobian matrix
J_1, J_2	rotational inertias
J_2	combined rotor and fluid inertia
k	machine capacity number; shaft torsional stiffness; spring constant
$K_{\#'S}$	geometrical coefficients
K	response gain
K_B	secondary circulation loss factor
K_C	controller proportional gain
L	flow path length

M	mass
$\dot{m}$, $\dot{M}$	mass flow rate
N	rotational speed (rpm)
P	fluid pressure
δP	elemental pressure
P_o	atmospheric pressure
$d\dot{P}$	elemental power
$\dot{P}$	power
PF	percentage fluid fill
$p\ (t+h)$	predicted numerical value of $y\ (t)$
Q_{IN}	fluid inflow rate to working compartment
Q_O , Q_{OUT}	fluid outflow rate from working compartment
Q_{CV} , Q_P	hydraulic oil flow rate through control valve and from hydraulic pump
r	radius from machine axis; position vector
r_V	distance from vortex centre
R	radius from machine axis (integrated)
R_C	cup geometric centre radius
R_H	cup outlet hold radius
R_I	cup inner radius
R_M	fluid vortex centre radius
R_O	cup outer radius
R_Y	air pocket centre radius
R_{EI}	inner fluid mean flow path radius
R_{EO}	outer fluid mean flow path radius
R_{CI}	air-water interface inner radius
R_{CO}	air-water interface outer radius
t	vane thickness; time
t_d	response dead time
T	shaft torque; controller time step
u	valve actuation signal
U	rotor tip linear velocity
v, $\dot{v}$	valve velocity, acceleration
V	volume; fluid absolute linear velocity
$\dot{V}$	fluid absolute linear acceleration
W	fluid relative linear velocity
$y\ (t)$	general function of time
z , $\dot{z}$, $\ddot{z}$	valve displacement, velocity and acceleration

Z	vane number; axial distance from vortex centre (cropped rotor analysis)
α	vane angle
β	angle of water entry to return ring (cropped rotor analysis)
γ	angle between two vectors
δ	relative angular displacement of shaft
ε	feedback system error signal
ζ	angle between position and radial acceleration
θ	angle around working compartment
θ_D	angle used in Fig. 3.5 to determine distance to air-water interface for pressure boundary condition
θ_1 , θ_2	angular displacements
$\dot{\theta}_1$, $\dot{\theta}_2$	angular velocities
$\ddot{\theta}_1$, $\ddot{\theta}_2$	angular acceleration
μ	angle used to determine machine acceleration cross product cofactor
λ	friction coefficient ($=4f$)
υ	fluid viscosity
ρ	fluid density
τ	dynamometer torque; response time constant
τ_D	controller derivative action time
τ_I	controller integral action time
ω	fluid angular velocity
ω_P	rotor angular velocity
ω_1 , ω_2	angular velocities
$\dot{\omega}$	fluid angular acceleration
$\dot{\omega}_P$	rotor angular acceleration
$\dot{\omega}_1$, $\dot{\omega}_2$	angular accelerations

Subscripts

A	centre of cup outlet hole; air
B	centre of cup outlet hole; bend loss coefficient
C	centre of cup outlet hole
CR	cropped rotor
D	drain annulus; drain position above outlet valve
F	friction; fluid
FS	flow straightener
H	rotor outlet hole radius
i	iteration counter
I	inner; inlet; incidence; input
IN	inner radius between rotor backs
L	lower (r < Rm) part of working compartment; loss
n	normal or radial
O	outer; outlet
OT	outer radius between rotor backs
OIL	back pressure control oil
R	rotor
REL	relative to rotating plane
S	stator
SC	secondary circulation
SS	steady state
t	tangential to fluid flow path in vane plane
U	upper (r > Rm) part of working compartment; unsteady state
WV, WR, WWR	cross product cofactors
xyz	relative to rotor control volume
θ	tangential to machine rotation in rotor plane

CHAPTER 1
INTRODUCTION

For more than a century hydraulic dynamometers have been used as power absorbers for engine test purposes. Development work has been mainly experimental, though much theoretical work has been done on the closely related fluid coupling and fluid torque converter. This latter work has been predominantly on the prediction of steady state performance maps. As transient testing has increased with the requirements of exhaust emissions driving cycle tests and the advent of computer control, the dynamic characteristics of the dynamometer must be studied more closely, particularly the phenomenon of self-emptying in open loop control mode. From this study the control requirements around the operating envelope can be determined.

A brief description of the operating action of hydraulic dynamometers precedes the presentation of the self-emptying phenomenon of hydraulic dynamometers and its implications. This is followed by a review of work on dynamometers and hydrokinetic machines, and an outline of the scope of the present thesis.

1.1 Self-Emptying Dynamometers

An hydraulic dynamometer has a working compartment shaped as an elliptic torus containing two sets of oppositely angled vanes. One set is mounted on a rotor driven by the engine under test, the other on the stator which is held stationary by the machine casing. These can be seen in Fig.1.1 illustrating typical Froude F type machine internals with water outlet holes are at the back of the rotor cups and the drain annulus between the rotor backs. The double sided rotor eliminates axial thrust loading. There are holes in the stator vanes to allow water inflow and atmospheric air venting (Fig.1.2); later machines have the outlet holes in the stator cup for greater hydrodynamic stability.

When rotating, the rotor vanes pump the fluid from the inner radius to the outer radius where it passes into the stator. From here it flows from the outer to the inner radius of the stator transmitting torque and returning to the inner radius of the rotor. This circuit flow

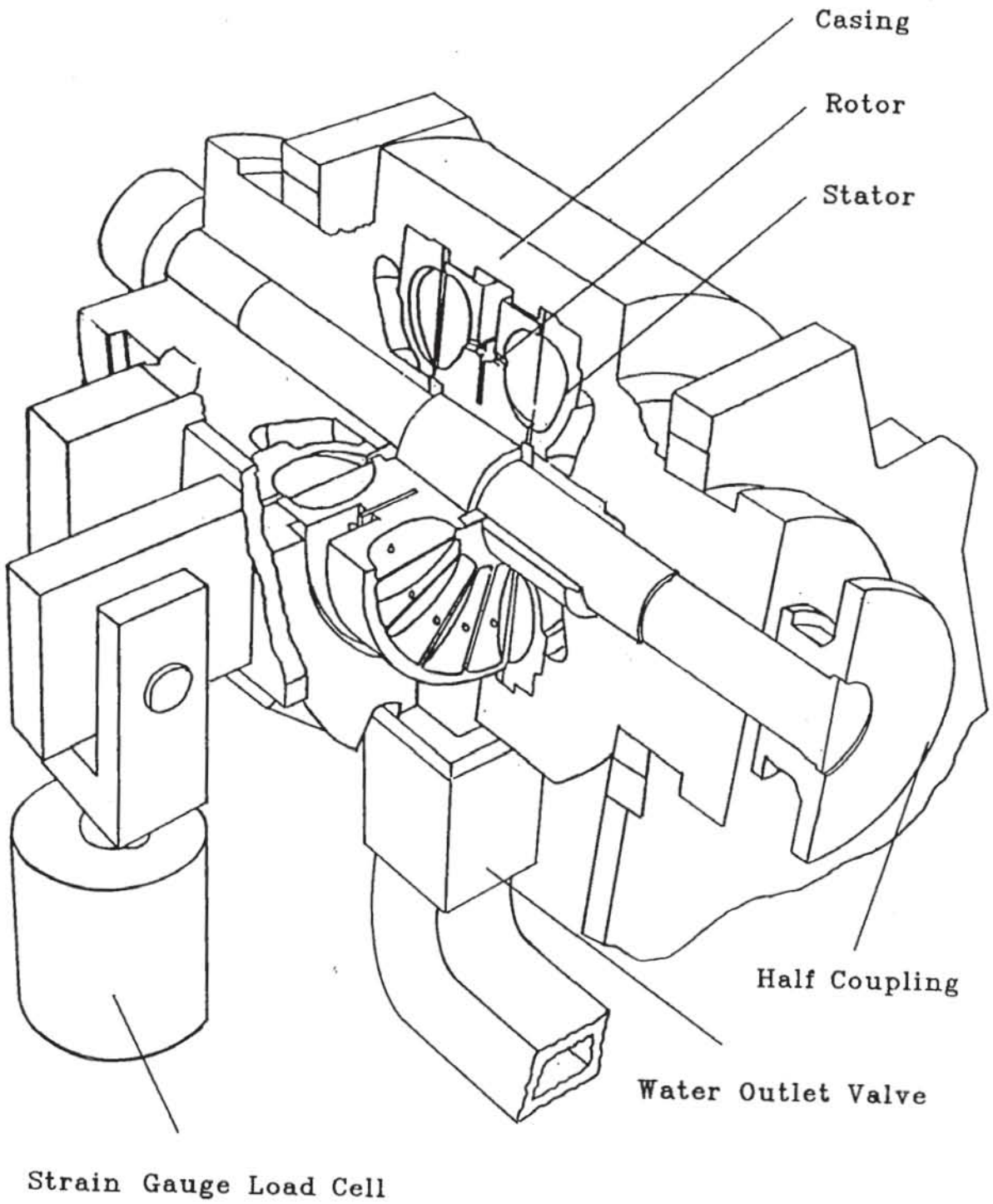

Figure 1.1: Cross-section Diagram of F0351Dynamometer

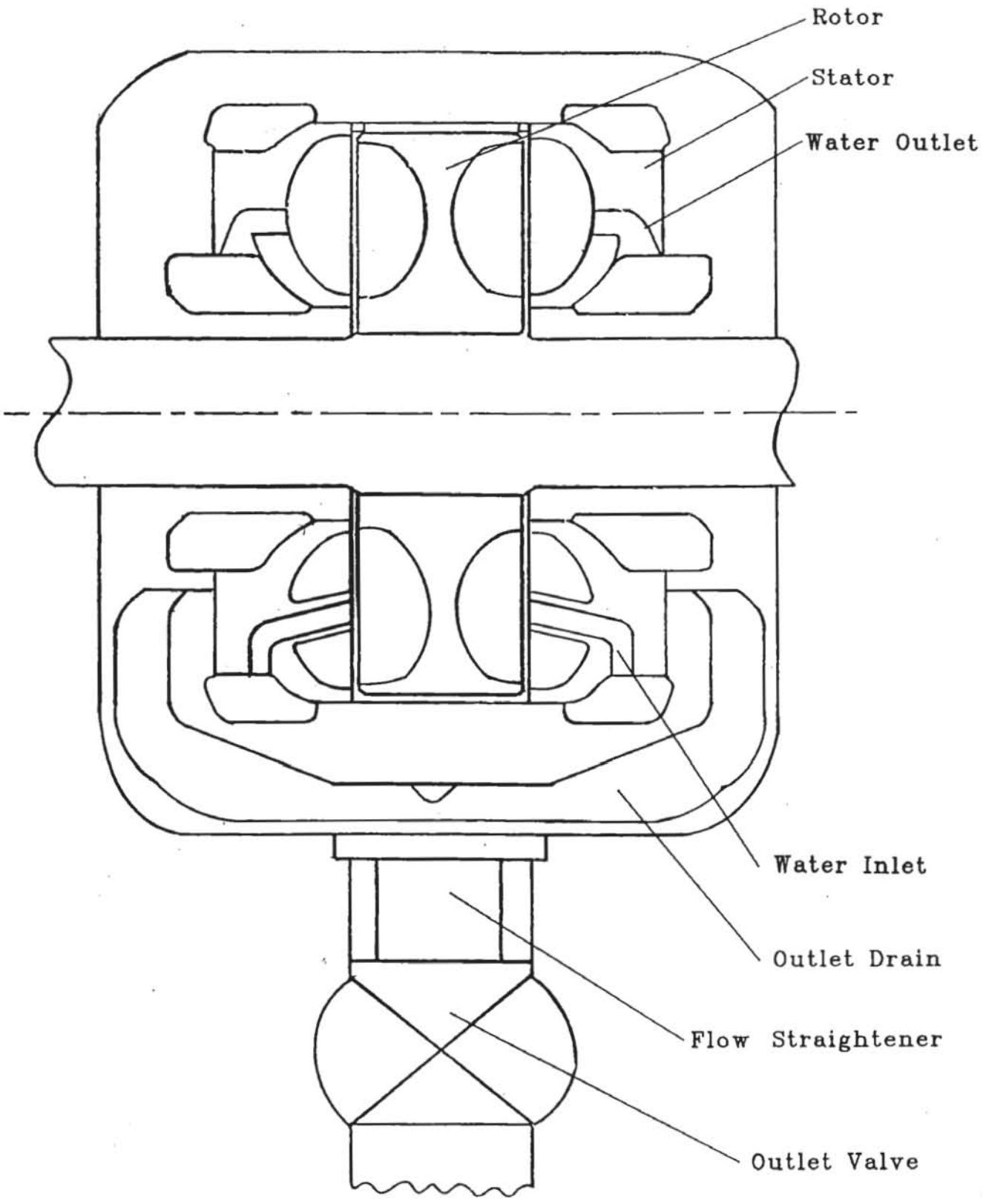

Figure 1.2: Stator Water Inlet and Outlet Holes

is superimposed on the rotational flow resulting in a helical flow path, as illustrated in Fig.1.3. Passing of the vanes disturbs this ideal flow pattern, generating turbulence. This combined with wall friction, fluid friction, incidence losses between rotor and stator, and eddies caused by the curved flow path, results in power being transferred to the internal energy of the working fluid. Hence it is necessary to maintain a sufficient fluid through-flow to limit the resultant temperature rise.

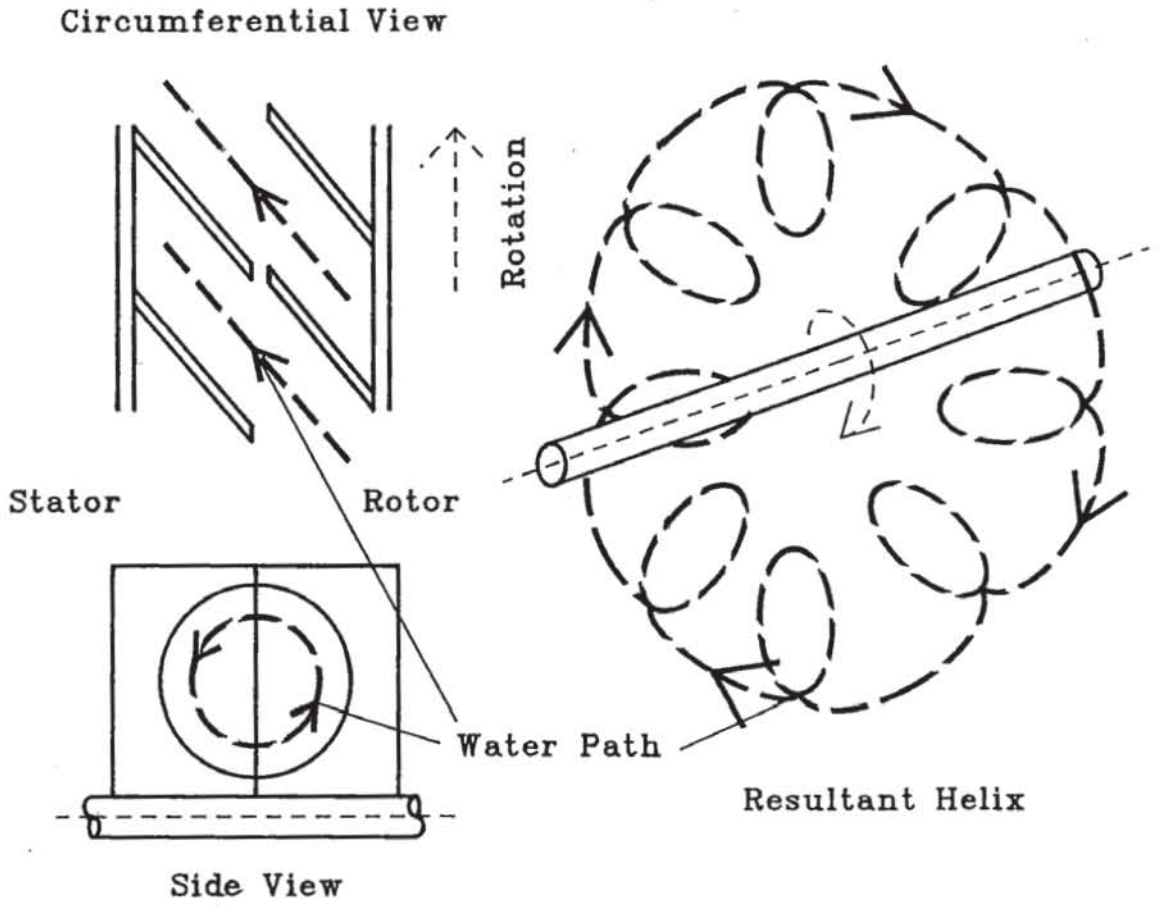

Figure 1.3: Dynamometer Vanes and Water Flow Path

The amount of torque produced by the machine is usually adjusted by either the use of a sluice gate between rotor and stator to reduce the area for fluid mass transfer, or by reducing the mass of fluid in the working compartment. Due to their superior transient response and reduced bulk, variable fill machines have superseded the sluice gate variety. The higher torque capacity to rotational inertia ratio of variable fill dynamometers also makes their performance superior to most electrical dynamometers in transient testing.

However when running under open-loop control the variable fill dynamometers display a torque characteristic as generalised in Fig.1.4

Initially torque increases with speed, but the pressure generated in the working compartment increases rapidly with speed until the fluid outflow rate is greater than the inflow and the machine begins emptying. As the volume of fluid in the working compartment is only a small fraction of the through-flow, a small difference in flow rates can produce dramatic effect on the torque developed. At higher speeds the torque begins increasing again, but this is shown later to be a dynamic effect of the machine accelerating and the rate of emptying decreasing, rather than increasing fluid fill.

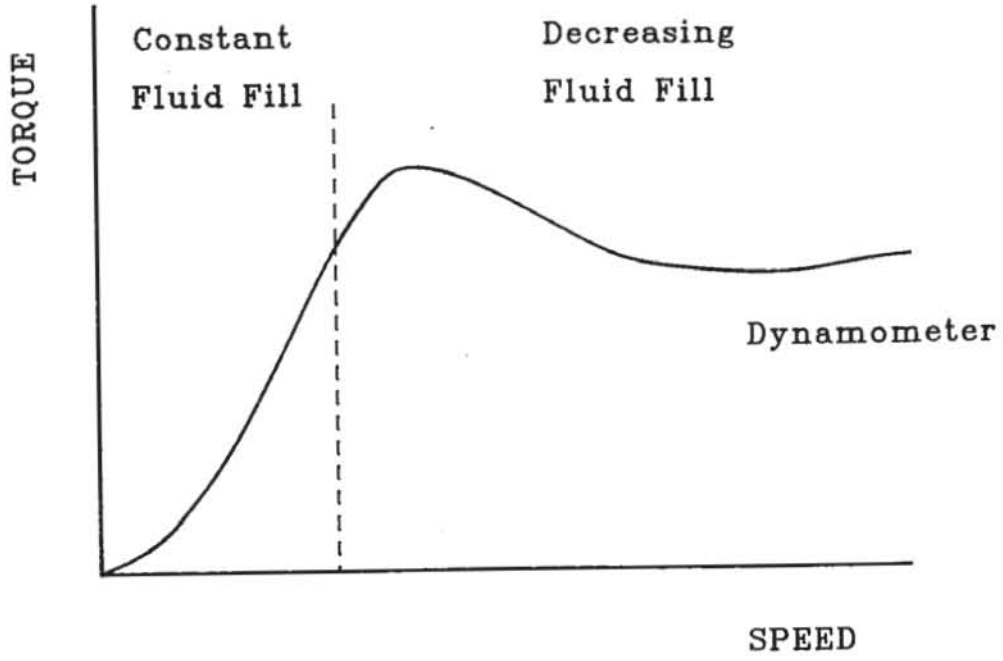

Figure 1.4: Typical Open Loop Torque Characteristic

When this characteristic is combined with a typical engine torque curve, as in Fig.1.5, the resultant problems become apparent. At set point A, where the torque gradient is greater for the dynamometer, a positive engine torque perturbation would increase the speed resulting in a greater dynamometer torque increase, which would slow the system back towards the set point. That is, the combination is self correcting. Where the dynamometer gradient is more negative, for example set point B, the increase in speed leads to decreased dynamometer torque, thus augmenting the accelerating torque and moving the system away from the desired set point. Similarly, a negative torque perturbation leads to a decrease in system

speed, an increase in dynamometer torque, and possible engine stall. Hence an increasing torque characteristic is desirable.

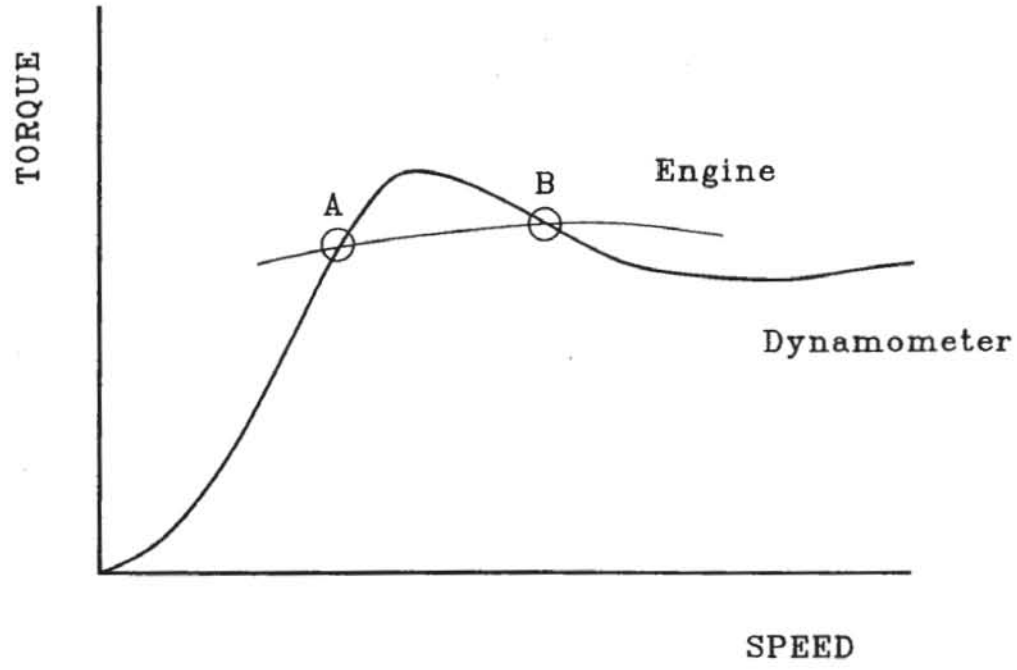

Figure 1.5: Combined Dynamometer and Engine Torque Characteristics

There are two methods of overcoming this problem; increase water inflow rate as speed increases, or provide rapidly increasing resistance to water outflow as speed increases. The former method involves: an inlet valve, which is controlled by rotor speed; or, an electrical or mechanical pump to increase inflow with speed. Outflow resistance methods include: a water outlet valve closed manually, by working compartment pressure feedback, or by shaft speed feedback (hydraulic or electrohydraulic); or, impellers on the back of the rotors to generate back pressure. It is desirable to study this self-emptying phenomenon and some methods of dealing with it so that improvements in dynamometer control can be made.

1.2 Historical Review

1.2.1 Dynamometers

In presenting his invention, the hydraulic dynamometer, in 1877 William Froude [1][1] gave a qualitative description of the vortex motion of the water within the machine. His original model used sluice gates to reduce the area available for fluid flow thus adjusting the torque developed by the full fill dynamometer. This method of load variation remained in widespread usage, although most modern machines now employ fill variation which was also discussed in Froude's presentation.

The first rigorous quantitative investigation[2] of dynamometers was by Rao [2] in 1968. He presented a mean flow path analysis of a fully filled machine and considered the effects of variation of blade angle, torus shape and dimensions, fluid properties, and loss coefficients on the torque capacity number. This work included shock and friction losses, but excluded blade thickness for most of the analysis. Knudsen and Countess [3] reported on hydrodynamic considerations of axial flow hydraulic dynamometers. While these operate in a different manner to the Froude type machine under study here, cavitation in dynamometers at high rotor tip velocities is also a major consideration in the design of Froude type dynamometers. Their paper discussed design procedures to minimize cavitation and proposed an experimental dynamometer research program.

A significant vibration problem in Froude type machines was reported by Mitsuhashi et al. [4] due to the combination of numbers of rotor and stator vanes. This work presented a linear analysis of the machine as a two degree of freedom system. Vibration was almost completely eliminated by increasing the number of rotor vanes by one. The effect of vane number on torque transmission was considered by Patki and Gill [5] using the classical hydrodynamic torque equation, though the pressure equation used to determine flow velocity is incomplete and incidence losses only qualitatively mentioned.

In order to investigate the self emptying phenomenon Raine [6] derived an integrated one-dimensional torque expression and a cup periphery pressure equation. He demonstrated that the cause of this emptying was an excessive decrease of cup fill rather than a degeneration of the cup water vortex action. His expressions allowed

---

1 Numbers in brackets denote references at the end of the thesis.

2 Rao's and others findings are compared to the author's investigation in Part II, while a brief comparison of the different approaches is given in the introduction of Part I.

for partial fill and the flow blockage due to vane thickness, but required the water velocity to be set as a function of rotor speed directly and pressure to be specified to calculate the water-air interface radii. Raine also discusses the practical implications of and solutions to these problems.

Raine's work was continued by Tan [7] to produce a quasi-dynamic model. Using a mass balance equation to determine the water-air interface radii and an energy balance on water outflow, he illustrated the falling torque characteristic. Results were presented for steady-state cases at various speeds where the water inflow and outflow were equal, and for quasi-dynamic cases (i.e. excluding rotational dynamics) with constant machine acceleration. Tan started to consider controller design by linearizing his equations about a set point, but concluded that system dynamics were necessary for adequate design.

Chiappini and Cipollone [8,9] used an experimental identification approach to give a discrete z-variable model of a linearized diesel engine and Froude G-type (inlet water pump to increase inflow with speed) dynamometer system. Caravani and Corcione [10] modelled D.C. and Eddy Current electric dynamometers also using an experimental identification approach.

1.2.2 Torque Converters and Fluid Couplings

Little other work has been reported on hydraulic dynamometers outside manufacturers' internal technical notes. However, a rich source of information exists for fluid couplings and torque converters developed first by Professor Föttinger circa 1908. Eksergian [11] investigated these machines using the mean flow path approach. Angular momentum, incidence loss and friction loss equations for each component were used to determine the useful operating range of acceptable efficiency. He also considered the effect of engine speed and torque, variation of machine circulating flow and the use of a fluid coupling as a torsional vibration damper.

Again using a mean flow path approach, Rolfe [12] analysed hydraulic couplings considering incidence and friction losses and fluid transfer from the working circuit to the reservoir and back. In addition to a theoretical approach, he used a transparent plastic model

to observe flow, concluding that a maximum vortex velocity around the working circuit occurred at 100% slip (i.e. dynamometer operating conditions).

Jandasek [13] and Qualman and Egbert [14] provided SAE design practises for torque converters and fluid couplings respectively, based on mean flow path analysis. These concluded that the design of the blading is of the utmost importance. Unequal inlet and exit angles for each component provided a higher torque capacity due to lower incidence losses.

More closely related to dynamometers, the hydrokinetic retarder's development is reviewed by Packer [15]. These share the same mode of operation as dynamometers, being power absorbers rather than transmitters. Both road and rail vehicles have incorporated these devices to allow faster hill descents and increase brake lining life. Numerous arrangements and placements of retarders in transmission systems have been developed, some of which are compared by Förster [16].

1.2.3 Analysis of Hydrodynamic Machines

In general, the analysis of hydrodynamic machines has varied from straightforward one dimensional design methods presented by Jandasek [13], Qualman and Egbert [14], Lucas and Rayner [17], Lucas [18], Szüle [19], and Nevrly [20] to the two dimensional fluid flow methods developed for both axial and radial flow turbomachines. The latter approaches stemmed from the work of Wu [21], Novak [22], and Marsh [23] and were classified as the Streamline Curvature Method and Matrix Through-flow Method. Reviews and comparisons of these two methods have been presented by Horlock and March [24,25], Bosman and Marsh [26], Davis and Millar [27], and Hirsch and Warzee [28]. Neal [29] applied the through-flow method to pump analysis, a similar case to dynamometers.

Andersson [30,31,32] used both one dimensional and two dimensional approaches to study torque converters. His one dimensional work began with a mean stream line approach, incorporating incidence and friction losses, in matrix form for computerisation. This was modified by the addition of equations in the direction transverse to the flow path. These allow for blade skew and

provide a check on the transverse force equilibrium required for the flow path analysis to be valid. Comparing this approach to both stream line curvature and finite element two dimensional methods, Andersson found that one dimensional theory is suitable when the external performance is of interest, and two dimensional theory when the flow pattern itself is being studied. The values of torque were less than 10% different with a greatly reduced computation requirement for one dimensional work.

The integrated one-dimensional approach was developed by Wallace and Whitfield with Sivalingam [33,34,35,36] and Patel [37,38,39]. Sivalingam [33] applied this model to torque converters and fluid couplings with and without core rings and of different blade angles and thicknesses. Couplings with baffle plates and partial fill, the two methods of torque adjustment, were also studied, as was a fully filled hydraulic retarder as a special case. Building on this Patel [37] developed a design procedure using the SAE design practises [13,14] for sizing torque converters and Sivalingam's model to produce refined performance prediction data. Patel also investigated the effect of geometric variations on the performance of hydrokinetic units, and flow visualisation using a transparent model.

Flow visualisation in partially filled fluid couplings had been presented by Ishihara et al [40] using a transparent machine with rectangular cross sections of various dimensions. The effect of different dimensions on the torque and thrust load characteristics were also studied. At stall, i.e. dynamometer conditions, the flow appeared to be an air-water mixture filling the working circuit, while at a slightly higher speed ratio a pocket of air remained at the centre of the circuit with aerated water flowing around the cups. Sivalingam [33] derived a pressure equation for the flow in the working compartment and used it to predict the profile of the air water interface. The latter concluded that an air core is formed as stall conditions are approached. However, the theoretical results predicted the four flow types found in Ishihara's visualisations, though the speed ratios varied. Numazawa [41] found during flow visualisation in torque converters that the pattern became smoother around the working circuit as the speed ratio approached stall.

Increasingly the dynamics of hydrokinetic machines has been investigated, with the work of Ishihara and Emori [42] leading the way. This work studied the transient characteristic of a torque converter

and clarified the damping effects by linearizing equations about a steady state operating point. A mean flow path analysis was used in conjunction with the equations of motion of the machine elements to analyse transients, while for vibration analysis the torque converter was simulated as a combination of mass, spring and damper elements. Meguid, May and Coleman [43] used mass, spring and beam elements to find the dynamic response of a fluid coupling.

The dynamics of torque converters, as part of a transmission system, have been of interest to automobile companies in such work as that of Kotwicki [44]. He produced a static non-linear terminal model of a torque converter to combine with differential equation models of engine and vehicle behaviour. The torque converter model used a mean streamline approach to obtain a torque expression as a function of pump and turbine speeds, which is simplified for the model. To obtain a consistent methodology in their vehicle studies many researchers have adopted bond graph modelling. The seminal reference on this method was presented by Karnopp and Rosenberg [45]. Hrovat and Tobler [46] applied this to torque converters as part of a power train, developing a system of dynamic equations for the machines including an unsteady torque equation.

1.3 Scope and Objectives of Thesis

The phenomenon of hydraulic dynamometers self emptying, the investigation of the effects of machine geometry variation, and the dynamic machine response to input perturbations under both open and closed loop control are the focal themes of this thesis.

In Part I, dynamometers are characterised by the application of integrated one dimensional theory and a vortex flow model. Given the accuracy of this approach, as reported by Andersson [30], and the flow patterns at stall, reported by various visualisations [40, 41], it is considered appropriate to the current investigation. The integrated one-dimensional approach developed by Wallace and Whitfield with Sivalingam [33,34,35,36] and Patel [37,38,39] was combined with the work of Raine [6] and Tan [7], then revised and expanded to form the basis of the dynamometer model. This was founded on a linear water velocity distribution due to a vortex action of constant angular velocity, and a balance between absorbed power and theoretically derived incidence, friction and turbulence losses. Chapter 2 presents an introduction to and comparison of one dimensional approaches, preceding the application of the theory to hydraulic dynamometers.

In the current work the derived torque equation is dynamic, allowing for both change of water fill and speed with time; the expressions used by Raine [6], Tan [7] and Sivalingam [33] can be seen as the steady state component. The determination of air-water interfaces under partial fill conditions is approached in a new manner in Chapter 3, while the derivations of a working compartment pressure expression includes terms due to acceleration and coriolis force not previously taken into account. The water outflow equation from Tan's work is modified and two additional water outflow paths analysed. Part I concludes with Chapter 4 showing the differences to the theoretical expressions if a machine with cropped rotor blades is being analysed.

The application of this theory to simulate dynamometer behaviour and the comparison of theoretical predictions with experimental test data are the themes of Part II, beginning with an investigation of static characteristics and the effect of geometric variations. This compares the current model's results to those of Rao [2] for geometry changes, and Tan [7] for steady *inflow equals outflow* mapping. Extensions to past studies are the consideration of twisted blades and the mapping of partial fill characteristics. A dynamic

representation of a dynamometer and engine inertia combination is derived in Chapter 6 as a system of first order differential equations, which are solved using the Adams-Bashforth predictor Adams-Moulton corrector method presented by Shampine and Gordon [47]. This characterisation is used as an open loop model to investigate the falling torque effect, and the subsequent rise at higher speeds. The latter effect is shown to be the result of system dynamics, as is the machine acceleration along a false hydraulic maximum. Both these characteristics were absent in Tan's work. The effect of input perturbations on the system are included in this study.

Two feedback systems, used to overcome the problem of self emptying, are modelled in Chapters 7 and 8. Firstly, a hydraulic back pressure water outflow valve which uses an oil pump driven by the dynamometer's shaft to close the outflow valve and a needle valve for load characteristic adjustment. Secondly, an electrohydraulically controlled butterfly outflow valve which uses a direct digital control representation of PID control on either dynamometer torque or speed feedback and requires varying control parameters around the operating envelope.

PART I

THEORETICAL ANALYSIS OF DYNAMOMETERS

CHAPTER 2
INTEGRATED ONE-DIMENSIONAL THEORY

Part I consists of three chapters. The first applies integrated one dimensional theory to the hydraulic dynamometer. In Chapter 3 the extra relationships to characterise machine behaviours are derived, and in the final chapter the differences in derivation for a cropped rotor machine are presented.

2.1 Introduction

The theoretical characterisation of turbomachines has been of interest to engineers for many years and with the advent of inexpensive computing power many techniques have been developed. The first hurdle is choosing the most appropriate technique for the task in hand. After utilizing both one and two dimensional theory in studying torque converters, Andersson [30] concluded that if performance prediction rather than fluid flow patterns is of interest one dimensional theory is more appropriate. For the purpose of this work an integrated one dimensional approach as developed by Wallace, Whitfield and Sivalingam [33,34,35,36] is used as the basis of the model in conjunction with the work of Raine [6] and Tan [7].

Classical theory for turbomachines gives the standard torque equation $T = kN^2D^5$, which is very convenient for the characterisation of geometrically similar machines once the capacity number, K, is determined. In practise the effects of speed and diameter have been found to vary with different indices. Rao [2] reasoned that the diameter index should be greater than 5 due to decreased relative roughness which is supported by Raine [6] who gives an empirical relationship of $T = kN^{1.8}D^{5.1}$. In several makes of dynamometer Rao also found the speed index to vary from 1.01 to 2.13, averaging at 1.62, concluding that the influence of incidence and friction effects must vary with speed.

The common theoretical approach has been the mean streamline (or flow path) method, which uses inner and outer effective radii and a uniform velocity distribution, as in Fig.2.1, to predict torque by

$$T = \dot{m}(V_{\theta O} R_{EO} - V_{\theta I} R_{EI}) \qquad (2.1)$$

where

$\dot{m}$ = mass flow rate

$V_{\theta O}, V_{\theta I}$ = outer and inner tangential water velocities

R_{EO}, R_{EI} = outer and inner effective radii

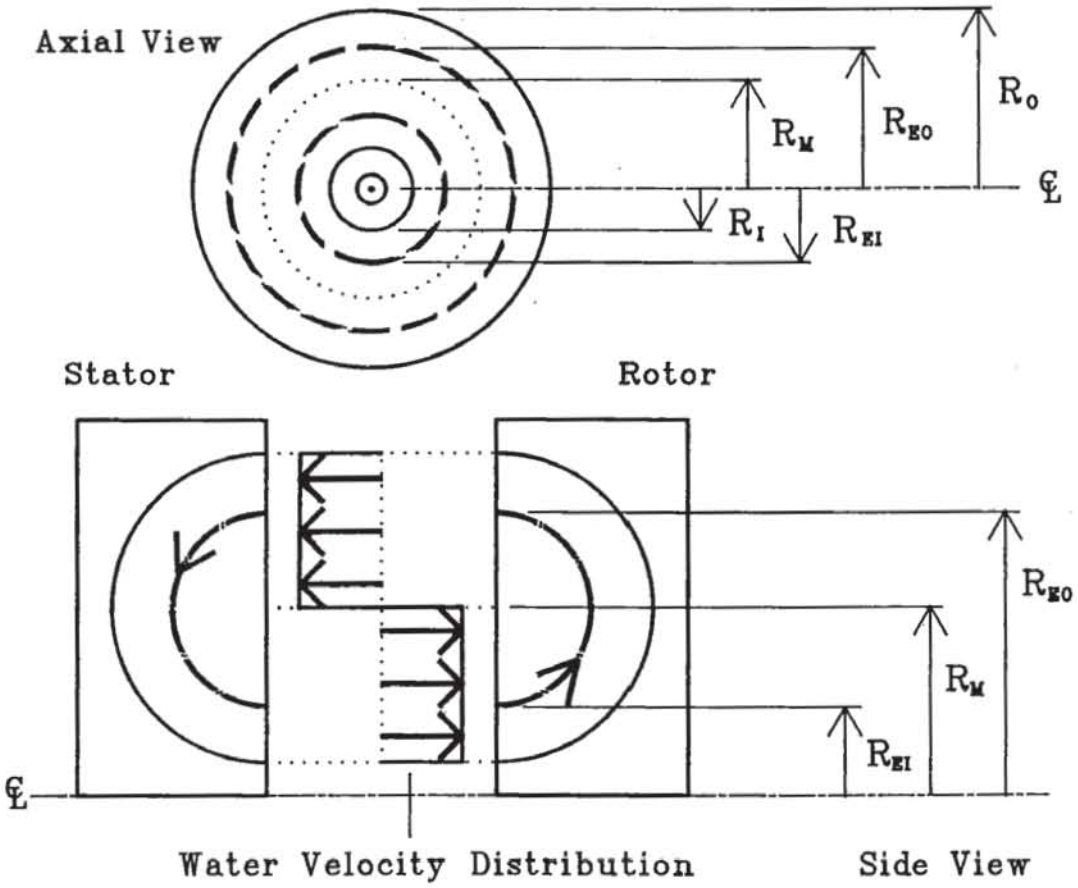

Figure 2.1: Uniform Velocity Distribution and Effective Radii Geometry

To satisfy continuity requirements the centre of the flow path, R_M, is found by equating the areas available for mass flow (excluding vane thickness for simplicity) to obtain

$$R_M = \sqrt{\frac{R_O^2 + R_I^2}{2}} \qquad (2.2)$$

The location of the inner and outer effective radii is usually obtained by a similar application to each flow area producing

$$R_{EO} = \sqrt{\frac{R_O^2 + R_M^2}{2}} \quad \text{and} \quad R_{EI} = \sqrt{\frac{R_I^2 + R_M^2}{2}}$$

These radii have also been calculated by equating the water kinetic energy transfers, Raine [6], leading to more complex expressions for

R_{EO} and R_{EI} . He uses a linear distributed velocity model for the water vortex.

The uniform velocity distribution has an unrealistic discontinuity at the centre, whereas Ishihara [40] and Numazawa [41] observed smooth flows around the working circuit at stall conditions. This smooth flow can be represented by a vortex of constant angular velocity, which results in a linear distributed flow, see Fig.2.2, as used by Whitfield, Wallace and Sivalingam and Raine. The flow velocity is proportional to the linear distance from the vortex centre. By equating the stator mass inflow and outflow rates the radius of the vortex centre is determined.

As an introduction to the application of the integrated one-dimensional approach the vortex centre of a fully filled axial vaned machine of zero blade thickness is derived and compared to that for the mean flow path theory above. A general expression for the quantity of interest is derived for a stream tube, as shown in Fig.2.2, and then integrated from the machine cup surface to either the vortex centre (full fill condition) or the air-water interface (partial fill condition). In this case the mass flow rate is being determined, so for the stream tube

$$\begin{aligned} d\dot{m} &= \textit{density} \times \textit{flow velocity} \times \textit{flow area} \\ &= \rho \times \omega(r - R_M) \times 2\pi r\, dr \end{aligned} \tag{2.3}$$

Integrating across the inlet,

$$\begin{aligned} \dot{m}_I &= \int_{R_M}^{R_O} 2\pi\rho\,\omega(r - R_M) r\, dr \\ &= 2\pi\rho\,\omega\left[\tfrac{1}{3}R_O^3 - \tfrac{1}{2}R_M R_O^2 + \tfrac{1}{6}R_M^3\right] \end{aligned} \tag{2.4}$$

Similarly for stator outflow,

$$\dot{m}_O = 2\pi\rho\,\omega\left[\tfrac{1}{3}R_I^3 - \tfrac{1}{2}R_M R_I^2 + \tfrac{1}{6}R_M^3\right] \tag{2.5}$$

Equating inflow and outflow yields

$$R_M = \frac{2}{3}\left[\frac{R_O^3 - R_I^3}{R_O^2 - R_I^2}\right] \tag{2.6}$$

This can be compared to Eqn.(2.2) for a Froude F020 machine (R_O = 102.5 mm, R_I = 43.5 mm), which gives a difference of just over 2%. Although not large in itself this difference is propagated through all the other calculations, for example the torque is dependent on R_M to

the fifth power, so its determination is required to be accurate for the approach chosen.

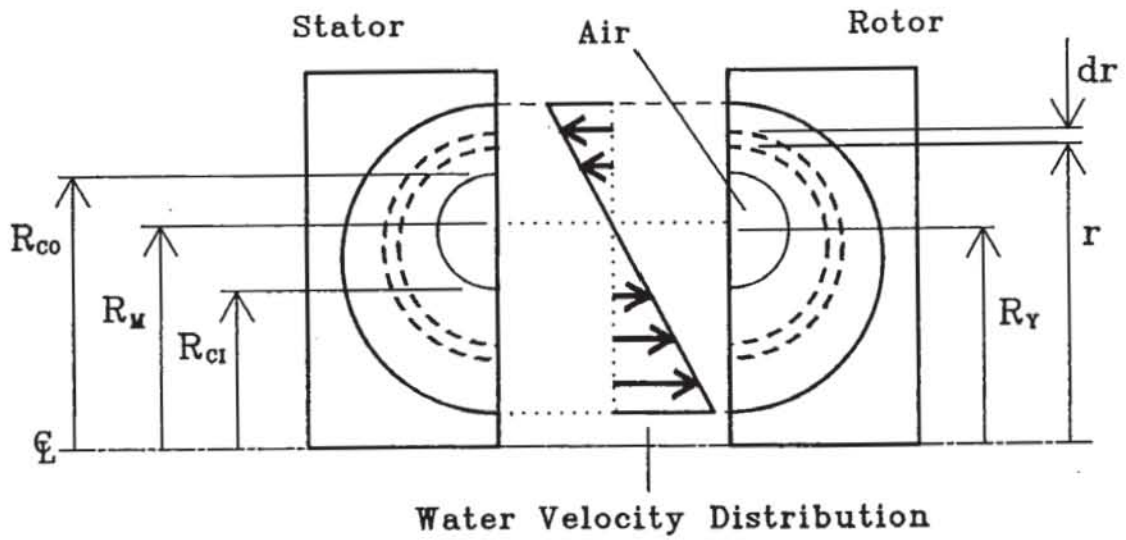

Figure 2.2: Linear Distributed Flow and Working Compartment Geometry

The application of the linear velocity distribution results in the velocity diagrams for the full rotor machine as shown in Fig.2.3. The magnitudes of the relative velocities is indicated on the diagram, but the directions at each point may need some clarification. At point 1 as the water just leaves the stator both the relative and absolute velocities are along the blade surface. Between the stator and rotor (point 2) the absolute velocity and that relative to the stator continue at the stator outlet angle, while the velocity relative to the rotor is influenced by the rotational motion. Having entered the rotor at point 3 the relative velocity is now along the rotor surface and the absolute velocity direction change is determined by the relative and rotational velocities. At rotor outlet (point 4) the relative velocity is still along the surface with the rotation contributing to the direction of the absolute velocity. Between components the rotor relative velocity continues at the rotor outlet angle, while the stator sees the absolute velocity, which

continues at the same angle as at point 4, as the velocity relative to it. Upon entering the stator the absolute and relative velocities remain coincident, but their direction has changed to that of the stator inlet angle.

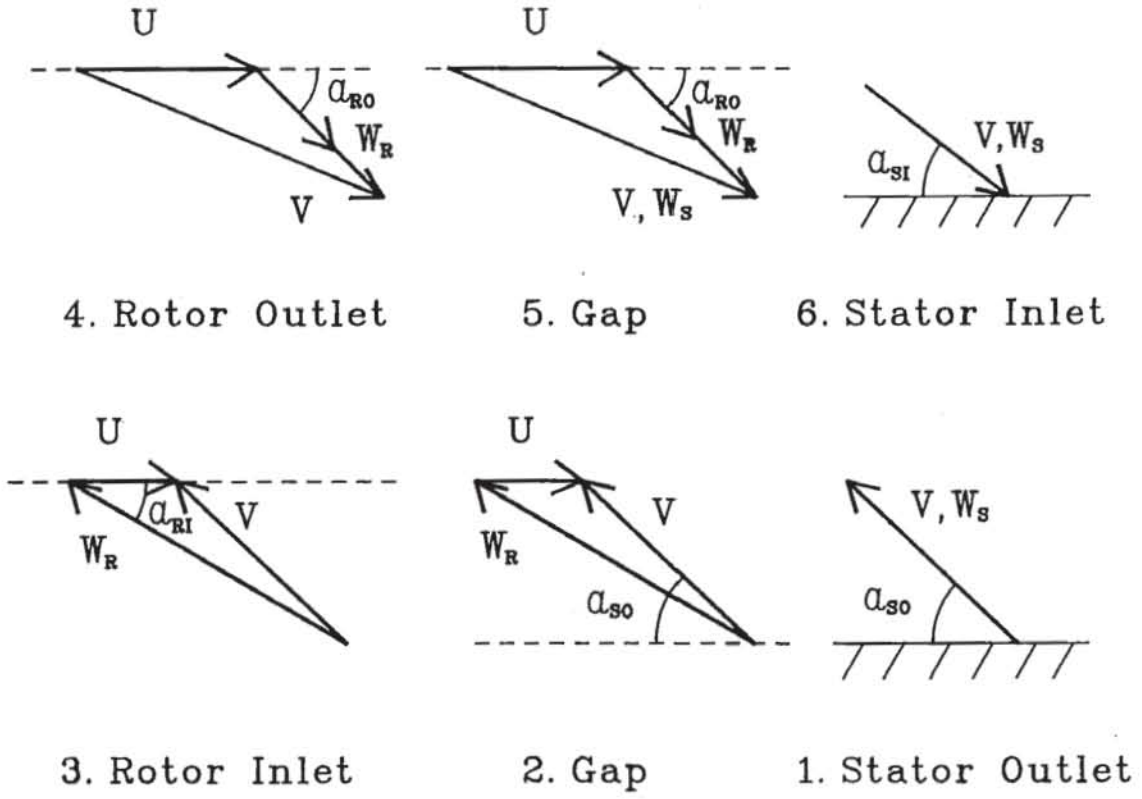

Figure 2.3: Full Rotor Dynamometer Velocity Diagrams

Due to the dynamometer usually operating in a partial fill condition and the vanes being considerably thicker than those of a torque converter or fluid coupling allowance for these two factors will be included in the theory from the outset. Sivalingam [33] concluded that blade thickness of 1.5 mm affected torque prediction by about 3~4%. However dynamometer vanes are considerably thicker for the same diameter of machine, so the blockage to flow area is significant.

In order to determine the vortex centre the principle of conservation of mass is applied to the stator in Section 2.3 with the inclusion of vane thickness and non-axial vanes as opposed to Eqn.(2.6). The torque developed is obtained from the conservation of angular momentum of the water flowing across the machine rotor (Section 2.4). Power input to the dynamometer is absorbed by the water, this energy

conversion process is represented in the model by three mechanisms: incidence loss, due to velocity changes between rotor and stator; friction loss, along the vane and toroid surfaces; and secondary circulation loss, caused by turbulence in the water flow from the curved flow path and vanes breaking the ideal helical flow. Section 2.2 shows how these energy loss equations and the torque equation are used in the application of conservation of energy to determine the angular velocity of the water vortex.

Before deriving the equations for the dynamometer, the initial assumptions are tabled below.

1. The water flow is modelled by a forced vortex of constant angular velocity in the plane of the machine vane, resulting in a velocity profile of linear distribution.
2. The vortex centre is determined for full water fill and is taken to be invariant as fill changes.
3. The working compartment is taken as giving a circular water flow path. In practice this is approximately true for most vane angles, though sometimes it becomes elliptic.
4. Boundaries between air and water are distinct, so the model is only dealing with single phase incompressible flow, though in fact the water is highly aerated.
5. Shearing of the vortex by passing vanes is not included, however the turbulence this causes is incorporated with the secondary circulation loss.
6. Vane angles are measured from the plane of the rotor in the direction of forward rotation, and positive velocities are in the direction of rotor rotation.
7. Disk friction and mechanical losses are not included.
8. The effect of sudden area changes in the gap between rotor and stator is omitted, though if sluice gate machines were being investigated some consideration of this may be necessary.
9. When analysing the water outflow to the drain, the drain annulus and passages are always full of water.

2.2 Conservation of Energy

There is no shaft power output from the dynamometer so all power input to the rotor must be transferred to the working fluid to maintain the conservation of energy. This transfer is by the methods of energy dissipation outlined above and results in the formation of eddies in the fluid and an increase in fluid temperature.

Input power is

$$\dot{P}_I = \tau \omega_P \tag{2.7}$$

where

τ = dynamometer torque

ω_P = rotor angular velocity

Both torque and energy dissipation power are functions of fluid fill percentage, fluid and rotor angular velocities, so in Section 2.4.1 Eqn.(2.18), a representation of the Euler equation, is obtained

$$\tau = K_1 \omega \omega_P + K_2 \omega^2 \tag{2.18}$$

where

K_1, K_2 = coefficients dependant on geometry and fill

ω = water angular velocity

and in Section 2.5.3 Eqn.(2.55).

$$\dot{P}_L = (K_{11} + K_{14})\omega \omega_P^2 + (K_{12} + K_{15})\omega^2 \omega_P + (K_{13} + K_{16} + K_F + K_{SC})\omega^3 \tag{2.55}$$

where

$K_{\#'S}$ = loss coefficients dependant on geometry and fill

Equating input and energy dissipation powers yields

$$\omega^2(K_{13} + K_{16} + K_F + K_{SC}) + \omega \omega_P(K_{12} + K_{15} - K_2) + \omega_P^2(K_{11} + K_{14} - K_1) = 0 \tag{2.8}$$

which is easily solved for the fluid vortex angular velocity, ω, using the quadratic formula. In general terms this yields a result of the form

$$\omega = \omega_P \, fn(K)$$

where

$fn(K)$ = combination of geometry and fill dependant coefficients

Hence for a given machine geometry and fluid fill the water angular velocity is directly proportional to rotor angular velocity.

2.3 Conservation of Mass

The vortex centre is determined by applying the principle of conservation of mass to the stator and is considered invariant as fluid fill varies. At full fill the mass inflow to and outflow from the stator are equal, and the effects of fluid inlet and outlet holes inconsequential. As outlined in Section 2.1 the quantity of interest, in this case mass flow, has a general streamtube expression derived for it, which is then integrated.

The mass flow between rotor and stator for a streamtube is generally,

$\dot{dm}$ = density x axial flow velocity x axial flow area

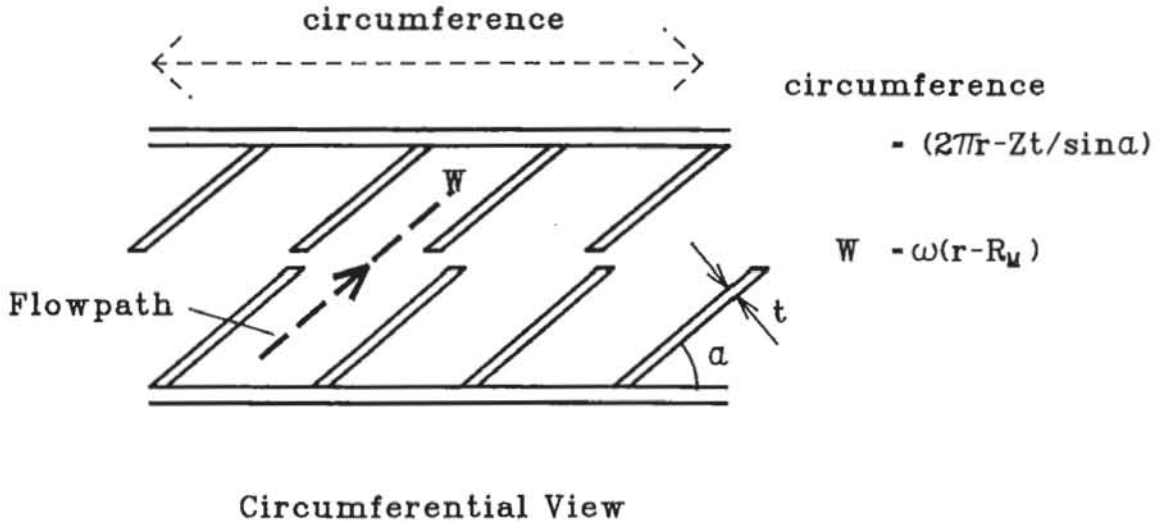

Figure 2.4: Vane Effect on Flow Area

Allowing for vane blockage, the axial flow area is the available circumference times the streamtube thickness (refer Fig.2.4),

$$dA = \left(2\pi r - \frac{Zt}{\sin\alpha}\right)dr$$

where

Z = vane number
t = vane thickness
α = vane angle

and the axial flow velocity is

$$W_A = \omega(r - R_M)\sin\alpha$$

Hence the elemental mass flow rate between components is

$$dm = \rho W_A\left(2\pi r - \frac{Zt}{\sin\alpha}\right)dr \qquad (2.9)$$

Therefore the elemental inflow to the stator is

$$d\dot{m}_{SI} = \rho\,\omega(r - R_M)\sin\alpha_{SI}\left(2\pi r - \frac{Z_S t}{\sin\alpha_{SI}}\right)dr$$

where

Z_S = stator vane number

α_{SI} = stator inlet angle

This is integrated from vortex centre to cup surface,

$$\dot{M}_{SI} = \int_{R_M}^{R_O} \rho\,\omega(r - R_M)\sin\alpha_{SI}\left(2\pi r - \frac{Z_S t}{\sin\alpha_{SI}}\right)dr$$

which yields

$$\dot{M}_{SI} = \rho\,\omega\sin\alpha_{SI}\left[2\pi\left(\tfrac{1}{3}r^3 - \tfrac{1}{2}r^2 R_M\right) - \frac{Z_S t}{\sin\alpha_{SI}}\left(\tfrac{1}{2}r^2 - rR_M\right)\right]_{R_M}^{R_O} \qquad (2.10)$$

Similarly for outflow from the stator,

$$\dot{M}_{SO} = \int_{R_I}^{R_M} \rho\,\omega(R_M - r)\sin\alpha_{SO}\left(2\pi r - \frac{Z_S t}{\sin\alpha_{SO}}\right)dr$$

yields

$$\dot{M}_{SO} = \rho\,\omega\sin\alpha_{SO}\left[2\pi\left(\tfrac{1}{2}r^2 R_M - \tfrac{1}{3}r^3\right) - \frac{Z_S t}{\sin\alpha_{SO}}\left(rR_M - \tfrac{1}{2}r^2\right)\right]_{R_I}^{R_M} \qquad (2.11)$$

Equating inflow (Eqn.(2.10)) and outflow (Eqn.(2.11)), and rearranging gives

$$\begin{aligned}\tfrac{2}{3}\pi\left(R_O^3\sin\alpha_{SI} - R_I^3\sin\alpha_{SO}\right) - \tfrac{1}{2}Z_S t\left(R_O^2 - R_I^2\right) \\ = \pi\sin\alpha_{SI}\left(R_M R_O^2 - \tfrac{1}{3}R_M^3\right) - \pi\sin\alpha_{SO}\left(R_M R_I^2 - \tfrac{1}{3}R_M^3\right) \\ - Z_S t R_M\left(R_O - R_I\right)\end{aligned} \qquad (2.12)$$

This can be solved for R_M using the Newton-Raphson method for finding a root.

If the stator vane angle is equal for inlet and outlet Eqn.(2.12) simplifies to

$$R_M = \frac{\frac{2}{3}\pi \sin\alpha_{so}\left(R_o^3 - R_I^3\right) - \frac{1}{2}Z_S t\left(R_o^2 - R_I^2\right)}{\pi \sin\alpha_{so}\left(R_o^2 - R_I^2\right) - Z_S t\left(R_o - R_I\right)} \qquad (2.13)$$

which can also be used as an initial value for the iteration if the dynamometer's vanes are twisted (i.e. unequal inlet and outlet angles). This equation is compared to Eqn.(2.6) for the F020 machine with axial vanes (R_O = 102.5 mm, R_I = 43.5 mm, t = 5.0 mm, Z_S = 12, $\alpha_{SI} = \alpha_{SO}$ = 90°), and the effect of vane blockage is found to move the vortex centre to a slightly larger radius. The constant thickness of the vanes has a greater blockage effect at the smaller radii, i.e. stator outlet.

2.4 Conservation of Angular Momentum

Treating the rotor as a control volume (Fig.2.5), to conserve angular momentum the torque input along the shaft must equal the rate of change of angular momentum of the fluid passing around the rotor. Previous work, Whitfield, Wallace and Sivalingam and Raine, has considered only the steady flow situation. However Fox and McDonald [48] derive a general control volume formulation for unsteady systems and then apply it to the basic laws of mechanics and thermodynamics to obtain control volume representations of these laws. Their equation for conservation of angular momentum is

$$\boldsymbol{r} \times \boldsymbol{F}_S + \iiint_{CV} \boldsymbol{r} \times \boldsymbol{g}\rho \, dV + \boldsymbol{T}_{Shaft} = \frac{\partial}{\partial t}\iiint_{CV} \boldsymbol{r} \times \boldsymbol{V}\, \rho \, dV + \iint_{CS} \boldsymbol{r} \times \boldsymbol{V}\, \rho \boldsymbol{V}_{xyz} . d\boldsymbol{A}$$

where

$\boldsymbol{F}_S$, $\boldsymbol{g}$	= surface and body forces on the fluid
$\boldsymbol{T}_{Shaft}$	= shaft torque
$\boldsymbol{V}$, $\boldsymbol{V}_{xyz}$	= absolute and relative fluid velocities
dV , $d\boldsymbol{A}$	= elemental volume and area
CV , CS	= control volume and surface

Surface forces are zero if viscosity is ignored, and symmetry allows the body forces to be neglected giving

$$\boldsymbol{T}_{Shaft} = \frac{\partial}{\partial t}\iiint_{CV} \boldsymbol{r} \times \boldsymbol{V}\, \rho dV + \iint_{CS} \boldsymbol{r} \times \boldsymbol{V}\, \rho \boldsymbol{V}_{xyz} . d\boldsymbol{A} \qquad (2.14)$$

for the rotor as shown in Fig.2.5. The first term on the right hand side is the time rate of change of angular momentum within the control volume, while the second is the net quantity passing through the control surface. Hence the latter term is the change in the angular momentum of the water between rotor inlet and outlet for steady flow as derived in previous work.

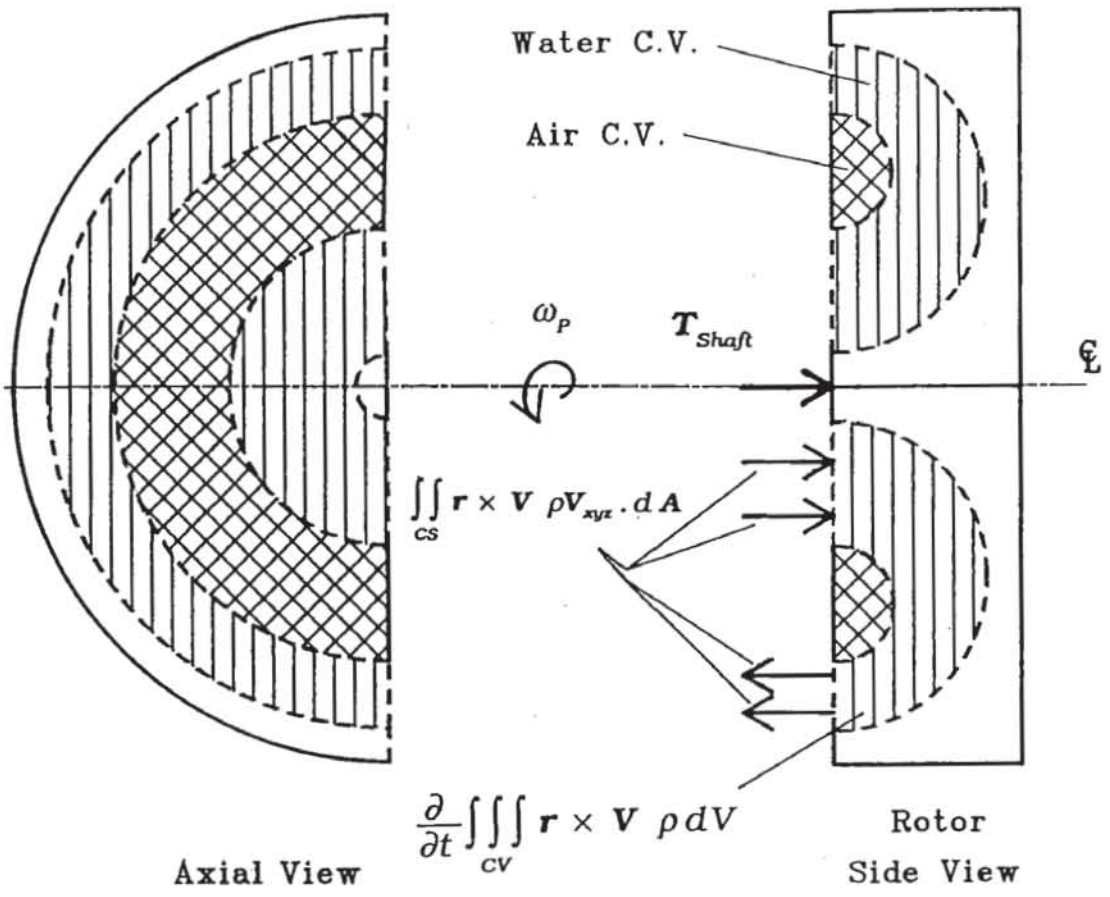

Figure 2.5: Rotor Control Volume and Angular Momentum Components

2.4.1 Steady Flow Component

The surface integral of Eqn.(2.14) is reduced to a single integral by replacing the elemental mass flow $\rho \mathbf{V}_{xyz}.d\mathbf{A}$ with the streamtube equivalents for relative velocity, $\mathbf{V}_{xyz} = W_A = \omega(r - R_M)\sin\alpha$, elemental area, $d\mathbf{A} = (2\pi r - \frac{Zt}{\sin\alpha})dr$, and tangential moment, $\mathbf{r} \times \mathbf{V} = rV_\theta$, and integrating from cup surface to air-water interface. The steady flow component becomes

$$\iint_{CS} \mathbf{r} \times \mathbf{V}\ \rho \mathbf{V}_{xyz} . d\mathbf{A} = \int_{R_{co}}^{R_o} r V_{\theta O}\, d\dot{m}_O - \int_{R_i}^{R_{ci}} r V_{\theta I}\, d\dot{m}_I \qquad (2.15)$$

where

$$d\dot{m}_O = \rho\,\omega(r - R_M)\sin\alpha_{RO}\left(2\pi r - \frac{Z_R t}{\sin\alpha_{RO}}\right)dr$$

$$d\dot{m}_I = \rho\,\omega(R_M - r)\sin\alpha_{RI}\left(2\pi r - \frac{Z_R t}{\sin\alpha_{RI}}\right)dr$$

and

$V_{\theta O}$, $V_{\theta I}$ = outer and inner tangential absolute velocities

R_{CO} , R_{CI} = outer and inner air-water interface radii

Referring to Fig.2.3 the tangential components of absolute water velocity are:

before rotor inlet (point 2)

$$V_{\theta I} = W_S \cos \alpha_{SO} = -\omega(R_M - r)\cos \alpha_{SO}$$

at rotor inlet (point 4)

$$V_{\theta O} = W_R \cos \alpha_{RO} + U = \omega(r - R_M)\cos \alpha_{RO} + \omega_P r$$

Hence the water angular momentum flowing into the rotor control volume is

$$\int_{R_I}^{R_{CI}} r V_{\theta I}\, d\dot{m}_I$$

$$= \int_{R_I}^{R_{CI}} r(-\omega(R_M - r)\cos \alpha_{SO})\rho\,\omega(R_M - r)\sin \alpha_{RI}\left(2\pi r - \frac{Z_R t}{\sin \alpha_{RI}}\right)dr$$

$$= -\rho\,\omega^2 \sin \alpha_{RI} \cos \alpha_{SO} \int_{R_I}^{R_{CI}} \left(2\pi r - \frac{Z_R t}{\sin \alpha_{RI}}\right)\left(rR_M^2 - 2r^2 R_M + r^3\right)dr$$

$$= -\rho\,\omega^2 \sin \alpha_{RI} \cos \alpha_{SO}\Big[\, 2\pi\left(\tfrac{1}{5}r^5 - \tfrac{1}{2}r^4 R_M + \tfrac{1}{3}r^3 R_M^2\right) \qquad (2.16)$$

$$- \frac{Z_R t}{\sin \alpha_{RI}}\left(\tfrac{1}{4}r^4 - \tfrac{2}{3}r^3 R_M + \tfrac{1}{2}r^2 R_M^2\right)\Big]_{R_I}^{R_{CI}}$$

That flowing out is

$$\int_{R_{CO}}^{R_O} r V_{\theta O}\, d\dot{m}_O$$

$$= \int_{R_{CO}}^{R_O} r\left(\omega(r - R_M)\cos \alpha_{RO} + \omega_P r\right)$$

$$\times \rho\,\omega(r - R_M)\sin \alpha_{RO}\left(2\pi r - \frac{Z_R t}{\sin \alpha_{RO}}\right)dr$$

$$= \rho\,\omega \sin \alpha_{RO} \int_{R_{CO}}^{R_O} \left(2\pi r - \frac{Z_R t}{\sin \alpha_{RO}}\right)(r^2 - rR_M)$$

$$\times \left(\omega(r - R_M)\cos \alpha_{RO} + \omega_P r\right)dr$$

$$= \rho\,\omega \sin \alpha_{RO}\Big\{\, \omega_P\Big[\, 2\pi\left(\tfrac{1}{5}r^5 - \tfrac{1}{4}r^4 R_M\right) - \frac{Z_R t}{\sin \alpha_{RO}}\left(\tfrac{1}{4}r^4 - \tfrac{1}{3}r^3 R_M\right)\Big]_{R_{CO}}^{R_O}$$

$$+ \omega \cos \alpha_{RO}\Big[\, 2\pi\left(\tfrac{1}{5}r^5 - \tfrac{1}{2}r^4 R_M + \tfrac{1}{3}r^3 R_M^2\right) \qquad (2.17)$$

$$- \frac{Z_R t}{\sin \alpha_{RO}}\left(\tfrac{1}{4}r^4 - \tfrac{2}{3}r^3 R_M + \tfrac{1}{2}r^2 R_M^2\right)\Big]_{R_{CO}}^{R_O}\Big\}$$

Substituting Eqns.(2.16) and (2.17) into Eqn.(2.15) to get the flow of angular momentum through the control surface and rearranging yields

$$\tau_{SS} = K_1 \omega \omega_P + K_2 \omega^2 \qquad (2.18)$$

where

$$K_1 = \rho \sin\alpha_{RO}\left[2\pi\left(\tfrac{1}{5} r^5 - \tfrac{1}{4} r^4 R_M\right) - \frac{Z_R t}{\sin\alpha_{RO}}\left(\tfrac{1}{4} r^4 - \tfrac{1}{3} r^3 R_M\right)\right]_{R_{co}}^{R_o}$$

$$K_2 = \rho \sin\alpha_{RO} \cos\alpha_{RO}\left[2\pi\left(\tfrac{1}{5} r^5 - \tfrac{1}{2} r^4 R_M + \tfrac{1}{3} r^3 R_M^2\right) - \frac{Z_R t}{\sin\alpha_{RO}}\left(\tfrac{1}{4} r^4 - \tfrac{2}{3} r^3 R_M + \tfrac{1}{2} r^2 R_M^2\right)\right]_{R_{co}}^{R_o}$$

$$+ \rho \sin\alpha_{RI} \cos\alpha_{SO}\left[2\pi\left(\tfrac{1}{5} r^5 - \tfrac{1}{2} r^4 R_M + \tfrac{1}{3} r^3 R_M^2\right) - \frac{Z_R t}{\sin\alpha_{RI}}\left(\tfrac{1}{4} r^4 - \tfrac{2}{3} r^3 R_M + \tfrac{1}{2} r^2 R_M^2\right)\right]_{R_I}^{R_{CI}}$$

Generally the torque calculation is only applied to the water in the working compartment, since water is approximately 1000 times more dense than air. The air torque contribution can be included by applying Eqn.(2.18) with R_O , R_I , R_{CO} , R_{CI} replaced by R_{CO} , R_{CI} , R_M , R_M (i.e. integration from air-water interface to vortex centre) and using the density of air. This contribution is found to be very small, even at low water fill. Hence it is not considered for the unsteady flow component, which itself is small even for water.

2.4.2 Unsteady Flow Component

To analyse the unsteady component of Eqn.(2.14) the integrated one-dimensional approach must be modified from that above. Due to these dynamometers operating with variable fill the time differential applies not only to the angular momentum within the control volume, but also to the boundary of the volume itself (the air-water interface). Before analysing the term

$$\frac{\partial}{\partial t}\iiint_{CV} \mathbf{r} \times \mathbf{V}\ \rho\, dV$$

the integrated technique is applied to the mass of the control volume,

$$\iiint_{CV} \rho\, dV$$

and compared to the result for an elliptical toroid to facilitate understanding of the more complex torque derivation.

The control volume geometry and elemental area are defined in cylindrical coordinates in Fig.2.6 for the rotor with integration required both radially and axially. By symmetry of the machine the elemental values are considered equal at all angles around the axis, and the triple integral is reduced to a double integral, allowing for the vane blockage, in Fig.2.6,

$$\iiint_{CV} \rho\, dV = \int_0^b \int_{g(x)}^{f(x)} \rho\left(2\pi r - \frac{Zt}{\sin\alpha}\right) dr\, dx - \int_0^{b_Y} \int_{gy(x)}^{fy(x)} \rho\left(2\pi r - \frac{Zt}{\sin\alpha}\right) dr\, dx \qquad (2.19)$$

where

$f(x)$, $g(x)$ = geometric functions defining the cup boundary of the control volume

$fy(x)$, $gy(x)$ = geometric functions defining the air-water interface boundary of the control volume

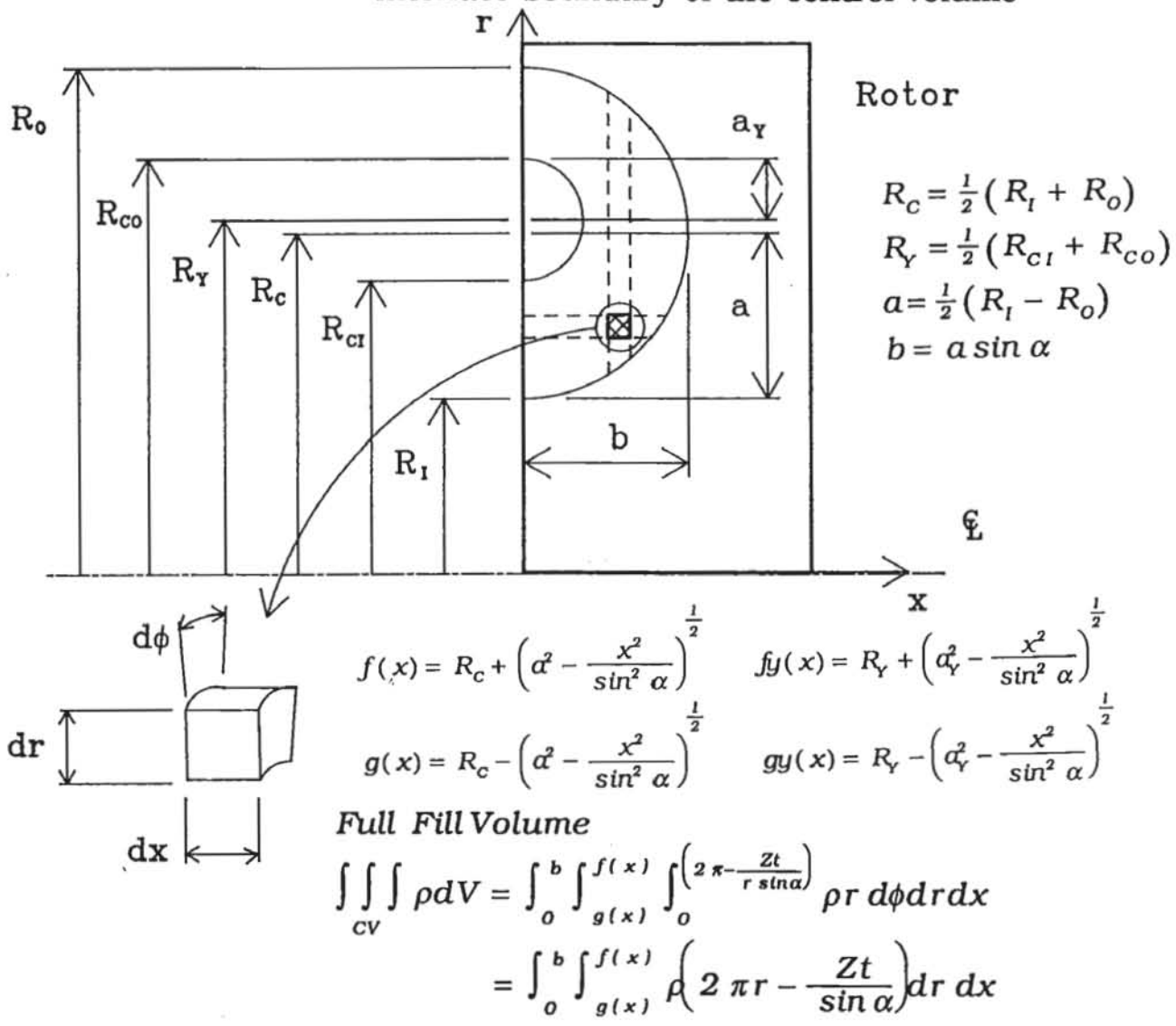

Figure 2.6: Mass Integral in Rotor Control Volume

For clarity the functions $f(x)$, $g(x)$, $fy(x)$ and $gy(x)$ are written f, g, fy and gy respectively henceforth. The first term of Eqn.(2.19) becomes

$$\int_0^b\int_g^f \rho\left(2\pi r - \frac{Zt}{\sin\alpha}\right)dr\,dx = \rho\int_0^b\left[\pi r^2 - \frac{Zt}{\sin\alpha}r\right]_g^f dx$$

$$= \rho\int_0^b\left[\pi(f^2 - g^2) - \frac{Zt}{\sin\alpha}(f - g)\right]dx \quad (2.20)$$

From the derivation in Appendix A,

$$(f^2 - g^2) = 4R_C\left(a^2 - \frac{x^2}{\sin^2\alpha}\right)^{\frac{1}{2}}$$

$$(f - g) = 2\left(a^2 - \frac{x^2}{\sin^2\alpha}\right)^{\frac{1}{2}}$$

leading to

$$\int_0^b\int_g^f \rho\left(2\pi r - \frac{Zt}{\sin\alpha}\right)dr\,dx = \rho\left(4\pi R_C - 2\frac{Zt}{\sin\alpha}\right)\int_0^b\left(a^2 - \frac{x^2}{\sin^2\alpha}\right)^{\frac{1}{2}} dx$$

Using the identity from Appendix B,

$$\int_0^b\left(a^2 - \frac{x^2}{\sin^2\alpha}\right)^{\frac{1}{2}} dx = \tfrac{1}{4}\pi ab$$

gives

$$\int_0^b\int_g^f \rho\left(2\pi r - \frac{Zt}{\sin\alpha}\right)dr\,dx = \rho\left(2\pi R_C - \frac{Zt}{\sin\alpha}\right)\tfrac{1}{2}\pi ab \quad (2.21)$$

for the rotor. If the stator is similarly analysed the mass in a fully filled machine is

$$M_F = \rho\left(2\pi R_C - \frac{Zt}{\sin\alpha}\right)\pi ab \quad (2.22)$$

the same as for an elliptical toroid of mean radius, R_C, with allowance for vane blockage. The same derivation applies to the second term of Eqn.(2.19), with fy, gy, a_Y, b_Y and R_Y replacing f, g, a, b, and R_C respectively, to give the mass of fluid displaced by air,

$$M_A = \rho\left(2\pi R_Y - \frac{Zt}{\sin\alpha}\right)\pi q_Y b_Y \quad (2.23)$$

Returning to the unsteady angular momentum term, symmetry is again used to reduce the triple integral,

$$\frac{\partial}{\partial t}\iiint_{CV} \mathbf{r} \times \mathbf{V}\ \rho\, dV = \frac{\partial}{\partial t}\int_o^b \int_g^f r V_\theta(r)\rho \left(2\pi r - \frac{Zt}{\sin\alpha}\right) dr\, dx \qquad (2.24)$$

where

$V_\theta(r)$ = tangential absolute velocity as a function of radius

Allowing for partial fill and using $C(r) = \rho(2\pi r - \frac{Zt}{\sin\alpha})$ for convenience,

$$\frac{\partial}{\partial t}\iiint_{CV} \mathbf{r} \times \mathbf{V}\ \rho\, dV$$

$$= \frac{\partial}{\partial t}\left\{\int_o^b \int_g^f r V_\theta(r)\, C(r) dr\, dx - \int_o^{b_Y} \int_{gy}^{fy} r V_\theta(r)\, C(r) dr\, dx\right\} \qquad (2.25)$$

At this stage consideration must be given to the fact that varying fill and speed result in the following values and functions being time dependant: a_Y, b_Y, R_Y, $fy(x)$, $gy(x)$, $V_\theta(r)$, ω, ω_p . Hence the second term on the right hand side of Eqn.(2.25) has time varying limits of integration as well as a time varying integrand. For functions of several variables Leibniz's rule, as given in Sokolnikoff and Redheffer [49], is applied to such integrations.

Leibniz's rule,

$$\frac{\partial}{\partial\alpha}\int_{u_o(\alpha)}^{u_1(\alpha)} f(x,\alpha)dx = f(u_1,\alpha)\frac{du_1}{d\alpha} - f(u_0,\alpha)\frac{du_0}{d\alpha} + \int_{u_o(\alpha)}^{u_1(\alpha)} f_\alpha(x,\alpha)dx$$

where

$$f_\alpha(x,\alpha) = \frac{\partial}{\partial\alpha} f(x,\alpha)$$

Applying to the second term,

$$\frac{\partial}{\partial t}\int_o^{b_Y} \int_{gy(x)}^{fy(x)} r V_\theta(r)\, C(r) dr\, dx$$

$$= \left(\int_{gy(b_Y)}^{fy(b_Y)} r V_\theta(r) C(r) dr\right)\frac{d(b_Y)}{dt} - \left(\int_{gy(0)}^{fy(0)} r V_\theta(r) C(r) dr\right)\frac{d(0)}{dt}$$

$$+ \int_o^{b_Y} \frac{\partial}{\partial t}\left(\int_{gy(x)}^{fy(x)} r V_\theta(r)\, C(r) dr\right) dx$$

But $fy(b_Y) = R_Y = gy(b_Y)$ by definition and the derivative of a constant is zero, so the first and second terms are equal to zero. Leibniz is applied again to the last term,

$$\int_0^{b_Y} \frac{\partial}{\partial t}\left(\int_{gy(x)}^{fy(x)} r V_\theta(r)\, C(r) dr\right) dx$$

$$= \int_0^{b_Y} \left\{ [fy V_\theta(fy)\, C(fy)] \frac{d(fy)}{dt} - [\, gy V_\theta(\, gy)\, C(\, gy)] \frac{d(\, gy)}{dt} + \int_{gy}^{fy} r \frac{\partial}{\partial t}(V_\theta(r))\, C(r) dr \right\} dx$$

Thus Eqn.(2.25) becomes

$$\frac{\partial}{\partial t} \int\int\int_{CV} \boldsymbol{r} \times \boldsymbol{V}\, \rho\, dV$$

$$= \int_0^b \int_g^f r \dot{V}_\theta(r)\, C(r) dr\, dx - \int_0^{b_Y} \int_{gy}^{fy} r \dot{V}_\theta(r)\, C(r) dr\, dx - \int_0^{b_Y} \{ [fy V_\theta(fy)\, C(fy)] \dot{fy} - [\, gy V_\theta(\, gy)\, C(\, gy)]\, \dot{gy} \} dx \qquad (2.26)$$

where

$$\dot{V}_\theta(r) = \frac{\partial}{\partial t}(V_\theta(r))$$

$$\dot{fy} = \frac{\partial}{\partial t}(fy(x))$$

$$\dot{gy} = \frac{\partial}{\partial t}(\, gy(x))$$

Before continuing with the mathematics the physical significance of these terms should be considered. The first two terms represent the change in angular momentum due to the acceleration of the rotor and water, while the third term represents the change due to the change in fluid fill in the machine (increase in volume occupied by air causes decrease in angular momentum).

This integral is evaluated term by term with the following identities listed again for convenience.

From Fig.2.6,

$$f = f(x) = R_c + \left(a^2 - \frac{x^2}{\sin^2 \alpha}\right)^{\frac{1}{2}} \qquad fy = fy(x) = R_Y + \left(a_Y^2 - \frac{x^2}{\sin^2 \alpha}\right)^{\frac{1}{2}}$$

$$g = g(x) = R_c - \left(a^2 - \frac{x^2}{\sin^2 \alpha}\right)^{\frac{1}{2}} \qquad gy = gy(x) = R_Y - \left(a_Y^2 - \frac{x^2}{\sin^2 \alpha}\right)^{\frac{1}{2}}$$

$$b = a \sin \alpha \qquad b_Y = a_Y \sin \alpha$$

$$R_c = \tfrac{1}{2}(R_o + R_I) \qquad R_Y = \tfrac{1}{2}(R_{co} + R_{cI})$$

From Eqn.(2.25),

$$C(r) = \rho\left(2\pi r - \frac{Zt}{\sin\alpha}\right)$$

and from Fig.2.3 absolute tangential velocity in the rotor is

$$V_\theta(r) = \omega(r - R_M)\cos\alpha + \omega_p r$$

hence,

$$\dot{V}_\theta(r) = \dot{\omega}(r - R_M)\cos\alpha + \dot{\omega}_p r$$

The first term of Eqn.(2.26) is therefore

$$\int_0^b\int_g^f r\dot{V}_\theta(r)\,C(r)\,dr\,dx$$

$$= \int_0^b\int_g^f\left[r(\dot{\omega}(r - R_M)\cos\alpha + \dot{\omega}_p r)\,\rho\left(2\pi r - \frac{Zt}{\sin\alpha}\right)\right]dr\,dx$$

$$= \rho\int_0^b\int_g^f\left[2\pi(\dot{\omega}\cos\alpha + \dot{\omega}_p r)\,r^3 - \frac{Zt}{\sin\alpha}(\dot{\omega}\cos\alpha + \dot{\omega}_p r)\,r^2 - 2\pi\dot{\omega}\cos\alpha\,R_M\,r^2 + \frac{Zt}{\sin\alpha}\dot{\omega}\cos\alpha\,R_M\,r\right]dr\,dx$$

$$= \rho\int_0^b\left[\dot{\omega}\cos\alpha\left(2\pi\left(\tfrac{1}{4}r^4 - \tfrac{1}{3}r^3 R_M\right) - \frac{Zt}{\sin\alpha}\left(\tfrac{1}{3}r^3 - \tfrac{1}{2}r^2 R_M\right)\right) + \dot{\omega}_p\left(2\pi\tfrac{1}{4}r^4 - \frac{Zt}{\sin\alpha}\tfrac{1}{3}r^3\right)\right]_g^f dx \qquad (2.27)$$

Referring to Appendix A,

$$(f^2 - g^2) = 4\,R_C\left(a^2 - \frac{x^2}{\sin^2\alpha}\right)^{\frac{1}{2}}$$

$$(f^3 - g^3) = 6\,R_C^2\left(a^2 - \frac{x^2}{\sin^2\alpha}\right)^{\frac{1}{2}} + 2\left(a^2 - \frac{x^2}{\sin^2\alpha}\right)^{\frac{3}{2}}$$

$$(f^4 - g^4) = 8\,R_C^3\left(a^2 - \frac{x^2}{\sin^2\alpha}\right)^{\frac{1}{2}} + 8\,R_C\left(a^2 - \frac{x^2}{\sin^2\alpha}\right)^{\frac{3}{2}}$$

and substituting into Eqn.(2.27),

$$\int_0^b\int_g^f r\dot{V}_\theta(r)\,C(r)\,dr\,dx$$

$$= \rho\int_0^b\left[\dot{\omega}\cos\alpha\left\{2\pi\left[\tfrac{1}{4}\left(8\,R_C^3\left(a^2 - \frac{x^2}{\sin^2\alpha}\right)^{\frac{1}{2}} + 8\,R_C\left(a^2 - \frac{x^2}{\sin^2\alpha}\right)^{\frac{3}{2}}\right)\right.\right.$$

$$\left.\left. - \tfrac{1}{3}R_M\left(6\,R_C^2\left(a^2 - \frac{x^2}{\sin^2\alpha}\right)^{\frac{1}{2}} + 2\left(a^2 - \frac{x^2}{\sin^2\alpha}\right)^{\frac{3}{2}}\right)\right]$$

$$-\frac{Zt}{\sin\alpha}\left[\tfrac{1}{3}\left(6\,R_C^2\left(a^2-\frac{x^2}{\sin^2\alpha}\right)^{\frac{1}{2}}+2\left(a^2-\frac{x^2}{\sin^2\alpha}\right)^{\frac{3}{2}}\right)\right.$$

$$\left.-\tfrac{1}{2}R_M\left(4\,R_C\left(a^2-\frac{x^2}{\sin^2\alpha}\right)^{\frac{1}{2}}\right)\right]\}$$

$$+\dot{\omega}_p\left\{\tfrac{1}{2}\pi\left(8\,R_C^3\left(a^2-\frac{x^2}{\sin^2\alpha}\right)^{\frac{1}{2}}+8\,R_C\left(a^2-\frac{x^2}{\sin^2\alpha}\right)^{\frac{3}{2}}\right)\right.$$

$$\left.-\frac{Zt}{\sin\alpha}\tfrac{1}{3}\left(6\,R_C^2\left(a^2-\frac{x^2}{\sin^2\alpha}\right)^{\frac{1}{2}}+2\left(a^2-\frac{x^2}{\sin^2\alpha}\right)^{\frac{3}{2}}\right)\right\}\Big]dx$$

Which rearranged is

$$\int_0^b\int_g^f r\dot{V}_\theta(r)\,C(r)\,dr\,dx$$

$$=\rho\int_0^b\Big[\dot{\omega}\cos\alpha\left\{2\left(R_C^2-R_C R_M\right)\left(2\pi R_C-\frac{Zt}{\sin\alpha}\right)\left(a^2-\frac{x^2}{\sin^2\alpha}\right)^{\frac{1}{2}}\right.$$

$$\left.+\left(4\pi R_C-\tfrac{4}{3}\pi R_M-\tfrac{2}{3}\frac{Zt}{\sin\alpha}\right)\left(a^2-\frac{x^2}{\sin^2\alpha}\right)^{\frac{3}{2}}\right\}$$

$$+\dot{\omega}_p\left\{\left(4\pi R_C^3-2\frac{Zt}{\sin\alpha}R_C^2\right)\left(a^2-\frac{x^2}{\sin^2\alpha}\right)^{\frac{1}{2}}\right.$$

$$\left.+\left(4\pi R_C-\tfrac{2}{3}\frac{Zt}{\sin\alpha}\right)\left(a^2-\frac{x^2}{\sin^2\alpha}\right)^{\frac{3}{2}}\right\}\Big]dx$$

Since only the factors $(a^2-\frac{x^2}{\sin^2\alpha})^{1/2}$ and $(a^2-\frac{x^2}{\sin^2\alpha})^{3/2}$ are functions of x, the remaining factors are moved outside the integral. In Appendix B the definite integrals of the two factors are determined yielding

$$\int_0^b\left(a^2-\frac{x^2}{\sin^2\alpha}\right)^{\frac{1}{2}}dx=\tfrac{1}{4}\pi\,ba$$

and

$$\int_0^b\left(a^2-\frac{x^2}{\sin^2\alpha}\right)^{\frac{3}{2}}dx=\tfrac{3}{16}\pi\,ba^3$$

Substituting these gives

$$\int_0^b \int_g^f r\dot{V}_\theta(r)\,C(r)\,dr\,dx$$

$$= \rho\Big[\dot{\omega}\cos\alpha\Big\{\tfrac{1}{2}\pi ba\Big(R_C^2 - R_C R_M\Big)\Big(2\pi R_C - \frac{Zt}{\sin\alpha}\Big) + \tfrac{1}{8}\pi ba^3\Big(6\pi R_C - \frac{Zt}{\sin\alpha} - 2\pi R_M\Big)\Big\} + \dot{\omega}_P\Big\{\tfrac{1}{2}\pi ba\Big(2\pi R_C - \frac{Zt}{\sin\alpha}\Big)R_C^2 + \tfrac{1}{8}\pi ba^3\Big(6\pi R_C - \frac{Zt}{\sin\alpha}\Big)\Big\}\Big] \quad (2.28)$$

By inspection, the second term of Eqn.(2.26) is the same as the first with $f(x)$, $g(x)$, R_C, b and a being replaced by $fy(x)$, $gy(x)$, R_Y, b_Y and a_Y respectively. Hence,

$$\int_0^{b_Y} \int_{gy}^{fy} r\dot{V}_\theta(r)\,C(r)\,dr\,dx$$

$$= \rho\Big[\dot{\omega}\cos\alpha\Big\{\tfrac{1}{2}\pi b_Y a_Y\Big(R_Y^2 - R_Y R_M\Big)\Big(2\pi R_Y - \frac{Zt}{\sin\alpha}\Big) + \tfrac{1}{8}\pi b_Y a_Y^3\Big(6\pi R_Y - \frac{Zt}{\sin\alpha} - 2\pi R_M\Big)\Big\} + \dot{\omega}_P\Big\{\tfrac{1}{2}\pi b_Y a_Y\Big(2\pi R_Y - \frac{Zt}{\sin\alpha}\Big)R_Y^2 + \tfrac{1}{8}\pi b_Y a_Y^3\Big(6\pi R_Y - \frac{Zt}{\sin\alpha}\Big)\Big\}\Big] \quad (2.29)$$

To evaluate the third term of Eqn.(2.26), the time derivatives of functions fy(x) and gy(x) are required,

$$\dot{fy} = \frac{\partial}{\partial t}(fy(x))$$

$$fy(x) = R_Y + \Big(a_Y^2 - \frac{x^2}{\sin^2\alpha}\Big)^{\frac{1}{2}}$$

therefore

$$\dot{fy} = \dot{R}_Y + a_Y\,\dot{a}_Y\Big(a_Y^2 - \frac{x^2}{\sin^2\alpha}\Big)^{-\frac{1}{2}}$$

and

$$\dot{gy} = \dot{R}_Y - a_Y\,\dot{a}_Y\Big(a_Y^2 - \frac{x^2}{\sin^2\alpha}\Big)^{-\frac{1}{2}}$$

The term is expanded,

$$\int_0^{b_Y}\Big\{[fyV_\theta(fy)\,C(fy)]\,\dot{fy} - [\,gyV_\theta(gy)\,C(gy)]\,\dot{gy}\Big\}dx$$

$$= \int_0^{b_Y}\Big\{\Big[fy(\omega\cos\alpha(fy - R_M) + \omega_P fy)\,\rho\Big(2\pi fy - \frac{Zt}{\sin\alpha}\Big)\Big]\dot{fy} - \Big[gy(\omega\cos\alpha(gy - R_M) + \omega_P gy)\,\rho\Big(2\pi gy - \frac{Zt}{\sin\alpha}\Big)\Big]\dot{g}y\Big\}dx$$

and rearranged,

$$\int_0^{b_Y} \{[fyV_\theta(fy)\,C(fy)]\,\dot{fy} - [\,gyV_\theta(\,gy\,)\,C(\,gy\,)]\,\dot{gy}\}dx$$

$$= \rho\int_0^{b_Y} \{\omega\cos\alpha[2\pi fy^3\,\dot{fy} - 2\pi R_M fy^2\,\dot{fy} - \frac{Zt}{\sin\alpha}fy^2\,\dot{fy} + R_M\frac{Zt}{\sin\alpha}fy\dot{fy}] + \omega_P[2\pi fy^3\,\dot{fy} - \frac{Zt}{\sin\alpha}fy^2\,\dot{fy}] - \omega\cos\alpha[2\pi\,gy^3\,\dot{gy} - 2\pi R_M\,gy^2\,\dot{gy} - \frac{Zt}{\sin\alpha}gy^2\,\dot{gy} + R_M\frac{Zt}{\sin\alpha}gy\,\dot{gy}] - \omega_P[2\pi\,gy^3\,\dot{gy} - \frac{Zt}{\sin\alpha}gy^2\,\dot{gy}]\}dx$$

to yield

$$\int_0^{b_Y} \{[fyV_\theta(fy)\,C(fy)]\,\dot{fy} - [\,gyV_\theta(\,gy\,)\,C(\,gy\,)]\,\dot{gy}\}dx$$

$$= \rho\int_0^{b_Y} \{\omega\cos\alpha[2\pi(fy^3\,\dot{fy} - gy^3\,\dot{gy}) - \left(2\pi R_M + \frac{Zt}{\sin\alpha}\right)(fy^2\,\dot{fy} - gy^2\,\dot{gy}) + R_M\frac{Zt}{\sin\alpha}(fy\,\dot{fy} - gy\,\dot{gy})] + \omega_P[2\pi(fy^3\,\dot{fy} - gy^3\,\dot{gy}) - \frac{Zt}{\sin\alpha}(fy^2\,\dot{fy} - gy^2\,\dot{gy})]\}dx \quad (2.30)$$

From Appendix C,

$$(fy\,\dot{fy} - gy\,\dot{gy}) = 2\,\dot{R}_Y\left(a_Y^2 - \frac{x^2}{\sin^2\alpha}\right)^{\frac{1}{2}} + 2\,R_Y\,a_Y\,\dot{a}_Y\left(a_Y^2 - \frac{x^2}{\sin^2\alpha}\right)^{-\frac{1}{2}}$$

$$(fy^2\,\dot{fy} - gy^2\,\dot{gy}) = (4\,R_Y\,\dot{R}_Y + 2\,a_Y\,\dot{a}_Y)\left(a_Y^2 - \frac{x^2}{\sin^2\alpha}\right)^{\frac{1}{2}} + 2\,R_Y^2\,a_Y\,\dot{a}_Y\left(a_Y^2 - \frac{x^2}{\sin^2\alpha}\right)^{-\frac{1}{2}}$$

$$(fy^3\,\dot{fy} - gy^3\,\dot{gy}) = (6\,R_Y^2\,\dot{R}_Y + 6\,R_Y\,a_Y\,\dot{a}_Y)\left(a_Y^2 - \frac{x^2}{\sin^2\alpha}\right)^{\frac{1}{2}} + 2\,R_Y^3\,a_Y\,\dot{a}_Y\left(a_Y^2 - \frac{x^2}{\sin^2\alpha}\right)^{-\frac{1}{2}} + 2\,\dot{R}_Y\left(a_Y^2 - \frac{x^2}{\sin^2\alpha}\right)^{\frac{3}{2}}$$

are substituted into Eqn.(2.30),

$$\int_0^{b_Y} \{[fyV_\theta(fy)\,C(fy)]\,\dot{fy} - [\,gyV_\theta(\,gy\,)\,C(\,gy\,)]\,\dot{gy}\}dx$$

$$= \rho\int_0^{b_Y} \{\omega\cos\alpha[2\pi(6\left(R_Y^2\,\dot{R}_Y + R_Y\,a_Y\,\dot{a}_Y\right)\left(a_Y^2 - \frac{x^2}{\sin^2\alpha}\right)^{\frac{1}{2}} + 2\,R_Y^3\,a_Y\,\dot{a}_Y\left(a_Y^2 - \frac{x^2}{\sin^2\alpha}\right)^{-\frac{1}{2}} + 2\,\dot{R}_Y\left(a_Y^2 - \frac{x^2}{\sin^2\alpha}\right)^{\frac{3}{2}})$$

$$-\left(2\pi R_M + \frac{Zt}{\sin\alpha}\right)\Big(2\Big(2 R_Y \dot{R}_Y + a_Y \dot{a}_Y\Big)\Big(a_Y^2 - \frac{x^2}{\sin^2\alpha}\Big)^{\frac{1}{2}} + 2 R_Y^2 a_Y \dot{a}_Y \Big(a_Y^2 - \frac{x^2}{\sin^2\alpha}\Big)^{-\frac{1}{2}} \Big)$$

$$+ R_M \frac{Zt}{\sin\alpha}\Big(2 \dot{R}_Y \Big(a_Y^2 - \frac{x^2}{\sin^2\alpha}\Big)^{\frac{1}{2}} + 2 R_Y a_Y \dot{a}_Y \Big(a_Y^2 - \frac{x^2}{\sin^2\alpha}\Big)^{-\frac{1}{2}} \Big) \Big]$$

$$+ \omega_P [2\pi\Big(6\Big(R_Y^2 \dot{R}_Y + R_Y a_Y \dot{a}_Y\Big)\Big(a_Y^2 - \frac{x^2}{\sin^2\alpha}\Big)^{\frac{1}{2}} + 2 R_Y^3 a_Y \dot{a}_Y \Big(a_Y^2 - \frac{x^2}{\sin^2\alpha}\Big)^{-\frac{1}{2}} + 2 \dot{R}_Y \Big(a_Y^2 - \frac{x^2}{\sin^2\alpha}\Big)^{\frac{3}{2}} \Big)$$

$$- \frac{Zt}{\sin\alpha}\Big(2\Big(2 R_Y \dot{R}_Y + a_Y \dot{a}_Y\Big)\Big(a_Y^2 - \frac{x^2}{\sin^2\alpha}\Big)^{\frac{1}{2}} + 2 R_Y^2 a_Y \dot{a}_Y \Big(a_Y^2 - \frac{x^2}{\sin^2\alpha}\Big)^{-\frac{1}{2}} \Big) \Big] \Big\} dx$$

As with the first term above only the factors of the form $(a_Y^2 - \frac{x^2}{\sin^2\alpha})^{n/2}$, $n = -1, 1, 3$ are functions of x, so the definite integrals are evaluated in Appendix B,

$$\int_0^{b_Y} \Big(a_Y^2 - \frac{x^2}{\sin^2\alpha}\Big)^{\frac{1}{2}} dx = \tfrac{1}{4}\pi b_Y a_Y$$

$$\int_0^{b_Y} \Big(a_Y^2 - \frac{x^2}{\sin^2\alpha}\Big)^{\frac{3}{2}} dx = \tfrac{3}{16}\pi b_Y a_Y^3$$

$$\int_0^{b_Y} \Big(a_Y^2 - \frac{x^2}{\sin^2\alpha}\Big)^{-\frac{1}{2}} dx = \tfrac{1}{2}\pi \sin\alpha$$

to give

$$\int_0^{b_Y} \Big\{ [f_Y V_\theta(f_Y)\, C(f_Y)]\, \dot{f}_Y - [\, g_Y V_\theta(\, g_Y)\, C(\, g_Y)]\, \dot{g}_Y \Big\} dx$$

$$= \rho \{ \omega \cos\alpha [2\pi (\tfrac{3}{2}\pi b_Y a_Y \Big(R_Y^2 \dot{R}_Y + R_Y a_Y \dot{a}_Y\Big) + \pi \sin\alpha R_Y^3 a_Y \dot{a}_Y + \tfrac{3}{8}\pi b_Y a_Y^3 \dot{R}_Y)$$

$$-\left(2\pi R_M + \frac{Zt}{\sin\alpha}\right)(\tfrac{1}{2}\pi b_Y a_Y \Big(2 R_Y \dot{R}_Y + a_Y \dot{a}_Y\Big) + \pi \sin\alpha R_Y^2 a_Y \dot{a}_Y)$$

$$+ R_M \frac{Zt}{\sin\alpha}(\tfrac{1}{2}\pi b_Y a_Y \dot{R}_Y + \pi \sin\alpha R_Y a_Y \dot{a}_Y)]$$

$$+ \omega_P[\ 2\pi\ (\ \tfrac{3}{2}\pi\, b_Y a_Y \left(R_Y^2\, \dot{R}_Y + R_Y a_Y\, \dot{a}_Y\right) + \pi \sin\alpha\, R_Y^3\, a_Y\, \dot{a}_Y + \tfrac{3}{8}\pi\, b_Y a_Y^3\, \dot{R}_Y\ ) - \frac{Zt}{\sin\alpha}(\ \tfrac{1}{2}\pi\, b_Y a_Y \left(2\, R_Y \dot{R}_Y + a_Y\, \dot{a}_Y\right) + \pi \sin\alpha\, R_Y^2\, a_Y\, \dot{a}_Y\ )\ ]\ \}$$ (2.31)

Hence from Eqns.(2.28), (2.29) and (2.31) the unsteady torque component is represented by

$$\tau_U = K_3\, \omega_P + K_4\, \omega + K_5\, \dot{\omega}_P + K_6\, \dot{\omega} \qquad (2.32)$$

where

$$K_3 = -\rho\ [\ 2\pi\ (\ \tfrac{3}{2}\pi\, b_Y a_Y \left(R_Y^2\, \dot{R}_Y + R_Y a_Y\, \dot{a}_Y\right) + \pi\, R_Y^3\, b_Y\, \dot{a}_Y + \tfrac{3}{8}\pi\, b_Y a_Y^3\, \dot{R}_Y\ ) - \frac{Zt}{\sin\alpha}\ (\ \tfrac{1}{2}\pi\, b_Y a_Y \left(2\, R_Y \dot{R}_Y + a_Y\, \dot{a}_Y\right) + \pi\, R_Y^2\, b_Y\, \dot{a}_Y\ )\ ]$$

$$K_4 = -\rho \cos\alpha\ [\ 2\pi\ (\ \tfrac{3}{2}\pi\, b_Y a_Y \left(R_Y^2\, \dot{R}_Y + R_Y a_Y\, \dot{a}_Y\right) + \pi\, R_Y^3\, b_Y\, \dot{a}_Y + \tfrac{3}{8}\pi\, b_Y a_Y^3\, \dot{R}_Y\ ) - \left(2\pi R_M + \frac{Zt}{\sin\alpha}\right)(\ \tfrac{1}{2}\pi\, b_Y a_Y \left(2\, R_Y \dot{R}_Y + a_Y\, \dot{a}_Y\right) + \pi\, R_Y^2\, b_Y\, \dot{a}_Y\ ) + R_M \frac{Zt}{\sin\alpha}\ (\ \tfrac{1}{2}\pi\, b_Y a_Y\, \dot{R}_Y + \pi R_Y\, b_Y\, \dot{a}_Y\ )\ ]$$

$$K_5 = \rho\ [\ \tfrac{1}{2}\pi\ (\ ba\left(2\pi R_C - \frac{Zt}{\sin\alpha}\right)R_C^2 - b_Y a_Y\left(2\pi R_Y - \frac{Zt}{\sin\alpha}\right)R_Y^2\ ) + \tfrac{1}{8}\pi\ (\ ba^3\left(6\pi R_C - \frac{Zt}{\sin\alpha}\right) - b_Y a_Y^3\left(6\pi R_Y - \frac{Zt}{\sin\alpha}\right)\ )\ ]$$

$$K_6 = \rho \cos\alpha\ [\ \tfrac{1}{2}\pi\ (\ ba\left(R_C^2 - R_C R_M\right)\left(2\pi R_C - \frac{Zt}{\sin\alpha}\right) - b_Y a_Y\left(R_Y^2 - R_Y R_M\right)\left(2\pi R_Y - \frac{Zt}{\sin\alpha}\right)\ ) + \tfrac{1}{8}\pi\ (\ ba^3\left(6\pi R_C - \frac{Zt}{\sin\alpha} - 2\pi R_M\right) - b_Y a_Y^3\left(6\pi R_Y - \frac{Zt}{\sin\alpha} - 2\pi R_M\right)\ )\ ]$$

Hence the shaft torque of dynamometer is given by Eqns.(2.14), (2.18) and (2.32),

$$\tau_{Shaft} = K_1\, \omega\, \omega_P + K_2\, \omega^2 + K_3\, \omega_P + K_4\, \omega + K_5\, \dot{\omega}_P + K_6\, \dot{\omega} \qquad (2.33)$$

2.5 Energy Dissipation

The principle of energy conservation is used in Section 2.2 to obtain the angular vortex velocity of the working fluid, by equating vortex input power to energy dissipation power. Three components are used to represent the dissipation process; incidence loss, friction loss, and secondary circulation loss. These are derived below.

2.5.1 Incidence Loss

As fluid passes between rotor and stator, energy losses occur due to the realignment of the velocity vector with the blading of component the fluid has just entered. This incidence, or shock, loss has been modelled several ways with comparisons given by Whitfield and Wallace [53] and Sivalingam [33]. The kinetic energy model, which bases the loss on the square of the change of tangential fluid velocity relative to the component being entered, is used here. There are incidence losses at entrance to both rotor and stator.
At rotor inlet,

$$d\dot{P}_{IR} = \tfrac{1}{2} d\dot{m}_{IR} \left(W_{R\theta 2} - W_{R\theta 3}\right)^2 \qquad (2.34)$$

where

$W_{R\theta 2}$ = tangential relative velocity just before rotor
$W_{R\theta 3}$ = tangential relative velocity just inside rotor
$d\dot{m}_{IR}$ = elemental fluid flow into rotor.

From Fig.2.3,

$$W_{R\theta 2} = -(\omega_P r + \omega(R_M - r)\cos\alpha_{SO})$$
$$W_{R\theta 3} = -(\omega(R_M - r)\cos\alpha_{RI})$$

and applying Eqn.(2.9) to the rotor inlet,

$$d\dot{m}_{IR} = \rho\,\omega(R_M - r)\sin\alpha_{RI}\left(2\pi r - \frac{Z_R t}{\sin\alpha_{RI}}\right)dr$$

the elemental loss at rotor inlet is integrated from R_I to R_{CI},

$$\dot{P}_{IR} = \int_{R_I}^{R_{CI}} \left[\tfrac{1}{2}\rho\,\omega(R_M - r)\sin\alpha_{RI}\left(2\pi r - \frac{Z_R t}{\sin\alpha_{RI}}\right)\right.$$
$$\left.\times\left(\omega_P r + \omega(R_M - r)\cos\alpha_{SO} - \omega(R_M - r)\cos\alpha_{RI}\right)^2\right]dr$$

Rearranging,

$$\dot{P}_{IR} = \tfrac{1}{2}\rho \sin\alpha_{RI}\int_{R_I}^{R_{CI}} \left(2\pi r - \frac{Z_R t}{\sin\alpha_{RI}}\right)[\,\omega\omega_P^2(R_M r^2 - r^3)$$
$$+ 2\omega^2\omega_P(\cos\alpha_{SO} - \cos\alpha_{RI})\left(R_M^2 r - 2R_M r^2 + r^3\right)$$
$$+ \omega^3(\cos\alpha_{SO} - \cos\alpha_{RI})^2\left(R_M^3 - 3R_M^2 r + 3R_M r^2 - r^3\right)]dr$$

which yields

$$\dot{P}_{IR} = K_{I1}\omega\omega_P^2 + K_{I2}\omega^2\omega_P + K_{I3}\omega^3 \qquad (2.35)$$

where

$$K_{I1} = \tfrac{1}{2}\rho \sin\alpha_{RI}\,[\,2\pi\left(\tfrac{1}{4}R_M r^4 - \tfrac{1}{5}r^5\right) - \frac{Z_R t}{\sin\alpha_{RI}}\left(\tfrac{1}{3}R_M r^3 - \tfrac{1}{4}r^4\right)]_{R_I}^{R_{CI}}$$

$$K_{I2} = \rho \sin\alpha_{RI}(\cos\alpha_{SO} - \cos\alpha_{RI})\,[\,2\pi\left(\tfrac{1}{3}R_M^2 r^3 - \tfrac{1}{2}R_M r^4 + \tfrac{1}{5}r^5\right)$$
$$- \frac{Z_R t}{\sin\alpha_{RI}}\left(\tfrac{1}{2}R_M^2 r^2 - \tfrac{2}{3}R_M r^3 + \tfrac{1}{4}r^4\right)]_{R_I}^{R_{CI}}$$

$$K_{I3} = \tfrac{1}{2}\rho \sin\alpha_{RI}(\cos\alpha_{SO} - \cos\alpha_{RI})^2$$
$$\times[\,2\pi\left(\tfrac{1}{2}R_M^3 r^2 - R_M^2 r^3 + \tfrac{3}{4}R_M r^4 - \tfrac{1}{5}r^5\right)$$
$$- \frac{Z_R t}{\sin\alpha_{RI}}\left(R_M^3 r - \tfrac{3}{2}R_M^2 r^2 + R_M r^3 - \tfrac{1}{4}r^4\right)]_{R_I}^{R_{CI}}$$

For stator inlet Eqn.(2.34) becomes

$$d\dot{P}_{IS} = \tfrac{1}{2}d\dot{m}_{IS}(W_{S\theta 5} - W_{S\theta 6})^2 \qquad (2.36)$$

where from Fig.2.3,

$$W_{S\theta 5} = (\omega_P r + \omega(r - R_M)\cos\alpha_{RO})$$
$$W_{S\theta 6} = (\omega(r - R_M)\cos\alpha_{SI})$$

and from Eqn.(2.9),

$$d\dot{m}_{IS} = \rho\,\omega(r - R_M)\sin\alpha_{SI}\left(2\pi r - \frac{Z_S t}{\sin\alpha_{SI}}\right)dr$$

The loss at stator inlet is therefore

$$\dot{P}_{IS} = \int_{R_{CO}}^{R_O}[\,\tfrac{1}{2}\rho\,\omega(r - R_M)\sin\alpha_{SI}\left(2\pi r - \frac{Z_S t}{\sin\alpha_{SI}}\right)$$
$$\times(\omega_P r + \omega(r - R_M)\cos\alpha_{RO} - \omega(r - R_M)\cos\alpha_{SI})^2\,]dr$$

$$= \tfrac{1}{2}\rho \sin\alpha_{SI}\int_{R_{CO}}^{R_O}\left(2\pi r - \frac{Z_S t}{\sin\alpha_{SI}}\right)[\,\omega\omega_P^2(r^3 - R_M r^2)$$
$$+ 2\omega^2\omega_P(\cos\alpha_{RO} - \cos\alpha_{SI})\left(r^3 - 2R_M r^2 + R_M^2 r\right)$$
$$+ \omega^3(\cos\alpha_{RO} - \cos\alpha_{SI})^2\left(r^3 - 3R_M r^2 + 3R_M^2 r - R_M^3\right)]dr$$

which yields

$$\dot{P}_{IS} = K_{I4}\,\omega\omega_P^2 + K_{I5}\,\omega^2\omega_P + K_{I6}\,\omega^3 \tag{2.37}$$

where

$$K_{I4} = \tfrac{1}{2}\rho\,\sin\alpha_{SI}\,[\,2\pi\left(\tfrac{1}{5}r^5 - \tfrac{1}{4}R_M\,r^4\right) - \frac{Z_S t}{\sin\alpha_{SI}}\left(\tfrac{1}{4}r^4 - \tfrac{1}{3}R_M\,r^3\right)\,]_{R_{co}}^{R_o}$$

$$K_{I5} = \rho\,\sin\alpha_{SI}(\cos\alpha_{RO} - \cos\alpha_{SI})\,[\,2\pi\left(\tfrac{1}{5}r^5 - \tfrac{1}{2}R_M\,r^4 + \tfrac{1}{3}R_M^2\,r^3\right) - \frac{Z_S t}{\sin\alpha_{SI}}\left(\tfrac{1}{4}r^4 - \tfrac{2}{3}R_M\,r^3 + \tfrac{1}{2}R_M^2\,r^2\right)\,]_{R_{co}}^{R_o}$$

$$K_{I6} = \tfrac{1}{2}\rho\,\sin\alpha_{SI}\,(\cos\alpha_{RO} - \cos\alpha_{SI})^2 \times [\,2\pi\left(\tfrac{1}{5}r^5 - \tfrac{3}{4}R_M\,r^4 + R_M^2\,r^3 - \tfrac{1}{2}R_M^3\,r^2\right) - \frac{Z_S t}{\sin\alpha_{SI}}\left(\tfrac{1}{4}r^4 - R_M\,r^3 + \tfrac{3}{2}R_M^2\,r^2 - R_M^3\,r\right)\,]_{R_{co}}^{R_o}$$

Combining Eqns.(2.35) and (2.37) gives the total incidence loss for the dynamometer of

$$\dot{P}_I = (K_{I1} + K_{I4})\,\omega\omega_P^2 + (K_{I2} + K_{I5})\,\omega^2\omega_P + (K_{I3} + K_{I6})\omega^3 \tag{2.38}$$

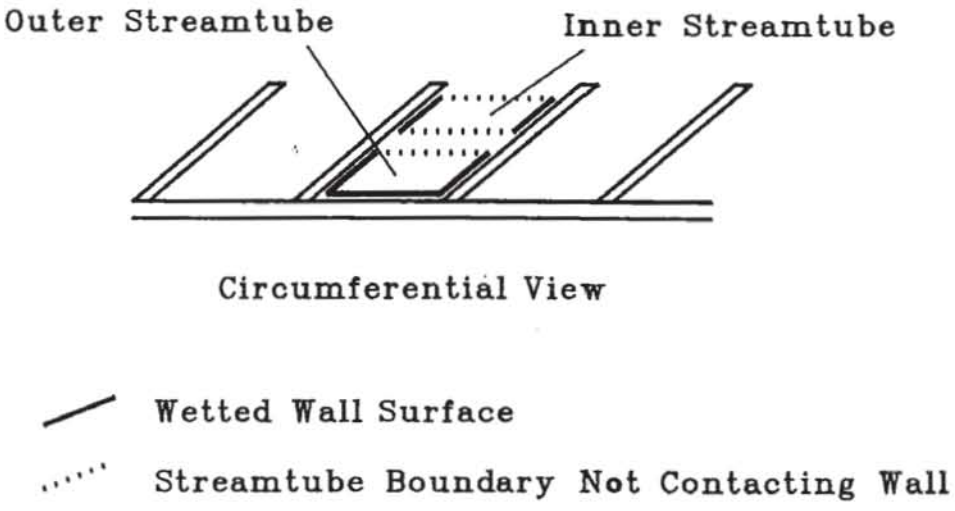

Figure 2.7: Friction Surfaces and Streamtubes

2.5.2 Friction Loss

Flow along the machine surfaces results in losses due to friction, that are represented by the commonly used pipe friction formula (Massey [54]),

$$d\dot{P}_F = d\dot{m}\frac{4 f\ LW^2}{2 d} \qquad (2.39)$$

where

L = flow path length
W = relative water velocity
d = hydraulic diameter $= 4\dfrac{\text{cross sectional area}}{\text{wetted perimeter}}$
f = friction factor
$\lambda_F = 4 f$

In Fig.2.7 it can be seen that the streamtubes adjacent to the machine wall surface (outer streamtubes) have a different wetted perimeters to those further up the blade surface (inner streamtubes), and so a different hydraulic diameter. Hence the two types are analysed separately. To simplify the analysis rotor and stator are divided into upper (further from axis) and lower halves, Fig.2.8.

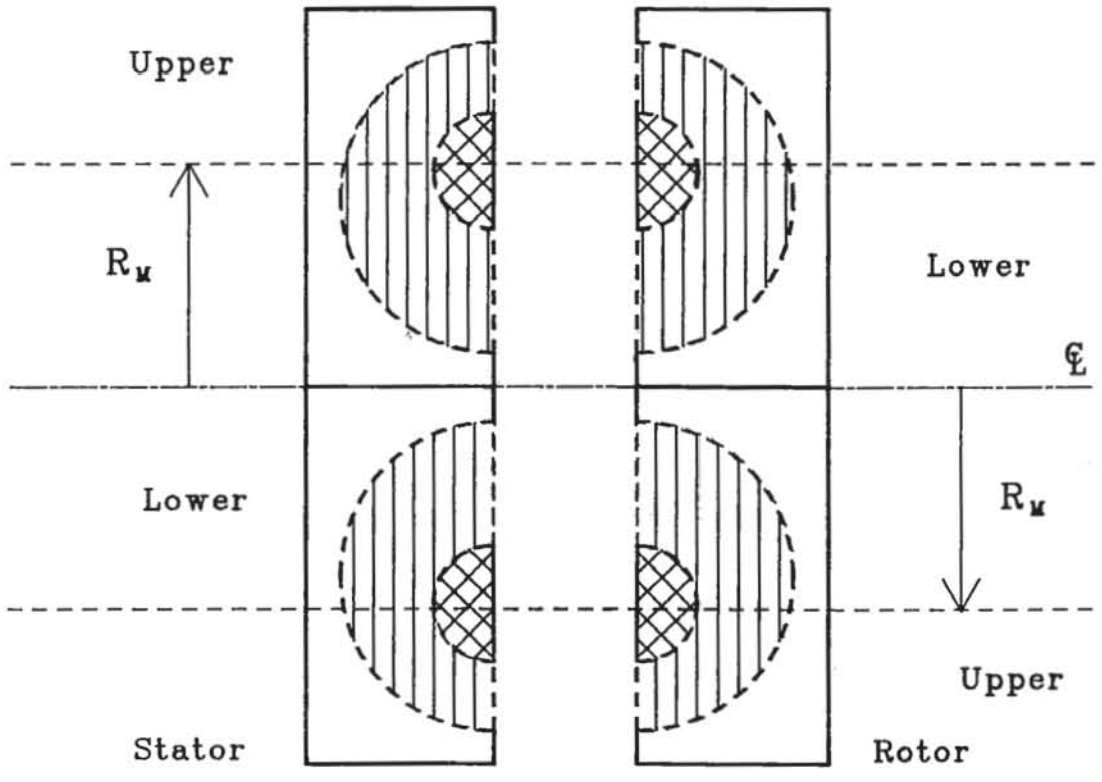

Figure 2.8: Rotor and Stator Quadrant Division

Outer Streamtubes

To account for the contact with the wall surface as well as the blade surfaces a streamtube of arbitrary thickness is used in Eqn.(2.39), and not an integrated thickness. For the lower half this thickness is arbitrarily $D_L = (R_M - R_I)/50$, and D_U (upper half) is defined by continuity. Considering the rotor with Eqn.(2.9),

$$\rho\,\omega(R_M - R_I)\,\sin\alpha_{RI}\left(2\pi R_I - \frac{Z_R t}{\sin\alpha_{RI}}\right)D_L = \rho\,\omega(R_O - R_M)\,\sin\alpha_{RO}\left(2\pi R_O - \frac{Z_R t}{\sin\alpha_{RO}}\right)D_{UR}$$

giving

$$D_{UR} = \frac{(R_M - R_I)\,\sin\alpha_{RI}\left(2\pi R_I - \frac{Z_R t}{\sin\alpha_{RI}}\right)}{(R_O - R_M)\,\sin\alpha_{RO}\left(2\pi R_O - \frac{Z_R t}{\sin\alpha_{RO}}\right)}D_L$$

Similarly for the stator,

$$D_{US} = \frac{(R_M - R_I)\,\sin\alpha_{SI}\left(2\pi R_I - \frac{Z_S t}{\sin\alpha_{SI}}\right)}{(R_O - R_M)\,\sin\alpha_{SO}\left(2\pi R_O - \frac{Z_S t}{\sin\alpha_{SO}}\right)}D_L$$

Considering the lower half of the rotor in Figs.2.7 and 2.8 gives

path length $\quad L_L = \frac{1}{2}\pi(R_M - R_I)$

hydraulic diameter $\quad d = 4\,\dfrac{\left(2\pi R_I - \frac{Z_R t}{\sin\alpha_{RI}}\right)D_L}{\left(2\pi R_I - \frac{Z_R t}{\sin\alpha_{RI}}\right) + 2\,Z_R\,D_L}$

relative velocity $\quad W = \omega(R_M - R_I)$

mass flowrate $\quad \dot{m} = \rho\,\omega(R_M - R_I)\,\sin\alpha_{RI}\left(2\pi R_I - \frac{Z_R t}{\sin\alpha_{RI}}\right)D_L$

Hence Eqn.(2.39) gives

$$\dot{P}_{FORL} = \tfrac{1}{2}\lambda_F L_L W^2 \frac{\rho\,\omega(R_M - R_I)\sin\alpha_{RI}\left(2\pi R_I - \dfrac{Z_R t}{\sin\alpha_{RI}}\right)D_L}{\left(4\dfrac{\left(2\pi R_I - \dfrac{Z_R t}{\sin\alpha_{RI}}\right)D_L}{\left(2\pi R_I - \dfrac{Z_R t}{\sin\alpha_{RI}}\right) + 2 Z_R D_L}\right)}$$

$$= \tfrac{1}{16}\lambda_F \rho\,\omega^3\pi\sin\alpha_{RI}(R_M - R_I)^4\left(2\pi R_I - \frac{Z_R t}{\sin\alpha_{RI}} + 2 Z_R D_L\right)$$

Which rearranged is

$$\dot{P}_{FORL} = K_{FORL}\,\omega^3 \tag{2.40}$$

where

$$K_{FORL} = \tfrac{1}{16}\lambda_F \rho\,\pi\,\sin\alpha_{RI}(R_M - R_I)^4\left(2\pi R_I - \frac{Z_R t}{\sin\alpha_{RI}} + 2 Z_R D_L\right)$$

For the upper rotor,

path length $L_U = \tfrac{1}{2}\pi(R_O - R_M)$

hydraulic diameter $d = 4\dfrac{\left(2\pi R_O - \dfrac{Z_R t}{\sin\alpha_{RO}}\right)D_{UR}}{\left(2\pi R_O - \dfrac{Z_R t}{\sin\alpha_{RO}}\right) + 2 Z_R D_{UR}}$

relative velocity $W = \omega(R_O - R_M)$

mass flowrate $\dot{m} = \rho\,\omega(R_O - R_M)\sin\alpha_{RO}\left(2\pi R_O - \dfrac{Z_R t}{\sin\alpha_{RO}}\right)D_{UR}$

which by the same rearrangement is

$$\dot{P}_{FORU} = K_{FORU}\,\omega^3 \tag{2.41}$$

where

$$K_{FORU} = \tfrac{1}{16}\lambda_F \rho\,\pi\,\sin\alpha_{RO}(R_O - R_M)^4\left(2\pi R_O - \frac{Z_R t}{\sin\alpha_{RO}} + 2 Z_R D_{UR}\right)$$

Similarly for the lower stator,

$$\dot{P}_{FOSL} = K_{FOSL}\,\omega^3 \tag{2.42}$$

where

$$K_{FOSL} = \tfrac{1}{16}\,\lambda_F\,\rho\,\pi\,\sin\alpha_{SO}\,(R_M - R_I)^4\left(2\pi R_I - \frac{Z_S t}{\sin\alpha_{SO}} + 2 Z_S D_L\right)$$

and the upper stator,

$$\dot{P}_{FOSU} = K_{FOSU}\,\omega^3 \tag{2.43}$$

where

$$K_{FOSU} = \tfrac{1}{16}\,\lambda_F\,\rho\,\pi\,\sin\alpha_{SI}\,(R_O - R_M)^4\left(2\pi R_O - \frac{Z_S t}{\sin\alpha_{SI}} + 2 Z_S D_{US}\right)$$

Inner Streamtubes

The elemental form of Eqn.(2.39) is used to determine the friction loss of these streamtubes and is integrated between the air-water interface and the limit of the outer streamtubes. Since the fluid is only contacting the blade surface the hydraulic diameter is markedly different from that of the outer streamtubes.

Beginning again with the lower rotor,

path length $\quad L = \tfrac{1}{2}\pi\,(R_M - r)$

hydraulic diameter $\quad d = 4\,\dfrac{\left(2\pi r - \dfrac{Z_R t}{\sin\alpha_{RI}}\right)dr}{2\,Z_R\,dr}$

relative velocity $\quad W = \omega(R_M - r)$

mass flowrate $\quad d\dot{m} = \rho\,\omega(R_M - r)\,\sin\alpha_{RI}\left(2\pi r - \dfrac{Z_R t}{\sin\alpha_{RI}}\right)dr$

and integrating Eqn.(2.39) gives

$$\dot{P}_{FIRL} = \int_{R_I + D_L}^{R_{CI}} \tfrac{1}{2}\lambda_F\,LW^2\,\frac{\rho\,\omega(R_M - r)\,\sin\alpha_{RI}\left(2\pi r - \dfrac{Z_R t}{\sin\alpha_{RI}}\right)}{\dfrac{2}{Z_R}\left(2\pi r - \dfrac{Z_R t}{\sin\alpha_{RI}}\right)}\,dr$$

$$= \tfrac{1}{8}\lambda_F Z_R \rho \pi \omega^3 \sin\alpha_{RI} \int_{R_I + D_L}^{R_{CI}} (R_M - r)^4 \, dr$$

$$= \tfrac{1}{8}\lambda_F Z_R \rho \pi \omega^3 \sin\alpha_{RI} \left[R_M^4 r - 2 R_M^3 r^2 + 2 R_M^2 r^3 - R_M r^4 + \tfrac{1}{5} r^5 \right]_{R_I + D_L}^{R_{CI}}$$

which yields

$$\dot{P}_{FIRL} = K_{FIRL} \omega^3 \tag{2.44}$$

where

$$K_{FIRL} = \tfrac{1}{8}\lambda_F Z_R \rho \pi \sin\alpha_{RI} \left[R_M^4 r - 2 R_M^3 r^2 + 2 R_M^2 r^3 - R_M r^4 + \tfrac{1}{5} r^5 \right]_{R_I + D_L}^{R_{CI}}$$

For the upper rotor,

path length $\quad L = \tfrac{1}{2}\pi (r - R_M)$

hydraulic diameter $\quad d = \dfrac{2}{Z_R}\left(2\pi r - \dfrac{Z_R t}{\sin\alpha_{RO}} \right)$

relative velocity $\quad W = \omega (r - R_M)$

mass flowrate $\quad \dot{m} = \rho \omega (r - R_M) \sin\alpha_{RO} \left(2\pi r - \dfrac{Z_R t}{\sin\alpha_{RO}} \right) dr$

which by the same rearrangement is

$$\dot{P}_{FIRU} = K_{FIRU} \omega^3 \tag{2.45}$$

where

$$K_{FIRU} = \tfrac{1}{8}\lambda_F Z_R \rho \pi \sin\alpha_{RO} \left[\tfrac{1}{5} r^5 - R_M r^4 + 2 R_M^2 r^3 - 2 R_M^3 r^2 + R_M^4 r \right]_{R_{CO}}^{R_O - D_{UR}}$$

Similarly for the lower stator,

$$\dot{P}_{FISL} = K_{FISL} \omega^3 \tag{2.46}$$

where

$$K_{FISL} = \tfrac{1}{8}\lambda_F Z_S \rho \pi \sin\alpha_{SO} \left[R_M^4 r - 2 R_M^3 r^2 + 2 R_M^2 r^3 - R_M r^4 + \tfrac{1}{5} r^5 \right]_{R_I + D_L}^{R_{CI}}$$

and the upper stator,

$$\dot{P}_{FISU} = K_{FISU}\,\omega^3 \tag{2.47}$$

where

$$K_{FISU} = \tfrac{1}{8}\lambda_F Z_S \rho \pi \sin\alpha_{SI}\left[\tfrac{1}{5}r^5 - R_M r^4 + 2R_M^2 r^3 - 2R_M^3 r^2 + R_M^4 r\right]_{R_{CO}}^{R_O - D_{US}}$$

Hence the total friction loss is the sum of Eqns.(2.40), (2.41), (2.42), (2.43), (2.44), (2.45), (2.46) and (2.47),

$$\dot{P}_F = K_F\,\omega^3 \tag{2.48}$$

where

$$K_F = K_{FORL} + K_{FORU} + K_{FOSL} + K_{FOSU} + K_{FIRL} + K_{FIRU} + K_{FISL} + K_{FISU}$$

2.5.3 Secondary Circulation Loss

Both the curved nature of the fluid flow path and the interruption of the ideal flow by the passing of vanes cause fluid circulation in other than the helical vortex of Fig.1.3. Flow around a bend results in a radial pressure gradient, and the operation of radical flow pumps (the rotor) forms a pressure gradient in the vane to vane direction, which give rise to eddy flows superimposed on the ideal helical flow. This is supplemented by turbulence from the vanes disrupting the flow.

To model these losses the common formula for pipe bends is used,

$$\dot{P}_{SC} = \tfrac{1}{2}K_B W^2\,\dot{dm} \tag{2.49}$$

where

W = relative water velocity

K_B = empirically derived loss coefficient.

Once more considering the rotor and stator as halves and integrating the general streamtube formulations. The lower rotor gives

$$\dot{P}_{SCRL} = \int_{R_I}^{R_{CI}} \tfrac{1}{2} K_B (\omega(R_M - r))^2 \rho\, \omega(R_M - r) \sin\alpha_{RI} \left(2\pi r - \frac{Z_R t}{\sin\alpha_{RI}}\right) dr$$

$$= \tfrac{1}{2} K_B \rho\, \omega^3 \sin\alpha_{RI} \int_{R_I}^{R_{CI}} (R_M - r)^3 \left(2\pi r - \frac{Z_R t}{\sin\alpha_{RI}}\right) dr$$

$$= \tfrac{1}{2} K_B \rho\, \omega^3 \sin\alpha_{RI} \left[2\pi \left(\tfrac{1}{2} R_M^3 r^2 - R_M^2 r^3 + \tfrac{3}{4} R_M r^4 - \tfrac{1}{5} r^5\right) - \frac{Z_R t}{\sin\alpha_{RI}} \left(R_M^3 r - \tfrac{3}{2} R_M^2 r^2 + R_M r^3 - \tfrac{1}{4} r^4\right) \right]_{R_I}^{R_{CI}}$$

which rearranged is

$$\dot{P}_{SCRL} = K_{SCRL}\, \omega^3 \tag{2.50}$$

where

$$K_{SCRL} = \tfrac{1}{2} K_B \rho \sin\alpha_{RI} \left[2\pi \left(\tfrac{1}{2} R_M^3 r^2 - R_M^2 r^3 + \tfrac{3}{4} R_M r^4 - \tfrac{1}{5} r^5\right) - \frac{Z_R t}{\sin\alpha_{RI}} \left(R_M^3 r - \tfrac{3}{2} R_M^2 r^2 + R_M r^3 - \tfrac{1}{4} r^4\right) \right]_{R_I}^{R_{CI}}$$

For the upper rotor,

$$\dot{P}_{SCRU} = \int_{R_{CO}}^{R_O} \tfrac{1}{2} K_B (\omega(r - R_M))^2 \rho\, \omega(r - R_M) \sin\alpha_{RO} \left(2\pi r - \frac{Z_R t}{\sin\alpha_{RO}}\right) dr$$

which yields

$$\dot{P}_{SCRU} = K_{SCRU}\, \omega^3 \tag{2.51}$$

where

$$K_{SCRU} = \tfrac{1}{2} K_B \rho \sin\alpha_{RO} \left[2\pi \left(\tfrac{1}{5} r^5 - \tfrac{3}{4} R_M r^4 + R_M^2 r^3 - \tfrac{1}{2} R_M^3 r^2\right) - \frac{Z_R t}{\sin\alpha_{RO}} \left(\tfrac{1}{4} r^4 - R_M r^3 + \tfrac{3}{2} R_M^2 r^2 - R_M^3 r\right) \right]_{R_{CO}}^{R_O}$$

Similarly for the lower stator,

$$\dot{P}_{SCSL} = K_{SCSL}\, \omega^3 \tag{2.52}$$

where

$$K_{SCSL} = \tfrac{1}{2} K_B \rho \sin\alpha_{SO} \left[2\pi \left(\tfrac{1}{2} R_M^3 r^2 - R_M^2 r^3 + \tfrac{3}{4} R_M r^4 - \tfrac{1}{5} r^5\right) - \frac{Z_S t}{\sin\alpha_{SO}} \left(R_M^3 r - \tfrac{3}{2} R_M^2 r^2 + R_M r^3 - \tfrac{1}{4} r^4\right) \right]_{R_I}^{R_{CI}}$$

and the upper stator,

$$\dot{P}_{SCSU} = K_{SCSU}\, \omega^3 \tag{2.53}$$

where

$$K_{SCSU} = \tfrac{1}{2} K_B \rho \sin\alpha_{SI} \left[2\pi \left(\tfrac{1}{5} r^5 - \tfrac{3}{4} R_M r^4 + R_M^2 r^3 - \tfrac{1}{2} R_M^3 r^2 \right) - \frac{Z_S t}{\sin\alpha_{SI}} \left(\tfrac{1}{4} r^4 - R_M r^3 + \tfrac{3}{2} R_M^2 r^2 - R_M^3 r \right) \right]_{R_{CO}}^{R_O}$$

So the total secondary circulation loss is the sum of Eqns.(2.50), (2.51), (2.52) and (2.53),

$$\dot{P}_{SC} = K_{SC} \omega^3 \qquad (2.54)$$

where

$$K_{SC} = K_{SCRL} + K_{SCRU} + K_{SCSL} + K_{SCSU}$$

The total energy dissipation is therefore the sum of Eqns.(2.38), (2.48) and (2.54),

$$\dot{P}_L = (K_{I1} + K_{I4}) \omega \omega_P^2 + (K_{I2} + K_{I5}) \omega^2 \omega_P + (K_{I3} + K_{I6} + K_F + K_{SC}) \omega^3 \qquad (2.55)$$

2.5.4 Empirical Loss Coefficients

In the previous two sections the friction and secondary circulation loss calculations require empirical loss coefficients. To determine the friction factor the approach used for fluid friction in pipes is adapted. The fluid flow area is considered as a rectangular duct (Fig.2.9) with a circumferential width at mean radius per fluid flow space given by,

$$X = (2\pi R_C - \frac{Zt}{\sin\alpha}) \qquad (2.56)$$

and depth by,

$$Y = \tfrac{1}{2} (R_O - R_I) \qquad (2.57)$$

These equations yield an equivalent hydraulic diameter of

$$d_h = 4 \times \frac{Y X \sin\alpha}{(2Y + X)} \qquad (2.58)$$

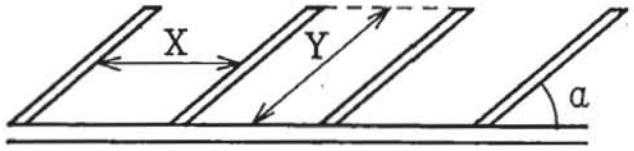

Circumferential View

Figure 2.9: Friction Factor Determination

For a Froude F020 dynamometer (R_o = 102.5 mm, R_i = 43.5 mm, t = 5.0 mm, Z (average) = 13, α = 45°) these equations give an equivalent hydraulic diameter of 27.0 mm. In Section 5.2.4 the effect of different surface roughnesses is investigated. As an example, a roughness height of 0.0127 mm is used, representing a fettled and ground finish on a sand cast cup. Later machines such as the F24 are investment cast leading to better surface finish (typically 0.003 mm roughness). By using the water angular velocity of 1577 rad/s at 1500 rpm for the F020, a Reynolds number of 1.1 x 10^6 is obtained (water kinematic viscosity of 1.14 x 10^{-6} m^2/s). The appropriate friction factor is then calculated from the Moody formula, Massey [51],

$$f = 0.001375 \ [1 + (20\,000 \frac{k}{d_h} + \frac{10^6}{Re})^{1/3} \ ]$$

where

k = surface roughness
d_h = hydraulic diameter
Re = Reynolds number
λ_F = $4f$ = friction constant used in Section 2.5.2

For the F020 the appropriate value of λ_F is 0.0171. Table 2.1 gives a summary of friction and secondary circulation loss for several dynamometers used in the following simulation chapters.

The values of the secondary circulation loss coefficient vary between types of machine. Sivalingam [33] reports a value of 0.45 as suitable for retarders as compared to 0.72 for fluid couplings. Applying a value of 0.45 to dynamometers leads to accurate torque predictions for cropped rotor and 90° vane machines in Section 5.2.1, but very low values for 45° vane machines. The 45° vane dynamometer has much lower fluid turbulence than the other two machines, due to the smoother flow path between rotor and stator than in the axial vane case, and to having the flow guided around the entire working circuit (unlike the cropped rotor machine). It is therefore surprising that Sivalingam believes that the secondary circulation losses should be of the same influence for 45° and axial vanes.

The F24 and other later model dynamometers have a reduced secondary circulation loss factor as a result of improved vane design leading to improved fluid flow and higher torque production. It should be noted that these empirical coefficients have been calculated for the case of a fully filled dynamometer running at a speed of 1500 rpm. These coefficients are expected to vary with both fill percentage and machine speed in practise, however for the purpose of this performance simulation they are taken as being constant.

MACHINE	FRICTION FACTOR λ_F	SECONDARY CIRCULATION FACTOR K_B
F020 45° vane	0.0171	0.22
F020 Cropped	0.0171	0.45
F020 90° vane	0.0171	0.45
F24 45° vane	0.0120	0.15

Table 2.1 Empirical Loss Coefficients for Dynamometer Simulations

CHAPTER 3
SUPPLEMENTARY EQUATIONS

In order to utilise the theory of Chapter 2 in an algorithm to simulate the self emptying behaviour of hydraulic dynamometers several supplementary equations are required. New methods for determining partial and varying fill are derived in Section 3.1, while the inclusion of acceleration, coriolis force and non-axial vanes in the derivation of water pressure in the working compartment (Section 3.2) extends previous work. The losses along the water outflow path are analysed for three flow paths in the final section of this chapter.

3.1 Partial and Varying Fill

Several of the theoretical derivations of the previous chapter use the air-water interface radii as integration limits, so a method of determining their position is necessary to apply the equations. For dynamic modelling the rate of change of fluid fill must also be quantified. The level of fluid in the working compartment is quantified as the percentage fill of the machine,

$$\text{Percentage Fill} = 1 - \frac{\text{Fluid mass displaced by air}}{\text{Maximum Fluid Mass possible}} \qquad (3.1)$$

In Section 2.4.2 these fluid masses are derived with reference to Fig.2.6,

maximum fluid mass,

$$M_F = \rho\ (2\pi\ R_C - \frac{Zt}{\sin\alpha})\pi\ ab \qquad (2.22)$$

mass displaced by air,

$$M_A = \rho\ (2\pi\ R_Y - \frac{Zt}{\sin\alpha})\pi\ a_Y b_Y \qquad (2.23)$$

where

$$R_C = \tfrac{1}{2}\,(R_O + R_I),\ a = \tfrac{1}{2}\,(R_O - R_I),\ b = \tfrac{1}{2}\,(R_O - R_I)\sin\alpha$$

and

$$R_Y = \tfrac{1}{2}(R_{CO} + R_{CI}),\ a_Y = \tfrac{1}{2}\ (R_{CO} - R_{CI}),\ b_Y = \tfrac{1}{2}\ (R_{CO} - R_{CI})\sin\alpha$$

Substituting into Eqn.(3.1) yields

$$PF = 1 - \frac{(R_{CO} - R_{CI})^2 \left(\pi(R_{CO} + R_{CI}) - \dfrac{Zt}{\sin\alpha}\right)}{(R_O - R_I)^2 \left(\pi(R_O + R_I) - \dfrac{Zt}{\sin\alpha}\right)} \qquad (3.2)$$

To allow for vane variations in the rotor and stator average values of vane number, 13, and angle, 45 deg., are used in the blockage factor of this expression.

At a given percentage fill the radii R_{CO} and R_{CI} define the air-water interface, and are determined by the simultaneous solution of two non-linear equations. The first is the definition of fluid percentage fill (Eqn.(3.2)), and the second is an application of the conservation of mass for the stator, as derived in Section 2.3, with the interface radii as integration limits rather than the vortex centre. Hence the mass inflow of Eqn.(2.10) becomes

$$\dot{M}_{SI} = \rho\,\omega\,\sin\alpha_{SI}\left[\,2\pi\left(\tfrac{1}{3}r^3 - \tfrac{1}{2}R_M\,r^2\right) - \frac{Z_S t}{\sin\alpha_{SI}}\left(\tfrac{1}{2}r^2 - R_M\,r\right)\right]_{R_{CO}}^{R_O}$$

and outflow (Eqn.(2.11)) is

$$\dot{M}_{SO} = \rho\,\omega\,\sin\alpha_{SO}\left[\,2\pi\left(\tfrac{1}{2}R_M\,r^2 - \tfrac{1}{3}r^3\right) - \frac{Z_S t}{\sin\alpha_{SO}}\left(R_M\,r - \tfrac{1}{2}r^2\right)\right]_{R_I}^{R_{CI}}$$

Equating inflow and outflow and rearranging gives

$$\begin{aligned} h(R_{CO}, R_{CI}) = {} & \tfrac{2}{3}\pi\left(\left(R_O^3 - R_{CO}^3\right)\sin\alpha_{SI} + \left(R_{CI}^3 - R_I^3\right)\sin\alpha_{SO}\right) \\ & - \pi R_M\left(\left(R_O^2 - R_{CO}^2\right)\sin\alpha_{SI} + \left(R_{CI}^2 - R_I^2\right)\sin\alpha_{SO}\right) \\ & - \tfrac{1}{2}Z_S t\left(R_O^2 - R_{CO}^2 + R_{CI}^2 - R_I^2\right) \\ & + Z_S t\,R_M\left(R_O - R_{CO} + R_{CI} - R_I\right) = 0 \end{aligned} \qquad (3.3)$$

The percentage fill definition (Eqn.(3.2)) is rearranged,

$$\begin{aligned} j(R_{CO}, R_{CI}) = {} & (R_{CO} - R_{CI})^2\left(\pi(R_{CO} + R_{CI}) - \frac{Zt}{\sin\alpha}\right) \\ & - (1 - PF)(R_O - R_I)^2\left(\pi(R_O + R_I) - \frac{Zt}{\sin\alpha}\right) = 0 \end{aligned} \qquad (3.4)$$

These are solved by Newton's method in two variables, Johnson and Riess [52], using the iteration

$$\begin{bmatrix} R_{CO_{t+1}} \\ R_{CI_{t+1}} \end{bmatrix} = \begin{bmatrix} R_{CO_t} \\ R_{CI_t} \end{bmatrix} - \boldsymbol{J}_t^{-1} \begin{bmatrix} h(R_{CO_t}, R_{CI_t}) \\ j(R_{CO_t}, R_{CI_t}) \end{bmatrix} \qquad (3.5)$$

where **J** is the Jacobi matrix,

$$\boldsymbol{J}_t = \begin{bmatrix} h_{R_{CO_t}} & h_{R_{CI_t}} \\ j_{R_{CO_t}} & j_{R_{CI_t}} \end{bmatrix}$$

the elements of which are the derivatives of $h\,(R_{CO}, R_{CI})$ and $j\,(R_{CO}, R_{CI})$ with respect to R_{CO} and R_{CI}.

$$h_{R_{CO}} = R_{CO}\,(2\pi R_M \sin\alpha_{SI} + Z_S t) - 2\pi \sin\alpha_{SI}\, R_{CO}^2 - Z_S t\, R_M$$

$$h_{R_{CI}} = 2\pi \sin\alpha_{SO}\, R_{CI}^2 - R_{CI}\,(2\pi R_M \sin\alpha_{SO} + Z_S t) + Z_S t\, R_M$$

$$j_{R_{CO}} = 2\,(R_{CO} - R_{CI})\left(\pi(R_{CO} + R_{CI}) - \frac{Zt}{\sin\alpha}\right) + \pi\,(R_{CO} - R_{CI})^2$$

$$j_{R_{CI}} = -2\,(R_{CO} - R_{CI})\left(\pi(R_{CO} + R_{CI}) - \frac{Zt}{\sin\alpha}\right) + \pi\,(R_{CO} - R_{CI})^2$$

After the matrix multiplication of the right hand side the iteration is

$$\begin{bmatrix} R_{CO_{t+1}} \\ R_{CI_{t+1}} \end{bmatrix} = \begin{bmatrix} R_{CO_t} \\ R_{CI_t} \end{bmatrix} - \frac{1}{\left(h_{R_{CO}} j_{R_{CI}} - j_{R_{CI}} h_{R_{CI}}\right)_t} \begin{bmatrix} j_{R_{CI}} h_t - h_{R_{CI}} j_t \\ -j_{R_{CO}} h_t + h_{R_{CO}} j_t \end{bmatrix} \qquad (3.6)$$

thus at any percentage fill the position of the air-water interface is evaluated.

If the dynamometer is not at steady state conditions the rate of change of percentage fill is obtained by comparing the mass flows into and out of the working compartment

$$\frac{d}{dt}(PF) = \frac{\rho Q_{IN} - \rho Q_{OUT}}{M_F} \qquad (3.7)$$

where

ρQ_{IN} = mass inflow rate
ρQ_{OUT} = mass outflow rate
M_F = maximum fluid mass in compartment (Eqn.(2.22))

The derivation of the unsteady torque component in Section 2.4.2 involves the time derivatives of the terms which define the air mass in the centre of the working compartment, the centre R_Y and radius a_Y. Substituting Eqns.(2.22) and (2.23) into the definition of percentage fill (Eqn.(3.1)) gives

$$PF = 1 - \frac{\rho\left(2\pi R_Y - \frac{Zt}{\sin\alpha}\right)\pi\, a_Y\, b_Y}{\rho\left(2\pi R_C - \frac{Zt}{\sin\alpha}\right)\pi ab}$$

which differentiated with respect to time is

$$\frac{d}{dt}(PF) = \frac{-1}{\left(2\pi R_C - \frac{Zt}{\sin\alpha}\right)a^2}\,\frac{d}{dt}\left(\left(2\pi R_Y - \frac{Zt}{\sin\alpha}\right)a_Y^2\right)$$

using $b = a\sin\alpha$ and $b_Y = a_Y \sin\alpha$ from Fig.2.6. Which leads to

$$\frac{d}{dt}(PF) = \frac{-1}{\left(2\pi R_C - \frac{Zt}{\sin\alpha}\right)a^2}\left(2\pi a_Y^2 \dot{R}_Y + \left(2\pi R_Y - \frac{Zt}{\sin\alpha}\right)2\, a_Y \dot{a}_Y\right) \quad (3.8)$$

Differentiating R_Y and a_Y gives

$$\dot{R}_Y = \tfrac{1}{2}\left(\dot{R}_{CO} + \dot{R}_{CI}\right) \quad (3.9)$$

$$\dot{a}_Y = \tfrac{1}{2}\left(\dot{R}_{CO} - \dot{R}_{CI}\right) \quad (3.10)$$

The derivatives of the interface radii, R_{CO} and R_{CI}, are interdependent but the relationship between them varies non linearly as the percentage fill changes, so rather than consume computer time obtaining the ratio of the derivatives iteratively for each torque calculation a constant ratio is substituted. Using constant values of percentage fill to provide radii values for a F24 machine (R_O = 121.0 mm, R_I = 51.2 mm, α = 45°) in Table 3.1, the ratio of the radii changes for different magnitude fill changes is calculated in Table 3.2.

% FILL	0	25	50	75	100
R_{CO} (mm)	121.0	117.5	113.2	107.3	91.49
R_{CI} (mm)	51.20	57.68	64.78	73.31	91.49

Table 3.1 Air-Water Interface Radii R_{CO}, R_{CI} for F24 machine

The average of these $\Delta R_{CO}/\Delta R_{CI}$ ratios is - 0.687 and is seen that the magnitude of both the percentage fill and change in fill effect this ratio. As both increase so does the ratio. Using a constant ratio introduces a small error to the unsteady torque component of Section 2.4.2, but it is found in Chapter 6 that the magnitude of the unsteady torque component relative to the steady component is so small that the inclusion of this simplification is of negligible effect.

Hence $\dot{R}_{CO} = -0.69\ \dot{R}_{CI}$ is substituted into Eqns.(3.9) and (3.10) which are rearranged to yield

$$\dot{R}_Y = -\frac{0.31}{1.69}\dot{a}_Y \qquad (3.11)$$

and using Eqn.(3.8) leads to

$$\dot{a}_Y = \frac{-\left(2\pi R_c - \frac{Zt}{\sin\alpha}\right)a^2}{\left(\left(2\pi R_Y - \frac{Zt}{\sin\alpha}\right)2\,a_Y - 2\pi a_Y^2 \frac{0.31}{1.69}\right)}\frac{d}{dt}(PF) \qquad (3.12)$$

Thus $\dot{a}_Y$ and $\dot{R}_Y$ are calculated from the rate of change of percentage fill and are used in the determination of unsteady torque.

FILL CHANGE	ΔR_{CO}	ΔR_{CI}	$\Delta R_{CO} / \Delta R_{CI}$
0 →25	3.50	-6.48	-0.540
0 →50	7.80	-13.6	-0.574
0 →75	13.7	-22.1	-0.620
0 →100	29.5	-40.3	-0.732
25 → 50	4.30	-7.10	-0.606
25 → 75	10.2	-15.6	-0.654
25 →100	26.0	-33.8	-0.769
50 → 75	5.90	-8.53	-0.692
50 →100	21.7	-26.7	-0.813
75 →100	15.8	-18.2	-0.868

Table 3.2 R_{CO}, R_{CI} changes for given fluid fill changes

3.2 Fluid Pressure

As the working fluid flows along the helical path (Fig.1.2) there is a variation in its pressure which has a significant effect on the self-emptying behaviour of the machine. The fluid pressure is lower in the stator than in the rotor, so dynamometers with water outlet holes in the stator empty at a much lower rate than those with rotor outlets. In Sections 5.4 and 5.5 the effects of water outlet position and fluid pressure on machine behaviour are considered.

Past work in this area does not meet the requirements of the current model, so a vector approach is used to allow pressure calculations around the working compartment at different vane angles. Patki and Gill [5] derive the fluid pressure as only due to the mechanical rotation of the machine, while Raine [6] and Tan [7] consider only the pressure caused by the vortex action of the water flowing around working compartment. Both the machine and the fluid rotation effects are included in Numazawa et al [41] in their mean flow path analysis of torque converters. However the most complete pressure analysis is by Sivalingam [33], who uses the pressure expression to define the free surface profile in partially filled fluid couplings. Although allowing for calculation at different points in the working compartment and including forces due to both machine and vortex rotation, Sivalingam's approach omits the effect of coriolis force while analysing a fluid element in a rotating reference frame. In the case of axial vaned machines this omission does not alter the analysis as the coriolis component is perpendicular to the plane in which the forces are analysed, but for other vane angles it must be included. Since the current work involves dynamic modelling the effect of dynamometer acceleration must now also be considered.

In order to calculate the fluid pressure the forces acting on a fluid element, lying in the plane of the machine vanes, are analysed. Thus the water flows around a circular vortex in the vane plane of reference, which itself rotates with the same speed as the machine element in which the fluid is being analysed. The fluid flow, the velocity vectors, and the acceleration vectors relative to the rotating vane plane are illustrated in Fig.3.1. Since the fluid is assumed to follow a curved path

around the vortex the forces acting on a fluid element must balance in the direction of the vortex centre[1].

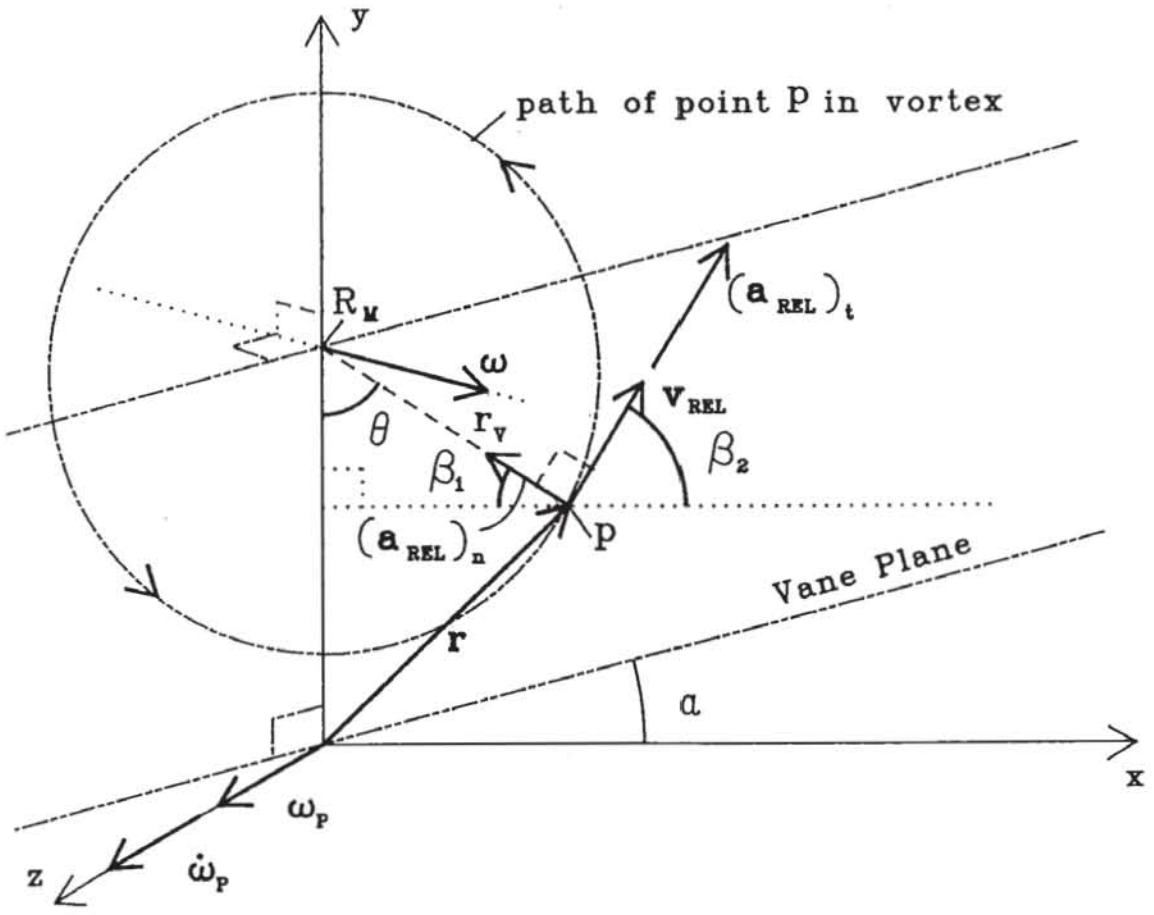

Figure 3.1: Fluid Position, Velocity and Acceleration Vectors

Referring to Fig.3.2 the net pressure force for an element of unit thickness is the sum of the force toward the vortex centre (the positive sign convention),

$$F_{PI} = (P + \delta P)\,\delta\theta\,(r_v + \delta r_v)$$

$$F_{PI} = P\,r_v\,\delta\theta + P\,\delta r_v\,\delta\theta + \delta P\,r_v\,\delta\theta + \delta P\,\delta r_v\,\delta\theta$$

and the force away from R_M,

$$F_{PO} = -P\,r_v\,\delta\theta - 2(P + k\,\delta P)\delta r_v \sin\left(\tfrac{1}{2}\delta\theta\right)$$

which yields

$$F_P = P\,r_v\,\delta\theta + P\,\delta r_v\,\delta\theta + \delta P\,r_v\,\delta\theta + \delta P\,\delta r_v\,\delta\theta - P\,r_v\,\delta\theta - 2(P + k\,\delta P)\delta r_v \sin\left(\tfrac{1}{2}\delta\theta\right)$$

---

1 The actual flow path is distorted from a circle as the centres of the dynamometer working compartment and the model vortex do not coincide (Section 2.1, Fig.2.2). As a result there is a small variation (0° - 9° depending on position around cup) between the relative velocity and acceleration vectors used here and the true vectors. In the case of the relative acceleration the exclusion of a small component of the tangential vector is compensated for by the radial component not being reduced. Hence the simplification only introduces a small error into the pressure determination.

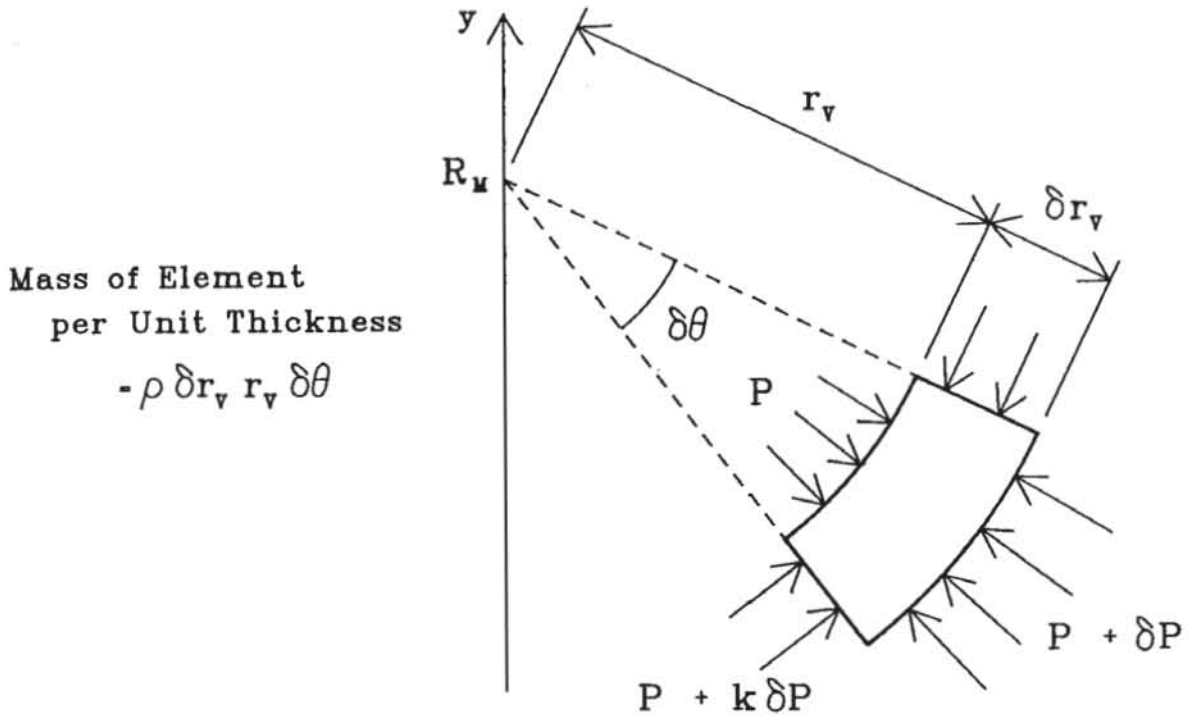

Figure 3.2: Pressure Forces on a Fluid Element

Using the approximation for small θ of *sin* θ and neglecting second order of smallness terms leaves

$$F_p = \delta P\, r_v\, \delta\theta \tag{3.13}$$

At a point P in a reference frame rotating with angular velocity ω_p, the acceleration components are

$$\boldsymbol{a} = \dot{\omega}_p \times \boldsymbol{r} + \omega_p \times (\omega_p \times \boldsymbol{r}) + 2\,\omega_p \times \boldsymbol{v}_{REL} + \boldsymbol{a}_{REL} \tag{3.14}$$

(Meriam [53]), shown in Fig.3.3 It should be noted that the direction of the vector cross products must be carefully evaluated as vane angle α and cup angle θ change, since the products usually lie in the rotor plane (X - Y plane in Fig.3.3) rather than the vane plane, but sometimes in the line of intersection. Therefore directional cofactors are geometrically determined to give the radial components of acceleration toward the vortex centre.

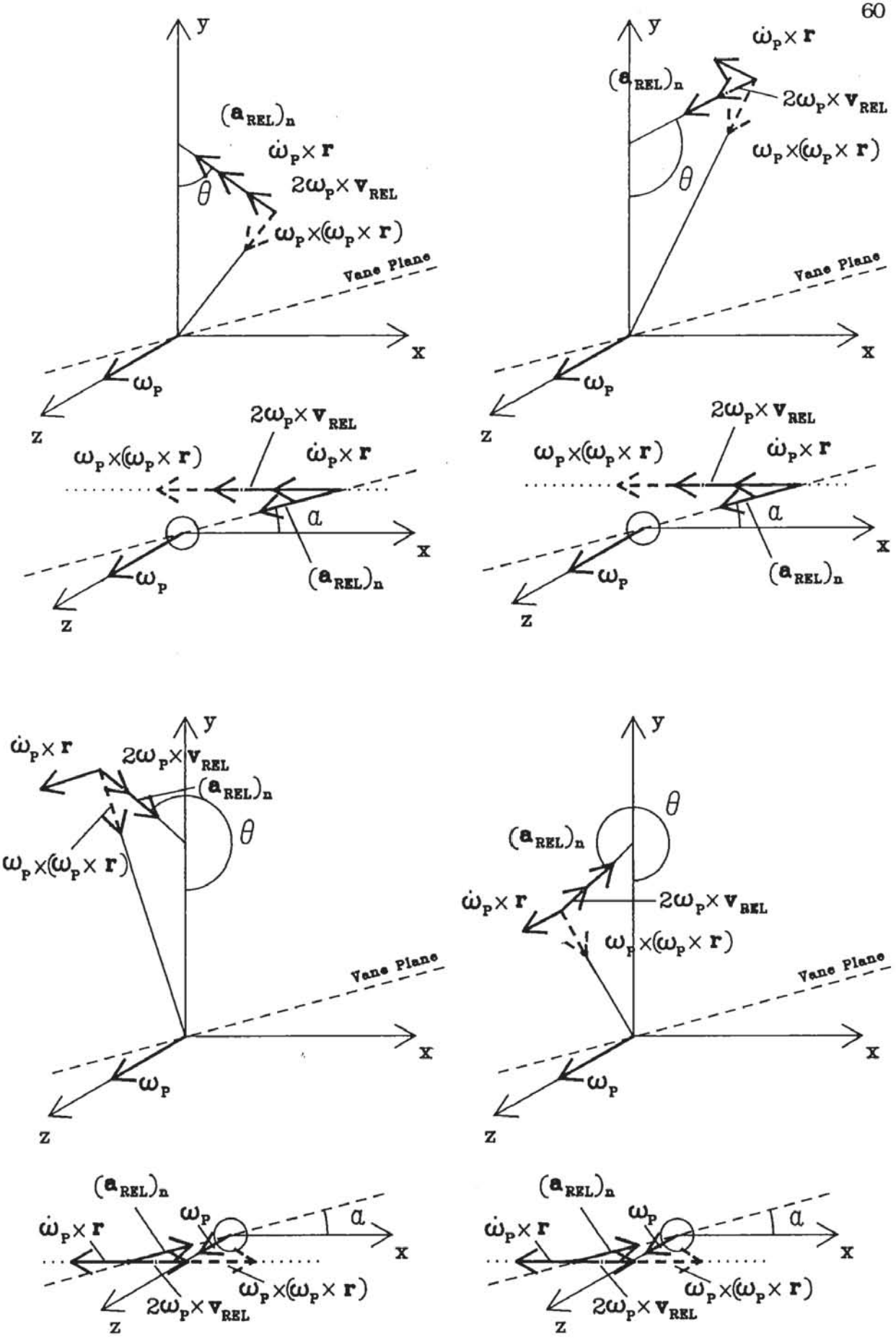

Figure 3.3: Fluid Acceleration and Vector Cross Products

The first cross product of Eqn.(3.14), $\dot{\omega}_P \times \boldsymbol{r}$, is due to the acceleration of the reference frame (rotor acceleration) and has a direction cofactor from Figs.3.3 and 3.4 of,

$$C_{WR} = K \cos\mu \cos\alpha \tag{3.15}$$

where

$$\mu = absolute(\zeta - 90°)$$

$$K = \begin{cases} 1, 0° < \theta < 180° \\ -1, \ 180° < \theta < 360° \\ 0, \theta = 0° \text{ or } 180° \end{cases}$$

In the case of the stator ($180° < \theta < 360°$) this term becomes zero, since the frame of reference is stationary at all times. Hence the second and third cross products are also zero for the stator region, though the direction cofactors are non-zero. The latter of these, coriolis acceleration $2\,\omega_P \times \boldsymbol{v}_{REL}$, has a cofactor

$$C_{WV} = \begin{cases} \cos\alpha, \theta \neq 0° \text{ or } 180° \\ 1 \quad , \theta = 0° \text{ or } 180° \end{cases} \tag{3.16}$$

as it is always in the rotor plane except at $\theta = 0°$ and 180° when it is in the line of intersection of the rotor and vane planes.

Attention must be paid to the direction cofactor of the machine rotation term, the second vector cross product $\omega_P \times (\omega_P \times \boldsymbol{r})$, because the final direction of this product varies from that of the negative $\boldsymbol{r}$ vector to the negative y axis direction as the vane angle α varies from 0° to 90° in Fig.3.4. The cosine rule is used to determine angle ζ,

$$\cos\zeta = \frac{r_V^2 + |R|^2 - R_M^2}{2\, r_V |R|} \tag{3.17}$$

with $|\boldsymbol{r}|$ the magnitude of vector $\boldsymbol{r}$; angle β is assumed to vary linearly with vane angle,

$$\beta = (180° - \zeta) - \frac{\alpha}{90°}(180° - \zeta - \theta) \tag{3.18}$$

As with the coriolis component the rotation product lies in the rotor plane and the line of intersection at $\theta = 0°$ and 180°.

Hence the machine rotation direction cofactor is

$$C_{WWR} = \begin{cases} -\cos\beta \cos\alpha, \theta \neq 0° \text{ or } 180° \\ -\cos\beta \quad , \theta = 0° \text{ or } 180° \end{cases} \tag{3.19}$$

where β is defined by Eqns.(3.17) and (3.18).

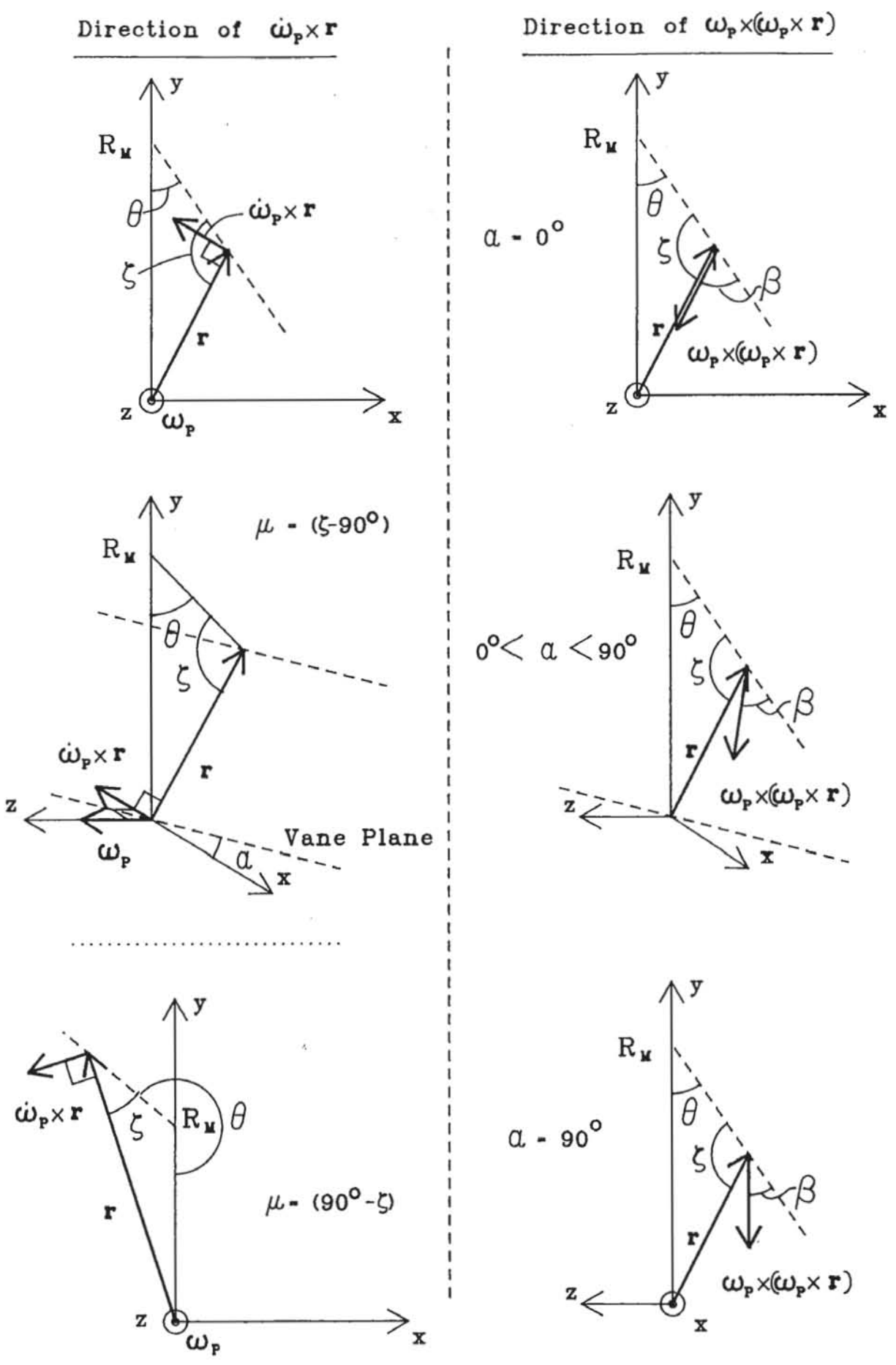

Figure 3.4: Directions of Vector Cross Product Radial Components

Finally from Eqn.(3.14) the acceleration relative to the reference frame $\boldsymbol{a}_{REL}$ (that due to the fluid vortex) is considered as radial and tangential components,

$$\boldsymbol{a}_{REL} = (\boldsymbol{a}_{REL})_n + (\boldsymbol{a}_{REL})_t$$

Having taken the fluid velocity as perpendicular to the radial direction, the acceleration component due to the fluid vortex is simply the centripetal acceleration, so the direction cofactor is unity for all angles.

The magnitude of a vector cross product is given by

$$\boldsymbol{a} \times \boldsymbol{b} = |a|\,|b|\,\sin\gamma$$

where

$$\gamma = \text{angle between } \boldsymbol{a} \text{ and } \boldsymbol{b} = \cos^{-1}\left(\frac{\boldsymbol{a}\cdot\boldsymbol{b}}{|\boldsymbol{a}|\,|\boldsymbol{b}|}\right)$$

$|\boldsymbol{a}|, |\boldsymbol{b}|$ = magnitudes of $\boldsymbol{a}$ and $\boldsymbol{b}$

From Fig.3.1 the vectors of Eqn.(3.14) are, in Cartesian coordinates,

position

$$\boldsymbol{r} = (r_V \sin\theta\cos\alpha,\ R_M - r_V\cos\theta,\ -r_V\sin\theta\sin\alpha)$$

relative velocity

$$\boldsymbol{v}_{REL} = (\omega r_V \cos\beta_2\cos\alpha,\ \omega r_V \sin\beta_2,\ -\omega r_V\cos\beta_2\sin\alpha)$$
$$= (\omega r_V\cos\theta\cos\alpha,\ \omega r_V\sin\theta,\ -\omega r_V\cos\theta\sin\alpha)$$

radial relative acceleration

$$(\boldsymbol{a}_{REL})_n = (-\omega^2 r_V\cos\beta_1\cos\alpha,\ \omega^2 r_V\sin\beta_1,\ \omega^2 r_V\cos\beta_1\sin\alpha)$$
$$= (-\omega^2 r_V\sin\theta\cos\alpha,\ \omega^2 r_V\cos\theta,\ \omega^2 r_V\sin\theta\sin\alpha)$$

machine rotational velocity

$$\omega_P = \begin{cases} (0, 0, \omega_P), & rotor \\ (0, 0, 0), & stator \end{cases}$$

machine rotational acceleration

$$\dot{\omega}_P = \begin{cases} (0, 0, \dot{\omega}_P), & rotor \\ (0, 0, 0), & stator \end{cases}$$

The magnitudes of which are

$$|\boldsymbol{r}| = \left(r_V^2 + R_M^2 - 2R_M r_V\cos\theta\right)^{\frac{1}{2}}$$
$$|\boldsymbol{v}_{REL}| = \omega r_V$$
$$|(\boldsymbol{a}_{REL})_n| = \omega^2 r_V$$
$$|\omega_P| = \begin{cases} \omega_P, & rotor \\ 0, & stator \end{cases}$$
$$|\dot{\omega}_P| = \begin{cases} \dot{\omega}_P, & rotor \\ 0, & stator \end{cases}$$

Hence the vector cross products are

$$\dot{\omega}_P \times \mathbf{r} = \dot{\omega}_P \left(r_V^2 + R_M^2 - 2 R_M r_V \cos\theta \right)^{\frac{1}{2}} \sin\gamma_A$$

where

$$\gamma_A = \cos^{-1}\left(\frac{-r_V \sin\theta \sin\alpha}{\left(r_V^2 + R_M^2 - 2 R_M r_V \cos\theta \right)^{\frac{1}{2}}} \right)$$

$$\omega_P \times \mathbf{r} = \omega_P \left(r_V^2 + R_M^2 - 2 R_M r_V \cos\theta \right)^{\frac{1}{2}} \sin\gamma_R$$

where

$$\gamma_R = \cos^{-1}\left(\frac{-r_V \sin\theta \sin\alpha}{\left(r_V^2 + R_M^2 - 2 R_M r_V \cos\theta \right)^{\frac{1}{2}}} \right)$$

$$\omega_P \times (\omega_P \times \mathbf{r}) = \omega_P^2 \left(r_V^2 + R_M^2 - 2 R_M r_V \cos\theta \right)^{\frac{1}{2}} \sin\gamma_R \sin\gamma_W$$

where

$\sin\gamma_W = 1$ as $(\omega_P \times \mathbf{r}) \perp \omega_P$

$$2\,\omega_P \times \mathbf{v}_{REL} = 2\,\omega_P\,\omega\, r_V \sin\gamma_V$$

where

$\gamma_V = \cos^{-1}(-\cos\theta \sin\alpha)$

Applying Newton's second law to the fluid element of Fig.3.2 in the radial direction,

net pressure force = mass × radial acceleration component

gives

$$\delta P\, r_V\, \delta\theta = \rho\, \delta r_V\, r_V\, \delta\theta \{ \dot{\omega}_P \left(r_V^2 + R_M^2 - 2 R_M r_V \cos\theta \right)^{\frac{1}{2}} \sin\gamma_A C_{WR} + \omega_P^2 \left(r_V^2 + R_M^2 - 2 R_M r_V \cos\theta \right)^{\frac{1}{2}} \sin\gamma_R C_{WWR} + 2\,\omega_P\,\omega\, r_V \sin\gamma_V C_{WV} + \omega^2 r_V \}$$

which rearranged is

$$\delta P = \rho \{ \omega^2 r_V + 2\,\omega_P \omega \sin\gamma_V C_{WV} r_V + \left(\dot{\omega}_P \sin\gamma_A C_{WR} + \omega_P^2 \sin\gamma_R C_{WWR} \right) \left(r_V^2 + R_M^2 - 2 R_M r_V \cos\theta \right)^{\frac{1}{2}} \} \delta r_V \qquad (3.20)$$

To integrate the last term of Eqn.(3.20) the substitutions

$$u = (r_V - R_M \cos\theta) \quad \text{and} \quad a^2 = R_M^2 (\cos^2\theta - 1)$$

are made, and the integration identity

$$\int (u^2 - a^2)^{\frac{1}{2}}\, du = \tfrac{1}{2}u(u^2 - a^2)^{\frac{1}{2}} - \tfrac{1}{2}a^2 \ln\left|u + (u^2 - a^2)^{\frac{1}{2}}\right| + C$$

is used. Note also,

$$\ln\left|u + (u^2 - a^2)^{\frac{1}{2}}\right| = \cosh^{-1}\left(\frac{u}{a}\right)$$

Thus Eqn.(3.20) is integrated,

$$\begin{aligned} P = \rho [& (\omega^2 + 2\,\omega_P\,\omega \sin\gamma_V\, C_{WV})\,\tfrac{1}{2} r_V^2 \\ & + (\dot{\omega}_P \sin\gamma_A\, C_{WR} + \omega_P^2 \sin\gamma_R\, C_{WWR}) \\ & \times \{ \tfrac{1}{2}(r_V - R_M \cos\theta)\left(r_V^2 + R_M^2 - 2\,R_M\, r_V \cos\theta\right)^{\frac{1}{2}} \\ & \quad -\tfrac{1}{2}(\cos^2\theta - 1) R_M^2 \\ & \quad \times \ln\left|(r_V - R_M \cos\theta) + \left(r_V^2 + R_M^2 - 2\,R_M\, r_V \cos\theta\right)^{\frac{1}{2}}\right| \}] + C \end{aligned} \qquad (3.21)$$

where C is the constant of integration.

The constant of integration is calculated by applying the boundary condition at the air-water interface, which is at atmospheric pressure due to the air vents in the dynamometer. As above the air pocket is assumed circular with

centre $R_Y = \frac{1}{2}(R_{CO} + R_{CI})$ and radius $a = \frac{1}{2}(R_{CO} - R_{CI})$.

For a given angle θ the point on the interface where pressure equals atmospheric pressure is calculated from Fig.3.5 using the sine rule,

$$r_o = a\frac{\sin\theta_D}{\sin\theta} \qquad (3.22)$$

where

$$\theta_D = 180° - (\theta_Y + \theta)$$

and

$$\sin\theta_Y = \frac{1}{a}(R_M - R_Y)\sin\theta \;, \quad \text{when } \theta > 180° \text{ put } \theta = (360° - \theta)$$

Applying the condition of atmospheric pressure P_O at radial distance r_O in Eqn.(3.21) gives

$$\begin{aligned} P_O = \rho [& (\omega^2 + 2\,\omega_P\,\omega \sin\gamma_V\, C_{WV})\,\tfrac{1}{2} r_O^2 \\ & + (\dot{\omega}_P \sin\gamma_A\, C_{WR} + \omega_P^2 \sin\gamma_R\, C_{WWR}) \\ & \times \{ \tfrac{1}{2}(r_O - R_M \cos\theta)\left(r_O^2 + R_M^2 - 2\,R_M\, r_O \cos\theta\right)^{\frac{1}{2}} \\ & \quad -\tfrac{1}{2}(\cos^2\theta - 1) R_M^2 \\ & \quad \times \ln\left|(r_O - R_M \cos\theta) + \left(r_O^2 + R_M^2 - 2\,R_M\, r_O \cos\theta\right)^{\frac{1}{2}}\right| \}] + C \end{aligned} \qquad (3.23)$$

Subtracting Eqn.(3.23) from Eqn.(3.21) gives the gauge pressure at any point along the radial direction of angle θ. Usually the surface of the working compartment wall is the point of interest, so a method of calculating distance r_v to the surface is given in Appendix D, as is a method for converting angles around the working compartment from its centre (more easily definable) to angles from the vortex centre.

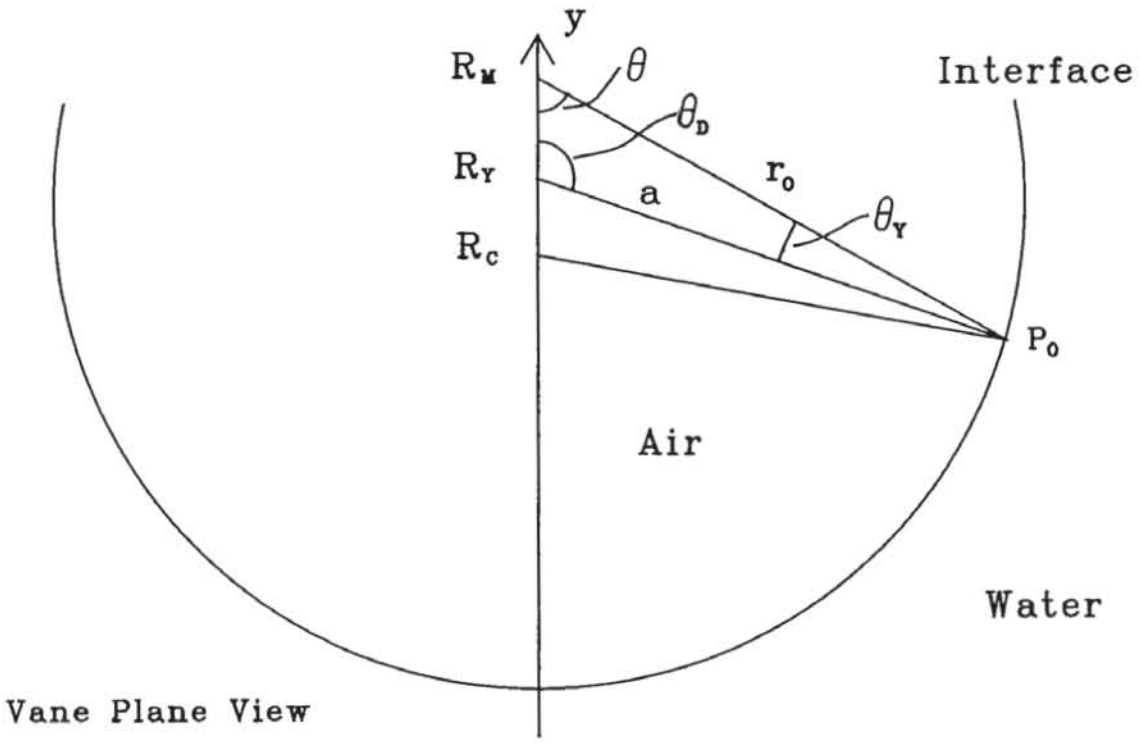

Figure 3.5: Determination of Distance to Air-Water Interface

3.3 Fluid Outflow from Working Compartment

Having calculated the fluid pressure in the working compartment, it is possible to determine the fluid outflow rate by analysing the outflow path using Bernoulli's energy equation with allowance for *pipe* energy losses (Massey [51]). This requires that the aeration of the water is disregarded so the fluid is of constant density, and that the drain passages are full at all times so the flow can be considered steady (no mass accumulation). Such a model is a great simplification of the complex turbulent two-phase flows occurring in the dynamometer and drain passages, but at the macroscopic level of machine performance prediction is sufficiently accurate to represent the emptying behaviour of hydraulic dynamometers.

There are three different outflow paths used on Froude F type dynamometers: from the back of the rotor cup (Fig.3.8); from the periphery of the working compartment (Fig.3.9); and from the back of the stator cup (Fig.3.10).

The first of these is analysed by Tan [7] and illustrates that the fluid pressure in the working compartment causes the self-emptying phenomenon.

3.3.1 Valve Characteristics

Before analysing the water outflow paths, suitable loss characteristics for the water outflow valves are determined in this section. Ideally there would be a linear relationship between the percentage of valve closure and the percentage of maximum torque produced by the dynamometer. The torque against valve closure characteristic for a F020 machine at 900 rpm (curve A), shown in Fig.3.6, is obtained from Froude experimental data [54]. To obtain this torque variation the valve pressure loss characteristic illustrated as curve A in Fig.3.7 is required. When used in tests, such as those in Section 6.3.1, over a range of speeds the distribution of torque curves for different valve closures compares very unfavourably with the experimental data over most of the range of valve closure. Therefore the curve B characteristic of Fig.3.7, which has a more even change in pressure loss over the closure range, is used. This results in the torque curve B in Fig.3.6 at 1500 rpm. In the tests of Section 6.3.1 this

characteristic shows reasonably accurate agreement with the experimental results over the range of speeds and valve closures. For greater accuracy pressure loss tests for valve different valve closures need to be conducted, since the curves obtained in Fig.3.6 can be influenced by many other factors. If, for example, a water outflow path from the back of the stator cup is used, the torque characteristic curve B becomes curve C, which is a significantly above that for a rotor cup outlet. The characteristic of curve B is used throughout this work, with the valve loss given by,

$$P_{L6} = \frac{1}{2} C_{LV} \left(\frac{Q_O}{A_A}\right)^2$$

where

$$C_{LV} = \begin{cases} K_{LV}(0.007144 + 0.5448\,x + 4.916\,x^2 \\ \qquad + 17.65\,x^3 - 23.34\,x^4 + 11.05\,x^5)\,, 0.3 \le x \le 1.0 \\ K_{LV}(0.1180\,x + 0.007144)\,, 0.0 \le x < 0.3 \end{cases}$$

K_{LV} = 630

x = the valve closure percentage.

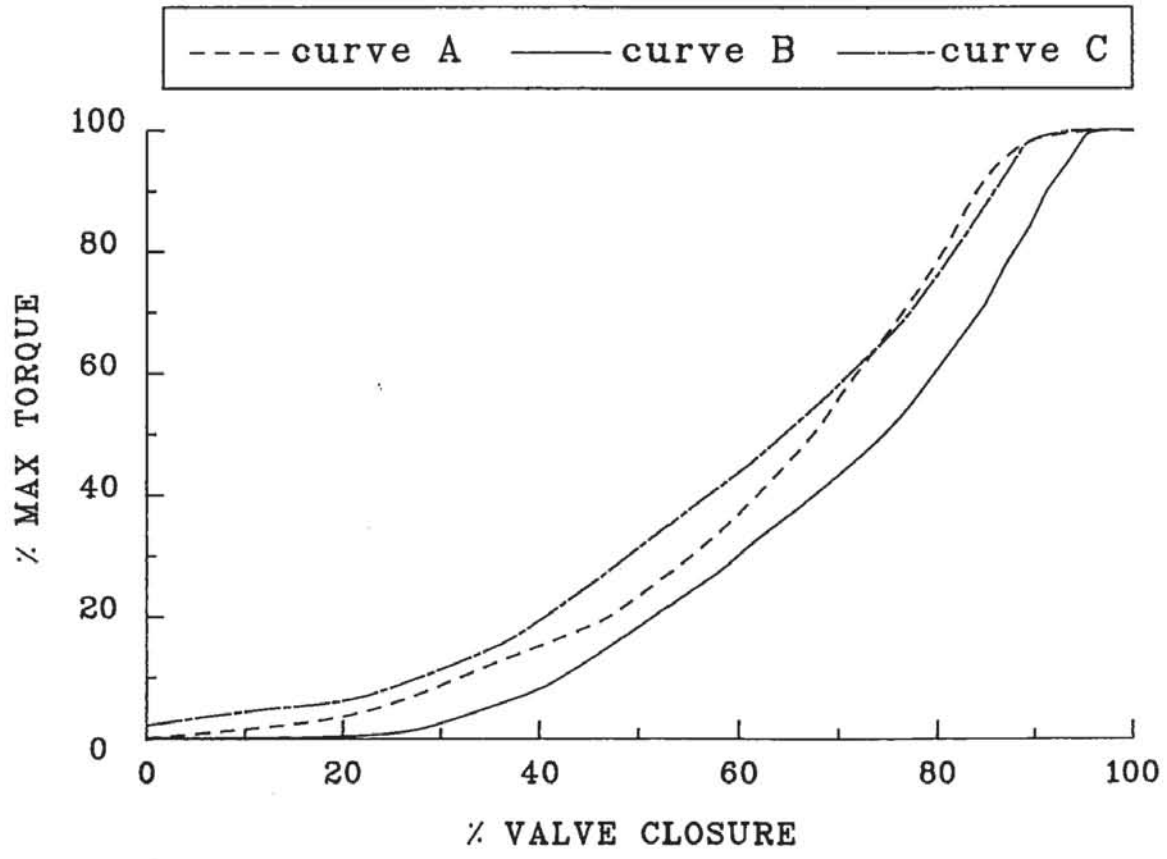

Figure 3.6: Torque against Water Outlet Valve Closure

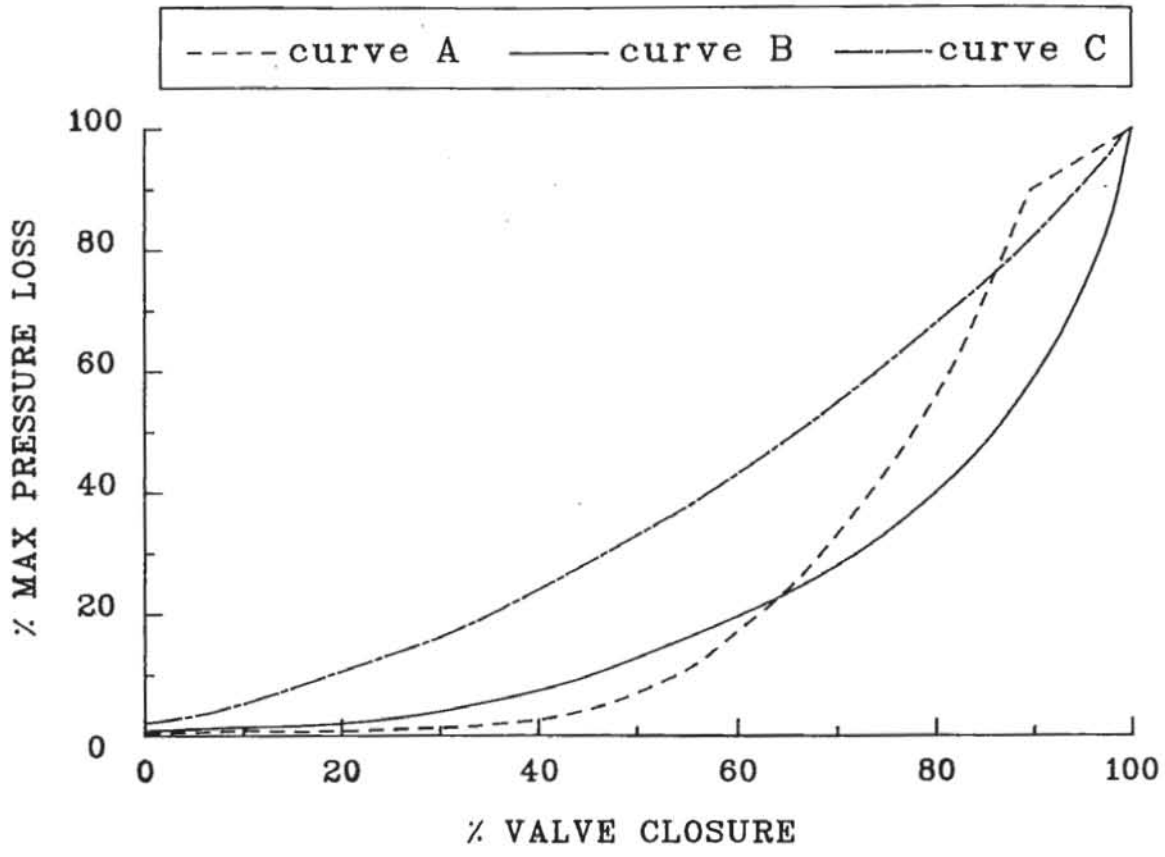

Figure 3.7: Valve Pressure Loss against Water Outlet Valve Closure

To simulate the oil driven back pressure valve machine in Chapter 7 this valve characteristic must be modified to allow for the higher full closure loss of the plug type valves used to control water outflow in these machines. Therefore the valve loss coefficient characteristic becomes,

$$C_{LV} = \begin{cases} K_{LV}(21.89X - 20.03), & 0.95 < x \le 1.0 \\ K_{LV}(0.007144 + 0.5448x + 4.916x^2 \\ \qquad + 17.65x^3 - 23.34x^4 + 11.05x^5), & 0.3 \le x \le 0.95 \\ K_{LV}(0.1180x + 0.007144), & 0.0 \le x < 0.3 \end{cases}$$

$$K_{LV} = 630$$

A loss characteristic is also required for the oil control system in the back pressure valve simulation. By comparing the distribution of torque characteristics obtained, using the above loss characteristics as the control valve characteristic, with the experimental torque characteristics of Fig.7.5 it is found that a more linear pressure loss with valve closure is required. Subsequently, the valve loss

characteristic below is found to provide a distribution of torque characteristics coincident with the experimental curves in Fig.7.5. The pressure loss for the oil control valve is,

$$P_{CV} = \frac{1}{2}\, C_{CV} \left(\frac{Q_{CV}}{A_{CV}}\right)^2$$

where

P_{CV} = valve pressure loss
Q_{CV} = flow rate through control valve
A_{CV} = area of oil line above valve

and

$$C_{CV} = \begin{cases} K_{CV}(7.865\,X - 6.756)\,, & 0.9 < x \le 1.0 \\ K_{CV}(5.193\,x^2 - 7.395\,x + 2.682)\,, & 0.7 < x \le 0.9 \\ K_{CV}(1.433\,x^3 - 1.734\,x^2 + 0.7203\,x - 0.09577)\,, & 0.3 < x \le 0.7 \\ K_{CV}(0.01165\,x^2 + 0.004729\,x + 0.000444)\,, & 0.0 \le x \le 0.3 \end{cases}$$

where

K_{CV} = 3.250×10^7

3.3.2 Rotor Cup Fluid Outlet

The flow from point C, the centre of the rotor cup outlet hole level with the machine surface, to point O, just below the outlet valve, as shown in Fig.3.8 is analysed using Bernoulli's equation (neglecting gravitational effects),

$$\frac{P_C}{\rho} + \tfrac{1}{2}V_C^2 = \frac{P_O}{\rho} + \tfrac{1}{2}V_O^2 + P_{Loss} \qquad (3.24)$$

where,

P_C = fluid pressure at point C, from Section 3.2
V_C = fluid velocity along the flow path being considered
P_O = fluid pressure at point O, taken to be atmospheric
V_O = fluid velocity in drain pipe
P_{Loss} = empirical pressure losses along the flow path

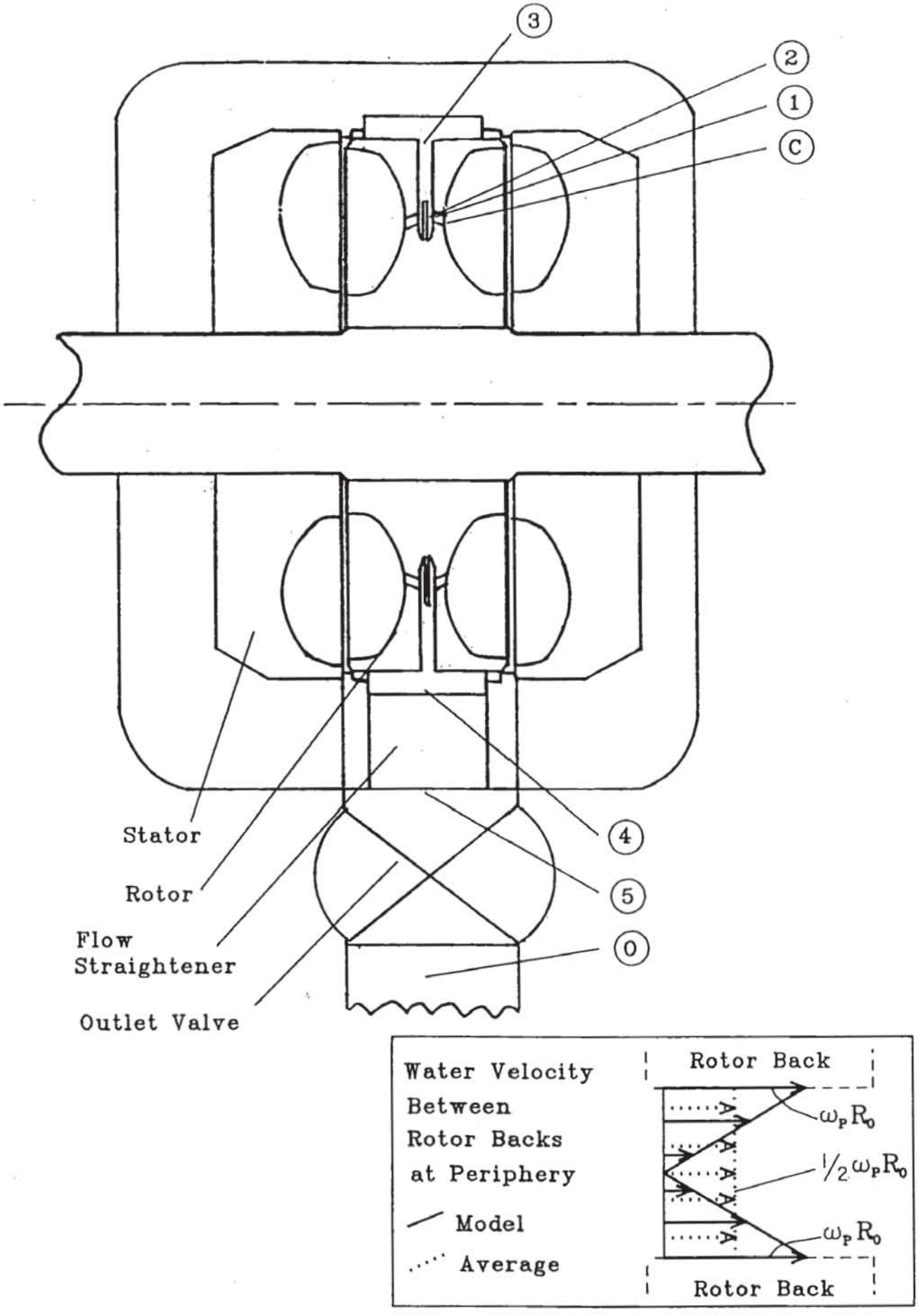

Figure 3.8: Water Outflow Path via Rotor Outlet

Generally the fluid velocities are represented as the outflow rate divided by the flow area, hence

$$V_O = \frac{Q_O}{A_O} \tag{3.25}$$

In the case of point C there is also a rotational component as the flow path is rotating with the rotor, so

$$V_C^2 = \left(\frac{Q_O}{A_C}\right)^2 + (\omega_P R_H)^2 \tag{3.26}$$

where

A_C = the combined area of outlet holes

R_H = radius of the holes from the centre of the shaft.

Tan uses the resultant velocity from combining the rotor motion and the vortex motion. The latter is perpendicular to the flowpath being considered so has no component in the direction of interest.

The empirical pressure losses are evaluated for each feature marked in Fig.3.8.

1/ Entry to drain holes; the standard loss (Massey [51]) is

$$P_{L1} = \tfrac{1}{2} C_{L1} \left(\frac{Q_O}{A_C}\right)^2 \qquad with \quad C_{L1} = 0.5$$

2/ Exit from drain holes; the standard loss (Massey [51]) is

$$P_{L2} = \tfrac{1}{2} C_{L2} \left(\frac{Q_O}{A_C}\right)^2 \qquad with \quad C_{L2} = 1.0$$

3/ Flow from inner to outer radius of drain ring; the fluid entering the drain ring will have a tangential component of velocity, disregarded by Tan, but as it moves outward this component decreases since there are no vanes to maintain the rotational motion. Modelling the tangential velocity as similar to a flow between two moving plates in Fig.3.8 gives an average tangential velocity component, while the radial component is the outflow rate divided by the flow area. Using the Bernoulli equation between inner and outer radius gives

$$\frac{P_{IN}}{\rho} + \tfrac{1}{2} V_{IN}^2 = \frac{P_{OT}}{\rho} + \tfrac{1}{2} V_{OT}^2$$

where

$$V_{IN}^2 = (\omega_P R_H)^2 + \left(\frac{Q_O}{2\pi R_H c}\right)^2$$

$$V_{OT}^2 = \left(\tfrac{1}{2}\omega_P R_O\right)^2 + \left(\frac{Q_O}{2\pi R_O c}\right)^2$$

with c the gap between the rotor backs. Thus,

$$\frac{(P_{IN} - P_{OT})}{\rho} = \tfrac{1}{2}\left(\left(\tfrac{1}{2}\omega_P R_O\right)^2 + \left(\frac{Q_O}{2\pi R_O c}\right)^2\right) - \tfrac{1}{2}\left(\left(\omega_P R_H\right)^2 + \left(\frac{Q_O}{2\pi R_H c}\right)^2\right)$$

which yields

$$P_{L3} = \tfrac{1}{2}\omega_P^2\left(\tfrac{1}{4}R_O^2 - R_H^2\right) + \frac{Q_O}{8\pi^2 c^2}\left(\frac{1}{R_O^2} - \frac{1}{R_H^2}\right)$$

4/ Flow around the drain annulus; this is a ring of increasing width in the direction of rotation around the circumference of the rotors. This flow is a mixture of flow around a bend and that in a diffuser, so it is analysed as a bend loss with allowance for the diffuser effect. The loss coefficient is calculated for a F020 machine (R_O = 102.5 mm, annulus width at outlet = 31 mm, annulus depth = 18 mm).

To calculate an equivalent hydraulic diameter the average width is used,

$$d_e = 4\,\frac{15.5 \times 18}{2 \times (15.5 + 18)} = 16.7 \text{ mm}$$

hence the bend radius of curvature is

$$R_C = 102.5 + 8.35 = 111 \text{ mm}$$

Ward-Smith [55] in his Fig.E24 gives bend loss coefficients for different geometries, and as the downstream distance for flow to re-establish is very short the values for $L_d / d_e + 1 = 1$ are relevant. In this case the aspect ratio is 1.72 and $R_C / h = 6.2$ which gives a loss coefficient of 0.2. The loss due to a diffuser is usually significantly higher than this value, but only a portion of the outflow experiences the diffuser effect, so the coefficient is only increased to 0.3.

$$P_{L4} = \tfrac{1}{2} C_{LD}\left(\frac{Q_O}{A_D}\right)^2 \qquad \text{with} \quad C_{LD} = 0.3$$

5/ The flow straightener; the loss for a flow straightener is given by Ward-Smith [55] as

$$C_{LFS} = [\,(\,\lambda\{0.872 - \frac{t}{d}0.0149 - \frac{d}{t}0.08\}\{1 - \lambda^{3.3}\} + \lambda^{4.3}\{1 + \left(\frac{t}{d}\right)^{\frac{1}{2}}0.134\}^{-1}\,)^{-1} - 1\,]^2$$

For this machine the porosity λ is 0.667 and thickness to hole diameter ratio t/d is 2.0 which gives a flow straightener loss of

$$P_{L5} = \tfrac{1}{2} C_{LFS}\left(\frac{Q_o}{A_A}\right)^2 \qquad with \quad C_{LFS} = 0.72$$

where

A_A = the area just before the straightener.

6/ The outlet valve; as the valve closes the pressure loss across the valve increases, so the loss coefficient is a function of the valve closure. For hydraulic dynamometers the outlet valve is usually a butterfly type valve, though plug type valves are used on machines using rotor shaft driven oil feedback systems. In Section 3.3.1, the valve loss characteristics are determined and so the water outflow valve loss is

$$P_{L6} = \tfrac{1}{2} C_{LV}\left(\frac{Q_o}{A_A}\right)^2$$

where for butterfly type valves,

$$C_{LV} = \begin{cases} K_{LV}(0.007144 + 0.5448x + 4.916x^2 \\ \qquad + 17.65x^3 - 23.34x^4 + 11.05x^5)\,, 0.3 \le x \le 1.0 \\ K_{LV}(0.1180x + 0.007144)\,, 0.0 \le x < 0.3 \end{cases}$$

with

K_{LV} = loss constant

x = percentage valve closure

and for plug type valves,

$$C_{LV} = \begin{cases} K_{LV}(21.89X - 20.03)\,, 0.95 < x \le 1.0 \\ K_{LV}(0.007144 + 0.5448x + 4.916x^2 \\ \qquad + 17.65x^3 - 23.34x^4 + 11.05x^5)\,, 0.3 \le x \le 0.95 \\ K_{LV}(0.1180x + 0.007144)\,, 0.0 \le x < 0.3 \end{cases}$$

Therefore, the empirical pressure losses are summed and substituted in Eqn.(3.24) with the velocities from Eqns.(3.25) and (3.26) to give

$$\frac{P_C}{\rho} + \tfrac{1}{2}\left(\left(\frac{Q_O}{A_C}\right)^2 + (\omega_P R_H)^2\right)$$
$$= \tfrac{1}{2}\left(\frac{Q_O}{A_O}\right)^2 + \left\{\tfrac{1}{2} C_{L1}\left(\frac{Q_O}{A_C}\right)^2 + \tfrac{1}{2} C_{L2}\left(\frac{Q_O}{A_C}\right)^2 + \tfrac{1}{2}\omega_P^2\left(\tfrac{1}{4} R_O^2 - R_H^2\right) + \frac{Q_O}{8\pi^2 c^2}\left(\frac{1}{R_O^2} - \frac{1}{R_H^2}\right) + \tfrac{1}{2} C_{LD}\left(\frac{Q_O}{A_D}\right)^2 + \tfrac{1}{2} C_{LFS}\left(\frac{Q_O}{A_A}\right)^2 + \tfrac{1}{2} C_{LV}\left(\frac{Q_O}{A_A}\right)^2\right\}$$

which rearranges to allow evaluation of the outflow rate Q_O,

$$\frac{P_C}{\rho} = \tfrac{1}{2} Q_O^2\left\{\frac{(C_{L1} + C_{L2} - 1)}{A_C^2} + \frac{C_{LD}}{A_D^2} + \frac{1}{4\pi^2 c^2}\left(\frac{1}{R_O^2} - \frac{1}{R_H^2}\right) + \frac{(C_{LFS} + C_{LV})}{A_A^2} + \frac{1}{A_O^2}\right\} + \tfrac{1}{2}\omega_P^2\left(\tfrac{1}{4} R_O^2 - 2 R_H^2\right) \quad (3.27)$$

3.3.3 Cup Periphery Fluid Outlet

In this arrangement the fluid leaves the working compartment between the rotor and stator with a tangential flow velocity component shown in Fig.3.9 as for a flow between a moving plate and a stationary plate. Hence, the flow velocity at point B is

$$V_B^2 = \left(\frac{Q_O}{A_B}\right)^2 + \left(\tfrac{1}{2}\omega_P R_O\right)^2 \quad (3.28)$$

where

A_B = the total gap area available for fluid outflow, generally designed to equal the combined area of outlet holes in the other outflow paths.

By inspection of Fig.3.9 there are several differences in the losses encountered from those in Fig.3.8.

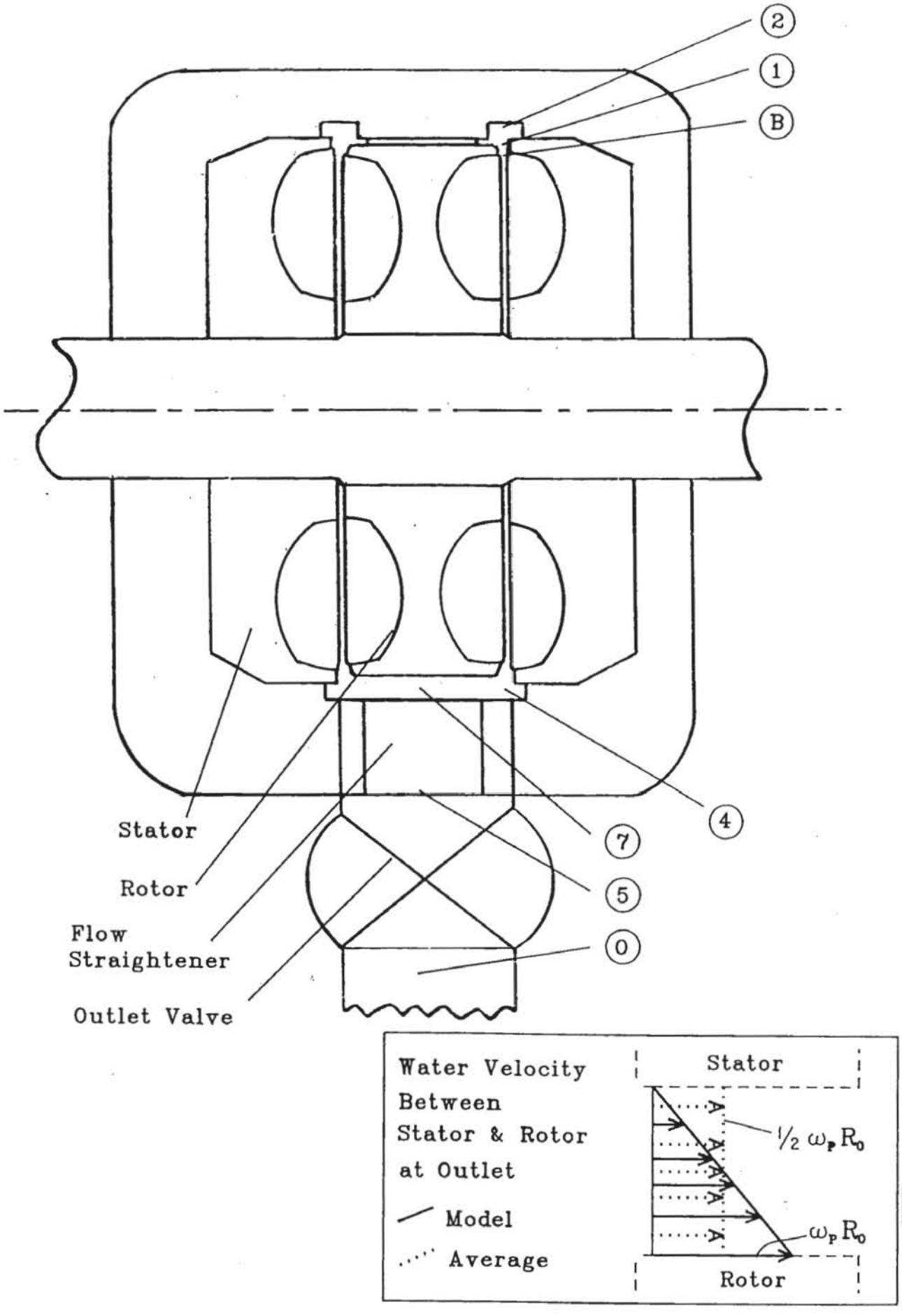

Figure 3.9: Water Outflow Path via Cup Periphery Outlet

1/ Entry to drain gap; as in Section 3.3.2,

$$P_{L1} = \tfrac{1}{2} C_{L1} \left(\frac{Q_O}{A_B} \right)^2 \qquad with \quad C_{L1} = 0.5$$

2/ Exit from drain gap; as in Section 3.3.2,

$$P_{L2} = \tfrac{1}{2} C_{L2} \left(\frac{Q_O}{A_B} \right)^2 \qquad with \quad C_{L2} = 1.0$$

4/ Flow around the drain annulus; similar to Section 3.3.2, except flow is split between the two annuli which are smaller. The loss is taken as that above,

$$P_{L4} = \tfrac{1}{2} C_{LD} \left(\frac{Q_O}{A_D} \right)^2 \qquad with \quad C_{LD} = 0.3$$

7/ Bend of two annuli into one outlet; using a standard bend loss,

$$P_{L7} = \tfrac{1}{2} C_{L7} \left(\frac{Q_O}{A_A} \right)^2 \qquad with \quad C_{L7} = 0.8$$

5/ The flow straightener; as in Section 3.3.2,

$$P_{L5} = \tfrac{1}{2} C_{LFS} \left(\frac{Q_O}{A_A} \right)^2 \qquad with \quad C_{LFS} = 0.72$$

6/ The outlet valve; as in Section 3.3.2,

$$P_{L6} = \tfrac{1}{2} C_{LV} \left(\frac{Q_O}{A_A} \right)^2 \qquad with \quad C_{LV} = fn(closure)$$

Thus, applying Eqn.(3.24) to the new flow path and again substituting for the flow velocities and pressure losses gives

$$\frac{P_B}{\rho} + \tfrac{1}{2} \left(\left(\frac{Q_O}{A_B} \right)^2 + \left(\tfrac{1}{2} \omega_P R_O \right)^2 \right)$$

$$= \tfrac{1}{2} \left(\frac{Q_O}{A_O} \right)^2 + \left\{ \tfrac{1}{2} C_{L1} \left(\frac{Q_O}{A_B} \right)^2 + \tfrac{1}{2} C_{L2} \left(\frac{Q_O}{A_B} \right)^2 + \tfrac{1}{2} C_{LD} \left(\frac{Q_O}{A_D} \right)^2 \right.$$

$$\left. + \tfrac{1}{2} C_{L7} \left(\frac{Q_O}{A_A} \right)^2 + \tfrac{1}{2} C_{LFS} \left(\frac{Q_O}{A_A} \right)^2 + \tfrac{1}{2} C_{LV} \left(\frac{Q_O}{A_A} \right)^2 \right\}$$

which yields

$$\frac{P_B}{\rho} = \tfrac{1}{2} Q_O^2 \left\{ \frac{(C_{L1} + C_{L2} - 1)}{A_B^2} + \frac{C_{LD}}{A_D^2} + \frac{(C_{L7} + C_{LFS} + C_{LV})}{A_A^2} + \frac{1}{A_O^2} \right\} - \tfrac{1}{8} \omega_P^2 R_O^2 \tag{3.29}$$

3.3.4 Stator Cup Fluid Outlet

Most late model dynamometers use a fluid outlet from the back of the stator cup (Fig.3.10) which gives a more stable behaviour. The water outlet flow at point A is

$$V_A^2 = \left(\frac{Q_O}{A_C} \right)^2 \tag{3.30}$$

So the initial flow velocity is less than for the previous cases, and the stator fluid pressures are less than for the same position on the rotor (Section 3.2) indicating that a lower outflow rate should occur. This is examined in Sections 5.4.1 and 5.5.1 .

Again the empirical losses are slightly changed.

1/ Entry to drain holes; as in Section 3.3.2,

$$P_{L1} = \tfrac{1}{2} C_{L1} \left(\frac{Q_O}{A_C} \right)^2 \qquad with \quad C_{L1} = 0.5$$

8/ Bend in drain holes; a bend loss with some turbulence,

$$P_{L8} = \tfrac{1}{2} C_{L8} \left(\frac{Q_O}{A_C} \right)^2 \qquad with \quad C_{L8} = 0.8$$

2/ Exit from drain holes; as in Section 3.3.2,

$$P_{L2} = \tfrac{1}{2} C_{L2} \left(\frac{Q_O}{A_C} \right)^2 \qquad with \quad C_{L2} = 0.8$$

as the exit is approximately a bellmouth opening.

9/ Entry into drain passage; a standard entry loss,

$$P_{L9} = \tfrac{1}{2} C_{L9} \left(\frac{Q_O}{A_A} \right)^2 \qquad with \quad C_{L9} = 0.5$$

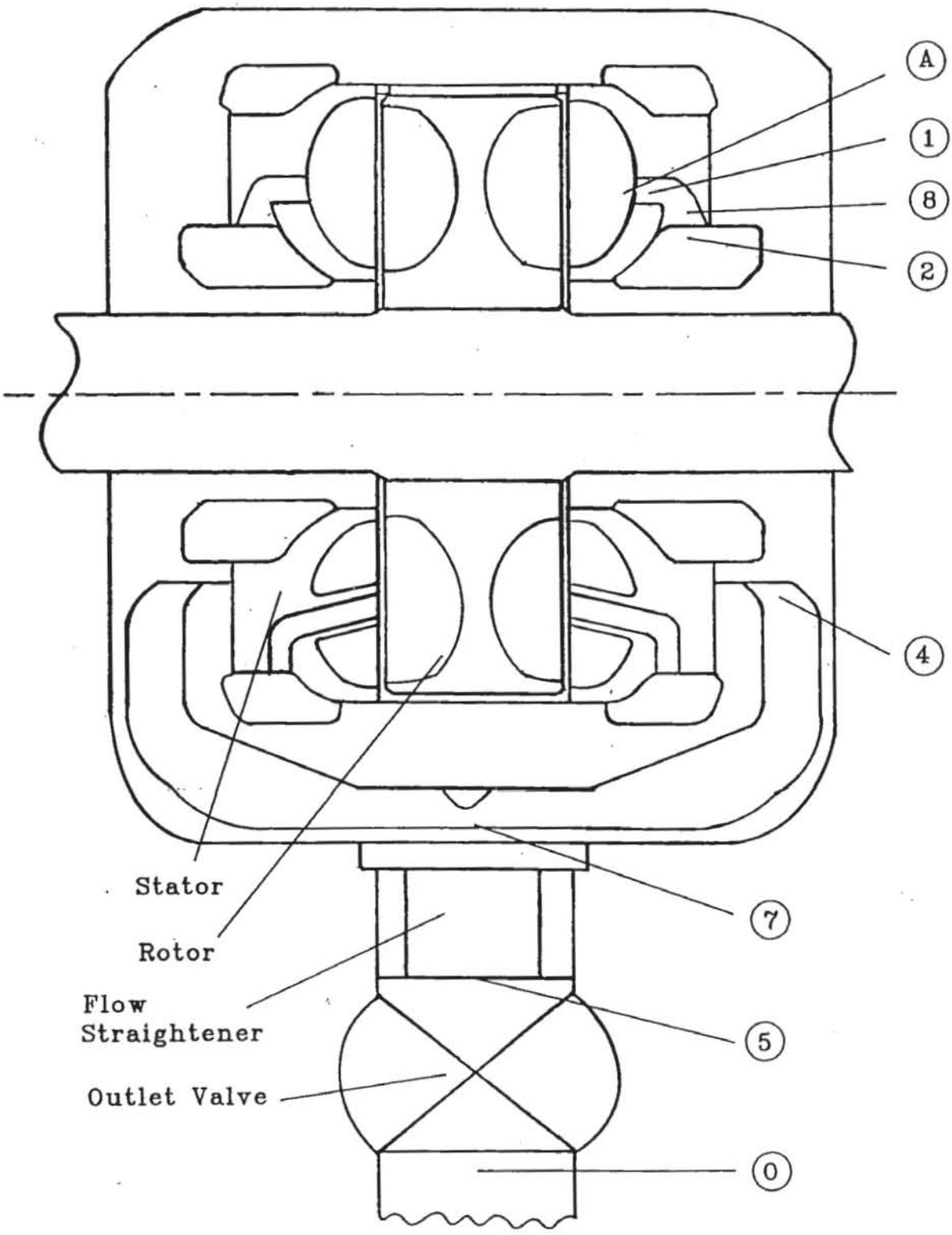

Figure 3.10: Water Outflow Path via Stator Outlet

7/ Bend into one outlet passage; as Section 3.3.3,

$$P_{L7} = \tfrac{1}{2} C_{L7} \left(\frac{Q_O}{A_A} \right)^2 \qquad with \quad C_{L7} = 0.8$$

5/ The flow straightener; as in Section 3.3.2,

$$P_{L5} = \tfrac{1}{2} C_{LFS} \left(\frac{Q_O}{A_A} \right)^2 \qquad with \quad C_{LFS} = 0.72$$

6/ The outlet valve; as in Section 3.3.2,

$$P_{L6} = \tfrac{1}{2} C_{LV} \left(\frac{Q_O}{A_A} \right)^2 \qquad with \quad C_{LV} = fn(closure)$$

Applying the Bernoulli equation, Eqn.(3.24), to this flow path and substituting for velocities and losses gives

$$\frac{P_A}{\rho} = \tfrac{1}{2} Q_O^2 \left\{ \frac{(C_{L1} + C_{L2} + C_{L8} - 1)}{A_C^2} + \frac{(C_{L9} + C_{L7} + C_{LFS} + C_{LV})}{A_A^2} + \frac{1}{A_O^2} \right\} \qquad (3.31)$$

CHAPTER 4
CROPPED ROTOR DYNAMOMETER

4.1 Introduction

In order that Froude hydraulic dynamometers can operate at higher speeds the rotor is cropped (Fig.4.1) to reduce rotational stresses, with the outer portion of rotor being replaced by a stationary return ring. Hence the characteristic torque operational envelope for the cropped rotor dynamometer is modified and a comparison with that for a full rotor machine is given in Fig.4.2; the torque increase with speed is at a much lower rate. This decrease in torque development is a result of the reduced angular momentum change in the water flowing across the new rotor.

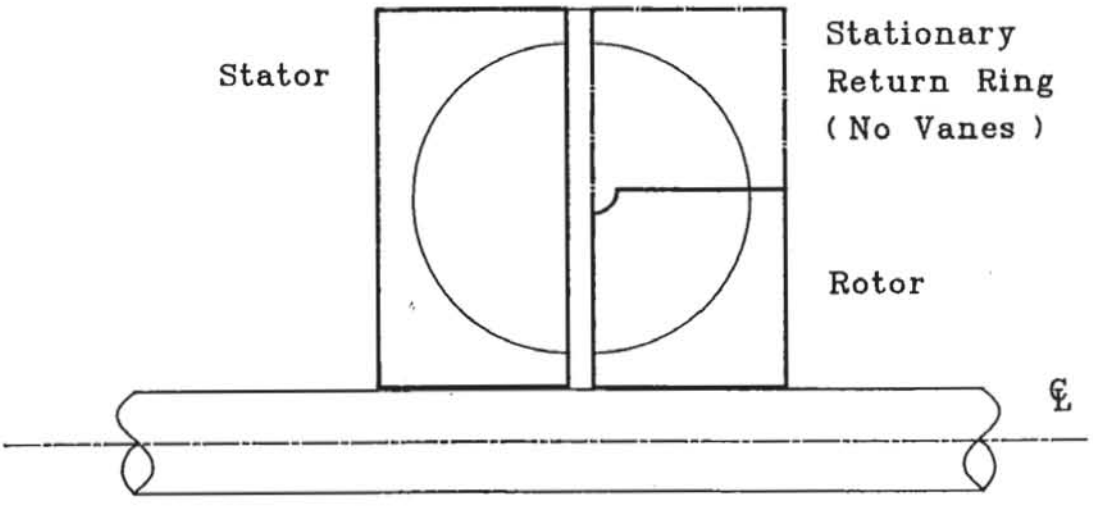

Figure 4.1: Cross Section of Cropped Rotor Dynamometer

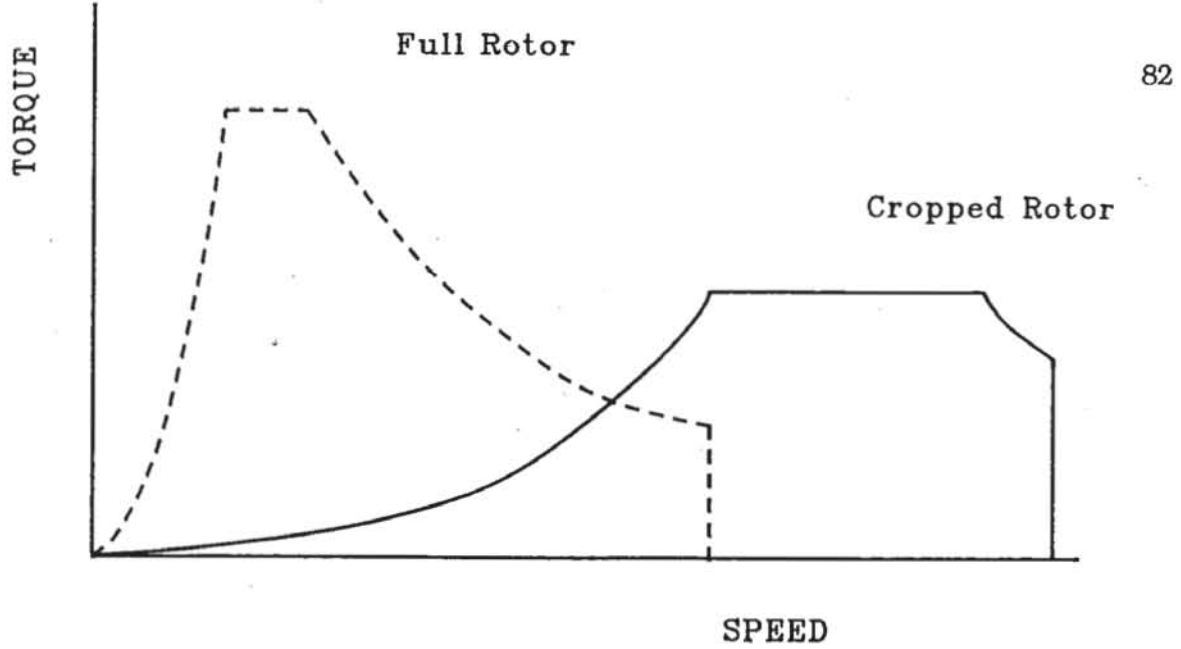

Figure 4.2: Comparison of Torque Characteristics for Full and Cropped Rotor Dynamometers

The rotor is designed so that the radius of the rotor tip is approximately at the theoretical water vortex centre radius[1], obtained by means of the root mean square of the inner and outer cup radii for a full rotor machine (refer Eqn.(2.2), Section 2.1). In the section of the working compartment which now becomes the return ring the vanes are removed to reduce losses. The reduction of losses leads to higher water vortex velocities, and so to a more efficient power absorption process. These geometric changes result in a new rotor exit velocity and some modification of the dynamometer theory derived in Chapters 2 and 3.

The velocity diagrams for the cropped rotor dynamometer when the linear velocity distribution model is applied are shown in Fig.4.3. As in Section 2.1 for the full rotor diagrams the directions of the water velocities at each point may require some clarification. Between the stator outlet and rotor inlet (points 1, 2, 3) the directions of the relative and absolute water velocities are the same as in the full rotor case. However at the rotor outlet (point 4) the relative water velocity is following the shape of the vane surface and is perpendicular to the rotor tip velocity, so the absolute velocity is the resultant of the two . Therefore the water passes into the return ring (point 5) at an angle not determined by the vane angle but by the ratio of the relative velocity to the rotor tip velocity[2]. As there are no vanes in the return ring the absolute velocity of the water is not altered at point 6, the return ring entry. The water maintains this direction but the curvature of the

---

1 The inside edge of cropped rotors near the water vortex centre is usually cut away (Fig.4.1) to avoid cavitation problems.

2 As in Section 3.2 for the fluid pressure calculation, the slight difference in working compartment and vortex model centre radii is disregarded (refer Chapter 3 Footnote 1).

working compartment brings this angle into the edge view of the velocities at the return ring outlet (points 7, 8), so the relative and absolute velocities are at the angle defined at rotor outlet as they approach the stator. In reality the angle is altered by the drag force from surface friction acting on the water. For modelling purposes this small change in direction is disregarded. As for the full rotor machine the relative and absolute velocities are in the direction of the stator inlet angle upon entering the stator (point 9). These new velocity diagrams modify the theoretical equations representing the dynamometer behaviour.

In the remaining sections of this chapter the alterations to the theory of Chapters 2 and 3 are presented. However, the application of Energy Conservation (Section 2.2) is unchanged, yielding a quadratic in ω, the fluid vortex angular velocity, Eqn.(2.8). The fluid vortex centre is determined by considering the inflow to and outflow from the stator for the Conservation of Mass (Section 2.3), so the radius is still obtained from Eqn.(2.12).

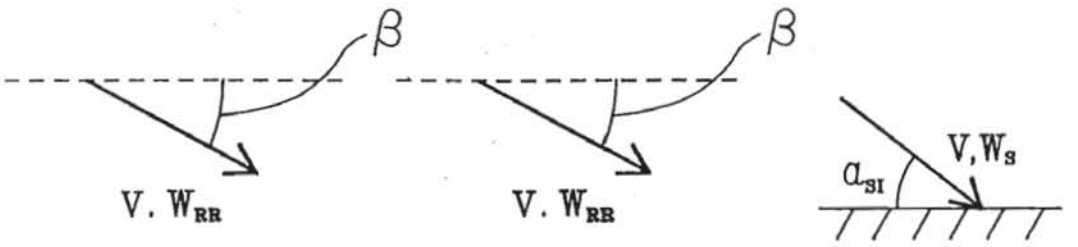

7. Return Ring Outlet

8. Gap

9. Stator Inlet

Plane View

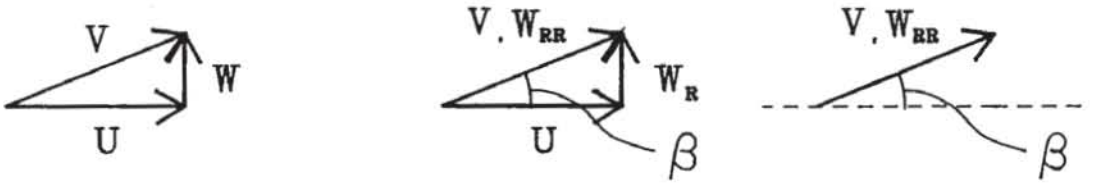

Edge View

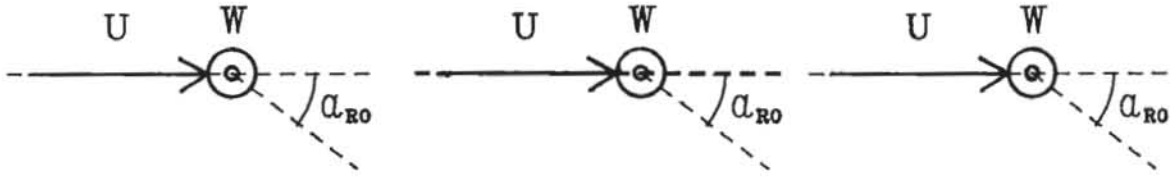

4. Rotor Outlet

5. Gap

6. Return Ring Inlet

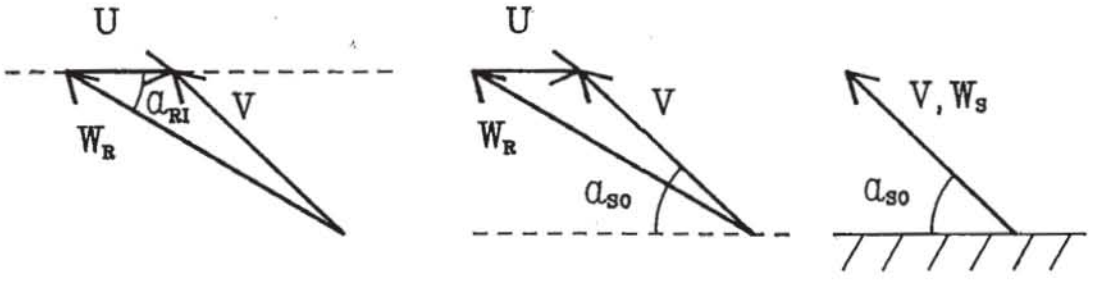

3. Rotor Inlet

2. Gap

1. Stator Outlet

Figure 4.3: Cropped Rotor Dynamometer Velocity Diagrams

4.2 Conservation of Angular Momentum

As in Section 2.4, the shaft input torque must equal the rate of change of angular momentum of the fluid across the rotor, so the rotor is the control volume (Fig.4.4). Thus the Conservation of Angular Momentum yields

$$\boldsymbol{T}_{Shaft} = \frac{\partial}{\partial t}\int\int\int_{CV} \boldsymbol{r} \times \boldsymbol{V}\ \rho dV + \int\int_{CS} \boldsymbol{r} \times \boldsymbol{V}\ \rho \boldsymbol{V}_{xyz} . d\boldsymbol{A} \qquad (2.14)$$

4.2.1 Steady Flow Component

The surface integral of Eqn.(2.14) is the steady flow torque component, and is reduced to a single integral by replacing the elemental mass flow with the streamtube equivalents (refer Section 2.4.1) to obtain

$$\int\int_{CS} \boldsymbol{r} \times \boldsymbol{V}\ \rho \boldsymbol{V}_{xyz} . d\boldsymbol{A} = \int_{OUTLET} r V_{\theta O}\, d\dot{m}_O - \int_{INLET} r V_{\theta I}\, d\dot{m}_I \qquad (4.1)$$

Comparing the cropped and full rotors shows that the inlets are the same. Consequently, the inlet integral is

$$\int_{R_I}^{R_{CI}} r V_{\theta I}\, d\dot{m}_I$$

$$= -\rho\,\omega^2 \sin\alpha_{RI} \cos\alpha_{SO}\Big[\, 2\pi\left(\tfrac{1}{5}r^5 - \tfrac{1}{2}r^4 R_M + \tfrac{1}{3}r^3 R_M^2\right) - \frac{Z_R t}{\sin\alpha_{RI}}\left(\tfrac{1}{4}r^4 - \tfrac{2}{3}r^3 R_M + \tfrac{1}{2}r^2 R_M^2\right)\Big]_{R_I}^{R_{CI}} \qquad (2.16)$$

At the outlet the control surface is now at a constant radius, and the integration is in the axial direction, as defined in Fig.4.4. The velocity model for the fluid vortex becomes $W = \omega z$, where z is the distance from the vortex centre taking into account the effect of vane angle, as illustrated for the limits of integration.

So the elemental mass flow is

$$d\dot{m}_O = \rho\,\omega\, z\left(2\pi R_M - \frac{Z_R t}{\sin\alpha_{RO}}\right)dz$$

and the tangential absolute fluid velocity component is

$$V_{\theta O} = \omega_P R_M$$

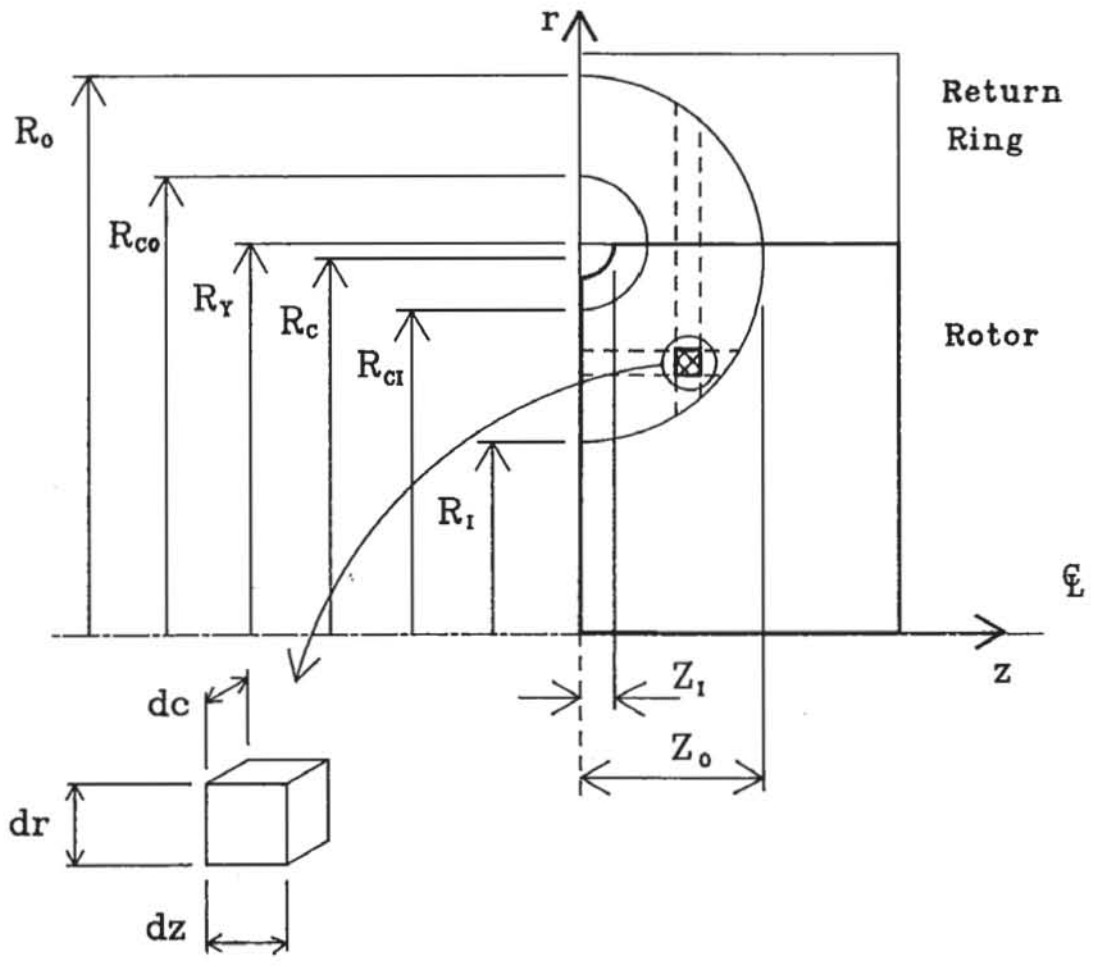

Figure 4.4: Cropped Rotor Control Volume

Hence, the fluid angular momentum flowing out of the cropped rotor control volume is

$$\int_{OUTLET} rV_{\theta O}\, dm_O = \int_{Z_I}^{Z_O} R_M\, \omega_P\, R_M\, \rho\, \omega\, z\left(2\pi R_M - \frac{Z_R t}{\sin\alpha_{RO}}\right)dz$$

where

Z_O = distance to cup surface

Z_I = distance to air-water interface
or rotor cut away

This yields

$$\int_{OUTLET} rV_{\theta O}\, dm_O$$

$$= \rho\left(2\pi R_M - \frac{Z_R t}{\sin\alpha_{RO}}\right)\omega\,\omega_P R_M^2\left[\tfrac{1}{2}z^2\right]_{Z_I}^{Z_O}$$

$$= \tfrac{1}{8}\rho\,\omega\omega_P\left(2\pi R_M - \frac{Z_R t}{\sin\alpha_{RO}}\right)R_M^2\sin^2\alpha_{RO}\left[\left(R_O - R_I\right)^2 - \left(R_{CO} - R_{CI}\right)^2\right] \quad (4.2)$$

Substituting Eqns.(2.16) and (4.2) into Eqn.(4.1) gives

$$\tau_{SSCR} = K_{1CR}\,\omega\,\omega_P + K_{2\,CR}\,\omega^2 \quad (4.3)$$

where

$$K_{1CR} = \tfrac{1}{8}\rho\sin^2\alpha_{RO}R_M^2\left(2\pi R_M - \frac{Z_R t}{\sin\alpha_{RO}}\right)\left[\left(R_O - R_I\right)^2 - \left(R_{CO} - R_{CI}\right)^2\right]$$

$$K_{2CR} = \rho\sin\alpha_{RI}\cos\alpha_{SO}\Big[2\pi\left(\tfrac{1}{5}r^5 - \tfrac{1}{2}r^4 R_M + \tfrac{1}{3}r^3 R_M^2\right) - \frac{Z_R t}{\sin\alpha_{RI}}\left(\tfrac{1}{4}r^4 - \tfrac{2}{3}r^3 R_M + \tfrac{1}{2}r^2 R_M^2\right)\Big]_{R_I}^{R_{CI}}$$

4.2.2 Unsteady Flow Component

To evaluate the unsteady component of Eqn.(2.14) the procedure of Section 2.4.2 is followed, though the geometric functions $f(x)$ and $fy(x)$, used as limits of integration, are constant in the case of a cropped rotor. Therefore, Eqn.(2.26) is taken as the start of the derivation of the unsteady torque,

$$\frac{\partial}{\partial t}\iiint_{CV} \mathbf{r}\times\mathbf{V}\,\rho\,dV$$

$$= \int_0^b\int_g^f r\dot{V}_\theta(r)\,C(r)\,dr\,dx - \int_0^{b_Y}\int_{gy}^{fy} r\dot{V}_\theta(r)\,C(r)\,dr\,dx$$

$$-\int_0^{b_Y}\{[fy V_\theta(fy)\,C(fy)]\dot{fy}-[gy V_\theta(gy)\,C(gy)]\,\dot{gy}\}dx \qquad (2.26)$$

From Section 2.4.2,

$$g = g(x) = R_C - \left(a^2 - \frac{x^2}{\sin^2\alpha}\right)^{\frac{1}{2}} \qquad gy = gy(x) = R_Y - \left(a_Y^2 - \frac{x^2}{\sin^2\alpha}\right)^{\frac{1}{2}}$$

$$b = a\sin\alpha \qquad b_Y = a_Y \sin\alpha$$

$$R_C = \tfrac{1}{2}(R_O + R_I) \qquad R_Y = \tfrac{1}{2}(R_{CO} + R_{CI})$$

$$C(r) = \rho\left(2\pi r - \frac{Zt}{\sin\alpha}\right)$$

$$V_\theta(r) = \omega(r - R_M)\cos\alpha + \omega_p r$$

$$\dot{V}_\theta(r) = \dot{\omega}(r - R_M)\cos\alpha + \dot{\omega}_p r$$

and from Fig.4.4,

$$f = f(x) = R_M \qquad fy = fy(x) = R_M$$

The first term of Eqn.(2.26) is integrated as before,

$$\int_0^b\int_g^f r\dot{V}_\theta(r)\,C(r)\,dr\,dx$$

$$= \rho\int_0^b\Big[\dot{\omega}\cos\alpha\left(2\pi\left(\tfrac{1}{4}r^4 - \tfrac{1}{3}r^3 R_M\right) - \frac{Zt}{\sin\alpha}\left(\tfrac{1}{3}r^3 - \tfrac{1}{2}r^2 R_M\right)\right)$$

$$+ \dot{\omega}_p\left(2\pi\tfrac{1}{4}r^4 - \frac{Zt}{\sin\alpha}\tfrac{1}{3}r^3\right)\Big]_g^f dx \qquad (2.27)$$

In Appendix E,

$$(f^2 - g^2) = R_M^2 - R_C^2 + 2R_C\left(a^2 - \frac{x^2}{\sin^2\alpha}\right)^{\frac{1}{2}} - \left(a^2 - \frac{x^2}{\sin^2\alpha}\right)$$

$$(f^3 - g^3) = R_M^3 - R_C^3 + 3R_C^2\left(a^2 - \frac{x^2}{\sin^2\alpha}\right)^{\frac{1}{2}}$$

$$- 3R_C\left(a^2 - \frac{x^2}{\sin^2\alpha}\right) + \left(a^2 - \frac{x^2}{\sin^2\alpha}\right)^{\frac{3}{2}}$$

$$(f^4 - g^4) = R_M^4 - R_C^4 + 4R_C^3\left(a^2 - \frac{x^2}{\sin^2\alpha}\right)^{\frac{1}{2}} - 6R_C^2\left(a^2 - \frac{x^2}{\sin^2\alpha}\right)$$

$$+ 4R_C\left(a^2 - \frac{x^2}{\sin^2\alpha}\right)^{\frac{3}{2}} - \left(a^2 - \frac{x^2}{\sin^2\alpha}\right)^2$$

are derived and substituted into Eqn.(2.27) to yield

$$\int_0^b\int_g^f r\dot{V}_\theta(r)\,C(r)\,dr\,dx$$

$$= \rho\int_0^b [\dot{\omega}\cos\alpha\{\tfrac{1}{2}\pi\left(R_M^4 - R_C^4\right) - \tfrac{1}{3}\left(2\pi R_M + \frac{Zt}{\sin\alpha}\right)\left(R_M^3 - R_C^3\right)$$

$$+ \tfrac{1}{2}\frac{Zt}{\sin\alpha}R_M\left(R_M^2 - R_C^2\right) + \left(R_C^2 - R_C R_M\right)\left(2\pi R_C - \frac{Zt}{\sin\alpha}\right)\left(a^2 - \frac{x^2}{\sin^2\alpha}\right)^{\frac{1}{2}}$$

$$+ \left(R_C\left(2\pi R_M + \frac{Zt}{\sin\alpha}\right) - 3\pi R_C^2 - \tfrac{1}{2}\frac{Zt}{\sin\alpha}R_M\right)\left(a^2 - \frac{x^2}{\sin^2\alpha}\right)$$

$$+ \left(2\pi R_C - \tfrac{2}{3}\pi R_M - \tfrac{1}{3}\frac{Zt}{\sin\alpha}\right)\left(a^2 - \frac{x^2}{\sin^2\alpha}\right)^{\frac{3}{2}} - \tfrac{1}{2}\pi\left(a^2 - \frac{x^2}{\sin^2\alpha}\right)^2\}$$

$$+ \dot{\omega}_p\{\tfrac{1}{2}\pi\left(R_M^4 - R_C^4\right) - \tfrac{1}{3}\frac{Zt}{\sin\alpha}\left(R_M^3 - R_C^3\right)$$

$$+ \left(2\pi R_C^3 - \frac{Zt}{\sin\alpha}R_C^2\right)\left(a^2 - \frac{x^2}{\sin^2\alpha}\right)^{\frac{1}{2}} + \left(\frac{Zt}{\sin\alpha}R_C - 3\pi R_C^2\right)\left(a^2 - \frac{x^2}{\sin^2\alpha}\right)$$

$$+ \left(2\pi R_C - \tfrac{1}{3}\frac{Zt}{\sin\alpha}\right)\left(a^2 - \frac{x^2}{\sin^2\alpha}\right)^{\frac{3}{2}} - \tfrac{1}{2}\pi\left(a^2 - \frac{x^2}{\sin^2\alpha}\right)^2\}]dx \qquad (4.4)$$

From Appendix B, the definite integrals of the factors in x are

$$\int_0^b 1\,dx = b$$

$$\int_0^b\left(a^2 - \frac{x^2}{\sin^2\alpha}\right)^{\frac{1}{2}}dx = \tfrac{1}{4}\pi\,ba$$

$$\int_0^b\left(a^2 - \frac{x^2}{\sin^2\alpha}\right)dx = \tfrac{2}{3}\pi\,ba^2$$

$$\int_0^b\left(a^2 - \frac{x^2}{\sin^2\alpha}\right)^{\frac{3}{2}}dx = \tfrac{3}{16}\pi\,ba^3$$

$$\int_0^b\left(a^2 - \frac{x^2}{\sin^2\alpha}\right)^2 dx = \tfrac{8}{15}\pi\,ba^4$$

Substituting into Eqn.(4.4) yields

$$\int_0^b\int_g^f r\dot{V}_\theta(r)\,C(r)\,dr\,dx$$

$$= \rho[\dot{\omega}\cos\alpha\{\tfrac{1}{2}\pi\,b\left(R_M^4 - R_C^4\right) - \tfrac{1}{3}b\left(2\pi R_M + \frac{Zt}{\sin\alpha}\right)\left(R_M^3 - R_C^3\right)$$

$$+ \tfrac{1}{2}\frac{Zt}{\sin\alpha}bR_M\left(R_M^2 - R_C^2\right) + \tfrac{1}{4}\pi ab\left(R_C^2 - R_C R_M\right)\left(2\pi R_C - \frac{Zt}{\sin\alpha}\right)$$

$$+\tfrac{2}{3}a^2 b\Big(R_C\Big(2\pi R_M+\frac{Zt}{\sin\alpha}\Big)-3\pi R_C^2-\tfrac{1}{2}\frac{Zt}{\sin\alpha}R_M\Big)$$
$$+\tfrac{3}{16}\pi a^3 b\Big(2\pi R_C-\tfrac{2}{3}\pi R_M-\tfrac{1}{3}\frac{Zt}{\sin\alpha}\Big)-\tfrac{4}{15}\pi a^4 b\}$$
$$+\dot{\omega}_p\{\tfrac{1}{2}\pi b\Big(R_M^4-R_C^4\Big)-\tfrac{1}{3}\frac{Zt}{\sin\alpha}b\Big(R_M^3-R_C^3\Big)$$
$$+\tfrac{1}{4}\pi ab\Big(2\pi R_C^3-\frac{Zt}{\sin\alpha}R_C^2\Big)+\tfrac{2}{3}a^2 b\Big(\frac{Zt}{\sin\alpha}R_C-3\pi R_C^2\Big) \qquad (4.5)$$
$$+\tfrac{3}{16}\pi a^3 b\Big(2\pi R_C-\tfrac{1}{3}\frac{Zt}{\sin\alpha}\Big)-\tfrac{4}{15}\pi a^4 b\}]$$

By similarity the second term of Eqn.(2.26) is

$$\int_0^{b_Y}\int_{gy}^{fy} r\dot{V}_\theta(r)\,C(r)\,dr\,dx$$
$$=\rho[\dot{\omega}\cos\alpha\{\tfrac{1}{2}\pi b_Y\Big(R_M^4-R_Y^4\Big)-\tfrac{1}{3}b_Y\Big(2\pi R_M+\frac{Zt}{\sin\alpha}\Big)\Big(R_M^3-R_Y^3\Big)$$
$$+\tfrac{1}{2}\frac{Zt}{\sin\alpha}b_Y R_M\Big(R_M^2-R_Y^2\Big)+\tfrac{1}{4}\pi q_Y b_Y\Big(R_Y^2-R_Y R_M\Big)\Big(2\pi R_Y-\frac{Zt}{\sin\alpha}\Big)$$
$$+\tfrac{2}{3}q_Y^2 b_Y\Big(R_Y\Big(2\pi R_M+\frac{Zt}{\sin\alpha}\Big)-3\pi R_Y^2-\tfrac{1}{2}\frac{Zt}{\sin\alpha}R_M\Big)$$
$$+\tfrac{3}{16}\pi q_Y^3 b_Y\Big(2\pi R_Y-\tfrac{2}{3}\pi R_M-\tfrac{1}{3}\frac{Zt}{\sin\alpha}\Big)-\tfrac{4}{15}\pi q_Y^4 b_Y\}$$
$$+\dot{\omega}_p\{\tfrac{1}{2}\pi b_Y\Big(R_M^4-R_Y^4\Big)-\tfrac{1}{3}\frac{Zt}{\sin\alpha}b_Y\Big(R_M^3-R_Y^3\Big)$$
$$+\tfrac{1}{4}\pi q_Y b_Y\Big(2\pi R_Y^3-\frac{Zt}{\sin\alpha}R_Y^2\Big)+\tfrac{2}{3}q_Y^2 b_Y\Big(\frac{Zt}{\sin\alpha}R_Y-3\pi R_Y^2\Big) \qquad (4.6)$$
$$+\tfrac{3}{16}\pi q_Y^3 b_Y\Big(2\pi R_Y-\tfrac{1}{3}\frac{Zt}{\sin\alpha}\Big)-\tfrac{4}{15}\pi q_Y^4 b_Y\}]$$

The third term of Eqn.(2.26) is simplified in the cropped rotor case as the function $fy\,(x)$ is constant with respect to time, so its derivative is zero. Hence, Eqn.(2.30) becomes

$$\int_0^{b_Y}\{[fyV_\theta(fy)\,C(fy)]\dot{fy}-[gyV_\theta(gy)\,C(gy)]\,\dot{gy}\}dx$$
$$=-\rho\int_0^{b_Y}\{\omega\cos\alpha[2\pi gy^3\,\dot{gy}-\Big(2\pi R_M+\frac{Zt}{\sin\alpha}\Big)gy^2\,\dot{gy}+R_M\frac{Zt}{\sin\alpha}gy\,\dot{gy}]$$
$$+\omega_p[2\pi gy^3\,\dot{gy}-\frac{Zt}{\sin\alpha}gy^2\,\dot{gy}]\}dx \qquad (4.7)$$

From Appendix C,

$$gy\,\dot{gy}=R_Y\dot{R}_Y+q_Y\dot{q}_Y-\dot{R}_Y\Big(q_Y^2-\frac{x^2}{\sin^2\alpha}\Big)^{\frac{1}{2}}-R_Y q_Y\dot{q}_Y\Big(q_Y^2-\frac{x^2}{\sin^2\alpha}\Big)^{-\frac{1}{2}}$$

$$gy^2\,\dot{g}y = R_Y^2\,\dot{R}_Y + 2R_Y q_Y\,\dot{q}_Y - \left(2R_Y\dot{R}_Y + a_Y\dot{a}_Y\right)\left(a_Y^2 - \frac{x^2}{\sin^2\alpha}\right)^{\frac{1}{2}}$$

$$- R_Y^2\,q_Y\,\dot{a}_Y\left(q_Y^2 - \frac{x^2}{\sin^2\alpha}\right)^{-\frac{1}{2}} + \dot{R}_Y\left(a_Y^2 - \frac{x^2}{\sin^2\alpha}\right)$$

$$gy^3\,\dot{g}y = R_Y^3\,\dot{R}_Y + 3R_Y^2 a_Y\,\dot{q}_Y - \left(3R_Y^2\dot{R}_Y + 3R_Y a_Y\,\dot{q}_Y\right)\left(a_Y^2 - \frac{x^2}{\sin^2\alpha}\right)^{\frac{1}{2}}$$

$$- R_Y^3\,q_Y\,\dot{a}_Y\left(q_Y^2 - \frac{x^2}{\sin^2\alpha}\right)^{-\frac{1}{2}} + \left(3R_Y\dot{R}_Y + a_Y\dot{q}_Y\right)\left(q_Y^2 - \frac{x^2}{\sin^2\alpha}\right)$$

$$- \dot{R}_Y\left(a_Y^2 - \frac{x^2}{\sin^2\alpha}\right)^{\frac{3}{2}}$$

are substituted into Eqn.(4.7) to give

$$\int_0^{b_Y}\left\{\left[fyV_\theta(fy)\,C(fy)\right]\dot{fy} - \left[gyV_\theta(gy)\,C(gy)\right]\dot{g}y\right\}dx$$

$$= -\rho\int_0^{b_Y}\{\omega\cos\alpha\,[\,2\pi\left(R_Y^3\dot{R}_Y + 3R_Y^2 a_Y\dot{a}_Y\right)$$

$$-\left(2\pi R_M + \frac{Zt}{\sin\alpha}\right)\left(R_Y^2\dot{R}_Y + 2R_Y a_Y\dot{q}_Y\right) + \frac{Zt}{\sin\alpha}R_M\left(R_Y\dot{R}_Y + q_Y\dot{a}_Y\right)$$

$$+\left(\left(2\pi R_M + \frac{Zt}{\sin\alpha}\right)\left(2R_Y\dot{R}_Y + q_Y\dot{a}_Y\right)\right.$$

$$\left. - 6\pi\left(R_Y\dot{R}_Y + R_Y a_Y\dot{q}_Y\right) - \frac{Zt}{\sin\alpha}R_M\dot{R}_Y\right)\left(a^2 - \frac{x^2}{\sin^2\alpha}\right)^{\frac{1}{2}}$$

$$+\left(\left(2\pi R_M + \frac{Zt}{\sin\alpha}\right)R_Y - 2\pi R_Y^2 - 2\frac{Zt}{\sin\alpha}R_M\right)R_Y\,q_Y\,\dot{a}_Y\left(a_Y^2 - \frac{x^2}{\sin^2\alpha}\right)^{-\frac{1}{2}}$$

$$+\left(2\pi\left(3R_Y\dot{R}_Y + q_Y\dot{a}_Y\right) - \left(2\pi R_M + \frac{Zt}{\sin\alpha}\right)\dot{R}_Y\right)\left(a_Y^2 - \frac{x^2}{\sin^2\alpha}\right)$$

$$\left. - 2\pi\dot{R}_Y\left(a_Y^2 - \frac{x^2}{\sin^2\alpha}\right)^{\frac{3}{2}}\right\}$$

$$+\omega_P\left\{2\pi\left(R_Y^3\dot{R}_Y + 3R_Y^2 a_Y\dot{a}_Y\right) - \frac{Zt}{\sin\alpha}\left(R_Y^2\dot{R}_Y + 2R_Y q_Y\dot{a}_Y\right)\right.$$

$$+\left(\frac{Zt}{\sin\alpha}\left(2R_Y\dot{R}_Y + a_Y\dot{q}_Y\right) - 6\pi\left(R_Y^2\dot{R}_Y + R_Y q_Y\dot{a}_Y\right)\right)\left(q_Y^2 - \frac{x^2}{\sin^2\alpha}\right)^{\frac{1}{2}}$$

$$+\left(\frac{Zt}{\sin\alpha} - 2\pi R_Y\right)R_Y^2 a_Y\dot{a}_Y\left(q_Y^2 - \frac{x^2}{\sin^2\alpha}\right)^{-\frac{1}{2}} - 2\pi\dot{R}_Y\left(a_y^2 - \frac{x^2}{\sin^2\alpha}\right)^{\frac{3}{2}}$$

$$\left.\left. + \left(2\pi\left(3R_Y\dot{R}_Y + q_Y\dot{a}_Y\right) - \frac{Zt}{\sin\alpha}\dot{R}_Y\right)\left(a_y^2 - \frac{x^2}{\sin^2\alpha}\right)\right\}\right]dx$$

(4.8)

The definite integrals are evaluated in Appendix C,

$$\int_0^{b_Y} 1\,dx = b_Y$$

$$\int_0^{b_Y}\left(a_Y^2 - \frac{x^2}{\sin^2\alpha}\right)^{\frac{1}{2}} dx = \tfrac{1}{4}\pi\, b_Y a_Y$$

$$\int_0^{b_Y}\left(a_Y^2 - \frac{x^2}{\sin^2\alpha}\right)^{-\frac{1}{2}} dx = \tfrac{1}{2}\pi \sin\alpha$$

$$\int_0^{b_Y}\left(a_Y^2 - \frac{x^2}{\sin^2\alpha}\right) dx = \tfrac{2}{3}\, b_Y a_y^2$$

$$\int_0^{b_Y}\left(a_Y^2 - \frac{x^2}{\sin^2\alpha}\right)^{\frac{3}{2}} dx = \tfrac{3}{16}\pi\, b_Y a_Y^3$$

and substituted into Eqn.(4.8) to yield

$$\begin{aligned}
&\int_0^{b_Y}\{[fyV_\theta(fy)\,C(fy)]\,\dot{fy} - [\,gyV_\theta(\,gy)\,C(\,gy)]\,\dot{gy}\}\,dx \\
&\quad = -\rho\,\{\,\omega\cos\alpha\,[\,2\pi\, b_Y\left(R_Y^3\,\dot{R}_Y + 3\,R_Y^2 a_Y\,\dot{a}_Y\right) \\
&\qquad - b_Y\left(2\pi R_M + \frac{Zt}{\sin\alpha}\right)\left(R_Y^2\,\dot{R}_Y + 2\,R_Y a_Y\,\dot{a}_Y\right) \\
&\qquad\qquad + \frac{Zt}{\sin\alpha} R_M\; b_Y\left(R_Y\,\dot{R}_Y + a_Y\,\dot{a}_Y\right) \\
&\qquad + \tfrac{1}{4}\pi\, a_Y\, b_Y\,(\left(2\pi R_M + \frac{Zt}{\sin\alpha}\right)(2\,R_Y\,\dot{R}_Y + a_Y\,\dot{a}_Y) \\
&\qquad\qquad - 6\pi\left(R_Y^2\,\dot{R}_Y + R_Y a_Y\,\dot{a}_Y\right) - \frac{Zt}{\sin\alpha} R_M\,\dot{R}_Y\,) \\
&\qquad + \tfrac{1}{2}\pi R_Y\, b_Y\,\dot{a}_Y\,(\left(2\pi R_M + \frac{Zt}{\sin\alpha}\right)R_Y - 2\pi R_Y^2 - 2\frac{Zt}{\sin\alpha} R_M\,) \\
&\quad + \tfrac{2}{3} a_Y^2\, b_Y\,(\,2\pi\left(3\,R_Y\,\dot{R}_Y + a_Y\,\dot{a}_Y\right) - \left(2\pi R_M + \frac{Zt}{\sin\alpha}\right)\dot{R}_Y\,) - \tfrac{3}{8}\pi^2\,\dot{R}_Y\, a_Y^3\, b_Y\,\} \\
&\quad + \omega_P\,[\,2\pi\, b_Y\left(R_Y^3\,\dot{R}_Y + 3\,R_Y^2 a_Y\,\dot{a}_Y\right) - \frac{Zt}{\sin\alpha} b_Y\left(R_Y^2\,\dot{R}_Y + 2\,R_Y a_Y\,\dot{a}_Y\right) \\
&\qquad + \tfrac{1}{4}\pi\, a_Y\, b_Y\,(\,\frac{Zt}{\sin\alpha}(2\,R_Y\,\dot{R}_Y + a_Y\,\dot{a}_Y) - 6\pi\left(R_Y^2\,\dot{R}_Y + R_Y a_Y\,\dot{a}_Y\right)\,) \\
&\qquad + \tfrac{1}{2}\pi R_Y^2\, b_Y\,\dot{a}_Y\left(\frac{Zt}{\sin\alpha} - 2\pi R_Y\right) \\
&\quad + \tfrac{2}{3} a_Y^2\, b_Y\,(\,2\pi\left(3\,R_Y\,\dot{R}_Y + a_Y\,\dot{a}_Y\right) - \frac{Zt}{\sin\alpha}\dot{R}_Y\,) + \tfrac{3}{8}\pi^2\,\dot{R}_Y\, a_Y^3\, b_Y\,]\,\}
\end{aligned} \tag{4.9}$$

Therefore, using Eqns.(4.5), (4.6) and (4.9) in Eqn.(2.26) the unsteady torque component is

$$\tau_{UCR} = K_{3CR}\,\omega_P + K_{4CR}\,\omega + K_{5CR}\,\dot{\omega}_P + K_{6CR}\,\dot{\omega} \tag{4.10}$$

where

$$K_{3CR} = -\rho [\ 2\pi\ b_Y \left(R_Y^3 \dot{R}_Y + 3 R_Y^2 a_Y \dot{a}_Y \right) - \frac{Zt}{\sin\alpha} b_Y \left(R_Y^2 \dot{R}_Y + 2 R_Y q_Y \dot{a}_Y \right)$$
$$+ \tfrac{1}{4}\pi\, a_Y\, b_Y \left(\frac{Zt}{\sin\alpha} \left(2 R_Y \dot{R}_Y + a_Y \dot{a}_Y \right) - 6\pi \left(R_Y^2 \dot{R}_Y + R_Y a_Y \dot{a}_Y \right) \right.$$
$$+ \tfrac{1}{2}\pi R_Y^2\, b_Y\, \dot{a}_Y \left(\frac{Zt}{\sin\alpha} - 2\pi R_Y \right) - \tfrac{3}{8}\pi^2 \dot{R}_Y a_Y^3 b_Y$$
$$\left. + \tfrac{2}{3} q_Y^2 b_Y \left(2\pi \left(3 R_Y \dot{R}_Y + a_Y \dot{a}_Y \right) - \frac{Zt}{\sin\alpha} \dot{R}_Y \right) \right]$$

$$K_{4CR} = -\rho \cos\alpha [\ 2\pi\ b_Y \left(R_Y^3 \dot{R}_Y + 3 R_Y^2 a_Y \dot{a}_Y \right) + \frac{Zt}{\sin\alpha} R_M\ b_Y \left(R_Y \dot{R}_Y + q_Y \dot{a}_Y \right)$$
$$- b_Y \left(2\pi R_M + \frac{Zt}{\sin\alpha} \right) \left(R_Y^2 \dot{R}_Y + 2 R_Y q_Y \dot{a}_Y \right)$$
$$+ \tfrac{1}{4}\pi q_Y b_Y \left(\left(2\pi R_M + \frac{Zt}{\sin\alpha} \right) \left(2 R_Y \dot{R}_Y + a_Y \dot{a}_Y \right) \right.$$
$$\left. - 6\pi \left(R_Y^2 \dot{R}_Y + R_Y a_Y \dot{a}_Y \right) - \frac{Zt}{\sin\alpha} R_M \dot{R}_Y \right)$$
$$+ \tfrac{1}{2}\pi R_Y b_Y \dot{a}_Y \left(\left(2\pi R_M + \frac{Zt}{\sin\alpha} \right) R_Y - 2\pi R_Y^2 - 2 \frac{Zt}{\sin\alpha} R_M \right)$$
$$+ \tfrac{2}{3} q_Y^2 b_Y \left(2\pi \left(3 R_Y \dot{R}_Y + q_Y \dot{a}_Y \right) - \left(2\pi R_M + \frac{Zt}{\sin\alpha} \right) \dot{R}_Y \right) - \tfrac{3}{8}\pi^2 \dot{R}_Y a_Y^3 b_Y\ ]$$

$$K_{5CR} = \rho [\ \tfrac{1}{2}\pi \left(b \left(R_M^4 - R_C^4 \right) - b_Y \left(R_M^4 - R_Y^4 \right) \right)$$
$$- \tfrac{1}{3} \frac{Zt}{\sin\alpha} \left(b \left(R_M^3 - R_C^3 \right) - b_Y \left(R_M^3 - R_Y^3 \right) \right) - \tfrac{4}{15}\pi \left(a^4 b - q_Y^4 b_Y \right)$$
$$+ \tfrac{1}{4}\pi \left(ab \left(2\pi R_C^3 - \frac{Zt}{\sin\alpha} R_C^2 \right) - q_Y b_Y \left(2\pi R_Y^3 - \frac{Zt}{\sin\alpha} R_Y^2 \right) \right)$$
$$+ \tfrac{2}{3} \left(a^2 b \left(\frac{Zt}{\sin\alpha} R_C - 3\pi R_C^2 \right) - a_Y^2 b_Y \left(\frac{Zt}{\sin\alpha} R_Y - 3\pi R_Y^2 \right) \right)$$
$$+ \tfrac{3}{16}\pi \left(a^3 b \left(2\pi R_C - \tfrac{1}{3} \frac{Zt}{\sin\alpha} \right) - q_Y^3 b_Y \left(2\pi R_Y - \tfrac{1}{3} \frac{Zt}{\sin\alpha} \right) \right)]$$

$$K_{6CR} = \rho \cos\alpha \left[\tfrac{1}{2}\pi \left(b \left(R_M^4 - R_C^4 \right) - b_Y \left(R_M^4 - R_Y^4 \right) \right) \right.$$
$$- \tfrac{1}{3} \left(2\pi R_M + \frac{Zt}{\sin\alpha} \right) \left(b \left(R_M^3 - R_C^3 \right) - b_Y \left(R_M^3 - R_Y^3 \right) \right)$$
$$+ \tfrac{1}{2} \frac{Zt}{\sin\alpha} R_M \left(b \left(R_M^2 - R_C^2 \right) - b_Y \left(R_M^2 - R_Y^2 \right) \right)$$
$$+ \tfrac{1}{4}\pi \left(ab \left(R_C^2 - R_M R_C \right) \left(2\pi R_C - \frac{Zt}{\sin\alpha} \right) \right.$$
$$\left. - q_Y b_Y \left(R_Y^2 - R_M R_Y \right) \left(2\pi R_Y - \frac{Zt}{\sin\alpha} \right) \right)$$
$$+ \tfrac{2}{3} \left(a^2 b \left(\left(2\pi R_M + \frac{Zt}{\sin\alpha} \right) R_C - 3\pi R_C^2 - \tfrac{1}{2} \frac{Zt}{\sin\alpha} R_M \right) \right.$$
$$\left. - q_Y^2 b_Y \left(\left(2\pi R_M + \frac{Zt}{\sin\alpha} \right) R_Y - 3\pi R_Y^2 - \tfrac{1}{2} \frac{Zt}{\sin\alpha} R_M \right) \right)$$
$$+ \tfrac{3}{16}\pi \left(a^3 b \left(2\pi R_C - \tfrac{2}{3}\pi R_M - \tfrac{1}{3} \frac{Zt}{\sin\alpha} \right) \right.$$
$$\left. \left. - q_Y^3 b_Y \left(2\pi R_Y - \tfrac{2}{3}\pi R_M - \tfrac{1}{3} \frac{Zt}{\sin\alpha} \right) \right) - \tfrac{4}{15}\pi \left(a^4 b - q_Y^4 b_Y \right) \right]$$

4.3 Energy Dissipation

4.3.1 Incidence Loss

Although there are three separate elements in the cropped rotor dynamometer, the absence of blading in the return ring results in there being a negligible incidence loss as the fluid passes from the rotor to the return ring. The inlet conditions to the rotor are the same as for the full rotor machine, so from Section 2.5.1 the rotor inlet loss is given by Eqn.(2.35)

$$\dot{P}_{IR} = K_{I1}\,\omega\,\omega_P^2 + K_{I2}\,\omega^2\,\omega_P + K_{I3}\,\omega^3 \qquad (2.35)$$

where

$$K_{I1} = \tfrac{1}{2}\rho\,\sin\alpha_{RI}\,\left[\,2\pi\left(\tfrac{1}{4}R_M\,r^4 - \tfrac{1}{5}r^5\right) - \frac{Z_R t}{\sin\alpha_{RI}}\left(\tfrac{1}{3}R_M\,r^3 - \tfrac{1}{4}r^4\right)\right]_{R_I}^{R_{CI}}$$

$$K_{I2} = \rho\,\sin\alpha_{RI}\,(\cos\alpha_{SO} - \cos\alpha_{RI})\left[\,2\pi\left(\tfrac{1}{3}R_M^2\,r^3 - \tfrac{1}{2}R_M\,r^4 + \tfrac{1}{5}r^5\right) - \frac{Z_R t}{\sin\alpha_{RI}}\left(\tfrac{1}{2}R_M^2\,r^2 - \tfrac{2}{3}R_M\,r^3 + \tfrac{1}{4}r^4\right)\right]_{R_I}^{R_{CI}}$$

$$K_{I3} = \tfrac{1}{2}\rho\,\sin\alpha_{RI}\,(\cos\alpha_{SO} - \cos\alpha_{RI})^2 \times\left[\,2\pi\left(\tfrac{1}{2}R_M^3\,r^2 - R_M^2\,r^3 + \tfrac{3}{4}R_M\,r^4 - \tfrac{1}{5}r^5\right) - \frac{Z_R t}{\sin\alpha_{RI}}\left(R_M^3\,r - \tfrac{3}{2}R_M^2\,r^2 + R_M\,r^3 - \tfrac{1}{4}r^4\right)\right]_{R_I}^{R_{CI}}$$

As the fluid passes around the return ring it will maintain the same velocity that it had upon leaving the rotor (Fig.4.3). Thus as the fluid approaches the stator inlet the tangential component of relative water velocity is

$$W_{S\theta S} = \omega_P\,R_M$$

The stator inlet loss is given by

$$d\dot{P}_{ISCR} = \tfrac{1}{2}\,d\dot{m}_{IS}\,(W_{S\theta S} - W_{S\theta 9})^2 \qquad (4.11)$$

where

$$W_{S\theta 9} = \omega(r - R_M)\cos\alpha_{SI}$$

and from Eqn.(2.9),

$$d\dot{m}_{IS} = \rho\,\omega(r - R_M)\,\sin\alpha_{SI}\left(2\pi r - \frac{Z_S t}{\sin\alpha_{SI}}\right)dr$$

By integrating Eqn.(4.11) the stator inlet loss is

$$\dot{P}_{ISCR} = \int_{R_{CO}}^{R_O} \tfrac{1}{2}\rho\,\omega(r - R_M)\,\sin\alpha_{SI}\left(2\pi r - \frac{Z_S t}{\sin\alpha_{SI}}\right) \times(\omega_P R_M - \omega(r - R_M)\cos\alpha_{SI})^2\,dr$$

$$= \tfrac{1}{2}\rho \sin\alpha_{SI} \int_{R_{co}}^{R_o} \left(2\pi r - \frac{Z_S t}{\sin\alpha_{SI}} \right)$$
$$\times [\, \omega \omega_P^2 \left(R_M^2 r - R_M^3 \right) - 2\omega^2 \omega_P \cos\alpha_{SI} \left(R_M r^2 - 2 R_m^2 r + R_M^3 \right)$$
$$+ \omega^3 \cos^2\alpha_{SI} \left(r^3 - 3 R_M r^2 + 3 R_M^2 r - R_M^3 \right)] dr$$

which yields

$$\dot{P}_{ISCR} = K_{I4\,CR}\, \omega \omega_P^2 + K_{I5\,CR}\, \omega^2 \omega_P + K_{I6\,CR}\, \omega^3 \qquad (4.12)$$

where

$$K_{I4\,CR} = \tfrac{1}{2}\rho \sin\alpha_{SI} \left[2\pi \left(\tfrac{1}{3} R_M^2 r^3 - \tfrac{1}{2} R_M^3 r^2 \right) - \frac{Z_S t}{\sin\alpha_{SI}} \left(\tfrac{1}{2} R_M^2 r^2 - R_M^3 r \right) \right]_{R_{co}}^{R_o}$$

$$K_{I5\,CR} = -\rho \sin\alpha_{SI} \cos\alpha_{SI} \left[2\pi \left(\tfrac{1}{4} R_M r^4 - \tfrac{2}{3} R_M^2 r^3 + \tfrac{1}{2} R_M^3 r^2 \right) \right.$$
$$\left. - \frac{Z_S t}{\sin\alpha_{SI}} \left(\tfrac{1}{3} R_M r^3 - R_M^2 r^2 + R_M^3 r \right) \right]_{R_{co}}^{R_o}$$

$$K_{I6\,CR} = \tfrac{1}{2}\rho \sin\alpha_{SI} \cos^2\alpha_{SI} \left[2\pi \left(\tfrac{1}{5} r^5 - \tfrac{3}{4} R_M r^4 + R_M^2 r^3 - \tfrac{1}{2} R_M^3 r^2 \right) \right.$$
$$\left. - \frac{Z_S t}{\sin\alpha_{SI}} \left(\tfrac{1}{4} r^4 - R_M r^3 + \tfrac{3}{2} R_M^2 r^2 - R_M^3 r \right) \right]_{R_{co}}^{R_o}$$

Hence, the total incidence loss for the cropped rotor dynamometer is

$$\dot{P}_{ICR} = \left(K_{I1} + K_{I4\,CR} \right) \omega \omega_P^2 + \left(K_{I2} + K_{I5\,CR} \right) \omega^2 \omega_P + \left(K_{I3} + K_{I6\,CR} \right) \omega^3 \qquad (4.13)$$

4.3.2 Friction Loss

This loss is calculated as in Section 2.5.2, however the upper rotor section is now the return ring. The absence of vanes results in differences to the friction losses in this section, though the losses for the other sections are unchanged.

For the outer streamtubes the thickness in the lower sections is $D_L = (R_M - R_I)/50$, and by continuity the upper thickness for the cropped rotor is

$$D_{URCR} = \frac{(R_M - R_I) \sin\alpha_{RI} \left(2\pi R_I - \dfrac{Z_R t}{\sin\alpha_{RI}} \right)}{(R_O - R_M) \sin\alpha_{RO} (2\pi R_O)} D_L$$

The value of the stator thickness remains the same.

To apply the pipe friction formula,

$$d\dot{P}_F = d\dot{m} \frac{4 f L W^2}{2 d} \qquad (2.39)$$

the parameters are

path length $L_U = \frac{1}{2}\pi(R_O - R_M)$

hydraulic diameter $d = 4\dfrac{2\pi R_O D_{URCR}}{2\pi R_O} = 4 D_{URCR}$

relative water velocity $W = \omega(R_O - R_M)$

mass flow rate

$$\dot{m} = \rho\,\omega(R_O - R_M)\sin\alpha_{RO}\left(2\pi R_O - \frac{Z_R t}{\sin\alpha_{RO}}\right)D_{URCR}$$

which yield

$$\dot{P}_{FORUCR} = K_{FORUCR}\,\omega^3 \tag{4.14}$$

where

$$K_{FORUCR} = \tfrac{1}{16}\lambda_F\,\rho\,\pi\,\sin\alpha_{RO}\,(R_O - R_M)^4\,(2\pi R_O)$$

Since there are no vanes in the return ring section there is no wall friction, thus the coefficient for the inner streamtubes is identically zero. Hence, the total friction loss is

$$\dot{P}_{FCR} = K_{FCR}\,\omega^3 \tag{4.15}$$

where

$$K_{FCR} = K_{FORL} + K_{FORUCR} + K_{FOSL} + K_{FOSU} + K_{FIRL} + K_{FIRU} + K_{FISL} + K_{FISU}$$

The coefficients K_{FORU} , K_{FORUCR}, K_{FOSL}, K_{FOSU} , K_{FIRL}, K_{FISL}, K_{FISU} are defined by Eqns.(2.40), (4.15), (2.42), (2.43), (2.44), (2.46), (2.47) respectively.

4.3.3 Secondary Circulation Loss

As with the friction losses the only difference for the cropped rotor machine is in the upper rotor section where there is no vane blockage. Therefore, the elemental mass flow is

$$d\dot{m}_{SUCR} = \rho\,\omega(r - R_M)\sin\alpha_{RO}(2\pi r)dr$$

So, applying Eqn.(2.49) the secondary circulation loss is

$$\dot{P}_{SCRUCR} = \int_{R_{CO}}^{R_O} \tfrac{1}{2}K_B\left(\omega(r - R_M)\right)^2 \rho\,\omega(r - R_M)\sin\alpha_{RO}(2\pi r)dr$$

$$= \tfrac{1}{2}K_B\rho\,\omega^3\sin\alpha_{RO}\left[\,2\pi\left(\tfrac{1}{5}r^5 - \tfrac{3}{4}R_M r^4 + R_M^2 r^3 - \tfrac{1}{2}R_M^3 r^2\right)\right]_{R_{CO}}^{R_O}$$

which yields

$$\dot{P}_{SCRUCR} = K_{SCRUCR}\ \omega^3 \tag{4.16}$$

where

$$K_{SCRUCR} = \tfrac{1}{2} K_B \rho\ \sin\alpha_{RO} \left[\ 2\pi \left(\tfrac{1}{5} r^5 - \tfrac{3}{4} R_M\, r^4 + R_M^2\, r^3 - \tfrac{1}{2} R_M^3\, r^2 \right) \right]_{R_{co}}^{R_o}$$

The total secondary circulation loss is

$$\dot{P}_{SCCR} = K_{SCCR}\ \omega^3 \tag{4.17}$$

where

$$K_{SCCR} = K_{SCRL} + K_{SCRUCR} + K_{SCSL} + K_{SCSU}$$

and the coefficients K_{SCRL} , K_{SCRUCR} , K_{SCSL} , K_{SCSU} are defined by Eqns.(2.50), (4.17), (2.52), (2.53) respectively.

4.4 Supplementary Equations

In Section 3.1 to determine parameters in the case of partial and varying fill an average value of blockage factor is used. By altering this factor to allow for the absence of vanes in the return ring the same equations and iteration is used to determine R_{CO} , R_{CI} , $\dot{R}_Y$, $\dot{a}_Y$ and the rate of change of fluid fill. To obtain the fluid pressure in the return ring section the machine rotation velocity and acceleration vectors are equated to zero, as they are for the stator, and Eqn.(3.23) of Section 3.2 is used.

For fluid outflow from the working compartment cropped rotor dynamometers use water outlet holes either at the periphery of the working compartment (Fig.4.5) or at the base of the stator cup (Fig.3.9). The latter case is analysed as in Section 3.3.4, but in the former case the outlet flow velocity is altered from that in Section 3.3.3 due to the return ring being stationary. Hence, referring to Fig.4.5 the flow velocity at point B is

$$V_B^2 = \left(\frac{Q_O}{A_B}\right)^2$$

The losses encountered on the outflow path are as in Section 3.3.3.

1./ Entry to drain gap;

$$P_{L1} = \tfrac{1}{2} C_{L1} \left(\frac{Q_O}{A_B}\right)^2 \qquad with \quad C_{L1} = 0.5$$

2./ Exit from drain gap;

$$P_{L2} = \tfrac{1}{2} C_{L2} \left(\frac{Q_O}{A_B}\right)^2 \qquad with \quad C_{L2} = 1.0$$

4./ Flow around drain annulus;

$$P_{L4} = \tfrac{1}{2} C_{LD} \left(\frac{Q_O}{A_D}\right)^2 \qquad with \quad C_{LD} = 0.3$$

7./ Bend of two annuli into one outlet;

$$P_{L7} = \tfrac{1}{2} C_{L7} \left(\frac{Q_O}{A_A}\right)^2 \qquad with \quad C_{L7} = 0.8$$

5./ Flow straightener;

$$P_{L5} = \tfrac{1}{2} C_{LFS} \left(\frac{Q_O}{A_A}\right)^2 \qquad with \quad C_{LFS} = 0.72$$

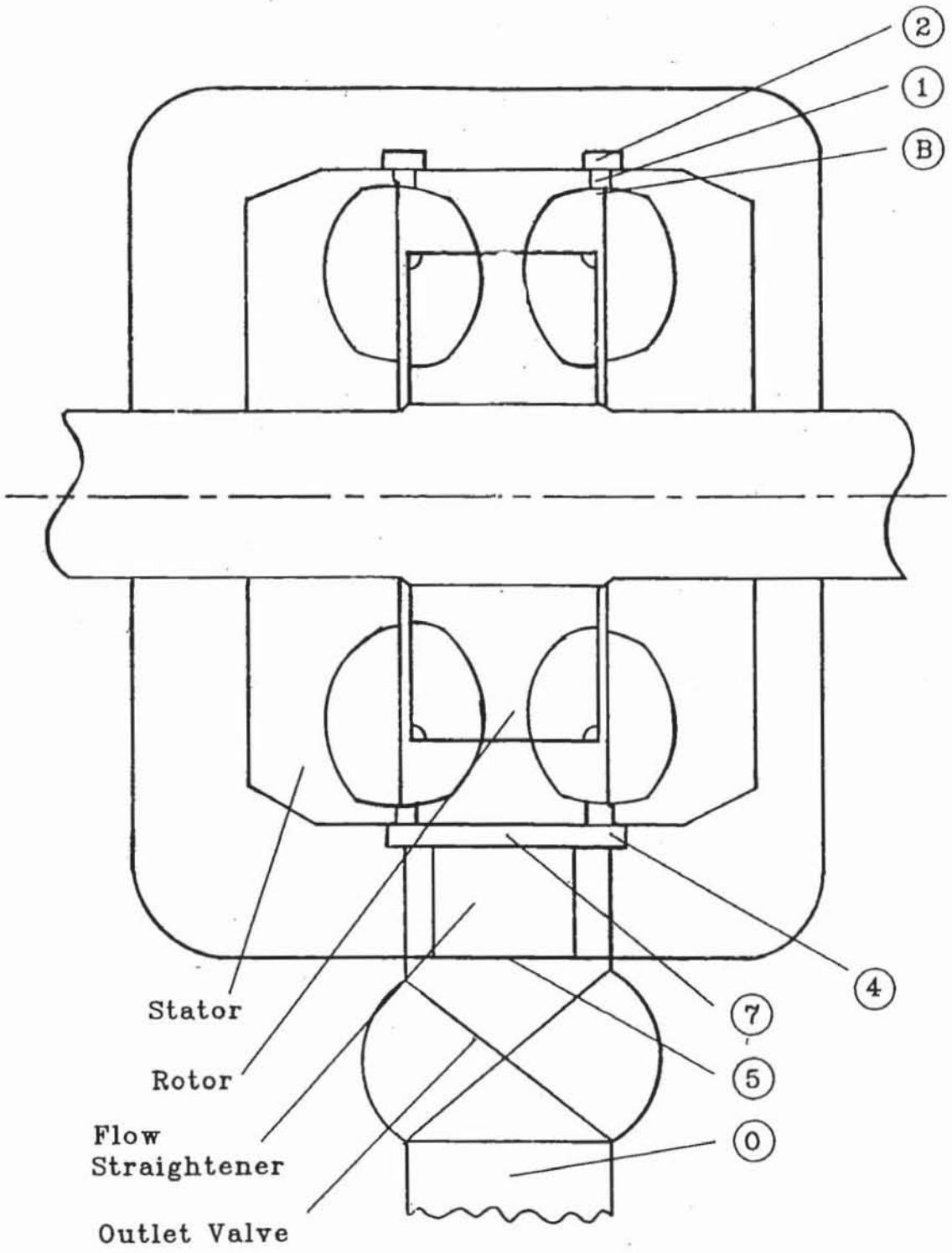

Figure 4.5: Water Outflow Path via Cup Periphery Outlet (Cropped Rotor)

6./ Outlet valve;

$$P_{L6} = \tfrac{1}{2} C_{LV} \left(\frac{Q_O}{A_A} \right)^2 \qquad with \quad C_{LV} = fn(closure)$$

Therefore, Eqn.(3.24) is applied to this flow path to get

$$\frac{P_B}{\rho} + \tfrac{1}{2}\left(\frac{Q_O}{A_B} \right)^2 = \tfrac{1}{2}\left(\frac{Q_O}{A_O} \right)^2 + \left\{ \tfrac{1}{2} C_{L1} \left(\frac{Q_O}{A_B} \right)^2 + \tfrac{1}{2} C_{L2} \left(\frac{Q_O}{A_B} \right)^2 + \tfrac{1}{2} C_{LD} \left(\frac{Q_O}{A_D} \right)^2 + \tfrac{1}{2} C_{L7} \left(\frac{Q_O}{A_A} \right)^2 + \tfrac{1}{2} C_{LFS} \left(\frac{Q_O}{A_A} \right)^2 + \tfrac{1}{2} C_{LV} \left(\frac{Q_O}{A_A} \right)^2 \right\}$$

which yields

$$\frac{P_B}{\rho} = \tfrac{1}{2} Q_O^2 \left\{ \frac{(C_{L1} + C_{L2} - 1)}{A_B^2} + \frac{C_{LD}}{A_D^2} + \frac{(C_{L7} + C_{LFS} + C_{LV})}{A_A^2} + \frac{1}{A_O^2} \right\} \quad (4.19)$$

PART II

DYNAMOMETER PERFORMANCE SIMULATION

CHAPTER 5
STEADY STATE SIMULATION

5.1 Introduction

Investigation of hydrokinetic machines usually involves the prediction of steady state performance maps. In this chapter the theory derived in Part I is used to simulate such steady state behaviour, both to compare with and to extend previous studies. Subsequent chapters apply the theory to a dynamic dynamometer simulation for both open and closed loop control configurations.

In order to predict the dynamometer performance the theory developed in the previous three chapters is formulated as a computer program. The machine theory equations form four subroutines, which are the machine performance kernel. This is the core of the dynamometer simulations: determining the water vortex centre radii (Section 2.3, Subroutine PART), solving for the air-water interface radii (Section 3.1, Subroutine PART); calculating the geometric equation coefficients for torque (Section 2.4, Subroutine KFACTS) and power losses (Section 2.5, Subroutine KFACTS); solving for water vortex velocity (Section 2.2, Subroutine VORVEL); and calculating torque, power, cup pressure (Section 3.2, Subroutine POWER), power losses and water outflow rate (Section 3.3, Subroutine POWER).

An overview of the steady state simulation program, from which performance maps are obtained, is presented in Fig.5.1. There is the straightforward constant percentage fill option for predictions at a given point or along lines of constant fill, and the water *inflow equals outflow* mapping option. In the latter option the fill is varied at each point to find the steady state point at which inflow and outflow are equal. By varying the speed, a map of points is obtained at which the water mass flow is balanced.

Firstly the effect of geometric variations in the machine on the maximum torque capacity is considered (Section 5.2). Since variation of fluid fill in the working compartment is an inherent feature of the hydraulic dynamometer's operation it is studied in Section 5.3. As a preliminary step towards illustrating the self-emptying phenomenon by means of steady state water *inflow equals outflow* mapping (Section

5.5), the distribution of fluid pressure around the working compartment is presented in Section 5.4.

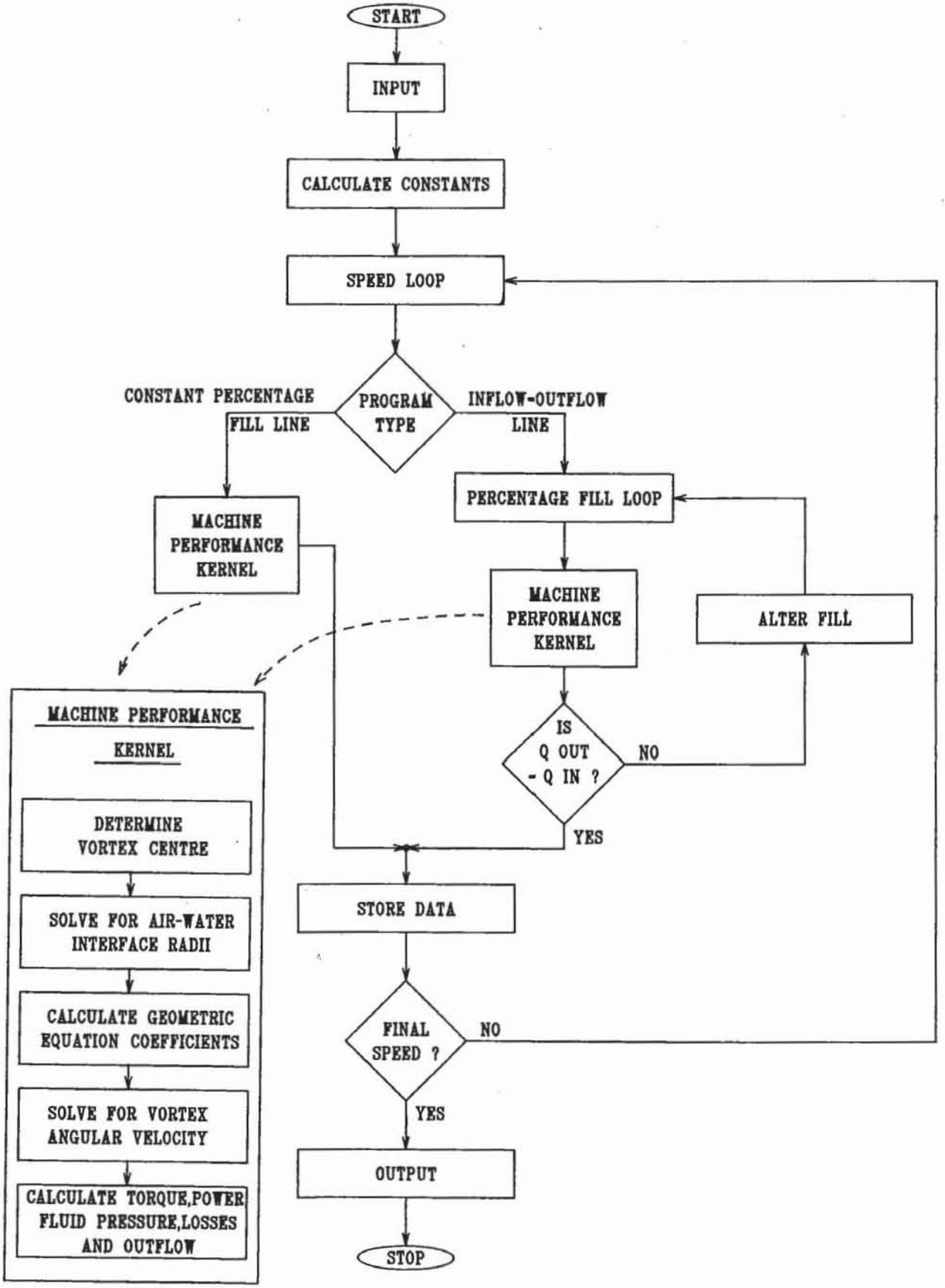

Figure 5.1: Structure of Steady State Program

5.2 Variations in Dynamometer Geometry

5.2.1 Working Compartment Size, Proportion and Speed

Although Froude [1] had found the index of torque against speed to be less than the fifth power of diameter, Rao [2] and Raine [6] report the index to be slightly greater than five. The latter proposition is more feasible since theoretical geometric derivations give the fifth power of diameter in torque equations, for example the steady state torque Eqn.(2.18) and the classical Turbomachinery equation, $T = kN^2D^5$, and then the effect of size on the loss mechanisms should be considered. If machine castings are taken as having constant surface roughness size, then the relative roughness and therefore the friction loss factor are lower on larger machines. Similarly the bend loss factor for secondary circulation is reduced as the bend radius is increased.

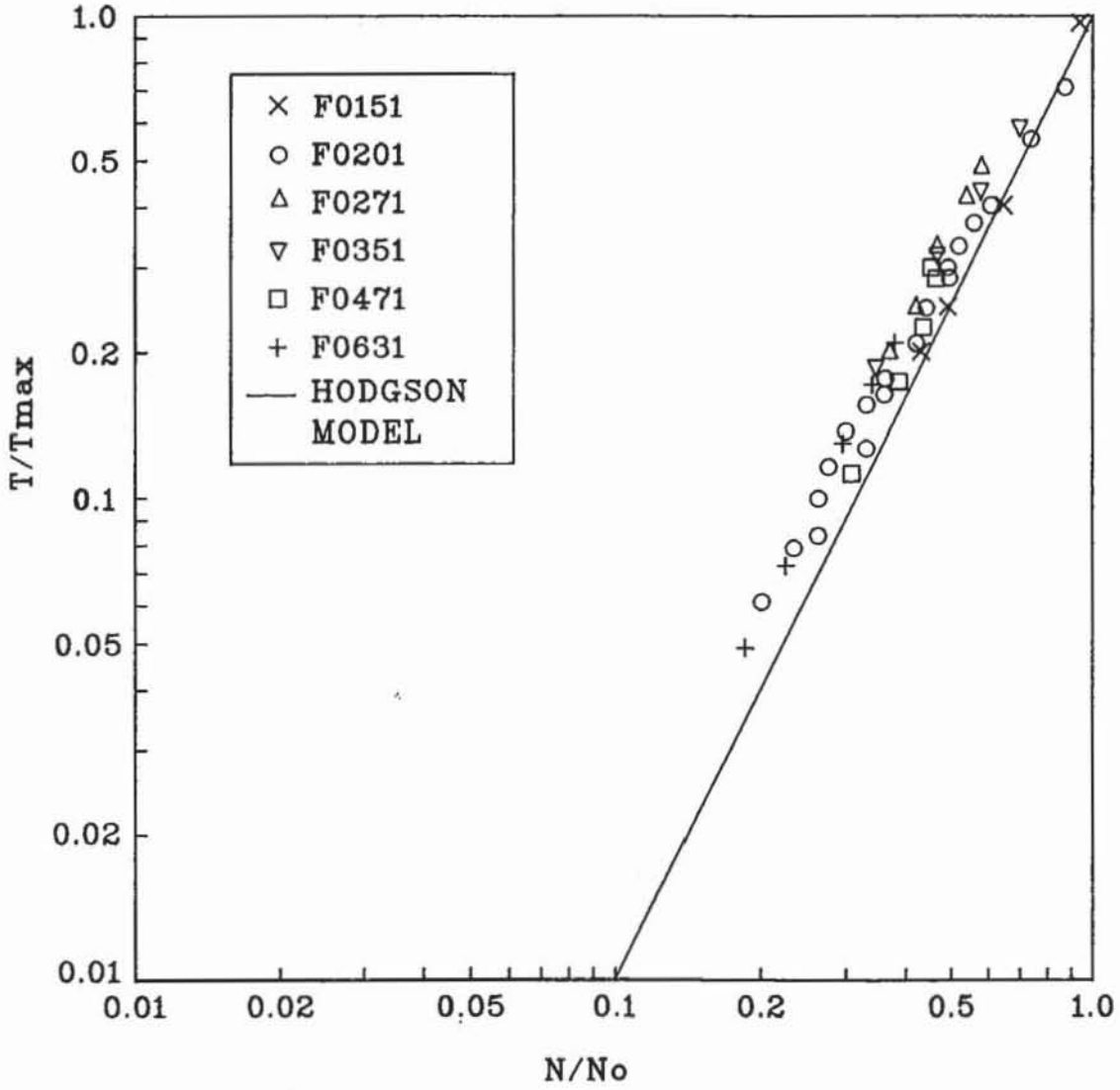

Figure 5.2: Comparison of Model Torque Predictions and Experimental Data for 45° Vane Full Rotor Dynamometer

However the maximum torque is taken to be proportional to the fifth power of diameter for scaling of Froude technical data [56] into a

non-dimensional plot to compare with the predicted performance. For standard 45° vane full rotor dynamometers there is close agreement as the maximum torque speed, N_o , is approached in Fig.5.2. Raine reports that Froude dynamometer design scaling from past performance is based on a speed index of 1.8 rather than the theoretical value of 2. This difference is illustrated by the gradient of the predicted line (power of 2) being slightly higher than the experimental lines for each machine, confirming Rao's findings on the actual speed effect on torque. As with the torque to diameter proportionality the empirical loss coefficients are affected by fluid fill variation and machine acceleration, so a slight difference between theoretical and experimental values is expected when using constant values for the model prediction.

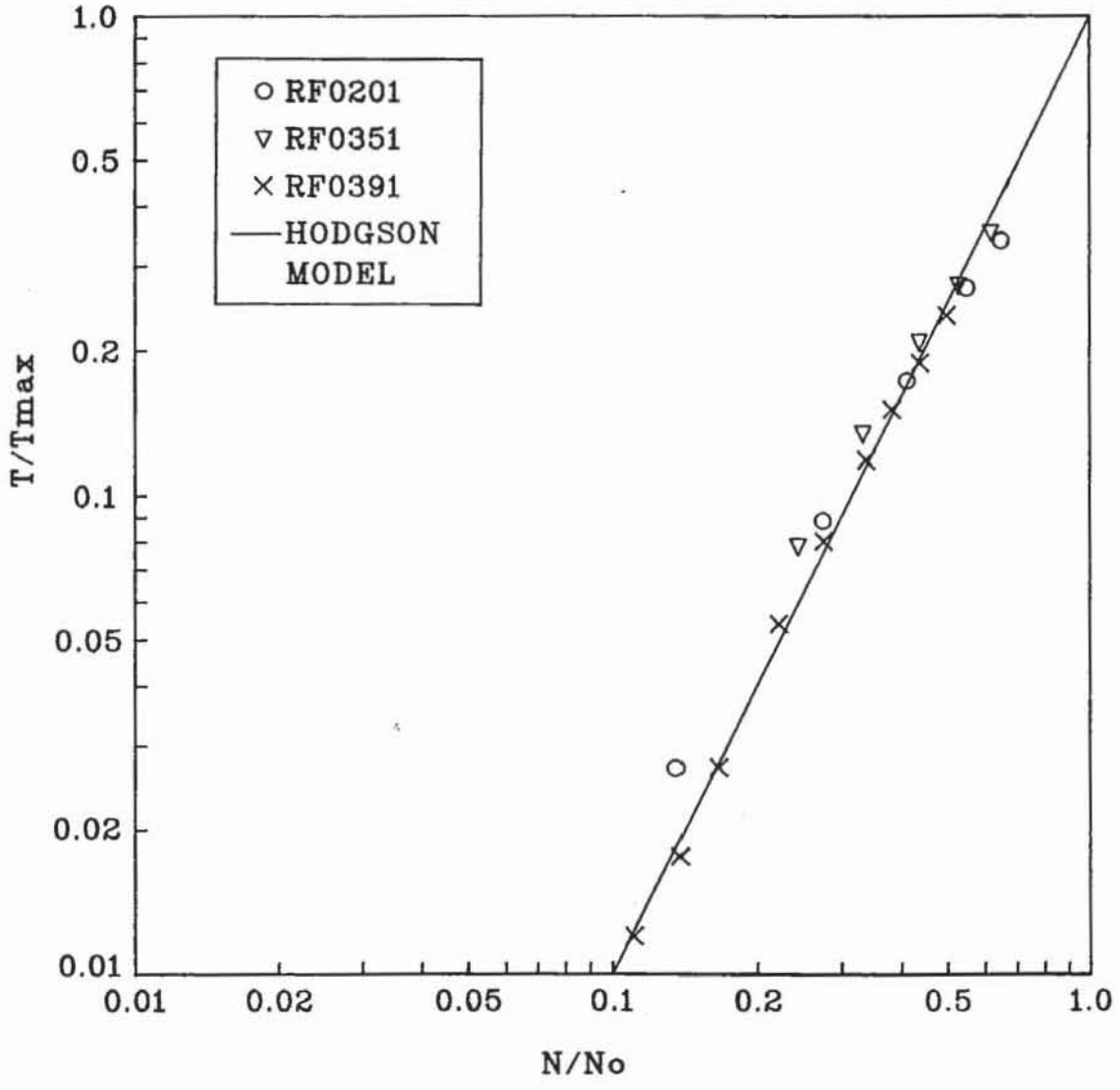

Figure 5.3: Comparison of Model Torque Predictions and Experimental Data for 90° Vane Full Rotor Dynamometer

Actual vane shape also affects the torque gradient as Fig.5.3 shows. The RF0391 reversible 90° vane full rotor dynamometer is a later machine than the other two and has an improved stator blade

shape, which results in a higher torque gradient against speed very close to the predicted line. For the 45° vane cropped rotor dynamometers the predicted torque gradient (Fig.5.4) is also very close results to the experimental data.

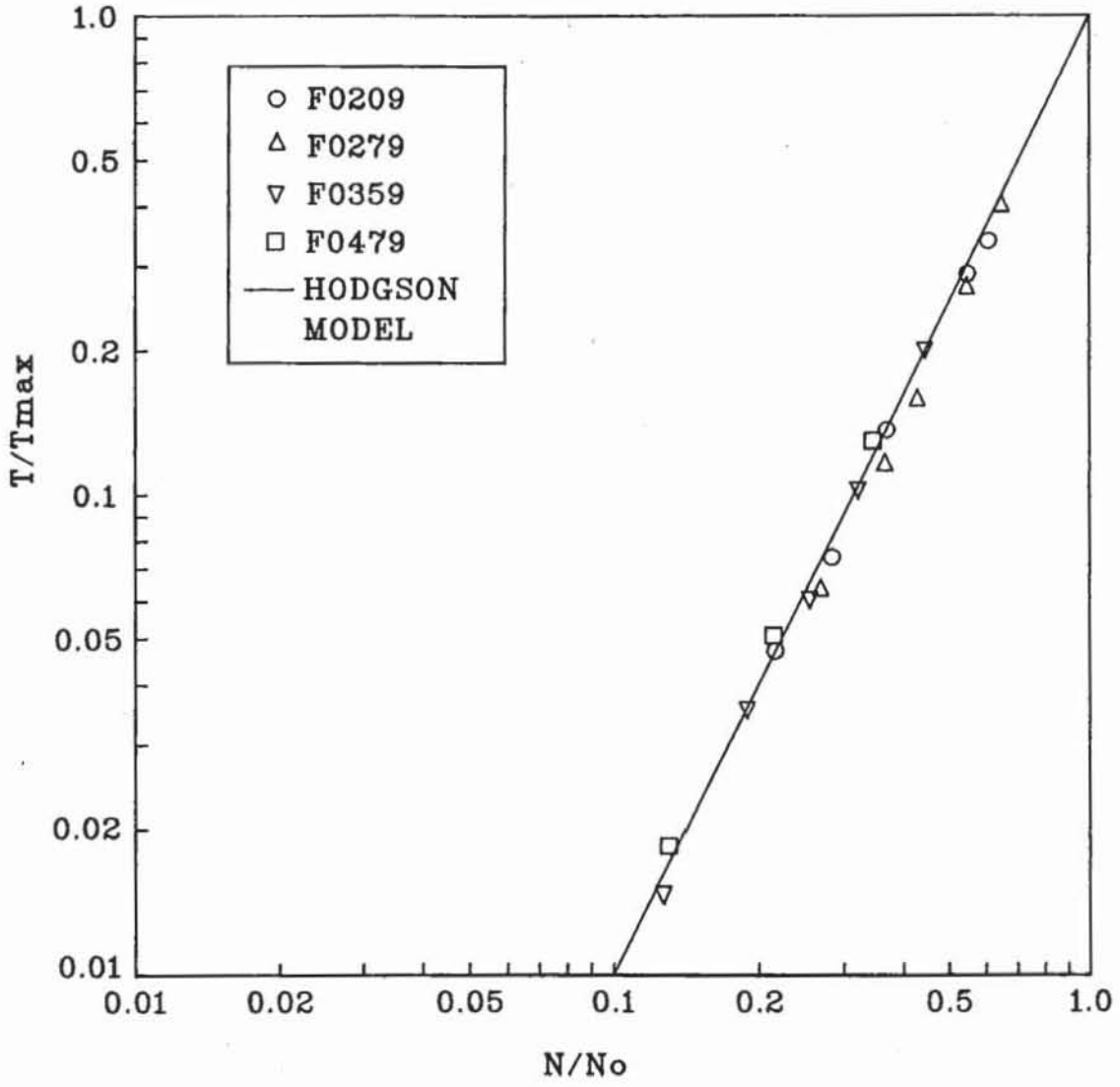

Figure 5.4: Comparison of Model Torque Predictions and Experimental Data for 45° Vane Cropped Rotor Dynamometer

As well as working compartment diameter, the ratio of outside radius to inside radius is very important in determining the torque capacity per unit diameter of a dynamometer. Using the F020 machine (45° vanes, R_o = 102.5 mm, R_i = 43.5 mm) as a reference, Fig.5.5 shows a very clearly defined optimum range for working compartment proportion. These results were obtained by setting a constant inner radius and varying the outer radius. The torque values are divided by the outer diameter to the fifth power, so that the size effect is removed from the comparison. As the ratio increases the geometric torque and loss factors increase, and therefore the torque produced increases.

However, the fluid vortex velocity, which is determined by the geometric factors, decreases with increasing ratio. The optimum peak shown is a combination of these two effects.

Through development work the Froude dynamometers (F020 R_O $/R_I$ = 2.36) are very close to the theoretical optimum of 2.15. Rao uses the ratio of inner to outer mean flowpath radii to find the optimum proportion as 0.71. This value is converted to a R_O $/R_I$ ratio of 2.30, using the figure he provides. There is a small variation in the R_O $/R_I$ values over the Froude range which contributes to the spread of experimental points in Fig.(5.2).

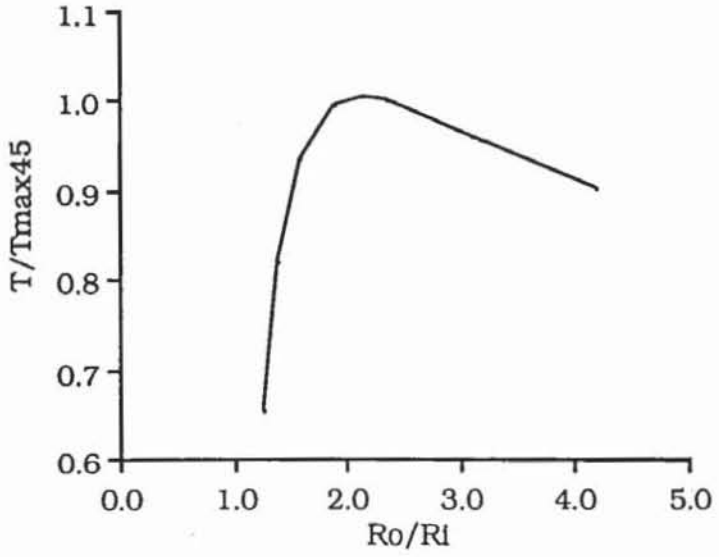

Figure 5.5: Optimum R_O $/R_I$ Working Compartment Proportion

5.2.2 Vane Angle

Altering the vane angles changes the torque capacity of the dynamometer. With flat equally angled vanes an optimum vane angle of 39° is predicted (Fig.5.6). Rao also found an optimum torque capacity at approximately at this angle. In practise however the torque increase of approximately 5% over the commonly used 45° vanes could be achieved by a 1% increase in diameter. Although having much lower torque 90° vanes (axial) are useful for bidirectional machines.

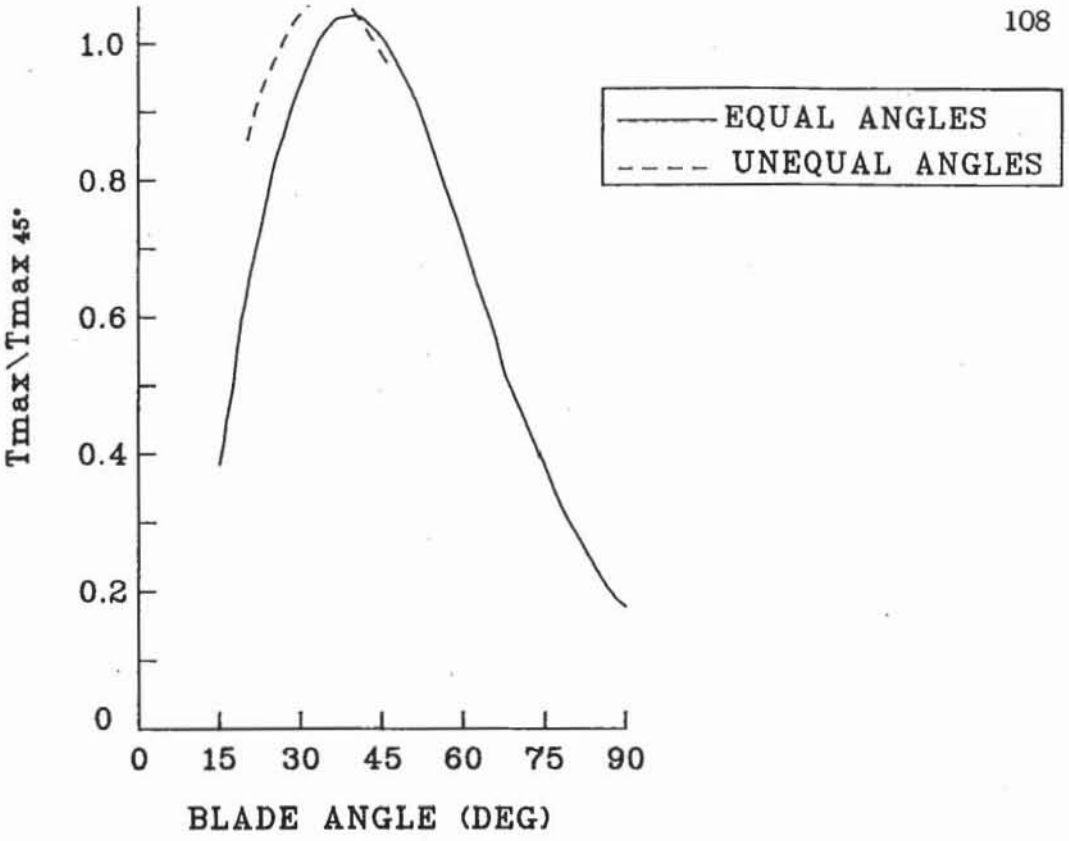

Figure 5.6: Optimum Vane Angle for Flat and Twisted Vanes

Both Qualman and Egbert [14] and Jandasek [13] stress the importance of blade design in fluid couplings and torque converters. They find that using helical rather than flat blades significantly increases the machine's torque capacity. To test vane shape for dynamometers the outlet angles for both rotor and stator are set to the optimum vane angle, and the inlet angles varied (Fig.5.6)[1]. The result was an optimum inlet angle of 35°, which gives a torque improvement of just more than 7% over the reference 45° vanes. Approximately half this improvement is achieved if an inlet angle of 40° is used with the 45° outlet angle. As in the case of flat equally angled blades this improvement is obtainable with a very small increase in machine diameter. The considerably smaller improvement from introducing helical vanes to dynamometers, as compared with fluid coupling and torque converter studies, is due to dynamometers having fewer and thicker vanes (as the vane angle gets lower the blockage factor increases reducing torque the improvements), and the work on other

---

1 When using the theory for non-equal vane angles care must be taken that mass flow rates between rotor and stator are not discontinuous due to the mathematics applied. Discontinuities can occur when the Conservation of Mass (Section 2.3) is applied to both rotor and stator. Equivalent expressions to those derived for the stator are obtained for the rotor water mass inflow and outflow rates. By inspection of Eqns.(2.10) and (2.11) the theoretical inflows and outflows are directly proportional to the vane angle at the point of interest. Hence if the vane angles vary between rotor and stator there can be an unrealistic discontuity of the mathematical values. The use of average values for mass flow is recommended, i.e. average of rotor outlet and stator inlet values, so that the investigation is not corrupted.

hydrokinetic machines using axial blades rather than 45° vanes as a reference, making the increase more marked.

5.2.3 Vane Number and Thickness

The effect of vane design on dynamometer performance is very important. Mitsuhashi et al [4] report the elimination of a serious vibrational problem in a Froude type dynamometer being achieved by increasing the number of rotor vanes by one. Their analysis shows the cause of vibration to be due to the combination of rotor and stator vane numbers. Ideally to avoid such problems the number of stator vanes should be one less than rotor vanes, with one of the numbers being a prime number (Rao).

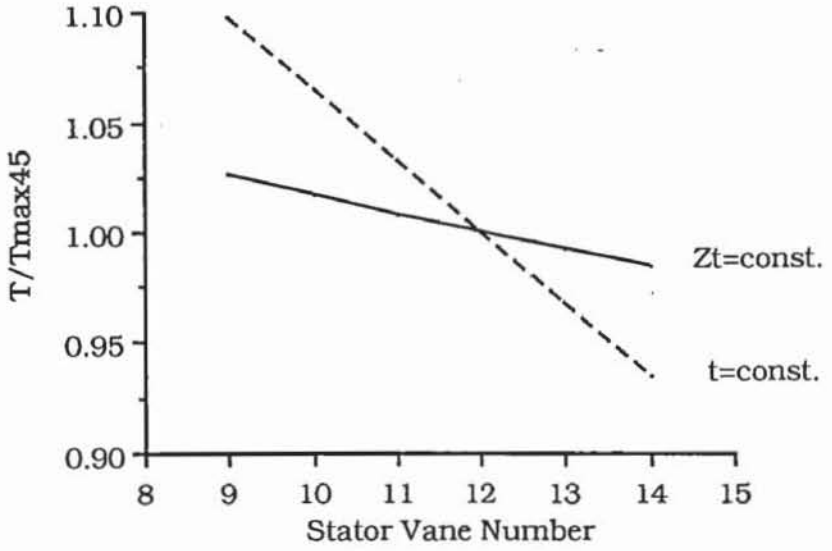

Figure 5.7: Effect of Vane Number on Torque Capacity

However Froude F type dynamometers generally have 14 rotor and 12 stator vanes. This arrangement results in approximately the same vane blockage for both rotor and stator, while allowing thicker stator vanes to accommodate the water inlet holes. Therefore the current study uses a difference of two while considering the effect of vane number and thickness on torque capacity. If the vane blockage factor[2] is held constant a slight increase in torque with decreasing

---

2 Vane blockage factor = vane number x vane thickness

vane number is shown in Fig.5.7. A much greater increase with decreasing vane number is indicated if a constant vane thickness value is used. In the first case the lower vane numbers result in a lower friction loss (linearly proportional; Section 2.5.2) and thus a higher torque. Holding the thickness constant results in decreased vane blockage as vane number decreases. Hence there is more area for mass flow leading to increased torque. In practise this increase would be reduced by an increase in secondary circulation losses as the vane number decreases, due to the fluid flow path deviating further from the ideal. A definitive conclusion can not be made on the resultant effect without experimental data, which is not presently available.

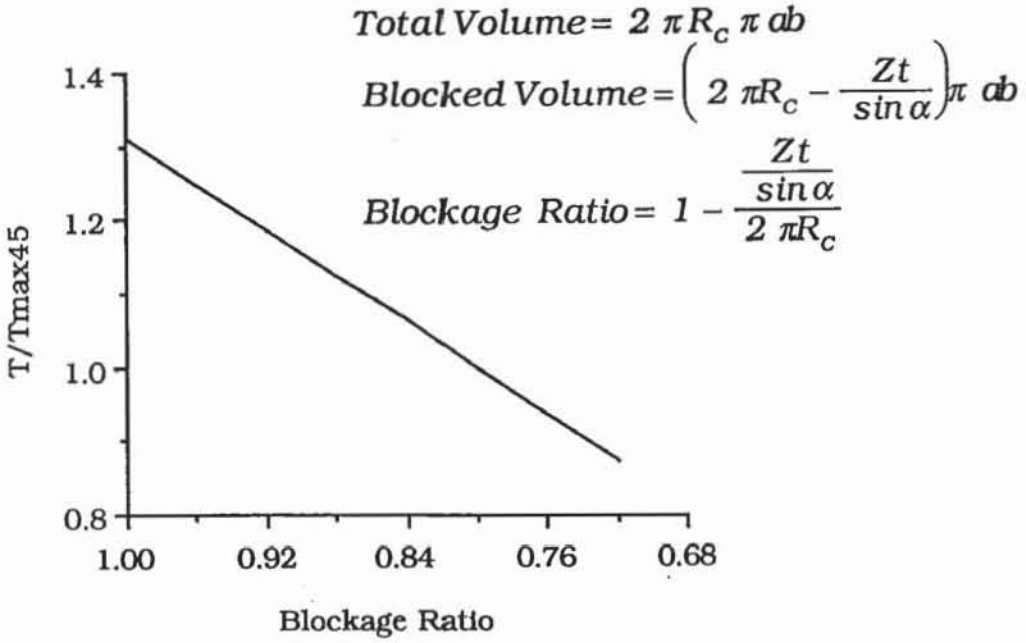

Figure 5.8: Effect of Vane Thickness on Torque Capacity

Given fixed vane numbers the effect on torque capacity of vane thickness is illustrated in Fig.5.8. Sivalingam [33] states that blade thickness is negligible for fluid couplings (thickness approx. 1.5 mm), however dynamometers have a minimum casting thickness of 4 mm (F24) and older machines use 5 mm (F020) or thicker vanes. Rao investigates the effect of blade thickness on his theoretical equations and deduces qualitatively that the torque capacity will decrease with increased vane blockage. In fact the difference in torque if vane thickness is ignored is 25-30%, which is very significant. Therefore vane thickness is an important consideration in hydraulic dynamometer design and is included throughout this work.

5.2.4 Surface Roughness

The stators and rotors of hydraulic dynamometers are cast, hence the surface finish has a noticeable effect on the torque produced by the machine. An appreciable increase in torque is obtained (Table 5.1) by the fettling and grinding (0.0127 mm roughness finish) of the as sand cast (0.127 mm roughness finish) machine elements. Later machines are produced by investment casting (0.003 mm roughness finish) resulting in further gains. Although torque increases more than linearly with decreasing surface roughness (Fig.5.9) the effort and cost of achieving very smooth surfaces places practical limits on the obtainable gains.

ROUGHNESS (mm)	FRICTION FACTOR	TORQUE (Nm)	FRACTION OF $T_{0.0127}$
0.1270	.0305	1253	0.841
0.1016	.0287	1280	0.859
0.0762	.0266	1313	0.881
0.0508	.0239	1358	0.911
0.0254	.0201	1426	0.957
0.0127	.0171	1490	1.000
0.0015	.0112	1612	1.086

Table 5.1: Influence of Surface Roughness on Maximum Torque at 1500 rpm for a F020 Dynamometer

5.2.5 Working Fluid

Rao states that generally a high density low viscosity fluid is preferable, but that the influence of viscosity on torque capacity is small. This assertion is confirmed by the results in Table 5.2, where large changes in viscosity have only a small effect on the friction factor. In contrast the differences in density have a major influence on the torque produced. In addition to having high density and low viscosity, water's high specific heat capacity results in lower through-flow rates than for other fluids for a given power input.

FLUID	DENSITY (kg/m^3)	VISCOSITY (m^3/s)	FRICTION FACTOR	TORQUE (Nm)
WATER	998.2	1.14×10^{-6}	.02013	1425
AUTO TRANS. OIL	863.4	3.52×10^{-5}	.02014	1233
SAE 20W/50	891.4	1.58×10^{-4}	.02016	1272

Table 5.2: Influence of Fluid Density and Viscosity on Maximum Torque at 1500 rpm for a F020 Dynamometer

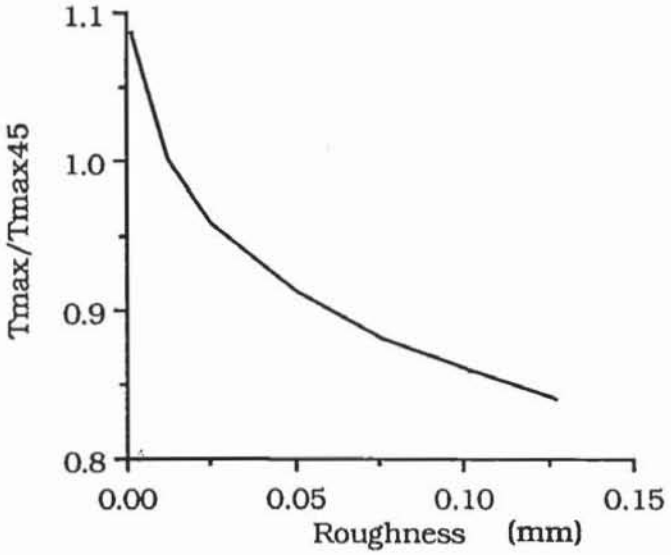

Figure 5.9: Effect of Machine Surface Roughness on Torque Capacity

5.3 Fluid Fill Variation

5.3.1 Fill Distribution Across Operating Envelope

For most of the time the variable fill type dynamometer is operating with its fluid fill less than 100%. Even accelerating up *the hydraulic maximum* curve is shown in Chapter 6 to be at less than full fill, so an appreciation of the variation of fill across the machine's operating envelope is vital to understanding the machine's behaviour. In Figs.5.10 and 5.11 lines of constant fluid fill are superimposed on Froude power against speed guarantee envelopes for the F020 full and cropped rotor dynamometers respectively. Similarly Fig.5.12 shows the F24 torque against speed guarantee envelope with constant fluid fill lines added.

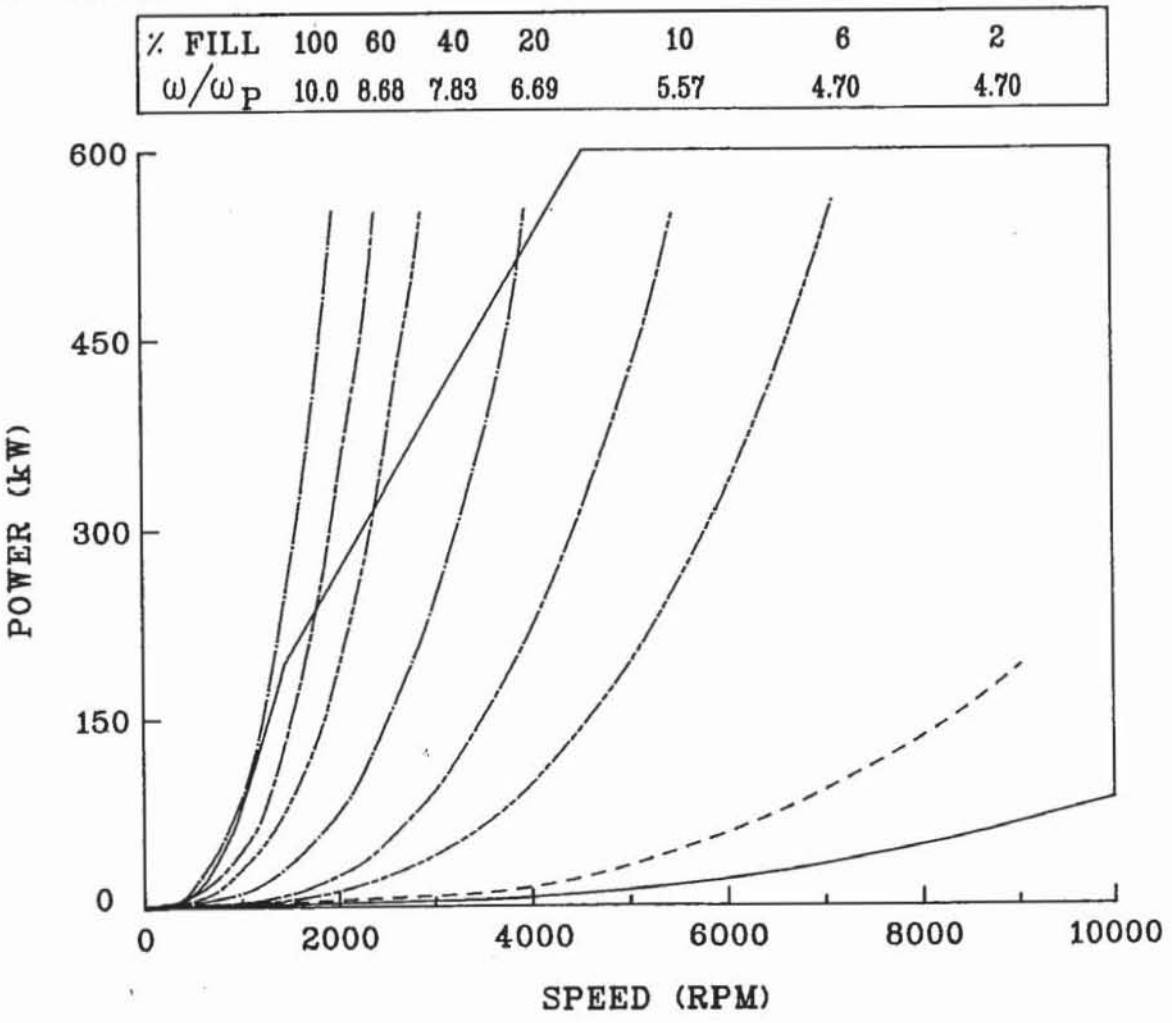

Figure 5.10: Distribution of Power Characteristics with Percentage Fill for F020 Dynamometer

The most notable characteristic of these illustrations is that the fill varies from 100% to 40% in a narrow band about the maximum guaranteed capacity line. Most of the operating envelope lies outside this band, so small changes of fluid fill in most operating regions mean

large movements from the desired set point unless carefully controlled. In the region of the maximum capacity the dynamometer is more *tolerant* of small fill variations, but the constant fill torque curves (Fig. 5.12) are much steeper in this region, so control requirements vary as the operating point moves around the operating envelope.

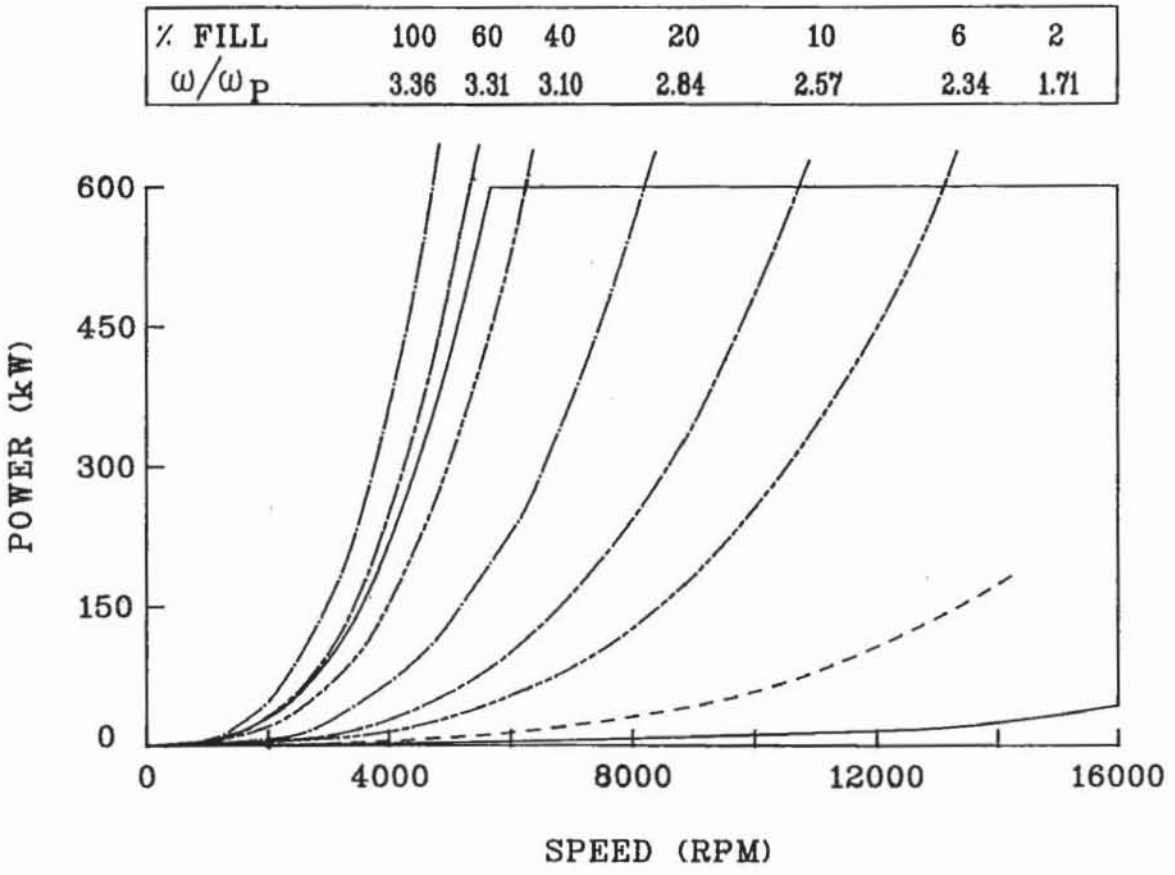

Figure 5.11: Distribution of Power Characteristics with Percentage Fill for F0209 Cropped Rotor Dynamometer

The high fill variation in the vicinity of the hydraulic maximum may account for the low values of torque Sivalingam presents in his comparison of theoretical and experimental values for a hydraulic retarder. Using the cited dimensions (R_o = 147 mm, R_i = 50 mm, t = 5 mm, α = 45°), lines of constant fill are presented in Fig.5.13 alongside Sivalingam's full fill line. Sivalingam's curves are scaled to allow for water (in the present work) rather than hydraulic oil as the working fluid; the ratio of torque capacities for water and automotive transmission oil of Section 5.2.5 is used for scaling. The results from Froude for the F0271 (R_o = 137.5 mm, R_i = 58.5 mm, t = 6.5 mm, α = 45°) and F24 (R_o = 121 mm, R_i = 51.2 mm, t = 4 mm, α = 45°) machines are also shown and indicate these two smaller machines

having greater torque capacity. Even allowing for the less than optimal proportions of the retarder (R_o/R_i = 2.94, refer Section 5.2.1), the author believes the experimental results supplied to Sivalingam to be either manufacturer guarantee figures or the result of acceleration tests, which can result in *maximum capacity* curves with less than 100% fill, as shown in Chapter 6. His predictions also exclude vane thickness effects, so are higher than they should be compared to the experimental data. Consequently, the secondary circulation loss constant used by Sivalingam for retarders is higher than that derived in Section 2.5.4 of this work.

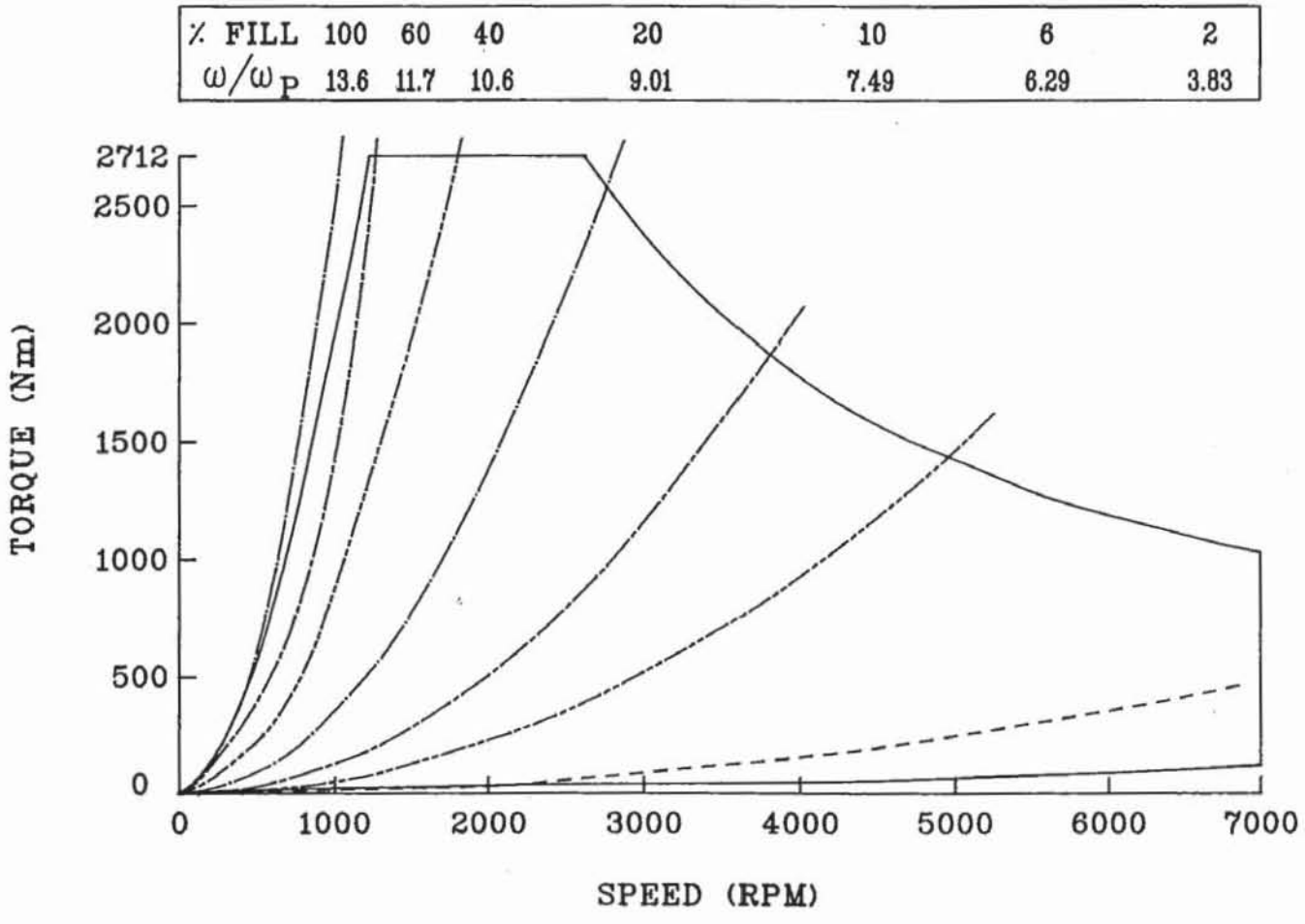

Figure 5.12: Distribution of Torque Characteristics with Percentage Fill for F24 Dynamometer

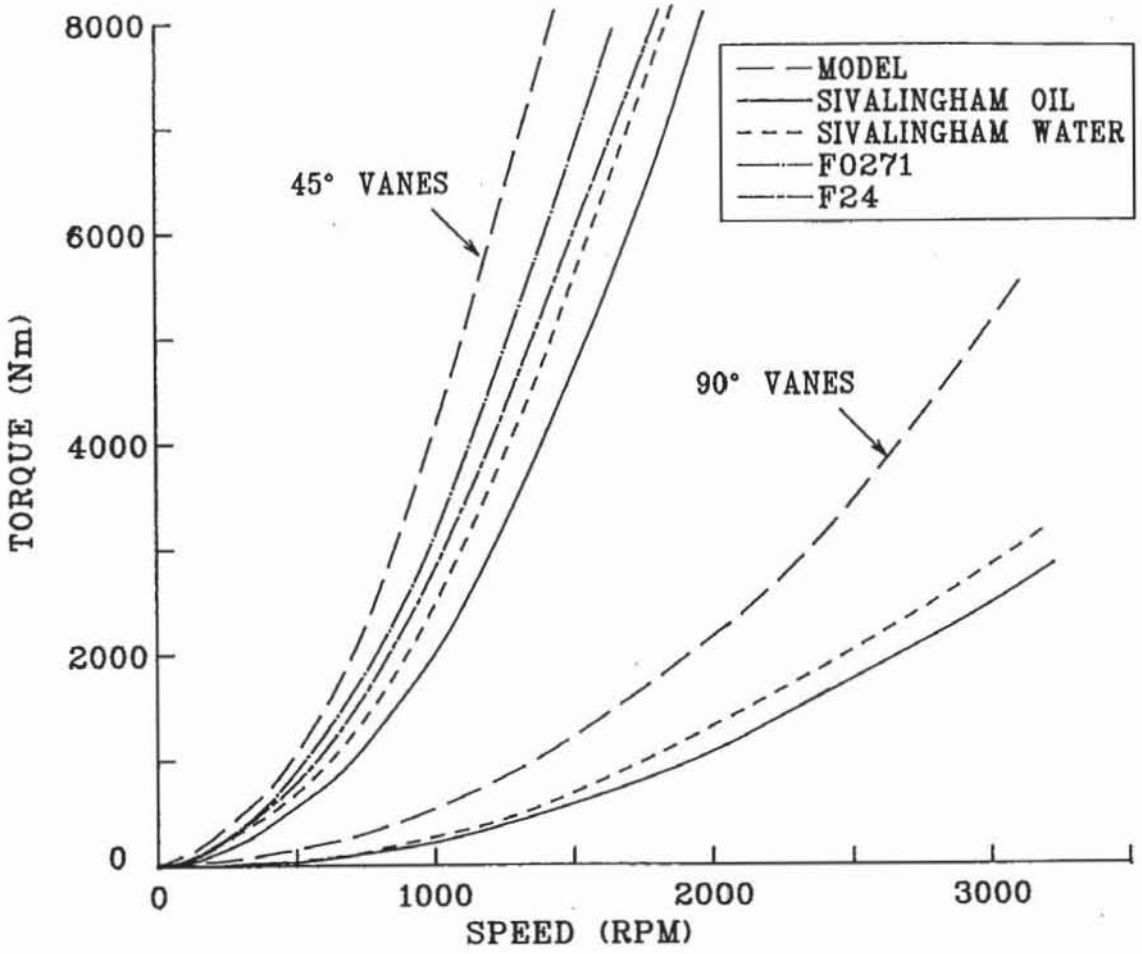

Figure 5.13: Comparison of Model Predictions with Sivalingam's Results for a Hydraulic Retarder

5.3.2 Fluid Velocity Distribution

The ratio of fluid angular vortex velocity to rotor speed (i.e. ω/ω_P) varies across the operating envelope with the percentage fluid fill (indicated in Figs.5.10, 5.11, 5.12). In Fig.5.14 this velocity ratio is plotted against fluid fill percentage. From 40% to 100% fill the variation of velocity ratio is almost linear. As shown in the previous section this range of fill only covers a small portion of the operating envelope. The decrease in velocity ratio is very rapid as fill decreases to zero. This variation of water velocity and therefore torque with fill contributes to the reduced speed index Raine reports for Froude design scaling (Section 5.2.1), as the highly aerated water in real machines is effectively lowering the percentage fill.

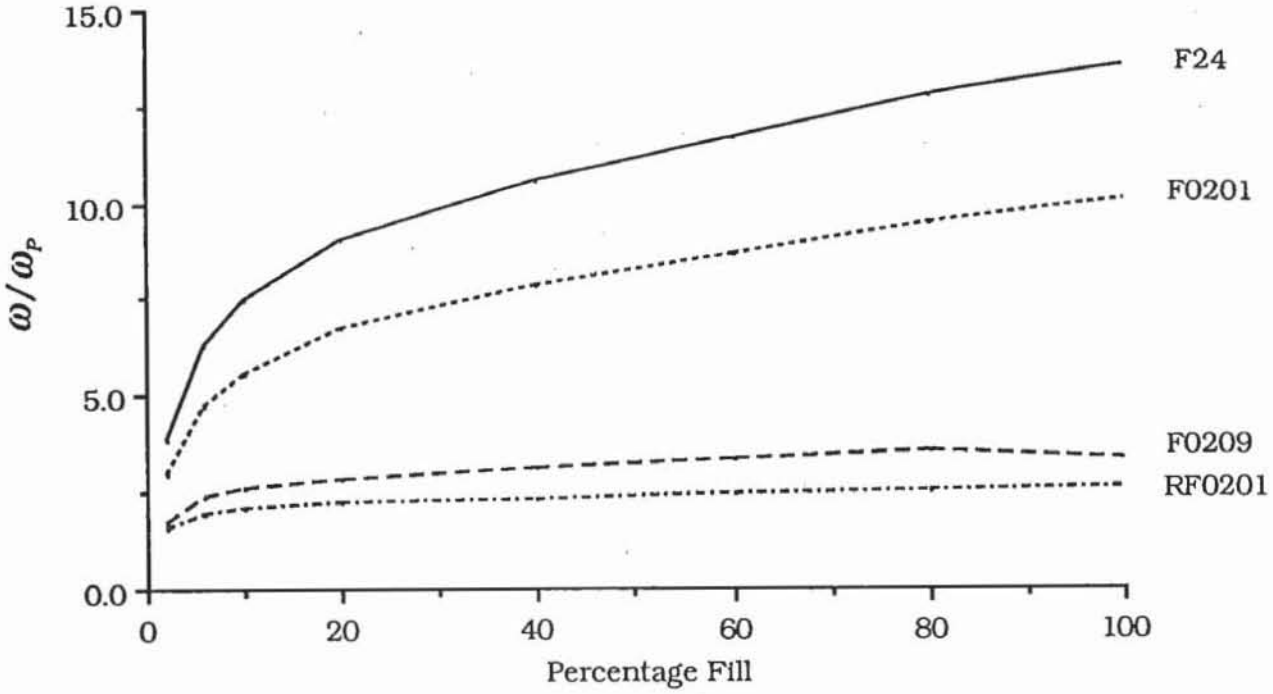

Figure 5.14: Variation of Water Velocity to Rotor Speed Ratio with Percentage Fill

At very low fills it is unlikely that the fluid in the working compartment is in a streamtube around the outside of the cups. More probably it is a spray circulating in a vortex, since even at a theoretical zero fill fluid is flowing into and out of the working compartment. Hence velocity ratio values at very low fill are taken only as indicative for the purposes of modelling machine torque. Similarly the values of air-water interface ratios (R_{co}/R_o and R_{ci}/R_o) at very low fill are not intended to be applicable to actual machines. However for modelling torque variation with fill, Fig.5.15 shows the variation of interface ratios with percentage fill for dynamometers with a R_o/R_i proportion of 2.36. Both F020 and F24 machines gave the same non-dimensional air-water interface radius against fluid fill characteristic.

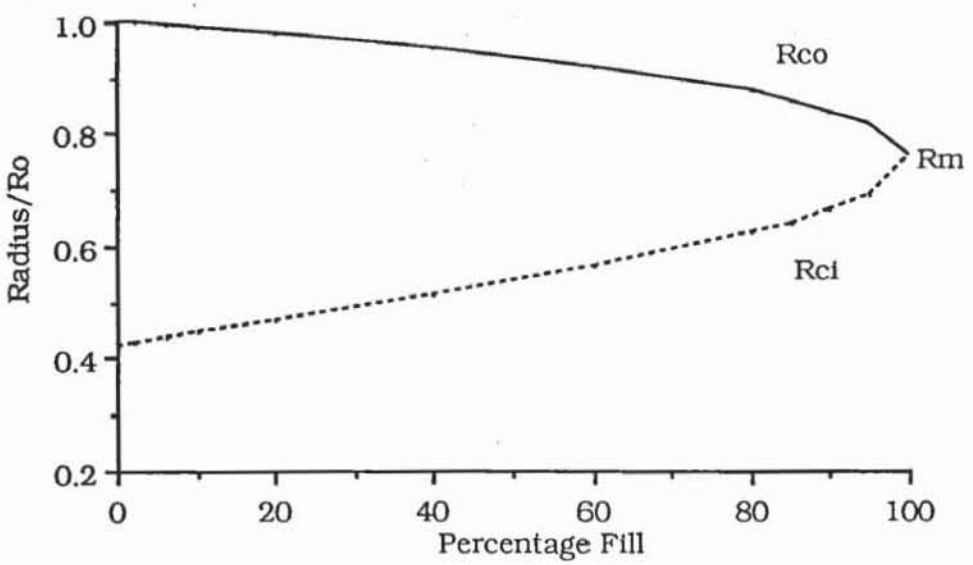

Figure 5.15: Variation of Air-Water Interface Radii with Percentage Fill

5.4 Pressure Variation

Using the pressure derivations of Section 3.2, the effect of changes in geometry, fluid fill and speed are investigated on the pressure at the cup surface in this section.

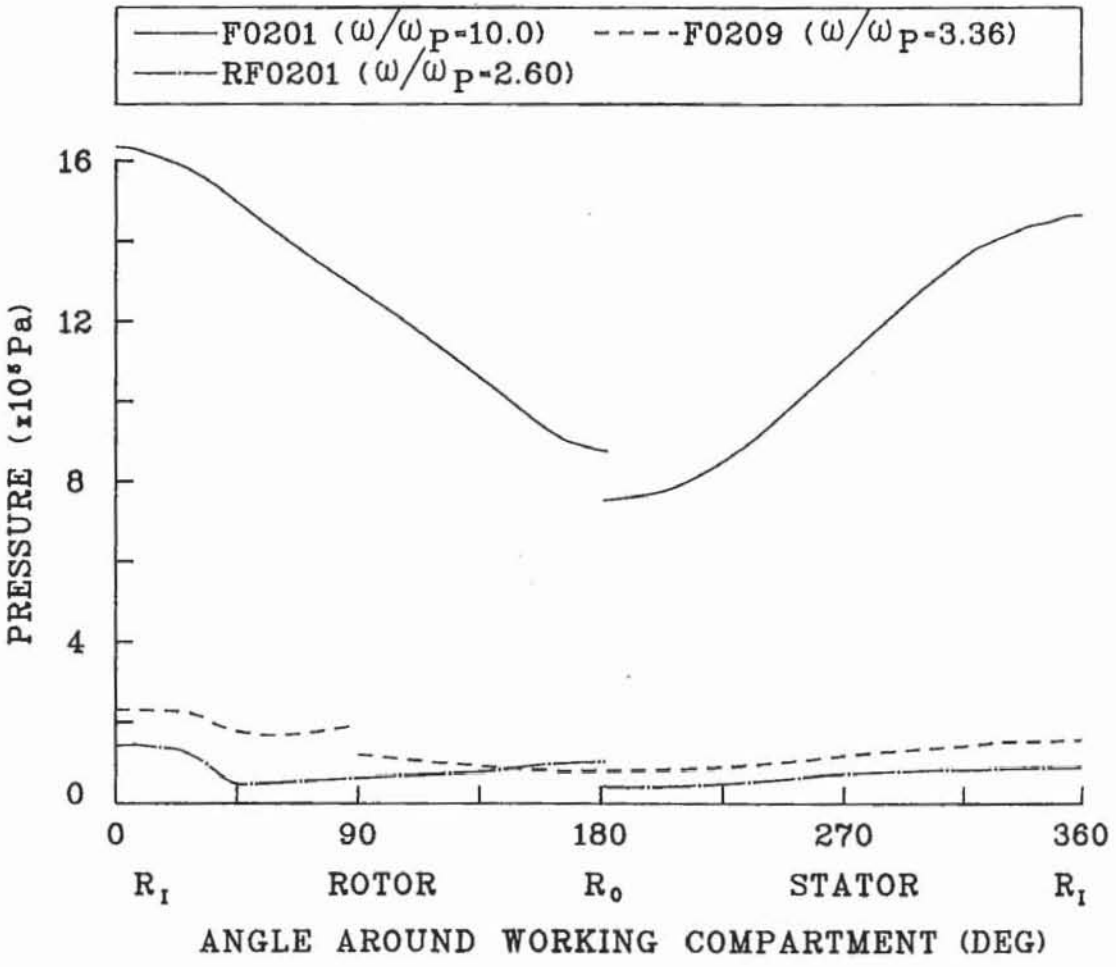

Figure 5.16: Fluid Pressure Distribution Around Working Compartment at 1500 rpm

5.4.1 Distribution Around Working Compartment

Intuitively the maximum fluid pressure in the rotor is expected at the outer radius, where the effect of machine rotation is the greatest. However as the fluid moves around the compartment the vortex action generates a greater pressure component at the inner radius of rotor

and stator. The result of this is shown in Fig.5.16[3]. For the stator pressures the smooth variation of the $\omega^2 \times r_v$ component[4] increases from the outer radius (180°) to the inner radius (360°). In the case of the rotor this is superimposed with a decreasing $\omega_p^2 \times r$ contribution towards the inner radius, giving a resultant pressure curve which is higher and more linear than that for the stator. Thus for the full rotor 45° vaned machine the maximum fluid pressures are predicted at the inner radius of the working compartment, as vortex velocity is approximately an order of magnitude greater than the machine rotational velocity.

The full rotor F0201 dynamometer has much higher working compartment pressure than the F0209 and RF0201 due to the much higher vortex velocity generated. With lower vortex to machine velocity ratios and altered geometry the cropped rotor and axial vaned machines display an initial decrease of pressure, due to the resultant vector products moving out of the pressure balance plane, around the rotor before it increases with radius to just below the value at the rotor inlet.

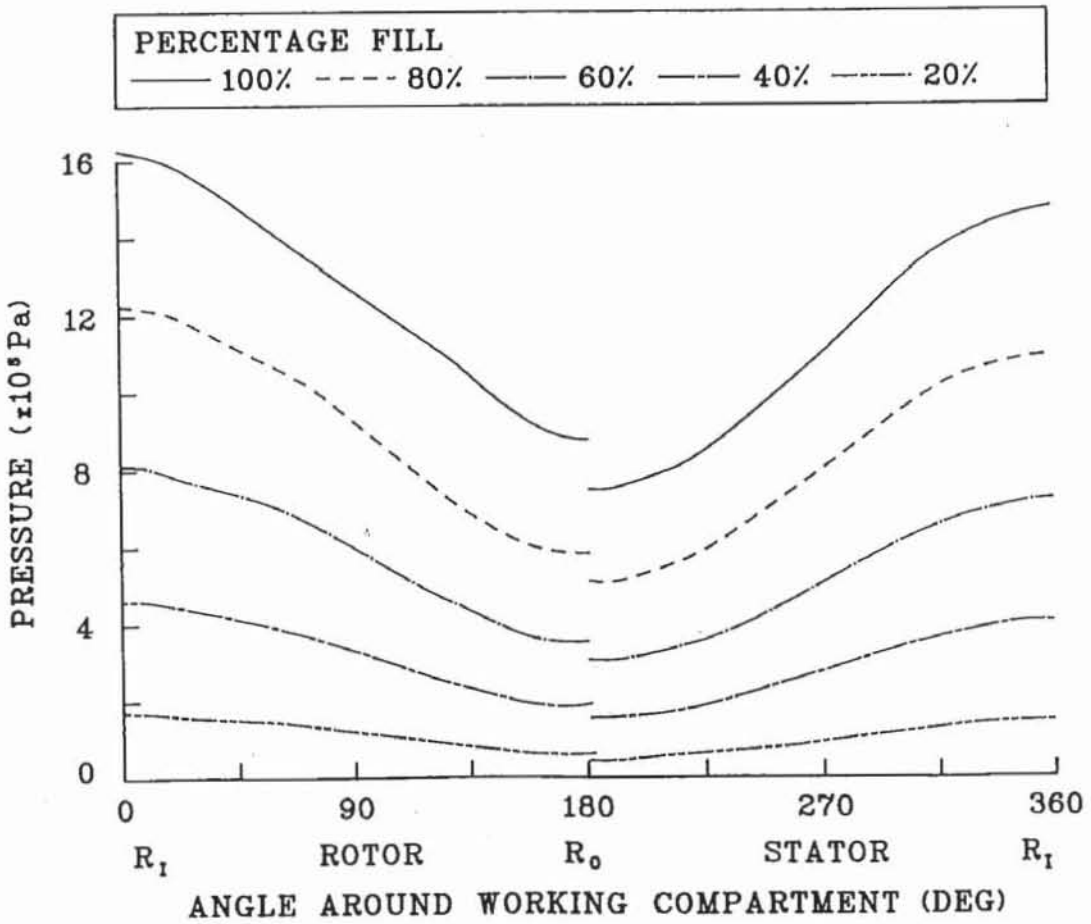

Figure 5.17: Variation of Fluid Pressure Distribution with Percentage Fill for F0201

---

3 The discontinuities between rotor and stator are in reality a more gradual change from one element characteristic to the other.

4 r_v is the distance from vortex centre to the point at which the pressure is being calculated, i.e. $(R_m - r)$

5.4.2 Pressure Variation With Fill

The characteristic pressure profile around the working compartment for the F0201 dynamometer is relatively unchanged as the level of fluid fill alters. Fig.5.17 shows a fairly even distribution of pressure profiles with varying fill. As the fluid fill decreases the pressure profile for the rotor resembles that for the stator more closely.

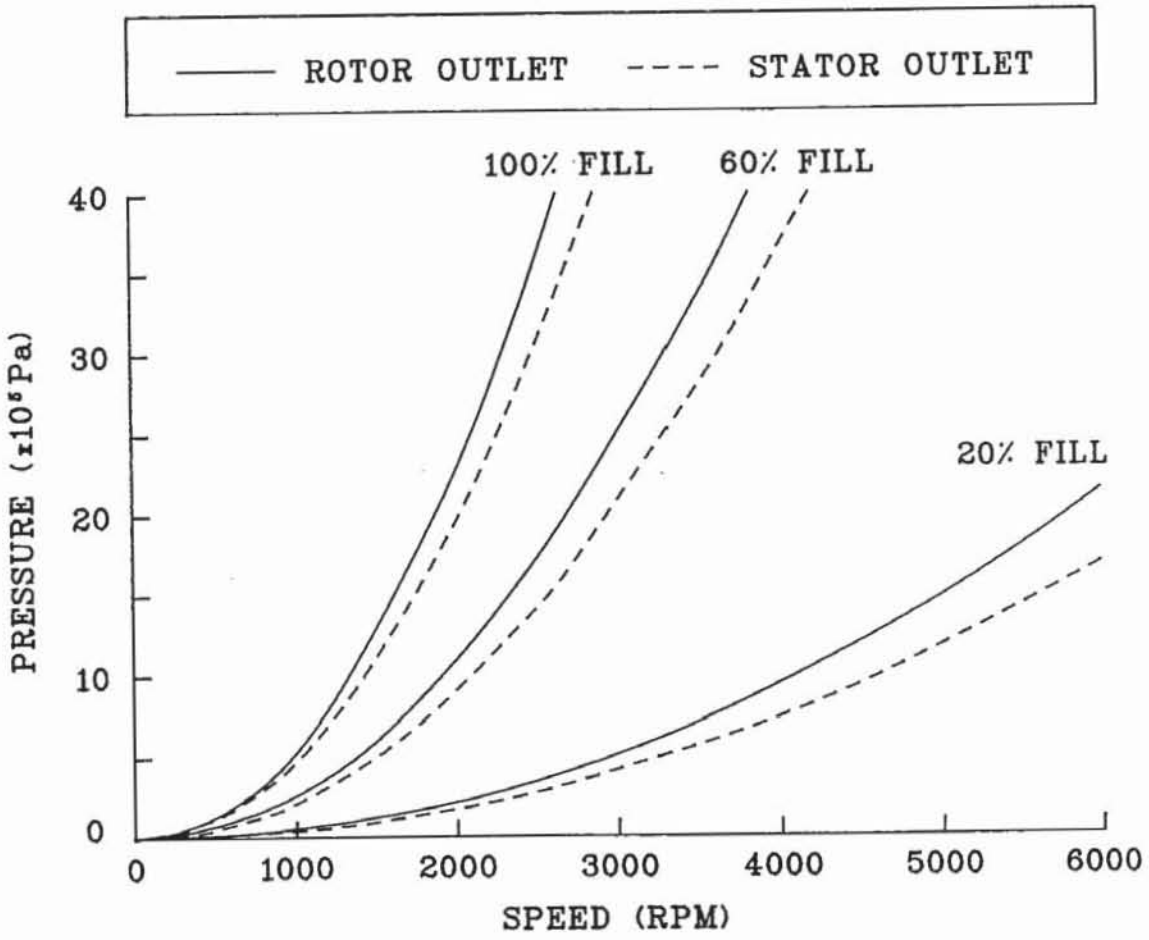

Figure 5.18: Fluid Outlet Hole Pressure Variation with Dynamometer Speed

The pressure at the water outlet hole in the dynamometer's working compartment varies with the square of speed (Fig.5.18), though the constant of proportionality decreases with fluid fill percentage. This figure also shows that the stator positioned water outlet holes have considerably lower fluid pressures in their vicinity than the rotor located holes in the F0201 machine. Hence there is less pressure to cause self-emptying if fluid outlets are positioned at the back of the stator cups. Another factor leading to the more stable behaviour of stator outlet machines over rotor outlet ones is that in all

dynamometers the water inlets are through the stator vanes into the vortex centre. The incoming water will therefore tend to join the rotor flow. A portion of the flow can be pumped out from rotor outlets without having to transfer angular momentum to the stator, resulting in a lower dynamometer absorption torque and a more pronounced self-emptying action.

5.5 Water Inflow Equals Outflow Mapping

Before incorporating the system dynamics into the model, the phenomenon of self-emptying is illustrated by mapping points at which the water inflow and outflow are equal. To find these points the fluid fill is taken as 100% until it is necessary to vary it at the given speed and machine parameter values to reduce the predicted water outflow rate to be equal to the set inflow rate.

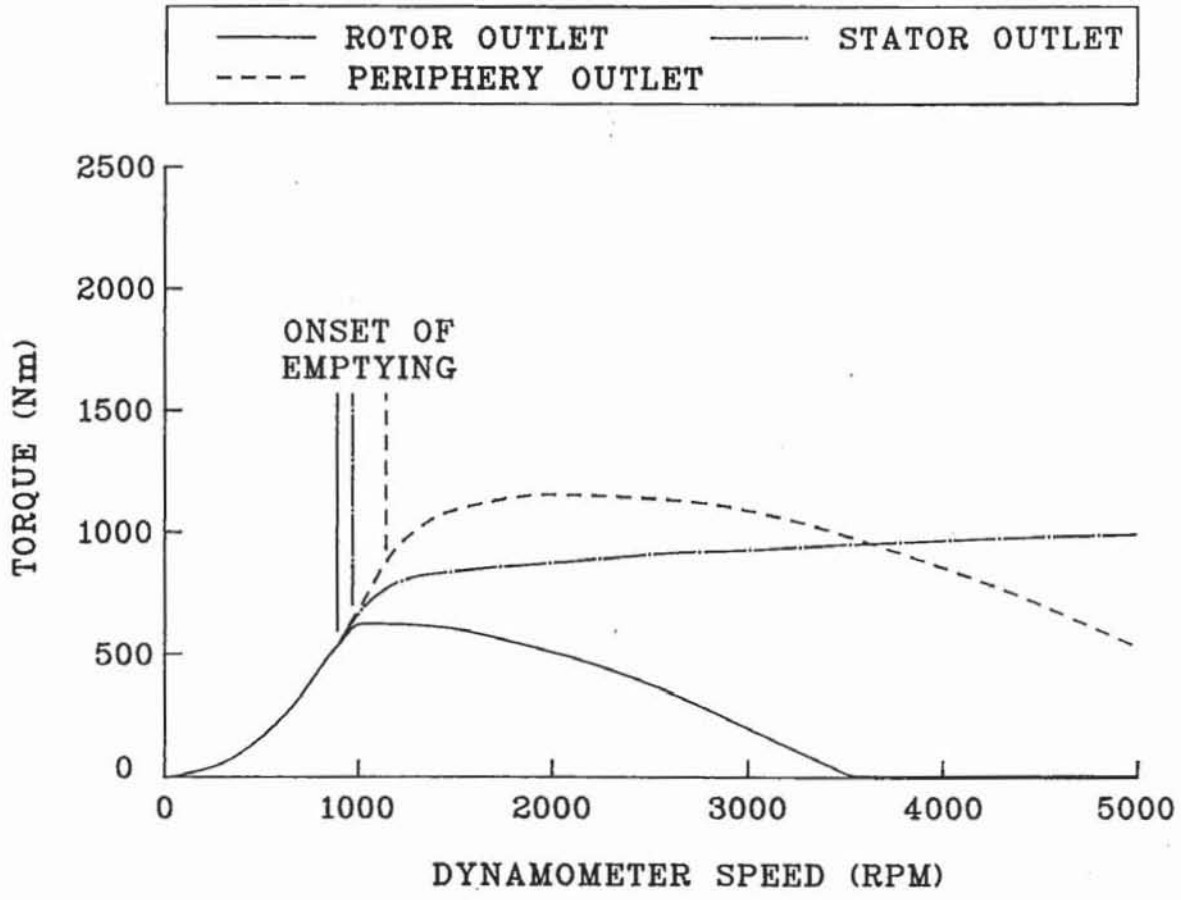

Figure 5.19: Dynamometer Torque-Speed Characteristics for Different Fluid Outflow Paths

5.5.1 Variation of Machine Parameters

In the previous section it is shown that the fluid pressure at the water outlet from the working compartment varies depending on the position of the outlet. The effect of this difference and the different outflow paths is shown in Fig.5.19. Both the curve for rotor cup outlet and that for cup periphery outlet display a falling torque characteristic, while the stator cup outlet shows a more stable torque curve. However

in all cases the fluid fill is decreasing with speed to maintain the water outflow rate equal to the inflow rate. Above each curve the fluid fill of the dynamometer would cause the outflow rate to exceed the inflow rate. Hence these curves are indicative of dynamometer behaviour, but in an actual test the machine has to be above the curves to have reducing fill. In Section 6 the dynamic dynamometer simulation illustrates this point.

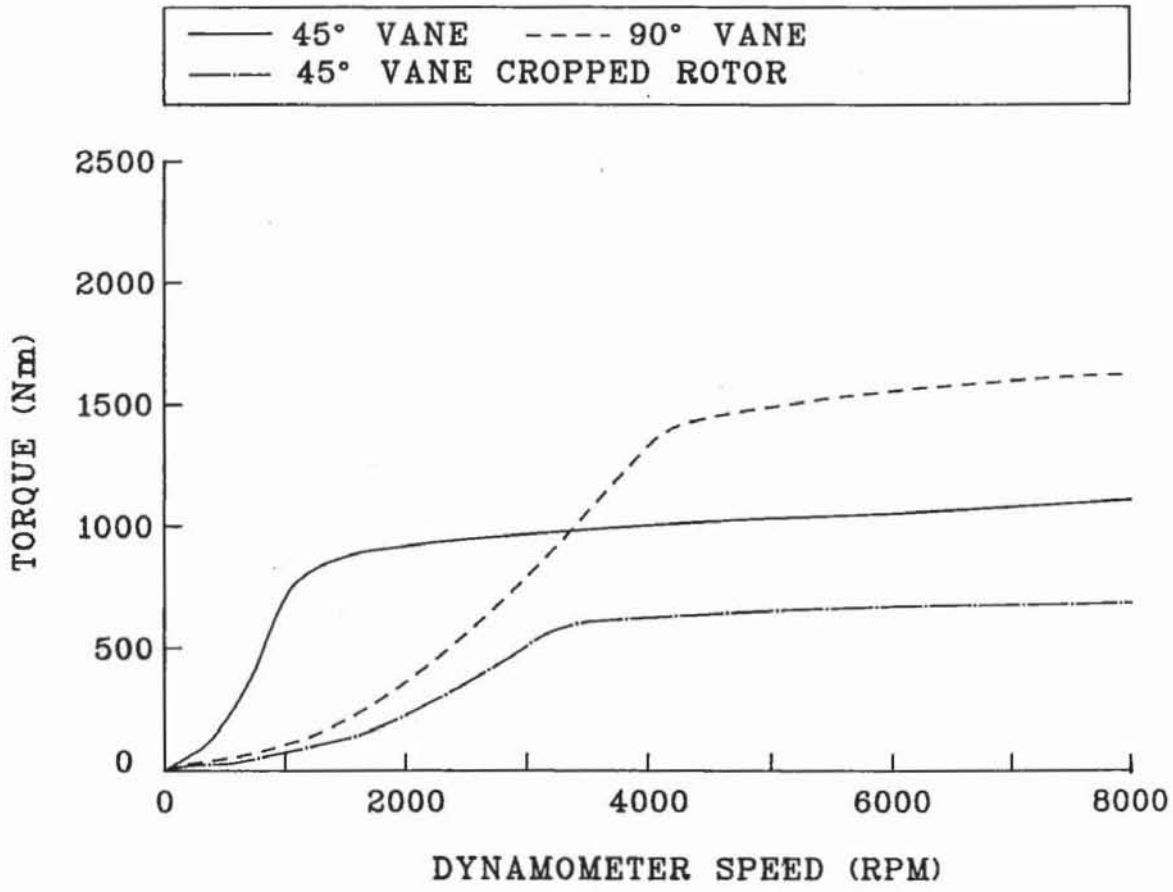

Figure 5.20: Dynamometer Torque-Speed Characteristics for Different Internal Machine Geometry

Using the same stator outlet hole position the behaviour of three dissimilar dynamometers is investigated in Fig.5.20, under identical test conditions. All the curves show a similar shape, but the axial vaned and cropped rotor machines have a much higher speed at which the fill begins decreasing to equalise the flow rates. That is, the rising maximum torque curve flattens out.

5.5.2 Variation of Water Flow Parameters

The dynamometer steady state characteristic is also affected by the closure of the water outlet valve and the water inflow rate. As the percentage valve closure[5] increases the map of outflow equal to inflow points moves to higher torque values and the speed at which fluid fill level begins decreasing is greater (Fig.5.21). At the given water inflow rate of 0.00505 m^3/s (4000 gph), which is the maximum for the F0201 machine, the higher valve closure maps are outside the dynamometer's guaranteed operating envelope as would be expected. However the values given by Tan put the map for 50% valve closure outside this envelope. Tan's higher valve closures predict excessively high torque values for this machine, which suggests either excessive outflow resistance through his valve model or a problem with his prediction of the speed at which cup emptying begins. This hypothesis is supported by the dynamic simulation of Section 6 and Tan's own quasi-dynamic simulation, where it is shown that the effect of acceleration on the self-emptying phenomenon is that the dynamometer torque characteristic increases beyond the steady state inflow equal to outflow to significantly higher torque/speed points before cup emptying begins. Thus if the Froude guaranteed operating envelope for the dynamometer incorporates actual dynamic operational performance the steady state theoretical predictions should fall within the envelope.

Similarly in studying the effect of increased water inflow rate (Fig.5.22) the torque curves of Tan's model are found to be excessively high compared to the machine operating envelope. His curves were produced for an outlet valve closure of only 60%, which is relatively low when the distribution of outflow resistance with valve closure is considered (Section 3.3). Tan's characteristic for a flow rate of 0.003786 m^3/s (3000 gph) is presented with the F0201 operating envelope and several characteristics for different flow rates from this simulation. As the inflow rate increases the dynamometer reaches a higher speed and torque at full fill before cup emptying occurs to maintain outflow equal to inflow. In reality dynamometers accelerate up a *maximum hydraulic* line lower than the 100% fill line, depending on the water inflow rate and valve closure, due to the dynamic effects of

---

5 Percentage valve closure is the percentage of valve travel from the fully open position to the fully closed position.

the acceleration run. A comparison of steady state, dynamic and experimental performance is made in Section 6.3.

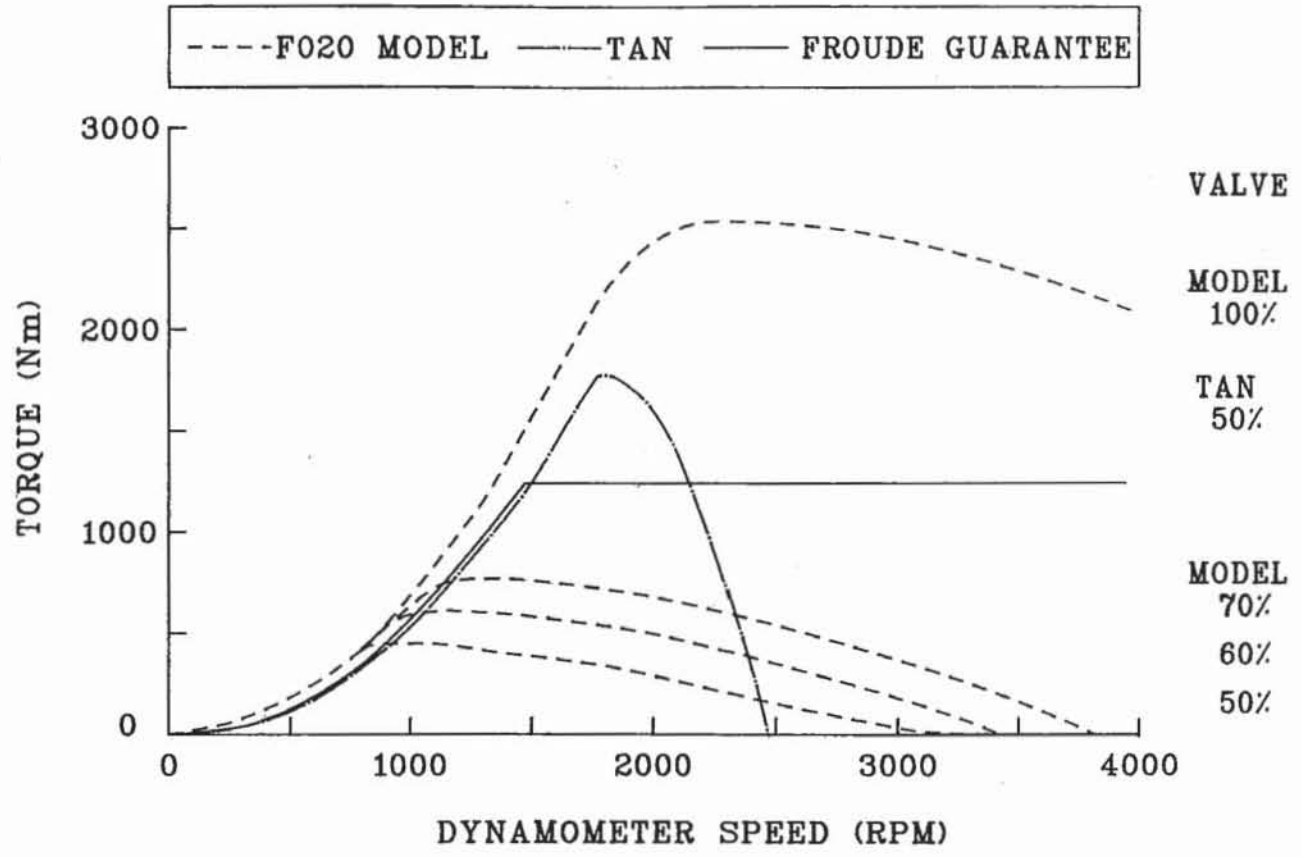

Figure 5.21: Valve Closure Effect on Torque-Speed Characteristic

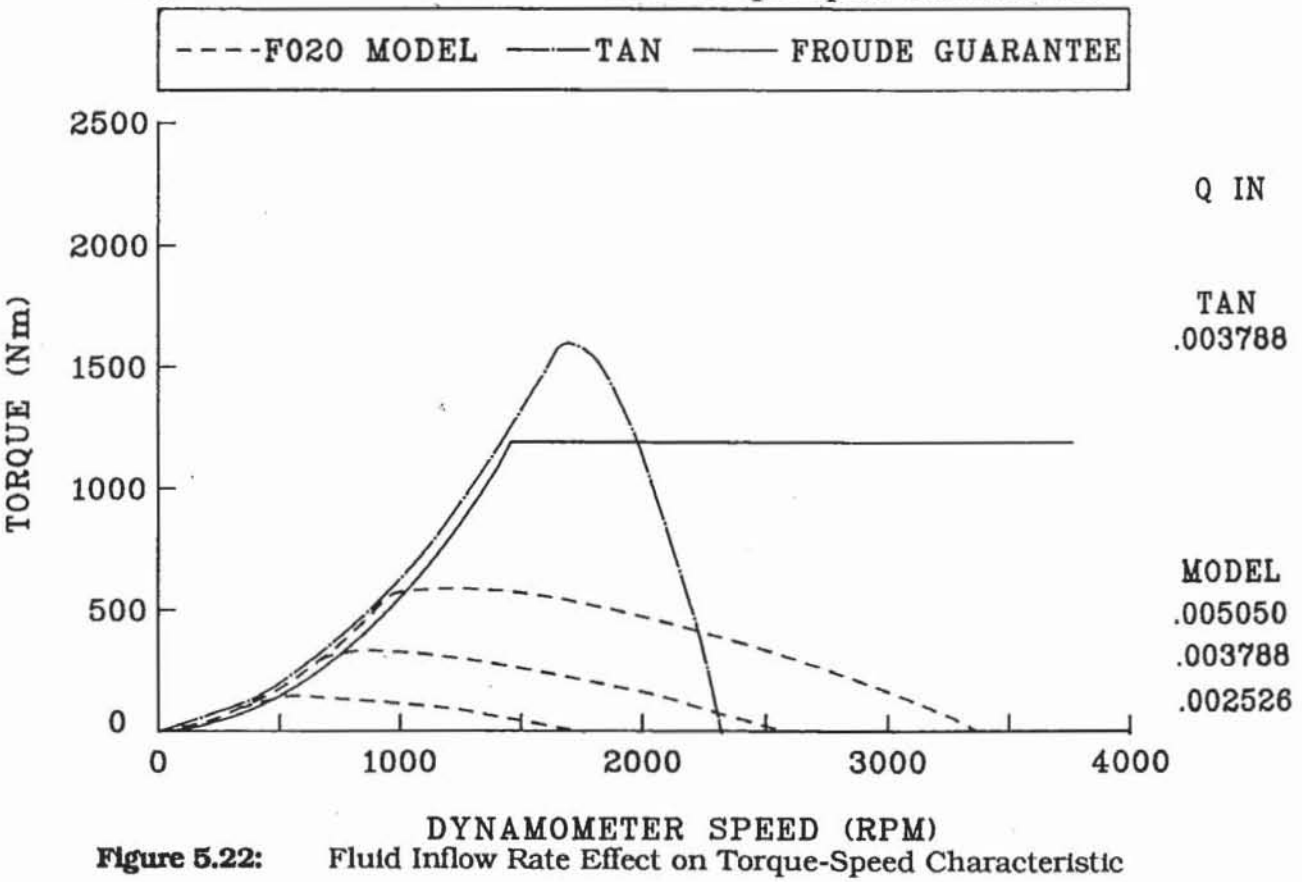

Figure 5.22: Fluid Inflow Rate Effect on Torque-Speed Characteristic

CHAPTER 6
DYNAMIC OPEN LOOP SIMULATION

6.1 Engine - Dynamometer System

6.1.1 Introduction

The steady-state investigation of hydrokinetic machines is very useful for comparative performance prediction of different machine geometries as in the previous chapter. However the influence of machine dynamics makes such models of limited value when considering machine responses to varying inputs and controller requirements. Hydraulic dynamometers are frequently used for transient testing of engines due to their low inertia to torque capacity ratio, so the inclusion of rotational dynamics is vital for both machine simulation and controller design.

Tan [7] presents a quasi-dynamic model which includes the rate of change of fill with time, but only operates at constant speed or acceleration excluding the inertial effects of the dynamometer. While this model illustrates the difference between static *inflow equals outflow* simulations (Section 5.5) and accelerating runs, it is inadequate for controller design. Tan recommends the inclusion of machine dynamics and the derivation of dynamic mathematical representations for torque and pressure to allow accurate dynamic analysis.

Ishihara and Emori [42] use a mean flow path analysis to study the transient response of torque converters. They solve the equations of motion numerically for slow transient phenomena and linearize the equations for perturbations about a steady state operating point. If external disturbances are at a rate of less than one pulse per two revolutions they find that the fluid inertia can be neglected. When considering a four-stroke combustion engine in the system this frequency threshold corresponds to the torque fluctuations of an engine with only one cylinder. Hence the fluid inertia should be included in an engine-hydraulic dynamometer model.

Hrovat and Tobler [46] also use a mean flow path approach, but include an unsteady torque representation for their bond graph model of a torque converter. This torque equation includes the fluid inertia,

but as with other torque converter and fluid coupling work does not have to allow for varying fluid fill in the working compartment. The effect of variable fill is that the torque equation is not only non-linear with speed (usually a squared relationship) but also with fluid fill level, itself a function of speed, acceleration and water outlet valve closure.

In order that the behaviour of the dynamometer model is consistent with experimental performance data the dynamics of an engine must be included as part of the overall system. Consequently the dynamic dynamometer representation includes an engine as an idealised power source capable of uniform, stepped, ramped, sinusoidal or other prespecified torque and speed characteristics. More complex engine models, involving the thermo and gas dynamics and engine control systems, have been developed. Benson [57] provides a theoretical base for such models, while Horlock and Winterbone [58] apply the theory to various situations. A specific example of this theory is utilised by Winterbone and Jai-In [59] for a variable geometry turbocharged diesel engine. Other models include the spark-ignition model of Dobner [60] and the diesel models of Tsai and Goyal [61], Kanamaru et al [62], and Jennings et al [63]. Such detailed engine modelling is outside the scope of the present work, which is specifically directed at the characterisation of hydraulic dynamometer performance.

6.1.2 Engine-Dynamometer System

In Fig.6.1 the engine-dynamometer system is modelled as a two rotor system connected by a flexible drive shaft of torsional stiffness k. Engine torque is the forcing function for the system, though engine speed can also be manipulated to represent engine speed control. The dynamometer is represented as a rotary power dissipator (damper) with a non-linear reaction torque characteristic and variable fluid fill.

The equations of motion for the systems are

$$J_1\ddot{\theta}_1 = T - k(\theta_1 - \theta_2) \tag{6.1}$$

and

$$J_2\ddot{\theta}_2 = k(\theta_1 - \theta_2) - \tau \tag{6.2}$$

where

J_1 , J_2 = polar inertia of engine and dynamometer
$\ddot{\theta}_1$, $\ddot{\theta}_2$ = angular accelerations of engine and dynamometer
k = shaft torsional stiffness
T = engine torque
τ = dynamometer torque

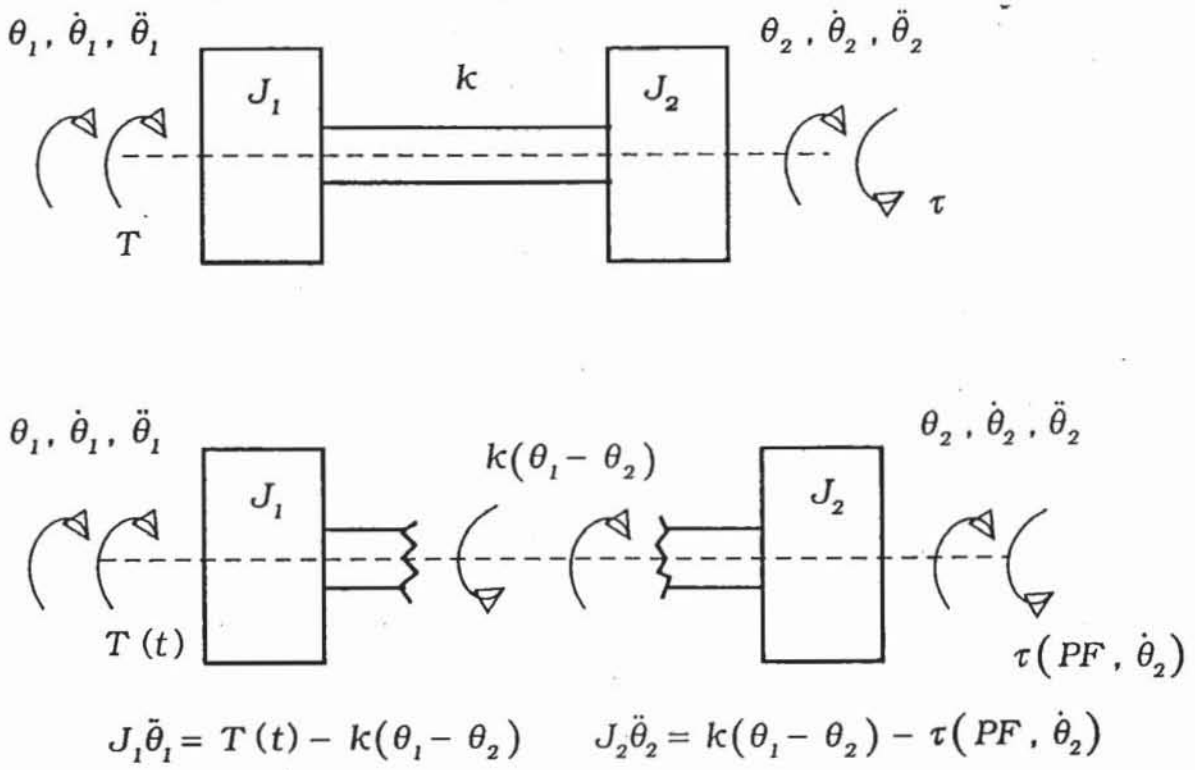

Figure 6.1: Two Rotor Representation of Engine-Dynamometer System

To simulate variable fill the equation governing the fluid fill percentage is derived in Section 3.1,

$$\frac{\partial}{\partial t}(PF) = \frac{\rho\, Q_{IN} - \rho\, Q_{OUT}}{M_F} \tag{3.7}$$

As the absolute angular displacements of the engine and dynamometer rotors are not of interest, only the relative displacement between them, the following identity is substituted into Eqns.(6.1) and (6.2),

$$\delta = \theta_1 - \theta_2 \tag{6.3}$$

A system of n^{th}-order differential equations is usually converted into a system of first-order equations to facilitate numerical solution, Johnson and Riess [52].
Therefore

$$\dot{\theta}_1 = \omega_1 \tag{6.4}$$

and

$$\dot{\theta}_2 = \omega_2 \tag{6.5}$$

are substituted into Eqns.(6.1) and (6.2) to yield

$$J_1 \dot{\omega}_1 = T - k\delta \tag{6.6}$$

and

$$J_2 \dot{\omega}_2 = k\delta - \tau \tag{6.7}$$

To solve these equations it is simpler to solve the time derivative of Eqn.(6.3) for δ than both Eqns.(6.4) and (6.5). Thus Eqn.(6.3) becomes

$$\dot{\delta} = \omega_1 - \omega_2 \tag{6.8}$$

By assuming the density of the operating fluid, usually water, to be constant throughout the dynamometer the change of fill equation, Eqn.(3.7) becomes

$$\frac{d}{dt}(PF) = \frac{1}{V_F}(Q_{IN} - Q_{OUT}) \tag{6.9}$$

where

V_F = maximum volume of fluid in the working compartment

Hence the engine dynamometer system is represented by four first-order differential equations,

$$\dot{\delta} = \omega_1 - \omega_2 \tag{6.8}$$

$$J_1 \dot{\omega}_1 = T - k\delta \tag{6.6}$$

$$J_2 \dot{\omega}_2 = k\delta - \tau \tag{6.7}$$

$$\frac{d}{dt}(PF) = \frac{1}{V_F}(Q_{IN} - Q_{OUT}) \tag{6.9}$$

The dynamometer torque τ is characterised in Section 2.4 as

$$\tau = K_1 \omega \omega_P + K_2 \omega^2 + K_3 \omega_P + K_4 \omega + K_5 \dot{\omega}_P + K_6 \dot{\omega} \tag{2.33}$$

The coefficients K_5 and K_6 represent the fluid inertia of the machine, which is a function of the fluid fill. It is shown in Section 2.2 that the fluid angular velocity is directly proportional to rotor angular velocity, so to incorporate Eqn.(2.33) into Eqn.(6.7) the fluid angular acceleration ω is taken as proportional to the rotor angular acceleration. Hence,

$$\tau = \tau_{14} + (K_5 + fn(K)\, K_6)\, \dot{\omega}_2 \qquad (6.10)$$

where

$$\tau_{14} = K_1 \omega \omega_P + K_2 \omega^2 + K_3 \omega_P + K_4 \omega$$

$fn(K)$ = geometric and fill dependent proportionality between fluid and rotor accelerations

Thus Eqn.(6.7) becomes

$$J_2^{'} \dot{\omega}_2 = k\,\delta - \tau_{14} \qquad (6.11)$$

with

$J_2^{'}$ = dynamometer rotor + fluid inertia

6.1.3 System Block Diagram

The system of first-order differential equations from the previous section is presented in block diagram form in Fig.6.2 to portray the non-linear interdependence of the system variables and how the feedback system acts to control the outputs. In this diagram the three physical system elements (engine rotor, shaft dynamometer rotor) and their interactions are discernible.

The engine rotor receives a torque input from the idealised power source and a torsional feedback from the shaft, which multiplied by the rotor inertia gives the angular acceleration. By integrating this variable the angular velocity of the engine is obtained. Another integration results in the angular displacement, which is passed on to the shaft. This displacement is compared with that of the dynamometer rotor by the shaft.[1] The displacement difference is passed as feedback to the engine rotor, and the driving torque transferred to the dynamometer rotor.

Several different inputs act on the model of the open loop dynamometer: driving torque from the shaft; water inflow rate; and outflow valve position. These inputs result in several outputs: dynamometer speed; dynamometer torque; and water outflow rate. However, it is not possible to obtain a simple transfer function across the dynamometer as the torque, water pressure and water outflow elements are very non-linear. Rather than linearize these three elements and lose much of the inherent character of machine

---

1 The shaft is modelled as an ideal torsional spring, so the stiffness of the couplings is combined with that of the shaft, and the rotational inertia of the shaft is included in the dynamometer inertia.

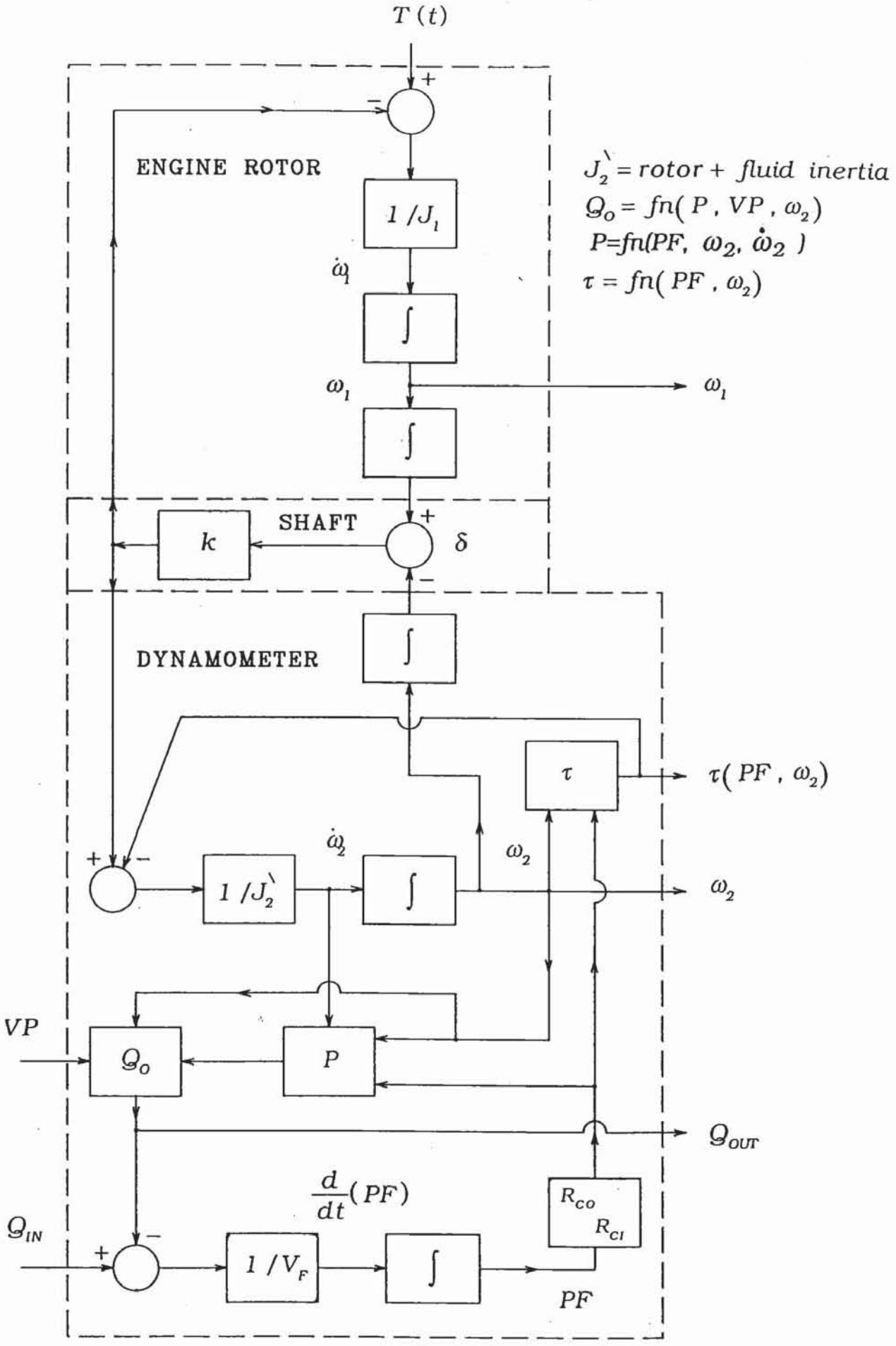

Figure 6.2: Block Diagram of Open Loop Engine-Dynamometer System

behaviour in a transfer function representation, these elements are retained and the system of differential equations solved in terms of the variables δ, ω_1, ω_2, PF. In practise the percentage fluid fill, PF, can not be measured, and the relative angular displacement, δ, would be very difficult to measure, so they are not shown as outputs of the system block diagram, whereas dynamometer torque and water outflow rate are tangible quantities.

The dynamometer is accelerated by the difference between the shaft driving torque and the fluid reactive torque. This acceleration and the rotor velocity, contribute to the pressure function and subsequently water outflow function, as do the fluid fill percentage and the outflow valve position. The value of fluid outflow is compared with the inflow rate to obtain the rate of change of fluid fill. Thus the fluid fill is determined, which contributes to the other non-linear element, the torque function. The interdependence of variables is apparent through several different loops.

It is obvious from Fig.6.2 that the only inputs which are directly alterable to control the dynamometer torque or speed outputs are the outflow valve positions (changing the water outflow rate) and the water inflow rate. These two methods are discussed in Section 1.1. In subsequent chapters dealing with closed loop dynamometer behaviour the feedback systems adjust the outflow valve position to effect control of the machine.

6.1.4 Program Implementation

Unlike the steady state simulation the dynamic simulation progresses from one time point to the next, so the values of machine speed and percentage fill are determined by the system of differential equations (Section 6.1.2, Subroutine F), and not predefined by the program input parameters. The machine performance kernel is the same as in Chapter 5, however now it is used to evaluate the dynamometer response at each time point and thus the values of the differential equations. These numerical values are used to solve the system of equations forward in time, as described in the following section. The kernel is also used to ensure that the set of initial conditions for the differential equations is consistent. In Fig. 6.3 the overall structure of the simulation is shown. Both the machine

performance kernel and the subroutine to calculate any time dependent constants (Subroutine STATUS) are called from within the equation solver (Subroutines DDE, DSTEP, DINTRP).

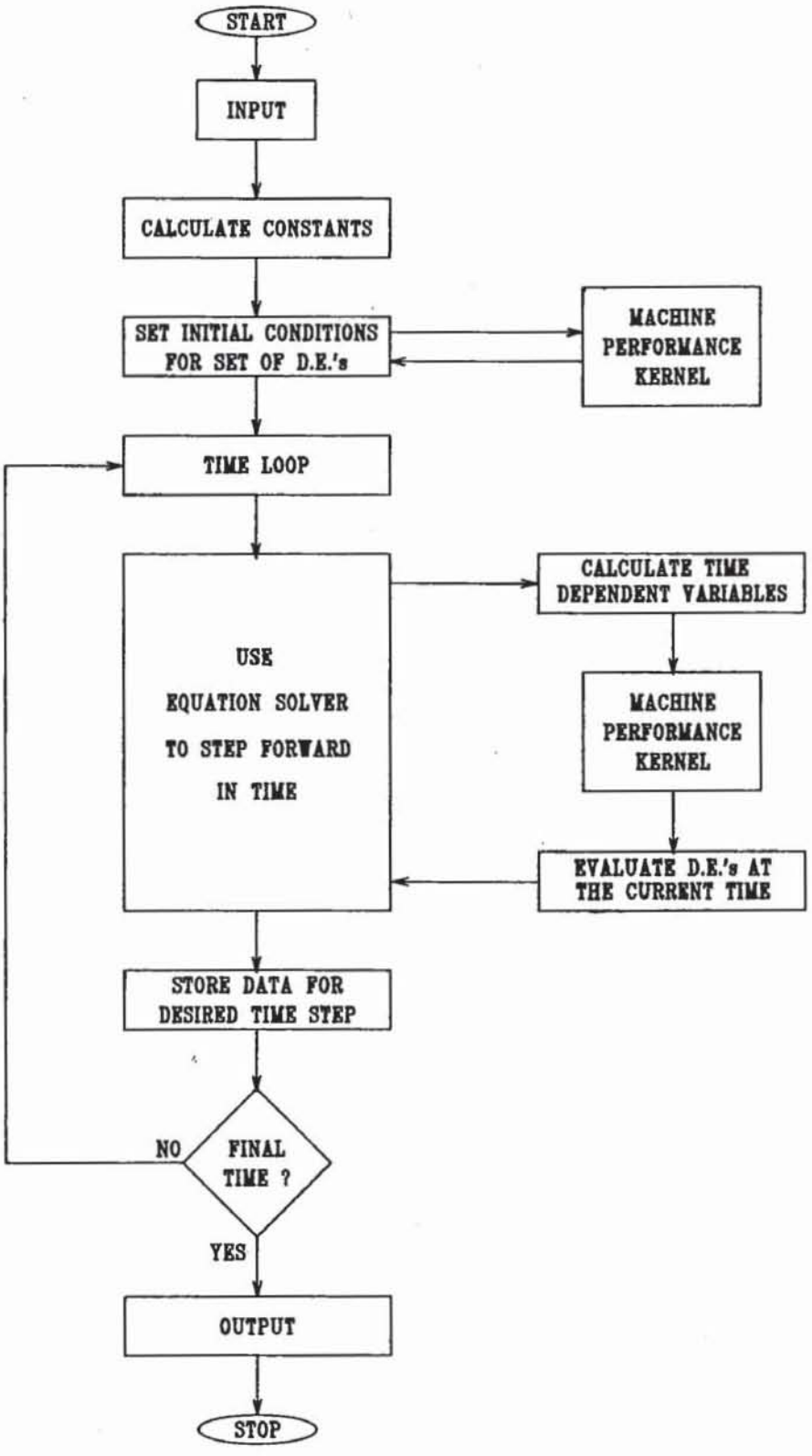

Figure 6.3: Structure of Open Loop Dynamic Program

6.2 Numerical Solution of Differential Equations

The system of differential equations, which model the engine dynamometer system, is a typical example of an initial value problem. Given the initial state of the system, the aim is to predict the value of the variables as time progresses. Due to the non linear nature of the system of equations, the solution is beyond the bounds of analytical analysis. Therefore numerical methods are used to solve the equations. Specifically, the Adams-Bashforth Predictor Adams-Moulton Corrector Method as presented by Shampine and Gordon [47]. These subroutines are incorporated with the dynamometer theory of earlier chapters to characterize the dynamic performance of the system.

A detailed description of these standard numerical methods is inappropriate for this thesis, but is readily available in Shampine and Gordon [47], Johnson and Riess [52], or any numerical analysis text. However a brief conceptual outline is presented below.

The basis of this numerical approach is to approximate with polynomials the functions which define the system variables (relative angular displacement, engine and dynamometer speeds, fluid fill). This polynomial is chosen to agree with value of the function (i.e. the variable) and its derivative at a given time T, in order to predict a value at a time greater than T.

For clarity the simplest method, Euler's method, is used as an example. In Fig.6.4 the next value is given by

$$\begin{aligned} y(t+h) &= y(t) + h f(t, y(t)) + O(h^2) \\ &= p(t+h) + O(h^2) \end{aligned} \qquad (6.12)$$

where

h	= size of the time step
$f(t, y(t))$	= the derivative of $y(t)$ at time t
$O(h^2)$	= the error between the actual and predicted values of $y(t+h)$
$p(t+h)$	= predicted value of $y(t+h)$

Eqn.(6.12) is explicit in the new variable value $y(t+h)$, but if the backward approach is taken the formula becomes implicit,

$$y(t+h) = y(t) + h f(t+h, y(t+h)) + O(h^2) \qquad (6.13)$$

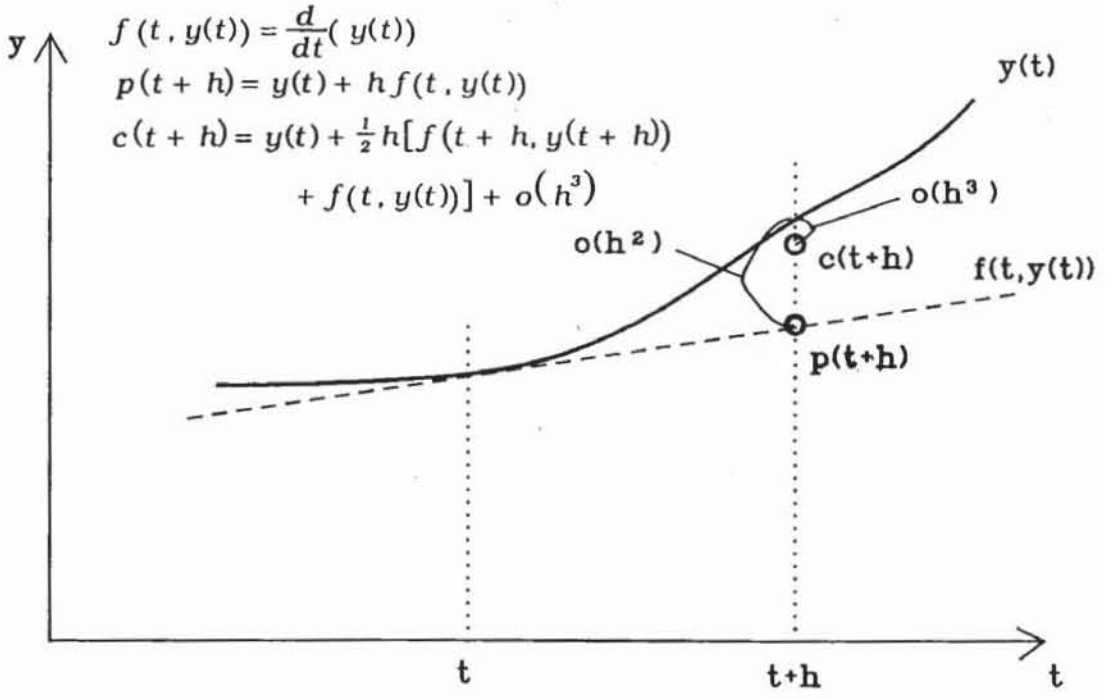

Figure 6.4: Numerical Approximation of a General Function

In this case of one step methods the truncation errors are the same, however as the order of the methods (the number of time step derivatives in the formulation) increases the truncation errors decrease more rapidly for implicit methods than for the equivalent explicit methods. Hence the explicit method (predictor) is used to predict a value at the new time, which is then used in an implicit method (corrector) to obtain a more accurate solution at that new time. Further to this advantage the corrector can conveniently be of one order higher than the predictor as only one evaluation of the derivative is necessary at the new time step since all other derivatives are the same as for the predictor calculation, reducing truncation error dramatically. In the example the corrector becomes

$$y(t+h) = y(t) + \tfrac{1}{2}h[f(t+h, y(t+h)) + f(t, y(t))] + O(h^3) = c(t+h) + O(h^3) \quad (6.14)$$

where

$c(t+h)$ = corrected value of $y(t+h)$

This formula is commonly known as the trapezoidal method.

By consideration of the predictor-corrector formulae, Eqns.(6.12) and (6.14), the magnitude of the truncation error is controlled by varying both the step size and the order of the formulae used. In their implementation of the Adams methods as predictor-corrector pairs Shampine and Gordon use variable order and step size, adjusted by the program itself, to contain the truncation error within the relative and absolute limits specified by the user. The criterion used is a combination of relative and absolute error limits,

$$|e_L| \leq relerr \times |y(t)| + abserr$$

where

$\|e_L\|$	= magnitude of local error
$\|y(t)\|$	= magnitude of computed variable
relerr, *abserr*	= relative and absolute error limits specified by the user

Pure error criteria can be obtained by putting the other limit to zero, but as the range of magnitudes of the system variables is large in this case equal limits are used in a mixed error criterion. The theory of error propagation and its control is covered extensively in Shampine and Gordon [47].

The appropriate sizes for the error limits vary from problem to problem, and are a balance between the desired precision of the answer, the computer time required for calculation, and the precision limits due to computer round off. To determine the appropriate limits for the engine-dynamometer problem several computer runs of the same test were made with different error limits, and a comparison was made of the variation of the system variables about their final steady state values.

The test involved the full closure of the water outlet valve, while input torque remained constant.

Machine Initial Conditions:

speed	= 1500 rpm
water inflow	= 0.00257 m^3/s
engine torque	= 148.4 Nm
fluid fill	= 18.03%
outflow valve closure	= 51.88%

Final Steady State Conditions:

speed = 485 rpm
torque = 148.4 Nm
fluid fill = 100%
relative shaft displacement = 0.00212 rad

	ABSOLUTE AND RELATIVE VARIATION				
ERROR LIMIT	SHAFT DISPL.	ENGINE SPEED	DYNR. SPEED	FLUID FILL	DYNR. TORQUE
1×10^{-2}	.00594	28.6	94.8	0.248	67.0
	280%	5.9%	19.5%	0.248%	45.0%
1×10^{-3}	.000635	0.97	4.36	0.291	3.30
	30.0%	0.20%	0.90%	0.291%	2.2%
1×10^{-4}	.000078	0.65	0.86	0.487	0.60
	3.7%	0.13%	0.18%	0.487%	0.40%
1×10^{-5}	.000006	0.46	0.45	0.343	0.40
	0.28%	0.09%	0.09%	0.343%	0.27%
1×10^{-6}	.000003	0.44	0.44	0.363	0.004
	0.14%	0.09%	0.09%	0.363%	0.27%
1×10^{-7}	.000003	0.44	0.44	0.519	0.003
	0.14%	0.09%	0.09%	0.519%	0.20%

Table 6.1: Absolute and Relative Variation of System Variables During Numerical Computation for Different Error Limits

In Table 6.1 the absolute variation given is the total peak-to-trough oscillation of the numerical output about the final steady state value. The variations are also presented as percentages of the final values. It is apparent that there is a point at which further reduction of the error limits does not result in more precision of the numerical computation. For this investigation it is considered appropriate that the variation in each of the four system variables is less than 1%, so limits of 1×10^{-5} are used. In other circumstances where the cost of computer time is more critical the limits could be increased to 1×10^{-4} since only the relative shaft displacement variation exceeds 1% and it is usually not of prime interest.

6.3 Influence of Dynamics (Open Loop)

In this section both the F0201 (R_o = 102.5 mm, R_i= 43.5 mm, t = 5.0 mm, α = 45°, J = 0.0931 kgm^2) and the F24 (R_o = 121 mm, R_i= 51.2 mm, t = 4.0 mm, α = 45°, J = 0.188 kgm^2) machines are used to study dynamometer dynamic characteristics. For comparisons with steady state results and previous studies the F020 is used, while the F24 predicted performance is compared with available experimental data. The driving torque input to the system for the tests is calculated to provide the required constant acceleration of the engine and dynamometer inertias.

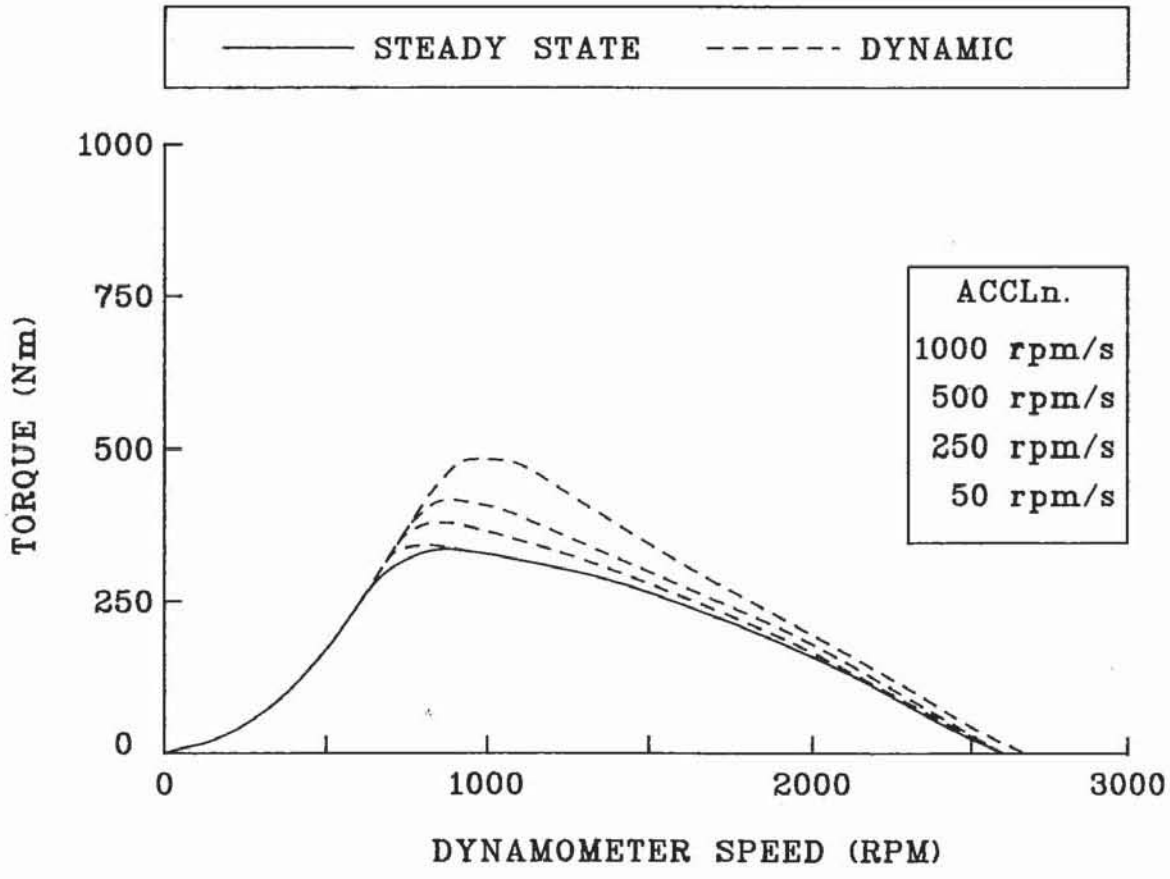

Figure 6.5: Comparison of Steady State and Acceleration Torque Characteristics

6.3.1 Comparison of Steady State and Acceleration Performance

In order to illustrate the effect acceleration has on the performance of a hydraulic dynamometer a series of test runs from a

stationary full fill start point are presented in Fig.6.5. The solid line is obtained using the water *inflow equals outflow* of Section 5.5, and represents a series of steady state points. This curve shows the characteristic falling torque of the dynamometer due to self-emptying. When the machine is accelerated from rest at only 50 rpm/s a deviation from the steady state curve appears. The fluid fill requires a finite time to respond to the higher speed and pressure, before the water inflow and outflow rates balance. At higher speeds as the fill decreases the performance curve tends toward the steady state case. The deviation becomes greater with increased acceleration. Tan's quasi-dynamic model also shows this behaviour with results qualitatively very similar to Fig.6.5, however once non-constant accelerations and system oscillations are encountered Tan's model cannot accurately predict system performance.

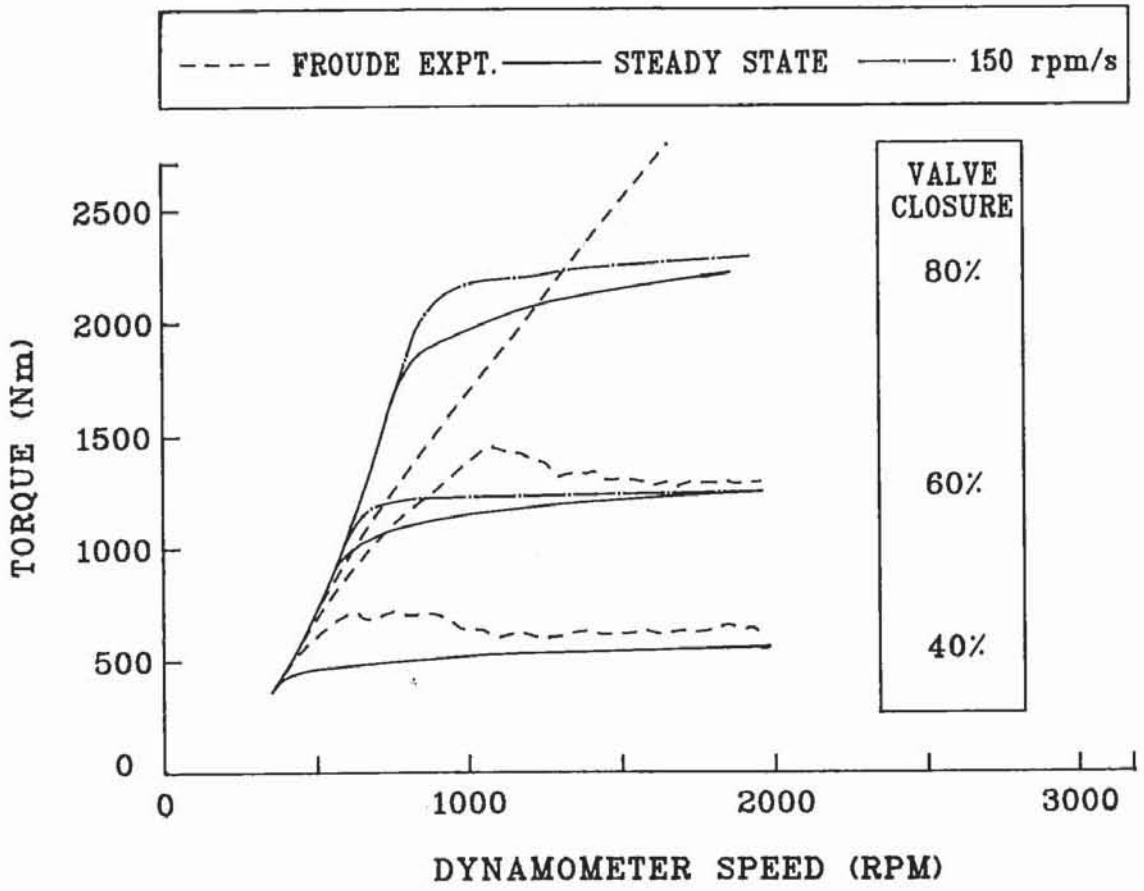

Figure 6.6: Comparison of Steady State and Dynamic Model Predictions with Experimental Valve Closure Tests; Q_{IN} = 0.003788 m^3/s

The difference between steady state and acceleration performance tests is further illustrated in Figs.6.6 and 6.7. A series of slow acceleration experimental curves (an approximation of the steady state open loop characteristics) from Froude for the F24 machine is presented with simulated steady state water inflow-equals-outflow and

low acceleration results for different outflow valve closures. Both the experimental and simulation results tend toward the same curves. The experimental curves were obtained using an eddy current coupling as a variable speed drive unit between the hydraulic dynamometer and a diesel engine, so the actual forcing function for the system differs somewhat from the simple speed ramp used for the simulation. The system response dependence on both initial conditions and forcing function during tests is examined in detail in Section 6.3.4.

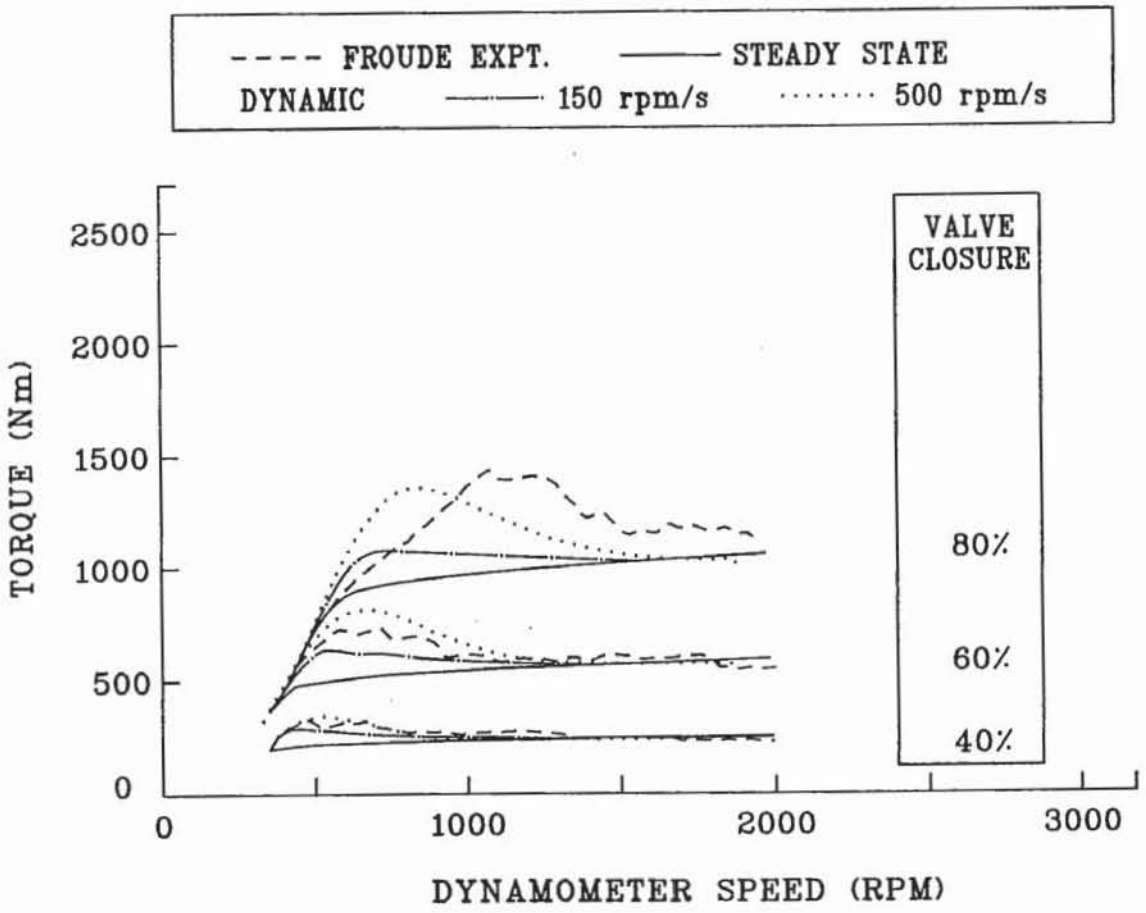

Figure 6.7: Comparison of Steady State and Dynamic Model Predictions with Experimental Valve Closure Tests; Q_{IN} = 0.002526 m^3/s

During the dynamic test simulations it is found that the torque contributions due to the unsteady torque components (K_3.,K_4,K_5.,K_6) are very small relative to the steady torque components (K_1.,K_2). The total unsteady contributions are generally less than 5% of the steady contributions, except when there is very low fluid fill (less than 2%). Under conditions of very low fluid fill the absolute magnitudes of the steady and unsteady torque components is very small, so the error caused by omitting the unsteady components is negligible. Hence for

almost all simulations these unsteady components can be ignored within the dynamic system model. However, they are included throughout the present work.

From these curves it is apparent that the distribution of valve pressure loss against the higher valve closures is low, and hence the valve characteristic presented in Section 3.3.1 should be less linear with steeper gradient as the valve approaches full closure.

6.3.2 Acceleration/Deceleration Hysteresis

The effect of the fluid response time is dependent on whether the dynamometer is accelerating or decelerating. Fig.6.8 shows the hysteresis which occurs when a dynamometer is accelerated at a constant valve closure and later decelerated from a point on that torque characteristic back to the starting point. In both the experimental and simulation curves the machine retains a higher fluid fill when accelerating, than it attains as it decelerates over the speed range for the same valve closure.

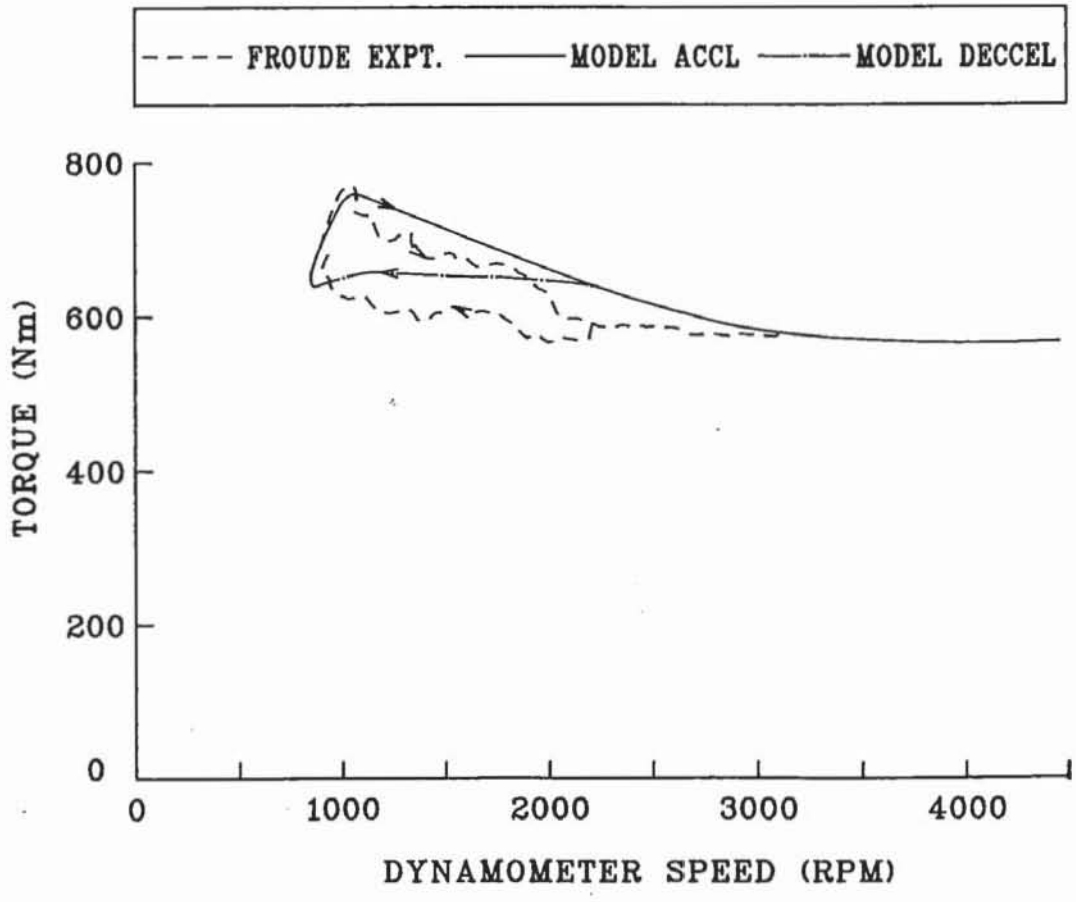

Figure 6.8: Comparison of Acceleration/Deceleration Hysteresis with Experimental Results

6.3.3 Torque Rise at Low Fill and High Speed

When a hydraulic dynamometer follows a falling torque characteristic, the torque curve begins rising again at higher speeds. This behaviour is shown in the experimental curves for a F020 machine in Fig.6.9. Insufficient information on the experimental conditions is available to simulate the test, so a generalised investigation of this phenomenon is made.

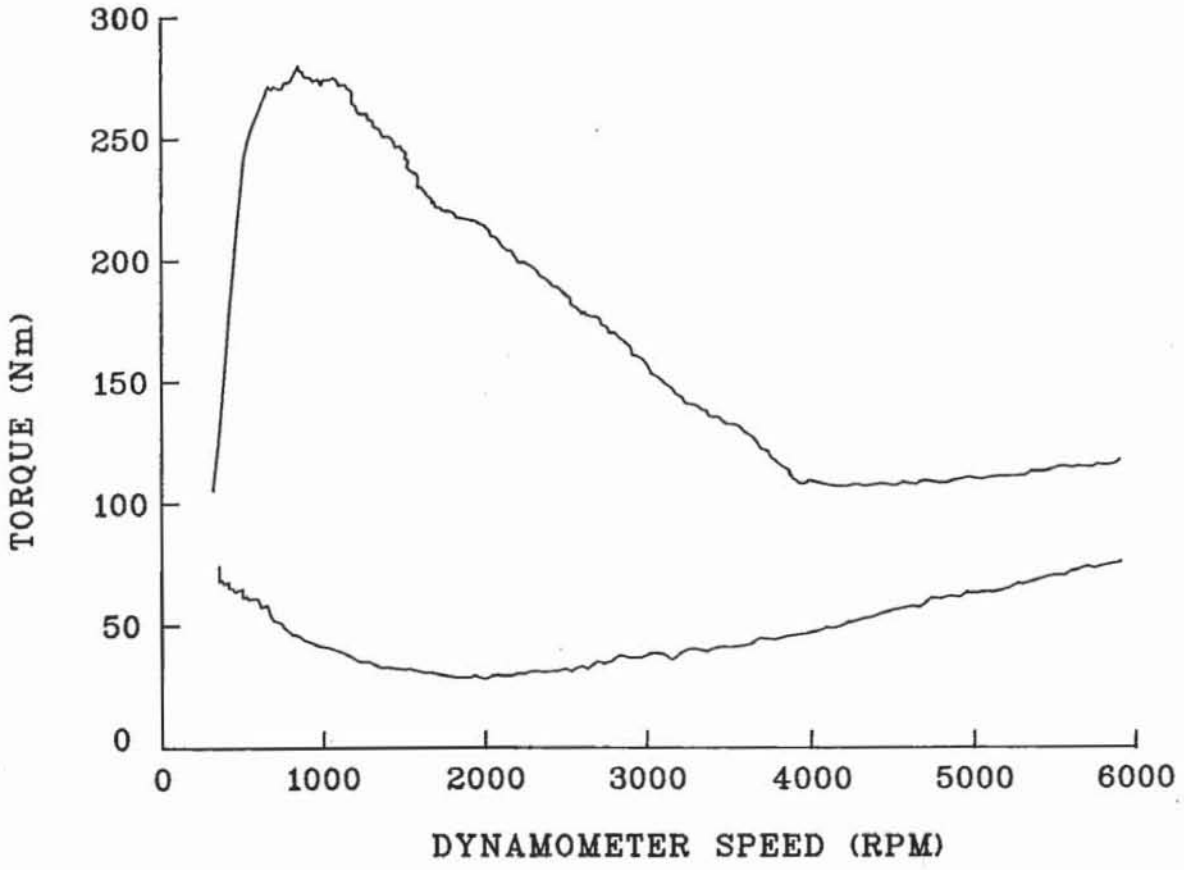

Figure 6.9: Experimental Example of Rising Torque at High Speed and Low Fill

A typical example of this is shown in Fig.6.10, where the minimum torque occurs at around 2800 rpm as the machine accelerates. This feature of the machine characteristic arises as the rate of self-emptying decreases, while the machine speed increases rapidly, producing a greater effect on the torque produced than that due to the decrease in fill. In the case presented the fill decreases from 100% to approximately 10% in the speed range 350 to 2000 rpm, yet from 2000 to 6000 rpm the fill only drops by little more than another 5%. The curves of water inflow and outflow clarify this

phenomenon. As the machine accelerates water outflow[2] increases, peaking as the decreasing fill in the dynamometer reduces the water pressure. Therefore the outflow rate reduces back towards the water inflow rate, reducing the rate of change of fill.

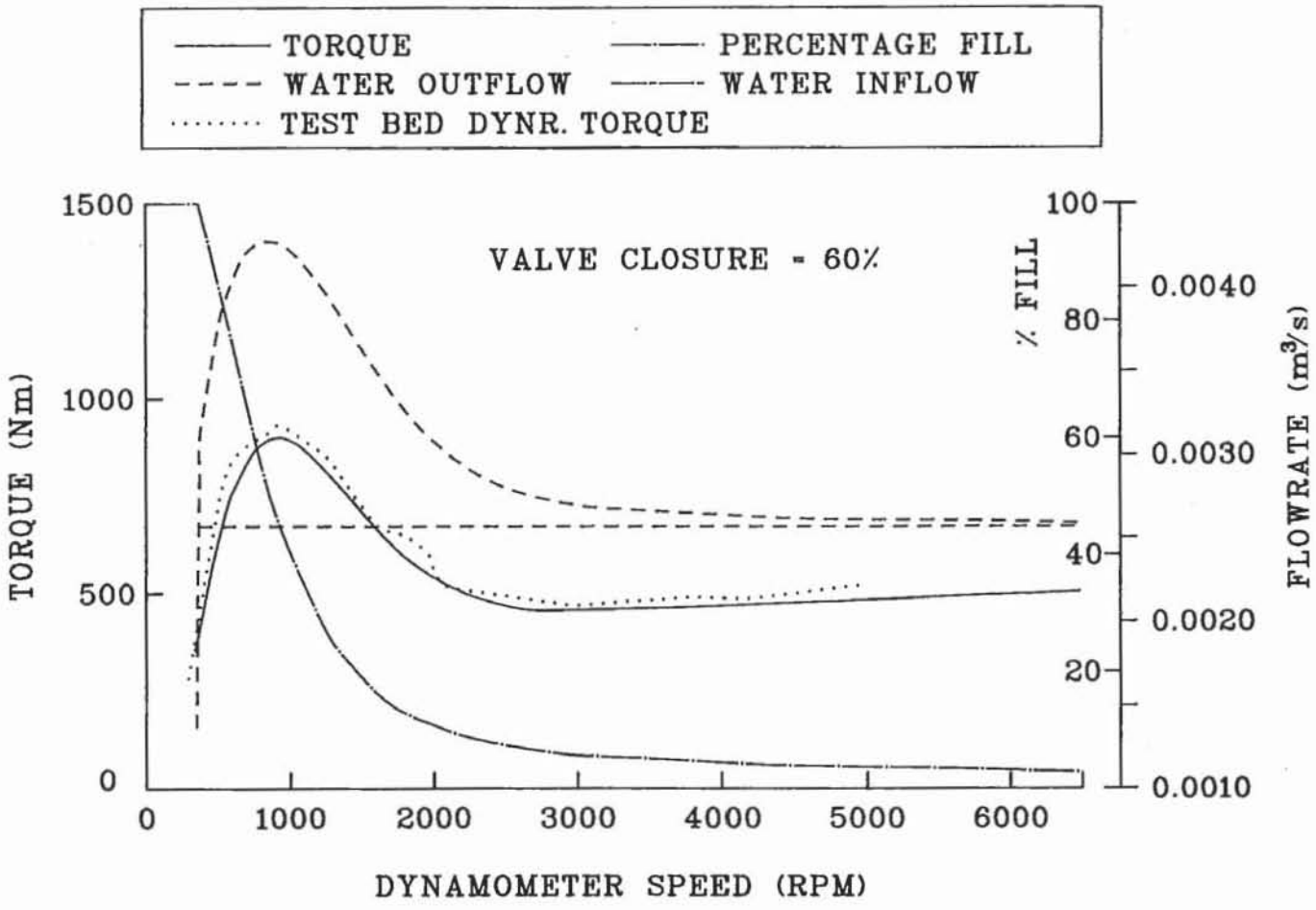

Figure 6.10: Rising Torque Characteristic Parameters Examined against Speed

In Fig.6.11 the variation of speed and fluid fill with time indicates how the speed increases rapidly, when self emptying occurs and the fill level has dropped considerably. Meanwhile the rate of decrease of fill has reduced, leading to a change in its degree of influence on the torque produced. Thus a torque minimum is reached, and then torque rises due to the speed effect. This behaviour is not predicted by steady state modelling.

---

2 The water outflow rate shown is the flow through the outflow valve. In the case of inflow exceeding outflow when the dynamometer is full, as occurs initially in Fig.6.9, the balance of the water exits the machine via the air vent holes in practice.

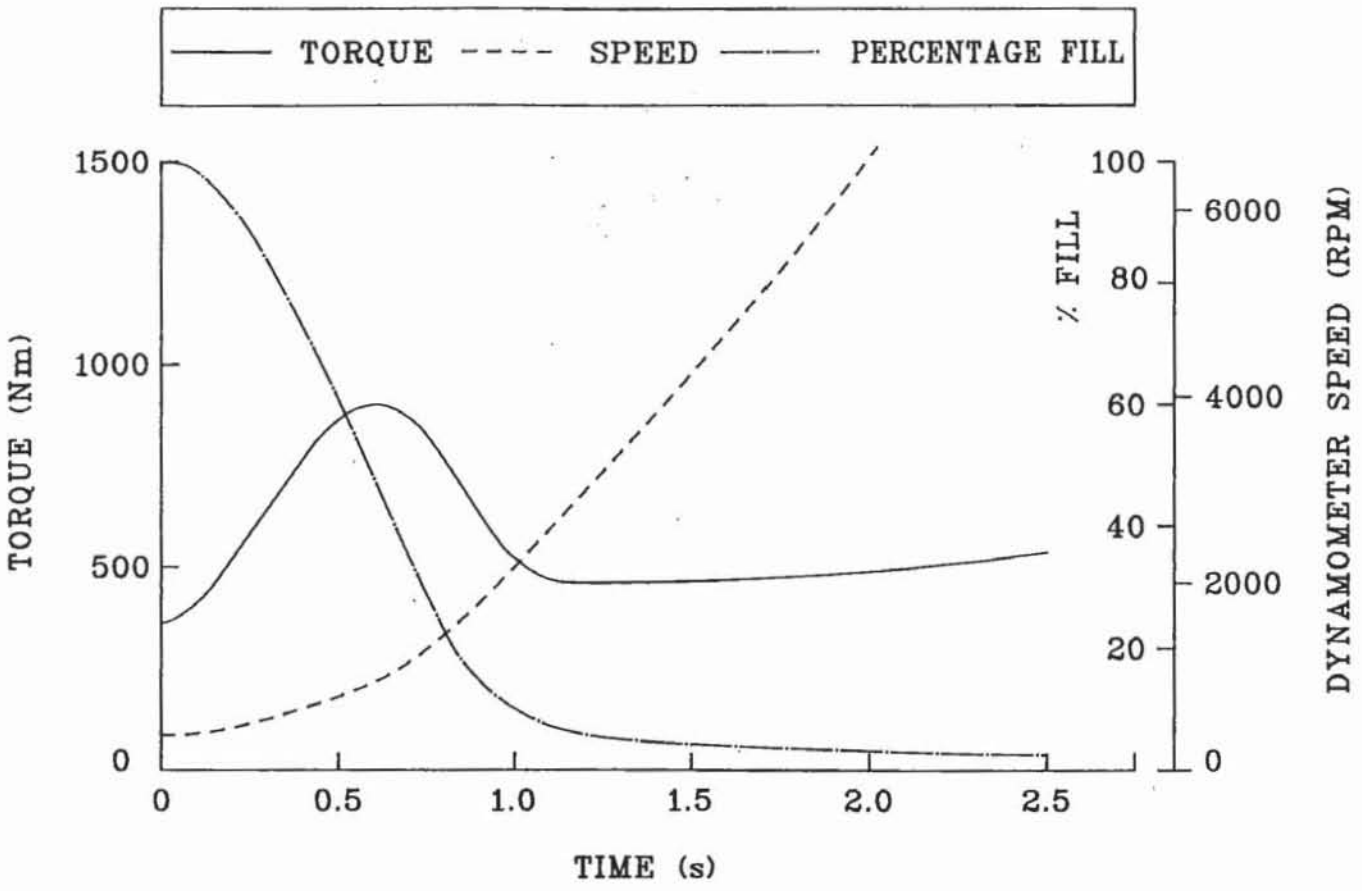

Figure 6.11: Rising Torque Characteristic Parameters Examined against Time

6.3.4 Effect of Initial Conditions and Forcing Function

Using a constant water outflow valve setting the dynamometer is accelerated to 1200 rpm from a stationary full fill point. A steady state water *inflow equals outflow* map of performance from the theoretical start point is presented for comparison with the acceleration curves of torque and fluid fill in Figs.6.12 and 6.13. As in Section 6.3.1 the curves show how the dynamometer retains more fluid as the acceleration rate is increased, causing higher torque values before the system heads back toward the steady state conditions.

The initial conditions are altered to a point (100 Nm and 350 rpm) off the steady state curve for that valve closure, and as the acceleration begins the valve is closed to the previous position. It is apparent that the resultant path is dependent on the acceleration. The torque curves tend toward those produced by the acceleration from rest, though as the acceleration is increased the deviation from the previous curves becomes greater. Even in the case of moderate

acceleration (500 rpm/s) the torque curve produced is significantly displaced from the steady state curve and appears as a *false hydraulic maximum*. This phenomenon has been experienced in practice when accelerating a system from engine idling.

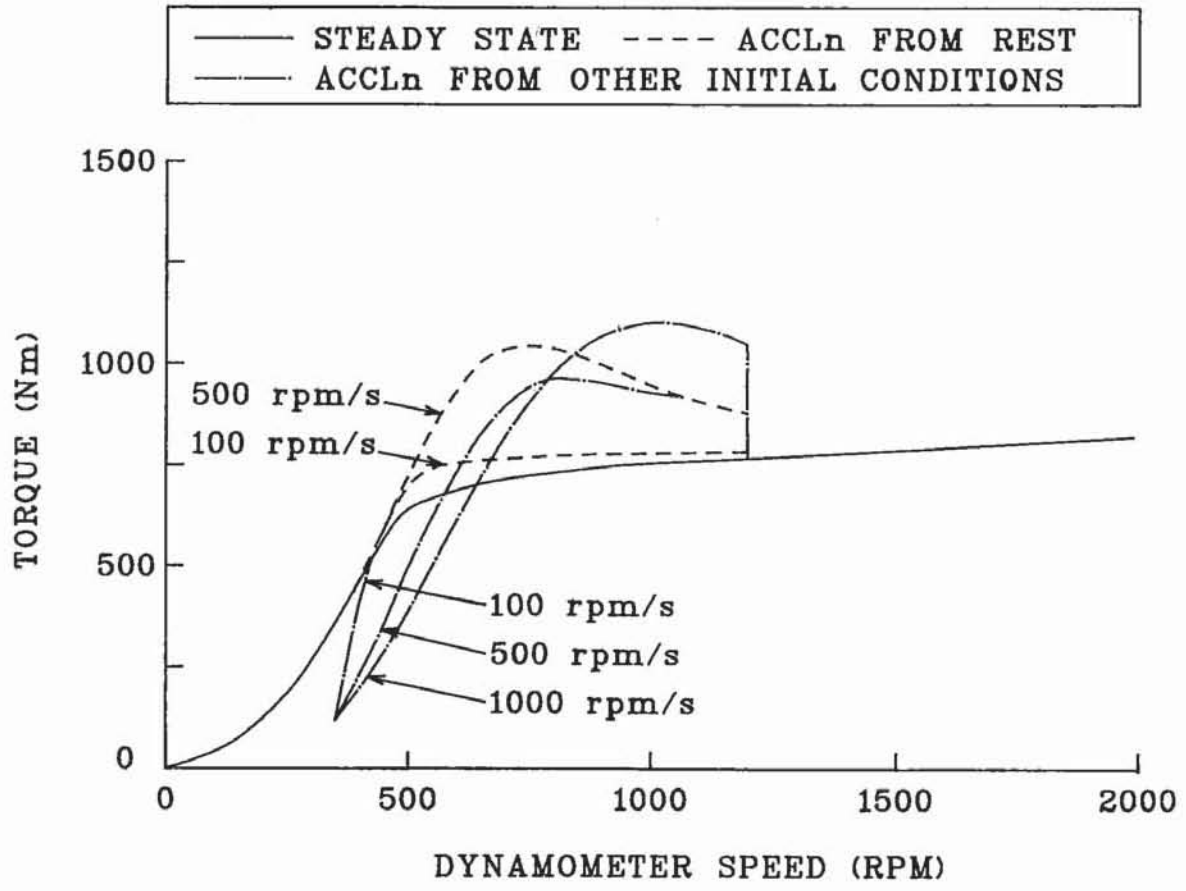

Figure 6.12: Effect of Driving Torque and Initial Conditions on Torque-Speed Characteristic

The explanation of this characteristic is found in Fig.6.13. In the slow acceleration case the fluid fill percentage reaches 100% and so the test path follows that of the *maximum* response for that acceleration. At greater accelerations the fill response is not fast enough to fill the machine before the increased speed causes the fill percentage to drop. The test path joins that from the previous tests at a much later point in the curve.

As would be expected the initial conditions affect the results of any test run, also the manner in which the system is forced through a test has a large influence on the results obtained.

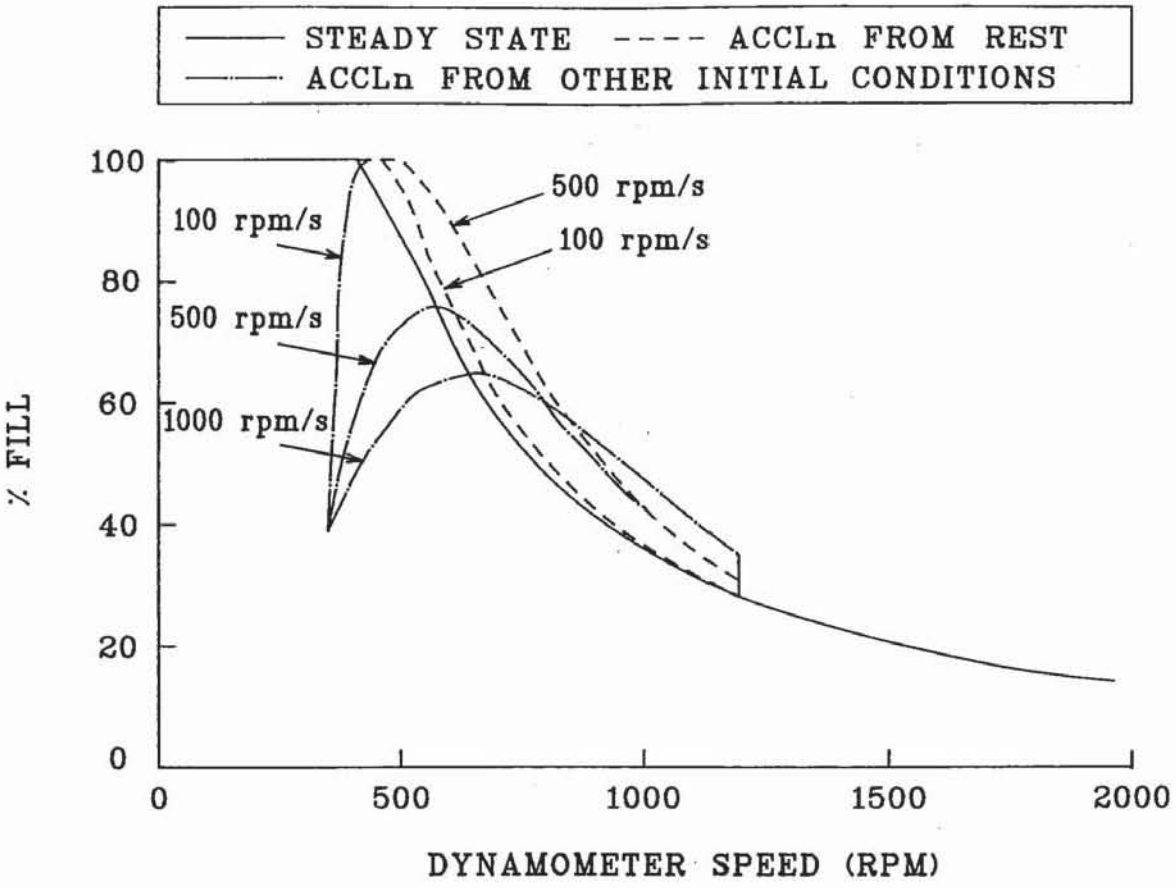

Figure 6.13: Effect of Driving Torque and Initial Conditions on Percentage Fill-Speed Characteristic

6.4 Response to Input Perturbations (Open Loop)

In this section the F24 dynamometer's response to changes in the inputs acting on it are investigated at several points to illustrate the variation in machine response across its operating envelope, i.e. the non-linearity of its behaviour. The five points used are illustrated in Fig.6.14 and tabulated below (Table 6.2). The spread of points allows the effects due to the differences in speed and percentage fill on the machine's responses to given perturbations to be observed.

In order that the dynamic response of the dynamometer is distinguishable from the system acceleration effects at the higher torque values an *engine* inertia of 2.5 kgm^2 is used in this section, except where stated otherwise. The tests of Sections 6.4.4 and 6.4.5 are repeated with an inertia of 0.2 kgm^2 in Section 8.2.1 showing the difference in dynamometer torque change and therefore the controller requirements.

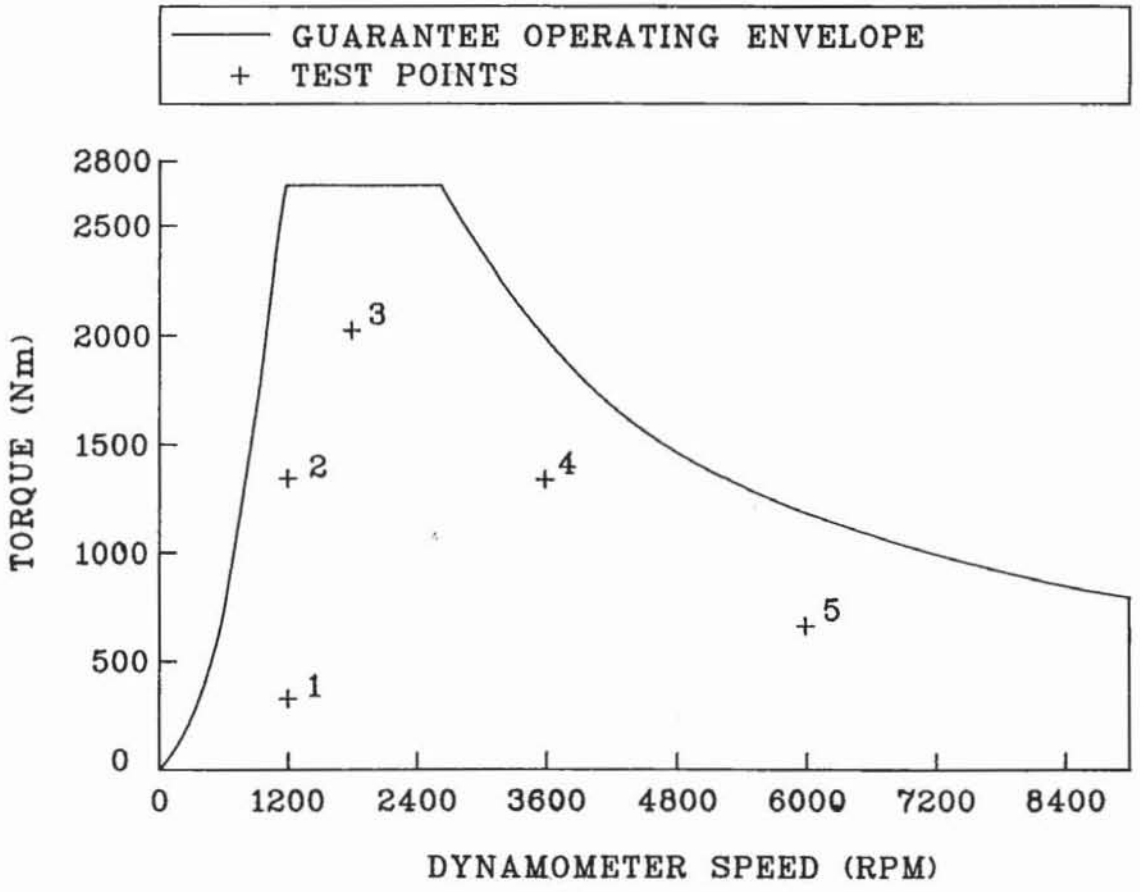

Figure 6.14: Map of Test Points for Open Loop Dynamic Models

POINT	TORQUE (Nm)	% RATED TORQUE	SPEED (rpm)	% VALVE CLOSURE	% FLUID FILL
1	339	12.5	1200	33.5	15.1
2	1356	50.0	1200	66.0	41.8
3	2034	75.0	1800	78.4	30.9
4	1356	50.0	3600	61.1	8.7
5	678	25.0	6000	40.8	3.0

Table 6.2: Dynamometer Parameter Values at Five Test Points

6.4.1 Fluctuations Due to Engine Firing

During the engine cycle the intermittent combustion in the cylinders leads to peaks in the torque output. For a single cylinder there is a large isolated peak followed by very low values for the remainder of the cycle. In a multi-cylinder engine this fluctuation becomes periodic about a mean value of torque; the objective of flywheel design is to smooth the engine output. For simplicity this engine driving torque variation for input to the system model is represented as a sinusoid, the period of which is dependent on both the number of engine cylinders and the engine speed,

$$T_E = T\left(1 + A_T \sin\left(\tfrac{1}{2} N_C \omega_E t\right)\right) \qquad (6.15)$$

where

T_E = engine torque output
T = mean engine torque
A_T = amplitude of engine torque fluctuations
N_C [3] = number of engine cylinders
ω_E = engine speed
t = time

Similarly if the model is to simulate a system driven by a speed controlled engine the equation used for the engine speed input to the system is,

$$\omega_E = \omega_{EM}\left(1 + A_W \sin\left(\tfrac{1}{2} N_C \omega_E t - \tfrac{1}{2}\pi\right)\right) \qquad (6.16)$$

---

3 To allow for the four stroke engine cycle there is a factor of 0.5 included in Eqn.(6.15).

where

ω_{EM} = mean engine speed

A_W = amplitude of engine speed fluctuation.

These equations are not used together as the basis for the dynamometer response, only as inputs for the separate test conditions.

The dynamometer's response is clearly dependent on both the number of cylinders and the amplitude of the fluctuation in comparison to the mean torque. This driving torque fluctuation appears reduced at the output from the engine since a large portion of it is required to accelerate the engine inertia. Therefore Table 6.3 shows the percentage of the driving torque variation which appears at the shaft for three tests.[4] For fluctuations of 25% of the mean torque value only 18% and 26% of the magnitudes, for 1 and 4 cylinder cases respectively, appear at the shaft and are transmitted to the dynamometer. The dynamometer responses are torque variations of 33% and 14% of the shaft input variation to the machine and phase lags of 90° compared to the driving sinusoid. The increase in cylinder numbers effectively gives the system inertias and fluid fill less time to respond to the fluctuations which leads to lower amplitude output variations. Thus the performance of the dynamometer as a vibration damper is dependant on the frequency of the vibration.

TEST	1	2	3
No. of CYLINDERS	1	4	4
A_T (% of mean T)	0.25	0.25	0.25
ENG. INERTIA (kgm^2)	1.0	0.5	2.5
ENG. PEAK ΔT (Nm)	84.7	84.7	84.6
ACCL. AT PEAK ΔT (rpm/s)	663	1200	294
ENG. ACCL. TORQUE (Nm)	69.4	62.7	77.1
DRIVE SHAFT PEAK ΔT (Nm)	15.3	22.0	7.5
SHAFT ΔT % of ENG. PEAK ΔT	18.1	26.0	8.9
DYNR. PEAK ΔT (Nm)	5.9	3.5	1.0
DYNR. ΔT % of SHAFT PEAK ΔT	38.6	15.9	13.3
DYNR. ΔT % of ENG. PEAK ΔT	7.0	4.1	1.2

Table 6.3 Percentage of Torque Fluctuation Transmitted to Dynamometer Output

---

4 These responses are typical for tests conducted at all five points and a range of fluctuation amplitudes from 1% to 50% for 1, 2, 4 and 6 cylinder engines.

When the engine inertia is increased in Test 3 the percentage of the driving torque fluctuation passed to the shaft is reduced, however the dynamometer response to the shaft peak is altered little . The dynamometer response is a very small percentage of the driving torque variation in all cases. Consequently for most test runs of multi-cylinder engines with flywheels the shaft torque fluctuation is considered negligible and for the remainder of the dynamometer dynamic investigation this fluctuation will be excluded.

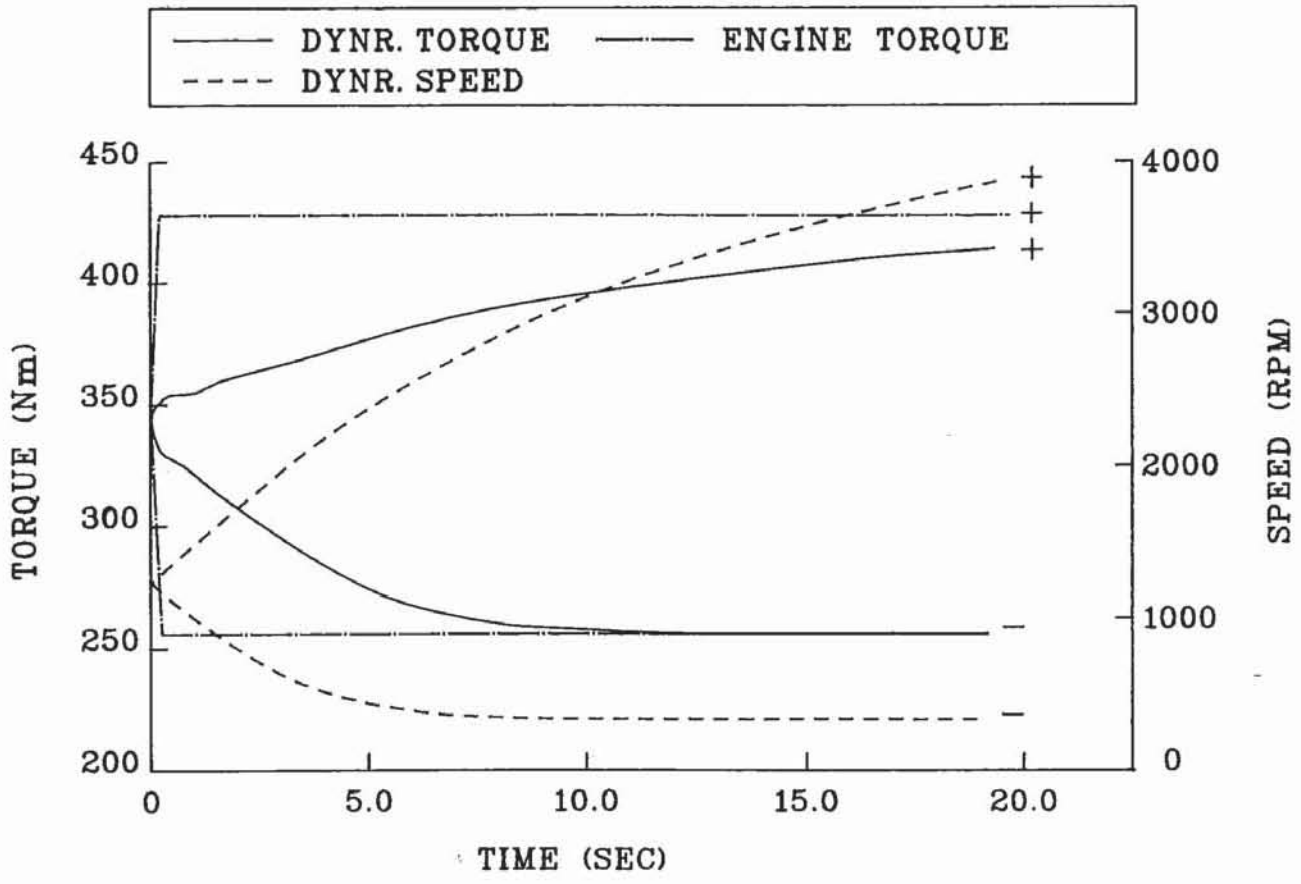

Figure 6.15: Dynamometer Torque and Speed Responses to a 10% Driving Torque Change

6.4.2 Engine Torque Change

A change in the engine torque driving the system excites a response in the dynamometer. Rather than using a pure step input to investigate the machine response a ramped step is used to represent the time required for torque to build up. The dynamometer responses

to increases and decreases of both 10 and 25 percent of the initial driving torque are typified by the curves of Figs.6.15 and 6.16[5]. For both increases and decreases the dynamometer torque follows the engine input torque, while the fluid fill follows sigmoidal curves to minimum and maximum values respectively.

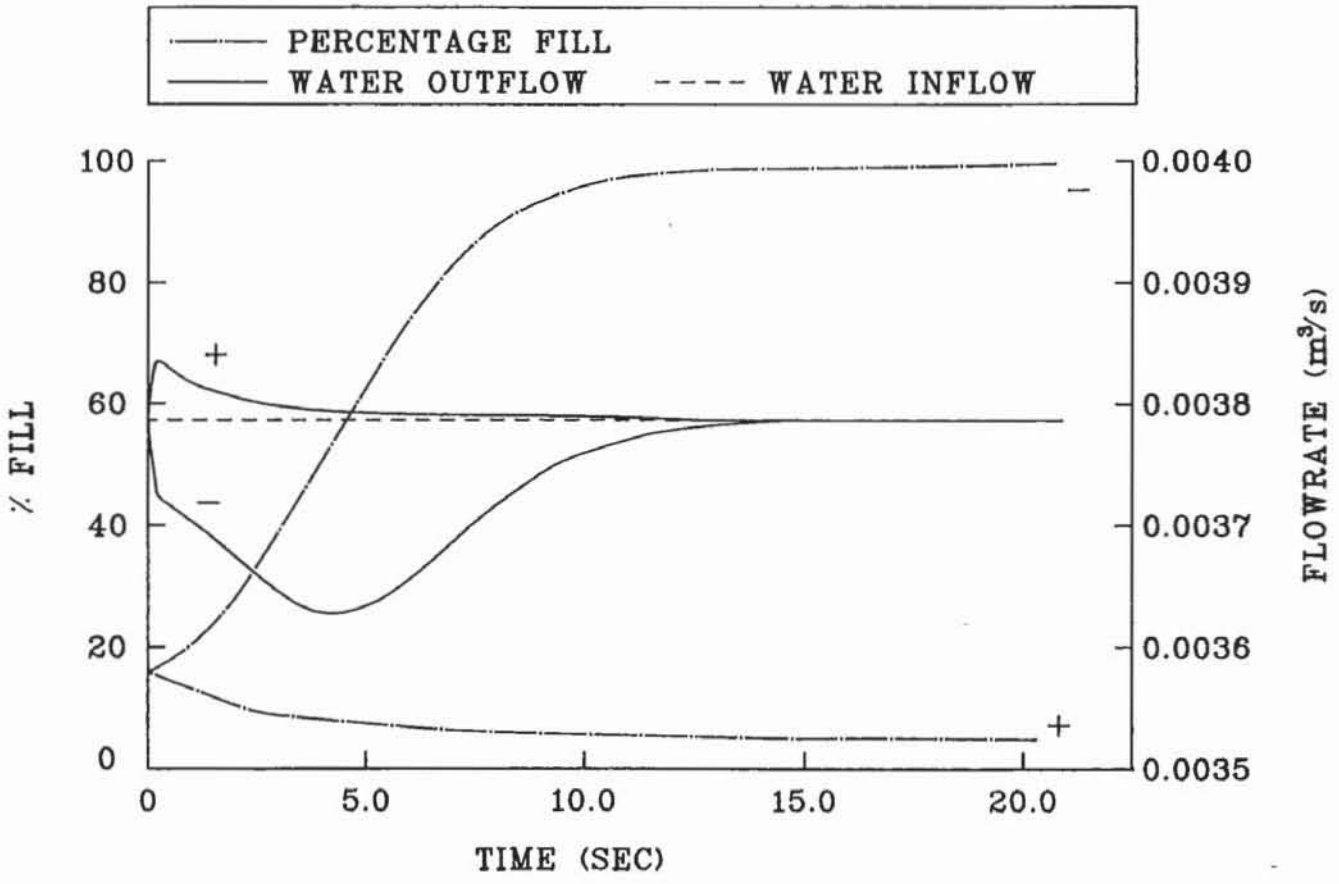

Figure 6.16: Fluid Outflow Rate and Percentage Fill Responses to a 10% Driving Torque Change

In Fig.6.17 the dynamometer responses to increases at the five test points show the torque following the same path for different sized changes at points 1, 4 and 5 where the initial percentage fluid fill is lower. However at the other points the torque response is driven over a peak into a falling torque characteristic which then rises again. The two different increases result in different torque characteristics, similar to the machine behaviour studied in Section 6.3.4.

---

5 These are responses to an increase and decrease of 25 percent at test point 1, using a constant ramp rate of 1000 Nm/s for both increases and decreases.

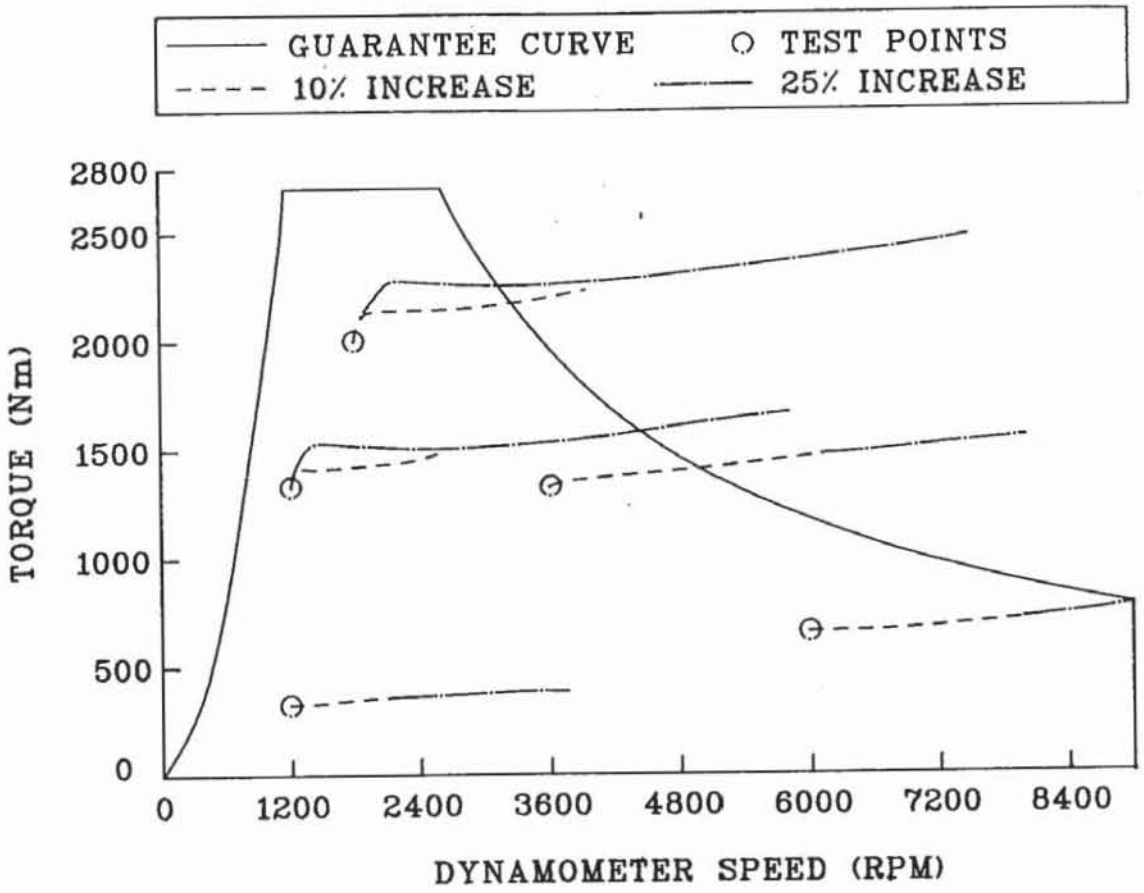

Figure 6.17: Torque-Speed Characteristics for 10% and 25% Increases in Driving Torque

6.4.3 Engine Speed Change

In practise an engine speed change is accompanied by a torque change, however here the effects due only to acceleration of the system are investigated to completely characterise the the dynamic behaviour of hydraulic dynamometers. The effect of change of the engine speed alone on the machine's performance is an increase in torque, for positive acceleration, followed by a break point when the driving acceleration stops, and a return towards the initial set torque.

In these tests the engine speed is subjected to positive and negative accelerations of 500 rpm/s to points 900 or 1200 rpm from the initial set point with no change to the driving torque. Figs. 6.18 and 6.19 show the results for test point 1. A much more gradual torque change is apparent for the positive acceleration rather than the

deceleration, due to the more gradual changes in the water outflow rate and consequently the percentage fill.

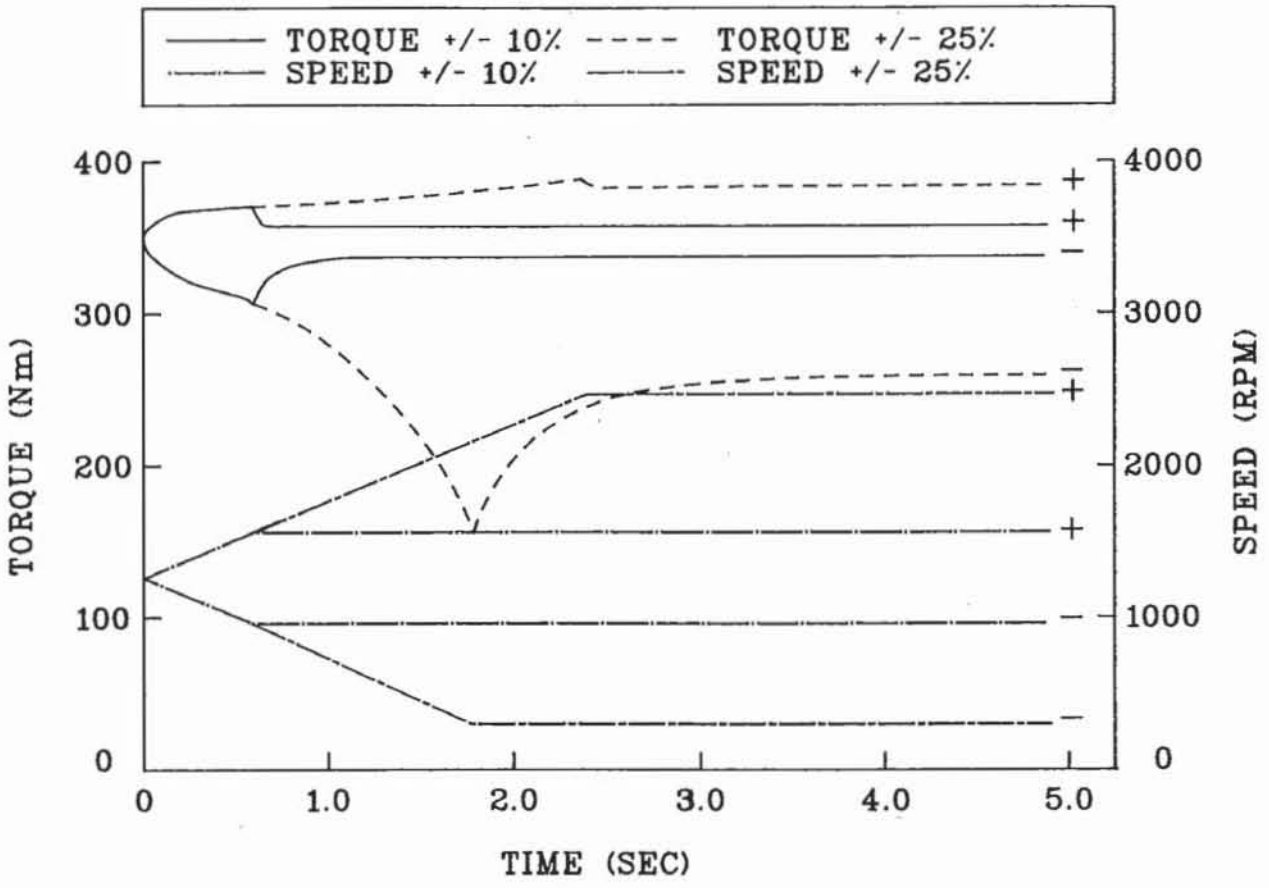

Figure 6.18: Dynamometer Torque and Speed Responses to Engine Speed Changes

As in Fig.6.17 above, the torque against speed characteristics for the different test points (Fig.6.20) varies depending upon the initial fluid fill in the case of both positive and negative accelerations. At lower fills (points 1, 4.,5) the torque curves are much flatter for both speed increases and decreases. While speed increases from the higher fill points show the dynamometer being driven over a torque peak into a falling characteristic which begins to rise again at a higher speed. A speed decrease from these points leads toward the maximum fill curve, though the torque drops rapidly with speed before reaching the torque maximum curve.

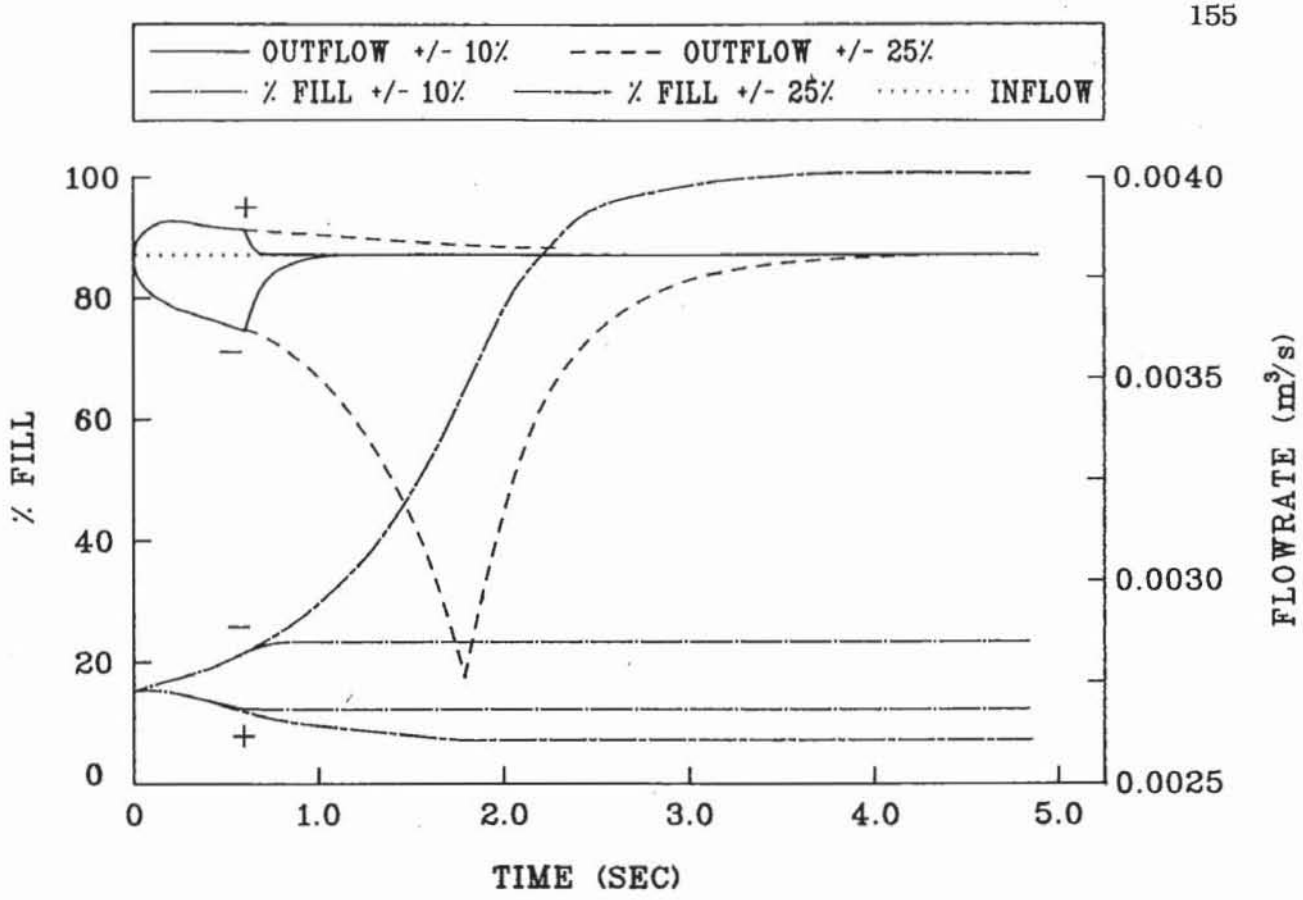

Figure 6.19: Fluid Outflow Rate and Percentage Fill Responses to Engine Speed Changes

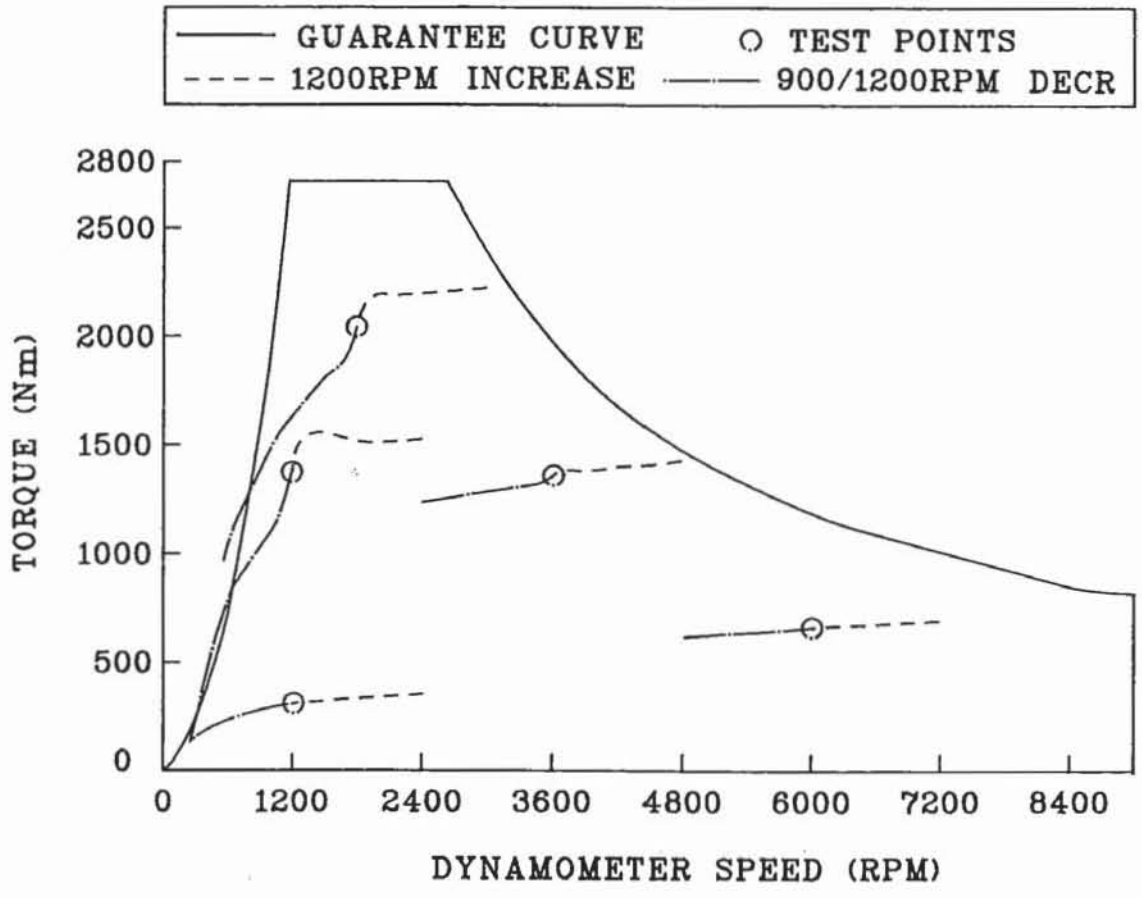

Figure 6.20: Torque-Speed Characteristics for Engine Speed Changes

6.4.4 Outflow Valve Closure (Constant Speed)

With the engine speed held constant the dynamometer water outflow valve is opened or closed[6] by 10 percent (of full movement) or to its extreme position. This disturbance simulates the control action of the valve when the engine is speed governed. Using test points 1 and 5 which have approximately the same initial valve closure, Fig.6.21 shows that for a 10 percent change of valve closure the effect on the dynamometer torque is very different between the points. Although point 5 has a much larger torque change, or *gain*, for this valve action its water fill change is much smaller. Consequently any control system design should take into account the way in which the torque gain varies around the operating envelope. This non-linearity of the dynamometer characteristic is confirmed by Table 6.4 of the 10 percent changes for all five test points. There appears to be a qualitative relation between the initial conditions[7] (fraction of rated torque and fraction of cup emptying speed) and the torque gain for a given valve closure.

POINT	FRACTION RATED TORQUE	FRACTION OF N_o	INITIAL VALVE CLOSURE %	TORQUE GAIN (Nm/10%)
10% CLOSURE				
1	.125	1.0	33.5	256
2	.500	1.0	66.0	416
3	.750	1.5	78.4	866
4	.500	3.0	61.1	424
5	.250	5.0	40.8	379
10% OPENING				
1	.125	1.0	33.5	-106
2	.500	1.0	66.0	-357
3	.750	1.5	78.4	-515
4	.500	3.0	61.1	-393
5	.250	5.0	40.8	-283

Table 6.4: Dynamometer Torque Gains at Constant Speed for 10 % Movement of Water Outflow Valve.

---

6 The valve considered is a butterfly valve with a slew time of 200 milliseconds for full action. Smaller valve changes are taken as requiring a direct proportion of that time.

7 F24 Dynamometer rated torque 2712 Nm and cup emptying speed 1200 rpm.

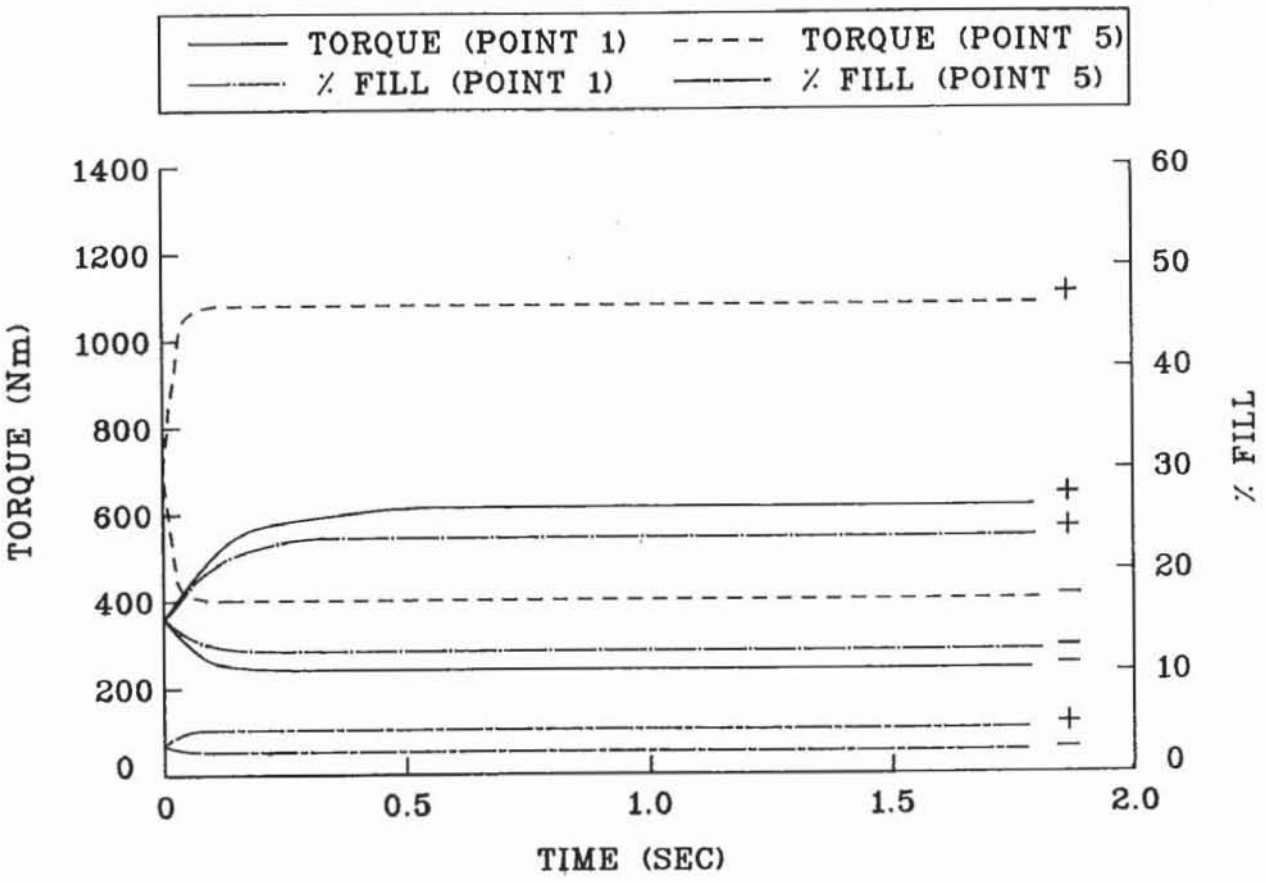

Figure 6.21: Dynamometer Torque and Percentage Fill Responses to 10% Valve Closure at Constant Speed

The effect of valve closure on the dynamometer's parameters at point 1 is illustrated in Fig.6.22. As the valve closes (either 10% or full closure) the water outflow rate drops and the fluid fill increases. When the valve movement ceases, the increasing fluid fill and therefore pressure in the working compartment returns the fluid outflow rate to equilibrium with the inflow rate. These changes result in a torque increase. For the 10 percent closure there is an increase to a new torque steady state, however closing the valve fully rapidly forces the dynamometer towards full fill and torque development above the rated value.

The time required for the torque build up to reach the maximum rated value at a given speed is dependent on the initial conditions, in a similar manner to the torque gains. Table 6.5 shows the results for the five test points, with the dynamometer taking longer to reach the rated torque the further away initially and less time at higher speed, depending upon the required change of fill and the rate of change of fill.

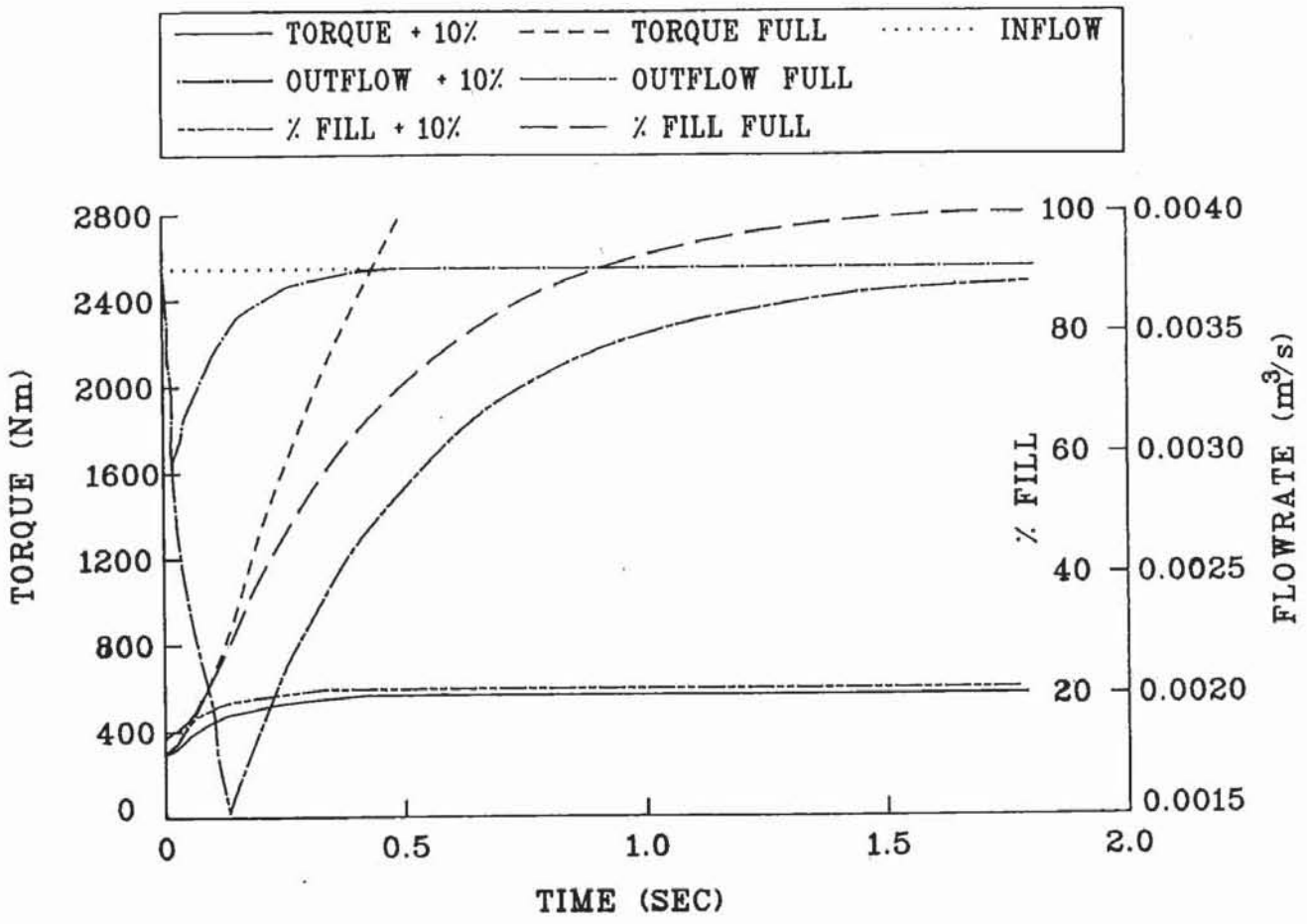

Figure 6.22: Dynamometer Torque, Percentage Fill and Outflow Rate Responses to 10% and Full Valve Closure Changes at Constant Speed

POINT	FRACTION RATED TORQUE	MAX. TORQUE AT SPEED (Nm)	REQUIRED FRACTION TORQUE CHANGE	ELAPSED TIME (s)
1	.125	2712	.875	.471
2	.500	2712	.500	.306
3	.750	2712	.250	.098
4	.500	1990	.234	.060
5	.250	1194	.190	.042

Table 6.5: Time to Reach Dynamometer Rated Torque at Speed[8] for Full Valve Closure

In the opposite case of the valve being opened fully the machine very rapidly empties to a minimum fill percentage. Hence the torque curve follows a sigmoidal curve, as does the percentage fill, typically

8 At points 4 and 5 the rated torque is less than 2712 Nm as the dynamometer operating envelope is also governed by a maximum power rating of 750 kW.

taking approximately 0.3 seconds to fall for the first three test points, and around half the time at points 4 and 5. Of note here is the fact that the minimum percentage fill is speed dependent, as Fig.6.23 illustrates. At higher speeds the cup pressure is greater for a given water fill, so producing a greater water outflow rate. Hence the water inflow and outflow rates reach equilibrium at a lower percentage fill.

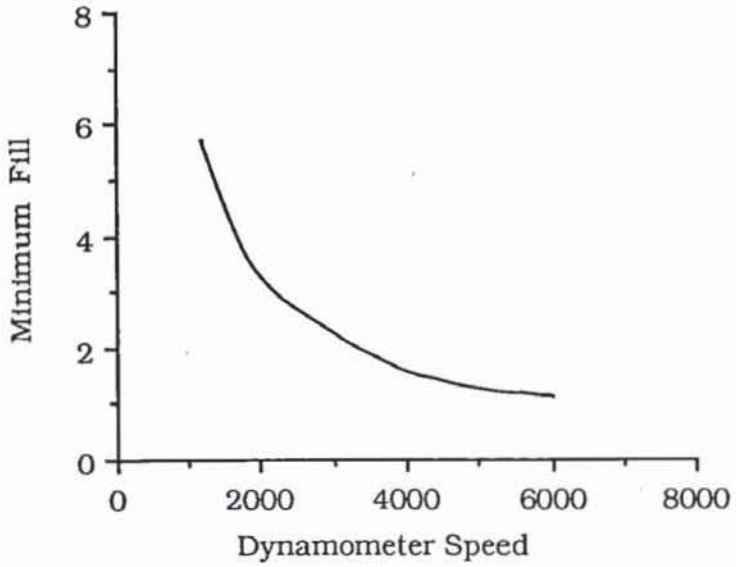

Figure 6.23: Minimum Percentage Fill against Speed

6.4.5 Valve Closure (Uncontrolled Speed)

When the engine speed is not controlled the speed of the whole system reacts to the dynamometer torque changes resulting from valve movement. Fig.6.24 shows how the closing of the valve by 10 or 25 percent (of full movement) results in a different response shape. Rather than a torque increase to a higher steady state value, the machine torque begins to increase until the torque build up slows the system. As a result the water fill increases rapidly (Fig.6.25), leading to the torque output dropping back to the original torque set point. Conversely, when the valve is opened the fill and torque drop which results in the system accelerating away and a gradually rising torque. Table 6.6 shows the torque gains at the five test points. These gains are measured to the response peaks and troughs rather than the final value as in the previous section. For the tests at lower speeds (points

1, 2, 3) the gains are smaller than those of Table 6.4. At higher speeds the gains are of a similar size those in the constant speed test.

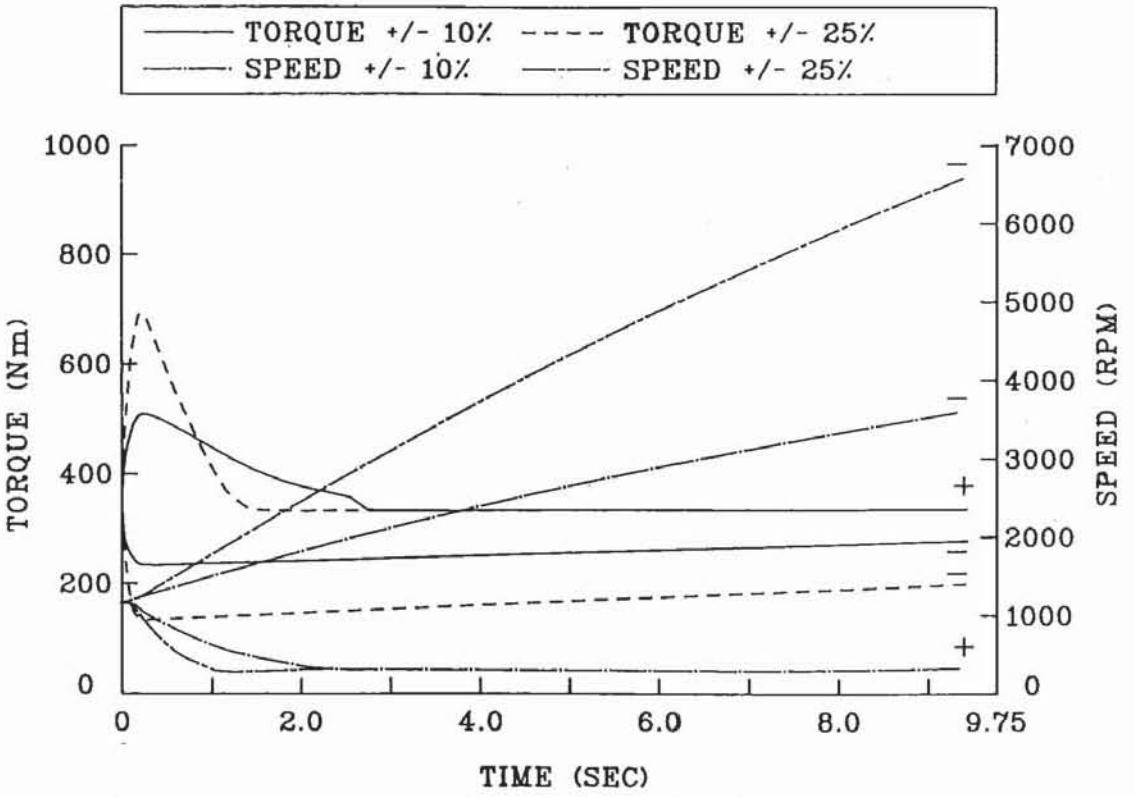

Figure 6.24: Dynamometer Torque and Speed Responses to 10% and 25% Valve Closure Changes with Uncontrolled Speed

POINT	FRACTION RATED TORQUE	FRACTION OF N_o	INITIAL VALVE CLOSURE %	TORQUE GAIN (Nm/10%)
10% CLOSURE				
1	.125	1.0	33.5	175
2	.500	1.0	66.0	117
3	.750	1.5	78.4	272
4	.500	3.0	61.1	353
5	.250	5.0	40.8	368
10% OPENING				
1	.125	1.0	33.5	-98
2	.500	1.0	66.0	-230
3	.750	1.5	78.4	-347
4	.500	3.0	61.1	-367
5	.25	5.0	40.8	-281

Table 6.6: Dynamometer Torque Gains at Constant Speed for 10 % Movement of Water Outflow Valve.

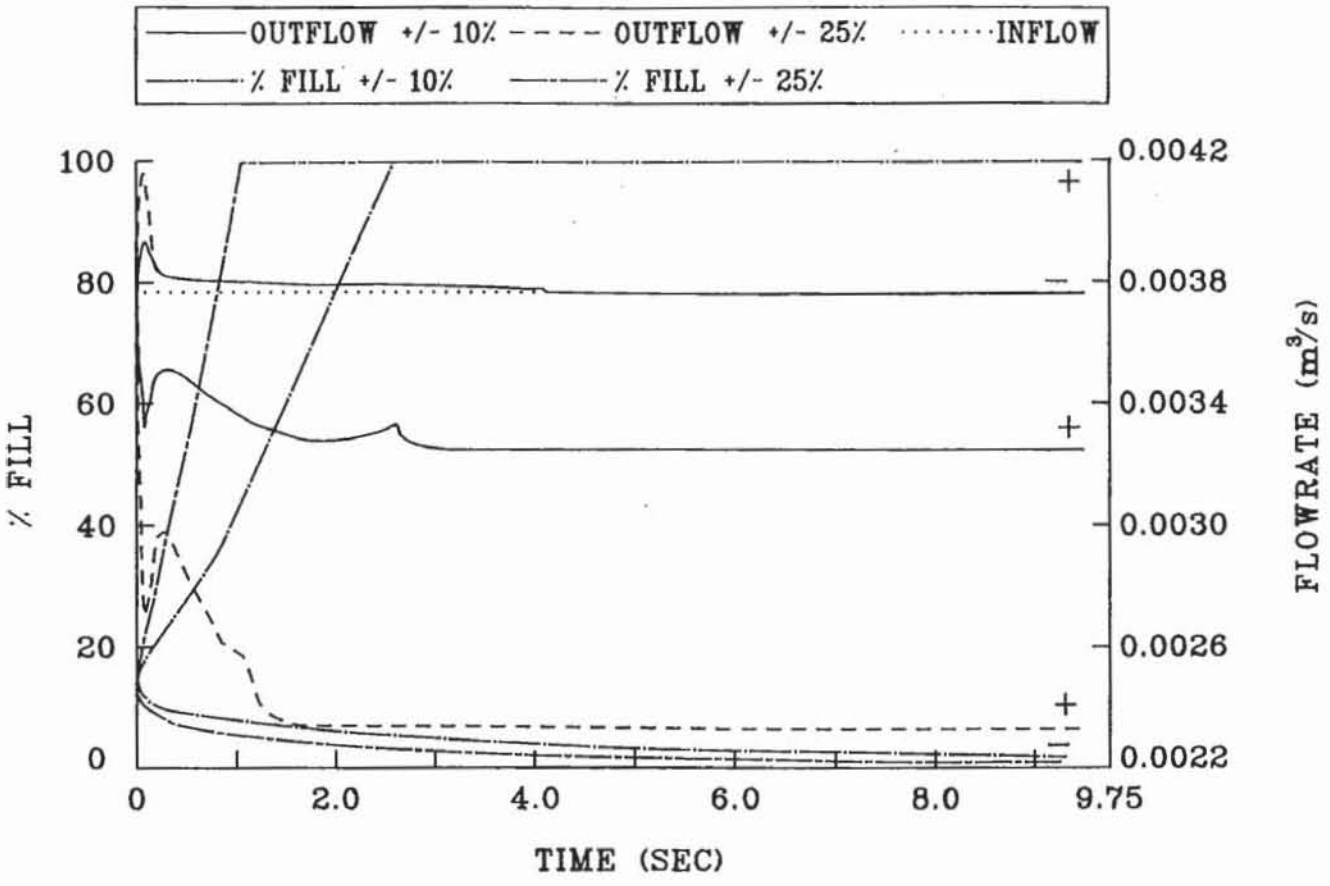

Figure 6.25: Fluid Outflow Rate and Percentage Fill Responses to 10% and 25% Valve Closure Changes with Uncontrolled Speed

6.4.6 Water Inflow Rate

During the normal operation of a hydraulic dynamometer the water inflow can experience fluctuations in its supply. Such disturbances affect the machine performance as does the magnitude of the water inflow rate (Section 5.5.2). To investigate these effects the inflow rate is subjected to increases and decreases of 10% of the initial value at the five test points while all other inputs are held constant. The tests use an initial inflow rate of 0.003788 m3/s (3000 gph) with a ramped change of 10% of this value occurring in 0.5 seconds.

While the inflow rate is increasing to its new value the dynamometer torque increases (Fig. 6.26). Once the new steady flow is reached the torque begins falling. Meanwhile the machine slows since the torque is greater than the driving torque. This deceleration results in the water outflow rate not reaching equilibrium with the inflow rate (Fig. 6.27). After initially following the increase of water inflow the

outflow rate decreases. Consequently the percentage fill increases, which tends to increase the torque and therefore further slow the system, i.e. unstable self-filling. The machine is moving onto a new flowrate characteristic (Section 5.5.2), but cannot find an equilibrium point. For a decrease in water inflow rate the machine's parameters behave in the opposite manner, though the response is stable since the water outflow rate continues to change with the inflow rate toward equilibrium once the new steady inflow rate is reached. Hence the system has found a stable point on a new flowrate characteristic.

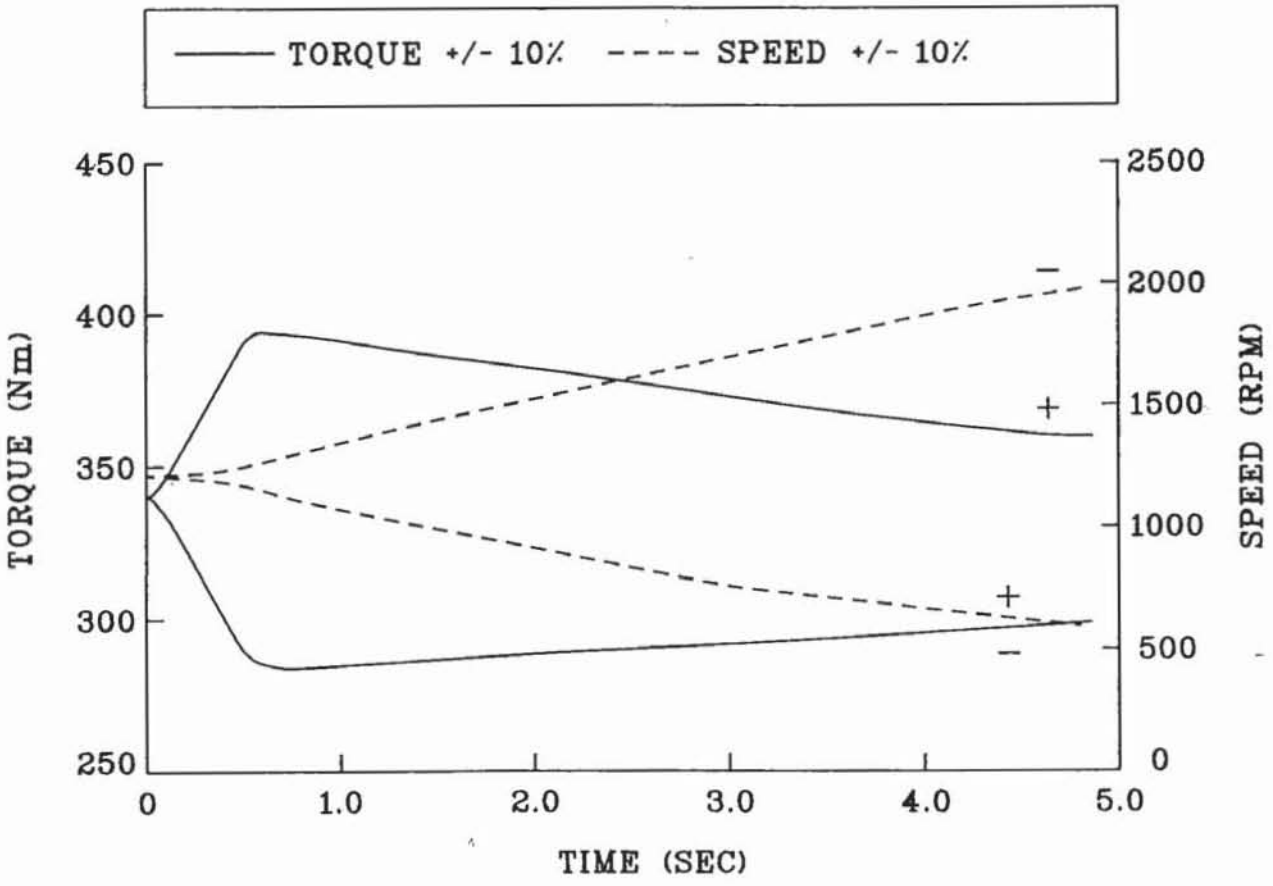

Figure 6.26: Dynamometer Torque and Speed Responses to 10% Fluid Inflow Rate Changes

In Table 6.7 the peak torque changes are shown for the test runs. The lower initial speed tests (points 1-3) indicate that the size of the torque change is dependent on the initial percentage fill of the dynamometer. Comparing the lower initial fill tests (points 1, 4, 5), the initial speed also has a significant effect on the change. This influence is illustrated by point 1 having considerably smaller torque

changes than points 4 and 5, which have much lower initial fill. The latter points lie in the region of the operating envelope where fill is generally low and small changes in fill have significant effects on the machine performance.

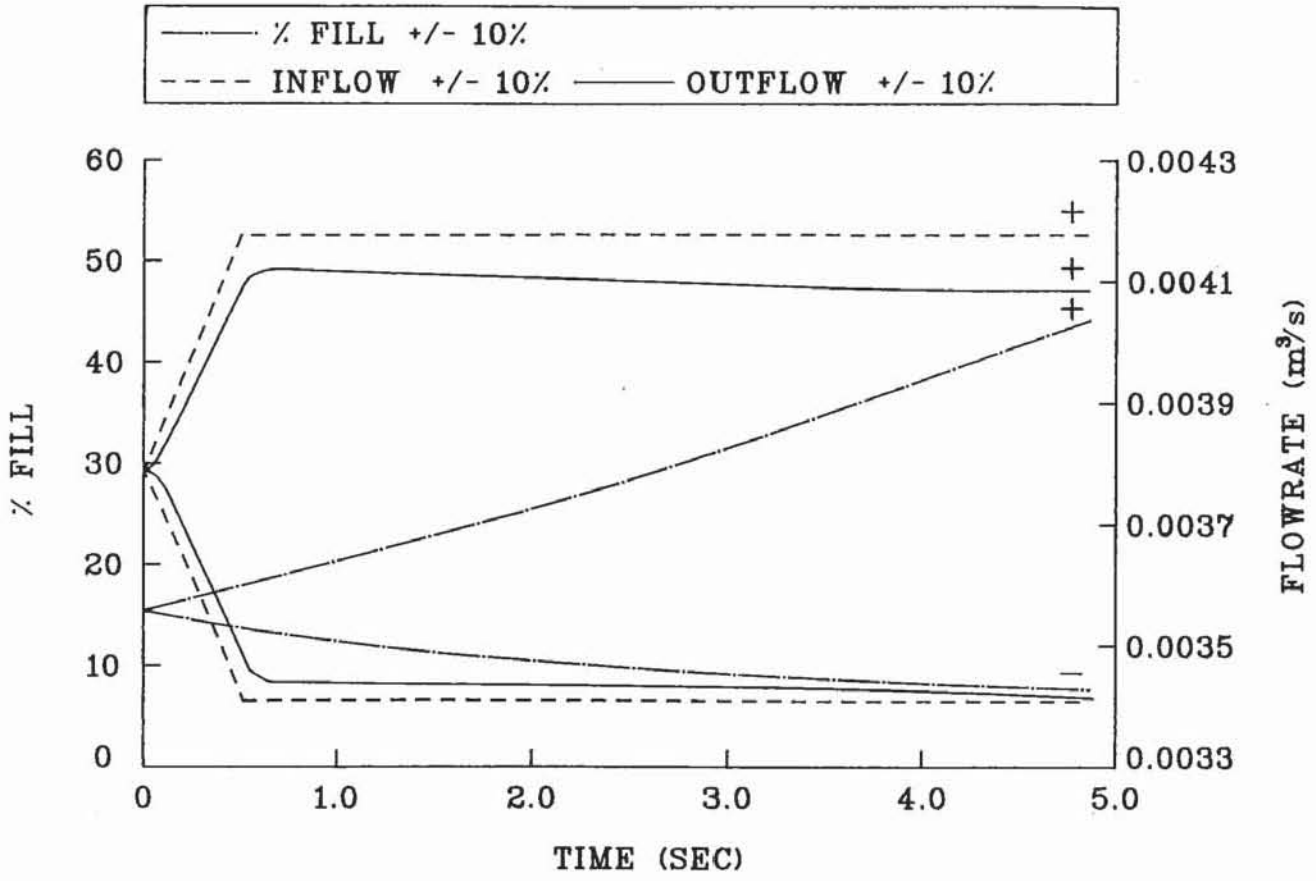

Figure 6.27: Fluid Outflow Rate and Percentage Fill Responses to 10% Fluid Inflow Rate Changes

POINT	INITIAL FILL %	INITIAL SPEED (rpm)	INFLOW RATE CHANGE	TORQUE CHANGE (Nm)
1	15.1	1200	+10%	53.8
			-10%	-53.8
2	41.8	1200	+10%	79.0
			-10%	-123
3	30.9	1800	+10%	142
			-10%	-210
4	8.7	3600	+10%	218
			-10%	-214
5	3.0	6000	+10%	119.2
			-10%	-110.5

Table 6.7 Dynamometer Torque Changes Due to Changes in Water Inflow Rate

CHAPTER 7
OIL DRIVEN BACK PRESSURE VALVE SIMULATION

7.1 Oil Driven Feedback System

7.1.1 Introduction

The previous two chapters investigated the open loop characteristics of hydraulic dynamometers using both steady state and dynamic simulations. When dynamometers are used for actual engine testing they usually have some form of feedback controller attached. Generally, the control device regulates the fluid fill by adjusting the closure of the water outflow valve. In this chapter the performance of a machine fitted with an oil driven back pressure valve is simulated.

Such a dynamometer produces a rising torque/speed characteristic for a fixed control valve setting, due to the resistance to water outflow increasing with the rotational speed of the dynamometer. The feedback control system for this arrangement is illustrated in Fig.7.1. A hydraulic oil pump is driven by the dynamometer shaft, drawing oil from a reservoir and discharging it back to the reservoir through a characterised control valve. The pressure generated in the oil line is transmitted along a dead leg to an oil chamber at the base of the valve assembly. By altering the shape of the valve head the outflow rate characteristic with valve closure can be varied. The valve response is also influenced by the light return spring and the inherent damping of the assembly. As shaft speed increases the increase in oil pressure tends to close the water outflow valve, while the increase in water pressure above the valve and any increase in machine fill tend to open the valve driving the feedback system toward an equilibrium position. Thus the control system is a dynamic subsystem which supplements the open loop dynamic simulation.

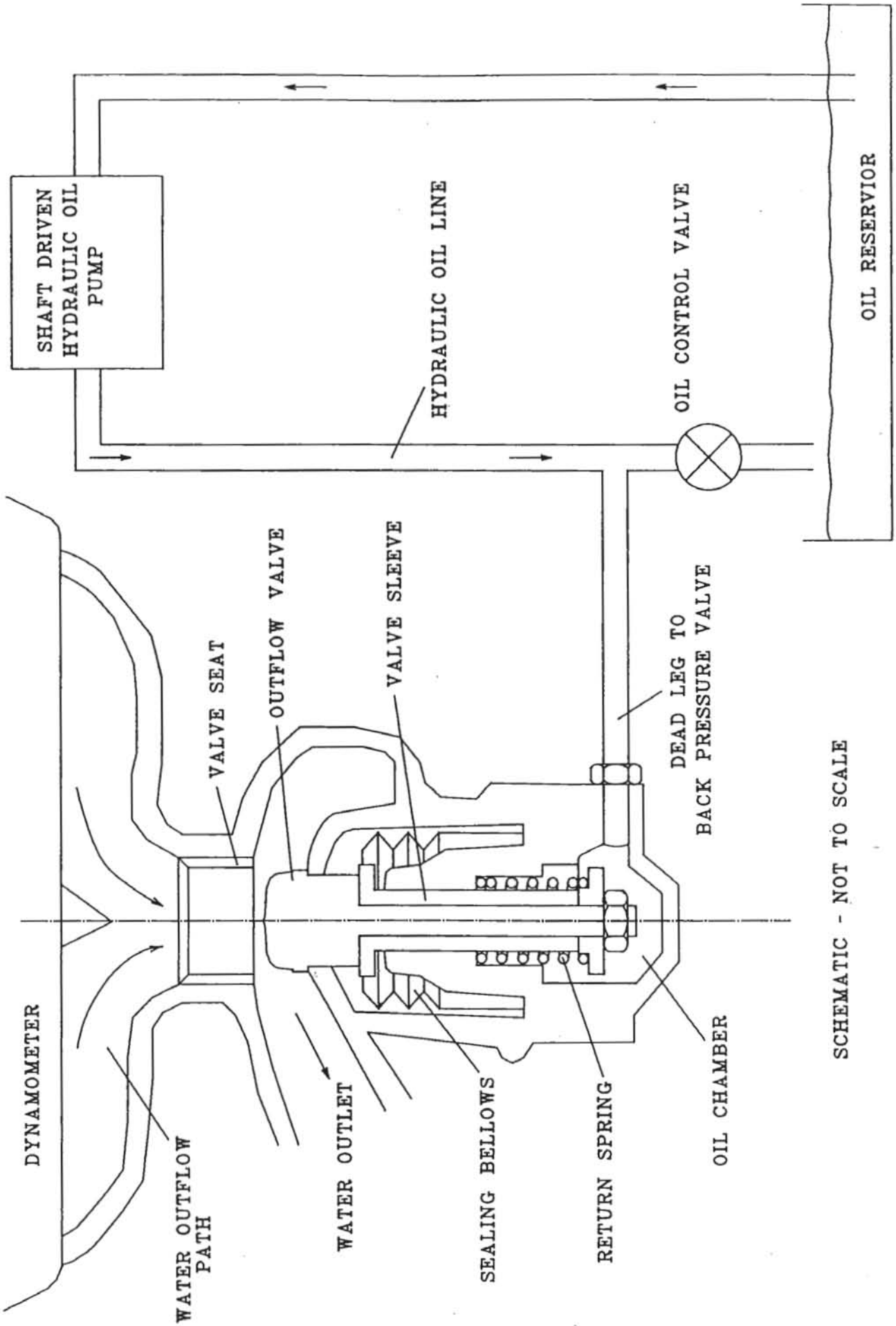

Figure 7.1: Back Pressure Valve Control System

7.1.2 Back Pressure Valve System

The dynamic open loop simulation of hydraulic dynamometers is based on the four first order differential equations derived in Section 6.1.2,

$$\dot{\delta} = \omega_1 - \omega_2 \tag{6.8}$$

$$J_1 \dot{\omega}_1 = T - k\delta \tag{6.6}$$

$$J_2' \dot{\omega}_2 = k\delta - \tau_{14} \tag{6.11}$$

$$\frac{d}{dt}(PF) = \frac{1}{V_F}(Q_{IN} - Q_{OUT}) \tag{6.9}$$

To these equations the representation of the feedback system is added to obtain the closed loop simulation. The back pressure valve arrangement as described in the previous section is modelled as a mass-spring-damper system, as shown in Fig.7.2, of which the equation of motion is

$$m\ddot{z} = P_{OIL} A_{CV} - P_D A_V - k z - c \dot{z} \tag{7.1}$$

where

$z, \dot{z}, \ddot{z}$ = displacement, velocity and acceleration of valve
k , c = spring and damping constants
m = mass of valve
P_{OIL} = hydraulic oil pressure acting over net area A_{CV}
P_D = water pressure above the valve acting on area A_V

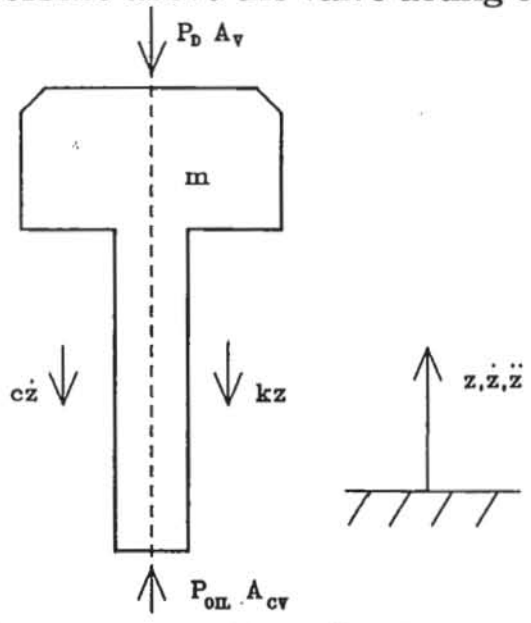

Figure 7.2: Representation of Back Pressure Valve

This second order differential equation is reduced to two first order differential equations, as in Section 6.1.2,

$$\dot{z} = v \tag{7.2}$$

and

$$m\dot{v} = P_{OIL} A_{CV} - P_D A_V - k z - c v \tag{7.3}$$

where

v = valve velocity

The water pressure above the valve is calculated from the working compartment outlet pressure by subtracting the pressure losses along the outflow path, as determined in Section 3.3. Another differential equation is used to determine the pressure in the hydraulic oil line. Using the definition of bulk modulus to allow for oil compressibility in Massey [51],

$$B = \frac{-\delta p}{\delta V / V}$$

where

B = bulk modulus of the hydraulic fluid

δp = pressure change due to a change of volume δV

V = overall volume of fluid

With V constant (assuming rigid walls for the hydraulic line), and δV equal to the difference in volume flow rates (into and out of the volume shown in Fig.7.3), the oil line pressure is given by

$$\frac{d}{dt}(P_{OIL}) = \frac{-B}{V}(Q_{CV} - Q_P) \tag{7.4}$$

where

Q_{CV} = oil flowrate through the control valve

Q_P = oil flowrate from the positive displacement hydraulic pump

$Q_P = N_P C_P$

N_P = pump revolutions per second

C_P = pump displaced volume per revolution

Thus the dynamic model of the back pressure valve controlled dynamometer consists of the seven first order differential equations, Eqns.(6.8), (6.6), (6.11), (6.9), (7.2), (7.3) and (7.4), which are solved as in Section 6.2 by the Adams-Bashforth Predictor Adams-Moulton Corrector Method of Shampine and Gordon [47], for any initial conditions and test runs.

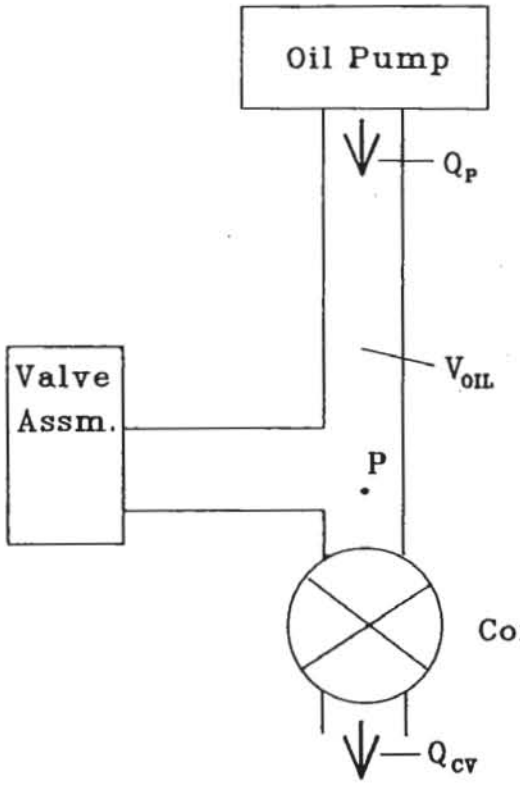

$$\frac{d}{dt}P = \frac{B}{V}(Q_P - Q_{CV})$$

$$B = -\frac{\delta P}{\delta V / V}$$

$$\delta P = -B\frac{\delta V}{V} = -\frac{B}{V}(Q_{CV} - Q_P)$$

$$Q_{CV} = A_{OIL}\left(\frac{2\,P_{OIL}}{C_{OIL}}\right)^{\frac{1}{2}}$$

Figure 7.3: Representation of Oil Control Pressure

7.1.3 System Block Diagram

The closed loop system is presented in Fig.7.4 as a block diagram. In Section 6.1.3 it is concluded that the open loop system can be controlled by either altering the water inflow rate or the water outflow valve closure. Clearly the back pressure valve arrangement affects control by the latter means. The overall dynamometer torque/speed characteristic is altered by the operator adjusting the oil control valve.

In the block diagram it is apparent that this control arrangement provides not only a direct speed feedback but also a feedback of the water pressure, which is dependent on percentage water fill as well as speed. These two feedbacks have opposing influences on the outflow valve, resulting in a very stable closed loop performance.

7.1.4 Program Implementation

By extending the system of differential equations to seven the oil driven back pressure valve is included to provide the closed loop simulation. Hence the routines to calculate the time-dependent constants (Subroutine STATUS) and the array of differential equation values (Subroutine F) are enlarged. Otherwise the program structure, as shown in Fig.7.5, is the same as for the open loop dynamic case.

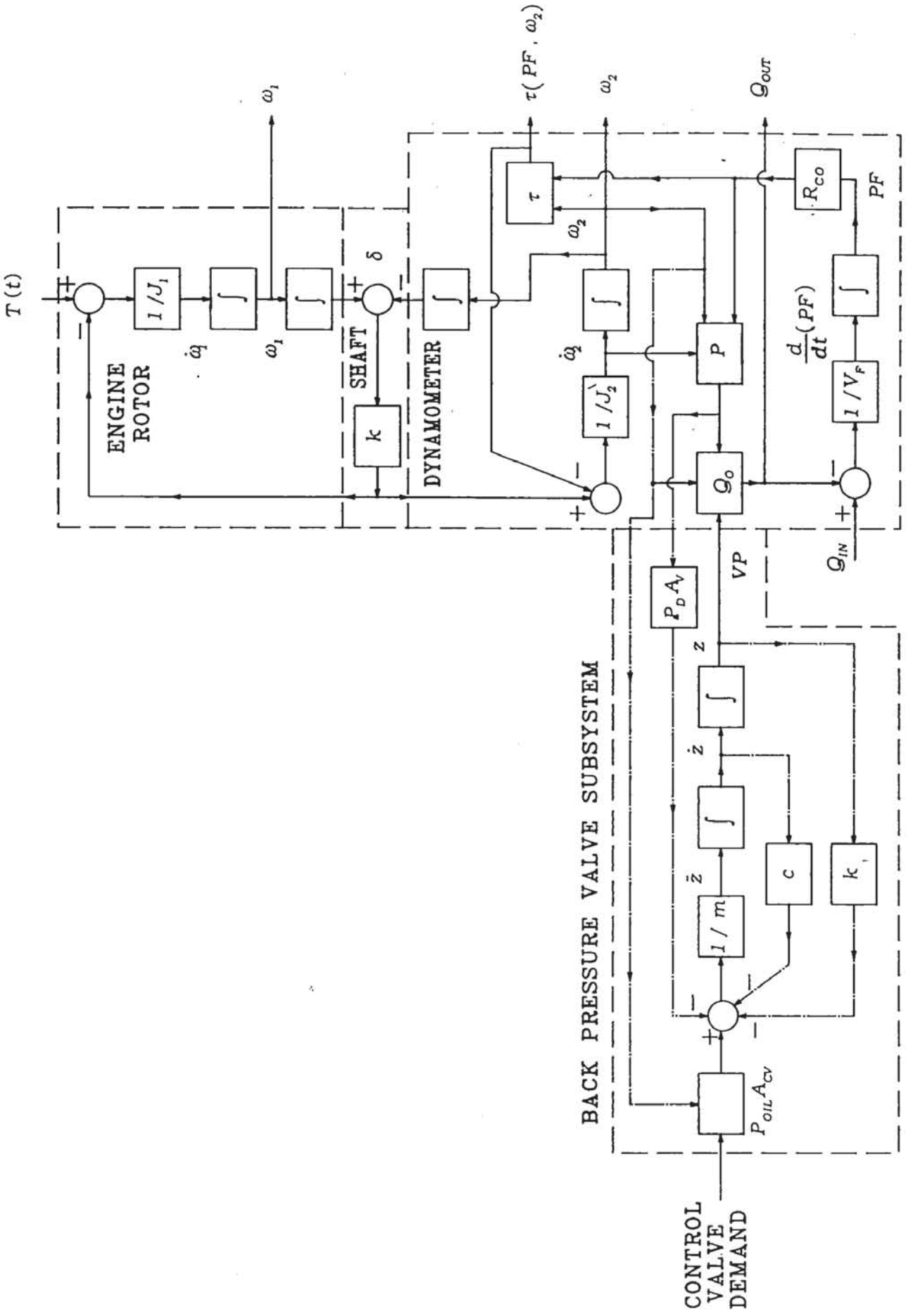

Figure 7.4: Block Diagram of Back Pressure Valve Closed Loop Engine-Dynamometer System

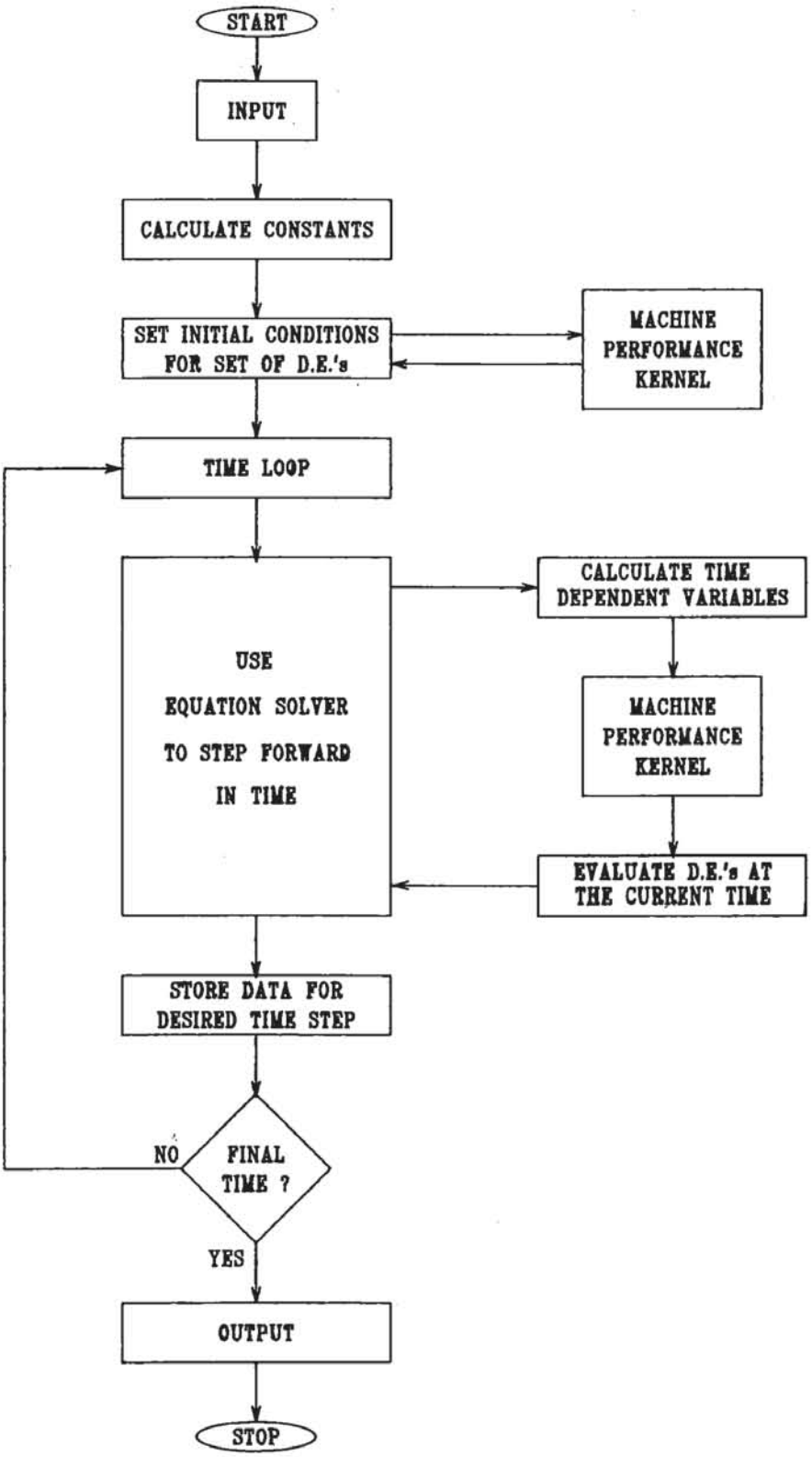

Figure 7.5: Structure of Back Pressure Valve Closed Loop Dynamic Program

7.2 Back Pressure Valve Performance

7.2.1 Constant Oil Control Valve Setting

For any given control valve setting the back pressure controlled dynamometer follows an increasing torque against speed characteristic. The pressure loss characteristic of the control valve determines the distribution of the torque characteristics. Using experimental data from Froude an appropriate control valve characteristic is determined in Section 3.3.1 which produces the series of torque characteristics, shown in Fig.7.6, across the operating envelope. The model prediction characteristics are coincident with the experimental curves in this figure. These torque characteristics for constant control valve setting are of a similar form to the lines of constant percentage fluid fill, indicating that the back pressure control valve system results in only a small variation of fluid fill with speed for a constant control setting.

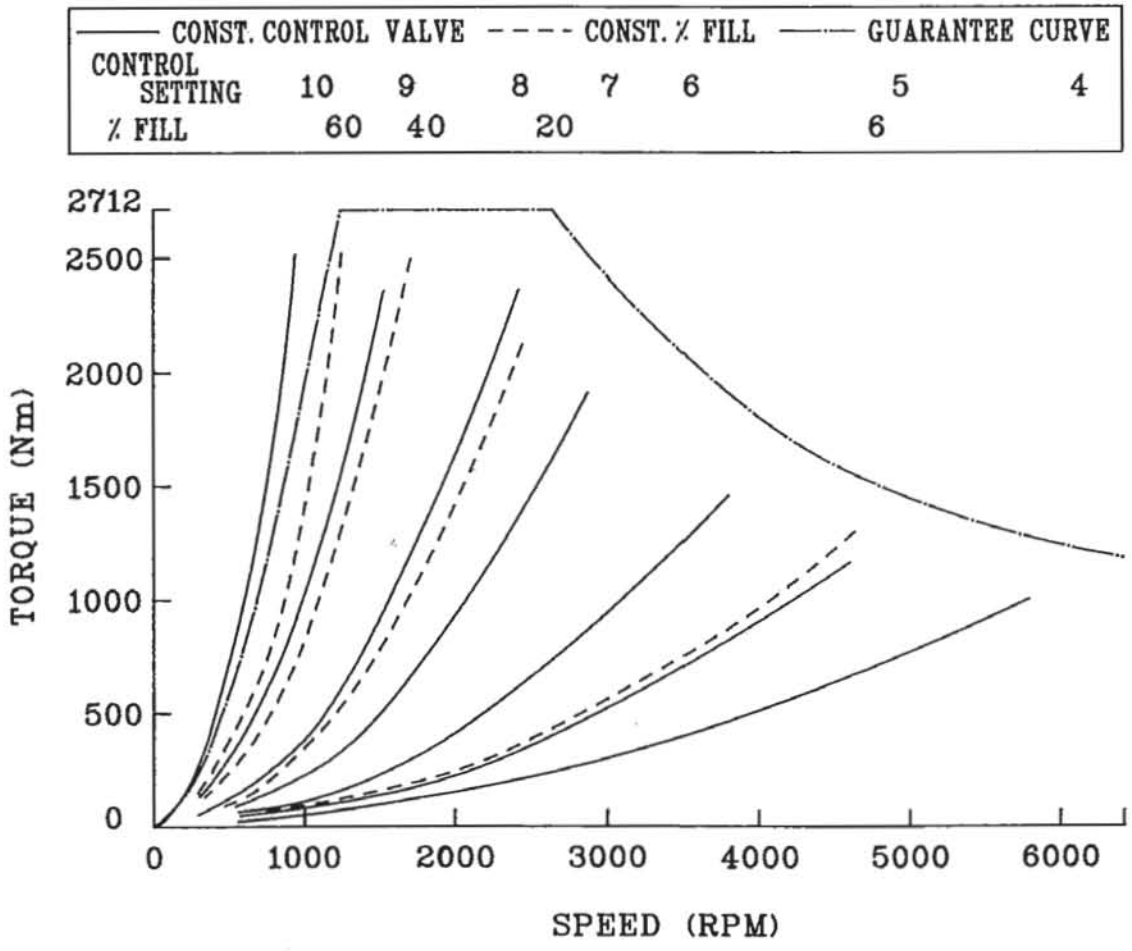

Figure 7.6: Constant Control Setting Torque-Speed Characteristics

7.2.2 Change of Control Valve Setting and/or Driving Torque

The effects of changes to the control valve setting and the driving torque input, occurring both together and independently, are studied in this section. Most straightforward of these changes is the case of an increase or decrease of control valve setting. For an increase or decrease of one turn from the initial setting[1] the system's torque response (Fig.7.7) is to rapidly move to the new constant setting characteristic with only a small speed change, before moving along the new torque characteristic to the driving torque value, which has remained constant throughout the test. Clearly the water outflow valve responds rapidly to the altered oil control pressure acting on it, leading to the effect of the change in the percentage water fill exceeding that of the acceleration of the rotating inertias (Fig.7.8).

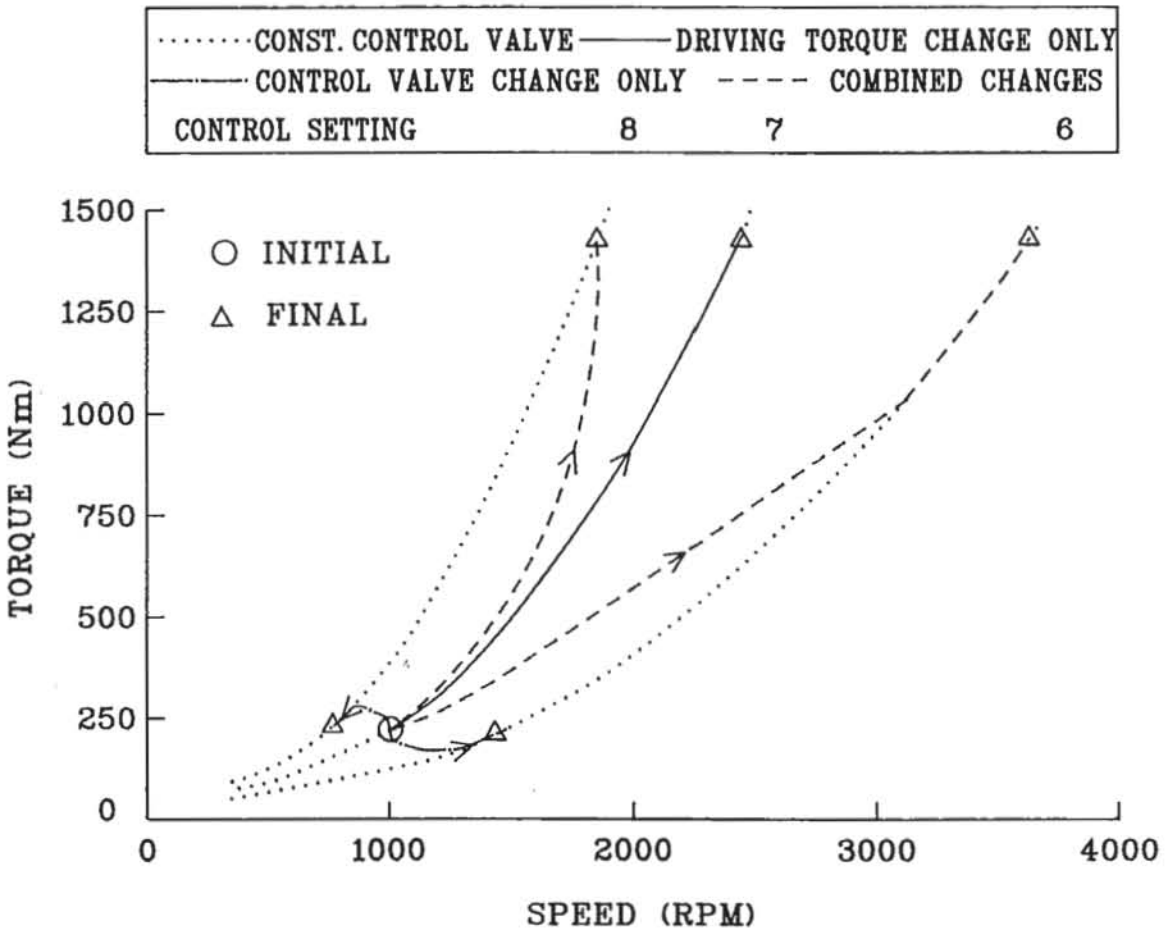

Figure 7.7: Torque-Speed Characteristics for Isolated and Combined Control Setting and Driving Torque Changes

---

1 For the analysis of this section the initial conditions are taken to be: control valve setting = 7; initial speed = 1000 rpm (uncontrolled during tests); initial driving torque (from engine inertia) = 208.5 Nm; engine inertia 5.0 kg m^2. Control valve changes to 6 or 8 are at the rate of 0.5 settings/s (i.e. a ramped change over 2.0 seconds) Driving torque change is to 1200 Nm at a rate of 1000 Nm/s (i.e. a ramped change over ≈ 1.0 seconds).

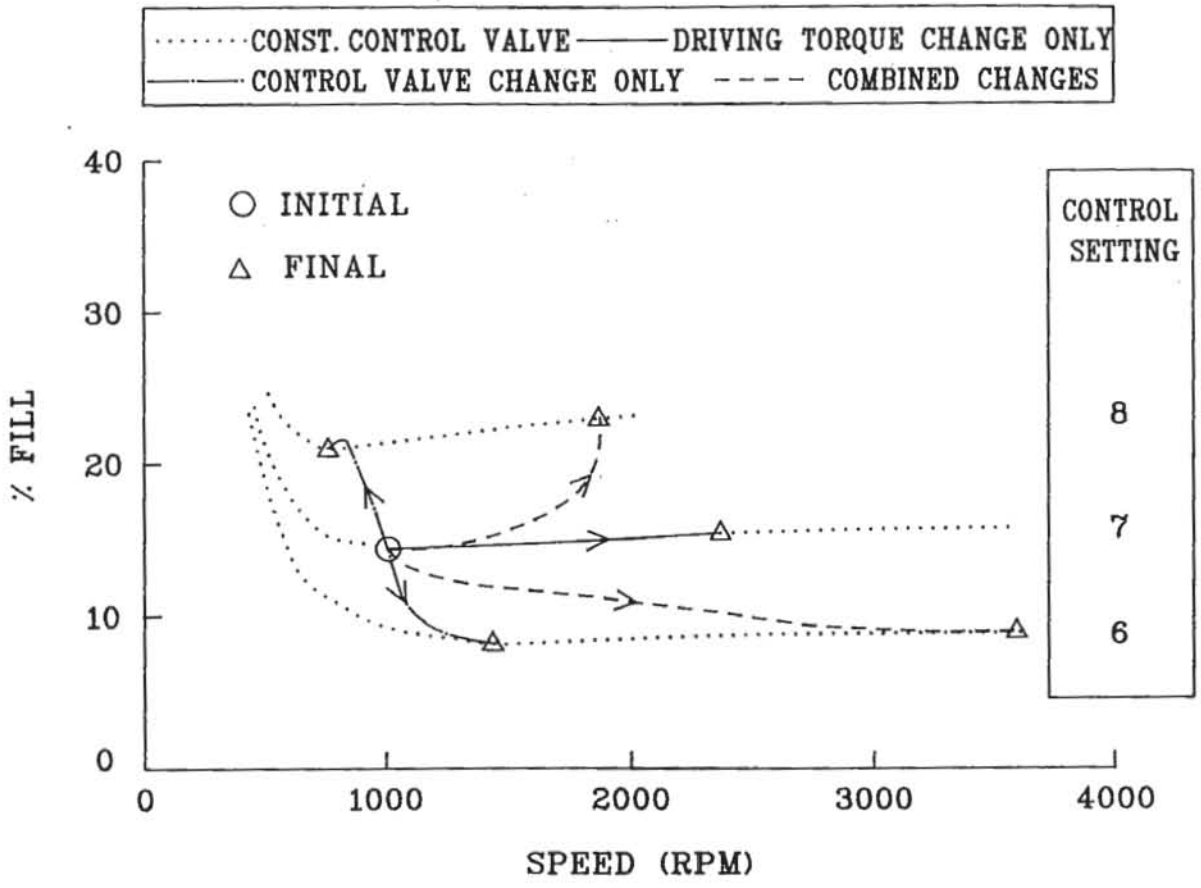

Figure 7.8: Percentage Fill-Speed Characteristics for Isolated and Combined Control Setting and Driving Torque Changes

In the latter stages of the control valve change tests the system behaves in the same manner as when there is simply a change in the driving torque input. Effectively this is the case, since the change in fluid fill has altered the dynamometer torque. The response to a change in the driving torque only is also shown in Fig.7.7. From the initial point the torque and speed increase along the characteristic curves for a control valve setting of seven, until equilibrium with the new driving torque is reached. When the parameters are presented against time both the water outflow valve (controlled by speed dependent oil system) and dynamometer torque curves follow sigmoidal curves due to the dynamometer speed change; such an acceleration is due to the increased torque acting on the rotating inertia (a second order subsystem). In contrast there is only a very slight increase in fluid fill percentage, thus the torque change is influenced almost entirely by the acceleration.

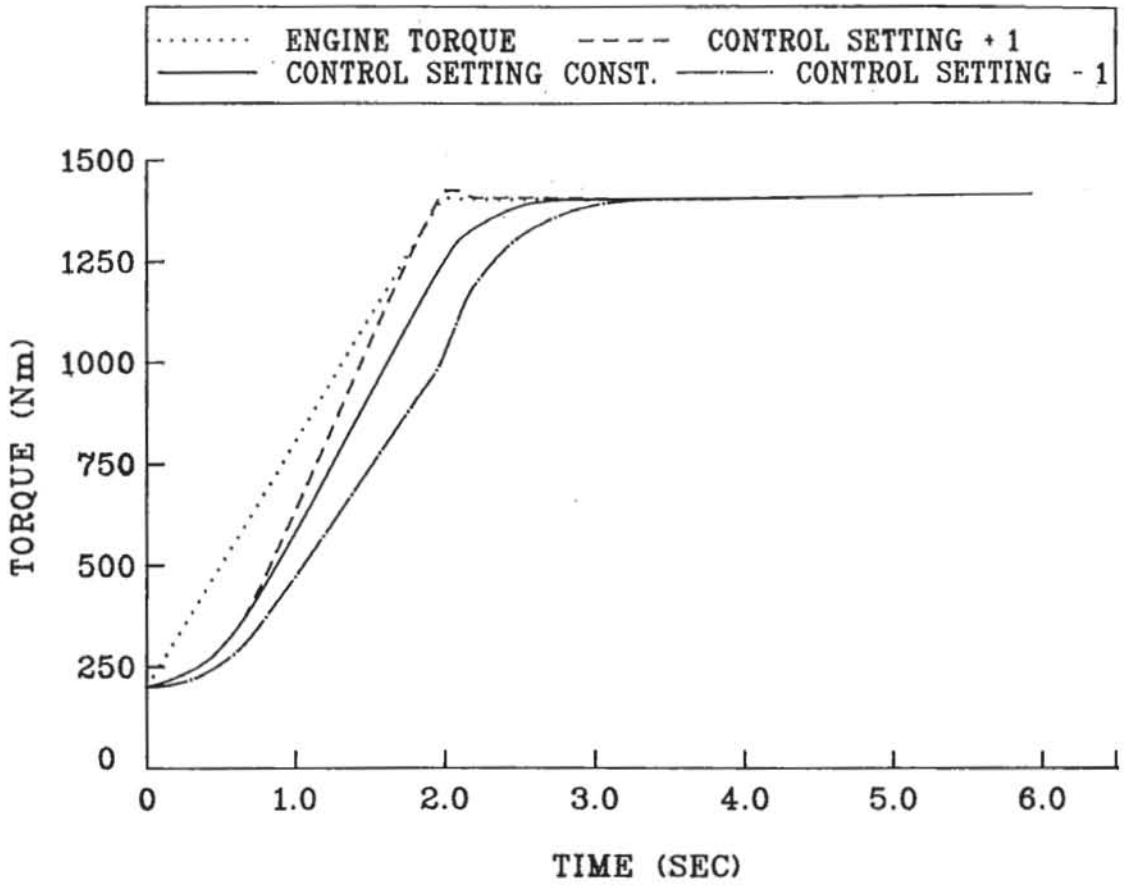

Figure 7.9: Dynamometer Torque Response to Combined Control Setting and Driving Torque Changes

If both the valve and torque changes are made simultaneously the system response is a combination of the previous two cases. The machine acceleration results in a greater speed change before the torque response aligns with the new valve setting characteristic. In the case of the valve setting increase, the multiple order nature of the system results in an over shoot and oscillation of the response before the new characteristic is adopted (Fig.7.9). Examination of the water outflow valve response in Fig.7.10 shows the oscillation occurring in this control subsystem as a consequence of the control valve closure. This overshoot causes the fluid fill percentage to rise sharply, before it settles on to a slightly increasing valve as for the case of only driving torque change. The oscillations in outflow valve and torque are both superimposed on sigmoidal curves similar to those for the case of an isolated driving torque change. When the valve setting is decreased (the valve opened) the response more rapidly reaches the new torque characteristic, producing a very clear breakpoint in the torque and percentage fill curves.

The response of the oil driven back pressure valve machines is characterised by a series of rising torque against speed curves. Primarily these dynamometers are intended for use along these curves with little adjustment of the control valve. If control valve adjustment is introduced to the test procedure, the resulting test characteristic is considerably influenced by the acceleration response to torque input changes as the system adjusts to the new control valve characteristic torque curve.

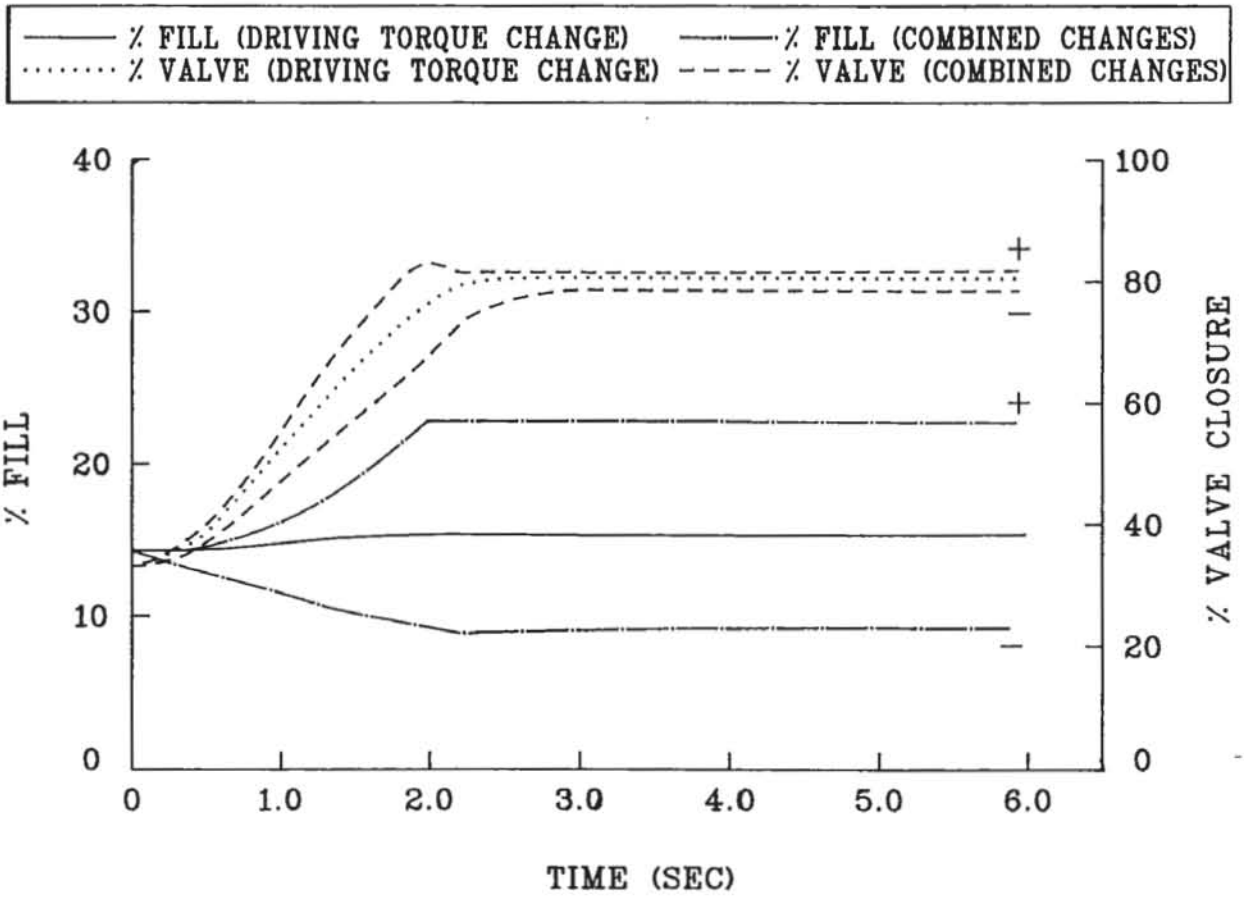

Figure 7.10: Fluid Outflow Valve Closure and Percentage Fill Responses to Combined Control Setting and Driving Torque Changes

The relationship between the component responses of any given change introduced to this system is dependent upon such factors as the two inertias, the outflow valve mass and damping (the spring is only a relatively light return spring). A smaller *engine* inertia would result in the whole system accelerating more rapidly and the acceleration effects merging more closely with the valve change effects. Therefore, when comparing the simulation to actual tests all experimental parameters must be considered.

CHAPTER 8
ELECTROHYDRAULIC VALVE MACHINE SIMULATION

8.1 Electrohydraulic Valve Feedback System

8.1.1 Introduction

In Chapter 7 a hydraulic oil pump is used to provide the system with a speed feedback and thus obtain a series of increasing torque characteristics against speed. However many situations require a more flexible control system. Such a system is provided by dynamometers with electrohydraulic valve control (Fig.8.1). An electrical controller (digital or analogue) receives feedback signals from the dynamometer and compares them to the required demands set on the operator's control panel. The *error* between the set point and the measured value is used to calculate a new activation signal for the servo driven butterfly valve that regulates the machine water outflow.

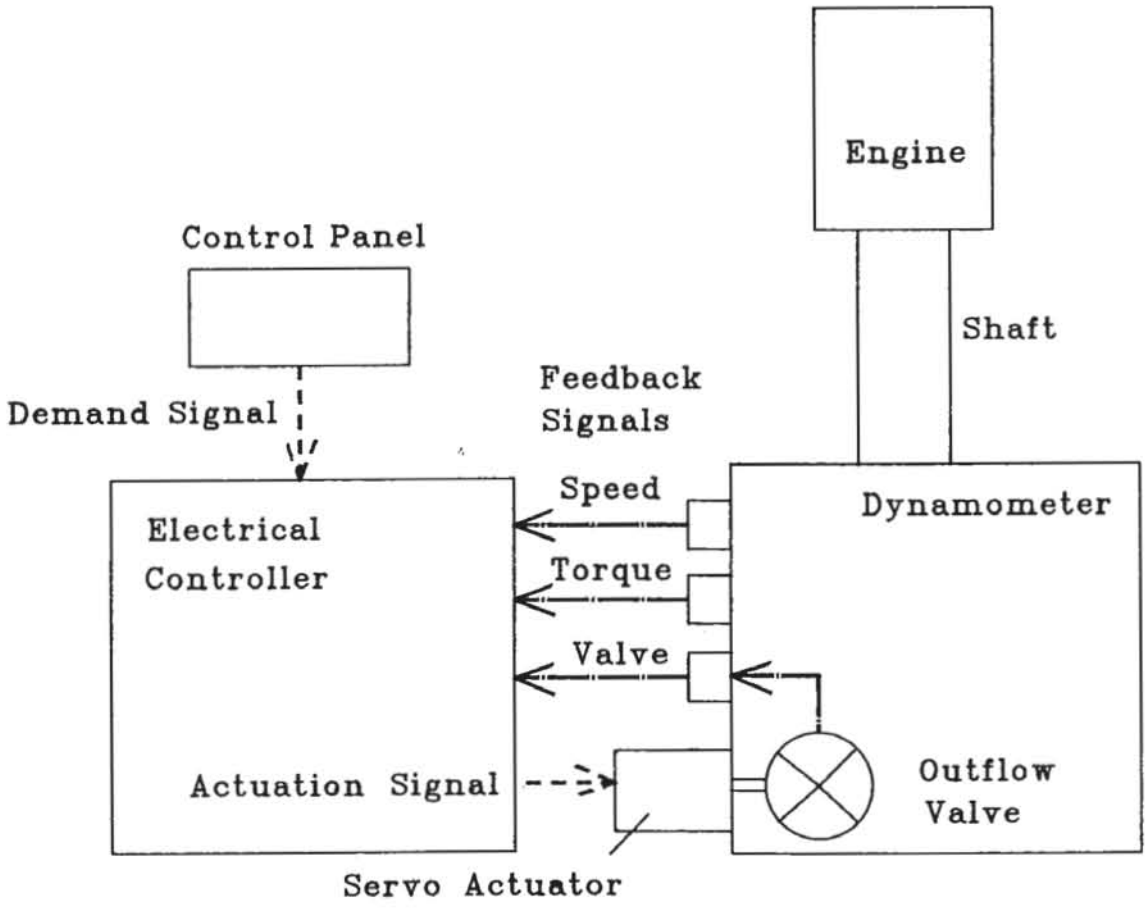

Figure 8.1: Electrohydraulic Valve Control System Schematic

Usually the required demand from the control panel is for valve position, torque, speed or power law control (Fig.8.2). Positional control is essentially open loop, as no consideration is taken of the speed and torque feedbacks. Only the valve position feedback is checked to determine that the servo is holding the correct position. For speed control the demand is inverted, since a speed increase requires dynamometer torque to be decreased by means of a lower valve closure. The speed feedback dictates system speed, while the system torque is determined by the engine throttle setting. With speed governed engines the dynamometer is used in torque control mode, utilising the torque feedback. In the case of the power law control mode the demand signal is sent into a function generator. The speed feedback enters the generator producing a torque demand, which is compared to the torque feedback signal.

From the error signal, produced by the demand and feedback signals, the controller calculates the new activation signal. For the torque and speed controllers this computation is achieved by means of the three term P.I.D. algorithm. The components of this method are proportional, integral and derivative. An in depth treatment of control algorithms is beyond the scope of this work, but is readily available in control texts such as Stephanopoulos [64] and Hougen [65]. Briefly, the effect of the three control elements are: proportional, accelerates the response to an error but produces an offset; integral, eliminates any offset, but is oscillatory (possibly leading to instability) and slows the system response; derivative, anticipates future errors and has a stabilising effect on oscillations allowing higher proportional gains to speed the overall response. The mathematical representation of such a control system is presented in the following section.

8.1.2 Representation of Feedback System

As described in the previous section and shown in Fig.8.2 the appropriate feedback signal is compared to the demand signal to provide an error input for the three term control amplifier. From this controller a valve demand signal is sent to the valve position control amplifier, which compares the positional feedback to the demand and sends an actuation signal to the servo valve. The valve controller is a

two term PD controller, giving a very fast response to errors in position.

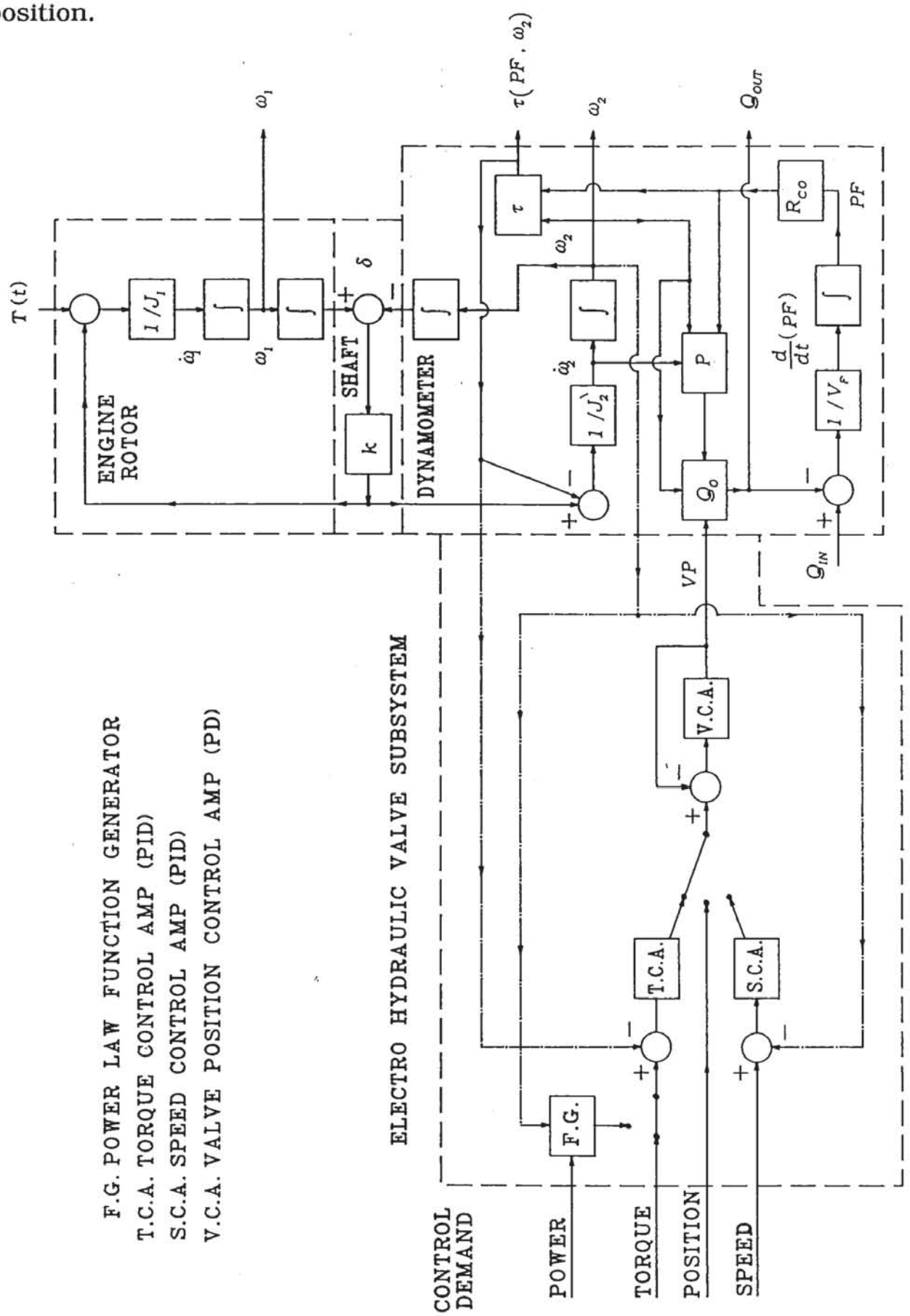

Figure 8.2: Block Diagram of Electrohydraulic Valve Closed Loop Engine-Dynamometer System

Both analogue and digital electronics are used to realise controller designs. In this work a digital representation suitable for direct digital control is modelled. At every control period[1] a new actuation signal is calculated based on the feedback and demand signals.

To introduce the mathematical representation the analogue control element responses to the error signal are defined. For proportional control the response is

$$u = u_0 + K_c \varepsilon \tag{8.1}$$

where

u = valve actuation signal
u_0 = initial valve actuation signal
K_c = proportion (controller) gain
ε = error signal = demand - feedback

The integral and derivative control responses are

$$\frac{1}{\tau_I}\int \varepsilon \, dt \quad and \quad \tau_D \frac{d}{dt}\varepsilon$$

respectively, where

τ_I = integral action time
τ_D = derivative action time.

These components combine to form the PID algorithm,

$$u = u_0 + K_c\left[\varepsilon + \frac{1}{\tau_I}\int \varepsilon \, dt + \tau_D \frac{d}{dt}\varepsilon\right] \tag{8.2}$$

A more detailed treatment of this analogue form is given in Chapter 13 of Stephanopoulos [64] with the following digital form in Chapter 30.

To apply this algorithm to a digital system a difference equation equivalent of the continuous Eqn.(8.2) is required, so the integral is represented as

$$\int \varepsilon \, dt = T \sum \varepsilon_K \qquad K = 0, 1, 2, 3, \ldots$$

and the derivative as

$$\frac{d}{dt}\varepsilon = \frac{1}{T}(\varepsilon_K - \varepsilon_{K-1})$$

---

1 The sampling rate for analogue to digital conversions must be at least twice the controller operating frequency. This work only considers the operating frequency taking the digital feedback to be a perfect representation of the analogue signal.

where T is the control time period equal to the interval $K\text{-}1$ to K. Hence Eqn.(8.2) becomes

$$u_K = u_O + K_C\left[\varepsilon_K + \frac{1}{\tau_I}T\sum_{1}^{K}\varepsilon_K + \frac{1}{T}\tau_D\,(\varepsilon_K - \varepsilon_{K-1})\right] \qquad (8.3)$$

By altering the gains on each element of the control equation the relative effects of each control component can be manipulated, so Eqn.(8.3) becomes

$$u_K = u_O + K_C\left[K_P\,\varepsilon_K + K_I\frac{1}{\tau_I}T\sum_{1}^{K}\varepsilon_K + K_D\frac{1}{T}\tau_D\,(\varepsilon_K - \varepsilon_{K-1})\right] \qquad (8.4)$$

For the valve position PD controller the control equation is

$$u_K = u_O + K_C\left[K_P\,\varepsilon_K + K_D\frac{1}{T}\tau_D\,(\varepsilon_K - \varepsilon_{K-1})\right] \qquad (8.5)$$

The Eqns.(8.3), (8.4) and (8.5) are the *position form* of the control algorithms. That is, at each time step the new actuation signal is calculated as an absolute value from the initial value and the subsequent errors. In the case of an acceleration test, for example, the system speed or torque may be less than the new dynamometer control demand for a long period. Using the above form of the equations the control action will become *saturated* (extreme valve position), and remain so even if the error returns to zero due to the effect of the integral summation term. This condition is known as *integral windup* . To prevent this occurring the control algorithms are used in an alternative form. In the *velocity form* of the equations only the change is actuation signal from the previous time step is calculated. Taking Eqn. (8.3), the change in PID control action between the K th and (K -1)th time steps is

$$\Delta u_K = u_K - u_{K-1}$$

$$\Delta u_K = K_C\left(1 + \frac{1}{\tau_I}T + \frac{1}{T}\tau_D\right)\varepsilon_K - K_C\left(1 + \frac{2}{T}\tau_D\right)\varepsilon_{K-1} + K_C\frac{1}{T}\tau_D\varepsilon_{K-2} \qquad (8.6)$$

where

ε_K = error signed at time step K

As above, relative gain constants are included to facilitate the investigation of the relative effects of the control components. Hence the PID algorithm (Eqn. (8.6)) is

$$u_K = u_{K-1} + K_C\left(K_P + K_I \frac{1}{\tau_I} T + K_D \frac{1}{T} \tau_D \right) \varepsilon_K$$
$$- K_C\left(K_P + K_D \frac{2}{T} \tau_D \right) \varepsilon_{K-1} + K_C K_D \frac{1}{T} \tau_D \varepsilon_{K-2} \qquad (8.7)$$

and the PD algorithm for valve position is

$$u_K = u_{K-1} + K_C\left(K_P + K_D \frac{1}{T} \tau_D \right) \varepsilon_K$$
$$- K_C\left(K_P + K_D \frac{2}{T} \tau_D \right) \varepsilon_{K-1} + K_C K_D \frac{1}{T} \tau_D \varepsilon_{K-2} \qquad (8.8)$$

8.1.3 Program Implementation

As with the open loop and back pressure valve machine dynamic simulations the core of this implementation (Fig.8.3) is the differential equation solver (Subroutines DDE, DSTEP, DINTRP), the set of four differential equations (Eqns.(6.8), (6.6), (6.11), (6.9) in Subroutine F), and the machine performance kernel as defined in Section 5.1. However to allow for the discrete controller action the main program decides whether the next time step is to a control action time or a required output time, and when to calculate a new controller actuation signal.

Provision is made in the program for the full use of varying relative gains as in Eqns.(8.4) and (8.5). In Section 8.2.1 the control parameters of this equation are determined using the Cohen-Coon criteria.

This model of the closed loop dynamometer considers the valve actuator system to respond perfectly, without considering the dynamics of the actuation system. Hence a full action slew time of 0.200 seconds is used to represent the valve movement. Any movement over less than the full range is considered to take a linear proportion of this time. Thus the valve actuation is determined by the signal from the speed/torque feedback loops (Section 8.1.2, Subroutine CONTOL) with the position control taken as responding rapidly and accurately. With appropriate data a model of the valve actuator system dynamics could be added to the program and the valve position controller incorporated.

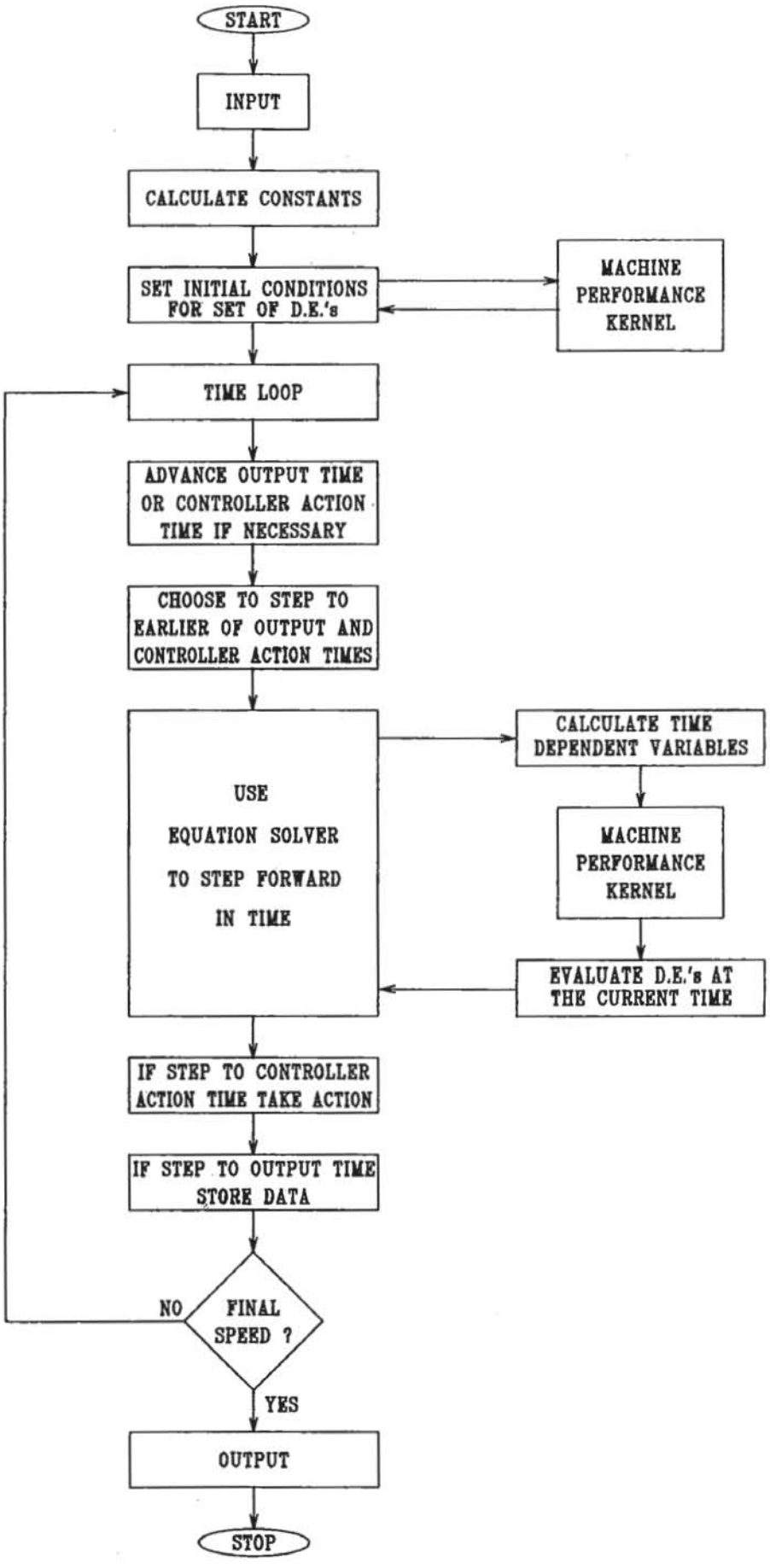

Figure 8.3: Structure of Electrohydraulic Valve Closed Loop Dynamic Program

8.2 Electrohydraulic Valve Performance

8.2.1 PID Controller Tuning

There are numerous combinations of values for the control parameters K_C, τ_I, τ_D and many criteria to determine the most suitable values for a given situation. A comparison of these methods is outside the scope of this thesis, but clearly the theoretical methods using a transfer function representation of the dynamometer system are not possible without linearizing and therefore seriously compromising the non-linear nature of the dynamic models. Since the open loop dynamic model is available to conduct tests an empirical method can be used to tune the controller parameters, while preserving the non-linear behaviour of the dynamometer.

Hence the very common *process reaction curve method* developed by Cohen and Coon is applied to the open loop dynamic model. A detailed treatment of this method is given in Stephanopoulos [64] and most other control texts, so only a brief outline is presented here. Under open loop control a step change is made to the outflow valve (the system control element), and the resulting torque and speed outputs recorded. Applying a step change to a physical system requires a finite time period in most situations, which actually results in a ramped step. Accordingly the valve closure tests of Sections 6.4.4 and 6.4.5, used to provide process reaction curves, incorporate a valve slew time of 0.2 seconds for full action into the step changes. The curves of torque and speed against time (Figs.6.21 and 6.24) have a sigmoidal shape. Cohen and Coon observed that such responses can be approximated by a first order plus dead time system (Fig.8.4). From the approximate response the three parameters are obtained for the first order plus dead time model,

$$G(s) \approx \frac{K\, e^{-t_d s}}{\tau s + 1}$$

where

$G(s)$ = modelled response
K = gain = output/input
τ = B/S, S= slope of sigmoidal response at point of inflection
t_d = dead time

This approximate model yields expressions for PID controller settings, according to Cohen and Coon, of

$$K_C = \frac{1}{K}\frac{\tau}{t_d}\left(\frac{4}{3} + \frac{t_d}{4\tau}\right)$$

$$\tau_I = t_d \frac{32 + 6t_d/\tau}{13 + 8t_d/\tau}$$

$$\tau_D = t_d \frac{4}{11 + 2t_d/\tau}$$

These parameter values are not regarded as optimal for any particular process, but as a good first approximation. On-line adjustment of these values tunes the controller to the specific test program.

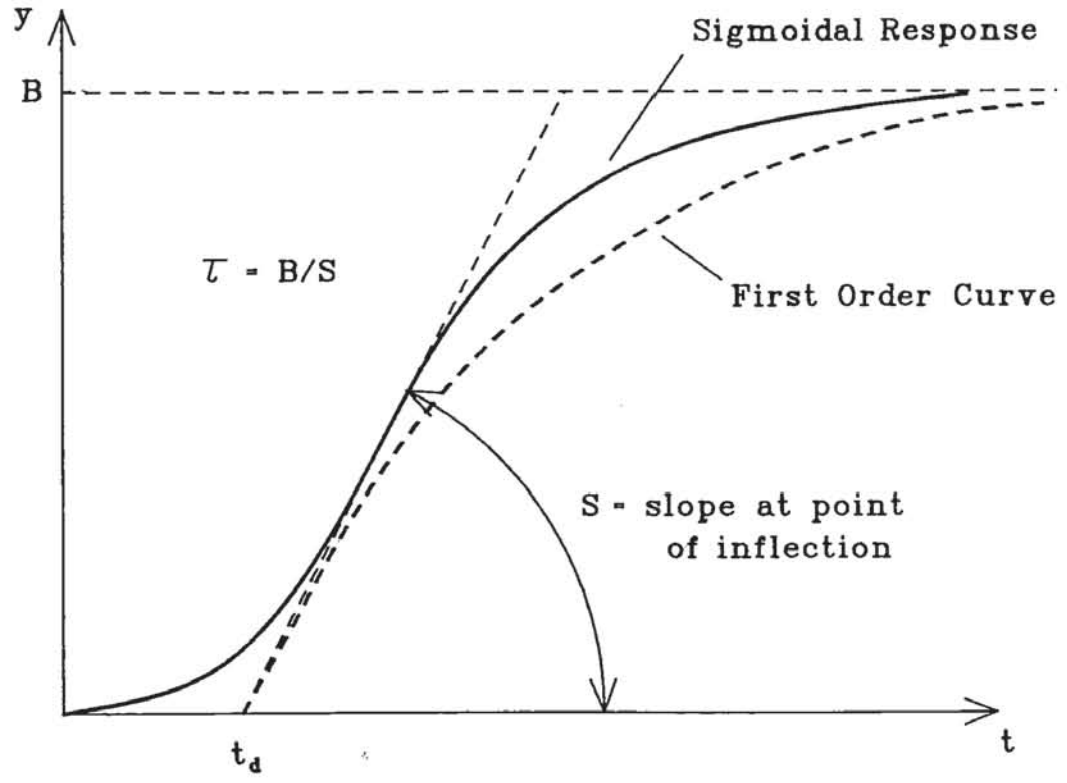

Figure 8.4: First Order Approximation to a Sigmoidal Response Curve

The tests of Section 6.4.4 and 6.4.5 provide the PID parameter values presented in Tables 8.1, 8.2 and 8.3. It is apparent that the appropriate control parameters vary as the fill and speed conditions change from point to point, which indicates non-linearity in the system. In the following section the effect on control performance of different control values at a given point is studied. Inappropriate values lead to unsatisfactory control. Hence setting the controller to the values suitable for the initial conditions leads to control problems if the

test involves a change in set point across the operating envelope. As would be expected the rate of dynamic response (dependant on system inertia) also influences the choice of controller parameters. Comparison of Tables 8.1 and 8.2 indicates that, for speed control, the selection criteria gives substantially different parameter values for the different engine inertias. The influence of the engine dynamic behaviour has further consequences if the engine is governed. The parameter values of Table 8.3 for torque control show some difference in K_C to those of Table 8.2. Hence the controlled engine characteristics must be considered in selecting dynamometer controller values in order that the system response is satisfactory.

POINT	K_C	τ_I	τ_D
SPEED CONTROL			
1	.0027	.15	.023
2	.0067	.14	.020
3	.0023	.14	.022
4	.0028	.086	.013
5	.0034	.071	.011
TORQUE CONTROL			
1	.010	.021	.0032
2	.012	.024	.0036
3	.0039	.028	.0043
4	.0040	.018	.0027
5	.0056	.014	.0021

Table 8.1: PID Controller Parameters Obtained with Uncontrolled Speed (Engine Inertia = 2.5 kgm^2)

The application of frequency response methods to the dynamometer dynamic behaviour would allow the use of the Ziegler-Nichols tuning technique (Stephanopoulos [64]) for the PID controller and comparison with the Cohen and Coon parameters. Should a dynamic transfer function model (empirical not theoretical) of the dynamometer be required rather than the time domain study of the present work, then the frequency response methods are generally regarded as more accurate.

POINT	K_C	τ_I	τ_D
SPEED CONTROL			
1	.0018	.062	.0094
2	.0075	.066	.0098
3	.0057	.037	.0055
4	.0088	.064	.0095
5	.0050	.084	.013
TORQUE CONTROL			
1	.013	.019	.0029
2	.015	.022	.0036
3	.012	.015	.0022
4	.0073	.019	.0029
5	.0071	.015	.0023

Table 8.2: PID Controller Parameters Obtained with Uncontrolled Speed (Engine Inertia = 0.2 kgm^2)

POINT	K_C	τ_I	τ_D
TORQUE CONTROL			
1	.0081	.020	.0029
2	.0084	.025	.0038
3	.0054	.016	.0023
4	.0024	.019	.0029
5	.0017	.014	.0022

Table 8.3: PID Controller Parameters Obtained with Constant Speed (Engine Inertia = 0.2 kgm^2)

8.2.2 Effect of Controller Parameter Variations

The use of Cohen and Coon criteria in the previous section is to locate good first approximations to the most suitable control values. In many control situations the actual test conditions and the desired system performance may require fine tuning of the controller. A series of simulations involving an increasing driving torque and an increasing speed control demand were performed to study the effect of parameter adjustments. The *base* test uses the Cohen and Coon parameter values for point 1, while subsequent tests alter the overall and relative gains of the control components (Eqns.(8.4) and (8.6)) by an order of

magnitude. Table 8.4 gives a summary of the system responses, as shown in Figs.8.5 and 8.6, to the different control parameters.

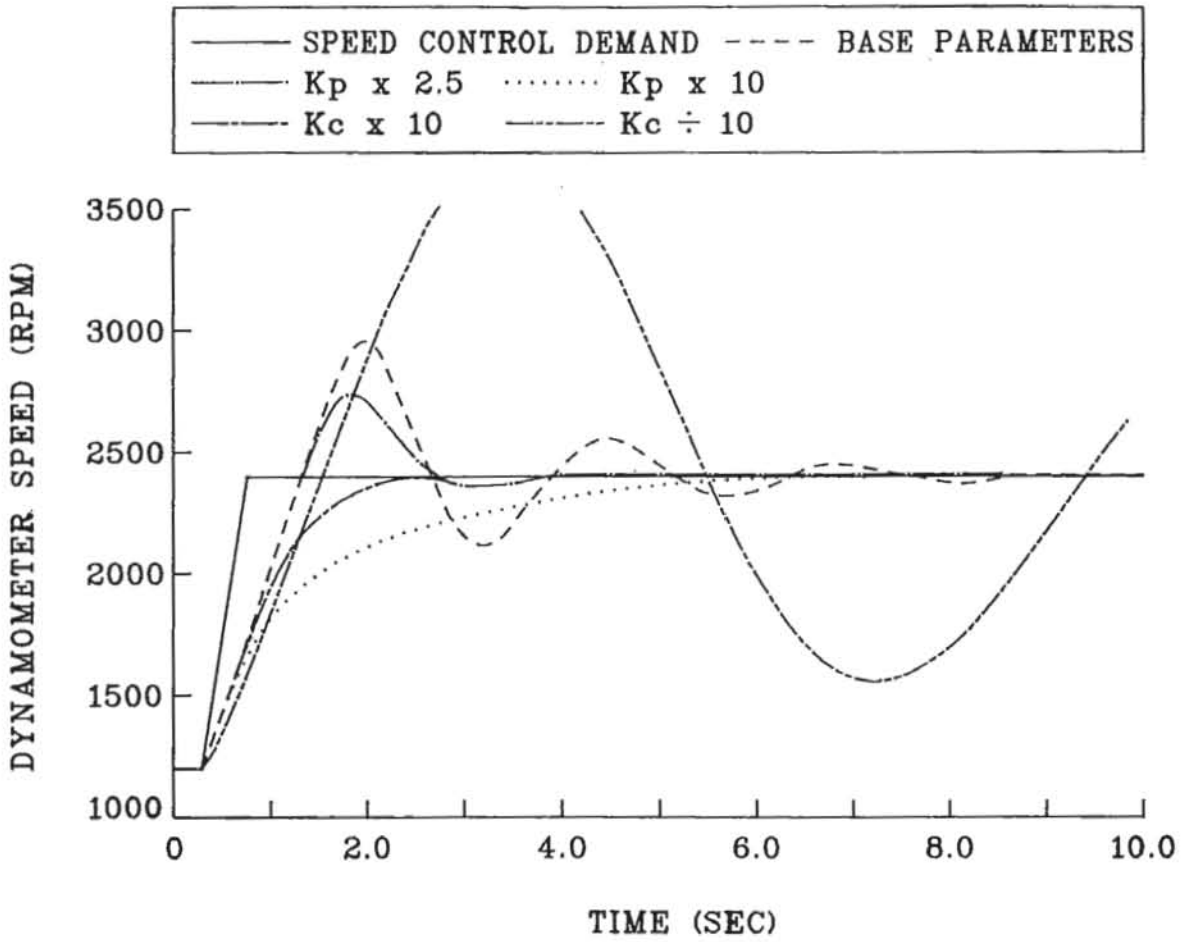

Figure 8.5: Dynamometer Speed Responses to a Speed Control Demand Change for Different Control Parameter Values

Test Inputs:

F24 dynamometer stator cup water outlet

engine torque ramp 250 Nm to 500 Nm @ 1000 Nm/s

speed control demand ramp 1200 rpm to 2400 rpm @ 6000 rpm/s

constant Q_{IN} = 0.003788 m^3/s

engine inertia[2] = 2.5 kgm^2

controller operating frequency = 30 Hz

BASE PARAMETERS	overshoot, then decaying oscillation	
GAIN	× 10	+ 10
K_C	over damped	very oscillatory
K_P	heavily over damped	oscillatory, slow decay
K_D	larger overshoot & oscillation	similar to base
K_I	constant small oscillation	large slow overshoot

Table 8.4: Summary of Speed Responses to Control Parameter Variation

2 The high inertia value is to slow the response in order that the controller effects are more obvious.

These results show considerable change in system response. For smaller changes in controller values the response change will be less, but as the test for a relative proportional gain increase of 2.5 times shows their effect on system performance is significant. The difference in Cohen and Coon parameters between points in the previous section is of a similar size to this smaller change, illustrating that undesirable oscillation of the response occurs with only a small change in control parameter values. It is therefore necessary to adjust the parameters as the set point moves across the operating envelope. The next development would be to provide this adjustment as a self-tuning algorithm for the controller.

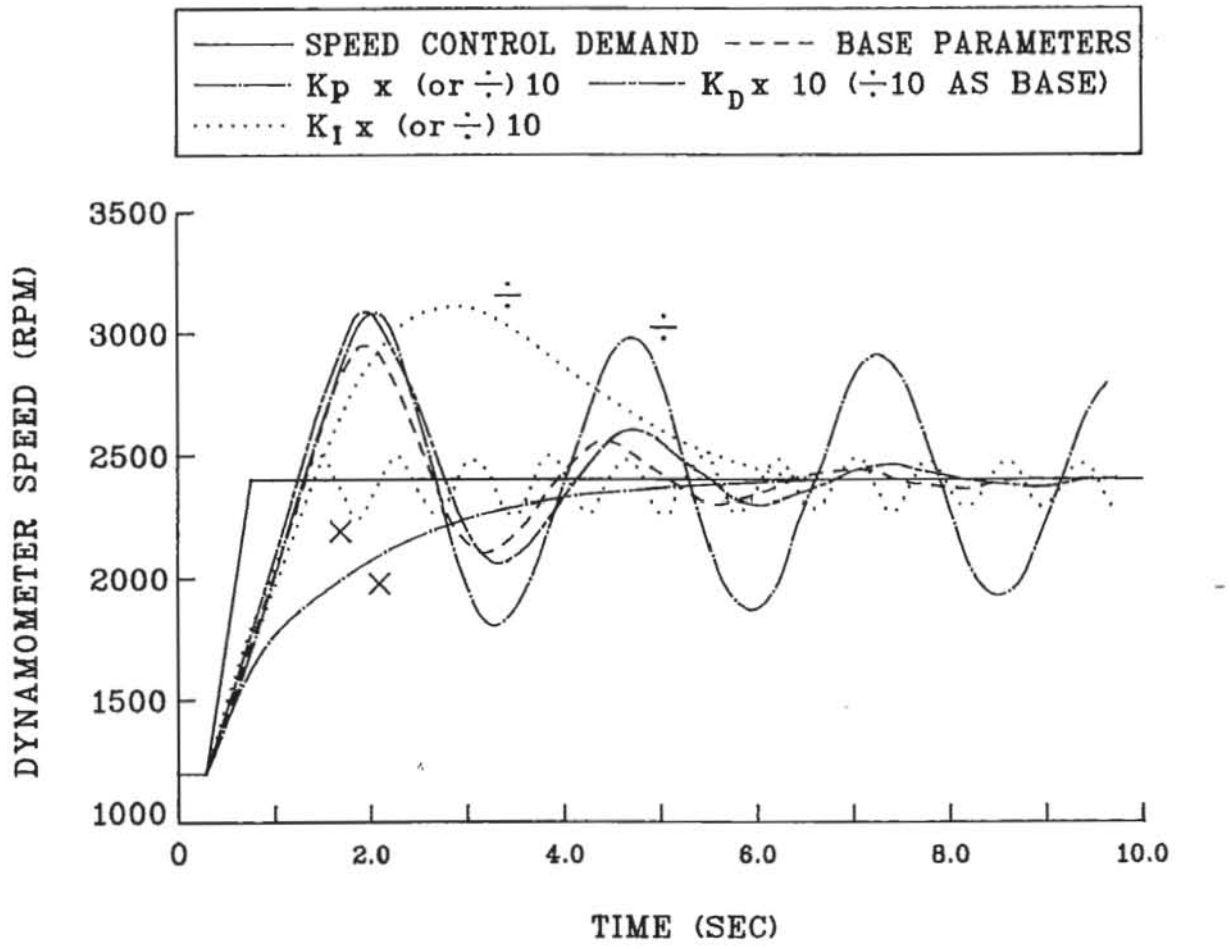

Figure 8.6: Dynamometer Speed Responses to a Speed Control Demand Change for Different Relative Control Parameter Values

8.2.3 Comparison of Open and Closed Loop Behaviour

The effect of the control system on the behaviour of the dynamometer is illustrated in Fig.8.7 which shows the the machine's torque and speed responses to an input torque increase with a constant speed control demand. Using the open loop results of Section 6.4.2 for a 25% ramped torque increase/decrease from test point 1, closed and open loop responses to an input torque change are compared. In the previous section it is shown that the Cohen and Coon values are too oscillatory for this system, so again the base parameters are varied and the results presented in Table 8.5. As intended the speed control prevents the system speed continually increasing.

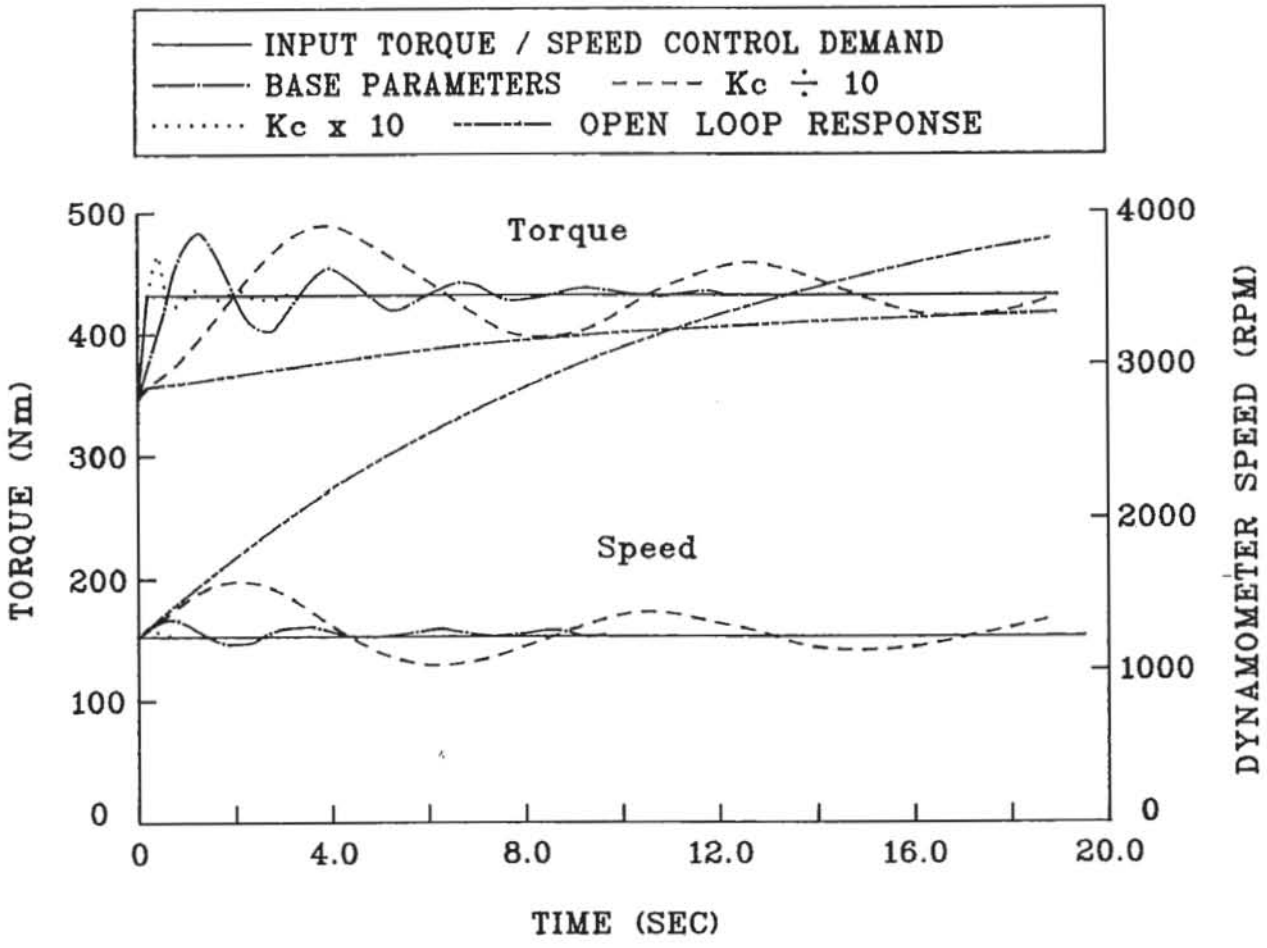

Figure 8.7: Dynamometer Torque and Speed Responses to an Input Torque Change for Different Control Parameter Values

In this application multiplying the overall PID response by a factor of 10 gave slightly under damped system behaviour, while in the previous section these values gave an over damped response. It is therefore necessary that the development of the self-tuning algorithm have consideration of the effect of control demand setting throughout

BASE K_C	Torque: overshoot, decaying oscillation Speed: small oscillation % Fill: small oscillation
$K_C \times 10$	Torque: overshoot, rapidly decaying oscillation Speed: almost constant % Fill: almost constant
$K_C + 10$	Torque: highly oscillatory, slowly decaying Speed: highly oscillatory, slowly decaying % Fill: highly oscillatory, slowly decaying
OPEN LOOP	Torque: gradually follows driving torque Speed: increase/decrease with +/- torque then levels % Fill: decrease/increase to min./max. with +/- torque

Table 8.5: Comparison of Open Loop and Different Closed Loop Control

CHAPTER 9
CONCLUSION

9.1 Conclusions

An accurate performance prediction model of variable fill hydraulic dynamometers is developed, and used to simulate both steady state and dynamic behaviour of several machines.

Based upon integrated one dimensional theory, the theoretical model includes unsteady flow torque components and determinations of partial and varying fluid fill not present in previous work. The dynamic fluid pressure equation and the fluid outflow rate calculation are more complete that those previously presented. A further advancement is the analysis of cropped rotor dynamometers. By formulating the engine-dynamometer system governing equations as a set of first order equations, a dynamic dynamometer simulation is created, which utilises numerical methods to solve for the system variable values with time.

Application of the machine theory for steady state investigation allows comparison of the present work with both previous studies and experimental results. The performance predictions of the model are found to be accurate with regard to the latter. The present work agrees with and extends Rao's findings in the case of geometric variations, and it is qualitatively similar to the results of Tan's steady state investigation of the self-emptying phenomenon. This steady state demonstration of the influences on machine self-emptying is a useful step towards the dynamic simulation.

From the steady state simulation it is confirmed that machine diameter and working compartment proportions are the dominant geometric influences on torque capacity. Further optimization of the flat 45° vanes leads to significantly less torque capacity increase than a small diameter increase. However the thickness of the dynamometer vanes is found to have a significant effect on torque. Their surface finish is also influential.

Consideration of partial fill conditions shows that the dynamometer characteristics for fluid fills from 100% to 40% lie in a narrow band about the Froude guaranteed maximum torque

characteristic. Hence most of the operating envelope is at lower fills, and therefore small changes in fill have a dramatic effect on torque production. Both the working compartment fluid pressure and the ratio of fluid vortex angular velocity to machine rotor velocity decrease with fill percentage.

Introducing system dynamics to the study of dynamometers provides a more accurate simulation of machine performance. The dynamic model indicates acceleration/deceleration torque hysteresis and torque rise at high speed and low fill following falling torque behaviour, which are not predicted by the steady state models. Other comparisons with the steady state work show the significance of dynamic factors such as acceleration rate, initial conditions and system driving torque function. These factors, particularly the system's initial conditions are also found to affect the dynamometer's response to input perturbations. It is found that the unsteady torque component contributions to the machine torque are relatively small compared with the steady torque components and can be neglected in most investigations.

The dynamometer's closed control loop behaviour is modelled for oil driven back pressure valve and electrohydraulic valve control systems. Comparison of the back pressure valve model with experimental data of torque characteristics for various control settings gives exact agreement. The electrohydraulic valve model is used to study the effect of changes to control system parameters, and to compare the closed and open loop behaviour. By using a common method of control system parameter selection, the variation of suitable values around the operating envelope is demonstrated. However in order to achieve satisfactory control, it is shown that not only the initial dynamometer speed and fill conditions are important, but also how those values and the controller demand setting change during the test must be considered.

9.2 Recommendations

Extension of the present study should focus on the inclusion of a comprehensive engine model and the development of a self tuning controller algorithm. As discussed earlier, much work has already been presented on complex engine models that could be modified to the engine-dynamometer system model.

Before production of a self tuning algorithm for use around the operating envelope, further investigation of dynamometer responses is necessary. The application of frequency response methods to the electrohydraulic valve model will allow the Ziegler-Nichols control parameters to be determined. Comparison of these values and consideration of the resultant system performance with those obtained by the process reaction method will allow determination of the most suitable control parameters. The variation of the controller demand setting throughout the test changes the values which are appropriate for the PID parameters, so this effect must also be studied. A self tuning algorithm can then be derived, leading to a hardware implementation.

The model could also be used to generate a simpler transfer function type model to represent dynamometers in models of engine test systems. Experimental work should be carried out to more precisely predict valve loss characteristics and fluid outflow path losses, and to further validate the model's predictions.

REFERENCES

1. **Froude, W.** *On a New Dynamometer for Measuring the Power Delivered to the Screws of Large Ships.* Proc. Inst. Mech. Eng., v72 pp 237-252 July 1877.
2. **Narayan Rao, N.N.** *The Basic Theory of Hydraulic Dynamometers & Retarders.* Trans. S.A.E., v77 n680178.
3. **Knudsen, D.D.; Countess, R.B.** *Hydrodynamic Considerations in Water Dynamometer Design.* Trans. S.A.E., v80 n710217.
4. **Mitsuhashi, K.; Takata, N.; Urushihara, A.; Endo, Y.; Kabayano, N.** *Vibration of Hydraulic Dynamometer and Resonant-Response Factor.* Mitsui Tech. Rev. (Japan), n84 pp26-35 1973.
5. **Patki, G.S.; Gill, B.S.** *The Effect of Number of Blades on the Performance of Hydrodynamic Couplings and Dynamometers.* Mech. Eng. Bull. (India), v7 n3 pp80-88 Sept. 1976.
6. **Raine, J.K.** *General Theory & Computer Simulation for F Type Dynamometer Performance.* Froude Eng. Ltd., Tech. Note n168 1977.
7. **Tan, K.C.** *Identification of a Hydraulic Dynamometer.* M.Sc. Thesis, Uni. of Manchester Inst. of Science and Technology, Oct. 1980.
8. **Chiappini, E.; Cipollone, R.** *A Mathematical Simulation of a Hydraulic Brake Diesel Engine Test Rig.* 2nd IAVD Congress on Vehicle Design & Components, Geneva, 4-6 Mar 1985. Int. J. of Vehicle Design, v6 n4-5 p665 Jul-Sept 1985.
9. **Chiappini, E.; Cipollone, R.** *Identification Procedure and Experimental Validation of a Hydraulic Brake Diesel Engine Test Rig.* 2nd IAVD Congress on Vehicle Design & Components, Geneva, Mar 4-6 1985. Int. J. of Vehicle Design, v6 n4-5 pp665-666 Jul-Sep 1985.
10. **Caravani, P.; Corcione, F.E.** *Modelling and Identification of a Dynamometer.* ISATA Conf. Publ., Rome, v1 n18 Sep 17-Oct 1 1976.

11. **Eksergian, R.** *The Fluid Torque Converter and Coupling.* J. Franklin Inst., v235 n5 pp441-478 May 1943.
12. **Rolfe, G.H.** *Research on the Hydraulic Coupling.* Proc. Inst. Mech. Eng., v183 pt1 n12 pp219-232 1968-69.
13. **Jandasek, V.J.** *Design of Single-Stage, Three-Element Torque Converter.* S.A.E. Advances in Eng., Design Practises for Passenger Car Automatic Transmissions, 2nd Ed., v5 pp201-226 1973.
14. **Qualman, J.W.; Egbert, E.L.** *Fluid Couplings.* S.A.E. Advances in Eng., Design Practises for Passenger Car Automatic Transmissions, 2nd Ed, v5 pp183-197 1973.
15. **Packer, M.B.** *Development of Hydrokinetic Retarders.* Inst. Mech. Eng. Conf. Publ. 1, C1/74 1974.
16. **Förster, H.-J.** *Retarders Built into Automatic Transmissions.* Inst. Mech. Eng. Conf. Publ. 1, C7/74 1974.
17. **Lucas, G.G.; Rayner, A.** *Torque Converter Design Calculations.* Automobile Eng., v60 n2 pp56-60 1970.
18. **Lucas, G.G.** *Torque Converter Design.* Automotive Eng. (London), v2 n4 1977.
19. **Szüle, D.** *General Relations for the Calculation of the Characteristics of a Hydrodynamic Torque Converter.* Proc. 4th Conf. on Fluid Machinery, Budapest, pp1397-1408 1972.
20. **Nevrly, J.** *Calculation of Characteristics of a Hydrodynamic Torque Converter in Unconventional Operational Ranges.* Proc. 5th Conf. on Fluid Machinery, Budapest, v2 pp 1975.
21. **Wu, C.H.** *A General Theory of Three Dimensional Flow in Subsonic and Supersonic Turbomachines of Axial-, Radial-, and Mixed-Flow Types.* NASA TN2604, Jan. 1952.
22. **Novak, R.A.** *Streamline Curvature Computing Procedure for Fluid Flow Problems.* Trans. ASME J. of Eng. for Power, v89 n4 pp478-490 1967.
23. **Marsh, H.** *A Digital Computer Program for the Through-Flow Fluid Mechanics in an Arbitrary Turbomachine, Using a Matrix Method.* Aero. Res. Council, R&M No 3509, 1968.
24. **Horlock, J.H.; Marsh, H.** *Flow Models for Turbomachines.* J. Mech. Eng. Science, v13 n5 pp358-368 1971.

25. **Horlock, J.H.; Marsh, H.** *Fluid Mechanics of Turbomachines: a Review.* Int. J. Heat and Fluid Flow, v3 n1 pp3-11 1982.

26. **Bosman, C.; Marsh, H.** *An Improved Method for Calculating the Flow in Turbomachines, Including a Consistent Loss Model.* J. Mech. Eng. Science, v16 n1 pp25-31 1974.

27. **Davis, W.R.; Millar, D.A.J.** *A Comparison of the Matrix and Streamline Curvature Methods of Axial Flow Turbomachinery Analysis, From a User's Point of View.* Trans. ASME J. of Eng. for Power, v97 n4 pp549-560 1975.

28. **Hirsch, Ch.; Warzee, G.** *A Finite-Element Method for Through-Flow Calculations in Turbomachines.* Trans. ASME J. of Fluids Eng., v98 n3 pp404-421 1976.

29. **Neal, A.N.** *Theoretical Methods for Analysing the Flow in Pumps.* Centrifugal Pumps - Hydraulic Design. Inst. Mech. Eng. Conf. Publ., C182/82 1982.

30. **Andersson, S.** *On Hydrodynamic Torque Converters.* Trans. Machine Elements Div., Lund Technical Uni., Sweden 1982.

31. **Andersson, S.** *Analysis of Multi-Element Torque Converter Transmissions.* Int. J. Mech. Sci., v28 n7 pp431-441 1986.

32. **Andersson, S.** *Assessment of the Blade Skew and the Through-Flow Velocity Gradients in Hydrodynamic Torque Converters.* Int. J. Mech. Sci., v29 n10-11 pp695-712 1987.

33. **Sivalingam, R.** *Flow Modelling and Computer Aided Design of Fluid Couplings and Torque Converters.* Ph.D. Thesis, University of Bath, 1978.

34. **Wallace, F.J.; Whitfield, A.; Sivalingam, R.** *A Theoretical Model for the Performance Prediction of Fully Filled Fluid Couplings.* Int. J. Mech. Sci. v20 pp335-347.

35. **Whitfield, A.; Sivalingam, R.; Wallace, F.J.** *Performance Prediction of Fluid Coupling with the Introduction of a Baffle Plate.* Int. J. Mech. Sci. v20 pp729-736.

36. **Whitfield, A.; Wallace, F.J.; Sivalingam, R.** *Performance Prediction Procedure for Three Element Torque Converters.* Int. J. Mech. Sci. v20 pp801-814.

37. **Patel, A.** *A Theoretical Model for the Design and Performance Prediction of Hydrokinetic Units.* Ph.D. Thesis, University of Bath, 1981.

38. **Whitfield, A; Wallace, F.J.; Patel, A.** *Performance Prediction of Multi Element Torque Converters.* Int. J. of Mech. Sci. v25 n2 pp77-85.

39. **Whitfield, A.; Wallace, F.J.; Patel, A.** *Design of Three Element Hydrokinetic Torque Converters.* Int. J. of Mech. Sci v25 n7 pp485-497.

40. **Ishihara, T.; Furuya, S.; Mori, K.** *Characteristics of Fluid Couplings.* Bull. J.S.M.E. v11 n45 pp496-508 1968.

41. **Numazawa, A.; Ushijima, F.; Fukumura, K.; Ishihara, T.** *An Experimental Analysis of Fluid Flow in a Torque Converter.* Trans. S.A.E. n830571.

42. **Ishihara, T.; Emori, R.I.** *Torque Converter as a Vibration Damper and its Transient Characteristics.* Trans S.A.E. n660368.

43. **Meguid, S.A.; May, W.; Coleman, P.T.** *A Computer-Aided Design Study of a Constant-fill Hydraulic Coupling.* Proc. Int. Conf. on Computer-Aided Production Eng., Edinburgh Apr. 1986.

44. **Kotwicki, A.J.** *Dynamic Models for Torque Converter Equipped Vehicles.* Trans S.A.E. n820393.

45. **Karnopp, D.; Rosenburg, R.** *System Dynamics: A Unified Approach.* John Wiley, New York, 1975.

46. **Hrovat, D.; Tobler, W.E.** *Bond Graph Modelling and Computer Simulation of Automotive Torque Converters.* J. Franklin Inst. v319 n1-2 pp93-114 1985.

47. **Shampine, L.F.; Gordon, M.K.** *Computer Solution of Ordinary Differential Equations - The Initial Value Problem.* Freeman & Co., San Francisco, 1975.

48. **Fox, R.W.; McDonald, A.T.** *Introduction to Fluid Mechanics.* John Wiley, 1973.

49. **Sokolnikoff, I.S.; Redheffer, R.M.** *Mathematics of Physics and Modern Engineering.* McGraw-Hill, 2nd Ed., 1966.

50. **Whitfield, A.; Wallace, F.J.** Study of Incidence Loss Models in Radial and Mixed-Flow Turbomachinery. Conf. on Heat & Fluid in Flow in Stream & Gas Turbine Plant 1973.

51. **Massey, B.S.** *Mechanics of Fluids.* Van Nostrand Reinhold, 4th Ed.

52. **Johnson, L.W.; Riess, R.D.** *Numerical Analysis.* Addison-Wesley, 2nd Ed, 1982.

53. **Meriam, J.L.** *Dynamics.* John Wiley, 2nd Ed., 1975.

54. **Raine, J.K.** *A Reappraisal of Froude Characterised Butterfly Valve Design.* Tech. Note 165, Froude Eng. Ltd., 1975.

55. **Ward-Smith, A.J.** *Internal Fluid Flow.* Clarendon Press, Oxford, 1980.

56. **Froude Eng. Ltd.**

Raine, J.K. *A Casing Pressure Law for DA Dynamometers,* Tech. Note 169, 1977.

Horrocks, R. *F0471 Dynamometer - Initial Running Tests,* Tech. Note 170, 1976

Raine, J.K. *Performance Tests and Control System Modifications on the Vickers Ltd. RFA 18 Dynrs. - a Casing Pressure Law for FA Dynrs.,* Tech. Note 175, 1976.

Dukes, B.J. *F0631 Performance,* Tech. Note 253, 1981.

Box, N. *Reversible F Type,* Tech. Note 260, 1981.

Dukes, B.J. *Performance of RF0351 Reversible Dynr.,* Tech. Note 263, 1981.

Dukes, B.J. *Performance of F Range 90° Cropped Rotor Machines,* Tech. Note 265, 1982.

57. **Benson, R.S.** *The Thermodynamics and Gas Dynamics of Internal- Combustion Engines, Vol. 1,* Oxford Press, 1982.

58. **Horlock, J.H.; Winterbone, D.E.** *The Thermodynamics and Gas Dynamics of Internal- Combustion Engines, Vol. 2,* Oxford Press, 1986.

59. **Winterbone, D.E.; Jai-In, S.** *Control Studies of an Automotive Turbocharged Diesel Engine with Variable Geometry Turbine,* Trans. S.A.E. n880485.

60. **Dobner, D.J.** *A Mathematical Engine Model for Development of Dynamic Engine Control.* Trans. S.A.E. n800054.

61. **Tsai, S-C.; Goyal, M.R.** *Dynamic Turbocharged Diesel Engine Model for Control Analysis and Design.* Trans S.A.E. n860455.

62. **Kanamaru, K.; Shimamoto, Y.; Choi, J-S.** *Computerised Simulation of Performances of a Two Stage Turbocharged Diesel Engine and its Application.* Japan S.A.E. Rev. pp20-26 Oct 1986.

63. **Jennings, M.J.; Blumberg, P.N.; Amann, R.W.** *A Dynamic Simulation of the Detroit Diesel Electronic Control System in Heavy Duty Truck Powertrains.* Trans. S.A.E. n861959.

64. **Stephanopoulos, G.** *Chemical Process Control.* Prentice-Hall 1984.

65. **Hougen, J.O.** *Measurements and Control Applications.* I.S.A. 2nd Ed. 1979.

66. **Leithold, L.** *The Calculus With Analytic Geometry.* Harper & Row 1976.

APPENDIX A
CUP BOUNDARY GEOMETRIC FUNCTION IDENTITIES

The geometric functions, f(x) and g(x), defining the cup boundary of the control volume are illustrated in Fig.2.6 and used to develop the following identities.

Upper Cup Boundary

$$f = f(x) = R_c + \left(a^2 - \frac{x^2}{\sin^2\alpha}\right)^{\frac{1}{2}}$$

$$f^2 = (f(x))^2 = R_c^2 + 2R_c\left(a^2 - \frac{x^2}{\sin^2\alpha}\right)^{\frac{1}{2}} + \left(a^2 - \frac{x^2}{\sin^2\alpha}\right)$$

$$f^3 = (f(x))^3 = R_c^3 + 3R_c^2\left(a^2 - \frac{x^2}{\sin^2\alpha}\right)^{\frac{1}{2}} + 3R_c\left(a^2 - \frac{x^2}{\sin^2\alpha}\right) + \left(a^2 - \frac{x^2}{\sin^2\alpha}\right)^{\frac{3}{2}}$$

$$f^4 = (f(x))^4 = R_c^4 + 4R_c^3\left(a^2 - \frac{x^2}{\sin^2\alpha}\right)^{\frac{1}{2}} + 6R_c^2\left(a^2 - \frac{x^2}{\sin^2\alpha}\right) + 4R_c\left(a^2 - \frac{x^2}{\sin^2\alpha}\right)^{\frac{3}{2}} + \left(a^2 - \frac{x^2}{\sin^2\alpha}\right)^2$$

Lower Cup Boundary

$$g = g(x) = R_c - \left(a^2 - \frac{x^2}{\sin^2\alpha}\right)^{\frac{1}{2}}$$

$$g^2 = (g(x))^2 = R_c^2 - 2R_c\left(a^2 - \frac{x^2}{\sin^2\alpha}\right)^{\frac{1}{2}} + \left(a^2 - \frac{x^2}{\sin^2\alpha}\right)$$

$$g^3 = (g(x))^3 = R_c^3 - 3R_c^2\left(a^2 - \frac{x^2}{\sin^2\alpha}\right)^{\frac{1}{2}} + 3R_c\left(a^2 - \frac{x^2}{\sin^2\alpha}\right) - \left(a^2 - \frac{x^2}{\sin^2\alpha}\right)^{\frac{3}{2}}$$

$$g^4 = (g(x))^4 = R_c^4 - 4R_c^3\left(a^2 - \frac{x^2}{\sin^2\alpha}\right)^{\frac{1}{2}} + 6R_c^2\left(a^2 - \frac{x^2}{\sin^2\alpha}\right) - 4R_c\left(a^2 - \frac{x^2}{\sin^2\alpha}\right)^{\frac{3}{2}} + \left(a^2 - \frac{x^2}{\sin^2\alpha}\right)^2$$

Hence the *Difference Identities*

$$(f - g) = 2\left(a^2 - \frac{x^2}{\sin^2\alpha}\right)^{\frac{1}{2}}$$

$$(f^2 - g^2) = 4R_c\left(a^2 - \frac{x^2}{\sin^2\alpha}\right)^{\frac{1}{2}}$$

$$(f^3 - g^3) = 6R_c^2\left(a^2 - \frac{x^2}{\sin^2\alpha}\right)^{\frac{1}{2}} + 2\left(a^2 - \frac{x^2}{\sin^2\alpha}\right)^{\frac{3}{2}}$$

$$(f^4 - g^4) = 8R_c^3\left(a^2 - \frac{x^2}{\sin^2\alpha}\right)^{\frac{1}{2}} + 8R_c\left(a^2 - \frac{x^2}{\sin^2\alpha}\right)^{\frac{3}{2}}$$

APPENDIX B
DEFINITE INTEGRALS

From Leithold [66] the following definite integral identities are obtained.

$$\int (a^2 - u^2)^{-\frac{1}{2}}\, du = \sin^{-1}\left(\frac{u}{a}\right) + C$$

$$\int (a^2 - u^2)^{\frac{1}{2}}\, du = \frac{1}{2}u(a^2 - u^2)^{\frac{1}{2}} + \frac{1}{2}a^2 \sin^{-1}\left(\frac{u}{a}\right) + C$$

$$\int (a^2 - u^2)^{\frac{3}{2}}\, du = \frac{-1}{8}u(2u^2 - 5a^2)(a^2 - u^2)^{\frac{1}{2}} + \frac{3}{8}a^4 \sin^{-1}\left(\frac{u}{a}\right) + C$$

These are used to evaluate the following expressions.

$$\int_0^b \left(a^2 - \frac{x^2}{\sin^2 \alpha}\right)^{-\frac{1}{2}} dx = \frac{1}{2}\pi \sin \alpha$$

$$\int_0^b \left(a^2 - \frac{x^2}{\sin^2 \alpha}\right)^{\frac{1}{2}} dx = \frac{1}{4}\pi\, ba$$

$$\int_0^b \left(a^2 - \frac{x^2}{\sin^2 \alpha}\right)^{\frac{3}{2}} dx = \frac{3}{16}\pi\, ba^3$$

The other definite integrals evaluated are

$$\int_0^b 1\, dx = b$$

$$\int_0^b \left(a^2 - \frac{x^2}{\sin^2 \alpha}\right) dx = \frac{2}{3}\, ba^2$$

$$\int_0^b \left(a^2 - \frac{x^2}{\sin^2 \alpha}\right)^2 dx = \frac{8}{15}\, ba^4$$

Similar identities are obtained for the air-water interface integrals by replacing a and b with a_Y and b_Y.

APPENDIX C
AIR-WATER INTERFACE TIME DERIVATIVE IDENTITIES

The air-water interface boundary is defined in Fig.2.6 by the geometric functions fy(x) and gy(x) and used to develop the following identities.

Upper Air-Water Interface Boundary

$$fy(x) = R_Y + \left(a_Y^2 - \frac{x^2}{\sin^2 \alpha}\right)^{\frac{1}{2}}$$

Lower Air-Water Interface Boundary

$$gy(x) = R_Y - \left(a_Y^2 - \frac{x^2}{\sin^2 \alpha}\right)^{\frac{1}{2}}$$

The *Time Derivatives* of these are

$$\dot{fy} = \dot{R}_Y + a_Y \dot{a}_Y \left(a_Y^2 - \frac{x^2}{\sin^2 \alpha}\right)^{-\frac{1}{2}}$$

$$\dot{gy} = \dot{R}_Y - a_Y \dot{a}_Y \left(a_Y^2 - \frac{x^2}{\sin^2 \alpha}\right)^{-\frac{1}{2}}$$

Which leads to the identities

$$fy\,\dot{fy} = R_Y \dot{R}_Y + a_Y \dot{a}_Y + \dot{R}_Y \left(a_Y^2 - \frac{x^2}{\sin^2 \alpha}\right)^{\frac{1}{2}} + R_Y a_Y \dot{a}_Y \left(a_Y^2 - \frac{x^2}{\sin^2 \alpha}\right)^{-\frac{1}{2}}$$

$$gy\,\dot{gy} = R_Y \dot{R}_Y + a_Y \dot{a}_Y - \dot{R}_Y \left(a_Y^2 - \frac{x^2}{\sin^2 \alpha}\right)^{\frac{1}{2}} - R_Y a_Y \dot{a}_Y \left(a_Y^2 - \frac{x^2}{\sin^2 \alpha}\right)^{-\frac{1}{2}}$$

and

$$(fy\,\dot{fy} - gy\,\dot{gy}) = 2\,\dot{R}_Y \left(a_Y^2 - \frac{x^2}{\sin^2 \alpha}\right)^{\frac{1}{2}} + 2\,R_Y a_Y \dot{a}_Y \left(a_Y^2 - \frac{x^2}{\sin^2 \alpha}\right)^{-\frac{1}{2}}$$

Similarly

$$fy^2\,\dot{fy} = R_Y^2\,\dot{R}_Y + 2\,R_Y q_Y\,\dot{q}_Y + \left(2\,R_Y\,\dot{R}_Y + a_Y\,\dot{a}_Y\right)\left(q_Y^2 - \frac{x^2}{\sin^2\alpha}\right)^{\frac{1}{2}}$$

$$+ R_Y^2\,q_Y\,\dot{a}_Y\left(q_Y^2 - \frac{x^2}{\sin^2\alpha}\right)^{-\frac{1}{2}} + \dot{R}_Y\left(q_Y^2 - \frac{x^2}{\sin^2\alpha}\right)$$

$$gy^2\,\dot{gy} = R_Y^2\,\dot{R}_Y + 2\,R_Y q_Y\,\dot{q}_Y - \left(2\,R_Y\,\dot{R}_Y + a_Y\,\dot{a}_Y\right)\left(q_Y^2 - \frac{x^2}{\sin^2\alpha}\right)^{\frac{1}{2}}$$

$$- R_Y^2\,q_Y\,\dot{a}_Y\left(q_Y^2 - \frac{x^2}{\sin^2\alpha}\right)^{-\frac{1}{2}} + \dot{R}_Y\left(q_Y^2 - \frac{x^2}{\sin^2\alpha}\right)$$

give

$$\left(fy^2\,\dot{fy} - gy^2\,\dot{gy}\right) = \left(4\,R_Y\,\dot{R}_Y + 2\,a_Y\,\dot{q}_Y\right)\left(q_Y^2 - \frac{x^2}{\sin^2\alpha}\right)^{\frac{1}{2}}$$

$$+ 2\,R_Y^2\,a_Y\,\dot{q}_Y\left(q_Y^2 - \frac{x^2}{\sin^2\alpha}\right)^{-\frac{1}{2}}$$

and

$$fy^3\,\dot{fy} = R_Y^3\,\dot{R}_Y + 3\,R_Y^2 a_Y\,\dot{q}_Y + \left(3\,R_Y^2\,\dot{R}_Y + 3\,R_Y a_Y\,\dot{q}_Y\right)\left(q_Y^2 - \frac{x^2}{\sin^2\alpha}\right)^{\frac{1}{2}}$$

$$+ R_Y^3\,q_Y\,\dot{a}_Y\left(q_Y^2 - \frac{x^2}{\sin^2\alpha}\right)^{-\frac{1}{2}} + \left(3\,R_Y\,\dot{R}_Y + a_Y\,\dot{q}_Y\right)\left(q_Y^2 - \frac{x^2}{\sin^2\alpha}\right)$$

$$+ \dot{R}_Y\left(q_Y^2 - \frac{x^2}{\sin^2\alpha}\right)^{\frac{3}{2}}$$

$$gy^3\,\dot{gy} = R_Y^3\,\dot{R}_Y + 3\,R_Y^2 a_Y\,\dot{q}_Y - \left(3\,R_Y^2\,\dot{R}_Y + 3\,R_Y a_Y\,\dot{q}_Y\right)\left(q_Y^2 - \frac{x^2}{\sin^2\alpha}\right)^{\frac{1}{2}}$$

$$- R_Y^3\,q_Y\,\dot{a}_Y\left(q_Y^2 - \frac{x^2}{\sin^2\alpha}\right)^{-\frac{1}{2}} + \left(3\,R_Y\,\dot{R}_Y + a_Y\,\dot{q}_Y\right)\left(q_Y^2 - \frac{x^2}{\sin^2\alpha}\right)$$

$$- \dot{R}_Y\left(q_Y^2 - \frac{x^2}{\sin^2\alpha}\right)^{\frac{3}{2}}$$

give

$$\left(fy^3\,\dot{fy} - gy^3\,\dot{gy}\right) = \left(6\,R_Y^2\,\dot{R}_Y + 6\,R_Y a_Y\,\dot{q}_Y\right)\left(q_Y^2 - \frac{x^2}{\sin^2\alpha}\right)^{\frac{1}{2}}$$

$$+ 2\,R_Y^3\,a_Y\,\dot{q}_Y\left(q_Y^2 - \frac{x^2}{\sin^2\alpha}\right)^{-\frac{1}{2}} + 2\,\dot{R}_Y\left(q_Y^2 - \frac{x^2}{\sin^2\alpha}\right)^{\frac{3}{2}}$$

APPENDIX D
CUP ANGLE TO VORTEX ANGLE CONVERSION

The calculation of working compartment fluid pressure uses an angle θ , defined from the vortex centre. During investigation of the fluid pressure variation around the compartment it is more convenient to present the results in terms of an angle θ_C from the centre (Fig.D.1). Having defined θ_C it is necessary to convert it to the equivalent θ value.

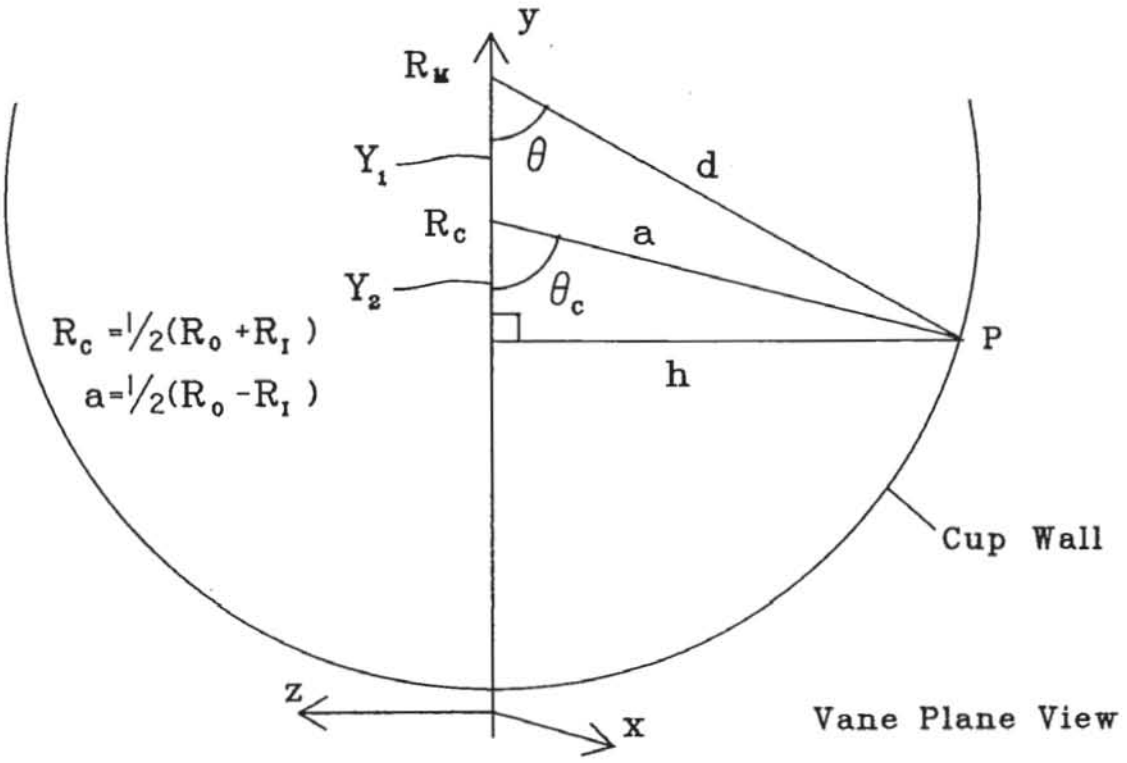

Figure D.1: Cup and Vortex Angle Conversion

From Fig.D.1 the following identities are obtained:

$$Y_1 = R_M - R_C$$
$$Y_2 = a\cos\theta_C$$
$$h = a\sin\theta_C$$

Hence the vortex angle is calculated by

$$\theta = \tan^{-1}(h/(Y_1 + Y_2))$$

As the angle θ_C increases around the working compartment both the numerator and denominator of this expression change sign, so several conditional statements are required in the computer implementation to ensure the correct value (between 0° and 360°) is calculated.

If $Y_1 + Y_2 = 0$ then,

$$\theta = 90° \text{ if } \theta_C < 180°$$

or $$\theta = 270° \text{ if } \theta_C > 180°.$$

If $\cos\theta_C < 0$ and $Y_1 + Y_2 < 0$ then,

$$\theta = 180° + \tan^{-1}(h/(Y_1 + Y_2)).$$

If $\cos\theta_C > 0$ and $\theta_C > 180°$ then,

$$\theta = 360° + \tan^{-1}(h/(Y_1 + Y_2)).$$

The casing radius d is calculated by Pythagoras' Theorem,

$$d = [\,(Y_1 + Y_2)^2 + h^2\,]^{1/2}$$

APPENDIX E
CROPPED ROTOR CUP BOUNDARY IDENTITIES

The rotor outlet control surface (refer Fig.4.4) is now at a constant radius, R_M , so the geometric function identities for the cup boundary are:

Upper Cup Boundary

$$f = f(x) = R_M$$
$$f^2 = (f(x))^2 = R_M^2$$
$$f^3 = (f(x))^3 = R_M^3$$
$$f^4 = (f(x))^4 = R_M^4$$

Lower Cup Boundary

$$g = g(x) = R_C - \left(a^2 - \frac{x^2}{\sin^2\alpha}\right)^{\frac{1}{2}}$$

$$g^2 = (g(x))^2 = R_C^2 - 2R_C\left(a^2 - \frac{x^2}{\sin^2\alpha}\right)^{\frac{1}{2}} + \left(a^2 - \frac{x^2}{\sin^2\alpha}\right)$$

$$g^3 = (g(x))^3 = R_C^3 - 3R_C^2\left(a^2 - \frac{x^2}{\sin^2\alpha}\right)^{\frac{1}{2}} + 3R_C\left(a^2 - \frac{x^2}{\sin^2\alpha}\right) - \left(a^2 - \frac{x^2}{\sin^2\alpha}\right)^{\frac{3}{2}}$$

$$g^4 = (g(x))^4 = R_C^4 - 4R_C^3\left(a^2 - \frac{x^2}{\sin^2\alpha}\right)^{\frac{1}{2}} + 6R_C^2\left(a^2 - \frac{x^2}{\sin^2\alpha}\right) - 4R_C\left(a^2 - \frac{x^2}{\sin^2\alpha}\right)^{\frac{3}{2}} + \left(a^2 - \frac{x^2}{\sin^2\alpha}\right)^2$$

Hence the *Difference Identities* are:

$$(f - g) = R_M - R_C + \left(a^2 - \frac{x^2}{\sin^2 \alpha}\right)^{\frac{1}{2}}$$

$$(f^2 - g^2) = R_M^2 - R_C^2 + 2 R_C \left(a^2 - \frac{x^2}{\sin^2 \alpha}\right)^{\frac{1}{2}} - \left(a^2 - \frac{x^2}{\sin^2 \alpha}\right)$$

$$(f^3 - g^3) = R_M^3 - R_C^3 + 3 R_C^2 \left(a^2 - \frac{x^2}{\sin^2 \alpha}\right)^{\frac{1}{2}}$$

$$- 3 R_C \left(a^2 - \frac{x^2}{\sin^2 \alpha}\right) + \left(a^2 - \frac{x^2}{\sin^2 \alpha}\right)^{\frac{3}{2}}$$

$$(f^4 - g^4) = R_M^4 - R_C^4 + 4 R_C^3 \left(a^2 - \frac{x^2}{\sin^2 \alpha}\right)^{\frac{1}{2}} - 6 R_C^2 \left(a^2 - \frac{x^2}{\sin^2 \alpha}\right)$$

$$+ 4 R_C \left(a^2 - \frac{x^2}{\sin^2 \alpha}\right)^{\frac{3}{2}} - \left(a^2 - \frac{x^2}{\sin^2 \alpha}\right)^2$$

APPENDIX F
PROGRAM LISTINGS
(EXAMINATION COPIES ONLY)

Both the steady state and open loop dynamic simulations are combined in the Fortran program DYNR, which is included in full in this appendix. The structures of these simulations are illustrated in Figs. 5.1 and 6.3, with descriptions in Sections 5.1 and 6.1.4.

Both the Back Pressure Valve and Electrohydraulic Valve closed loop programs, BPV and EHV respectively, are presented in abridged form to highlight those sections (other than input and output routines) which are substantially different from the DYNR program. The structures of BPV and EHV are given in Figs. 7.5 and 8.3 (descriptions Sections 7.1.4 and 8.1.3).

```
C
C     ################################################
C     ################################################
C     ##                                            ##
C     ##  DDDDDDD   YY      YY NNN       NN RRRRRR   ##
C     ##   DD    DD  YY    YY  NNNN      NN RR    RR  ##
C     ##   DD     DD  YY  YY   NN NN     NN RR     RR ##
C     ##   DD     DD   YYYY    NN  NN    NN RR    RR  ##
C     ##   DD     DD    YY     NN   NN   NN RRRRRR    ##
C     ##   DD     DD   YY      NN    NN  NN RRRR      ##
C     ##   DD     DD  YY       NN     NN NN RR RR     ##
C     ##   DD    DD  YY        NN      NNNN RR   RR   ##
C     ##  DDDDDDD   YY         NN       NNN RR    RR  ##
C     ##                                            ##
C     ##        COPYRIGHT 1989 P.G. HODGSON          ##
C     ##                                            ##
C     ################################################
C     ################################################
C
C          TORQUE/POWER vs. SPEED CHARACTERISTIC FOR
C
C             PARTIAL-FILL HYDRAULIC DYNAMOMETRS
C
C                    PROGRAM VERSION 1.0
C
C                     DATE:  JULY 1989
C
C                    AUTHOR: P.G. HODGSON
C
C                  UNIVERSITY OF CANTERBURY
C
C
C     INITIALISATION BLOCK
C     ********************
      BLOCK DATA DYDATA
C
      IMPLICIT DOUBLE PRECISION (A-H,O-Z)
C
      COMMON/FLG1/IPGM,ISS,IMAC,IRTR,IOUT,ITQSTT,IOPUT(6),ICES,IFUL,ICOM
      COMMON/FLG2/IT,INTS,IV,IVST,IVR,IVAR(4),MNQQ,ICS,ICLC
      COMMON/GEO1/RO,RI,RINERT,BRI,BRO,BSI,BSO,ZR,ZS,BT,FFAC,BFAC
      COMMON/GEO2/PI,RHO,ARHO,PO,RC,RM,VF,ENGINT,CYLN,FNN,SHSTFF
      COMMON/RUN1/RTFI,RTCR,PFIN,PFFI,PFCR
      COMMON/RUN2/CPIN,CPFI,CPCR,CPT,SMIN,SMAX,SICR,ST
      COMMON/RUN3/QIIN,QIFI,QICR,QIT,TQIN,TQFI,TQCR,TQT
      COMMON/SCON/CES,AA,CLFS,CLV,SCL,CL,PBFAC,PFFAC,RTS,WRV
      COMMON/VAR1/PERF,RCO,RCI,DYNERT,QIN,CP,P1,DP,QOUT
      COMMON/VAR2/W,WP,WE,THETA1,THETA2,DELTA,ACH2O,ACRTR,ACENG
      COMMON/VAR3/TOR,POW,ETOR,EPOW,EPHI,DDTDEL,DDTPF
      COMMON/ARR1/TQFAC(6),PIFAC(3),PLOSS(3),TQCMPT(6),SPRES(26)
C
      DATA IPGM,ISS,IMAC,IRTR,IOUT,ITQSTT/1,0,4,0,2,0/
      DATA (IOPUT(K),K=1,6),ICES,IFUL,ICOM,MNQQ,ICS,ICLC/12*0/
      DATA IT,INTS,IV,IVST,IVR,(IVAR(K),K=1,4)/0,1,0,1,1,4*0/
      DATA RO,RI,RINERT,BRI,BRO,BSI,BSO/121.D0,51.2D0,.188D0,4*45.D0/
      DATA ZR,ZS,BT,FFAC,BFAC/14.D0,12.D0,4.D0,.015D0,.22D0/
      DATA PI,RHO,ARHO,PO/3.1415927D0,998.2D0,1.1D0,101325.D0/
      DATA RC,RM,VF,ENGINT,CYLN,FNN,SHSTFF/3*0.D0,2.D0,6.D0,.025D0,7.D4/
      DATA RTFI,RTCR,PFIN,PFFI,PFCR/5*0.D0/
      DATA CPIN,CPFI,CPCR,CPT,SMIN,SMAX,SICR,ST/8*0.D0/
      DATA QIIN,QIFI,QICR,QIT,TQIN,TQFI,TQCR,TQT/8*0.D0/
      DATA CES,AA,CLFS,CLV,SCL,CL,PBFAC,PFFAC,RTS,WRV/10*0.D0/
      DATA PERF,RCO,RCI,DYNERT,QIN,CP,P1,DP,QOUT/3*0.D0,.188D0,5*0.D0/
      DATA W,WP,WE,THETA1,THETA2,DELTA,ACH2O,ACRTR,ACENG/9*0.D0/
      DATA TOR,POW,ETOR,EPOW,EPHI,DDTDEL,DDTPF/7*0.D0/
      DATA (TQFAC(K),K=1,6),(PIFAC(K),K=1,3),(PLOSS(K),K=1,3)/12*0.D0/
      DATA (TQCMPT(K),K=1,6),(SPRES(K),K=1,26)/32*0.D0/
C
      END
C
C     MAIN PROGRAM
C     ************
      PROGRAM DYNR
C
      IMPLICIT DOUBLE PRECISION (A-H,O-Z)
C
      EXTERNAL F
      DIMENSION Y(20),YP(20),YPEXT(20)
```

```
C
C     ################################################
C     ################################################
C     ##                                            ##
C     ##  DDDDDDD   YY      YY NNN       NN RRRRRR    ##
C     ##   DD    DD  YY    YY  NNNN      NN RR    RR   ##
C     ##   DD     DD  YY  YY   NN NN     NN RR     RR  ##
C     ##   DD     DD   YYYY    NN  NN    NN RR    RR   ##
C     ##   DD     DD    YY     NN   NN   NN RRRRRR     ##
C     ##   DD     DD   YY      NN    NN  NN RRRR       ##
C     ##   DD     DD  YY       NN     NN NN RR RR      ##
C     ##   DD    DD  YY        NN      NNNN RR   RR    ##
C     ##  DDDDDDD   YY         NN       NNN RR     RR  ##
C     ##                                            ##
C     ##        COPYRIGHT 1989 P.G. HODGSON          ##
C     ##                                            ##
C     ################################################
C     ################################################
C
C          TORQUE/POWER vs. SPEED CHARACTERISTIC FOR
C
C             PARTIAL-FILL HYDRAULIC DYNAMOMETRS
C
C                    PROGRAM VERSION 1.0
C
C                     DATE:  JULY 1989
C
C                    AUTHOR: P.G. HODGSON
C
C                  UNIVERSITY OF CANTERBURY
C
C
C     INITIALISATION BLOCK
C     ********************
      BLOCK DATA DYDATA
C
      IMPLICIT DOUBLE PRECISION (A-H,O-Z)
C
      COMMON/FLG1/IPGM,ISS,IMAC,IRTR,IOUT,ITQSTT,IOPUT(6),ICES,IFUL,ICOM
      COMMON/FLG2/IT,INTS,IV,IVST,IVR,IVAR(4),MNQQ,ICS,ICLC
      COMMON/GEO1/RO,RI,RINERT,BRI,BRO,BSI,BSO,ZR,ZS,BT,FFAC,BFAC
      COMMON/GEO2/PI,RHO,ARHO,PO,RC,RM,VF,ENGINT,CYLN,FNN,SHSTFF
      COMMON/RUN1/RTFI,RTCR,PFIN,PFFI,PFCR
      COMMON/RUN2/CPIN,CPFI,CPCR,CPT,SMIN,SMAX,SICR,ST
      COMMON/RUN3/QIIN,QIFI,QICR,QIT,TQIN,TQFI,TQCR,TQT
      COMMON/SCON/CES,AA,CLFS,CLV,SCL,CL,PBFAC,PFFAC,RTS,WRV
      COMMON/VAR1/PERF,RCO,RCI,DYNERT,QIN,CP,P1,DP,QOUT
      COMMON/VAR2/W,WP,WE,THETA1,THETA2,DELTA,ACH2O,ACRTR,ACENG
      COMMON/VAR3/TOR,POW,ETOR,EPOW,EPHI,DDTDEL,DDTPF
      COMMON/ARR1/TQFAC(6),PIFAC(3),PLOSS(3),TQCMPT(6),SPRES(26)
C
      DATA IPGM,ISS,IMAC,IRTR,IOUT,ITQSTT/1,0,4,0,2,0/
      DATA (IOPUT(K),K=1,6),ICES,IFUL,ICOM,MNQQ,ICS,ICLC/12*0/
      DATA IT,INTS,IV,IVST,IVR,(IVAR(K),K=1,4)/0,1,0,1,1,4*0/
      DATA RO,RI,RINERT,BRI,BRO,BSI,BSO/121.D0,51.2D0,.188D0,4*45.D0/
      DATA ZR,ZS,BT,FFAC,BFAC/14.D0,12.D0,4.D0,.015D0,.22D0/
      DATA PI,RHO,ARHO,PO/3.1415927D0,998.2D0,1.1D0,101325.D0/
      DATA RC,RM,VF,ENGINT,CYLN,FNN,SHSTFF/3*0.D0,2.D0,6.D0,.025D0,7.D4/
      DATA RTFI,RTCR,PFIN,PFFI,PFCR/5*0.D0/
      DATA CPIN,CPFI,CPCR,CPT,SMIN,SMAX,SICR,ST/8*0.D0/
      DATA QIIN,QIFI,QICR,QIT,TQIN,TQFI,TQCR,TQT/8*0.D0/
      DATA CES,AA,CLFS,CLV,SCL,CL,PBFAC,PFFAC,RTS,WRV/10*0.D0/
      DATA PERF,RCO,RCI,DYNERT,QIN,CP,P1,DP,QOUT/3*0.D0,.188D0,5*0.D0/
      DATA W,WP,WE,THETA1,THETA2,DELTA,ACH2O,ACRTR,ACENG/9*0.D0/
      DATA TOR,POW,ETOR,EPOW,EPHI,DDTDEL,DDTPF/7*0.D0/
      DATA (TQFAC(K),K=1,6),(PIFAC(K),K=1,3),(PLOSS(K),K=1,3)/12*0.D0/
      DATA (TQCMPT(K),K=1,6),(SPRES(K),K=1,26)/32*0.D0/
C
      END
C
C     MAIN PROGRAM
C     ************
      PROGRAM DYNR
C
      IMPLICIT DOUBLE PRECISION (A-H,O-Z)
C
      EXTERNAL F
      DIMENSION Y(20),YP(20),YPEXT(20)
```

```
C
      COMMON/FLG1/IPGM,ISS,IMAC,IRTR,IOUT,ITQSTT,IOPUT(6),ICES,IFUL,ICOM
      COMMON/FLG2/IT,INTS,IV,IVST,IVR,IVAR(4),MNQQ,ICS,ICLC
      COMMON/GEO1/RO,RI,RINERT,BRI,BRO,BSI,BSO,ZR,ZS,BT,FFAC,BFAC
      COMMON/GEO2/PI,RHO,ARHO,PO,RC,RM,VF,ENGINT,CYLN,FNN,SHSTFF
      COMMON/RUN1/RTFI,RTCR,PFIN,PFFI,PFCR
      COMMON/RUN2/CPIN,CPFI,CPCR,CPT,SMIN,SMAX,SICR,ST
      COMMON/RUN3/QIIN,QIFI,QICR,QIT,TQIN,TQFI,TQCR,TQT
      COMMON/SCON/CES,AA,CLFS,CLV,SCL,CL,PBFAC,PFFAC,RTS,WRV
      COMMON/VAR1/PERF,RCO,RCI,DYNERT,QIN,CP,P1,DP,QOUT
      COMMON/VAR2/W,WP,WE,THETA1,THETA2,DELTA,ACH2O,ACRTR,ACENG
      COMMON/VAR3/TOR,POW,ETOR,EPOW,EPHI,DDTDEL,DDTPF
      COMMON/ARR1/TQFAC(6),PIFAC(3),PLOSS(3),TQCMPT(6),SPRES(26)
C
C OPEN OUTPUT, PLOT DATA & STORAGE FILES
      OPEN(2,FILE='[HODGSON.DATAA]OOUT.GPH',STATUS='OLD')
      OPEN(6,FILE='[HODGSON.DATAA]OOUT.DAT',STATUS='OLD')
      OPEN(8,FILE='[HODGSON.DATAA]ONUM.DAT',STATUS='OLD')
      OPEN(9,STATUS='SCRATCH',FORM='UNFORMATTED')
C READ INPUT, SET UP PROGRAM & CALC. INVARIANT CONSTANTS
      CALL INPUT()
      CALL CONSTS()
C
C PROGRAM OPTIONS
C
      IF(IPGM.LE.5)THEN
C DYNAMIC
        IF(ITQSTT.EQ.1)CALL TQSTRT()
        T=0.D0
        RELERR=1.D-5
        ABSERR=1.D-5
C        PRINT *,' ENTER RELERR,ABSERR'
C        READ(*,*)RELERR,ABSERR
        IF(ISS.NE.1)THEN
          DYNERT=DYNERT+ENGINT
        END IF
C INITIAL CONDITIONS
        CALL STATUS(1,T,T)
        CALL PART()
        CALL KFACTS()
        CALL VORVEL()
        CALL POWER()
        DELTA=0.D0
        IF(ISS.EQ.1)DELTA=ETOR/SHSTFF
        Y(1)=DELTA
        WP=WE
        Y(2)=WE
        Y(3)=WP
        Y(4)=PERF
C STORE DATA
        EPOW=ETOR*WE
        WRITE(9)SCL,CL,PBFAC,PFFAC,RTS,WRV
        WRITE(9)PERF,RCO,RCI,DYNERT,QIN,CP,P1,DP,QOUT
        WRITE(9)W,WP,WE,THETA1,THETA2,DELTA,ACH2O,ACRTR,ACENG
        WRITE(9)TOR,POW,ETOR,EPOW,EPHI,DDTDEL,DDTPF
        WRITE(9)(TQFAC(K),K=1,6),(PIFAC(K),K=1,3)
        WRITE(9)(PLOSS(K),K=1,3),(TQCMPT(K),K=1,6),(SPRES(K),K=1,26)
C SOLVE D.E.S FOR EACH TIME STEP
        IFLAG=1
        IOVF=0
        DO 1000 IT=2,INTS
          TOUT=RTCR*DFLOAT(IT-1)
 1300     CONTINUE
          CALL DDE(F,4,Y,T,TOUT,RELERR,ABSERR,IFLAG)
 1333     IF(IFLAG.EQ.2)THEN
            IF(ISS.NE.1)Y(1)=0.D0
            DELTA=Y(1)
            WE=Y(2)
            WP=Y(3)
            PERF=Y(4)
            CALL F(T,T,Y,YPEXT)
            DDTDEL=YPEXT(1)
            ACENG=YPEXT(2)
            ACRTR=YPEXT(3)
            DDTPF=YPEXT(4)
C STORE DATA
            EPOW=ETOR*WE
            WRITE(9)SCL,CL,PBFAC,PFFAC,RTS,WRV
            WRITE(9)PERF,RCO,RCI,DYNERT,QIN,CP,P1,DP,QOUT
```

```
            WRITE(9)W,WP,WE,THETA1,THETA2,DELTA,ACH2O,ACRTR,ACENG
            WRITE(9)TOR,POW,ETOR,EPOW,EPHI,DDTDEL,DDTPF
            WRITE(9)(TQFAC(K),K=1,6),(PIFAC(K),K=1,3)
      WRITE(9)(PLOSS(K),K=1,3),(TQCMPT(K),K=1,6),(SPRES(K),K=1,26)
          ELSE
            IF(IFLAG.EQ.3)PRINT *,' ERROR TOLER. TOO SMALL'
            IF(IFLAG.EQ.4)PRINT *,' TOO MANY STEPS. IT= ',IT
            IF(IFLAG.EQ.5)PRINT *,' EQUATIONS STIFF. IT= ',IT
            IF(IFLAG.EQ.6)PRINT *,' INCORRECT INPUT'
            IF(IFLAG.NE.6)IOVF=IOVF+1
          END IF
          IF(IFLAG.EQ.3.OR.IFLAG.EQ.4.OR.IFLAG.EQ.5)GOTO 1300
          PRINT *, ' TIMESTEP COMPLETE.  IT= ',IT
 1000   CONTINUE
      ELSE
C STATIC
C VARIATION LOOP
        DO 1100 IV=1,IVST
          CALL STATUS(2,0.D0,0.D0)
C SPEED LOOP
          DO 1200 IT=1,INTS
            WP=SMIN+SICR*DFLOAT(IT-1)
            IF(WP.GT.SMAX)WP=SMAX
            IF(IPGM.EQ.8)THEN
C CONSTANT PERCENTAGE FILL
              CALL PART()
              CALL KFACTS()
              CALL VORVEL()
                IF(ICOM.EQ.1)ISAV=1
                IF(ICOM.EQ.1)GOTO 1000
              CALL POWER()
            ELSE
C STATIC QIN=QOUT LINE
              CALL STFLOW()
            END IF
C STORE DATA
            WRITE(9)SCL,CL,PBFAC,PFFAC,RTS,WRV
            WRITE(9)PERF,RCO,RCI,DYNERT,QIN,CP,P1,DP,QOUT
            WRITE(9)W,WP,WE,THETA1,THETA2,DELTA,ACH2O,ACRTR,ACENG
            WRITE(9)TOR,POW,ETOR,EPOW,EPHI,DDTDEL,DDTPF
            WRITE(9)(TQFAC(K),K=1,6),(PIFAC(K),K=1,3)
      WRITE(9)(PLOSS(K),K=1,3),(TQCMPT(K),K=1,6),(SPRES(K),K=1,26)
 1200     CONTINUE
 1100   CONTINUE
      END IF
      IF(ISAV.EQ.1)ICOM=1
C OUTPUT INPUT & RESULTS
 8888 CONTINUE
      CALL OUTPUT()
C      IF(IOPUT(6).EQ.1)CALL AAAA()
C CLOSE FILES
      CLOSE(2)
      CLOSE(6)
      CLOSE(8)
      CLOSE(9)
C END PROGRAM
      PRINT *,' EXTRA DDE CALLS = ',IOVF
      PRINT *,' ***** PROGRAM EXECUTION COMPLETE *****'
      PRINT *,' ***** PROGRAM EXECUTION COMPLETE *****'
      PRINT *,' ***** PROGRAM EXECUTION COMPLETE *****'
 9999 STOP
      END
C
C
C
C     SUBROUTINE F
C     ************
C     THIS ROUTINE CALCULATES THE DE'S AT ANY TIME STEP
C
      SUBROUTINE F(X,XXOLD,Y,YP)
C
      IMPLICIT DOUBLE PRECISION (A-H,O-Z)
      DIMENSION Y(20),YP(20)
C
      COMMON/FLG1/IPGM,ISS,IMAC,IRTR,IOUT,ITQSTT,IOPUT(6),ICES,IFUL,ICOM
      COMMON/FLG2/IT,INTS,IV,IVST,IVR,IVAR(4),MNQQ,ICS,ICLC
      COMMON/GEO1/RO,RI,RINERT,BRI,BRO,BSI,BSO,ZR,ZS,BT,FFAC,BFAC
      COMMON/GEO2/PI,RHO,ARHO,PO,RC,RM,VF,ENGINT,CYLN,FNN,SHSTFF
      COMMON/RUN1/RTFI,RTCR,PFIN,PFFI,PFCR
```

```
      COMMON/RUN2/CPIN,CPFI,CPCR,CPT,SMIN,SMAX,SICR,ST
      COMMON/RUN3/QIIN,QIFI,QICR,QIT,TQIN,TQFI,TQCR,TQT
      COMMON/SCON/CES,AA,CLFS,CLV,SCL,CL,PBFAC,PFFAC,RTS,WRV
      COMMON/VAR1/PERF,RCO,RCI,DYNERT,QIN,CP,P1,DP,QOUT
      COMMON/VAR2/W,WP,WE,THETA1,THETA2,DELTA,ACH2O,ACRTR,ACENG
      COMMON/VAR3/TOR,POW,ETOR,EPOW,EPHI,DDTDEL,DDTPF
      COMMON/ARR1/TQFAC(6),PIFAC(3),PLOSS(3),TQCMPT(6),SPRES(26)
C
      IF(ISS.NE.1)Y(1)=0.D0
      DELTA=Y(1)
      WE=Y(2)
      WP=Y(3)
      PERF=Y(4)
      CALL STATUS(1,X,XXOLD)
      CALL PART()
      CALL KFACTS()
      CALL VORVEL()
      CALL POWER()
      STOR=TQCMPT(1)+TQCMPT(2)+TQCMPT(3)+TQCMPT(4)
      RWWP=W/WP
      YP(1)=WE-WP
      IF(IPGM.EQ.1)THEN
        IF(ISS.EQ.1)THEN
         YP(2)=(ETOR-SHSTFF*DELTA)/ENGINT
         YP(3)=(SHSTFF*DELTA-STOR)
         YP(3)=YP(3)/(DYNERT+2.D0*(TQFAC(5)+RWWP*TQFAC(6)))
        ELSE
         YP(2)=(ETOR-STOR)/(DYNERT+2.D0*(TQFAC(5)+RWWP*TQFAC(6)))
         YP(3)=(ETOR-STOR)/(DYNERT+2.D0*(TQFAC(5)+RWWP*TQFAC(6)))
        END IF
      END IF
      IF(IPGM.EQ.2)THEN
         YP(2)=SICR
        IF(ISS.EQ.1)THEN
         YP(3)=(SHSTFF*DELTA-STOR)
         YP(3)=YP(3)/(DYNERT+2.D0*(TQFAC(5)+RWWP*TQFAC(6)))
        ELSE
         YP(3)=YP(2)
        END IF
      END IF
      YP(4)=(QIN-QOUT)/VF
C
      ACRTR=YP(3)
      ACH2O=RWWP*ACRTR
      TQCMPT(5)=2.D0*TQFAC(5)*ACRTR
      TQCMPT(6)=2.D0*TQFAC(6)*ACH2O
      TOR=TQCMPT(1)+TQCMPT(2)+TQCMPT(3)+TQCMPT(4)+TQCMPT(5)+TQCMPT(6)
      POW=TOR*WP
      RETURN
      END
C
C
C
C
C
C     SUBROUTINE CONSTS
C     *****************
C     THIS ROUTINE CALCULATES THE TIME INDEPENDENT CONSTANTS
C
      SUBROUTINE CONSTS()
C
      IMPLICIT DOUBLE PRECISION (A-H,O-Z)
C
      COMMON/FLG1/IPGM,ISS,IMAC,IRTR,IOUT,ITQSTT,IOPUT(6),ICES,IFUL,ICOM
      COMMON/FLG2/IT,INTS,IV,IVST,IVR,IVAR(4),MNQQ,ICS,ICLC
      COMMON/GEO1/RO,RI,RINERT,BRI,BRO,BSI,BSO,ZR,ZS,BT,FFAC,BFAC
      COMMON/GEO2/PI,RHO,ARHO,PO,RC,RM,VF,ENGINT,CYLN,FNN,SHSTFF
      COMMON/RUN1/RTFI,RTCR,PFIN,PFFI,PFCR
      COMMON/RUN2/CPIN,CPFI,CPCR,CPT,SMIN,SMAX,SICR,ST
      COMMON/RUN3/QIIN,QIFI,QICR,QIT,TQIN,TQFI,TQCR,TQT
      COMMON/SCON/CES,AA,CLFS,CLV,SCL,CL,PBFAC,PFFAC,RTS,WRV
      COMMON/VAR1/PERF,RCO,RCI,DYNERT,QIN,CP,P1,DP,QOUT
      COMMON/VAR2/W,WP,WE,THETA1,THETA2,DELTA,ACH2O,ACRTR,ACENG
      COMMON/VAR3/TOR,POW,ETOR,EPOW,EPHI,DDTDEL,DDTPF
      COMMON/ARR1/TQFAC(6),PIFAC(3),PLOSS(3),TQCMPT(6),SPRES(26)
C
C     CONVERT PERF,CP,QIN,SPEED,DEMAND TORQUE
C
      CPIN=CPIN/100.D0
```

```
      CPFI=CPFI/100.D0
      CPCR=CPCR/100.D0
      SMIN=SMIN*PI/30.D0
      SMAX=SMAX*PI/30.D0
      SICR=SICR*PI/30.D0
      PFIN=PFIN/100.D0
      PFFI=PFFI/100.D0
      PFCR=PFCR/100.D0
C
      CP=CPIN
      WE=SMIN
      WP=SMIN
      QIN=QIIN
      ETOR=TQIN
      PERF=PFIN
      DYNERT=RINERT
C
      IF(CP.GT.1.D0)CP=1.D0
      IF(CP.LT.0.D0)CP=0.D0
      IF(PERF.GE.1.D0)PERF=1.D0
      IF(PERF.LE.0.D0)PERF=0.D0
      IFUL=0
      IF(PERF.GE.1.0)IFUL=1
C
C     CONVERT BLADE ANGLES
C
      BRI=BRI*PI/180.D0
      BRO=BRO*PI/180.D0
      BSI=BSI*PI/180.D0
      BSO=BSO*PI/180.D0
C
C     CALCULATE TIME STEPS & CALC. LOOPS
C     INTS & IVST CALCED IN INPUT()
C
C     LOSS COEFF.,AREAS ,OUTLET RADIUS (RC), CMPT. VOLUME (VF)
C
         RC=(RO+RI)/2.D0
         CL1=0.5D0
         CL2=1.D0
         IF(IOUT.EQ.2)CL2=0.8D0
         CLD=0.3D0
         CL6=0.8D0
         CL7=0.8D0
         CL8=0.5D0
         CLFS=0.72D0
         A0=0.054D0*0.036D0
         A1=PI*0.004D0*0.004D0*28.D0
         IF(IOUT.EQ.1)A1=PI*0.0055D0*0.0055D0*24.D0
         AD=0.018D0*0.031D0/2.D0
         AA=A0
         CG=0.01D0
      SCL=(CL1+CL2-1.D0)/A1**2+1.D0/A0**2+CLD/AD**2
      IF(IOUT.EQ.0)SCL=SCL+((1.D3/RO)**2-(1.D3/RC)**2)/(4.D0*(PI*CG)**2)
      IF(IOUT.EQ.1)SCL=SCL+CL6/AA**2
      IF(IOUT.EQ.2)SCL=(CL1+CL2+CL7-1.D0)/A1**2+1.D0/A0**2+(CL6+CL8)/AA*
     1*2
      IF(IRTR.EQ.1)THEN
        A=(ZR/DSIN(BRI)+ZR/DSIN(BRO))/2.D0
        A=(A+ZS/DSIN(BSI)+ZS/DSIN(BSO))/4.D0
      ELSE
        A=(ZR/DSIN(BRI)+ZR/DSIN(BRO)+ZS/DSIN(BSI)+ZS/DSIN(BSO))/4.D0
      END IF
      BAV=(BRI+BRO+BSI+BSO)/4.D0
      VF=((RO-RI)**2)*(2.D0*PI*RC-A*BT)*PI*SIN(BAV)/4.D9
C
      RETURN
      END
C
C
C
C
C
C     SUBROUTINE STATUS
C     *****************
C     THIS ROUTINE CALCULATES THE CHANGES TO VALVE,SPEED,QIN
C     WITH TIME AND THE VALVE LOSS
C
      SUBROUTINE STATUS(III,XX,TT)
C
```

```
      IMPLICIT DOUBLE PRECISION (A-H,O-Z)
C
      COMMON/FLG1/IPGM,ISS,IMAC,IRTR,IOUT,ITQSTT,IOPUT(6),ICES,IFUL,ICOM
      COMMON/FLG2/IT,INTS,IV,IVST,IVR,IVAR(4),MNQQ,ICS,ICLC
      COMMON/GEO1/RO,RI,RINERT,BRI,BRO,BSI,BSO,ZR,ZS,BT,FFAC,BFAC
      COMMON/GEO2/PI,RHO,ARHO,PO,RC,RM,VF,ENGINT,CYLN,FNN,SHSTFF
      COMMON/RUN1/RTFI,RTCR,PFIN,PFFI,PFCR
      COMMON/RUN2/CPIN,CPFI,CPCR,CPT,SMIN,SMAX,SICR,ST
      COMMON/RUN3/QIIN,QIFI,QICR,QIT,TQIN,TQFI,TQCR,TQT
      COMMON/SCON/CES,AA,CLFS,CLV,SCL,CL,PBFAC,PFFAC,RTS,WRV
      COMMON/VAR1/PERF,RCO,RCI,DYNERT,QIN,CP,P1,DP,QOUT
      COMMON/VAR2/W,WP,WE,THETA1,THETA2,DELTA,ACH2O,ACRTR,ACENG
      COMMON/VAR3/TOR,POW,ETOR,EPOW,EPHI,DDTDEL,DDTPF
      COMMON/ARR1/TQFAC(6),PIFAC(3),PLOSS(3),TQCMPT(6),SPRES(26)
C
      IF(III.EQ.1)THEN
C APPLY TIME CHANGES OF PERF,CP,QIN
C
        CP=CPIN
        IF(XX.GE.CPT.AND.IVAR(1).NE.1)THEN
          IF(IVAR(1).EQ.2)CP=CPFI
          IF(IVAR(1).EQ.3)CP=CP+CPCR*(XX-CPT)
          IF(CP.GT.CPFI.AND.CPFI.GT.CPIN)CP=CPFI
          IF(CP.LT.CPFI.AND.CPFI.LT.CPIN)CP=CPFI
        END IF
C
          IF(IPGM.EQ.2)WE=SMIN
        IF(IPGM.EQ.2.AND.XX.GE.ST.AND.IVAR(2).NE.1)THEN
          IF(IVAR(2).EQ.2)WE=SMAX
          IF(IVAR(2).EQ.3)WE=WE+SICR*(XX-ST)
          IF(WE.GT.SMAX.AND.SMAX.GT.SMIN)WE=SMAX
          IF(WE.LT.SMAX.AND.SMAX.LT.SMIN)WE=SMAX
        END IF
          IF(IPGM.EQ.2)WE=WE*(1.D0+FNN*DSIN(CYLN*WE*XX/2.D0-PI/2.D0))
          IF(IPGM.EQ.2.AND.ISS.NE.1)WP=WE
C
          QIN=QIIN
        IF(XX.GE.QIT.AND.IVAR(3).NE.1)THEN
          IF(IVAR(3).EQ.2)QIN=QIFI
          IF(IVAR(3).EQ.3)QIN=QIN+QICR*(XX-QIT)
          IF(QIN.GT.QIFI.AND.QIFI.GT.QIIN)QIN=QIFI
          IF(QIN.LT.QIFI.AND.QIFI.LT.QIIN)QIN=QIFI
        END IF
C
          ETOR=TQIN
        IF(XX.GE.TQT.AND.IVAR(4).NE.1)THEN
          IF(IVAR(4).EQ.2)ETOR=TQFI
          IF(IVAR(4).EQ.3)ETOR=ETOR+TQCR*(XX-TQT)
          IF(ETOR.GT.TQFI.AND.TQFI.GT.TQIN)ETOR=TQFI
          IF(ETOR.LT.TQFI.AND.TQFI.LT.TQIN)ETOR=TQFI
        END IF
          ETOR=ETOR*(1.D0+FNN*DSIN(CYLN*WE*XX/2.D0))
C
      END IF
C
      IF(III.EQ.2)THEN
        IF(IVR.EQ.1)THEN
          CP=CPIN+CPCR*DFLOAT(IV-1)
          IF(CP.GT.CPFI)CP=CPFI
        END IF
        IF(IVR.EQ.2)THEN
          PERF=PFIN+PFCR*DFLOAT(IV-1)
          IF(PERF.GT.PFFI)PERF=PFFI
        END IF
        IF(IVR.EQ.3)THEN
          QIN=QIIN+QICR*DFLOAT(IV-1)
          IF(QIN.GT.QIFI)QIN=QIFI
        END IF
      END IF
      IF(CP.GT.1.D0)CP=1.D0
      IF(CP.LT.0.D0)CP=0.D0
      IF(PERF.GE.1.D0)PERF=1.D0
      IF(PERF.LE.0.D0)PERF=0.D0
      IFUL=0
      IF(PERF.GE.1.0)IFUL=1
C
C     LOSS COEFF.
C
         FC=.007144D0+.54479D0*CP-4.9163D0*CP**2+17.653D0*CP**3
```

```
         FC=FC-23.342D0*CP**4+11.052D0*CP**5
           IF(CP.LT.0.3D0)FC=0.007144D0+0.118D0*CP
        CLV=630.D0*FC
       CL=SCL+(CLFS+CLV)/AA**2
C
       RETURN
       END
C
C
C
C
C      SUBROUTINE KFACTS
C      *****************
C      THIS SUBROUTINE CALCULATES THE K FACTORS FOR THE
C      TORQUE,INCIDENCE,FRICTION,& SECONDARY CIRCULATION EQNS.
C
       SUBROUTINE KFACTS()
C
       IMPLICIT DOUBLE PRECISION (A-H,K,O-Z)
C
       COMMON/FLG1/IPGM,ISS,IMAC,IRTR,IOUT,ITQSTT,IOPUT(6),ICES,IFUL,ICOM
       COMMON/FLG2/IT,INTS,IV,IVST,IVR,IVAR(4),MNQQ,ICS,ICLC
       COMMON/GEO1/RO,RI,RINERT,BRI,BRO,BSI,BSO,ZR,ZS,BT,FFAC,BFAC
       COMMON/GEO2/PI,RHO,ARHO,PO,RC,RM,VF,ENGINT,CYLN,FNN,SHSTFF
       COMMON/RUN1/RTFI,RTCR,PFIN,PFFI,PFCR
       COMMON/RUN2/CPIN,CPFI,CPCR,CPT,SMIN,SMAX,SICR,ST
       COMMON/RUN3/QIIN,QIFI,QICR,QIT,TQIN,TQFI,TQCR,TQT
       COMMON/SCON/CES,AA,CLFS,CLV,SCL,CL,PBFAC,PFFAC,RTS,WRV
       COMMON/VAR1/PERF,RCO,RCI,DYNERT,QIN,CP,P1,DP,QOUT
       COMMON/VAR2/W,WP,WE,THETA1,THETA2,DELTA,ACH2O,ACRTR,ACENG
       COMMON/VAR3/TOR,POW,ETOR,EPOW,EPHI,DDTDEL,DDTPF
       COMMON/ARR1/TQFAC(6),PIFAC(3),PLOSS(3),TQCMPT(6),SPRES(26)
C
C      DEFINE FUNCTIONS FOR ROUTINE
C
       F5(AB)=AB**5.0
       D2(BB,CB)=BB**2-CB**2
       D3(DB,EB)=DB**3-EB**3
       D4(FB,GB)=FB**4-GB**4
       D5(PB,QB)=PB**5.0-QB**5.0
C
C
       F51(A,B,C)=D5(A,B)/5.D0-D4(A,B)*C+2.D0*D3(A,B)*C*C-2.D0*D2(A,B)*C*
      1C*C
       F52(A,B,C)=D5(A,B)/5.D0-3.D0*D4(A,B)*C/4.D0+D3(A,B)*C*C-D2(A,B)/2.
      2D0*C*C*C
       F53(A,B,C)=D5(A,B)/5.D0-D4(A,B)*C/2.D0+D3(A,B)/3.D0*C*C
       F54(A,B,C)=D5(A,B)/5.D0-D4(A,B)*C/4.D0
       F41(A,B,C)=D4(A,B)/4.D0-D3(A,B)*C+3.D0*D2(A,B)/2.D0*C*C-(A-B)*C**3
       F42(A,B,C)=D4(A,B)/4.D0-2.D0*D3(A,B)*C/3.D0+D2(A,B)/2.D0*C*C
       F43(A,B,C)=D4(A,B)/4.D0-D3(A,B)*C/3.D0
       F32(A,B,C)=(D3(A,B)/3.D0-D2(A,B)/2.D0*C)*C*C
       F31(A,B,C)=D3(A,B)/3.D0-C*D2(A,B)+(A-B)*C*C
       F21(A,B,C)=(D2(A,B)/2.D0-(A-B)*C)*C*C
       FOU(A,B,C,D,E)=(2.D0*PI*A-B+2.D0*C*D)*DSIN(E)
C
C
C      DETERMINE BLOCKAGE CONSTANTS
C
       BLKRI=ZR*BT/DSIN(BRI)
       BLKRO=ZR*BT/DSIN(BRO)
       BLKSI=ZS*BT/DSIN(BSI)
       BLKSO=ZS*BT/DSIN(BSO)
C
C      CALCULATE CONSTANTS FOR ROUTINE
C
       DL=(RM-RI)/50.D0
       DU=DL*(RM-RI)/(RO-RM)
       DUR=DU*DSIN(BRI)/DSIN(BRO)*(2.D0*PI*RI-BLKRI)/(2.D0*PI*RO-BLKRO)
       DUS=DU*DSIN(BSI)/DSIN(BSO)*(2.D0*PI*RI-BLKSI)/(2.D0*PI*RO-BLKSO)
       R1=RI+DL
       R3=RO-DU
       RP=RHO*PI
       RF=RHO*FFAC/8.D0*PI
       RK=RHO*BFAC
C
C      CHOOSE FULL OR CROPPED ROTOR
C
       IF(IRTR.EQ.1)THEN
```

```
C                       *** CROPPED ROTOR ***
C
C     CALCULATE TORQUE EQN. FACTORS
C
        TQF=RCO-RCI
        IF((RCO-RCI).LT.16.D0)TQF=16.D0
      TQFAC(1)=RHO/8.D0*RM*RM*(2.D0*PI*RM-BLKRO)*(D2((RO-RI),TQF))
      TQFAC(1)=TQFAC(1)*DSIN(BRO)*DSIN(BRO)
        TQF=RCI
        IF(RCI.GT.(RM-10.D0))TQF=RM-10.D0
      TQ22=2.D0*PI*F53(TQF,RI,RM)-BLKRI*F42(TQF,RI,RM)
      TQFAC(2)=RHO*TQ22*DSIN(BRI)*DCOS(BSO)
        TQF1=16.D0
        TQF2=RCO-RCI
        IF(TQF2.LT.TQF1)TQF2=TQF1
      ATQ1=ARHO/8.D0*RM*RM*(2.D0*PI*RM-BLKRO)*(D2(TQF2,TQF1))
      ATQ1=ATQ1*DSIN(BRO)*DSIN(BRO)
        TQF1=RM-10.D0
        TQF2=RCI
        IF(TQF2.GT.TQF1)TQF2=TQF1
      ATQ2=2.D0*PI*F53(TQF1,TQF2,RM)-BLKRI*F42(TQF1,TQF2,RM)
      ATQ2=ARHO*ATQ2*DSIN(BRI)*DCOS(BSO)
      TQFAC(1)=TQFAC(1)+ATQ1
      TQFAC(2)=TQFAC(2)+ATQ2
C
C     CALCULATE INCIDENCE LOSS FACTORS
C
      KI1=BLKRI/2.D0*F43(RCI,RI,RM)-PI*F54(RCI,RI,RM)*DSIN(BRI)
      KI4=(PI*F32(RO,RCO,RM)-BLKSI/2.D0*F21(RO,RCO,RM))*DSIN(BSI)
      PIFAC(1)=RHO*(KI1+KI4)
C
      KI2=2.D0*PI*F53(RCI,RI,RM)-BLKRI*F42(RCI,RI,RM)
      KI2=KI2*(DCOS(BSO)-DCOS(BRI))*DSIN(BRI)
      KI5=RM*(2.D0*PI*F42(RO,RCO,RM)-BLKSI*F31(RO,RCO,RM))
      KI5=KI5*DCOS(BSI)*DSIN(BSI)
      PIFAC(2)=RHO*(KI2-KI5)
C
      KI3=BLKRI*F41(RCI,RI,RM)-2.D0*PI*F52(RCI,RI,RM)
      KI3=KI3*(DCOS(BSO)-DCOS(BRI))**2*DSIN(BRI)
      KI6=2.D0*PI*F52(RO,RCO,RM)-BLKSI*F41(RO,RCO,RM)
      KI6=KI6*DCOS(BSI)**2*DSIN(BSI)
      PIFAC(3)=RHO/2.D0*(KI3+KI6)
C
C     CALCULATE FRICTION LOSS FACTOR
C
      KF1=ZR*DSIN(BRI)*(F51(RCI,RI+DL,RM)+(RCI-RI-DL)*RM**4)
      KF5=ZS*DSIN(BSO)*(F51(RCI,RI+DL,RM)+(RCI-RI-DL)*RM**4)
      KF7=ZS*DSIN(BSI)*(F51(RO-DUS,RCO,RM)+(RO-DUS-RCO)*RM**4)
      KFO=KF1+KF5+KF7
C
      KF26=FOU(RI,BLKRI,ZR,DL,BRI)+FOU(RI,BLKSO,ZS,DL,BSO)
      KF26=KF26*(RM-RI)**4.0
      KF48=FOU(RO,0.D0,0.D0,DU,BRO)+FOU(RO,BLKSI,ZS,DU,BSI)
      KF48=KF48*(RO-RM)**4.0
      KFE=KF26+KF48
      PFFAC=RF*(KFO+KFE/2.0D0)
C
C     CALCULATE SECONDARY CIRCULATION LOSS FACTOR
C
      KB1=(BLKRI/2.D0*F41(RCI,RI,RM)-PI*F52(RCI,RI,RM))*DSIN(BRI)
      KB2=PI*F52(RO,RCO,RM)*DSIN(BRO)
      KB3=(BLKSO/2.D0*F41(RCI,RI,RM)-PI*F52(RCI,RI,RM))*DSIN(BSO)
      KB4=(PI*F52(RO,RCO,RM)-BLKSI/2.D0*F41(RO,RCO,RM))*DSIN(BSI)
      PBFAC=RK*(KB1+KB2+KB3+KB4)
C
      ELSE
C           *** FULL ROTOR ***
C
C     CALCULATE TORQUE EQN. FACTORS
C
      TQFAC(1)=(2.D0*PI*F54(RO,RCO,RM)-BLKRO*F43(RO,RCO,RM))*DSIN(BRO)
      TQFAC(1)=RHO*TQFAC(1)
      TQ21=2.D0*PI*F53(RO,RCO,RM)-BLKRO*F42(RO,RCO,RM)
      TQ21=TQ21*DSIN(BRO)*DCOS(BRO)
      TQ22=2.D0*PI*F53(RCI,RI,RM)-BLKRI*F42(RCI,RI,RM)
      TQ22=TQ22*DSIN(BRI)*DCOS(BSO)
      TQFAC(2)=RHO*(TQ21+TQ22)
      ATQ1=(2.D0*PI*F54(RCO,RM,RM)-BLKRO*F43(RCO,RM,RM))*DSIN(BRO)
      ATQ1=ARHO*ATQ1
```

```
      ATQ21=2.D0*PI*F53(RCO,RM,RM)-BLKRO*F42(RCO,RM,RM)
      ATQ21=ATQ21*DSIN(BRO)*DCOS(BRO)
      ATQ22=2.D0*PI*F53(RM,RCI,RM)-BLKRI*F42(RM,RCI,RM)
      ATQ22=ATQ22*DSIN(BRI)*DCOS(BSO)
      ATQ2=ARHO*(ATQ21+ATQ22)
      TQFAC(1)=TQFAC(1)+ATQ1
      TQFAC(2)=TQFAC(2)+ATQ2
      IF(IPGM.LE.5)THEN
        ALP=(BRO+BRI)/2.D0
        A=(RO-RI)/2.D0
        B=A*DSIN(ALP)
        AY=(RCO-RCI)/2.D0
        BY=AY*DSIN(ALP)
        RY=(RCO+RCI)/2.D0
        PAB=PI*A*B/2.D0
        PA3B=PAB*A*A/4.D0
        PAYB=PI*AY*BY/2.D0
        PAY3B=PAYB*AY*AY/4.D0
        ZTSA=ZR*BT/DSIN(ALP)
        PRCZ=(2.D0*PI*RC-ZTSA)
        P6RCZ=PRCZ+4.D0*PI*RC
        PRCZR=P6RCZ-2.D0*PI*RM
        PRYZ=(2.D0*PI*RY-ZTSA)
        P6RYZ=PRYZ+4.D0*PI*RY
        PRYZR=P6RYZ-2.D0*PI*RM
        DAY=2.D0*AY*(PRYZ-PI*AY*.31D0/1.69D0)
        IF(DAY.LT.1.D-6)DAY=1.D-6
        DAY=-DDTPF*PRCZ*A*A/DAY
        DRY=-DAY*.31D0/1.69D0
        PBYDA=PI*BY*DAY
        RYSAY=RY*(RY*DRY+AY*DAY)
        RY2AY=2.D0*RY*DRY+AY*DAY
C
        TQ3=2.D0*PI*(3.D0*PAYB*RYSAY+PBYDA*RY*RY*RY+3.D0*PAY3B*DRY)
        TQFAC(3)=-RHO*(TQ3-ZTSA*(RY2AY*PAYB+PBYDA*RY*RY))
        TQ4=TQ3-(2.D0*PI*RM+ZTSA)*(RY2AY*PAYB+PBYDA*RY*RY)
        TQFAC(4)=-RHO*DCOS(ALP)*(TQ4+RM*ZTSA*(DRY*PAYB+PBYDA*RY))
        TQ5=PAB*PRCZ*RC*RC-PAYB*PRYZ*RY*RY
        TQFAC(5)=RHO*(TQ5+PA3B*P6RCZ-PAY3B*P6RYZ)
        TQ6=PAB*(RC*RC-RM*RC)*PRCZ-PAYB*(RY*RY-RM*RY)*PRYZ
        TQFAC(6)=RHO*DCOS(ALP)*(TQ6+PA3B*PRCZR-PAY3B*PRYZR)
      END IF
C
C     CALCULATE INCIDENCE LOSS FACTORS
C
      KI1=(BLKRI/2.D0*F43(RCI,RI,RM)-PI*F54(RCI,RI,RM))*DSIN(BRI)
      KI4=(PI*F54(RO,RCO,RM)-BLKSI/2.D0*F43(RO,RCO,RM))*DSIN(BSI)
      PIFAC(1)=RHO*(KI1+KI4)
C
      KI2=2.D0*PI*F53(RCI,RI,RM)-BLKRI*F42(RCI,RI,RM)
      KI2=KI2*(DCOS(BSO)-DCOS(BRI))*DSIN(BRI)
      KI5=2.D0*PI*F53(RO,RCO,RM)-BLKSI*F42(RO,RCO,RM)
      KI5=KI5*(DCOS(BRO)-DCOS(BSI))*DSIN(BSI)
      PIFAC(2)=RHO*(KI2+KI5)
C
      KI3=BLKRI*F41(RCI,RI,RM)-2.D0*PI*F52(RCI,RI,RM)
      KI3=KI3*(DCOS(BSO)-DCOS(BRI))**2*DSIN(BRI)
      KI6=2.D0*PI*F52(RO,RCO,RM)-BLKSI*F41(RO,RCO,RM)
      KI6=KI6*(DCOS(BRO)-DCOS(BSI))**2*DSIN(BSI)
      PIFAC(3)=RHO/2.D0*(KI3+KI6)
C
C     CALCULATE FRICTION LOSS FACTOR
C
      KF1=ZR*DSIN(BRI)*(F51(RCI,RI+DL,RM)+(RCI-RI-DL)*RM**4)
      KF3=ZR*DSIN(BRO)*(F51(RO-DUR,RCO,RM)+(RO-DUR-RCO)*RM**4)
      KF5=ZS*DSIN(BSO)*(F51(RCI,RI+DL,RM)+(RCI-RI-DL)*RM**4)
      KF7=ZS*DSIN(BSI)*(F51(RO-DUS,RCO,RM)+(RO-DUS-RCO)*RM**4)
      KFO=KF1+KF3+KF5+KF7
C
      KF26=FOU(RI,BLKRI,ZR,DL,BRI)+FOU(RI,BLKSO,ZS,DL,BSO)
      KF26=KF26*(RM-RI)**4.0
      KF48=FOU(RO,BLKRO,ZR,DU,BRO)+FOU(RO,BLKSI,ZS,DU,BSI)
      KF48=KF48*(RO-RM)**4.0
      KFE=KF26+KF48
      PFFAC=RF*(KFO+KFE/2.0D0)
C
C     CALCULATE SECONDARY CIRCULATION LOSS FACTOR
C
      KB1=(BLKRI/2.D0*F41(RCI,RI,RM)-PI*F52(RCI,RI,RM))*DSIN(BRI)
```

```
      KB2=(PI*F52(RO,RCO,RM)-BLKRO/2.D0*F41(RO,RCO,RM))*DSIN(BRO)
      KB3=(BLKSO/2.D0*F41(RCI,RI,RM)-PI*F52(RCI,RI,RM))*DSIN(BSO)
      KB4=(PI*F52(RO,RCO,RM)-BLKSI/2.D0*F41(RO,RCO,RM))*DSIN(BSI)
      PBFAC=RK*(KB1+KB2+KB3+KB4)
C
      END IF
C
C     CORRECTION FOR RO,RI,RM IN mm
C
      TQFAC(1)=TQFAC(1)*1.D-15
      TQFAC(2)=TQFAC(2)*1.D-15
      TQFAC(3)=TQFAC(3)*1.D-15
      TQFAC(4)=TQFAC(4)*1.D-15
      TQFAC(5)=TQFAC(5)*1.D-15
      TQFAC(6)=TQFAC(6)*1.D-15
      PIFAC(1)=PIFAC(1)*1.D-15
      PIFAC(2)=PIFAC(2)*1.D-15
      PIFAC(3)=PIFAC(3)*1.D-15
      PFFAC=PFFAC*1.D-15
      PBFAC=PBFAC*1.D-15
C
      RETURN
      END
C
C
C
C
C
C     SUBROUTINE VORVEL
C     *****************
C     THIS SUBROUTINE SOLVES FOR THE VORTEX VELOCITY
C     UDSING THE QUADRATIC FORMULA
C
      SUBROUTINE VORVEL()
C
      IMPLICIT DOUBLE PRECISION (A-H,O-Z)
C
      COMMON/FLG1/IPGM,ISS,IMAC,IRTR,IOUT,ITQSTT,IOPUT(6),ICES,IFUL,ICOM
      COMMON/FLG2/IT,INTS,IV,IVST,IVR,IVAR(4),MNQQ,ICS,ICLC
      COMMON/GEO1/RO,RI,RINERT,BRI,BRO,BSI,BSO,ZR,ZS,BT,FFAC,BFAC
      COMMON/GEO2/PI,RHO,ARHO,PO,RC,RM,VF,ENGINT,CYLN,FNN,SHSTFF
      COMMON/RUN1/RTFI,RTCR,PFIN,PFFI,PFCR
      COMMON/RUN2/CPIN,CPFI,CPCR,CPT,SMIN,SMAX,SICR,ST
      COMMON/RUN3/QIIN,QIFI,QICR,QIT,TQIN,TQFI,TQCR,TQT
      COMMON/SCON/CES,AA,CLFS,CLV,SCL,CL,PBFAC,PFFAC,RTS,WRV
      COMMON/VAR1/PERF,RCO,RCI,DYNERT,QIN,CP,P1,DP,QOUT
      COMMON/VAR2/W,WP,WE,THETA1,THETA2,DELTA,ACH2O,ACRTR,ACENG
      COMMON/VAR3/TOR,POW,ETOR,EPOW,EPHI,DDTDEL,DDTPF
      COMMON/ARR1/TQFAC(6),PIFAC(3),PLOSS(3),TQCMPT(6),SPRES(26)
C
C     CALCULATE THE COEFFIENTS
C
      A=(PIFAC(3)+PFFAC+PBFAC)
      B=((PIFAC(2)-TQFAC(2))*WP)
      C=((PIFAC(1)-TQFAC(1))*(WP**2))
C
C     CHECK IF SQUARE ROOT IS COMPLEX
C
      ICOM=0
      BSD=B**2-4.0D0*A*C
      IF(BSD.LT.0.0D0)THEN
        WRITE(*,4911)
 4911   FORMAT(' **********-ROOTS FOR VELOCITY ARE COMPLEX-**********')
        ICOM=1
      ELSE
C
C     SOLVE FOR VELOCITTY
C
        RBS=DSQRT(BSD)
        W=(-B+RBS)/(2.0D0*A)
      END IF
C
      RETURN
      END
C
C
C
C
C
```

```
C     SUBROUTINE POWER
C     ****************
C     THIS SUBROUTINE CALCULATES TORQUE,POWER,CUP
C     PRESSURES AND LOSSES
C
      SUBROUTINE POWER()
C
      IMPLICIT DOUBLE PRECISION (A-H,O-Z)
C
      COMMON/FLG1/IPGM,ISS,IMAC,IRTR,IOUT,ITQSTT,IOPUT(6),ICES,IFUL,ICOM
      COMMON/FLG2/IT,INTS,IV,IVST,IVR,IVAR(4),MNQQ,ICS,ICLC
      COMMON/GEO1/RO,RI,RINERT,BRI,BRO,BSI,BSO,ZR,ZS,BT,FFAC,BFAC
      COMMON/GEO2/PI,RHO,ARHO,PO,RC,RM,VF,ENGINT,CYLN,FNN,SHSTFF
      COMMON/RUN1/RTFI,RTCR,PFIN,PFFI,PFCR
      COMMON/RUN2/CPIN,CPFI,CPCR,CPT,SMIN,SMAX,SICR,ST
      COMMON/RUN3/QIIN,QIFI,QICR,QIT,TQIN,TQFI,TQCR,TQT
      COMMON/SCON/CES,AA,CLFS,CLV,SCL,CL,PBFAC,PFFAC,RTS,WRV
      COMMON/VAR1/PERF,RCO,RCI,DYNERT,QIN,CP,P1,DP,QOUT
      COMMON/VAR2/W,WP,WE,THETA1,THETA2,DELTA,ACH2O,ACRTR,ACENG
      COMMON/VAR3/TOR,POW,ETOR,EPOW,EPHI,DDTDEL,DDTPF
      COMMON/ARR1/TQFAC(6),PIFAC(3),PLOSS(3),TQCMPT(6),SPRES(26)
C
      TQCMPT(1)=2.D0*TQFAC(1)*WP*W
      TQCMPT(2)=2.D0*TQFAC(2)*(W**2)
      TQCMPT(3)=2.D0*TQFAC(3)*WP
      TQCMPT(4)=2.D0*TQFAC(4)*W
      IF(IPGM.GT.5.OR.IT.LE.1)THEN
        TQCMPT(5)=2.D0*TQFAC(5)*ACRTR
        TQCMPT(6)=2.D0*TQFAC(6)*ACH2O
        TOR=TQCMPT(1)+TQCMPT(2)+TQCMPT(3)+TQCMPT(4)+TQCMPT(5)+TQCMPT(6)
        POW=TOR*WP
      END IF
      SAVEWP=WP
C
      PL1=PIFAC(1)*WP**2
      PL2=PIFAC(2)*W*WP
      PL3=PIFAC(3)*W**2
      PLOSS(1)=2.D0*W*(PL1+PL2+PL3)
      PLOSS(2)=2.D0*PFFAC*(W**3)
      PLOSS(3)=2.D0*PBFAC*(W**3)
C
C     ROTOR TIP SPEED, H2O RELATIVE VELO. & VORTEX PRESSURE (GAUGE)
C
      IF(IRTR.EQ.1)THEN
        RTS=WP*RM/1.D3
        WRV=W*(RO-RI)/2.D3*DSIN(BRO)
      ELSE
        RTS=WP*RO/1.D3
        WRV=W*(RO-RM)/1.D3
      END IF
C     PRESSURE
C     SET LOOP RANGE
      IF(IOPUT(5).EQ.1)THEN
        IP1=1
        IP2=26
      ELSE
        IF(IOUT.EQ.0)THEN
          IP1=7
          IP2=7
        ELSE
          IF(IOUT.EQ.1)THEN
            IP1=13
            IP2=13
          ELSE
            IP1=19
            IP2=19
          END IF
        END IF
      END IF
      R1=(RO-RI)/2.D0
      R2=RM-(RO+RI)/2.D0
      DO 6000 K=IP1,IP2
        THC=REAL(K-1)*PI/12.D0
C ALLOW FOR GAP BETWEEN ROTOR AND STATOR
        IF(K.EQ.1)THC=PI/180.D0
        IF(K.EQ.13)THC=179.D0*PI/180.D0
        IF(K.EQ.25)THC=359.D0*PI/180.D0
C        IF(K.EQ.26)THC=PI
        IF(K.EQ.26)THC=181.D0*PI/180.D0
```

```
        COC=DCOS(THC)
C CONVERT ANGLES ROUND CUP TO ANGLES FROM VORTEX CENTRE
        IF(DABS((R1*COC-R2)/RM).LT.0.0005D0)THEN
          TH=PI/2.D0
          IF(K.GT.13)TH=TH*3.D0
        ELSE
          IF(COC.LT.0.D0.AND.DABS(R1*COC).GT.R2)THEN
            TH=PI+DATAN(R1*DSIN(THC)/(R2+R1*COC))
          ELSE
            IF(COC.GT.0.D0.AND.K.GT.13)THEN
              TH=2.D0*PI+DATAN(R1*DSIN(THC)/(R2+R1*COC))
            ELSE
              TH=DATAN(R1*DSIN(THC)/(R2+R1*COC))
            END IF
          END IF
        END IF
        CO=DCOS(TH)
        CTHC=DABS(DCOS(PI-THC-TH))
        AL=BRI+(BRO-BRI)*DBLE(K-1)/12.D0
        IF(IRTR.EQ.1)THEN
          IF(K.GT.7)WP=0.D0
          AL=BRI+(BRO-BRI)*DBLE(K-1)/6.D0
          IF(K.GT.7)AL=BRO
        END IF
        IF(K.GT.13)WP=0.D0
        IF(K.GT.13)AL=BSI+(BSO-BSI)*DBLE(K-1)/12.D0
        SAL=DSIN(AL)
        CAL=DABS(DCOS(AL))
C CALC. BOUNDARY CONDITION AT THIS ANGLE
C     FREE SURFACE RADIUS
        BB=(RM-(RCO+RCI)/2.D0)*DCOS(TH)
        CB=(RM-(RCO+RCI)/2.D0)**2-((RCO-RCI)/2.D0)**2
        XO=BB+DSQRT(BB**2-CB)
C     CALC. COMMON VALUES
        RAM=DSQRT(XO**2+RM**2-2.D0*RM*XO*CO)
        XR=XO-RM*CO
        GV=DACOS(-CO*SAL)
        GR=DACOS(-XO*SAL*DSIN(TH)/RAM)
        GA=DACOS(-XO*SAL*DSIN(TH)/RAM)
        XXO=XO
        IF(DABS(XO).LT.1.D-6)XXO=1.D-6
        CZETA=(XO**2+RAM**2-RM**2)/(2.D0*XXO*RAM)
        IF(CZETA.GT.1.D0)CZETA=1.D0
        IF(CZETA.LT.-1.D0)CZETA=-1.D0
        ZETA=DACOS(CZETA)
        BETA=(PI-ZETA)-(AL/PI*2.D0)*(PI-ZETA-TH)
        CBETA=DCOS(BETA)
C     DIRECTION AND COEFFIENT OF R*WP**2 VECTOR
C       IF(K.EQ.1.OR.K.EQ.13.OR.K.GT.24)THEN
C         CWV=1.D0
C         CWWR=-CBETA
C         CWR=0.D0
C         PRES=XR*RAM/2.D0
C       ELSE
          CWV=CAL
          CWWR=-CBETA*CAL
          IF(AL.GT.(PI/2.D0-0.0001D0))CWWR=-CBETA
          CWR=CAL*DCOS(DABS(ZETA-PI/2.D0))
          IF(K.GT.13)CWR=-CWR
      PRES=XR/2.D0*RAM+(1-(DCOS(TH))**2)*RM**2/2.D0*DLOG(DABS(XR+RAM))
C       END IF
      BDC=((W*W+2.D0*WP*W*DSIN(GV)*CWV)*XO*XO/2.D0)
      BDC=BDC+(ACRTR*DSIN(GA)*CWR+WP*WP*DSIN(GR)*CWWR)*DABS(PRES)
C  CALC. PRESSURE AT CUP SURFACE
C     CASING RADIUS
        BB=(RM-(RO+RI)/2.D0)*DCOS(TH)
        CB=(RM-(RO+RI)/2.D0)**2-((RO-RI)/2.D0)**2
        XC=BB+DSQRT(BB**2-CB)
C     CALC. COMMON VALUES
        RAM=DSQRT(XC**2+RM**2-2.D0*RM*XC*CO)
        XR=XC-RM*CO
        GV=DACOS(-CO*SAL)
        GR=DACOS(-XC*SAL*DSIN(TH)/RAM)
        GA=DACOS(-XC*SAL*DSIN(TH)/RAM)
        XXC=XC
        IF(DABS(XC).LT.1.D-6)XXC=1.D-6
        CZETA=(XC**2+RAM**2-RM**2)/(2.D0*XXC*RAM)
        IF(CZETA.GT.1.D0)CZETA=1.D0
        IF(CZETA.LT.-1.D0)CZETA=-1.D0
```

```
        ZETA=DACOS(CZETA)
        BETA=(PI-ZETA)-(AL/PI*2.D0)*(PI-ZETA-TH)
        CBETA=DCOS(BETA)
C     DIRECTION AND COEFFIENT OF R*WP**2 VECTOR
C        IF(K.EQ.1.OR.K.EQ.13.OR.K.GT.24)THEN
C          CWV=1.D0
C          CWWR=-CBETA
C          CWR=0.D0
C          PRES=XR*RAM/2.D0
C        ELSE
          CWV=CAL
          CWWR=-CBETA*CAL
          IF(AL.GT.(PI/2.D0-0.0001D0))CWWR=-CBETA
          CWR=CAL*DCOS(DABS(ZETA-PI/2.D0))
          IF(K.GT.13)CWR=-CWR
      PRES=XR/2.D0*RAM+(1-(DCOS(TH))**2)*RM**2/2.D0*DLOG(DABS(XR+RAM))
C        END IF
      SPRE=((W*W+2.D0*WP*W*DSIN(GV)*CWV)*XC*XC/2.D0)
      SPRE=SPRE+(ACRTR*DSIN(GA)*CWR+WP*WP*DSIN(GR)*CWWR)*DABS(PRES)-BDC
      SPRES(K)=RHO*SPRE*1.D-6
 6000 CONTINUE
      WP=SAVEWP
C
      IF(IOUT.EQ.0)PWP2=((RO/2.D3)**2-2.D0*(RC/1.D3)**2)*WP**2
      P1=SPRES(7)
      IF(IOUT.EQ.1)P1=SPRES(13)
      IF(IOUT.EQ.2)P1=SPRES(19)
      IF(IPGM.LE.5)THEN
        IF(IOUT.EQ.0)QO=(2.D0*P1/RHO-PWP2)/CL
        IF(IOUT.EQ.1.AND.IRTR.EQ.0)QO=(2.D0*P1/RHO+(WP*RO/2.D3)**2)/CL
        IF(IOUT.EQ.1.AND.IRTR.EQ.1)QO=(2.D0*P1/RHO)/CL
        IF(IOUT.EQ.2)QO=(2.D0*P1/RHO)/CL
        IF(QO.LE.0.D0)THEN
          QOUT=0.D0
        ELSE
          QOUT=DSQRT(QO)
        END IF
        DP=P1-RHO/2.D0*(QOUT**2)*SCL
      END IF
      IF(IPGM.GT.5)DP=P1-RHO/2.D0*(QIN**2)*SCL
      IF(IOUT.EQ.0)DP=DP-RHO/2.D0*PWP2
      IF(IOUT.EQ.1.AND.IRTR.EQ.0)DP=DP+RHO/2.D0*(WP*RO/2.D3)**2
C
      RETURN
      END
C
C
C
C     SUBROUTINE PART
C     ***************
C     THIS SUBROUTINE CALCULATES RM,RCI,RCO
C
      SUBROUTINE PART()
C
      IMPLICIT DOUBLE PRECISION (A-H,O-Z)
C
      COMMON/FLG1/IPGM,ISS,IMAC,IRTR,IOUT,ITQSTT,IOPUT(6),ICES,IFUL,ICOM
      COMMON/FLG2/IT,INTS,IV,IVST,IVR,IVAR(4),MNQQ,ICS,ICLC
      COMMON/GEO1/RO,RI,RINERT,BRI,BRO,BSI,BSO,ZR,ZS,BT,FFAC,BFAC
      COMMON/GEO2/PI,RHO,ARHO,PO,RC,RM,VF,ENGINT,CYLN,FNN,SHSTFF
      COMMON/RUN1/RTFI,RTCR,PFIN,PFFI,PFCR
      COMMON/RUN2/CPIN,CPFI,CPCR,CPT,SMIN,SMAX,SICR,ST
      COMMON/RUN3/QIIN,QIFI,QICR,QIT,TQIN,TQFI,TQCR,TQT
      COMMON/SCON/CES,AA,CLFS,CLV,SCL,CL,PBFAC,PFFAC,RTS,WRV
      COMMON/VAR1/PERF,RCO,RCI,DYNERT,QIN,CP,P1,DP,QOUT
      COMMON/VAR2/W,WP,WE,THETA1,THETA2,DELTA,ACH2O,ACRTR,ACENG
      COMMON/VAR3/TOR,POW,ETOR,EPOW,EPHI,DDTDEL,DDTPF
      COMMON/ARR1/TQFAC(6),PIFAC(3),PLOSS(3),TQCMPT(6),SPRES(26)
C
C     CALCULATE CENTRE OF FORCED VORTEX
C
        BLKSI=ZS*BT/DSIN(BSI)
        BLKSO=ZS*BT/DSIN(BSO)
      IF(IT.LE.1.AND.(IPGM.NE.9.OR.MNQQ.EQ.1))THEN
      RNUM=2.D0*PI/3.D0*(RO**3-RI**3)*DSIN(BSO)-ZS*BT/2.D0*(RO**2-RI**2)
       RDEN=PI*(RO**2-RI**2)*DSIN(BSO)-ZS*BT*(RO-RI)
      RM=RNUM/RDEN
        IF(DABS(BSO-BSI).GT.0.02D0)THEN
          X=RM
```

```
          DO 5000 M=1,20
        F=2.D0*PI/3.D0*(RO**3*DSIN(BSI)-RI**3*DSIN(BSO))
        F=F-ZS*BT/2.D0*(RO*RO-RI*RI)-DSIN(BSI)*PI*(RM*RO*RO-RM**3/3.D0)
        F=F+DSIN(BSO)*PI*(RM*RI*RI-RM**3/3.D0)+ZS*BT*RM*(RO-RI)
        FX=ZS*BT*(RO-RI)+DSIN(BSO)*PI*(RI*RI-RM*RM)
        FX=FX-DSIN(BSI)*PI*(RO*RO-RM*RM)
        SGN=1.D0
        IF(FX.LT.0.D0)SGN=-1.D0
        IF(DABS(FX).LT.0.001D0)FX=0.001D0*SGN
              Y=X-F/FX
              IF(DABS((Y-X)/X).LT.0.0001D0)GOTO 5001
              X=Y
              RM=Y
 5000       CONTINUE
 5001       CONTINUE
            RM=Y
          END IF
        END IF
           IF(IFUL.EQ.1)THEN
             RCO=RM
             RCI=RM
           END IF
           IF(PERF.LE.0.D0)THEN
             RCO=RO
             RCI=RI
           END IF
C
        IF(IFUL.LT.1.AND.PERF.GT.0.D0)THEN
C
C       RCI & RCO FOR M=1 BELOW
           FA=3.125D0*(1.D0-PERF)
           FB=4.000D0*(1.D0-PERF)
            IF(PERF.LT.0.92D0)FB=1.5467D0-1.3333D0*PERF
            IF(PERF.LT.0.92D0)FA=1.3053D0-1.1471D0*PERF
            IF(PERF.LT.0.74D0)FB=1.0919D0-0.7188D0*PERF
            IF(PERF.LT.0.75D0)FA=1.0825D0-0.850D0*PERF
            IF(PERF.LT.0.42D0)FB=1.D0-0.5D0*PERF
            IF(PERF.LT.0.55D0)FA=1.D0-0.7D0*PERF
        RCI=RM-FA*(RM-RI)
        RCO=RM+FB*(RO-RM)
C
        IF(RCO.LT.RM)RCO=RM
        IF(RCO.GT.RO)RCO=RO
        IF(RCI.GT.RM)RCI=RM
        IF(RCI.LT.RI)RCI=RI
C
C       RE-CALCULATE RCI USING VOLUME FILL & RCO USING CONTINUITY
C       EXCEPT FOR FULL-FILL OR ZERO-FILL CASES
C
        X=RCO
        Y=RCI
        BI=PI
        BAV=(BRI+BRO+BSI+BSO)/4.D0
        CON=VF*4.D9/PI/SIN(BAV)/10.D0
        CONI=(1.D0-PERF)*CON*10.D0
        D=RM
        AO=2.D0*PI/3.D0
        BO=RM*PI
        DAA=DSIN(BSI)
        DBB=DSIN(BSO)
        SGN=(RO**2/2.D0-RM*RO)-(RI**2/2.D0-RM*RI)
        CO=ZS*BT
        CONO=BO*(DAA*(RO**2)-DBB*(RI**2))+CO*SGN
        CONO=CONO-AO*(DAA*(RO**3)-DBB*(RI**3))
        CI=ZP*BT*(1.D0/DSIN(BRO)+1.D0/DSIN(BRI))
          IF(IRTR.EQ.1)CI=CI/2.D0
        CI=(CI+ZS*BT*(1.D0/DSIN(BSO)+1.D0/DSIN(BSI)))/4.0D0
C
C       USE SIMULTANEOUS ITERATION
        DO 5100 M=1,20
              SGN=(X**2/2.D0-D*X)-(Y**2/2.D0-D*Y)
           F=AO*(DAA*X**3-DBB*Y**3)-BO*(DAA*X**2-DBB*Y**2)-CO*SGN+CONO
           G=((X+Y)*BI-CI)*((X-Y)**2)-CONI
        IF(DABS(F/CON).LE.0.0005D0.AND.DABS(G/CON).LE.0.0005D0)GOTO 5101
C       CALC. DERIVATIVES OF F & G
           FX=3.0D0*AO*DAA*(X**2)-2.0D0*BO*DAA*X-CO*(X-D)
           FY=2.0D0*BO*DBB*Y-3.0D0*AO*DBB*(Y**2)-CO*(D-Y)
           GX=2.0D0*(X-Y)*((X+Y)*BI-CI)+BI*((X-Y)**2)
           GY=BI*((X-Y)**2)-2.0D0*(X-Y)*((X+Y)*BI-CI)
```

```
C     CALC. NEW X & Y
         RDEN=FX*GY-GX*FY
           SGN=1.0D0
           IF(RDEN.LT.0.0D0)SGN=(-1.0D0)
           IF(DABS(RDEN).LT.0.01D0)RDEN=0.01D0*SGN
         X=X-(GY*F-FY*G)/RDEN
         Y=Y-(FX*G-GX*F)/RDEN
 5100 CONTINUE
 5101 CONTINUE
         RCO=(X)
         RCI=(Y)
C
      IF(RCO.LT.RM)RCO=RM
      IF(RCO.GT.RO)RCO=RO
C
      IF(RCI.GT.RM)RCI=RM
      IF(RCI.LT.RI)RCI=RI
C
      END IF
C  CALCULATE WATER INERTIA FOR SOLID BODY ROTATION
C  NOT REQUIRED AS TQFAC(5) &(6) COVER THIS
C       IF(IPGM.LE.5)THEN
C         R1=(RO-RI)/2.D3
C         R2=(RCO-RCI)/2.D3
C         RRC=RC/1.D3
C         IF(R2.GT.0.D0)THEN
C           WINERT=(R1**2)*(RRC**2+.75D0*(R1**2))
C           WINERT=WINERT-(RRC**2+.75D0*(R2**2))*(R2**2)
C         ELSE
C           WINERT=(R1**2)*(RRC**2+.75D0*(R1**2))
C         END IF
C         WINERT=4.D0*RHO*(PI**2)*RRC*WINERT
C         TINERT=RINERT+WINERT
C       END IF
C       DYNERT=TINERT
C       IF(ISS.NE.1)THEN
C         DYNERT=DYNERT+ENGINT
C       END IF
C
      RETURN
      END
C
C
C
C
C
C     SUBROUTINE TQSTRT
C     *****************
C     THIS SUBROUTINE FINDS THE VALVE CLOSURE POSITION FOR A
C     GIVEN TORQUE & SPEED SET POINT
C
      SUBROUTINE TQSTRT()
C
      IMPLICIT DOUBLE PRECISION (A-H,O-Z)
C
      COMMON/FLG1/IPGM,ISS,IMAC,IRTR,IOUT,ITQSTT,IOPUT(6),ICES,IFUL,ICOM
      COMMON/FLG2/IT,INTS,IV,IVST,IVR,IVAR(4),MNQQ,ICS,ICLC
      COMMON/GEO1/RO,RI,RINERT,BRI,BRO,BSI,BSO,ZR,ZS,BT,FFAC,BFAC
      COMMON/GEO2/PI,RHO,ARHO,PO,RC,RM,VF,ENGINT,CYLN,FNN,SHSTFF
      COMMON/RUN1/RTFI,RTCR,PFIN,PFFI,PFCR
      COMMON/RUN2/CPIN,CPFI,CPCR,CPT,SMIN,SMAX,SICR,ST
      COMMON/RUN3/QIIN,QIFI,QICR,QIT,TQIN,TQFI,TQCR,TQT
      COMMON/SCON/CES,AA,CLFS,CLV,SCL,CL,PBFAC,PFFAC,RTS,WRV
      COMMON/VAR1/PERF,RCO,RCI,DYNERT,QIN,CP,P1,DP,QOUT
      COMMON/VAR2/W,WP,WE,THETA1,THETA2,DELTA,ACH2O,ACRTR,ACENG
      COMMON/VAR3/TOR,POW,ETOR,EPOW,EPHI,DDTDEL,DDTPF
      COMMON/ARR1/TQFAC(6),PIFAC(3),PLOSS(3),TQCMPT(6),SPRES(26)
C
      T=0.D0
      ETOR=ETOR*(1.D0+FNN*DSIN(CYLN*WE*T/2.D0))
      IF(IPGM.EQ.2)WE=WE*(1.D0+FNN*DSIN(CYLN*WE*T/2.D0-PI/2.D0))
      IF(IPGM.EQ.2)WP=WE
C
      CP1=0.0D0
      CP2=1.0D0
      CP=CP1
      CALL STATUS(0,0.D0,0.D0)
      CALL STFLOW()
           IF(ICOM.EQ.1)ISAV=1
```

```
          IF(ICOM.EQ.1)RETURN
      DT1=TOR
      CP=CP2
      CALL STATUS(0,0.D0,0.D0)
      CALL STFLOW()
           IF(ICOM.EQ.1)ISAV=1
           IF(ICOM.EQ.1)RETURN
      DT2=TOR
      CP=CPIN
      PERF=PFIN
      DO 4500 MMM=1,100
        CALL STATUS(0,0.D0,0.D0)
        CALL STFLOW()
            IF(ICOM.EQ.1)ISAV=1
            IF(ICOM.EQ.1)RETURN
          DT=ETOR
          IF(DT.LT.0.01D0)DT=0.01D0
        IF(DABS((TOR-ETOR)/DT).LT.0.0001D0)GOTO 4501
        IF((CP2-CP1).LT.1.D-7)GOTO 4501
        IF(TOR.GT.ETOR)THEN
          CP2=CP
          DT2=TOR
        ELSE
          CP1=CP
          DT1=TOR
        END IF
        DEN=(DT2-DT1)
        IF(DEN.LT.1.D-6)DEN=1.D-6
        DNCP=CP+(ETOR-TOR)*(CP2-CP1)/DEN
          IF(DNCP.GE.CP2.OR.DNCP.LE.CP1)DNCP=(CP1+CP2)/2.0D0
        CP=DNCP
          IF(CP.GT.1.D0)CP=1.D0
          IF(CP.LT.0.D0)CP=0.D0
 4500 CONTINUE
 4501 CONTINUE
      CPIN=CP
      PFIN=PERF
C
      RETURN
      END
C
C
C     SUBROUTINE STFLOW
C     *****************
C     THIS SUBROUTINE FINDS QIN=QOUT PERF FOR GIVEN
C     VAVLE CLOSURE & SPEED
C
      SUBROUTINE STFLOW()
C
      IMPLICIT DOUBLE PRECISION (A-H,O-Z)
C
      COMMON/FLG1/IPGM,ISS,IMAC,IRTR,IOUT,ITQSTT,IOPUT(6),ICES,IFUL,ICOM
      COMMON/FLG2/IT,INTS,IV,IVST,IVR,IVAR(4),MNQQ,ICS,ICLC
      COMMON/GEO1/RO,RI,RINERT,BRI,BRO,BSI,BSO,ZR,ZS,BT,FFAC,BFAC
      COMMON/GEO2/PI,RHO,ARHO,PO,RC,RM,VF,ENGINT,CYLN,FNN,SHSTFF
      COMMON/RUN1/RTFI,RTCR,PFIN,PFFI,PFCR
      COMMON/RUN2/CPIN,CPFI,CPCR,CPT,SMIN,SMAX,SICR,ST
      COMMON/RUN3/QIIN,QIFI,QICR,QIT,TQIN,TQFI,TQCR,TQT
      COMMON/SCON/CES,AA,CLFS,CLV,SCL,CL,PBFAC,PFFAC,RTS,WRV
      COMMON/VAR1/PERF,RCO,RCI,DYNERT,QIN,CP,P1,DP,QOUT
      COMMON/VAR2/W,WP,WE,THETA1,THETA2,DELTA,ACH2O,ACRTR,ACENG
      COMMON/VAR3/TOR,POW,ETOR,EPOW,EPHI,DDTDEL,DDTPF
      COMMON/ARR1/TQFAC(6),PIFAC(3),PLOSS(3),TQCMPT(6),SPRES(26)
C
      ICHAG=0
      SLOP=0.6
      SLOP1=0.09
      IF(IRTR.EQ.1)SLOP=0.4
C
      DO 4600 MNQQ=1,100
        IF(IPGM.EQ.9.AND.IT.EQ.1.AND.MNQQ.EQ.1)IFUL=1
        CALL PART()
        CALL KFACTS()
        CALL VORVEL()
          IF(ICOM.EQ.1)ISAV=1
          IF(ICOM.EQ.1)RETURN
        CALL POWER()
C CUP PRESS. FROM ENERGY EQN. (QIN=QOUT) TO FIND CORRECT FILL
        IF(IOUT.EQ.0)PWP2=((RO/2.D3)**2-2.D0*(RC/1.D3)**2)*WP**2
```

```
        IF(IOUT.EQ.0)P=RHO*((QIN**2)*CL+PWP2)/2.0D0
        IF(IOUT.EQ.0)P1=SPRES(7)
        IF(IOUT.GT.0)P=RHO*((QIN**2)*CL)/2.0D0
        IF(IOUT.EQ.1.AND.IRTR.EQ.0)P=P-RHO*((WP*RO/2.D3)**2)/2.D0
        IF(IOUT.EQ.1)P1=SPRES(13)
        IF(IOUT.EQ.2)P1=SPRES(19)
        DE=W*W
          IF(DE.LE.1.D0)DE=1.0D0
        DX=(P1-P)/DE
C USE PERF & DX TO DETERMINE EQUIL. STATE
        IF(PERF.GE.1.0D0)THEN
          IF(DABS(DX).LE.0.002D0)THEN
            CES=WP
            ICES=1
            GOTO 4601
          ELSE
            IF(DX.LT.0.0D0)GOTO 4601
C ESTIMATE PERF AS NO LONGER ON HYDRAULIC MAX.
            PERF=1.D0-DX*SLOP
              IF(PERF.GT.1.D0)PERF=1.D0
              IF(PERF.LT.0.D0)PERF=0.D0
              IFUL=0
              IF(PERF.GE.1.D0)IFUL=1
          END IF
        ELSE
          IF(IPGM.EQ.9.AND.IT.EQ.1.AND.MNQQ.EQ.1)THEN
C ESTIMATE PERF ON FIRST STATIC LOOP
            PERF=1.D0-DX*SLOP
              IF(PERF.GT.1.D0)PERF=1.D0
              IF(PERF.LT.0.D0)PERF=0.D0
              IFUL=0
              IF(PERF.GE.1.D0)IFUL=1
          ELSE
C FIND EQUIL. STATE IN PARTIAL FILL REGION
            IF(DABS(P1/PO).LE.0.001D0.AND.DX.GE.0.D0)GOTO 4601
            IF(DABS(DX).LE.0.00001D0.AND.P1.GE.0.D0)GOTO 4601
          IF(PERF.LT.0.001D0.AND.DX.GT.0.D0.AND.P1.GE.0.D0)GOTO 4601
C          IF(PERF.LT.0.01D0.AND.MNQQ.GE.15)GOTO 4601
            SPERF=PERF
            CPF=DX*SLOP
            IF(ABS(DX).LT.0.01D0)CPF=CPF/4.D0
            IF(P1.LT.0.D0.OR.ICHAG.EQ.1)CPF=P1/PO*SLOP1
              IF(MNQQ.GE.15)CPF=CPF/2.D0
              IF(MNQQ.GE.35)CPF=CPF/2.D0
            PERF=PERF-CPF
              IF(PERF.GT.1.D0)PERF=1.D0
              IF(PERF.LT.0.D0)PERF=0.D0
              IFUL=0
              IF(PERF.GE.1.D0)IFUL=1
            IF(P.LT.0.D0.AND.DX.GT.0.D0)ICHAG=1
            IF(PERF.LT.0.003D0)PERF=0.D0
          END IF
        END IF
 4600 CONTINUE
      PERF=SPERF
 4601 CONTINUE
C
      RETURN
      END
C
C
C
C     SUBROUTINE INPUT
C     ****************
C     THIS SUBROUTINE READS THE INPUT FOR THE PROGRAM
C     AND COMPARES ARRAY REQUIREMENTS WITH AVAILABLE STORAGE
C
      SUBROUTINE INPUT()
C
      IMPLICIT DOUBLE PRECISION (A-H,O-Z)
      INTEGER*4 IWAIT,IW2
      CHARACTER*1 YN
C
      COMMON/FLG1/IPGM,ISS,IMAC,IRTR,IOUT,ITQSTT,IOPUT(6),ICES,IFUL,ICOM
      COMMON/FLG2/IT,INTS,IV,IVST,IVR,IVAR(4),MNQQ,ICS,ICLC
      COMMON/GEO1/RO,RI,RINERT,BRI,BRO,BSI,BSO,ZR,ZS,BT,FFAC,BFAC
      COMMON/GEO2/PI,RHO,ARHO,PO,RC,RM,VF,ENGINT,CYLN,FNN,SHSTFF
      COMMON/RUN1/RTFI,RTCR,PFIN,PFFI,PFCR
      COMMON/RUN2/CPIN,CPFI,CPCR,CPT,SMIN,SMAX,SICR,ST
```

```
      COMMON/RUN3/QIIN,QIFI,QICR,QIT,TQIN,TQFI,TQCR,TQT
      COMMON/SCON/CES,AA,CLFS,CLV,SCL,CL,PBFAC,PFFAC,RTS,WRV
      COMMON/VAR1/PERF,RCO,RCI,DYNERT,QIN,CP,P1,DP,QOUT
      COMMON/VAR2/W,WP,WE,THETA1,THETA2,DELTA,ACH2O,ACRTR,ACENG
      COMMON/VAR3/TOR,POW,ETOR,EPOW,EPHI,DDTDEL,DDTPF
      COMMON/ARR1/TQFAC(6),PIFAC(3),PLOSS(3),TQCMPT(6),SPRES(26)
C
C     SET UP SCREEN
C
      PRINT *,'  ################################################'
      PRINT *,'  ################################################'
      PRINT *,'  ##                                            ##'
      PRINT *,'  ##  DDDDDDD   YY      YY NNN      NN RRRRRR    ##'
      PRINT *,'  ##   DD    DD  YY    YY  NNNN     NN RR    RR   ##'
      PRINT *,'  ##   DD     DD  YY  YY   NN NN    NN RR     RR  ##'
      PRINT *,'  ##   DD     DD   YYYY    NN  NN   NN RR    RR   ##'
      PRINT *,'  ##   DD     DD    YY     NN   NN  NN RRRRRR     ##'
      PRINT *,'  ##   DD     DD    YY     NN    NN NN RRRR       ##'
      PRINT *,'  ##   DD     DD  YY       NN     NN NN RR RR     ##'
      PRINT *,'  ##   DD    DD  YY        NN      NNN RR   RR    ##'
      PRINT *,'  ##  DDDDDDD   YY         NN       NN RR     RR  ##'
      PRINT *,'  ##                                            ##'
      PRINT *,'  ##        COPYRIGHT 1989 P.G. HODGSON         ##'
      PRINT *,'  ##                                            ##'
      PRINT *,'  ################################################'
      PRINT *,'  ################################################'
      PRINT *,'                                                  '
      PRINT *,'       TORQUE/POWER vs. SPEED CHARACTERISTIC FOR  '
      PRINT *,'                                                  '
      PRINT *,'          PARTIAL-FILL HYDRAULIC DYNAMOMETRS      '
      PRINT *,'                                                  '
      PRINT *,'               PROGRAM VERSION 1.0                '
      PRINT *,'                 DATE:  JULY 1989                 '
      PRINT *,'               AUTHOR: P.G. HODGSON               '
      PRINT *,'             UNIVERSITY OF CANTERBURY             '
C
C     INPUT DATA
C
 2010 CONTINUE
      WRITE(*,2020)
      WRITE(*,2022)
      WRITE(*,2024)
      WRITE(*,2026)
 2020 FORMAT(/' ENTER PROGRAM OPTION:  DYNAMIC            STATIC')
 2022 FORMAT('                        1=INPUT TORQUE     8=CONST. PERF')
 2024 FORMAT('                        2=INPUT SPEED      9=QIN=QOUT')
 2026 FORMAT('                        3=INPUT POWER LAW')
      READ(*,*)IPGM
      IF(IPGM.LT.1.OR.IPGM.GT.9)GOTO 2010
      IF(IPGM.GT.3.AND.IPGM.LT.8)GOTO 2010
      IF(IPGM.LE.5)THEN
        WRITE(*,2028)
 2028   FORMAT(' INCLUDE SHAFT STIFFNESS ? [Y] or N ')
        YN='Y'
        READ(*,'(A1)')YN
        ISS=1
        IF(YN.EQ.'N')ISS=0
      END IF
C
      WRITE(*,2030)
 2030 FORMAT(/' CHOOSE MACHINE TYPE'/' OR MANUAL DATA ENTRY:'T24'1-F020'
     1/T24'2-F020 AV'/T24'3-F020 CR'/T24'4-F24'/T24'5-F24 AV'/T24'6-F24
     2CR'/T24'7-F35'/T24'50-MANUAL')
      READ(*,*)IMAC
      IF(IMAC.GE.50)THEN
        WRITE(*,2032)
        WRITE(*,2034)
 2032   FORMAT(/' ENTER ROTOR TYPE: 0=FULL BLADED ROTOR')
 2034   FORMAT(T20'1=90deg. CROPPED ROTOR')
        READ(*,*)IRTR
        IF(IRTR.NE.1)IRTR=0
C
        WRITE(*,2036)
 2036   FORMAT(/' GEOMETRIC PARAMETERS'/' ********************')
        WRITE(*,2038)
 2038 FORMAT(/' ENTER RO,RI,BRI,BRO,BSI,BSO,ZR,ZS,BT,INERTIA,FFAC,BFAC')
        READ(*,*)RO,RI,BRI,BRO,BSI,BSO,ZR,ZS,BT,RINERT,FFAC,BFAC
      ELSE
      IF(IMAC.EQ.1)OPEN(7,FILE='[HODGSON.DATAA]F020.DAT',STATUS='OLD')
```

```
      IF(IMAC.EQ.2)OPEN(7,FILE='[HODGSON.DATAA]F020AV.DAT',STATUS='OLD')
      IF(IMAC.EQ.3)OPEN(7,FILE='[HODGSON.DATAA]F020CR.DAT',STATUS='OLD')
      IF(IMAC.EQ.4)OPEN(7,FILE='[HODGSON.DATAA]F24.DAT',STATUS='OLD')
      IF(IMAC.EQ.5)OPEN(7,FILE='[HODGSON.DATAA]F24AV.DAT',STATUS='OLD')
      IF(IMAC.EQ.6)OPEN(7,FILE='[HODGSON.DATAA]F24CR.DAT',STATUS='OLD')
      IF(IMAC.EQ.7)OPEN(7,FILE='[HODGSON.DATAA]F35.DAT',STATUS='OLD')
      IF(IMAC.EQ.8)OPEN(7,FILE='[HODGSON.DATAA]F35AV.DAT',STATUS='OLD')
        READ(7,*)RO,RI,BRI,BRO,BSI,BSO,ZR,ZS,BT,IRTR,RINERT,FFAC,BFAC
        CLOSE(7)
      END IF
        WRITE(*,2039)
 2039 FORMAT(/' ENTER ** ENGINE INERTIA ** ')
        READ(*,*)ENGINT
C
      WRITE(*,2040)
      WRITE(*,2042)
 2040 FORMAT(/' ENTER WATER OUTLET POSITION: 0=ROTOR CUP')
 2042 FORMAT(T31'1=TOP OF WORKING CMPT.'/T31'2=STATOR CUP')
      READ(*,*)IOUT
      IF(IOUT.NE.1.AND.IOUT.NE.2)IOUT=0
C
      PRINT *,'ENTER No. OF ENG CYLINDERS & FLUCTUATION AMPLITUDE'
      READ(*,*)CYLN,FNN
C      ENGINT=0.3D0
C      IF(CYLN.EQ.4.D0)ENGINT=0.2D0
C      IF(CYLN.EQ.2.D0)ENGINT=0.12D0
C      IF(CYLN.EQ.1.D0)ENGINT=0.08D0
C
 2049 WRITE(*,2050)
 2050 FORMAT(/' RUN PARAMETERS'/' **************')
      IF(IPGM.LE.5)THEN
        WRITE(*,2052)
 2052   FORMAT(/' RUN LENGTH (SEC), STEP LENGTH (SEC)')
        READ(*,*)RTFI,RTCR
      ELSE
        WRITE(*,2054)
 2054   FORMAT(/' MIN. SPEED, MAX. SPEED, INCREMENT (rpm)')
        READ(*,*)SMIN,SMAX,SICR
      END IF
C
C     CHECK NUMBER OF TIME/SPEED STEPS
C
      YN='Y'
      IF(IPGM.LE.5)INTS=IDNINT(RTFI/RTCR)+1
      IF(IPGM.GT.5)INTS=IDNINT((SMAX-SMIN)/SICR)+1
      IF(INTS.GT.100)THEN
        WRITE(*,2056)
        WRITE(*,2058)
 2056   FORMAT(T6'***MORE THAN 100 TIME/SPEED STEPS***')
 2058   FORMAT(T6'     IS THIS OKAY ?  [Y] or N')
        READ(*,'(A1)')YN
      END IF
      IF(YN.EQ.'N')GOTO 2049
C
      WRITE(*,2060)
 2060 FORMAT(/' M/C INPUT VALUES'/' ****************')
C
      IF(IPGM.LE.5)THEN
C
C     DYNAMIC CASE
C
        WRITE(*,2070)
        WRITE(*,2072)
 2070   FORMAT(/' ENTER TYPES OF RUN TIME CHANGES')
 2072   FORMAT(T8'(1)-NO CHANGE    (2)-STEP CHANGE'/T8'(3)-RAMP CHANGE
     3(4)-PROGRAM DEFINED FUNCTION')
        WRITE(*,2074)
 2074   FORMAT('  VALVE CLOSURE')
        READ(*,*)IVAR(1)
        WRITE(*,2076)
 2076   FORMAT('  QIN')
        READ(*,*)IVAR(3)
          WRITE(*,2078)
 2078     FORMAT('  DEMAND TORQUE')
          READ(*,*)IVAR(4)
        IF(IPGM.EQ.2)THEN
          WRITE(*,2082)
 2082     FORMAT('  SPEED')
          READ(*,*)IVAR(2)
```

```
      END IF
        WRITE(*,2080)
 2080   FORMAT(/' ENTER 1 TO DEFINE TORQUE & SPEED START POINT')
        READ(*,*)ITQSTT
      DO 2100 K=1,4
         IF(IVAR(K).LT.2.OR.IVAR(K).GT.4)IVAR(K)=1
 2100 CONTINUE
C
      IF(ITQSTT.NE.1)WRITE(*,2110)
      IF(ITQSTT.EQ.1)WRITE(*,2112)
 2110 FORMAT(/' INITIAL VALVE CLOSURE')
 2112 FORMAT(/' APPROXIMATE INITIAL VALVE CLOSURE')
      READ(*,*)CPIN
      IF(IVAR(1).NE.1)THEN
        WRITE(*,2114)
 2114   FORMAT(' FINAL VALVE CLOSURE')
        READ(*,*)CPFI
        IF(IVAR(1).EQ.3)THEN
          WRITE(*,2116)
 2116     FORMAT(' RATE OF RAMP INCREASE PER SECOND')
          READ(*,*)CPCR
        END IF
        WRITE(*,2118)
 2118   FORMAT(' TIME OF CHANGE (SEC)')
        READ(*,*)CPT
      END IF
      WRITE(*,2120)
 2120 FORMAT(/' INITIAL SPEED (RPM)')
      READ(*,*)SMIN
      IF(IVAR(2).NE.1.AND.IPGM.EQ.2)THEN
        WRITE(*,2122)
 2122   FORMAT(' FINAL SPEED (RPM)')
        READ(*,*)SMAX
        IF(IVAR(2).EQ.3)THEN
          WRITE(*,2116)
          READ(*,*)SICR
        END IF
        WRITE(*,2118)
        READ(*,*)ST
      END IF
      WRITE(*,2130)
 2130 FORMAT(/' INITIAL WATER INFLOW RATE (M3/SEC)')
      READ(*,*)QIIN
      IF(IVAR(3).NE.1)THEN
        WRITE(*,2132)
 2132   FORMAT(' FINAL WATER INFLOW RATE (M3/SEC)')
        READ(*,*)QIFI
        IF(IVAR(3).EQ.3)THEN
          WRITE(*,2116)
          READ(*,*)QICR
        END IF
        WRITE(*,2118)
        READ(*,*)QIT
      END IF
        WRITE(*,2140)
 2140   FORMAT(/' INITIAL DEMAND TORQUE (Nm)')
        READ(*,*)TQIN
        IF(IVAR(4).NE.1)THEN
          WRITE(*,2142)
 2142     FORMAT(' FINAL DEMAND TORQUE (Nm)')
          READ(*,*)TQFI
          IF(IVAR(4).EQ.3)THEN
            WRITE(*,2116)
            READ(*,*)TQCR
          END IF
          WRITE(*,2118)
          READ(*,*)TQT
        END IF
      IF(ITQSTT.NE.1)WRITE(*,2150)
      IF(ITQSTT.EQ.1)WRITE(*,2152)
 2150 FORMAT(/' INITIAL PERCENTAGE WATER FILL')
 2152 FORMAT(/' APPROXIMATE INITIAL PERCENTAGE WATER FILL')
      READ(*,*)PFIN
    ELSE
C
C     STATIC CASE
C
 2159 WRITE(*,2160)
 2160 FORMAT(/' ENTER VARIATION REQUIRED'/T8'(0)-NONE'/T8'(1)-VALVE CLOS
```

```
     4URE'/T8'(2)-PERCENTAGE FILL'/T8'(3)-QIN')
        READ(*,*)IVR
        IF(IVR.NE.1.AND.IVR.NE.2.AND.IVR.NE.3)IVR=0
C
 2161   CONTINUE
        IF(IPGM.EQ.9)THEN
          PFIN=100.0
          IF(IVR.EQ.0.OR.IVR.EQ.2)THEN
            WRITE(*,2162)
 2162       FORMAT(/' ENTER: CP,QIN')
            READ(*,*)CPIN,QIIN
          ELSE
            IF(IVR.EQ.1)THEN
              WRITE(*,2164)
 2164         FORMAT(' ENTER CPMIN,CPMAX,CPICR,QIN')
              READ(*,*)CPIN,CPFI,CPCR,QIIN
            END IF
            IF(IVR.EQ.3)THEN
              WRITE(*,2166)
 2166         FORMAT(' ENTER: QINMIN,QINMAX,QINICR,CP')
              READ(*,*)QIIN,QIFI,QICR,CPIN
            END IF
          END IF
        ELSE
          IF(IVR.NE.2)THEN
            WRITE(*,2170)
 2170       FORMAT(/' ENTER: PERF,QIN')
            READ(*,*)PFIN,QIIN
          ELSE
            WRITE(*,2172)
 2172       FORMAT(' ENTER: PERFMIN,PERFMAX,PERFICR,QIN')
            READ(*,*)PFIN,PFFI,PFCR,QIIN
          END IF
        END IF
        YN='Y'
        IF(IVR.NE.0)THEN
          IF(IVR.EQ.1)IVST=IDNINT((CPFI-CPIN)/CPCR)+1
          IF(IVR.EQ.2)IVST=IDNINT((PFFI-PFIN)/PFCR)+1
          IF(IVR.EQ.3)IVST=IDNINT((QIFI-QIIN)/QICR)+1
          IF(IVST.GT.10)THEN
            WRITE(*,2174)
            WRITE(*,2058)
 2174       FORMAT(T6'***MORE THAN 10 VARIATION STEPS***')
            READ(*,'(A1)')YN
          END IF
        ELSE
          IVST=1
        END IF
        IF(YN.EQ.'N')GOTO 2159
      END IF
C
C     OUTPUT REQUIRED
C
      WRITE(*,2180)
      WRITE(*,2182)
      WRITE(*,2184)
 2180 FORMAT(/T6' ENTER REQUIRED OUTPUT')
 2182 FORMAT(T6' 0 IF OUTPUT NOT REQD. (#,#,#,#,#,# IN ORDER)')
 2184 FORMAT(T6' RESULTS,INTERMEDIATE,COMPONENTS,FACTORS,PRESS. DISTR.')
      READ(*,*)(IOPUT(K),K=1,5)
C
C     PLOTTING REQUIRED
C
      WRITE(*,2186)
 2186 FORMAT(/T6' ENTER 1 IF RESULTS PLOTTING FILE REQUIRED')
      READ(*,*)IOPUT(6)
C
      PRINT *,' *****INPUT COMPLETE * PROGRAM RUNNING*****'
      PRINT *,' *****INPUT COMPLETE * PROGRAM RUNNING*****'
      PRINT *,' *****INPUT COMPLETE * PROGRAM RUNNING*****'
C
      RETURN
      END
C
C
C
C
C
C     SUBROUTINE OUTPUT
```

```
C     *****************
C     THIS SUBROUTINE OUTPUTS THE INPUT, RESULTS, &/OR INTERMEDIATE
C     VALUES TO THE SCREEN & PRINTER IF REQUIRED
C
      SUBROUTINE OUTPUT()
C
      IMPLICIT DOUBLE PRECISION (A-H,O-Z)
C
      CHARACTER*6 CTYP
      CHARACTER CNO*10,CSTEP*12,CRAMP*12,CFUNC*32,CRATE*21,CTIME*22
      DATA CNO/'NO CHANGE'/,CSTEP/'STEP CHANGE'/,CRAMP/'RAMP CHANGE'/
      DATA CFUNC/'PROGRAM DEFINED FUNCTION CHANGE'/
      DATA CRATE/'RATE OF INCREASE'/,CTIME/'CHANGE OCCURS AT'/
C
      COMMON/FLG1/IPGM,ISS,IMAC,IRTR,IOUT,ITQSTT,IOPUT(6),ICES,IFUL,ICOM
      COMMON/FLG2/IT,INTS,IV,IVST,IVR,IVAR(4),MNQQ,ICS,ICLC
      COMMON/GEO1/RO,RI,RINERT,BRI,BRO,BSI,BSO,ZR,ZS,BT,FFAC,BFAC
      COMMON/GEO2/PI,RHO,ARHO,PO,RC,RM,VF,ENGINT,CYLN,FNN,SHSTFF
      COMMON/RUN1/RTFI,RTCR,PFIN,PFFI,PFCR
      COMMON/RUN2/CPIN,CPFI,CPCR,CPT,SMIN,SMAX,SICR,ST
      COMMON/RUN3/QIIN,QIFI,QICR,QIT,TQIN,TQFI,TQCR,TQT
      COMMON/SCON/CES,AA,CLFS,CLV,SCL,CL,PBFAC,PFFAC,RTS,WRV
      COMMON/VAR1/PERF,RCO,RCI,DYNERT,QIN,CP,P1,DP,QOUT
      COMMON/VAR2/W,WP,WE,THETA1,THETA2,DELTA,ACH2O,ACRTR,ACENG
      COMMON/VAR3/TOR,POW,ETOR,EPOW,EPHI,DDTDEL,DDTPF
      COMMON/ARR1/TQFAC(6),PIFAC(3),PLOSS(3),TQCMPT(6),SPRES(26)
C
C     CONVERT ANGLES,SPEEDS,VALVE CLOSURE,PERF FOR PRINTING OR PLOTTING
C
      BRI=180.D0/PI*BRI
      BRO=180.D0/PI*BRO
      BSI=180.D0/PI*BSI
      BSO=180.D0/PI*BSO
      CPIN=CPIN*100.D0
      CPFI=CPFI*100.D0
      CPCR=CPCR*100.D0
      SMIN=SMIN/PI*30.D0
      SMAX=SMAX/PI*30.D0
      SICR=SICR/PI*30.D0
      PFIN=PFIN*100.D0
      PFFI=PFFI*100.D0
      PFCR=PFCR*100.D0
C
C     CHECK IF OUTPUT REQUIRED
C
      IT=IOPUT(1)+IOPUT(2)+IOPUT(3)+IOPUT(4)+IOPUT(5)+IOPUT(6)
      IF(IT.EQ.0)RETURN
C
C     TITLE  &  WARNINGS
C
C      GOTO 5533
        WRITE(6,3001)
        WRITE(6,3002)
        WRITE(6,3003)
        WRITE(6,3004)
        WRITE(6,3005)
        WRITE(6,3006)
        WRITE(6,3007)
        WRITE(6,3008)
        WRITE(6,3009)
        WRITE(6,3010)
        WRITE(6,3011)
        WRITE(6,3012)
        WRITE(6,3013)
        WRITE(6,3014)
        WRITE(6,3015)
        WRITE(6,3016)
        WRITE(6,3017)
        WRITE(6,3018)
        WRITE(6,3019)
        WRITE(6,3020)
        WRITE(6,3021)
        WRITE(6,3022)
        WRITE(6,3023)
        WRITE(6,3024)
        WRITE(6,3025)
        WRITE(6,3026)
 5533 CONTINUE
      IF(IPGM.LE.5)THEN
```

```
        WRITE(6,3030)
        IF(IPGM.EQ.1)WRITE(6,3032)
        IF(IPGM.EQ.2)WRITE(6,3034)
        IF(IPGM.EQ.3)WRITE(6,3036)
        IF(ISS.NE.1)WRITE(6,3037)
        IF(ISS.EQ.1)WRITE(6,3038)
      ELSE
        WRITE(6,3040)
        IF(IPGM.EQ.8)WRITE(6,3042)
        IF(IPGM.EQ.9)WRITE(6,3044)
      END IF
      IF(IMAC.EQ.1)CTYP='  F020'
      IF(IMAC.EQ.2)CTYP='F020AV'
      IF(IMAC.EQ.3)CTYP='F020CR'
      IF(IMAC.EQ.4)CTYP='   F24'
      IF(IMAC.EQ.5)CTYP=' F24AV'
      IF(IMAC.EQ.6)CTYP=' F24CR'
      IF(IMAC.EQ.7)CTYP='   F35'
      IF(IMAC.EQ.8)CTYP=' F35AV'
      WRITE(6,3050)CTYP
      IF(IRTR.EQ.0)WRITE(6,3052)
      IF(IRTR.EQ.1)WRITE(6,3054)
      IF(IOUT.EQ.0)WRITE(6,3056)
      IF(IOUT.EQ.1)WRITE(6,3058)
      IF(IOUT.EQ.2)WRITE(6,3060)
C
      LPRD=38
C      LPRD=20
C
C
      IF(ICOM.EQ.1)THEN
        WRITE(*,3019)
        WRITE(*,3021)
        WRITE(*,3066)
        WRITE(*,3066)
        WRITE(*,3066)
        WRITE(6,3066)
        WRITE(6,3066)
        WRITE(6,3066)
        LPRD=42
      END IF
C
C     TITLE FORMATS
C
 3001 FORMAT('  ##################################################')
 3002 FORMAT('  ##################################################')
 3003 FORMAT('  ##                                              ##')
 3004 FORMAT('  ##  DDDDDDD   YY      YY NNN       NN RRRRRR    ##')
 3005 FORMAT('  ##   DD    DD  YY    YY  NNNN      NN RR    RR   ##')
 3006 FORMAT('  ##   DD     DD  YY  YY   NN NN     NN RR     RR  ##')
 3007 FORMAT('  ##   DD     DD   YYYY    NN  NN    NN RR    RR   ##')
 3008 FORMAT('  ##   DD     DD    YY     NN   NN   NN RRRRRR     ##')
 3009 FORMAT('  ##   DD     DD   YY      NN    NN  NN RRRR       ##')
 3010 FORMAT('  ##   DD     DD  YY       NN     NN NN RR RR      ##')
 3011 FORMAT('  ##   DD    DD  YY        NN      NNNN RR   RR    ##')
 3012 FORMAT('  ##  DDDDDDD   YY         NN       NNN RR     RR  ##')
 3013 FORMAT('  ##                                              ##')
 3014 FORMAT('  ##        COPYRIGHT 1989 P.G. HODGSON           ##')
 3015 FORMAT('  ##                                              ##')
 3016 FORMAT('  ##################################################')
 3017 FORMAT('  ##################################################')
 3018 FORMAT('                                                   ')
 3019 FORMAT('       TORQUE/POWER vs. SPEED CHARACTERISTIC FOR   ')
 3020 FORMAT('                                                   ')
 3021 FORMAT('          PARTIAL-FILL HYDRAULIC DYNAMOMETRS       ')
 3022 FORMAT('                                                   ')
 3023 FORMAT('                PROGRAM VERSION 1.0                ')
 3024 FORMAT('                  DATE:  JULY 1989                 ')
 3025 FORMAT('                AUTHOR: P.G. HODGSON               ')
 3026 FORMAT('              UNIVERSITY OF CANTERBURY             ')
 3030 FORMAT(//T4'DYNAMIC          DYNAMIC          DYNAMIC')
 3032 FORMAT(' INPUT TORQUE     INPUT TORQUE     INPUT TORQUE')
 3034 FORMAT(' INPUT SPEED      INPUT SPEED      INPUT SPEED')
 3036 FORMAT(' INPUT POWER LAW  INPUT POWER LAW  INPUT POWER LAW ')
 3037 FORMAT(/' SHAFT STIFFNESS NOT INCLUDED')
 3038 FORMAT(/' SHAFT STIFFNESS INCLUDED')
 3040 FORMAT(//T4' STATIC            STATIC            STATIC')
 3042 FORMAT(' CONST PERF LINE   CONST PERF LINE    CONST PERF LINE')
 3044 FORMAT('  QIN=QOUT LINE     QIN=QOUT LINE      QIN=QOUT LINE')
```

```
 3050 FORMAT(//' MACHINE:  ',A6,/' ################')
 3052 FORMAT(' FULL BLADED ROTOR')
 3054 FORMAT(' 90deg CROPPED ROTOR')
 3056 FORMAT(' ROTOR CUP WATER OUTLET')
 3058 FORMAT(' TOP OF CMPT. WATER OUTLET')
 3060 FORMAT(' STATOR CUP WATER OUTLET')
 3066 FORMAT(/' *****-SOME VELOCITIES ARE COMPLEX-*****')
C
C     OUTPUT INPUT DATA
C
      WRITE(6,3070)
      WRITE(6,3072)RO,RI,RINERT
      WRITE(6,3074)BRI,BRO,ZR,BT
      WRITE(6,3076)BSI,BSO,ZS,BT
      IF(IPGM.LE.5)WRITE(6,3078)ENGINT,SHSTFF
      IF(IPGM.LE.5)WRITE(6,3079)CYLN,FNN
      WRITE(6,3080)FFAC,BFAC
      WRITE(6,3082)
      IF(IPGM.LE.5)WRITE(6,3084)RTFI,RTCR
      IF(IPGM.GT.5)WRITE(6,3086)SMIN,SMAX,SICR
      WRITE(6,3088)
      LPRD=LPRD+14
      IF(IPGM.LE.5)LPRD=LPRD+1
      IF(IPGM.LE.5)THEN
        WRITE(6,3090)CPIN
        IF(IVAR(1).EQ.1)THEN
          WRITE(6,3092)CNO
        ELSE
          IF(IVAR(1).EQ.2)WRITE(6,3094)CSTEP,CPFI
          IF(IVAR(1).EQ.3)WRITE(6,3094)CRAMP,CPFI
          IF(IVAR(1).EQ.3)WRITE(6,3096)CRATE,CPCR
          IF(IVAR(1).EQ.4)WRITE(6,3098)CFUNC,CPFI
          WRITE(6,3102)CTIME,CPT
        END IF
        WRITE(6,3104)SMIN
        IF(IPGM.EQ.2)THEN
        IF(IVAR(2).EQ.1)THEN
          WRITE(6,3092)CNO
        ELSE
          IF(IVAR(2).EQ.2)WRITE(6,3106)CSTEP,SMAX
          IF(IVAR(2).EQ.3)WRITE(6,3106)CRAMP,SMAX
          IF(IVAR(2).EQ.3)WRITE(6,3108)CRATE,SICR
          IF(IVAR(2).EQ.4)WRITE(6,3110)CFUNC,SMAX
          WRITE(6,3102)CTIME,ST
        END IF
        END IF
        WRITE(6,3112)QIIN
        IF(IVAR(3).EQ.1)THEN
          WRITE(6,3092)CNO
        ELSE
          IF(IVAR(3).EQ.2)WRITE(6,3114)CSTEP,QIFI
          IF(IVAR(3).EQ.3)WRITE(6,3114)CRAMP,QIFI
          IF(IVAR(3).EQ.3)WRITE(6,3116)CRATE,QICR
          IF(IVAR(3).EQ.4)WRITE(6,3118)CFUNC,QIFI
          WRITE(6,3102)CTIME,QIT
        END IF
          WRITE(6,3120)TQIN
        IF(IVAR(4).EQ.1)THEN
          WRITE(6,3092)CNO
        ELSE
          IF(IVAR(4).EQ.2)WRITE(6,3122)CSTEP,TQFI
          IF(IVAR(4).EQ.3)WRITE(6,3122)CRAMP,TQFI
          IF(IVAR(4).EQ.3)WRITE(6,3124)CRATE,TQCR
          IF(IVAR(4).EQ.4)WRITE(6,3126)CFUNC,TQFI
          WRITE(6,3102)CTIME,TQT
        END IF
        WRITE(6,3128)PFIN
        LPRD=LPRD+5+IVAR(1)+IVAR(2)+IVAR(3)+IVAR(4)
      ELSE
        IF(IVR.EQ.0)THEN
          WRITE(6,3090)CPIN
          WRITE(6,3128)PFIN
          WRITE(6,3112)QIIN
        END IF
        IF(IVR.EQ.1)THEN
          WRITE(6,3090)CPIN
          WRITE(6,3130)CPFI,CPCR
          WRITE(6,3128)PFIN
          WRITE(6,3112)QIIN
```

```
        END IF
        IF(IVR.EQ.2)THEN
          WRITE(6,3128)PFIN
          WRITE(6,3130)PFFI,PFCR
          WRITE(6,3090)CPIN
          WRITE(6,3112)QIIN
        END IF
        IF(IVR.EQ.3)THEN
          WRITE(6,3112)QIIN
          WRITE(6,3132)QIFI,QICR
          WRITE(6,3090)CPIN
          WRITE(6,3128)PFIN
        END IF
        LPRD=LPRD+3
        IF(IVR.GT.0)LPRD=LPRD+1
      END IF
      IF(IOPUT(6).NE.0)THEN
        IMOD=1
        WRITE(2,3071)IMOD,IPGM,IMAC,IRTR,IOUT
        WRITE(2,3071)IVAR(1),IVAR(2),IVAR(3),IVAR(4),INTS
        WRITE(2,3073)RO,RI,RINERT,BRI,BRO,BSI,BSO,ZR,ZS,BT,FFAC,BFAC
        WRITE(2,3073)PI,RHO,PO,RC,RM,VF,ENGINT,CYLN,FNN,SHSTFF
        WRITE(2,3073)RTFI,RTCR,PFIN,PFFI,PFCR
        WRITE(2,3073)CPIN,CPFI,CPCR,CPT,SMIN,SMAX,SICR,ST
        WRITE(2,3073)QIIN,QIFI,QICR,QIT,TQIN,TQFI,TQCR,TQT
      END IF
 3071 FORMAT(10(I4,TR1))
 3073 FORMAT(12(E11.4,TR1))
C
C     INPUT DATA FORMATS
C
 3070 FORMAT(/' INPUT DATA'/' **********'//' GEOMETRIC:')
 3072 FORMAT(T6'OUTER RADIUS   ',F10.3,' mm   INNER RADIUS   ',F10.3,' m
     1m    INERTIA   ',E11.4,' kgm2')
 3074 FORMAT(T6'ROTOR  BLADES: INLET ',F7.2,' deg   OUTLET ',F7.2,' deg
     2   No. ',F5.1,'   THICKNESS ',F10.3,' mm')
 3076 FORMAT(T6'STATOR BLADES: INLET ',F7.2,' deg   OUTLET ',F7.2,' deg
     3   No. ',F5.1,'   THICKNESS ',F10.3,' mm')
 3078 FORMAT(T6'ENG INERTIA ',E11.4,' kgm2  SHAFT STIFF ',E11.4,' Nm')
 3079 FORMAT(T6'No. OF CYLINDERS ',F5.1,' FLUCTUATION AMPLITUDE ',E11.4)
 3080 FORMAT(T6'FRICTION FACTOR ',E10.3,'   BEND LOSS FACTOR ',E10.3)
 3082 FORMAT(/' RUN TIME:')
 3084 FORMAT(T6'RUN LENGTH ',F8.3,' sec  IN STEPS OF',F8.3,' sec')
 3086 FORMAT(T6'FROM ',F10.2,' rpm  TO ',F10.2,' rpm  IN ',F10.2,' rpm
     4STEPS')
 3088 FORMAT(/' MACHINE INPUT:')
 3090 FORMAT(T6'VALVE CLOSURE INITIAL ',F7.2,' %')
 3092 FORMAT(T6,A10)
 3094 FORMAT(T6,A12,'TO'TR8,F7.2,' %')
 3096 FORMAT(T6,A21,' ',F8.3,' %/sec')
 3098 FORMAT(T6,A32,'TO ',F7.2,' %')
 3102 FORMAT(T6,A22,F8.3,' sec')
 3104 FORMAT(T6'INPUT SPEED INITIAL',F10.2,' rpm')
 3106 FORMAT(T6,A12,'TO'TR5,F10.2,' rpm')
 3108 FORMAT(T6,A20,F11.3,' rpm/sec')
 3110 FORMAT(T6,A32,'TO ',F10.2,' rpm')
 3112 FORMAT(T6'WATER INFLOW INITIAL ',E11.4,' m3/sec')
 3114 FORMAT(T6,A12,'TO ',E11.4,' m3/sec')
 3116 FORMAT(T6,A21,E12.5,' m3/sec/sec')
 3118 FORMAT(T6,A32,'TO ',E11.4,' m3/sec')
 3120 FORMAT(T6'DEMAND TORQUE INITIAL',E11.4,' Nm')
 3122 FORMAT(T6,A12,'TO'TR7,E11.4,' Nm')
 3124 FORMAT(T6,A20,E12.5,' Nm/sec')
 3126 FORMAT(T6,A32,'TO ',E11.4,' Nm')
 3128 FORMAT(T6'WATER PERCENTAGE FILL INITIAL ',F7.2,' %')
 3130 FORMAT(T6'VARIES TO ',F7.2,' %  IN STEPS OF ',F7.2,' %')
 3132 FORMAT(T6'VARIES TO ',E11.4,' m3/s  IN STEPS OF ',E11.4,' m3/s')
C
      IF(LPRD.GE.58)THEN
        LPRD=LPRD-58
      ELSE
        LP=57-LPRD
        DO 3850 I=1,LP
          WRITE(6,3135)
 3135     FORMAT(' ')
 3850   CONTINUE
        LPRD=-1
      END IF
C
```

```
C     OUTPUT RESULTS
C
      IF(IPGM.LE.5)IVST=1
C
      IF(IOPUT(1).NE.0.OR.IOPUT(6).NE.0)THEN
        IV=1
        WRITE(6,3140)
        LPRD=LPRD+3
        REWIND(9)
        DO 3000 IV=1,IVST
          CALL HEAD(LPRD,54)
          IF(IPGM.LE.5)WRITE(6,3142)
          IF(IPGM.GT.5)WRITE(6,3144)
          LPRD=LPRD+2
          DO 3100 IT=1,INTS
            READ(9)SCL,CL,PBFAC,PFFAC,RTS,WRV
            READ(9)PERF,RCO,RCI,DYNERT,QIN,CP,P1,DP,QOUT
            READ(9)W,WP,WE,THETA1,THETA2,DELTA,ACH2O,ACRTR,ACENG
            READ(9)TOR,POW,ETOR,EPOW,EPHI,DDTDEL,DDTPF
            READ(9)(TQFAC(K),K=1,6),(PIFAC(K),K=1,3)
          READ(9)(PLOSS(K),K=1,3),(TQCMPT(K),K=1,6),(SPRES(K),K=1,26)
            TIME=RTCR*DFLOAT(IT-1)
            WP=WP/PI*30.D0
            POW=POW/1.D3
            P1=P1/1.D3
            DP=DP/1.D3
            CP=CP*100.D0
            PERF=PERF*100.D0
            IF(LPRD.EQ.58)THEN
              IF(IPGM.LE.5)WRITE(6,3142)
              IF(IPGM.GT.5)WRITE(6,3144)
              LPRD=2
            END IF
        IF(IPGM.LE.5)WRITE(6,3146)TIME,WP,TOR,POW,W,PERF,CP,P1,DP,QOUT,QIN
        IF(IPGM.GT.5)WRITE(6,3148)WP,TOR,POW,W,PERF,CP,P1,DP
              IF(IOPUT(6).NE.0)THEN
                 WE=WE/PI*30.D0
                 EPHI=EPHI*100.D0
                 EPOW=EPOW/1.D3
                 ACRTR=ACRTR/PI*30.D0
                 ACENG=ACENG/PI*30.D0
                 DDTPF=DDTPF*100.D0
                IF(IPGM.LE.5)THEN
       WRITE(2,3147)TIME,WP,TOR,POW,W,PERF,CP,P1,DP,QOUT,QIN,WE,EPHI,ETOR
     5             ,EPOW,DELTA,ACH2O,ACRTR,ACENG,DDTDEL,DDTPF
                 ELSE
                   WRITE(2,3147)WP,TOR,POW,W,PERF,CP,P1,DP
                END IF
              END IF
              LPRD=LPRD+1
 3100       CONTINUE
 3000     CONTINUE
          IF(IPGM.LE.5)THEN
            REWIND(9)
            CALL HEAD(LPRD,54)
            WRITE(6,3150)
            LPRD=LPRD+2
            DO 3200 IT=1,INTS
              READ(9)SCL,CL,PBFAC,PFFAC,RTS,WRV
              READ(9)PERF,RCO,RCI,DYNERT,QIN,CP,P1,DP,QOUT
              READ(9)W,WP,WE,THETA1,THETA2,DELTA,ACH2O,ACRTR,ACENG
              READ(9)TOR,POW,ETOR,EPOW,EPHI,DDTDEL,DDTPF
              READ(9)(TQFAC(K),K=1,6),(PIFAC(K),K=1,3)
            READ(9)(PLOSS(K),K=1,3),(TQCMPT(K),K=1,6),(SPRES(K),K=1,26)
              TIME=RTCR*DFLOAT(IT-1)
              WE=WE/PI*30.D0
              EPHI=EPHI*100.D0
              EPOW=EPOW/1.D3
              ACRTR=ACRTR/PI*30.D0
              ACENG=ACENG/PI*30.D0
              DDTPF=DDTPF*100.D0
              IF(LPRD.EQ.58)THEN
                WRITE(6,3150)
                LPRD=2
              END IF
       WRITE(6,3152)TIME,WE,EPHI,ETOR,EPOW,DELTA,ACH2O,ACRTR,ACENG,
     5              DDTDEL,DDTPF
              LPRD=LPRD+1
 3200       CONTINUE
```

```
        END IF
      END IF
C
C     RESULTS FORMATS
C
 3140 FORMAT(/' RESULTS'/' *******')
 3142 FORMAT(T5'TIME'T15'SPEED'T25'TORQUE'T37'POWER'T47'WATER VELO'T60'%
     6 FILL'T68'VALVE %'T77'CUP PRESS'T88'DRAIN PRESS'T104'QOUT'T116'QIN
     7'/T5'(sec)'T15'(rpm)'T26'(Nm)'T38'(kW)'T48'(rad/sec)'T79'(kPa)'T91
     8'(kPa)'T102'(m3/sec)'T114'(m3/sec)')
 3144 FORMAT(T15'SPEED'T26'TORQUE'T38'POWER'T48'WATER VELO'T60'% FILL'T6
     98'VALVE %'T77'CUP PRESS'T88'DRAIN PRESS'/T15'(rpm)'T27'(Nm)'T39'(k
     1W)'T49'(rad/sec)'T79'(kPa)'T91'(kPa)')
 3146 FORMAT(T2,F8.3,TR1,F10.2,3(TR1,E11.4),2(TR1,F8.3),4(TR1,E11.4))
 3147 FORMAT(8(E11.4,TR1))
 3148 FORMAT(T11,F10.2,3(TR1,E11.4),2(TR1,F8.3),2(TR1,E11.4))
 3150 FORMAT(/T5'TIME'T13'ENG SPEED'T23'ENG THROT'T33'ENG TORQ'T45'ENG P
     2OWR'T58'DELTA'T69'H2O ACCL'T80'DYNR ACCL'T92'ENG ACCL'T103'd/dt(DE
     3LTA)'T115'd/dt(% FILL)'/T5'(sec)'T15'(rpm)'T35'(Nm)'T47'(kW)'T69'(
     4rad/s2)'T81'(rpm/s)'T93'(rpm/s)')
 3152 FORMAT(T2,F8.3,TR1,F10.2,TR1,F8.3,8(TR1,E11.4))
C
C     OUTPUT INTERMEDIATE VALUES
C
      IF(IOPUT(2).NE.0)THEN
        IV=1
        CALL HEAD(LPRD,50)
        WRITE(6,3160)
        LPRD=LPRD+3
        REWIND(9)
        DO 3300 IV=1,IVST
          CALL HEAD(LPRD,54)
          WRITE(6,3162)
          WRITE(6,3164)
          LPRD=LPRD+2
          DO 3400 IT=1,INTS
            READ(9)SCL,CL,PBFAC,PFFAC,RTS,WRV
            READ(9)PERF,RCO,RCI,DYNERT,QIN,CP,P1,DP,QOUT
            READ(9)W,WP,WE,THETA1,THETA2,DELTA,ACH2O,ACRTR,ACENG
            READ(9)TOR,POW,ETOR,EPOW,EPHI,DDTDEL,DDTPF
            READ(9)(TQFAC(K),K=1,6),(PIFAC(K),K=1,3)
          READ(9)(PLOSS(K),K=1,3),(TQCMPT(K),K=1,6),(SPRES(K),K=1,26)
            WP=WP/PI*30.D0
            PERF=PERF*100.D0
            RRTS=RTS
            IF(RRTS.LT.1.D-10)RRTS=1.D-10
            RATIO=WRV/RRTS
            IF(LPRD.EQ.58)THEN
              WRITE(6,3162)
              WRITE(6,3164)
              LPRD=2
            END IF
            WRITE(6,3166)WP,PERF,RM,RCO,RCI,RTS,WRV,RATIO,DYNERT,SCL,CL
            LPRD=LPRD+1
 3400     CONTINUE
 3300   CONTINUE
      END IF
C
C     INTERMEDIATE VALUE FORMATS
C
 3160 FORMAT(/' INTERMEDIATE'/' ************')
 3162 FORMAT(T6'SPEED'T15'% FILL'T26'RM'T38'RCO'T50'RCI'T60'ROTOR TIP'T7
     63'H2O REL'T86'RATIO'T97'INERTIA'T110'SCL'T123'CL')
 3164 FORMAT(T6'(rpm)'T25'(mm)'T38'(mm)'T50'(mm)'T62'(m/s)'T74'(m/s)')
 3166 FORMAT(T2,F10.2,TR1,F8.3,9(TR1,E11.4))
C
C     OUTPUT COMPONENTS
C
      IF(IOPUT(3).NE.0)THEN
        IV=1
        CALL HEAD(LPRD,50)
        WRITE(6,3170)
        LPRD=LPRD+3
        REWIND(9)
        DO 3500 IV=1,IVST
          CALL HEAD(LPRD,54)
          WRITE(6,3172)
          WRITE(6,3174)
          LPRD=LPRD+2
```

```
          DO 3600 IT=1,INTS
            READ(9)SCL,CL,PBFAC,PFFAC,RTS,WRV
            READ(9)PERF,RCO,RCI,DYNERT,QIN,CP,P1,DP,QOUT
            READ(9)W,WP,WE,THETA1,THETA2,DELTA,ACH2O,ACRTR,ACENG
            READ(9)TOR,POW,ETOR,EPOW,EPHI,DDTDEL,DDTPF
            READ(9)(TQFAC(K),K=1,6),(PIFAC(K),K=1,3)
          READ(9)(PLOSS(K),K=1,3),(TQCMPT(K),K=1,6),(SPRES(K),K=1,26)
            WP=WP/PI*30.D0
            PERF=PERF*100.D0
            IF(LPRD.EQ.58)THEN
              WRITE(6,3172)
              WRITE(6,3174)
              LPRD=2
            END IF
            WRITE(6,3176)WP,PERF,(TQCMPT(K),K=1,6),(PLOSS(K),K=1,3)
            LPRD=LPRD+1
 3600     CONTINUE
 3500   CONTINUE
      END IF
C
C     COMPONENT VALUE FORMATS
C
 3170 FORMAT(/' COMPONENTS'/' **********')
 3172 FORMAT(T6'SPEED'T15'% FILL'T25'TQCMPT'T37'TQCMPT'T49'TQCMPT'T61'TQ
     7CMPT'T73'TQCMPT'T85'TQCMPT'T97'PLOSS'T109'PLOSS'T121'PLOSS')
 3174 FORMAT(T6'(rpm)'T26'WP*W'T38'W**2'T51'WP'T63'W'T72'd/dt(WP)'T85'd/
     8dt(W)'T97'(ICD)'T109'(FRC)'T121'(SEC)')
 3176 FORMAT(T2,F10.2,TR1,F8.3,9(TR1,E11.4))
C
C     OUTPUT FACTORS
C
      IF(IOPUT(4).NE.0)THEN
        IV=1
        CALL HEAD(LPRD,50)
        WRITE(6,3180)
        LPRD=LPRD+3
        REWIND(9)
        DO 3700 IV=1,IVST
          CALL HEAD(LPRD,54)
          WRITE(6,3182)
          WRITE(6,3184)
          LPRD=LPRD+2
          DO 3800 IT=1,INTS
            READ(9)SCL,CL,PBFAC,PFFAC,RTS,WRV
            READ(9)PERF,RCO,RCI,DYNERT,QIN,CP,P1,DP,QOUT
            READ(9)W,WP,WE,THETA1,THETA2,DELTA,ACH2O,ACRTR,ACENG
            READ(9)TOR,POW,ETOR,EPOW,EPHI,DDTDEL,DDTPF
            READ(9)(TQFAC(K),K=1,6),(PIFAC(K),K=1,3)
          READ(9)(PLOSS(K),K=1,3),(TQCMPT(K),K=1,6),(SPRES(K),K=1,26)
            WP=WP/PI*30.D0
            IF(LPRD.EQ.58)THEN
              WRITE(6,3182)
              WRITE(6,3184)
              LPRD=2
            END IF
      WRITE(6,3186)WP,(TQFAC(K),K=1,6),(PIFAC(K),K=1,3),PBFAC,PFFAC
            LPRD=LPRD+1
 3800     CONTINUE
 3700   CONTINUE
      END IF
C
C     FACTOR FORMATS
C
 3180 FORMAT(/' FACTORS'/' *******')
 3182 FORMAT(T6'SPEED'T16'TQFAC'T27'TQFAC'T38'TQFAC'T49'TQFAC'T60'TQFAC'
     9T71'TQFAC'T82'PIFAC'T93'PIFAC'T104'PIFAC'T115'PBFAC'T126'PFFAC')
 3184 FORMAT(T6'(rpm)'T16'WP*W'T27'W**2'T39'WP'T51'W'T59'd/dt(WP)'T70'd/
     1dt(W)'T81'W*WP**2'T92'WP*W**2'T104'W**3')
 3186 FORMAT(T2,F10.2,11(E11.4))
C
C     OUTPUT PRESSURE DISTRIBUTION
C
      IF(IOPUT(5).NE.0)THEN
        IV=1
        CALL HEAD(LPRD,45)
        WRITE(6,3190)
        LPRD=LPRD+3
        REWIND(9)
        DO 3900 IV=1,IVST
```

```
          DO 3950 IT=1,INTS
            READ(9)SCL,CL,PBFAC,PFFAC,RTS,WRV
            READ(9)PERF,RCO,RCI,DYNERT,QIN,CP,P1,DP,QOUT
            READ(9)W,WP,WE,THETA1,THETA2,DELTA,ACH2O,ACRTR,ACENG
            READ(9)TOR,POW,ETOR,EPOW,EPHI,DDTDEL,DDTPF
            READ(9)(TQFAC(K),K=1,6),(PIFAC(K),K=1,3)
          READ(9)(PLOSS(K),K=1,3),(TQCMPT(K),K=1,6),(SPRES(K),K=1,26)
            WP=WP/PI*30.D0
            PERF=PERF*100.D0
            DO 3975 I=1,26
              SPRES(I)=SPRES(I)/1.D3
 3975       CONTINUE
            CALL HEAD(LPRD,50)
            WRITE(6,3192)IT,WP,PERF
            WRITE(6,3194)
            WRITE(6,3196)(SPRES(K),K=1,7)
            WRITE(6,3198)
            WRITE(6,3196)(SPRES(K),K=8,13)
            WRITE(6,3202)
            WRITE(6,3196)SPRES(26),(SPRES(K),K=14,19)
            WRITE(6,3204)
            WRITE(6,3196)(SPRES(K),K=20,25)
            LPRD=LPRD+9
 3950     CONTINUE
 3900   CONTINUE
      END IF
C
C     PRESSURE FORMATS
C
 3190 FORMAT(/' PRESSURES'/' *********')
 3192 FORMAT(' IV= ',I3,T10'SPEED = ',F10.2,T35'% FILL = ',F8.3)
 3194 FORMAT(T2'ROTOR ANGLE (deg)'T25'0'T36'15'T48'30'T60'45'T72'60'T84'
     275'T96'90')
 3196 FORMAT(T14'(kPa)',7(TR1,E11.4))
 3198 FORMAT(T14'(deg)'T23'105'T35'120'T47'135'T59'150'T71'165'T83'180')
 3202 FORMAT(T2'STATOR ANGLE(deg)'T23'180'T35'195'T47'210'T59'225'T71'2
     340'T83'255'T95'270')
 3204 FORMAT(T14'(deg)'T23'285'T35'300'T47'315'T59'330'T71'345'T83'360')
C
      RETURN
      END
C
      SUBROUTINE HEAD(I,J)
      IF(I.LT.58.AND.I.GT.J)THEN
        LP=58-I
        DO 3851 K=1,LP
          WRITE(6,3136)
 3136     FORMAT(' ')
 3851   CONTINUE
        I=0
      ELSE
        IF(I.EQ.58)I=0
      END IF
      RETURN
      END
C
C
C
C     SUBROUTINE AAAA
C     ***************
C     THIS ROUTINE CALLS PLOT79 AND GRAPHS THE OUTPUT
C
C    EQUATION SOLVERS
C    ****************
C
C
      SUBROUTINE LMT(YLMT)
C
C   LMT  LIMITS THE VALUES OF THE VARIABLES DDE IS SOLVING FOR
C
      IMPLICIT DOUBLE PRECISION (A-H,O-Z)
      DIMENSION YLMT(20)
C
C      YLMT(1)=0.D0
C
      IF(YLMT(2).LT.0.D0)YLMT(2)=0.D0
      IF(YLMT(3).LT.0.D0)YLMT(3)=0.D0
      IF(IRTR.EQ.0)THEN
        IF(YLMT(2).GT.838.D0)YLMT(2)=838.D0
```

```
        IF(YLMT(3).GT.838.D0)YLMT(3)=838.D0
      ELSE
        IF(YLMT(2).GT.1571.D0)YLMT(2)=1571.D0
        IF(YLMT(3).GT.1571.D0)YLMT(3)=1571.D0
      END IF
      IF(YLMT(4).LT.0.D0)YLMT(4)=0.D0
      IF(YLMT(4).GT.1.D0)YLMT(4)=1.D0
      RETURN
      END
C
C
C
      SUBROUTINE DDE(F,NEQN,Y,T,TOUT,RELERR,ABSERR,IFLAG)
C
C   DE  INTEGRATES A SYSTEM OF UP TO 20 FIRST ORDER O.D.E.S
C       OF THE FORM
C            DY(I)/DT = F(T,Y(1),Y(2),...,Y(NEQN))
C            Y(I) GIVEN AT T
C   THE SUBROUTINE INTEGRATES FROM T TO TOUT. ON RETURN THE
C   PARAMETERS IN THE CALL LIST ARE INITIALIZED FOR CONTINUING THE
C   INTEGRATION. THE USER HAS ONLY TO DEFINE A NEW VALUE TOUT
C   AND CALL DE AGAIN.
C
C   THIS CODE IS COMPLETELY EXPLAINED AND DOCUMENTED IN THE TEXT,
C   COMPUTER SOLUTION OF ORDINARY DIFFERENTIAL EQUATIONS:  THE INITIAL
C   VALUE PROBLEM  BY L. F. SHAMPINE AND M. K. GORDON.
C
      IMPLICIT DOUBLE PRECISION (A-H,O-Z)
      LOGICAL STIFF,CRASH,START
      EXTERNAL F,DSTEP,DINTRP
      DIMENSION Y(NEQN),YY(20),WT(20),PHI(20,16),P(20),YP(20)
      DIMENSION YPOUT(20),PSI(12)
C
C*********************************************************************
C*  THE ONLY MACHINE DEPENDENT CONSTANT IS BASED ON THE MACHINE UNIT   *
C*  ROUNDOFF ERROR  U  WHICH IS THE SMALLEST POSITIVE NUMBER SUCH THAT *
C*  1.0+U .GT. 1.0 .  U  MUST BE CALCULATED AND  FOURU=4.0*U  INSERTED *
C*  IN THE FOLLOWING DATA STATEMENT BEFORE USING  DE .  THE ROUTINE    *
C*  MACHIN  CALCULATES  U .  FOURU  AND  TWOU=2.0*U  MUST ALSO BE      *
C*  INSERTED IN SUBROUTINE  STEP  BEFORE CALLING  DE                   *
      DATA FOURU /.5552E-16/
C*********************************************************************
C
C   THE CONSTANT  MAXNUM  IS THE MAXIMUM NUMBER OF STEPS ALLOWED IN ONE
C   CALL TO  DE .  THE USER MAY CHANGE THIS LIMIT BY ALTERING THE
C   FOLLOWING STATEMENT
C
      DATA MAXNUM/500/
C            ***            ***            ***
C   TEST FOR IMPROPER PARAMETERS
C
      IF(NEQN .LT. 1 .OR. NEQN .GT. 20) GO TO 10
      IF(T .EQ. TOUT)GOTO 10
      IF(RELERR .LT. 0.D0  .OR.  ABSERR .LT. 0.D0) GO TO 10
      EPS = DMAX1(RELERR,ABSERR)
      IF(EPS .LE. 0.D0) GO TO 10
      IF(IFLAG .EQ. 0) GO TO 10
      ISN = ISIGN(1,IFLAG)
      IFLAG = IABS(IFLAG)
      IF(IFLAG .EQ. 1) GO TO 20
      IF(T .NE. TOLD) GO TO 10
      IF(IFLAG .GE. 2  .AND.  IFLAG .LE. 5) GO TO 20
   10 IFLAG = 6
      RETURN
C
C   ON EACH CALL SET INTERVAL OF INTEGRATION AND COUNTER FOR NUMBER OF
C   STEPS.  ADJUST INPUT ERROR TOLERANCES TO DEFINE WEIGHT VECTOR FOR
C   SUBROUTINE  STEP
C
   20 DEL = TOUT - T
      ABSDEL = DABS(DEL)
      TEND = T + 10.D0*DEL
      IF(ISN .LT. 0) TEND = TOUT
      NOSTEP = 0
      KLE4 = 0
      STIFF = .FALSE.
      RELEPS = RELERR/EPS
      ABSEPS = ABSERR/EPS
      IF(IFLAG .EQ. 1) GO TO 30
```

```
      IF(ISNOLD .LT. 0) GO TO 30
      IF(DELSGN*DEL .GT. 0.D0) GO TO 50
C
C   ON START AND RESTART ALSO SET WORK VARIABLES X AND YY(*), STORE THE
C   DIRECTION OF INTEGRATION AND INITIALIZE THE STEP SIZE
C
   30 START = .TRUE.
      X = T
      DO 40 L = 1,NEQN
   40   YY(L) = Y(L)
      DELSGN = DSIGN(1.D0,DEL)
      H = DSIGN(DMAX1(DABS(TOUT-X),FOURU*DABS(X)),TOUT-X)
C
C   IF ALREADY PAST OUTPUT POINT, INTERPOLATE AND RETURN
C
   50 IF(DABS(X-T) .LT. ABSDEL) GO TO 60
      IIFUL=0
      IF(Y(4).GE.1.D0.AND.YP(4).GE.0.D0)IIFUL=1
      CALL DINTRP(X,YY,TOUT,Y,YPOUT,NEQN,KOLD,PHI,PSI)
      IF(Y(4).LT.1.D0.AND.IIFUL.EQ.1)Y(4)=1.D0
      IFLAG = 2
      T = TOUT
      TOLD = T
      ISNOLD = ISN
      RETURN
C
C   IF CANNOT GO PAST OUTPUT POINT AND SUFFICIENTLY CLOSE,
C   EXTRAPOLATE AND RETURN
C
   60 IF(ISN .GT. 0  .OR.  DABS(TOUT-X) .GE. FOURU*DABS(X)) GO TO 80
      H = TOUT - X
      CALL F(X,X,YY,YP)
      DO 70 L = 1,NEQN
   70   Y(L) = YY(L) + H*YP(L)
      IFLAG = 2
      T = TOUT
      TOLD = T
      ISNOLD = ISN
      RETURN
C
C   TEST FOR TOO MANY STEPS
C
   80 IF(NOSTEP .LT. MAXNUM) GO TO 100
      IFLAG = ISN*4
      IF(STIFF) IFLAG = ISN*5
      DO 90 L = 1,NEQN
   90   Y(L) = YY(L)
      T = X
      TOLD = T
      ISNOLD = 1
      RETURN
C
C   LIMIT STEP SIZE, SET WEIGHT VECTOR AND TAKE A STEP
C
  100 H = DSIGN(DMIN1(DABS(H),DABS(TEND-X)),H)
      DO 110 L = 1,NEQN
  110   WT(L) = RELEPS*DABS(YY(L)) + ABSEPS
      CALL DSTEP(X,YY,F,NEQN,H,EPS,WT,START,
     1  HOLD,K,KOLD,CRASH,PHI,P,YP,PSI)
C
C   TEST FOR TOLERANCES TOO SMALL
C
      IF(.NOT.CRASH) GO TO 130
      IFLAG = ISN*3
      RELERR = EPS*RELEPS
      ABSERR = EPS*ABSEPS
      DO 120 L = 1,NEQN
  120   Y(L) = YY(L)
      T = X
      TOLD = T
      ISNOLD = 1
      RETURN
C
C   AUGMENT COUNTER ON NUMBER OF STEPS AND TEST FOR STIFFNESS
C
  130 NOSTEP = NOSTEP + 1
      KLE4 = KLE4 + 1
      IF(KOLD .GT. 4) KLE4 = 0
      IF(KLE4 .GE. 50) STIFF = .TRUE.
```

```
      GO TO 50
      END
      SUBROUTINE DSTEP(X,Y,F,NEQN,H,EPS,WT,START,
     1  HOLD,K,KOLD,CRASH,PHI,P,YP,PSI)
C
C   SUBROUTINE  STEP  INTEGRATES A SYSTEM OF FIRST ORDER ORDINARY
C   DIFFERENTIAL EQUATIONS ONE STEP NORMALLY FROM X TO X+H, USING A
C   MODIFIED DIVIDED DIFFERENCE FORM OF THE ADAMS PECE FORMULAS.  LOCAL
C   EXTRAPOLATION IS USED TO IMPROVE ABSOLUTE STABILITY AND ACCURACY.
C   THE CODE ADJUSTS ITS ORDER AND STEP SIZE TO CONTROL THE LOCAL ERROR
C   PER UNIT STEP IN A GENERALIZED SENSE.  SPECIAL DEVICES ARE INCLUDED
C   TO CONTROL ROUNDOFF ERROR AND TO DETECT WHEN THE USER IS REQUESTING
C   TOO MUCH ACCURACY.
C
C   THIS CODE IS COMPLETELY EXPLAINED AND DOCUMENTED IN THE TEXT,
C   COMPUTER SOLUTION OF ORDINARY DIFFERENTIAL EQUATIONS:  THE INITIAL
C   VALUE PROBLEM  BY L. F. SHAMPINE AND M. K. GORDON.
C
C
C   THE PARAMETERS REPRESENT:
C      X -- INDEPENDENT VARIABLE
C   Y(*) -- SOLUTION VECTOR AT X
C      YP(*) -- DERIVATIVE OF SOLUTION VECTOR AT  X  AFTER SUCCESSFUL
C           STEP
C      NEQN -- NUMBER OF EQUATIONS TO BE INTEGRATED
C      H -- APPROPRIATE STEP SIZE FOR NEXT STEP.  NORMALLY DETERMINED BY
C           CODE
C      EPS -- LOCAL ERROR TOLERANCE.  MUST BE VARIABLE
C      WT(*) -- VECTOR OF WEIGHTS FOR ERROR CRITERION
C      START -- LOGICAL VARIABLE SET .TRUE. FOR FIRST STEP,  .FALSE.
C           OTHERWISE
C      HOLD -- STEP SIZE USED FOR LAST SUCCESSFUL STEP
C      K -- APPROPRIATE ORDER FOR NEXT STEP (DETERMINED BY CODE)
C      KOLD -- ORDER USED FOR LAST SUCCESSFUL STEP
C      CRASH -- LOGICAL VARIABLE SET .TRUE. WHEN NO STEP CAN BE TAKEN,
C           .FALSE. OTHERWISE.
C   THE ARRAYS  PHI,  PSI  ARE REQUIRED FOR THE INTERPOLATION SUBROUTINE
C   INTRP .  THE ARRAY   P  IS INTERNAL TO THE CODE.
C
C   INPUT TO  STEP
C
C      FIRST CALL --
C
C   THE USER MUST PROVIDE STORAGE IN HIS DRIVER PROGRAM FOR ALL ARRAYS
C   IN THE CALL LIST, NAMELY
C
C     DIMENSION Y(NEQN),WT(NEQN),PHI(NEQN,16),P(NEQN),YP(NEQN),PSI(12)
C
C   THE USER MUST ALSO DECLARE  START  AND  CRASH  LOGICAL VARIABLES
C   AND  F  AN EXTERNAL SUBROUTINE, SUPPLY THE SUBROUTINE  F(X,Y,YP)
C   TO EVALUATE
C      DY(I)/DX = YP(I) = F(X,Y(1),Y(2),...,Y(NEQN))
C   AND INITIALIZE ONLY THE FOLLOWING PARAMETERS:
C      X -- INITIAL VALUE OF THE INDEPENDENT VARIABLE
C      Y(*) -- VECTOR OF INITIAL VALUES OF DEPENDENT VARIABLES
C      NEQN -- NUMBER OF EQUATIONS TO BE INTEGRATED
C      H -- NOMIAL STEP SIZE INDICATING DIRECTION OF INTEGRATION
C           AND MAXIMUM SIZE OF STEP.  MUST BE VARIABLE
C      WT(*) -- VECTOR OF NON-ZERO WEIGHTS FOR ERROR CRITERION
C      START -- .TRUE.
C
C   STEP REQUIRES THE L2 NORM OF THE VECTOR WITH COMPONENTS
C   LOCAL ERROR(L)/WT(L) BE LESS THAN  EPS  FOR A SUCCESSFUL STEP.  THE
C   ARRAY  WT  ALLOWS THE USER TO SPECIFY AN ERROR TEST APPROPRIATE
C   FOR THIS PROBLEM.  FOR EXAMPLE,
C      WT(L) = 1.0  SPECIFIES ABSOLUTE ERROR,
C            = DABS(Y(L))  ERROR RELATIVE TO THE MOST RECENT VALUE OF THE
C                 L-TH COMPONENT OF THE SOLUTION,
C            = DABS(YP(L))  ERROR RELATIVE TO THE MOST RECENT VALUE OF
C                 THE L-TH COMPONENT OF THE DERIVATIVE,
C            = DMAX1(WT(L),DABS(Y(L)))  ERROR RELATIVE TO THE LARGEST
C                 MAGNITUDE OF L-TH COMPONENT OBTAINED SO FAR,
C            = DABS(Y(L))*RELERR/EPS + ABSERR/EPS  SPECIFIES A MIXED
C                 RELATIVE-ABSOLUTE TEST WHERE  RELERR  IS RELATIVE
C                 ERROR  ABSERR  IS ABSOLUTE ERROR AND  EPS =
C                 DMAX1(RELERR,ABSERR)
C
C   SUBSEQUENT CALLS --
C
```

```
C   SUBROUTINE  STEP  IS DEDSIGNED SO THAT ALL INFORMATION NEEDED TO
C   CONTINUE THE INTEGRATION, INCLUDING THE STEP SIZE  H  AND THE ORDER
C   K , IS RETURNED WITH EACH STEP.  WITH THE EXCEPTION OF THE STEP
C   SIZE, THE ERROR TOLERANCE, AND THE WEIGHTS, NONE OF THE PARAMETERS
C   SHOULD BE ALTERED.  THE ARRAY  WT  MUST BE UPDATED AFTER EACH STEP
C   TO MAINTAIN RELATIVE ERROR TESTS LIKE THOSE ABOVE.  NORMALLY THE
C   SOLUTION INTERPOLATED THERE WITH SUBROUTINE  INTRP .  IF IT IS
C   IMPOSSIBLE TO INTEGRATE BEYOND THE ENDPOINT, THE STEP SIZE MAY BE
C   REDUCED TO HIT THE ENDPOINT SINCE THE CODE WILL NOT TAKE A STEP
C   LARGER THAN THE  H  INPUT.  CHANGING THE DIRECTION OF INTEGRATION,
C   I.E., THE DSIGN OF  H , REQUIRES THE USER SET  START = .TRUE. BEFORE
C   CALLING  STEP  AGAIN.  THIS IS THE ONLY SITUATION IN WHICH  START
C   SHOULD BE ALTERED.
C
C   OUTPUT FROM  STEP
C
C      SUCCESSFUL STEP --
C
C   THE SUBROUTINE RETURNS AFTER EACH SUCCESSFUL STEP WITH  START  AND
C   CRASH  SET .FALSE. .  X  REPRESENTS THE INDEPENDENT VARIABLE
C   ADVANCED ONE STEP OF LENGTH  HOLD  FROM ITS VALUE ON INPUT AND  Y
C   THE SOLUTION VECTOR AT THE NEW VALUE OF  X .  ALL OTHER PARAMETERS
C   REPRESENT INFORMATION CORRESPONDING TO THE NEW  X  NEEDED TO
C   CONTINUE THE INTEGRATION.
C
C      UNSUCCESSFUL STEP --
C
C   WHEN THE ERROR TOLERANCE IS TOO SMALL FOR THE MACHINE PRECISION,
C   THE SUBROUTINE RETURNS WITHOUT TAKING A STEP AND  CRASH = .TRUE.
C   AN APPROPRIATE STEP SIZE AND ERROR TOLERANCE FOR CONTINUING ARE
C   ESTIMATED AND ALL OTHER INFORMATION IS RESTORED AS UPON INPUT
C   BEFORE RETURNING.  TO CONTINUE WITH THE LARGER TOLERANCE, THE USER
C   JUST CALLS THE CODE AGAIN.  A RESTART IS NEITHER REQUIRED NOR
C   DESIRABLE.
C
      IMPLICIT DOUBLE PRECISION (A-H,O-Z)
      LOGICAL START,CRASH,PHASE1,NORND
      EXTERNAL F,DINTRP
      DIMENSION Y(NEQN),WT(NEQN),PHI(NEQN,16),P(NEQN),YP(NEQN),PSI(NEQN)
      DIMENSION ALPHA(12),BETA(12),SIG(13),W(12),V(12),G(13),
     1  GSTR(13),TWO(13)
C***********************************************************************
C*  THE ONLY MACHINE DEPENDENT CONSTANTS ARE BASE ON THE MACHINE UNIT  *
C*  ROUDOFF ERROR  U  WHICH IS THE SMALLEST POSITIVE NUMBER SUCH THAT  *
C*  1.0+U .GT. 1.0  .  THE USER MUST CALCULATE  U  AND INSERT          *
C*  TWOU=2.0*U  AND  FOURU=4.0*U  IN THE DATA STATEMENT BEFORE CALLING *
C*  THE CODE.  THE ROUTINE  MACHIN  CALCULATES  U .                    *
      DATA TWOU,FOURU/.2776E-16,.5552E-16/
C***********************************************************************
      DATA TWO/2.D0,4.D0,8.D0,16.D0,32.D0,64.D0,128.D0,256.D0,512.D0,
     1  1024.D0,2048.D0,4096.D0,8192.D0/
      DATA GSTR/0.5D0,0.0833D0,0.0417D0,0.0264D0,0.0188D0,0.0143D0,0.01
     114D0,0.00936D0,0.00789D0,0.00679D0,0.00592D0,0.00524D0,0.00468D0/
      DATA G(1),G(2)/1.D0,0.5D0/,SIG(1)/1.D0/
C
C
C       ***     BEGIN BLOCK 0     ***
C   CHECK IF STEP SIZE OR ERROR TOLERANCE IS TOO SMALL FOR MACHINE
C   PRECISION.  IF FIRST STEP, INITIALIZE PHI ARRAY AND ESTIMATE A
C   STARTING STEP SIZE.
C                    ***
C
C   IF STEP SIZE IS TOO SMALL, DETERMINE AN ACCEPTABLE ONE
C
      CRASH=.TRUE.
      IF(DABS(H) .GE. FOURU*DABS(X)) GO TO 5
      H=DSIGN(FOURU*DABS(X),H)
      RETURN
    5 P5EPS=0.5D0*EPS
C
C   IF ERROR TOLERANCE IS TOO SMALL, INCREASE IT TO AN ACCEPTABLE VALUE
C
      ROUND=0.D0
      DO 10 L=1,NEQN
   10   ROUND=ROUND+(Y(L)/WT(L))**2
      ROUND=TWOU*DSQRT(ROUND)
      IF(P5EPS .GE. ROUND) GO TO 15
      EPS=2.D0*ROUND*(1.D0+FOURU)
      RETURN
```

```
   15 CRASH=.FALSE.
      IF(.NOT.START) GO TO 99
C
C   INITIALIZE.  COMPUTE APPROPRIATE STEP SIZE FOR FIRST STEP
C
      CALL F(X,X,Y,YP)
      SUM=0.D0
      DO 20 L=1,NEQN
        PHI(L,1)=YP(L)
        PHI(L,2)=0.D0
   20   SUM=SUM+(YP(L)/WT(L))**2
      SUM=DSQRT(SUM)
      ABSH=DABS(H)
      IF(EPS .LT. 16.D0*SUM*H*H) ABSH=0.25D0*DSQRT(EPS/SUM)
      H=DSIGN(DMAX1(ABSH,FOURU*DABS(X)),H)
      HOLD=0.D0
      K=1
      KOLD=0
      START=.FALSE.
      PHASE1=.TRUE.
      NORND=.TRUE.
      IF(P5EPS .GT. 100.D0*ROUND) GO TO 99
      NORND=.FALSE.
      DO 25 L=1,NEQN
   25   PHI(L,15)=0.D0
   99 IFAIL=0
C       ***     END BLOCK 0     ***
C
C       ***     BEGIN BLOCK 1     ***
C   COMPUTE COEFFICIENTS OF FORMULAS FOR THIS STEP.  AVOID COMPUTING
C   THOSE QUANTITIES NOT CHANGED WHEN STEP SIZE IS NOT CHANGED.
C                ***
C
  100 KP1=K+1
      KP2=K+2
      KM1=K-1
      KM2=K-2
C
C   NS IS THE NUMBER OF STEPS TAKEN WITH SIZE H, INCLUDING THE CURRENT
C   ONE.  WHEN K.LT.NS, NO COEFFICIENTS CHANGE
C
      IF(H .NE. HOLD) NS=0
      NS=MIN0(NS+1,KOLD+1)
      NSP1=NS+1
      IF (K .LT. NS) GO TO 199
C
C   COMPUTE THOSE COMPONENTS OF ALPHA(*),BETA(*),PSI(*),SIG(*) WHICH
C   ARE CHANGED
C
      BETA(NS)=1.D0
      REALNS=NS
      ALPHA(NS)=1.D0/REALNS
      TEMP1=H*REALNS
      SIG(NSP1)=1.D0
      IF(K .LT. NSP1) GO TO 110
      DO 105 I=NSP1,K
         IM1=I-1
         TEMP2=PSI(IM1)
         PSI(IM1)=TEMP1
         BETA(I)=BETA(IM1)*PSI(IM1)/TEMP2
         TEMP1=TEMP2+H
         ALPHA(I)=H/TEMP1
         REALI=I
  105 SIG(I+1)=REALI*ALPHA(I)*SIG(I)
  110 PSI(K)=TEMP1
C
C   COMPUTE COEFFICIENTS G(*)
C
C   INITIALIZE V(*) AND SET W(*).  G(2) IS SET IN DATA STATEMENT
C
      IF(NS .GT. 1) GO TO 120
      DO 115 IQ=1,K
        TEMP3=IQ*(IQ+1)
        V(IQ)=1.D0/TEMP3
  115   W(IQ)=V(IQ)
      GO TO 140
C
C   IF ORDER WAS RAISED, UPDATE DIAGONAL PART OF V(*)
C
```

```
  120 IF(K .LE. KOLD) GO TO 130
      TEMP4=K*KP1
      V(K)=1.D0/TEMP4
      NSM2=NS-2
      IF(NSM2 .LT. 1) GO TO 130
      DO 125 J=1,NSM2
        I=K-J
  125   V(I)=V(I)-ALPHA(J+1)*V(I+1)
C
C   UPDATE V(*) AND SET W(*)
C
  130 LIMIT1=KP1-NS
      TEMP5=ALPHA(NS)
      DO 135 IQ =1,LIMIT1
        V(IQ)=V(IQ)-TEMP5*V(IQ+1)
  135   W(IQ)=V(IQ)
      G(NSP1)=W(1)
C
C   COMPUTE THE G(*) IN THE WORK VECTOR W(*)
C
  140 NSP2=NS+2
      IF(KP1 .LT. NSP2) GO TO 199
      DO 150 I=NSP2,KP1
        LIMIT2=KP2-I
        TEMP6=ALPHA(I-1)
        DO 145 IQ=1,LIMIT2
  145     W(IQ)=W(IQ)-TEMP6*W(IQ+1)
  150   G(I)=W(1)
  199 CONTINUE
C       ***     END BLOCK 1     ***
C
C       ***     BEGIN BLOCK 2     ***
C   PREDICT A SOLUTION P(*), EVALUATE DERIVATIVES USING PREDICTED
C   SOLUTION, ESTIMATE LOCAL ERROR AT ORDER K AND ERRORS AT ORDERS K,
C   K-1,K-2 AS IF CONSTANT STEP SIZE WERE USED.
C                   ***
C
C   CHANGE PHI TO PHI STAR
C
      IF(K .LT. NSP1) GO TO 215
      DO 210 I=NSP1,K
        TEMP1=BETA(I)
        DO 205 L=1,NEQN
  205   PHI(L,I)=TEMP1*PHI(L,I)
  210 CONTINUE
C
C   PREDICT SOLUTION AND DIFFERENCES
C
  215 DO 220 L=1,NEQN
        PHI(L,KP2) =PHI(L,KP1)
        PHI(L,KP1) =0.D0
  220   P(L)=0.D0
      DO 230 J=1,K
        I=KP1-J
        IP1=I+1
        TEMP2=G(I)
        DO 225 L=1,NEQN
          P(L)=P(L)+TEMP2*PHI(L,I)
CCCCCC          CALL LMT(P)
  225     PHI(L,I)=PHI(L,I)+PHI(L,IP1)
  230   CONTINUE
      IF(NORND) GO TO 240
      DO 235 L=1,NEQN
        TAU=H*P(L)-PHI(L,15)
        P(L)=Y(L)+TAU
CCCCCC        CALL LMT(P)
  235   PHI(L,16)=(P(L)-Y(L))-TAU
      GO TO 250
  240 DO 245 L=1,NEQN
  245   P(L)=Y(L)+H*P(L)
CCCCCC      CALL LMT(P)
  250 XOLD=X
      X=X+H
      ABSH=DABS(H)
      CALL F(X,X,P,YP)
C
C   ESTIMATE ERRORS AT ORDERS K,K-1,K-2
C
      ERKM2=0.D0
```

```
      ERKM1=0.D0
      ERK=0.D0
      DO 265 L=1,NEQN
        TEMP3=1.D0/WT(L)
        TEMP4=YP(L)-PHI(L,1)
        IF(KM2) 265,260,255
  255 ERKM2=ERKM2+((PHI(L,KM1)+TEMP4)*TEMP3)**2
  260 ERKM1=ERKM1+((PHI(L,K)+TEMP4)*TEMP3)**2
  265 ERK=ERK+(TEMP4*TEMP3)**2
      IF(KM2)280,275,270
  270 ERKM2=ABSH*SIG(KM1)*GSTR(KM2)*DSQRT(ERKM2)
  275 ERKM1=ABSH*SIG(K)*GSTR(KM1)*DSQRT(ERKM1)
  280 TEMP5=ABSH*DSQRT(ERK)
      ERR=TEMP5*(G(K)-G(KP1))
      ERK=TEMP5*SIG(KP1)*GSTR(K)
      KNEW=K
C
C   TEST IF ORDER SHOULD BE LOWERED
C
      IF(KM2)299,290,285
  285 IF(DMAX1(ERKM1,ERKM2) .LE. ERK) KNEW=KM1
      GO TO 299
  290 IF(ERKM1 .LE. 0.5D0*ERK) KNEW=KM1
C
C   TEST IF STEP SUCCESSFUL
C
  299 IF(ERR .LE. EPS) GO TO 400
C       ***     END BLOCK 2     ***
C
C       ***     BEGIN BLOCK 3     ***
C   THE STEP IS UNSUCCESSFUL.  RRSTORE  X, PHI(*,*), PSI(*) .
C   IF THIRD CONSECUTIVE FAILURE, SET ORDER TO ONE.  IF STEP FAILS MORE
C   THAN THREE TIMES, CONSIDER AN OPTIMAL STEP SIZE.  DOUBLE ERROR
C   TOLERANCE AND RETURN IF ESTIMATED STE SIZE IS TOO SMALL FOR MACHINE
C   PRECISION.
C                   ***
C
C   RESTORE X, PHI(*,*$ AND PSI(*)
C
      PHASE1=.FALSE.
      X=XOLD
      DO 310 I=1,K
        TEMP1=1.D0/BETA(I)
        IP1=I+1
        DO 305 L=1,NEQN
  305     PHI(L,I)=TEMP1*(PHI(L,I)-PHI(L,IP1))
  310   CONTINUE
      IF(K .LT. 2) GO TO 320
      DO 315 I=2,K
  315   PSI(I-1)=PSI(I)-H
C
C   ON THIRD FAILURE, SET ORDER TO ONE.  THEREAFTER, USE OPTIMAL STEP
C   SIZE
C
  320 IFAIL=IFAIL+1
      TEMP2=0.5D0
      IF(IFAIL-3) 335,330,325
  325 IF(P5EPS .LT. 0.25D0*ERK) TEMP2=DSQRT(P5EPS/ERK)
  330 KNEW=1
  335 H=TEMP2*H
      K=KNEW
      IF(DABS(H) .GE. FOURU*DABS(X)) GO TO 340
      CRASH=.TRUE.
      H=DSIGN(FOURU*DABS(X),H)
      EPS=EPS+EPS
      RETURN
  340 GO TO 100
C       ***     END BLOCK 3     ***
C
C       ***     BEGIN BLOCK 4     ***
C   THE STEP IS SUCCESSFUL.  CORRECT THE PREDICTED SOLUTION,EVALUATE
C   THE DERIVATIVES USING THE CORRECTED SOLUTION AND UPDATE THE
C   DIFFERENCES.  DETERMINE BEST ORDER AND STEP SIZE FOR NEXT STEP
C                   ***
  400 KOLD=K
      HOLD=H
C
C   CORRECT AND EVALUATE
C
```

```
      TEMP1=H*G(KP1)
      IF(NORND) GO TO 410
      DO 405 L=1,NEQN
        RHO=TEMP1*(YP(L)-PHI(L,1))-PHI(L,16)
        Y(L)=P(L)+RHO
        CALL LMT(Y)
  405   PHI(L,15)=(Y(L)-P(L))-RHO
      GO TO 420
  410 DO 415 L=1,NEQN
  415   Y(L)=P(L)+TEMP1*(YP(L)-PHI(L,1))
      CALL LMT(Y)
  420 CALL F(X,XOLD,Y,YP)
C
C   UPDATE DIFFERENCES FOR NEXT STEP
C
      DO 425 L=1,NEQN
        PHI(L,KP1)=YP(L)-PHI(L,1)
  425   PHI(L,KP2) =PHI(L,KP1)-PHI(L,KP2)
      DO 435 I=1,K
        DO 430 L=1,NEQN
  430     PHI(L,I)=PHI(L,I)+PHI(L,KP1)
  435   CONTINUE
C
C   ESTIMATE ERROR AT ORDER K+1 UNLESS
C     IN FIRST PHASE WHEN ALWAYS RAISE ORDER,
C     ALREADY DECIDED TO LOWER ORDER,
C     STEP SIZE NOT CONSTANT SO ESTIMATE UNRELIABLE
C
      ERKP1=0.D0
      IF(KNEW .EQ. KM1  .OR.  K .EQ. 1) PHASE1=.FALSE.
      IF(PHASE1) GO TO 450
      IF(KNEW .EQ. KM1) GO TO 455
      IF(KP1 .GT. NS) GO TO 460
      DO 440 L=1,NEQN
  440   ERKP1=ERKP1+(PHI(L,KP2)/WT(L))**2
      ERKP1=ABSH*GSTR(KP1)*DSQRT(ERKP1)
C
C   USING ESTIMATED ERROR AT ORDER K+1, DETERMINE APPROPRIATE ORDER
C   FOR NEXT STEP
C
      IF(K .GT. 1) GO TO 445
      IF(ERKP1 .GE. 0.5D0*ERK) GO TO 460
      GO TO 450
  445 IF(ERKM1 .LE. DMIN1(ERK,ERKP1)) GO TO 455
      IF(ERKP1 .GE. ERK  .OR.  K .EQ. 12) GO TO 460
C
C   HERE ERKM1 .LT. ERK .LT. DMAX1(ERKM1,ERKM2) ELSE ORDER WOULD HAVE
C   BEEN LOWERED IN BLOCK 2.  THUS ORDER IS TO BE RAISED
C
C   RAISE ORDER
C
  450 K=KP1
      ERK=ERKP1
      GO TO 460
C
C   LOWER ORDER
C
  455 K=KM1
      ERK=ERKM1
C
C   WITH NEW ORDER DETERMINE APPROPRIATE STEP SIZE FOR NEXT STEP
C
  460 HNEW=H+H
      IF(PHASE1) GO TO 465
      IF(P5EPS .GE. ERK*TWO(K+1)) GO TO 465
      HNEW=H
      IF(P5EPS .GE. ERK) GO TO 465
      TEMP2=K+1
      R=(P5EPS/ERK)**(1.D0/TEMP2)
      HNEW=ABSH*DMAX1(0.5D0,DMIN1(0.9D0,R))
      HNEW=DSIGN(DMAX1(HNEW,FOURU*DABS(X)),H)
  465 H =HNEW
      RETURN
C       ***     END BLOCK 4     ***
      END
C
C
C
C
```

```
C
      SUBROUTINE DINTRP(X,Y,XOUT,YOUT,YPOUT,NEQN,KOLD,PHI,PSI)
C
C   THE METHODS IN SUBROUTINE  STEP  APPROXIMATE THE SOLUTION NEAR  X
C   BY A POLYNOMIAL.  SUBROUTINE  INTRP  APPROXIMATES THE SOLUTION AT
C   XOUT  BY EVALUATING THE POLYNOMIAL THERE.  INFORMATION DEFINING THIS
C   POLYNOMIAL IS PASSED FROM  STEP  SO  INTRP  CANNOT BE USED ALONE.
C
C   THIS CODE IS COMPLETELY EXPLAINED AND DOCUMENTED IN THE TEXT,
C   COMPUTER SOLUTION OF ORDINARY DIFFERENTIAL EQUATIONS:  THE INITIAL
C   VALUE PROBLEM  BY L. F. SHAMPINE AND M. K. GORDON.
C
C   INPUT TO INTRP --
C
C   THE USER PROVIDES STORAGE IN THE CALLING PROGRAM FOR THE ARRAYS IN
C   THE CALL LIST
C   AND DEFINES
C      XOUT -- POINT AT WHICH SOLUTION IS DESIRED.
C   THE REMAINING PARAMETERS ARE DEFINED IN  STEP  AND PASSED TO  INTRP
C   FROM THAT SUBROUTINE
C
C   OUTPUT FROM  INTRP --
C
C      YOUT(*) -- SOLUTION AT  XOUT
C      YPOUT(*) -- DERIVATIVE OF SOLUTION AT  XOUT
C   THE REMAINING PARAMETERS ARE RETURNED UNALTERED FROM THEIR INPUT
C   VALUES.  INTEGRATION WITH  STEP  MAY BE CONTINUED
C
      IMPLICIT DOUBLE PRECISION (A-H,O-Z)
      DIMENSION Y(NEQN),YOUT(NEQN),YPOUT(NEQN),PHI(NEQN,16),PSI(12)
      DIMENSION G(13),W(13),RHO(13)
      DATA G(1)/1.0/,RHO(1)/1.0/
C
      HI=XOUT-X
      KI=KOLD+1
      KIP1=KI+1
C
C   INITIALIZE W(*) FOR COMPUTING G(*)
C
      DO 5 I=1,KI
        TEMP1=I
    5   W(I)=1.D0/TEMP1
      TERM=0.D0
C
C   COMPUTE G(*)
C
      DO 15 J=2,KI
        JM1=J-1
        PSIJM1=PSI(JM1)
        GAMMA=(HI+TERM)/PSIJM1
        ETA =HI/PSIJM1
        LIMIT1=KIP1-J
        DO 10 I=1,LIMIT1
   10     W(I)=GAMMA*W(I)-ETA*W(I+1)
        G(J)=W(1)
        RHO(J)=GAMMA*RHO(JM1)
   15   TERM=PSIJM1
C
C   INTERPOLATE
C
      DO 20 L=1,NEQN
        YPOUT(L)=0.D0
   20   YOUT(L)=0.D0
      DO 30 J=1,KI
        I=KIP1-J
        TEMP2=G(I)
        TEMP3=RHO(I)
        DO 25 L=1,NEQN
          YOUT(L)=YOUT(L)+TEMP2*PHI(L,I)
   25     YPOUT(L)=YPOUT(L)+TEMP3*PHI(L,I)
   30   CONTINUE
      DO 35 L=1,NEQN
   35  YOUT(L)=Y(L)+HI*YOUT(L)
      RETURN
      END
C
```

```
C      ################################################
C      ################################################
C      ##                                            ##
C      ##     BBBBB        PPPPPP     VV        VV    ##
C      ##     BB   BB      PP   PP     V         V     ##
C      ##     BB   BB      PP    PP    VV       VV     ##
C      ##     BBBBB        PP   PP      V      V      ##
C      ##     BB   BB      PPPPP        VV    VV      ##
C      ##     BB    BB     PP             V   V       ##
C      ##     BB    BB     PP             VV VV       ##
C      ##     BB   BB      PP              V V        ##
C      ##     BBBBBB       PP               V         ##
C      ##                                            ##
C      ##        COPYRIGHT 1990 P.G. HODGSON         ##
C      ##                                            ##
C      ################################################
C      ################################################
C
C           TORQUE/POWER vs. SPEED CHARACTERISTIC FOR
C
C              PARTIAL-FILL HYDRAULIC DYNAMOMETRS
C
C                 BACK PRESSURE VALVE CONTROL
C
C                     PROGRAM VERSION 1.0
C
C                      DATE:  APRIL 1990
C
C                     AUTHOR: P.G. HODGSON
C
C                   UNIVERSITY OF CANTERBURY
C
C
C
C     MAIN PROGRAM
C     ************
      PROGRAM BPV
C
      IMPLICIT DOUBLE PRECISION (A-H,O-Z)
C
      EXTERNAL F
      DIMENSION Y(20),YP(20),YPEXT(20)
C
      COMMON/FLG1/IPGM,ISS,IMAC,IRTR,IOUT,ITQSTT,IOPUT(6),ICES,IFUL,ICOM
      COMMON/FLG2/IT,INTS,IV,IVST,IVR,IVAR(4),MNQQ,ICS,ICLC
      COMMON/GEO1/RO,RI,RINERT,BRI,BRO,BSI,BSO,ZR,ZS,BT,FFAC,BFAC
      COMMON/GEO2/PI,RHO,ARHO,PO,RC,RM,VF,ENGINT,CYLN,FNN,SHSTFF
      COMMON/RUN1/RTFI,RTCR,PFIN,PFFI,PFCR
      COMMON/RUN2/CVIN,CVFI,CVCR,CVT,SMIN,SMAX,SICR,ST
      COMMON/RUN3/QIIN,QIFI,QICR,QIT,TQIN,TQFI,TQCR,TQT
      COMMON/SCON/CES,AA,CLFS,CLV,SCL,CL,PBFAC,PFFAC,RTS,WRV
      COMMON/VAR1/PERF,RCO,RCI,DYNERT,QIN,CP,P1,DP,QOUT
      COMMON/VAR2/W,WP,WE,THETA1,THETA2,DELTA,ACH2O,ACRTR,ACENG
      COMMON/VAR3/TOR,POW,ETOR,EPOW,EPHI,DDTDEL,DDTPF
      COMMON/CON1/VA,VV,VZ,POIL,CLOIL,CV,RGOP,QCV,DPOIL
      COMMON/CON2/PCP,RKS,DC,RMV,AOIL,ACV,AV,POMX,VMXT,BMO,VOIL
      COMMON/ARR1/TQFAC(6),PIFAC(3),PLOSS(3),TQCMPT(6),SPRES(26)
C
C OPEN OUTPUT, PLOT DATA & STORAGE FILES
      OPEN(2,FILE='[HODGSON.DATAA]OUT.GPH',STATUS='OLD')
      OPEN(6,FILE='[HODGSON.DATAA]OUT.DAT',STATUS='OLD')
      OPEN(8,FILE='[HODGSON.DATAA]NUM.DAT',STATUS='OLD')
      OPEN(9,STATUS='SCRATCH',FORM='UNFORMATTED')
C READ INPUT, SET UP PROGRAM & CALC. INVARIANT CONSTANTS
      CALL INPUT()
      CALL CONSTS()
C DYNAMIC
       IF(ITQSTT.EQ.1.OR.ITQSTT.EQ.2)CALL TQSTRT()
       T=0.D0
       RELERR=1.D-5
       ABSERR=1.D-5
C       PRINT *,' ENTER RELERR,ABSERR'
C       READ(*,*)RELERR,ABSERR
       IF(ISS.NE.1)THEN
         DYNERT=DYNERT+ENGINT
         ENGINT=DYNERT
       END IF
C INITIAL CONDITIONS
       CALL STATUS(1,T,T)
```

```
        CALL PART()
        CALL KFACTS()
        CALL VORVEL()
        CALL POWER()
        DELTA=0.D0
        IF(ISS.EQ.1)DELTA=ETOR/SHSTFF
        Y(1)=DELTA
        WP=WE
        Y(2)=WE
        Y(3)=WP
        Y(4)=PERF
        Y(5)=VZ
        Y(6)=VV
        QCV=WP/2.D0/PI*PCP
        RGOP=CLOIL/2.D0*(QCV/AOIL)**2
        POIL=RGOP
        IF(POIL.GT.POMX)POIL=POMX
        Y(7)=POIL
C STORE DATA
        EPOW=ETOR*WE
        WRITE(9)SCL,CL,PBFAC,PFFAC,RTS,WRV
        WRITE(9)PERF,RCO,RCI,DYNERT,QIN,CP,P1,DP,QOUT
        WRITE(9)W,WP,WE,THETA1,THETA2,DELTA,ACH2O,ACRTR,ACENG
        WRITE(9)TOR,POW,ETOR,EPOW,EPHI,DDTDEL,DDTPF
        WRITE(9)VA,VV,VZ,POIL,CLOIL,CV,RGOP,QCV,DPOIL
        WRITE(9)(TQFAC(K),K=1,6),(PIFAC(K),K=1,3)
        WRITE(9)(PLOSS(K),K=1,3),(TQCMPT(K),K=1,6),(SPRES(K),K=1,26)
C SOLVE D.E.S FOR EACH TIME STEP
        IFLAG=1
        IOVF=0
        DO 1000 IT=2,INTS
          TOUT=RTCR*DFLOAT(IT-1)
 1300     CONTINUE
          CALL DDE(F,7,Y,T,TOUT,RELERR,ABSERR,IFLAG)
 1333     IF(IFLAG.EQ.2)THEN
            IF(ISS.NE.1)Y(1)=0.D0
            DELTA=Y(1)
            WE=Y(2)
            WP=Y(3)
            PERF=Y(4)
            VZ=Y(5)
            VV=Y(6)
            POIL=Y(7)
            CALL F(T,T,Y,YPEXT)
            DDTDEL=YPEXT(1)
            ACENG=YPEXT(2)
            ACRTR=YPEXT(3)
            DDTPF=YPEXT(4)
            VV=YPEXT(5)
            VA=YPEXT(6)
            DPOIL=YPEXT(7)
C STORE DATA
            EPOW=ETOR*WE
            WRITE(9)SCL,CL,PBFAC,PFFAC,RTS,WRV
            WRITE(9)PERF,RCO,RCI,DYNERT,QIN,CP,P1,DP,QOUT
            WRITE(9)W,WP,WE,THETA1,THETA2,DELTA,ACH2O,ACRTR,ACENG
            WRITE(9)TOR,POW,ETOR,EPOW,EPHI,DDTDEL,DDTPF
            WRITE(9)VA,VV,VZ,POIL,CLOIL,CV,RGOP,QCV,DPOIL
            WRITE(9)(TQFAC(K),K=1,6),(PIFAC(K),K=1,3)
      WRITE(9)(PLOSS(K),K=1,3),(TQCMPT(K),K=1,6),(SPRES(K),K=1,26)
          ELSE
            IF(IFLAG.EQ.3)PRINT *,' ERROR TOLER. TOO SMALL'
            IF(IFLAG.EQ.4)PRINT *,' TOO MANY STEPS. IT= ',IT
            IF(IFLAG.EQ.5)PRINT *,' EQUATIONS STIFF. IT= ',IT
            IF(IFLAG.EQ.6)PRINT *,' INCORRECT INPUT'
            IF(IFLAG.NE.6)IOVF=IOVF+1
          END IF
          IF(IFLAG.EQ.3.OR.IFLAG.EQ.4.OR.IFLAG.EQ.5)GOTO 1300
          PRINT *, ' TIMESTEP COMPLETE.  IT= ',IT
 1000   CONTINUE
      IF(ISAV.EQ.1)ICOM=1
C OUTPUT INPUT & RESULTS
 8888 CONTINUE
      CALL OUTPUT()
C      IF(IOPUT(6).EQ.1)CALL AAAA()
C CLOSE FILES
      CLOSE(2)
      CLOSE(6)
      CLOSE(8)
```

```
      CLOSE(9)
C END PROGRAM
      PRINT *,' EXTRA DDE CALLS = ',IOVF
      PRINT *,' ***** PROGRAM EXECUTION COMPLETE *****'
      PRINT *,' ***** PROGRAM EXECUTION COMPLETE *****'
      PRINT *,' ***** PROGRAM EXECUTION COMPLETE *****'
 9999 STOP
      END
C
C
C
C     SUBROUTINE F
C     ************
C     THIS ROUTINE CALCULATES THE DE'S AT ANY TIME STEP
C
      SUBROUTINE F(X,XXOLD,Y,YP)
C
      IMPLICIT DOUBLE PRECISION (A-H,O-Z)
      DIMENSION Y(20),YP(20)
C
      COMMON/FLG1/IPGM,ISS,IMAC,IRTR,IOUT,ITQSTT,IOPUT(6),ICES,IFUL,ICOM
      COMMON/FLG2/IT,INTS,IV,IVST,IVR,IVAR(4),MNQQ,ICS,ICLC
      COMMON/GEO1/RO,RI,RINERT,BRI,BRO,BSI,BSO,ZR,ZS,BT,FFAC,BFAC
      COMMON/GEO2/PI,RHO,ARHO,PO,RC,RM,VF,ENGINT,CYLN,FNN,SHSTFF
      COMMON/RUN1/RTFI,RTCR,PFIN,PFFI,PFCR
      COMMON/RUN2/CVIN,CVFI,CVCR,CVT,SMIN,SMAX,SICR,ST
      COMMON/RUN3/QIIN,QIFI,QICR,QIT,TQIN,TQFI,TQCR,TQT
      COMMON/SCON/CES,AA,CLFS,CLV,SCL,CL,PBFAC,PFFAC,RTS,WRV
      COMMON/VAR1/PERF,RCO,RCI,DYNERT,QIN,CP,P1,DP,QOUT
      COMMON/VAR2/W,WP,WE,THETA1,THETA2,DELTA,ACH2O,ACRTR,ACENG
      COMMON/VAR3/TOR,POW,ETOR,EPOW,EPHI,DDTDEL,DDTPF
      COMMON/CON1/VA,VV,VZ,POIL,CLOIL,CV,RGOP,QCV,DPOIL
      COMMON/CON2/PCP,RKS,DC,RMV,AOIL,ACV,AV,POMX,VMXT,BMO,VOIL
      COMMON/ARR1/TQFAC(6),PIFAC(3),PLOSS(3),TQCMPT(6),SPRES(26)
C
      IF(ISS.NE.1)Y(1)=0.D0
      DELTA=Y(1)
      WE=Y(2)
      WP=Y(3)
      PERF=Y(4)
      VZ=Y(5)
      VV=Y(6)
      CP=VZ/VMXT
        IF(CP.GT.1.D0)CP=1.D0
        IF(CP.LT.0.D0)CP=0.D0
      POIL=Y(7)
      CALL STATUS(1,X,XXOLD)
      CALL PART()
      CALL KFACTS()
      CALL VORVEL()
      CALL POWER()
      STOR=TQCMPT(1)+TQCMPT(2)+TQCMPT(3)+TQCMPT(4)
      RGOP=CLOIL/2.D0*(WP/2.D0/PI*PCP/AOIL)**2
      CQCV=2.D0/CLOIL*POIL
        IF(CQCV.LT.0.D0)CQCV=0.D0
      QCV=AOIL*DSQRT(CQCV)
      RWWP=W/WP
C DERIVATIVES CALC
      YP(1)=WE-WP
      IF(IPGM.EQ.1)THEN
        IF(ISS.EQ.1)THEN
          YP(2)=(ETOR-SHSTFF*DELTA)/ENGINT
          YP(3)=(SHSTFF*DELTA-STOR)
          YP(3)=YP(3)/(DYNERT+2.D0*(TQFAC(5)+RWWP*TQFAC(6)))
        ELSE
          YP(2)=(ETOR-STOR)/(ENGINT+2.D0*(TQFAC(5)+RWWP*TQFAC(6)))
          YP(3)=(ETOR-STOR)/(DYNERT+2.D0*(TQFAC(5)+RWWP*TQFAC(6)))
        END IF
      END IF
      IF(IPGM.EQ.2)THEN
        YP(2)=SICR
        IF(ISS.EQ.1)THEN
          YP(3)=(SHSTFF*DELTA-STOR)
          YP(3)=YP(3)/(DYNERT+2.D0*(TQFAC(5)+RWWP*TQFAC(6)))
        ELSE
          YP(3)=YP(2)
        END IF
      END IF
      YP(4)=(QIN-QOUT)/VF
```

```
      YP(5)=VV
      YP(6)=(POIL*ACV-DP*AV-DC*VV-RKS*VZ)/RMV
      YP(7)=BMO/(VOIL+CP*VMXT*AOIL)*(WP/2.D0/PI*PCP-QCV)
C
      ACRTR=YP(3)
      ACH2O=RWWP*ACRTR
      TQCMPT(5)=2.D0*TQFAC(5)*ACRTR
      TQCMPT(6)=2.D0*TQFAC(6)*ACH2O
      TOR=TQCMPT(1)+TQCMPT(2)+TQCMPT(3)+TQCMPT(4)+TQCMPT(5)+TQCMPT(6)
      POW=TOR*WP
      RETURN
      END
C
C
C
C
C
C     SUBROUTINE CONSTS
C     *****************
C     THIS ROUTINE CALCULATES THE TIME INDEPENDENT CONSTANTS
C
      SUBROUTINE CONSTS()
C
      IMPLICIT DOUBLE PRECISION (A-H,O-Z)
C
      COMMON/FLG1/IPGM,ISS,IMAC,IRTR,IOUT,ITQSTT,IOPUT(6),ICES,IFUL,ICOM
      COMMON/FLG2/IT,INTS,IV,IVST,IVR,IVAR(4),MNQQ,ICS,ICLC
      COMMON/GEO1/RO,RI,RINERT,BRI,BRO,BSI,BSO,ZR,ZS,BT,FFAC,BFAC
      COMMON/GEO2/PI,RHO,ARHO,PO,RC,RM,VF,ENGINT,CYLN,FNN,SHSTFF
      COMMON/RUN1/RTFI,RTCR,PFIN,PFFI,PFCR
      COMMON/RUN2/CVIN,CVFI,CVCR,CVT,SMIN,SMAX,SICR,ST
      COMMON/RUN3/QIIN,QIFI,QICR,QIT,TQIN,TQFI,TQCR,TQT
      COMMON/SCON/CES,AA,CLFS,CLV,SCL,CL,PBFAC,PFFAC,RTS,WRV
      COMMON/VAR1/PERF,RCO,RCI,DYNERT,QIN,CP,P1,DP,QOUT
      COMMON/VAR2/W,WP,WE,THETA1,THETA2,DELTA,ACH2O,ACRTR,ACENG
      COMMON/VAR3/TOR,POW,ETOR,EPOW,EPHI,DDTDEL,DDTPF
      COMMON/CON1/VA,VV,VZ,POIL,CLOIL,CV,RGOP,QCV,DPOIL
      COMMON/CON2/PCP,RKS,DC,RMV,AOIL,ACV,AV,POMX,VMXT,BMO,VOIL
      COMMON/ARR1/TQFAC(6),PIFAC(3),PLOSS(3),TQCMPT(6),SPRES(26)
C
C     CONVERT PERF,CP,QIN,SPEED,DEMAND TORQUE
C
      CVIN=CVIN/10.D0
      CVFI=CVFI/10.D0
      CVCR=CVCR/10.D0
      SMIN=SMIN*PI/30.D0
      SMAX=SMAX*PI/30.D0
      SICR=SICR*PI/30.D0
      PFIN=PFIN/100.D0
      PFFI=PFFI/100.D0
      PFCR=PFCR/100.D0
C
      CV=CVIN
      WE=SMIN
      WP=SMIN
      QIN=QIIN
      ETOR=TQIN
      PERF=PFIN
      DYNERT=RINERT
C
      IF(CV.GT.1.D0)CV=1.D0
      IF(CV.LT.0.D0)CV=0.D0
      IF(PERF.GE.1.D0)PERF=1.D0
      IF(PERF.LE.0.D0)PERF=0.D0
      IFUL=0
      IF(PERF.GE.1.0)IFUL=1
C
C     CONVERT BLADE ANGLES
C
      BRI=BRI*PI/180.D0
      BRO=BRO*PI/180.D0
      BSI=BSI*PI/180.D0
      BSO=BSO*PI/180.D0
C
C     CALCULATE TIME STEPS & CALC. LOOPS
C     INTS & IVST CALCED IN INPUT()
C
C     LOSS COEFF.,AREAS ,OUTLET RADIUS (RC), CMPT. VOLUME (VF)
C
```

```
          RC=(RO+RI)/2.D0
          CL1=0.5D0
          CL2=1.D0
          IF(IOUT.EQ.2)CL2=0.8D0
          CLD=0.3D0
          CL6=0.8D0
          CL7=0.8D0
          CL8=0.5D0
          CLFS=0.72D0
          A0=0.054D0*0.036D0
          A1=PI*0.004D0*0.004D0*28.D0
          IF(IOUT.EQ.1)A1=PI*0.0055D0*0.0055D0*24.D0
          AD=0.018D0*0.031D0/2.D0
          AA=A0
          CG=0.01D0
        SCL=(CL1+CL2-1.D0)/A1**2+1.D0/A0**2+CLD/AD**2
        IF(IOUT.EQ.0)SCL=SCL+(1.D3/RO**2-1.D3/RC**2)/(4.D0*(PI*CG)**2)
        IF(IOUT.EQ.1)SCL=SCL+CL6/AA**2
        IF(IOUT.EQ.2)SCL=(CL1+CL2+CL7-1.D0)/A1**2+1.D0/A0**2+(CL6+CL8)/AA*
       1*2
        IF(IRTR.EQ.1)THEN
          A=(ZR/DSIN(BRI)+ZR/DSIN(BRO))/2.D0
          A=(A+ZS/DSIN(BSI)+ZS/DSIN(BSO))/4.D0
        ELSE
          A=(ZR/DSIN(BRI)+ZR/DSIN(BRO)+ZS/DSIN(BSI)+ZS/DSIN(BSO))/4.D0
        END IF
        BAV=(BRI+BRO+BSI+BSO)/4.D0
        VF=((RO-RI)**2)*(2.D0*PI*RC-A*BT)*PI*SIN(BAV)/4.D9
C
C CONSTANTS FOR CONTROL SYSTEM
        PCP=1.2D-6
        BMO=1380.D6
        POMX=4.83D6
        RKS=5.9D3
        RMV=.76
        DC=5.0D0*2.D0*DSQRT(RMV*RKS)
        VMXT=0.02D0
        AOIL=PI/4.D0*(0.0066D0)**2
        VOIL=AOIL*1.5D0
        ACV=PI/4.D0*(0.02353D0)**2
        AV=PI/4.D0*(0.04193D0)**2
C
        RETURN
        END
C
C
C
C
C
C     SUBROUTINE STATUS
C     *****************
C     THIS ROUTINE CALCULATES THE CHANGES TO VALVE,SPEED,QIN
C     WITH TIME AND THE VALVE LOSS
C
      SUBROUTINE STATUS(III,XX,TT)
C
      IMPLICIT DOUBLE PRECISION (A-H,O-Z)
C
      COMMON/FLG1/IPGM,ISS,IMAC,IRTR,IOUT,ITQSTT,IOPUT(6),ICES,IFUL,ICOM
      COMMON/FLG2/IT,INTS,IV,IVST,IVR,IVAR(4),MNQQ,ICS,ICLC
      COMMON/GEO1/RO,RI,RINERT,BRI,BRO,BSI,BSO,ZR,ZS,BT,FFAC,BFAC
      COMMON/GEO2/PI,RHO,ARHO,PO,RC,RM,VF,ENGINT,CYLN,FNN,SHSTFF
      COMMON/RUN1/RTFI,RTCR,PFIN,PFFI,PFCR
      COMMON/RUN2/CVIN,CVFI,CVCR,CVT,SMIN,SMAX,SICR,ST
      COMMON/RUN3/QIIN,QIFI,QICR,QIT,TQIN,TQFI,TQCR,TQT
      COMMON/SCON/CES,AA,CLFS,CLV,SCL,CL,PBFAC,PFFAC,RTS,WRV
      COMMON/VAR1/PERF,RCO,RCI,DYNERT,QIN,CP,P1,DP,QOUT
      COMMON/VAR2/W,WP,WE,THETA1,THETA2,DELTA,ACH2O,ACRTR,ACENG
      COMMON/VAR3/TOR,POW,ETOR,EPOW,EPHI,DDTDEL,DDTPF
      COMMON/CON1/VA,VV,VZ,POIL,CLOIL,CV,RGOP,QCV,DPOIL
      COMMON/CON2/PCP,RKS,DC,RMV,AOIL,ACV,AV,POMX,VMXT,BMO,VOIL
      COMMON/ARR1/TQFAC(6),PIFAC(3),PLOSS(3),TQCMPT(6),SPRES(26)
C
      IF(III.EQ.1)THEN
C APPLY TIME CHANGES OF PERF,CV,QIN
C
          CV=CVIN
        IF(XX.GE.CVT.AND.IVAR(1).NE.1)THEN
          IF(IVAR(1).EQ.2)CV=CVFI
```

```
          IF(IVAR(1).EQ.3)CV=CV+CVCR*(XX-CVT)
          IF(CV.GT.CVFI.AND.CVFI.GT.CVIN)CV=CVFI
          IF(CV.LT.CVFI.AND.CVFI.LT.CVIN)CV=CVFI
        END IF
          IF(IPGM.EQ.2)WE=SMIN
        IF(IPGM.EQ.2.AND.XX.GE.ST.AND.IVAR(2).NE.1)THEN
          IF(IVAR(2).EQ.2)WE=SMAX
          IF(IVAR(2).EQ.3)WE=WE+SICR*(XX-ST)
          IF(WE.GT.SMAX.AND.SMAX.GT.SMIN)WE=SMAX
          IF(WE.LT.SMAX.AND.SMAX.LT.SMIN)WE=SMAX
        END IF
        IF(IPGM.EQ.2)WE=WE*(1.D0+FNN*DSIN(CLYN*WE*XX/2.D0-PI/2.D0))
        IF(IPGM.EQ.2.AND.ISS.NE.1)WP=WE
          QIN=QIIN
        IF(XX.GE.QIT.AND.IVAR(3).NE.1)THEN
          IF(IVAR(3).EQ.2)QIN=QIFI
          IF(IVAR(3).EQ.3)QIN=QIN+QICR*(XX-QIT)
          IF(QIN.GT.QIFI.AND.QIFI.GT.QIIN)QIN=QIFI
          IF(QIN.LT.QIFI.AND.QIFI.LT.QIIN)QIN=QIFI
        END IF
          ETOR=TQIN
        IF(XX.GE.TQT.AND.IVAR(4).NE.1)THEN
          IF(IVAR(4).EQ.2)ETOR=TQFI
          IF(IVAR(4).EQ.3)ETOR=ETOR+TQCR*(XX-TQT)
          IF(ETOR.GT.TQFI.AND.TQFI.GT.TQIN)ETOR=TQFI
          IF(ETOR.LT.TQFI.AND.TQFI.LT.TQIN)ETOR=TQFI
        END IF
        ETOR=ETOR*(1.D0+FNN*DSIN(CYLN*WE*XX/2.D0))
      END IF
C
      IF(CV.GT.1.2D0)CV=1.2D0
      IF(CV.LT.0.D0)CV=0.D0
      IF(CP.GT.1.D0)CP=1.D0
      IF(CP.LT.0.D0)CP=0.D0
      IF(PERF.GE.1.D0)PERF=1.D0
      IF(PERF.LE.0.D0)PERF=0.D0
      IFUL=0
      IF(PERF.GE.1.0)IFUL=1
C
C     LOSS COEFF. THRU WATER OUTLET
C
         FC=.007144D0+.54479D0*CP-4.9163D0*CP**2+17.653D0*CP**3
         FC=FC-23.342D0*CP**4+11.052D0*CP**5
           IF(CP.GT.0.95D0)FC=21.888D0*CP-20.031D0
           IF(CP.LT.0.3D0)FC=0.007144D0+0.118D0*CP
        CLV=630.D0*FC
      CL=SCL+(CLFS+CLV)/AA**2
C
C     LOSS COEFF. THRU OIL CONTROL VALVE
C
      IF(CV.GT.0.9D0)FC=7.7649D0*CV-6.7555D0
      IF(CV.LE.0.9D0.AND.CV.GT.0.7D0)THEN
        FC=2.68205D0-7.39542D0*CV+5.19343D0*CV**2
      END IF
      IF(CV.LE.0.7D0.AND.CV.GT.0.3D0)THEN
        FC=-0.09577D0+0.72031D0*CV-1.73444D0*CV**2+1.4330D0*CV**3
      END IF
      IF(CV.LE.0.3D0)THEN
        FC=0.000444D0+0.004729D0*CV+0.01165D0*CV**2
      END IF
      CLOIL=3.250D7*FC
C
      RETURN
      END
C
```

```
C
C      ################################################
C      ################################################
C      ##                                            ##
C      ##     EEEEEEE    HH      HH    VV       VV    ##
C      ##     EE         HH      HH    VV       VV    ##
C      ##     EE         HH      HH     VV     VV     ##
C      ##     EEEEE      HH      HH     VV     VV     ##
C      ##     EE         HHHHHHHHHH      VV   VV      ##
C      ##     EE         HH      HH      VV   VV      ##
C      ##     EE         HH      HH       VV VV       ##
C      ##     EE         HH      HH       VV VV       ##
C      ##     EEEEEEE    HH      HH        VVV        ##
C      ##                                            ##
C      ##        COPYRIGHT 1990 P.G. HODGSON         ##
C      ##                                            ##
C      ################################################
C      ################################################
C
C           TORQUE/POWER vs. SPEED CHARACTERISTIC FOR
C
C              PARTIAL-FILL HYDRAULIC DYNAMOMETRS
C
C                ELECTRO-HYDRAULIC CONTROL VALVE
C
C                     PROGRAM VERSION 1.0
C
C                      DATE:  MAY 1990
C
C                     AUTHOR: P.G. HODGSON
C
C                   UNIVERSITY OF CANTERBURY
C
C
C     MAIN PROGRAM
C     ************
      PROGRAM EHV
C
      IMPLICIT DOUBLE PRECISION (A-H,O-Z)
C
      EXTERNAL F
      DIMENSION Y(20),YP(20),YPEXT(20)
C
      COMMON/FLG1/IPGM,ISS,IMAC,IRTR,IOUT,ITQSTT,IOPUT(6),ICES,IFUL,ICOM
      COMMON/FLG2/IT,INTS,IV,IVST,IVR,IVAR(4),MNQQ,ICS,ICLC
      COMMON/GEO1/RO,RI,RINERT,BRI,BRO,BSI,BSO,ZR,ZS,BT,FFAC,BFAC
      COMMON/GEO2/PI,RHO,ARHO,PO,RC,RM,VF,ENGINT,CYLN,FNN,SHSTFF
      COMMON/RUN1/RTFI,RTCR,PFIN,PFFI,PFCR
      COMMON/RUN2/CPIN,CPFI,CPCR,CPT,SMIN,SMAX,SICR,ST
      COMMON/RUN3/QIIN,QIFI,QICR,QIT,TQIN,TQFI,TQCR,TQT
      COMMON/SCON/CES,AA,CLFS,CLV,SCL,CL,PBFAC,PFFAC,RTS,WRV
      COMMON/VAR1/PERF,RCO,RCI,DYNERT,QIN,CP,P1,DP,QOUT
      COMMON/VAR2/W,WP,WE,THETA1,THETA2,DELTA,ACH2O,ACRTR,ACENG
      COMMON/VAR3/TOR,POW,ETOR,EPOW,EPHI,DDTDEL,DDTPF
      COMMON/ARR1/TQFAC(6),PIFAC(3),PLOSS(3),TQCMPT(6),SPRES(26)
      COMMON/CON1/IOTP,ICTR,IDYCON,ICVOP,KONVAR
      COMMON/CON2/TCONTR,TOUTP,WPD,TORD,CPD,CPOLD,CPNEW
      COMMON/CON3/CPDIN,CPDFI,CPDCR,CPDT,WPDIN,WPDFI,WPDCR,WPDT
      COMMON/CON4/TORDIN,TORDFI,TORDCR,TORDT
      COMMON/CON5/CKCV,CKPV,CKDV,TDV,CKCS,CKPS,CKIS,CKDS,TDS,TIS
      COMMON/CON6/CKCT,CKPT,CKIT,CKDT,TDT,TIT,CONCR,VSLEW
C
C OPEN OUTPUT, PLOT DATA & STORAGE FILES
      OPEN(2,FILE='[HODGSON.DATAA]OUT.GPH',STATUS='OLD')
      OPEN(6,FILE='[HODGSON.DATAA]OUT.DAT',STATUS='OLD')
      OPEN(8,FILE='[HODGSON.DATAA]NUM.DAT',STATUS='OLD')
      OPEN(9,STATUS='SCRATCH',FORM='UNFORMATTED')
C READ INPUT, SET UP PROGRAM & CALC. INVARIANT CONSTANTS
      CALL INPUT()
      CALL CONSTS()
C DYNAMIC
       IF(ITQSTT.EQ.1)CALL TQSTRT()
       T=0.D0
       TOUTP=0.D0
       TCONTR=0.D0
       RELERR=1.D-5
       ABSERR=1.D-5
C       PRINT *,' ENTER RELERR,ABSERR'
C       READ(*,*)RELERR,ABSERR
```

```
        IF(ISS.NE.1)THEN
          DYNERT=DYNERT+ENGINT
          ENGINT=DYNERT
        END IF
C INITIAL CONDITIONS
        CALL STATUS(1,T,T)
        CALL PART()
        CALL KFACTS()
        CALL VORVEL()
        CALL POWER()
        DELTA=0.D0
        IF(ISS.EQ.1)DELTA=ETOR/SHSTFF
        Y(1)=DELTA
        WP=WE
        Y(2)=WE
        Y(3)=WP
        Y(4)=PERF
C STORE DATA
        EPOW=ETOR*WE
        WRITE(9)SCL,CL,PBFAC,PFFAC,RTS,WRV
        WRITE(9)PERF,RCO,RCI,DYNERT,QIN,CP,P1,DP,QOUT
        WRITE(9)W,WP,WE,THETA1,THETA2,DELTA,ACH2O,ACRTR,ACENG
        WRITE(9)TOR,POW,ETOR,EPOW,EPHI,DDTDEL,DDTPF
        WRITE(9)(TQFAC(K),K=1,6),(PIFAC(K),K=1,3)
        WRITE(9)(PLOSS(K),K=1,3),(TQCMPT(K),K=1,6),(SPRES(K),K=1,26)
C
C SOLVE D.E.S FOR EACH TIME STEP
C
        IFLAG=1
        IOVF=0
        IOTP=1
        ICTR=1
C
        DO 1000 IT=2,INTS
C ADVANCE OUTPUT AND/OR CONTROLLER TIMES IF NECESSARY
 1313     CONTINUE
          IF(IOTP.EQ.1)THEN
            TOUTP=RTCR*DFLOAT(IT-1)
            IOTP=0
          END IF
          IF(ICTR.EQ.1)THEN
            TCONTR=TCONTR+CONCR
            ICTR=0
          END IF
C CHOOSE TO STEP TO EARLIER OF OUTPUT AND CONTROLLER TIMES
          IF(TOUTP.LE.TCONTR)THEN
            TOUT=TOUTP
            IOTP=1
            IF(TOUTP.EQ.TCONTR)ICTR=1
          ELSE
            TOUT=TCONTR
            ICTR=1
          END IF
C CALL EQUATION SOLVER
 1300     CONTINUE
          CALL DDE(F,4,Y,T,TOUT,RELERR,ABSERR,IFLAG)
C CHECK RETURN STATUS AND TAKE APPROPRIATE ACTION
 1333     IF(IFLAG.EQ.2)THEN
            IF(ISS.NE.1)Y(1)=0.D0
            DELTA=Y(1)
            WE=Y(2)
            WP=Y(3)
            PERF=Y(4)
            CALL F(T,T,Y,YPEXT)
            DDTDEL=YPEXT(1)
            ACENG=YPEXT(2)
            ACRTR=YPEXT(3)
            DDTPF=YPEXT(4)
C CALL CONTROLLER ROUTINE
            IF(ICTR.EQ.1)CALL CONTOL()
C STORE DATA
            IF(IOTP.EQ.1)THEN
              EPOW=ETOR*WE
              WRITE(9)SCL,CL,PBFAC,PFFAC,RTS,WRV
              WRITE(9)PERF,RCO,RCI,DYNERT,QIN,CP,P1,DP,QOUT
              WRITE(9)W,WP,WE,THETA1,THETA2,DELTA,ACH2O,ACRTR,ACENG
              WRITE(9)TOR,POW,ETOR,EPOW,EPHI,DDTDEL,DDTPF
              WRITE(9)(TQFAC(K),K=1,6),(PIFAC(K),K=1,3)
      WRITE(9)(PLOSS(K),K=1,3),(TQCMPT(K),K=1,6),(SPRES(K),K=1,26)
```

```
          END IF
        ELSE
          IF(IFLAG.EQ.3)PRINT *,' ERROR TOLER. TOO SMALL'
          IF(IFLAG.EQ.4)PRINT *,' TOO MANY STEPS. IT= ',IT
          IF(IFLAG.EQ.5)PRINT *,' EQUATIONS STIFF. IT= ',IT
          IF(IFLAG.EQ.6)PRINT *,' INCORRECT INPUT'
          IF(IFLAG.NE.6)IOVF=IOVF+1
        END IF
        IF(IFLAG.EQ.3.OR.IFLAG.EQ.4.OR.IFLAG.EQ.5)GOTO 1300
        IF(IOTP.EQ.0)GOTO 1313
        PRINT *, ' TIMESTEP ',IT,' COMPLETE'
 1000   CONTINUE
      IF(ISAV.EQ.1)ICOM=1
C OUTPUT INPUT & RESULTS
 8888 CONTINUE
      CALL OUTPUT()
C      IF(IOPUT(6).EQ.1)CALL AAAA()
C CLOSE FILES
      CLOSE(2)
      CLOSE(6)
      CLOSE(8)
      CLOSE(9)
C END PROGRAM
      PRINT *,' EXTRA DDE CALLS = ',IOVF
      PRINT *,' ***** PROGRAM EXECUTION COMPLETE *****'
      PRINT *,' ***** PROGRAM EXECUTION COMPLETE *****'
      PRINT *,' ***** PROGRAM EXECUTION COMPLETE *****'
 9999 STOP
      END
C
C
C
C     SUBROUTINE F
C     ************
C     THIS ROUTINE CALCULATES THE DE'S AT ANY TIME STEP
C
      SUBROUTINE F(X,XXOLD,Y,YP)
C
      IMPLICIT DOUBLE PRECISION (A-H,O-Z)
      DIMENSION Y(20),YP(20)
C
      COMMON/FLG1/IPGM,ISS,IMAC,IRTR,IOUT,ITQSTT,IOPUT(6),ICES,IFUL,ICOM
      COMMON/FLG2/IT,INTS,IV,IVST,IVR,IVAR(4),MNQQ,ICS,ICLC
      COMMON/GEO1/RO,RI,RINERT,BRI,BRO,BSI,BSO,ZR,ZS,BT,FFAC,BFAC
      COMMON/GEO2/PI,RHO,ARHO,PO,RC,RM,VF,ENGINT,CYLN,FNN,SHSTFF
      COMMON/RUN1/RTFI,RTCR,PFIN,PFFI,PFCR
      COMMON/RUN2/CPIN,CPFI,CPCR,CPT,SMIN,SMAX,SICR,ST
      COMMON/RUN3/QIIN,QIFI,QICR,QIT,TQIN,TQFI,TQCR,TQT
      COMMON/SCON/CES,AA,CLFS,CLV,SCL,CL,PBFAC,PFFAC,RTS,WRV
      COMMON/VAR1/PERF,RCO,RCI,DYNERT,QIN,CP,P1,DP,QOUT
      COMMON/VAR2/W,WP,WE,THETA1,THETA2,DELTA,ACH2O,ACRTR,ACENG
      COMMON/VAR3/TOR,POW,ETOR,EPOW,EPHI,DDTDEL,DDTPF
      COMMON/ARR1/TQFAC(6),PIFAC(3),PLOSS(3),TQCMPT(6),SPRES(26)
      COMMON/CON1/IOTP,ICTR,IDYCON,ICVOP,KONVAR
      COMMON/CON2/TCONTR,TOUTP,WPD,TORD,CPD,CPOLD,CPNEW
      COMMON/CON3/CPDIN,CPDFI,CPDCR,CPDT,WPDIN,WPDFI,WPDCR,WPDT
      COMMON/CON4/TORDIN,TORDFI,TORDCR,TORDT
      COMMON/CON5/CKCV,CKPV,CKDV,TDV,CKCS,CKPS,CKIS,CKDS,TDS,TIS
      COMMON/CON6/CKCT,CKPT,CKIT,CKDT,TDT,TIT,CONCR,VSLEW
C
      IF(ISS.NE.1)Y(1)=0.D0
      DELTA=Y(1)
      WE=Y(2)
      WP=Y(3)
      PERF=Y(4)
      CALL STATUS(1,X,XXOLD)
      CALL PART()
      CALL KFACTS()
      CALL VORVEL()
      CALL POWER()
      STOR=TQCMPT(1)+TQCMPT(2)+TQCMPT(3)+TQCMPT(4)
C DERIVATIVES CALC
      RWWP=W/WP
      YP(1)=WE-WP
      IF(IPGM.EQ.1)THEN
        IF(ISS.EQ.1)THEN
         YP(2)=(ETOR-SHSTFF*DELTA)/ENGINT
         YP(3)=(SHSTFF*DELTA-STOR)
         YP(3)=YP(3)/(DYNERT+2.D0*(TQFAC(5)+RWWP*TQFAC(6)))
```

```
        ELSE
         YP(2)=(ETOR-STOR)/(ENGINT+2.D0*(TQFAC(5)+RWWP*TQFAC(6)))
         YP(3)=(ETOR-STOR)/(DYNERT+2.D0*(TQFAC(5)+RWWP*TQFAC(6)))
        END IF
      END IF
      IF(IPGM.EQ.2)THEN
         YP(2)=SICR
        IF(ISS.EQ.1)THEN
         YP(3)=(SHSTFF*DELTA-STOR)
         YP(3)=YP(3)/(DYNERT+2.D0*(TQFAC(5)+RWWP*TQFAC(6)))
        ELSE
         YP(3)=YP(2)
        END IF
      END IF
      YP(4)=(QIN-QOUT)/VF
C
      ACRTR=YP(3)
      ACH2O=RWWP*ACRTR
      TQCMPT(5)=2.D0*TQFAC(5)*ACRTR
      TQCMPT(6)=2.D0*TQFAC(6)*ACH2O
      TOR=TQCMPT(1)+TQCMPT(2)+TQCMPT(3)+TQCMPT(4)+TQCMPT(5)+TQCMPT(6)
      POW=TOR*WP
      RETURN
      END
C
C
C
C
C     SUBROUTINE CONTOL
C     *****************
C     THIS ROUTINE SIMULATES THE CONTROL ACTIONS OF THE PID
C     ROUTINES FOR THE ELECTROHYDRAULIC OUTLET VALVE SYSTEM
C
      SUBROUTINE CONTOL()
C
      IMPLICIT DOUBLE PRECISION (A-H,O-Z)
C
      COMMON/FLG1/IPGM,ISS,IMAC,IRTR,IOUT,ITQSTT,IOPUT(6),ICES,IFUL,ICOM
      COMMON/FLG2/IT,INTS,IV,IVST,IVR,IVAR(4),MNQQ,ICS,ICLC
      COMMON/GEO1/RO,RI,RINERT,BRI,BRO,BSI,BSO,ZR,ZS,BT,FFAC,BFAC
      COMMON/GEO2/PI,RHO,ARHO,PO,RC,RM,VF,ENGINT,CYLN,FNN,SHSTFF
      COMMON/RUN1/RTFI,RTCR,PFIN,PFFI,PFCR
      COMMON/RUN2/CPIN,CPFI,CPCR,CPT,SMIN,SMAX,SICR,ST
      COMMON/RUN3/QIIN,QIFI,QICR,QIT,TQIN,TQFI,TQCR,TQT
      COMMON/SCON/CES,AA,CLFS,CLV,SCL,CL,PBFAC,PFFAC,RTS,WRV
      COMMON/VAR1/PERF,RCO,RCI,DYNERT,QIN,CP,P1,DP,QOUT
      COMMON/VAR2/W,WP,WE,THETA1,THETA2,DELTA,ACH2O,ACRTR,ACENG
      COMMON/VAR3/TOR,POW,ETOR,EPOW,EPHI,DDTDEL,DDTPF
      COMMON/ARR1/TQFAC(6),PIFAC(3),PLOSS(3),TQCMPT(6),SPRES(26)
      COMMON/CON1/IOTP,ICTR,IDYCON,ICVOP,KONVAR
      COMMON/CON2/TCONTR,TOUTP,WPD,TORD,CPD,CPOLD,CPNEW
      COMMON/CON3/CPDIN,CPDFI,CPDCR,CPDT,WPDIN,WPDFI,WPDCR,WPDT
      COMMON/CON4/TORDIN,TORDFI,TORDCR,TORDT
      COMMON/CON5/CKCV,CKPV,CKDV,TDV,CKCS,CKPS,CKIS,CKDS,TDS,TIS
      COMMON/CON6/CKCT,CKPT,CKIT,CKDT,TDT,TIT,CONCR,VSLEW
C
      TTT=CONCR
C
C VELOCITY OR POSITION FORM OF CONTROL EQUATIONS
C
      IF(ICVOP.EQ.1)THEN
C VELOCITY FORM
C SPEED CONTROL: PID
      IF(IDYCON.EQ.2)THEN
        E2=WP-WPD
      CPD=CPD+CKCS*(CKPS+CKIS*TTT/TIS+CKDS*TDS/TTT)*E2
      CPD=CPD-CKCS*(CKPS+CKDS*2.D0*TDS/TTT)*E2M1+CKCS*CKDS*TDS/TTT*E2M2
        E2M2=E2M1
        E2M1=E2
      END IF
C TORQUE CONTROL: PID
      IF(IDYCON.EQ.3)THEN
        E3=TORD-TOR
      CPD=CPD+CKCT*(CKPT+CKIT*TTT/TIT+CKDT*TDT/TTT)*E3
      CPD=CPD-CKCT*(CKPT+CKDT*2.D0*TDT/TTT)*E3M1+CKCT*CKDT*TDT/TTT*E3M2
        E3M2=E3M1
        E3M1=E3
      END IF
C VALVE CONTROL: PD
```

```
      CPOLD=CP
      E1=CPD-CP
      CPNEW=CP+CKCV*(CKPV+CKDV*TDV/TTT)*E1+CKCV*CKDV*TDV/TTT*E1M2
      CPNEW=CPNEW-CKCV*(CKPV+CKDV*2.D0*TDV/TTT)*E1M1
      E1M2=E1M1
      E1M1=E1
C
      ELSE
C POSITION FORM
C SPEED CONTROL: PID
      IF(IDYCON.EQ.2)THEN
        E2=WP-WPD
        SK2=SK2+E2
       CPD=CPDIN+CKCS*(CKPS*E2+CKIS*TTT*SK2/TIS+CKDS*TDS*(E2-E2OLD)/TTT)
        E2OLD=E2
      END IF
C TORQUE CONTROL: PID
      IF(IDYCON.EQ.3)THEN
        E3=TORD-TOR
        SK3=SK3+E3
       CPD=CPDIN+CKCT*(CKPT*E3+CKIT*TTT*SK3/TIT+CKDT*TDT*(E3-E3OLD)/TTT)
        E3OLD=E3
      END IF
C VALVE CONTROL: PD
      CPOLD=CP
      E1=CPD-CP
      CPNEW=CPIN+CKCV*(CKPV*E1+CKDV*TDV*(E1-E1OLD)/TTT)
      E1OLD=E1
C
      END IF
C
      RETURN
      END
C
C
C
C
C
C     SUBROUTINE CONSTS
C     *****************
C     THIS ROUTINE CALCULATES THE TIME INDEPENDENT CONSTANTS
C
      SUBROUTINE CONSTS()
C
      IMPLICIT DOUBLE PRECISION (A-H,O-Z)
C
      COMMON/FLG1/IPGM,ISS,IMAC,IRTR,IOUT,ITQSTT,IOPUT(6),ICES,IFUL,ICOM
      COMMON/FLG2/IT,INTS,IV,IVST,IVR,IVAR(4),MNQQ,ICS,ICLC
      COMMON/GEO1/RO,RI,RINERT,BRI,BRO,BSI,BSO,ZR,ZS,BT,FFAC,BFAC
      COMMON/GEO2/PI,RHO,ARHO,PO,RC,RM,VF,ENGINT,CYLN,FNN,SHSTFF
      COMMON/RUN1/RTFI,RTCR,PFIN,PFFI,PFCR
      COMMON/RUN2/CPIN,CPFI,CPCR,CPT,SMIN,SMAX,SICR,ST
      COMMON/RUN3/QIIN,QIFI,QICR,QIT,TQIN,TQFI,TQCR,TQT
      COMMON/SCON/CES,AA,CLFS,CLV,SCL,CL,PBFAC,PFFAC,RTS,WRV
      COMMON/VAR1/PERF,RCO,RCI,DYNERT,QIN,CP,P1,DP,QOUT
      COMMON/VAR2/W,WP,WE,THETA1,THETA2,DELTA,ACH2O,ACRTR,ACENG
      COMMON/VAR3/TOR,POW,ETOR,EPOW,EPHI,DDTDEL,DDTPF
      COMMON/ARR1/TQFAC(6),PIFAC(3),PLOSS(3),TQCMPT(6),SPRES(26)
      COMMON/CON1/IOTP,ICTR,IDYCON,ICVOP,KONVAR
      COMMON/CON2/TCONTR,TOUTP,WPD,TORD,CPD,CPOLD,CPNEW
      COMMON/CON3/CPDIN,CPDFI,CPDCR,CPDT,WPDIN,WPDFI,WPDCR,WPDT
      COMMON/CON4/TORDIN,TORDFI,TORDCR,TORDT
      COMMON/CON5/CKCV,CKPV,CKDV,TDV,CKCS,CKPS,CKIS,CKDS,TDS,TIS
      COMMON/CON6/CKCT,CKPT,CKIT,CKDT,TDT,TIT,CONCR,VSLEW
C
C     CONVERT PERF,CP,QIN,SPEED,ENG TORQUE
C
      CPIN=CPIN/100.D0
      SMIN=SMIN*PI/30.D0
      SMAX=SMAX*PI/30.D0
      SICR=SICR*PI/30.D0
      PFIN=PFIN/100.D0
      PFFI=PFFI/100.D0
      PFCR=PFCR/100.D0
C
      CP=CPIN
      WE=SMIN
      WP=SMIN
      QIN=QIIN
```

```
      ETOR=TQIN
      PERF=PFIN
      DYNERT=RINERT
C
      IF(CP.GT.1.D0)CP=1.D0
      IF(CP.LT.0.D0)CP=0.D0
      IF(PERF.GE.1.D0)PERF=1.D0
      IF(PERF.LE.0.D0)PERF=0.D0
      IFUL=0
      IF(PERF.GE.1.0)IFUL=1
C
C CONVERT CONTROLLER INPUT
      CONCR=1.D0/CONCR
      WPDIN=WPDIN*PI/30.D0
      WPDCR=WPDCR*PI/30.D0
      WPDFI=WPDFI*PI/30.D0
      CPDIN=CPDIN/100.D0
      CPDFI=CPDFI/100.D0
      CPDCR=CPDCR/100.D0
C
      WPD=WPDIN
      TORD=TORDIN
      CPD=CPDIN
      CPNEW=CP
      CPOLD=CP
C
      IF(CPD.GT.1.D0)CPD=1.D0
      IF(CPD.LT.0.D0)CPD=0.D0
C
C     CONVERT BLADE ANGLES
C
      BRI=BRI*PI/180.D0
      BRO=BRO*PI/180.D0
      BSI=BSI*PI/180.D0
      BSO=BSO*PI/180.D0
C
C     CALCULATE TIME STEPS & CALC. LOOPS
C     INTS & IVST CALCED IN INPUT()
C
C     LOSS COEFF.,AREAS ,OUTLET RADIUS (RC), CMPT. VOLUME (VF)
C
         RC=(RO+RI)/2.D0
         CL1=0.5D0
         CL2=1.D0
         IF(IOUT.EQ.2)CL2=0.8D0
         CLD=0.3D0
         CL6=0.8D0
         CL7=0.8D0
         CL8=0.5D0
         CLFS=0.72D0
         A0=0.054D0*0.036D0
         A1=PI*0.004D0*0.004D0*28.D0
         IF(IOUT.EQ.1)A1=PI*0.0055D0*0.0055D0*24.D0
         AD=0.018D0*0.031D0/2.D0
         AA=A0
         CG=0.01D0
      SCL=(CL1+CL2-1.D0)/A1**2+1.D0/A0**2+CLD/AD**2
      IF(IOUT.EQ.0)SCL=SCL+(1.D3/RO**2-1.D3/RC**2)/(4.D0*(PI*CG)**2)
      IF(IOUT.EQ.1)SCL=SCL+CL6/AA**2
      IF(IOUT.EQ.2)SCL=(CL1+CL2+CL7-1.D0)/A1**2+1.D0/A0**2+(CL6+CL8)/AA*
     1*2
      IF(IRTR.EQ.1)THEN
        A=(ZR/DSIN(BRI)+ZR/DSIN(BRO))/2.D0
        A=(A+ZS/DSIN(BSI)+ZS/DSIN(BSO))/4.D0
      ELSE
        A=(ZR/DSIN(BRI)+ZR/DSIN(BRO)+ZS/DSIN(BSI)+ZS/DSIN(BSO))/4.D0
      END IF
      BAV=(BRI+BRO+BSI+BSO)/4.D0
      VF=((RO-RI)**2)*(2.D0*PI*RC-A*BT)*PI*SIN(BAV)/4.D9
C
      RETURN
      END
C
C
C
C
C
C     SUBROUTINE STATUS
C     *****************
```

```
C     THIS ROUTINE CALCULATES THE CHANGES TO VALVE,SPEED,QIN
C     WITH TIME AND THE VALVE LOSS
C
      SUBROUTINE STATUS(III,XX,TT)
C
      IMPLICIT DOUBLE PRECISION (A-H,O-Z)
C
      COMMON/FLG1/IPGM,ISS,IMAC,IRTR,IOUT,ITQSTT,IOPUT(6),ICES,IFUL,ICOM
      COMMON/FLG2/IT,INTS,IV,IVST,IVR,IVAR(4),MNQQ,ICS,ICLC
      COMMON/GEO1/RO,RI,RINERT,BRI,BRO,BSI,BSO,ZR,ZS,BT,FFAC,BFAC
      COMMON/GEO2/PI,RHO,ARHO,PO,RC,RM,VF,ENGINT,CYLN,FNN,SHSTFF
      COMMON/RUN1/RTFI,RTCR,PFIN,PFFI,PFCR
      COMMON/RUN2/CPIN,CPFI,CPCR,CPT,SMIN,SMAX,SICR,ST
      COMMON/RUN3/QIIN,QIFI,QICR,QIT,TQIN,TQFI,TQCR,TQT
      COMMON/SCON/CES,AA,CLFS,CLV,SCL,CL,PBFAC,PFFAC,RTS,WRV
      COMMON/VAR1/PERF,RCO,RCI,DYNERT,QIN,CP,P1,DP,QOUT
      COMMON/VAR2/W,WP,WE,THETA1,THETA2,DELTA,ACH2O,ACRTR,ACENG
      COMMON/VAR3/TOR,POW,ETOR,EPOW,EPHI,DDTDEL,DDTPF
      COMMON/ARR1/TQFAC(6),PIFAC(3),PLOSS(3),TQCMPT(6),SPRES(26)
      COMMON/CON1/IOTP,ICTR,IDYCON,ICVOP,KONVAR
      COMMON/CON2/TCONTR,TOUTP,WPD,TORD,CPD,CPOLD,CPNEW
      COMMON/CON3/CPDIN,CPDFI,CPDCR,CPDT,WPDIN,WPDFI,WPDCR,WPDT
      COMMON/CON4/TORDIN,TORDFI,TORDCR,TORDT
      COMMON/CON5/CKCV,CKPV,CKDV,TDV,CKCS,CKPS,CKIS,CKDS,TDS,TIS
      COMMON/CON6/CKCT,CKPT,CKIT,CKDT,TDT,TIT,CONCR,VSLEW
C
      IF(III.EQ.1)THEN
C APPLY TIME CHANGES OF QIN,ENG SPEED,ENG TORQUE
C
        IF(IPGM.EQ.2)WE=SMIN
      IF(IPGM.EQ.2.AND.XX.GE.ST.AND.IVAR(2).NE.1)THEN
        IF(IVAR(2).EQ.2)WE=SMAX
        IF(IVAR(2).EQ.3)WE=WE+SICR*(XX-ST)
        IF(WE.GT.SMAX.AND.SMAX.GT.SMIN)WE=SMAX
        IF(WE.LT.SMAX.AND.SMAX.LT.SMIN)WE=SMAX
      END IF
        IF(IPGM.EQ.2)WE=WE*(1.D0+FNN*DSIN(CYLN*WE*XX/2.D0-PI/2.D0))
        IF(IPGM.EQ.2.AND.ISS.NE.1)WP=WE
        QIN=QIIN
      IF(XX.GE.QIT.AND.IVAR(3).NE.1)THEN
        IF(IVAR(3).EQ.2)QIN=QIFI
        IF(IVAR(3).EQ.3)QIN=QIN+QICR*(XX-QIT)
        IF(QIN.GT.QIFI.AND.QIFI.GT.QIIN)QIN=QIFI
        IF(QIN.LT.QIFI.AND.QIFI.LT.QIIN)QIN=QIFI
      END IF
        ETOR=TQIN
      IF(XX.GE.TQT.AND.IVAR(4).NE.1)THEN
        IF(IVAR(4).EQ.2)ETOR=TQFI
        IF(IVAR(4).EQ.3)ETOR=ETOR+TQCR*(XX-TQT)
        IF(ETOR.GT.TQFI.AND.TQFI.GT.TQIN)ETOR=TQFI
        IF(ETOR.LT.TQFI.AND.TQFI.LT.TQIN)ETOR=TQFI
      END IF
        ETOR=ETOR*(1.D0+FNN*DSIN(CYLN*WE*XX/2.D0))
C APPLY TIME CHANGES OF CONTROLLER DEMANDS
      IF(IDYCON.EQ.1)THEN
        CPD=CPDIN
      IF(XX.GE.CPDT.AND.KONVAR.GT.1)THEN
        IF(KONVAR.EQ.2)CPD=CPDFI
        IF(KONVAR.EQ.3)CPD=CPD+CPDCR*(XX-CPDT)
        IF(CPD.GT.CPDFI.AND.CPDFI.GT.CPDIN)CPD=CPDFI
        IF(CPD.LT.CPDFI.AND.CPDFI.LT.CPDIN)CPD=CPDFI
      END IF
      END IF
      IF(IDYCON.EQ.2)THEN
        WPD=WPDIN
      IF(XX.GE.WPDT.AND.KONVAR.GT.1)THEN
        IF(KONVAR.EQ.2)WPD=WPDFI
        IF(KONVAR.EQ.3)WPD=WPD+WPDCR*(XX-WPDT)
        IF(WPD.GT.WPDFI.AND.WPDFI.GT.WPDIN)WPD=WPDFI
        IF(WPD.LT.WPDFI.AND.WPDFI.LT.WPDIN)WPD=WPDFI
      END IF
      END IF
      IF(IDYCON.EQ.3)THEN
        TORD=TORDIN
      IF(XX.GE.TORDT.AND.KONVAR.GT.1)THEN
        IF(KONVAR.EQ.2)TORD=TORDFI
        IF(KONVAR.EQ.3)TORD=TORD+TORDCR*(XX-TORDT)
        IF(TORD.GT.TORDFI.AND.TORDFI.GT.TORDIN)TORD=TORDFI
        IF(TORD.LT.TORDFI.AND.TORDFI.LT.TORDIN)TORD=TORDFI
```

```
          END IF
          END IF
          VACUT=VSLEW*DABS(CPNEW-CPOLD)
          IF(VACUT.GE.(XX-TCONTR+CONCR).AND.CPNEW.NE.CPOLD)THEN
            CP=CPOLD+(XX-TCONTR+CONCR)/VACUT*(CPNEW-CPOLD)
          ELSE
            CP=CPNEW
          END IF
        END IF
C
        IF(CPD.GT.1.D0)CPD=1.D0
        IF(CPD.LT.0.D0)CPD=0.D0
        IF(CP.GT.1.D0)CP=1.D0
        IF(CP.LT.0.D0)CP=0.D0
C
C       LOSS COEFF.
C
           FC=.007144D0+.54479D0*CP-4.9163D0*CP**2+17.653D0*CP**3
           FC=FC-23.342D0*CP**4+11.052D0*CP**5
             IF(CP.LT.0.3D0)FC=0.007144D0+0.118D0*CP
          CLV=630.D0*FC
        CL=SCL+(CLFS+CLV)/AA**2
C
        RETURN
        END
```